U.PORTO

3º Ciclo

Biologia Básica e Aplicada

The Role of Insulin Resistance in Metabolic Reprogramming and Lineage Commitment

Dário Lúcio Ferreira de Jesus

2018

D

U.PORTO

Dário Lúcio Ferreira de Jesus. The Role of Insulin Resistance in Metabolic Reprogramming and Lineage Commitment

D.ICBAS **2018**

The Role of Insulin Resistance in Metabolic Reprogramming and Lineage Commitment
Dário Lúcio Ferreira de Jesus

SEDE ADMINISTRATIVA
INSTITUTO DE CIÊNCIAS BIOMÉDICAS ABEL SALAZAR
FACULDADE DE CIÊNCIAS
FACULDADE DE MEDICINA

DÁRIO LÚCIO FERREIRA DE JESUS

THE ROLE OF INSULIN RESISTANCE IN METABOLIC REPROGRAMMING AND LINEAGE COMMITMENT

Tese de Candidatura ao grau de Doutor em Biologia Básica e Aplicada submetida ao Instituto de Ciências Biomédicas Abel Salazar da Universidade do Porto.

Orientador – Doutor Rohit N Kulkarni
Categoria – Professor Catedrático
Afiliação – Joslin Diabetes Center and Harvard Medical School

Coorientador – Doutora Amélia M Silva
Categoria – Professora Auxiliar
Afiliação – Universidade de Trás-os-Montes e Alto Douro

Coorientador – Doutora Carmen Jerónimo
Categoria – Professora Associada Convidada com Agregação
Afiliação – Instituto de Ciências Biomédicas Abel Salazar da Universidade do Porto

All the experimental work presented here was conducted in the context of the Graduate Program in Areas of Basic and Applied Biology (GABBA) – 11st Edition at the Joslin Diabetes Center and Harvard Medical School and financially supported by the Portuguese Foundation for Science and Technology (FCT) – Fellowship #SFRH/BD/ 51699/2011, Albert Renold Travel Fellowship, FLAD grant for Research Internship, and by the Harvard Stem Cell Institute (HSCI) and National Institute of Health (NIH) grants R01 DK67536, R01 DK103215 and UC4 DK116278.

The following articles were used to write this thesis:

De Jesus DF*, Gupta, MK*, Kahraman S, Valdez IA, Shamsi F, Yi L, Swensen, AC, Tseng, YH, Qian, WJ, Kulkarni RN. Insulin receptor-mediated signaling regulates pluripotency markers and lineage differentiation. Molecular Metabolism. DOI:org/10.1016/j.molmet.2018.09.003, 2018. (*co-first authors).

De Jesus DF, Orime K, Dirice E, Kaminska D, Wang CH, Hu J, Mannisto V, Silva AM, Tseng YH, Pihlajamaki J, Kulkarni RN. NREP bridges TGF-β Signaling and Lipid Metabolism in the Epigenetic Programming of NAFLD. *In revision.*

Other articles published during my PhD:

Dirice E, Kahraman S, Jiang W, El Ouaamari A, **De Jesus DF**, Teo A, Hu J, Kawamori D, Gaglia J, Mathis D, Kulkarni RN. Soluble factors secreted by T-cells promote β-cell proliferation. Diabetes 63:188-202, 2014.

Kahraman S*, Dirice E*, **De Jesus DF**, Hu J, Kulkarni RN. Maternal insulin resistance and transient hyperglycemia impacts the metabolic and endocrine phenotypes of offspring. APJ - Endocrinology and Metabolism DOI: 10.1152/ajpendo.00210.2014, 2014. (*co-first authors).

De Jesus DF, Kulkarni RN. Epigenetic modifiers of islet function and mass. TEM 25(12): 628-636, 2015.

El Ouaamari A, Zhou J, Liew CW, Shirakawa J, Dirice E, Gedeon N, Kahraman S, **De Jesus DF**, Bhatt S, Kim JS, Clauss TRW, Camp DG, Smith RD, Qian WJ and Kulkarni RN. Compensatory Islet Response to Insulin Resistance Revealed by Quantitative Proteomics. J. Proteome Res 14(8):3111-22, 2015.

Gupta MK, Teo AKK, Rao TN, Bhatt S, Kleinridders A, Shirakawa, J, Takatani T, **De Jesus DF,** Windmueller R, Wagers AJ, Kulkarni RN. Excessive cellular proliferation negatively impacts reprogramming efficiency of human fibroblasts. Stem Cells Trans Med DOI: 10.5966/sctm.2014-0217.

El Ouaamari A, Dirice E, Gedeon N, Hu J, Zhou JY, Shirakawa J, Hou L, Goodman J, Karampelias C, Qiang G, Boucher J, Martinez R,Gritsenko MA, **De Jesus DF**, Kahraman S, Bhatt S, Smith RD, Beer H, Jungtrakoon P, Gong Y, Goldfine AB, Liew CW, Doria A, Andersson O, Qian WJ, Remold-O'Donnell E, and Kulkarni RN. SerpinB1 Promotes Pancreatic β-Cell Proliferation. Cell Metabolism 23:1-12, 2016.

Shirakawa J*, **De Jesus DF***, and Kulkarni RN. Exploring inter-organ crosstalk to uncover mechanisms that regulate β-cell function and mass. Eur J Clin Nutr 7(7): 896-903, 2017. (*co-first authors).

Aos meus pais,

Alípio e Armanda

Acknowledgments

Acknowledgments

Without the guidance and support from the following people, this adventure could never have happened. I would like to express my gratitude to my mentor and PhD supervisor Rohit N. Kulkarni for his support and encouragement throughout all these years. It's a privilege and uniquely rare to find a mentor that never clips our wings. I would like to thank Amélia Silva for her co-supervision, guidance, and above all, for her friendship. Amélia was fundamental for my successful Fulbright application which brought me to the US for the first time in 2010. That paved the way for my acceptance in GABBA and totally shaped my future. She is a truly inspiring and graceful person. I thank my co-supervisor and GABBA alumni, Carmen Jerónimo for her advice and help with many of the bureaucratic paperwork we had to fill during these years.

I wish to thank my colleagues and friends in the lab. Other labs at Joslin sometimes tell us we are loud, that we laugh a lot, that we party a lot. What they probably don't know is that we are just normal people.

Nothing of this could be possible without the GABBA. It is such a privilege to be in this family (yes, because it is clearly not only a PhD program). GABBA challenge us and give us critical thinking skills. Thank you to the 15th edition of GABBA. I would like to thank the former but especially the current GABBA director Prof. António Amorim. His book, "*A Espécie das Origens*", was the very first scientific book I read back at the high school. I was far from imagining I would end up in a PhD program directed by him. I would like to thank Prof. Maria de Sousa. I could not believe when she called me around 9 pm in Boston (2 am in Lisbon!) telling me I was accepted in the program. She has been a truly inspiration for the whole GABBA. I thank Catarina Carona for the unmeasurable efforts in taking care of everything.

A big thank to my "*cem segundas intencões*" friends. Porto is just an empty city if I don't see you there.

Obrigado aos meus pais e irmãos por todo o apoio. A receita lá de casa para a vida sempre foi muito simples: trabalho, honestidade e carácter. Cresci e durante muito tempo não percebi porque os meus pais tinham de trabalhar tanto e não percebia porque nunca gozavam de férias como tantas outras familias. Percebo hoje e só lhes posso estar grato.

Elisa, grazie di cuore per l'affetto e il tuo supporto. Lascia che il pane non finisca mai nella nostra vita.

Abstract

Abstract

The insulin receptor (IR) belongs to the tyrosine kinase family of transmembrane signaling proteins that collectively are fundamentally important regulators of cell differentiation, growth, and metabolism. The insulin receptor signaling has unique and broad physiological and biochemical functions that include the development of nonalcoholic fatty liver disease (NAFLD) and the regulation of pluripotency and differentiation of pluripotent stem cells.

The prevalence of NAFLD is increasing worldwide in parallel with the obesity epidemic. We aimed to investigate the impact of paternal and maternal insulin resistance on the metabolic phenotypes of their offspring to identify the underlying genetic and epigenetic contributors of NAFLD. To this end, we used the liver-specific insulin receptor knockout (LIRKO) mouse, a unique non-dietary model manifesting insulin resistance. In this thesis we show that parental insulin resistance reprograms several members of the TGF-β family including the neuronal regeneration-related protein (NREP). NREP modulates the expression of *PPARγ*, *SREBP1c* and *SREBP2*, while acting on ATP-citrate lyase in a phospho-AKT dependent manner to regulate hepatic triglyceride and cholesterol metabolism. The reduced hepatic expression of *NREP* in patients with hepatic steatosis, and significant correlations between the low serum NREP levels and the presence of steatosis and NASH highlight the translational relevance of our findings in the context of recent preclinical trials implicating ATP-citrate lyase in NAFLD progression.

Next, we focused on the importance of IR-mediated signaling in pluripotency and differentiation. Therefore, in the second part of this thesis, we aimed to investigate the significance of IR dependent and independent signaling pathways involved in pluripotency and differentiation. Expression of several pluripotency markers were upregulated in IRKO iPSCs and phosphoproteomics confirmed the novel IR-mediated regulation of the global pluripotency network including key proteins involved in growth and embryonic development. Thus, IRKO iPSCs provide an opportunity to explore the crosstalk of IR signaling with key pluripotency related signaling pathways in the maintenance of pluripotency and lineage determination.

Keywords: *NAFLD, Insulin resistance, metabolic reprogramming, lineage commitment.*

Resumo

Resumo

O receptor de insulina (IR) pertence à família dos recetores tirosina cinase, proteínas transmembranares, fundamentais para a regulação de diferenciação celular, crescimento e metabolismo. A sinalização da insulina mediada pelo IR está implicada na regulação de vários processos fisiológicos e bioquímicos únicos que incluem o desenvolvimento de fígado gordo não alcoólico e a regulação dos factores de pluripotência e diferenciação.

A prevalência de fígado gordo não alcoólico está a aumentar mundialmente e de uma forma paralela à epidemia da obesidade. O nosso objectivo foi investigar o impacto da insulino-resistência paternal ou maternal na primeira geracão e identificar os mecanismos genéticos e epigenéticos envolvidos no desenvolvimento de fígado gordo não alcoólico. Neste trabalho, demonstramos que a insulino-resistência parental afeta vários membros da família TGF-β, incluíndo *regeneration-related protein* (NREP). NREP regula a expressão genética de *PPARγ*, *SREBP1c* e *SREBP2*, controlando em simultâneo a ATP-citrato liase através da regulação da fosforilação da AKT, regulando desta forma o metabolismo hepático de triglicéridos e colesterol. A redução da expressão genética de *NREP* e a correlação entre níveis baixos de NREP e presença de esteatose e esteato-hepatite não alcoólica salientam a importância dos nossos resultados num contexto de vários ensaios experimentais envolvendo a *ATP-citrato liase* e a progressão de esteatose hepática não alcoólica.

Em seguida estudámos a importância da sinalização da insulina na manutenção da pluripotência e diferenciação. Assim, na segunda parte desta tese investigámos a importância da sinalização directa e indirecta do receptor de insulina envolvida na regulação da pluripotência e diferenciação. A expressão de vários marcadores de pluripotência foram aumentados, nas células estaminais pluripotentes induzidas (iPSCs) sem o receptor de insulina (IRKO), e através de fosfo-proteómica confirmámos o papel de IR na regulação da rede global de pluripotência incluíndo proteínas cruciais relacionadas com crescimento e desenvolvimento. Assim, as IRKO iPSCs oferecem uma oportunidade para explorar a interconnectividade da sinalização da insulina com as principais vias de sinalização relacionadas com a manutenção da pluripotência e diferenciação .

Palavras-chave: *esteatose hepática, insulino-resistência, reprogramação metabólica, diferenciação.*

Table of Contents

Table of Contents

List of Abbreviations

List of Abbreviations

ACLY	ATP citrate lyase
AKT	Protein kinase B
BER	Base excision repair
CpG	5'—C—phosphate—G—3'
DNMT	DNA methyltransferase
eIF3b	Eukaryotic translation initiation factor 3 subunit B
EMT	Epithelial–mesenchymal transition
ERK	Extracellular signal–regulated kinases
ESCs	Embryonic stem cells
FASN	Fatty acid synthase
GSK3	Glycogen synthase kinase 3
IGF1	Insulin-like growth factor
iPSCs	Induced pluripotent stem cells
IR	Insulin receptor
KLF4	Kruppel like factor 4
LAP	Latency associated protein
LIF	Leukemia inhibitory factor
LIRKO	Liver-specific insulin receptor knock-out
MEK	Mitogen-activated protein kinase kinase 1
NAFLD	Non-alcoholic fatty liver disease
NANOG	Homeobox transcription factor nanog
NASH	Non-alcoholic steatohepatitis
NREP	Neuronal regeneration related protein
OCT4	Octamer-binding transcription factor 4
PGC1A	Peroxisome proliferator-activated receptor gamma coactivator 1-alpha
Pi3K	Phosphoinositide 3-kinase
PPARA	Peroxisome Proliferator Activated Receptor Alpha

PPARG	Peroxisome proliferator-activated receptor gamma
ROS	Reactive oxygen species
SOX2	Sex determining region Y-box 2
SREBP1	Sterol regulatory element-binding protein 1
SREBP2	Sterol regulatory element-binding protein 2
STAT3	Signal transducer and activator of transcription 3
TET	Ten-eleven translocation
TGF	Transforming growth factor

Chapter I - Introduction

Section 1

1. Developmental Priming and Non-Alcoholic Fatty Liver Disease (NAFLD)

1.1 Prevalence and etiology of NAFLD

Nonalcoholic fatty liver disease (NAFLD) is a clinical condition characterized by excess liver fat accumulation (>5% of liver weight). It is emerging as one of the most prevalent pathophysiological conditions among liver diseases and constitutes an enormous burden to healthcare systems (Brumbaugh and Friedman 2013; Bush, Golabi et al. 2017; Younossi, Anstee et al. 2018).

Prevalence estimates of NAFLD reach up to 10% among children in western populations. NAFLD diagnosis increases with aging and the number of adolescents with the disease has doubled in the last 30 years (Brumbaugh and Friedman 2013; Li, Reynolds et al. 2015). Pediatric and adult NAFLD increase the risk of several clinical conditions such as metabolic disease, insulin resistance, diabetes, hypertension among others (Li, Reynolds et al. 2015; Bush, Golabi et al. 2017). However, NAFLD in children presents some unique characteristics that differentiate it from adults. For example, while adults favor fat accumulation in a perivenular fashion in the liver, pediatric fat accumulation is mostly in the periportal regions and is usually associated with inflammation and advanced liver disease (Brumbaugh and Friedman 2013; Li, Reynolds et al. 2015; Bush, Golabi et al. 2017; Younossi, Anstee et al. 2018).

NAFLD can be characterized by the presence of simple fat accumulation–i.e. steatosis, or co-exists with inflammation and ballooning which together constitute steatohepatitis (NASH). A subset of these patients progress to fibrosis and ultimately develops cirrhosis and hepatocellular carcinoma. While initial observations considered this transition a sequential process, it is now accepted that the pathogenesis of simple steatosis and NASH is mediated by different molecular mechanisms (Li, Reynolds et al. 2015). Overall, the accumulation of fat in hepatocytes is achieved by four main mechanisms: a) increased free fatty acid uptake, b) increased *de novo* lipogenesis, c) decreased beta-oxidation, and d) decreased hepatic VLDL-triglyceride secretion (Buzzetti, Pinzani et al. 2016; Eslam, Valenti et al. 2018). In NASH the progression of steatosis and inflammation may constitute a parallel mechanism that feedbacks with each other. Only 20% of the NAFLD patient's progress rapidly to liver fibrosis or

cirrhosis and 5% of patients with NAFLD succumb from liver-derived complications (Figure 1). The observed heterogeneity in NAFLD might lie in earlier origins of the disease in some patients and the metabolic phenotypes might be transmitted from parents to offspring to impact the risk and etiology of NAFLD progression (Brumbaugh and Friedman 2013; Bush, Golabi et al. 2017).

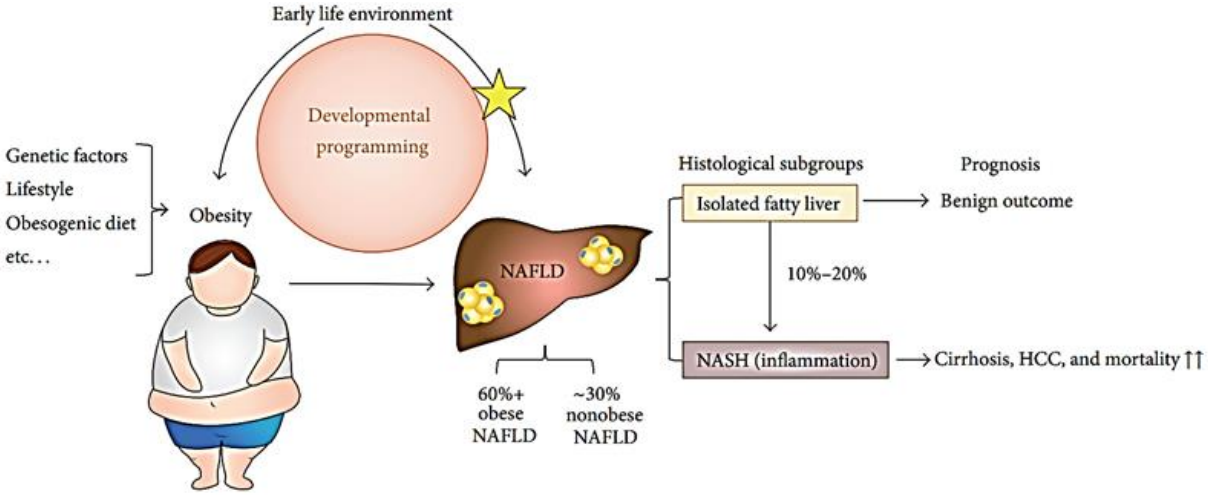

Figure 1: Graphical representation of non-alcoholic fatty-liver disease (NAFLD). NAFLD programming can be secondary to the development of obesity and associated co-morbidities or as a direct consequence of early life environment such as paternal and/or maternal effects. More than 60% of patients with NAFLD are obese; however, a large percentage (~30%) develops NAFLD independent of obesity. About 10-20% of the cases progress into the most severe forms of NAFLD–NASH, characterized by lipid accumulation and inflammation. Patients with nonalcoholic steatohepatitis (NASH) may progress into cirrhosis and hepatocellular carcinoma (HCC). Figure adapted from (Li, Reynolds et al. 2015).

1.2 Hereditability of NAFLD

The complex etiology of NAFLD likely involves genomic and environmental interactions (Eslam, Valenti et al. 2018; Younossi, Anstee et al. 2018). Several experimental approaches have confirmed the strong genetic component underlying the development of NAFLD. First, family studies have demonstrated that fatty liver is significantly more common in siblings and parents of children with NAFLD (Schwimmer, Celedon et al. 2009). These

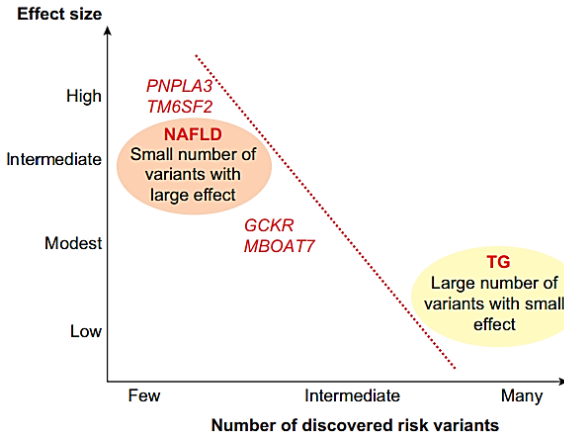

Figure 2: NAFLD risk variants. Graphical representation of the genes possessing risk variants and their effect size compared to loci associated with circulating triglycerides levels (TG). Figure adapted from (Eslam, Valenti et al. 2018).

data together with other reports have demonstrated that familial factors are an important element in the development of NAFLD. Twin studies have further strengthened the notion of NAFLD hereditability. A cross-sectional study analyzing 42 pairs of monozygotic and 18 dizygotic twins has found a strong positive correlation of hepatic steatosis and fibrosis between monozygotic twins (Loomba, Schork et al. 2015). Recently, genome-wide association studies (GWAS) have identified several risk variants mainly affecting genes involved in lipid metabolism (Figure 2) (reviewed in: (Eslam, Valenti et al. 2018)). The variants with largest effect are related to four genes: patatin-like phospholipase domain-containing protein 3 (PNPLA3), transmembrane 6 superfamily member 2 (TM6SF2), glucokinase regulatory gene (GCKR) and membrane bound O-acyltransferase domain containing 7 (MBOAT7) (Eslam, Valenti et al. 2018; Younossi, Anstee et al. 2018) .

1.3 Epigenetic mechanisms in the developmental programming of NAFLD

DNA methylation is an evolutionary conserved mechanism that implies the addition of a methyl group to the 5´ position of the cytosine pyrimidine ring (5-mC). Roughly, 70% of all CpG dinucleotides (CpGs) are methylated, and most of the unmethylated CpGs are clustered in “CpG islands” (Suzuki and Bird 2008). CpG islands are CG enriched segments and are often situated close to the promoter regions of the genes, and can influence the affinity of transcription factors to the DNA binding sites (Suzuki and Bird 2008). DNA methylation is established and maintained by DNA methyltransferase enzymes (DNMTs). There are different classes of DNMTs with different molecular functions, e.g. the role of DNMT1 is to maintain the DNA methylation pattern, while DNMT3a and 3b generate new methylation patterns (*de novo* methylation) (Mazzio and Soliman 2012). DNA hypermethylation is generally associated with gene silencing while DNA hypomethylation correlates with gene activation. DNA demethylation was thought to occur due to a lack or reduction of DNMTs, until the discovery of three families of enzymes (e.g. TET (Tet methylcytosine dioxygenase 1), AID/APOBEC (activation-induced deaminase/apolipoprotein B), and BER (base-excision repair glycosylases)) that were associated with active and dynamic DNA demethylation (Zhu 2009; Bhutani, Burns et al. 2011; Williams, Christensen et al. 2012).

The molecular mechanisms involved in the developmental programming of NAFLD are multifactorial and involve epigenetic pathways. Paternal but mostly maternal-associated effects have been reported to reshape DNA methylation

landscapes in offspring to modulate hepatic *de novo* lipogenesis, mitochondrial and endoplasmic reticulum function and adaptation to inflammation.

NAFLD is characterized by an excessive storage of triacylglycerol (TAG), inflammation and liver damage. Donnelly et al. (2005) used stable isotopes to identify the hepatic lipid sources in NAFLD patients. Among liver TAG ~56% were derived from serum free-fatty acids, ~26% from *de novo* lipogenesis and ~15% from diet (Donnelly, Smith et al. 2005). Male offspring exposed to western diet during the prenatal and post-weaning periods present hepatic accumulation of cholesterol and triglycerides associated with increased *de novo* lipogenesis and alterations in DNA methylation of important metabolic genes such as fatty-acid synthase (*Fasn*) (Pruis, Lendvai et al. 2014).

Mitochondria are essential for energy generation and are the primary sites for lipid β-oxidation. In NAFLD mitochondrial β-oxidation increases to compensate the high lipid demand (Li, Reynolds et al. 2015). This increment leads to an augmentation in ROS production that ultimately contributes to progression of NAFLD leading to inflammation, fibrosis and cell death (Li, Reynolds et al. 2015). Peroxisome proliferator-activated receptor γ coactivator 1α gene (PGC1α) activates peroxisome proliferator-activated receptor alpha (PPARα) and is essential for mitochondrial biogenesis and proper lipid β-oxidation and respiratory function (Lin, Handschin et al. 2005). Indeed, liver samples collected from NALFD patients revealed increased DNA methylation of the PGC1α promoter that negatively correlated with PGC1α mRNA (Sookoian, Rosselli et al. 2010). Furthermore, maternal HFD in rodents during pregnancy decreases liver mtDNA copy number and decreases the expression of PGC1α (Burgueño, Cabrerizo et al. 2013). Paternal effects were also reported to affect liver lipid metabolism. Offspring of fathers fed a low-protein diet exhibit increased expression of several genes involved in cholesterol biosynthesis and manifest changes in DNA methylation of PPARα (Carone, Fauquier et al. 2010).

Recent work has also demonstrated DNA methylation alterations in known fibrotic genes in patients with NAFLD (Zeybel, Hardy et al. 2015). Further studies are needed to fully elucidate the importance of DNA methylation in NAFLD development.

1.4 The TGF-β – NREP signaling axis

Neuronal regeneration-related protein (NREP) is an 8kD highly conserved protein with a PEST domain responsible for its fast ubiquitin-dependent degradation (Studler, Glowinski et al. 1993; Taylor, Hudson et al. 2000; Stradiot, Mannaerts et al.

2018). NREP is highly expressed in several brain regions that exhibit active postnatal neurogenesis and intense synaptic activity such as cerebellum, hippocampus and the olfactory bulb (Studler, Glowinski et al. 1993; Taylor, Hudson et al. 2000; Stradiot, Mannaerts et al. 2018).

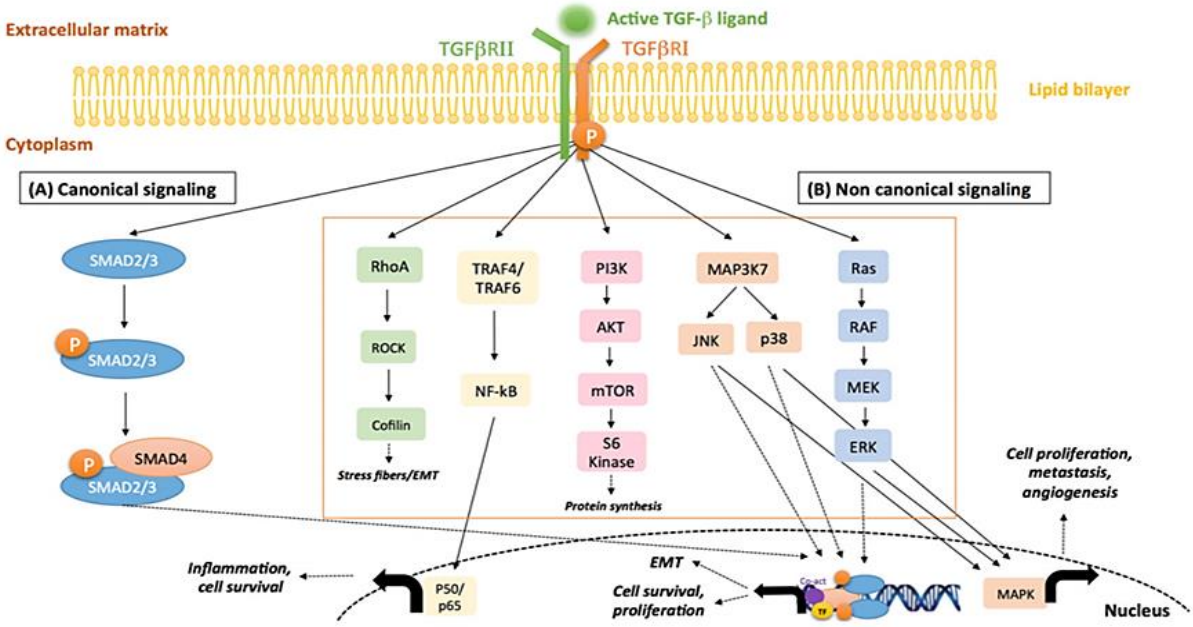

Figure 3: Canonical and non-canonical pathways involved in TGF-β signaling. (A) In the canonical signaling branch TGF-β binds to TGF-β receptor 2 which in turn activates TGF-β receptor 1 signaling through SMAD2-3 protein. (B) In the non-canonical pathway TGF-β can signal through various branches including the phosphatidylinositide 3-kinase (PI3K) and AKT to control protein synthesis, Figure adapted from (Costanza, Umelo et al. 2017).

NREP is a naturally disordered protein and requires binding partners to acquire tertiary structure (Taylor, Hudson et al. 2000). NREP interacts with several cytoskeletal proteins such as Filamin A, non-muscle myosin heavy chain 9 (MYH9) and with the eukaryotic translation initiation factor 3, subunit B (eIF3b) (Stradiot, Mannaerts et al. 2018). NREP has been also shown to modulate the TGF-β pathway (Stradiot, Mannaerts et al. 2018). In summary, TGF-β1 binds to TGF-β1/2 receptors and signals through the canonical and non-canonical pathways controlling various biological functions (Figure 3) such as epithelial-to-mesenchymal transition (EMT) and the conversion of fibroblast and mesenchymal cells into myofibroblasts (Costanza, Umelo et al. 2017; Stradiot, Mannaerts et al. 2018). The precise mechanism by which NREP regulates the TGF-β pathway is not entirely elucidated and includes different results in different systems (Figure 4) (reviewed in: (Stradiot, Mannaerts et al. 2018)). NREP was found to interact with the TGF-β latent associated protein (LAP) and to control TGF-β autoinduction by regulating the expression levels of TGF-β1 and 2 (Paliwal, Shi et al.

2004). Furthermore, Pan and colleagues (Pan, Zhe et al. 2002) reported that NREP overexpression in myofibroblasts inhibits TGF-β1 and TGF-β2 receptors and a decrease in fibrotic markers. These results were the first suggesting that NREP prevents fibrosis (Pan, Zhe et al. 2002). The relevance of NREP-TGF-β axis in the development of NAFLD is further strengthened by reports linking TGF-β signaling with lipid metabolism. TGF-β signaling was shown to induce stearoyl-CoA desaturase (SCD) expression and control lipid metabolism (Samuel, Nagineni et al. 2002). Furthermore, TGF-β signaling promotes lipid accumulation and decreased β-oxidation in hepatocytes in a mechanism that requires signaling through TGF-β receptor 2 (Yang, Roh et al. 2014).

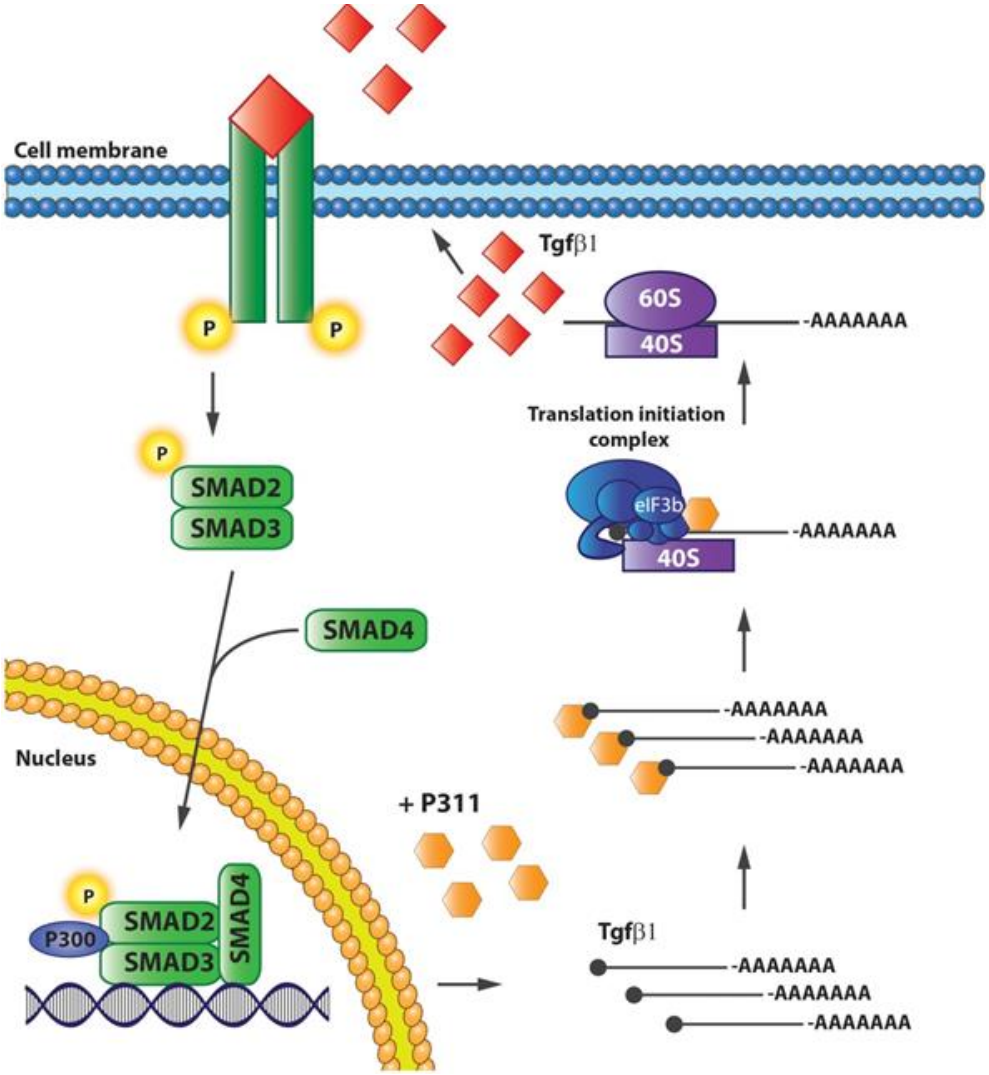

Figure 4: Proposed model of NREP (also known as P311) stimulated TGF-β1 translation. NREP binds to the TGF-β1 mRNA and eukaryotic translation initiation factor 3, to regulate the translation of TGF-β1. Figure adapted from (Stradiot, Mannaerts et al. 2018).

Section 2

2. Mechanisms Underlying the Maintenance of Pluripotency and Lineage Determination

2.1 Transcription Factors Modulating the Maintenance of Pluripotency

Embryonic stem cells (ESCs) are derived from the inner cell mass (ICM) of blastocysts during development and require specific *in vitro* culture conditions to maintain pluripotency and the capacity to self-renew (Chen, Cheng et al. 2017). On the other hand, differentiated cells can be reprogrammed to an embryonic-like state by the transfer of specific transcription factors (Takahashi and Yamanaka 2006). These cells were designated by Takahashi and Yamanaka (2006) as induced pluripotent stem cells (iPSCs). The latter cells possess a great value for basic research and a potential for future clinical interventions (Zhao and Jin 2017). In the past decade a lot of effort was allocated in understanding the factors and pathways controlling pluripotency and differentiation capacity of ESCs and iPSCs. Pluripotency is defined as the capacity of a cell to differentiate into the three germ layers (e.g. ectoderm, endoderm and mesoderm) (Chen, Cheng et al. 2017). There are multiple transcription factors, particularly Oct4, Sox2, Nanog and Klf4, that act in complex and counter-regulatory manners to control pluripotency, (Takahashi and Yamanaka 2016; Zhao and Jin 2017).

Oct4 belongs to the POU family and is a master regulator of pluripotency (Sterneckert, Höing et al. 2012). Oct4 is specifically expressed in pluripotent cells and its expression is sufficient to induce pluripotency in somatic cells (Sterneckert, Höing et al. 2012). Recently, Oct4 has been proposed to be more than a master regulator of pluripotency (Sterneckert, Höing et al. 2012). Indeed,

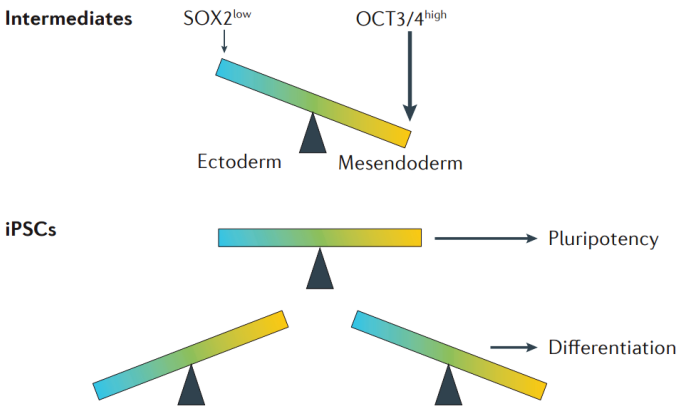

Figure 5: SOX2 and OCT3/4 balance controls pluripotency and differentiation. For example, high levels of Oct4 and low levels of Sox2 induce a transient mesodermal feature which is essential for progression of reprogramming. However the maintenance of pluripotency requires careful equilibration of the levels of cell-fate factors. Figure adapted from (Takahashi and Yamanaka 2016).

while moderate Oct4 expression enables derivation and maintenance of pluripotency, Oct4 overexpression induces differentiation into mesoderm and endoderm lineages (Niwa, Miyazaki et al. 2000). This complex fine-tuning mechanism involves secondary transcription factors (Figure 5).

Sox2 belongs to the Sox family of transcription factors and has a highly conserved high-mobility-group (HMG) DNA binding domain (Zhang and Cui 2014). Sox2 has been shown to be fundamental for embryonic development but it has several different functional effects due to the diverse number of interactions with other cofactors (Zhang and Cui 2014). Reduced levels of Sox2 leads to loss of pluripotency but this can be rescued via overexpression of Oct4, suggesting it has a secondary role to Oct4 in maintaining pluripotency (Zhang and Cui 2014; Chen, Cheng et al. 2017).

Several Kruppel-like factors (Klf) act to control pluripotency (Hall, Guo et al. 2009; Chen, Cheng et al. 2017). Klf4 acts in combination with the core regulatory circuit Oct4/Sox2/Nanog to prevent ESC differentiation and to maintain pluripotency (Chen, Cheng et al. 2017). Oct4 acts with Stat3 signaling in the direct regulation of Klf transcriptional factors which reinforce the pluripotent state of ESCs (Hall, Guo et al. 2009).

Nanog is a homeodomain transcription factor that plays a role in maintaining pluripotency and is important in mouse embryonic development (Chen, Cheng et al. 2017). Chromatin immunoprecipitation experiments revealed that Oct4 and Nanog overlap substantially in the downstream targets (Loh, Wu et al. 2006). Many of these targets are involved in control of pluripotency, self-renewal and cell fate determination (Loh, Wu et al. 2006). While Sox2 and Oct4 expression is relatively uniform, the levels of Nanog fluctuate between states of high expression and lower expression in ESCs (Navarro, Festuccia et al. 2012). Indeed, Nanog auto-repression is the main mechanism of Nanog transcription switching and is virtually independent of Oct4 and Sox2 (Navarro, Festuccia et al. 2012). Consistent with these findings, recently, Nanog was shown to be dispensable for the formation of iPSCs under proper culture conditions (Schwarz, Bar-Nur et al. 2014). Indeed, Nanog-deficient iPSCs generate teratomas and chimeric mice (Schwarz, Bar-Nur et al. 2014).

2.2 Signaling Pathways Regulating Pluripotency and Differentiation

Mouse ESCs were first progressively cultured *in vitro* in 1981 after the development of a “feeder-system”, consisting of a lower layer of inactivated fibroblasts (Evans and Kaufman 1981). The essential factor secreted by fibroblasts is leukemia inhibitory factor (LIF) and serum can be exchanged by the use of bone morphogenetic protein 4 (BMP4) (Ye, Liu et al. 2014). BMP4 is dispensable in a 2i system (Ye, Liu et al. 2014) which involves the addition of two inhibitors: CHIR99021–a glycogen synthase kinase 3 (GSK3) inhibitor, and PD032901–mitogen activated kinase kinase (MEK) inhibitor. LIF/2i systems are widely used to generate and maintain mouse ESCs and iPSCs (Ye, Liu et al. 2014).

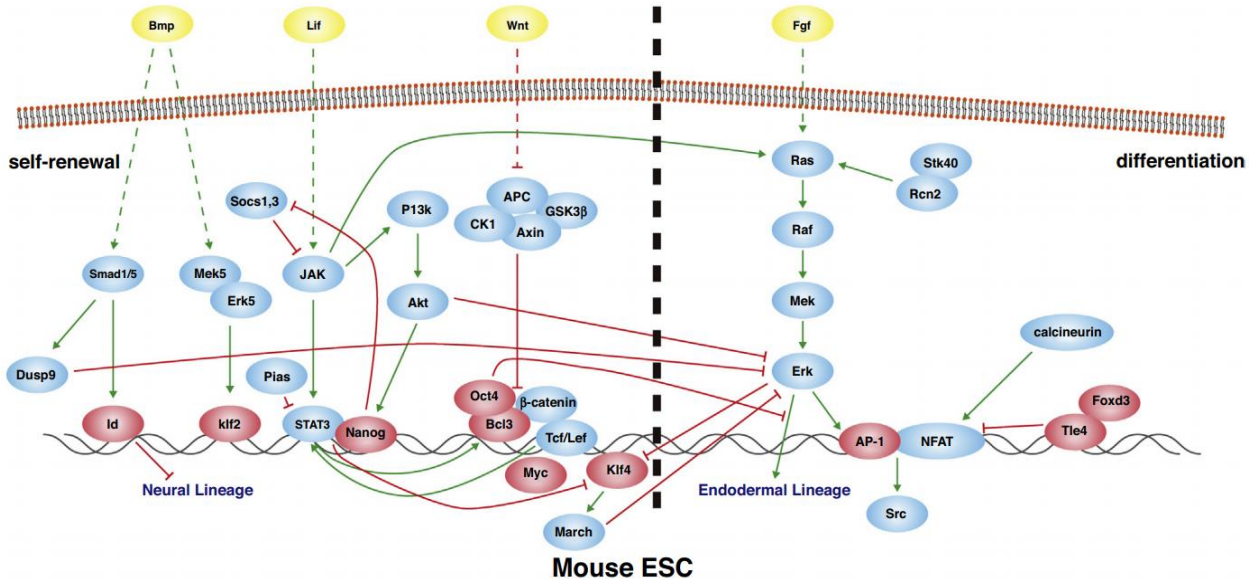

Figure 6: Graphical representation depicting the mouse ESC self-renewal and differentiation. Several pathways including Lif/Stat3, Bmp and Wnt act to control pluripotency and self-renewal. LIF induces phosphorylation of Jak which block differentiation by inactivating Erk signaling and promotes maintenance of pluripotency by acting on PI3k/Akt pathway. Dashed lines represent indirect interactions. Red lines depict inhibition and green activation. Yellow circles represent external factors and red circles mark the transcription factors that regulate the activity of each pathway. Blue circles represent other components of the represented signaling pathways. Figure extracted from (Zhao and Jin 2017).

LIF binds to the heterodimeric LIF/gp130 receptors resulting in the phosphorylation of gp130-associated Jak kinases (pJak) which in turn signals through a vast network of intracellular proteins including Stat3, PI3K-Akt and Erk/Mapk (Figure 6) (Zhao and Jin 2017). Stat3 is phosphorylated by LIF and translocates to the nucleus where it regulates the expression of Klf4 and the transcription factor CP2 like 1(Tfcp211) (Zhao and Jin 2017). B cell leukemia/lymphoma 3 (Bcl3) is another

important pluripotency regulator downstream of the LIF/Stat3 pathway. LIF promotes Bcl3 expression which interacts with Oct4 and β-catenin to regulate the promoter activity of Oct4 and Nanog (Ye, Liu et al. 2014; Chen, Cheng et al. 2017; Zhao and Jin 2017). PI3k-Akt signaling also contributes to the regulation of stemness by two opposite mechanisms. First, PI3k-Akt inhibits the Mapk/Erk signaling pathway to blocking differentiation; second it acts to promote T box 3 (Tbx3) activity and increase Nanog expression leading to ESC pluripotency and proliferation (Chen, Cheng et al. 2017). The downstream signaling events mediating the mechanisms of Erk/Mapk signaling in regulating pluripotency and differentiation are not entirely understood. There are several lines of evidence demonstrating that Erk/Mapk signaling negatively regulates several pluripotency factors such as Nanog and Tbx3, however, a low basal activity level of Erk/Mapk is required for ESC maintenance (Chen, Guo et al. 2015). Indeed, Erk may exhibit functions independent of Mek, which explains, in part, the discrepancies in ESC renewal when Mek is inhibited versus the effects of knocking out Erk (Chen, Guo et al. 2015). Continued efforts are underway to fully dissect the signals regulating the core pluripotency network.

2.3 Role of Insulin Signaling in Pluripotency and Differentiation

Insulin receptor (IR) is a tetrameric protein with kinase activity consisting of two α-subunits and two β-subunits (Figure 7) (Saltiel and Kahn 2001; De Meyts and Whittaker 2002; Belfiore, Frasca et al. 2009). IR belongs to a family of tyrosine kinases receptors that include insulin-like growth factor receptor (IGF-1R) (De Meyts and Whittaker 2002). There are several downstream targets of IR. Among them, the insulin receptor substrate proteins (IRS) are central for the downstream signaling of the insulin and IGF-1 and link IR/IGF1R signaling to important

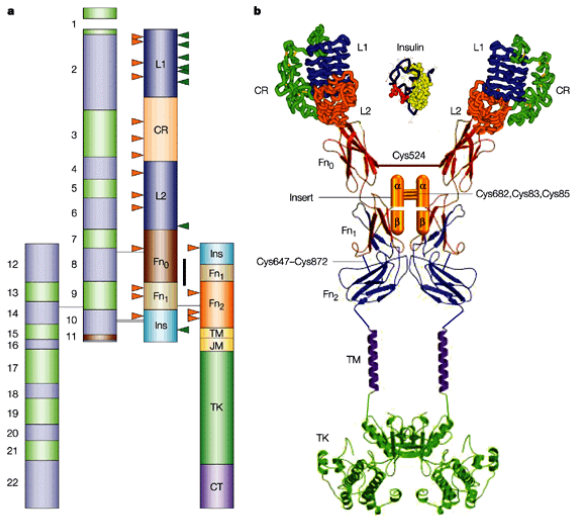

Figure 7: Structure of α and b subunits of IR. The left part of the image "**a**" represents the boundaries of the 22 exons of the IR gene and the right part correspond to predicted boundaries of the protein modules. The image "**b**" represents the tridimensional scheme of the modular organization of the IR protein (De Meyts and Whittaker 2002).

phosphorylation cascades (Saltiel and Kahn 2001; Taguchi and White 2008).

Insulin signaling is fundamental for the maintenance of cell homeostasis in virtually every tissue in mammals. Loss of insulin signaling in pancreatic beta-cells results in insulin secretory defects similar to that in type 2 diabetes (Kulkarni, Brüning et al. 1999), while its loss in hepatocytes leads to severe hepatic dysfunction (Michael, Kulkarni et al. 2000). In the brain insulin signaling controls energy disposal, metabolism and reproduction (Brüning, Gautam et al. 2000), while in the white adipose tissue insulin receptor ablation protects against obesity and associated glucose intolerance (Blüher, Michael et al. 2002).

Insulin and IGF1 act with other several growth factors to modulate differentiation and proliferation of pluripotent stem cells during development (Liu, Kumar et al. 1997). The importance of IR-mediated signaling in pluripotency maintenance and differentiation has been virtually unexplored. The focus has been mainly about the role of IGF1R and the involvement of PI3K-Akt (Figure 8) (Yu and Cui 2016). IGF1R is fundamental for the survival and clonogenicity of human ESCs (Bendall, Stewart et al. 2007), IGF1R blockade by the use of shRNAs or blocking antibodies leads to reduced self-renewal of ESCs and induces differentiation (Wang, Schulz et al. 2007). While blocking IGF1R attenuates differentiation of hepatocytes, the concomitant blocking of IGF1R and IR reduces the activation of AKT and further impairs the differentiation of hepatocytes from human ESCs, suggesting a synergistic role of IGF1 and insulin in maintaining pluripotency and regulating differentiation (Magner, Jung et al. 2013). Recently, Iovino and colleagues derived human iPSCs from fibroblasts of patients with genetic insulin resistance and consequent impairments in

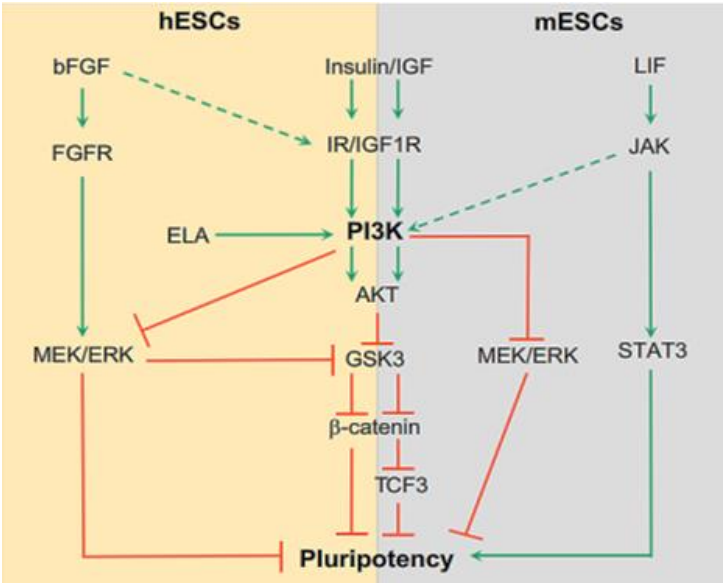

Figure 8: Involvement of insulin/IGF1 signaling in the regulation of pluripotency of mESC and hESC. PI3K/AKT signaling maintains pluripotency through inhibition of MEK/ERK signalling. In mESCs, PI3K/AKT may be activated by the LIF/JAK pathway to inhibit GSK3 signalling in addition to inhibition of MEK/ERK. Green arrows represent activation, red arrows represent inhibition. Dashed arrows represent non-canonical induction by other pathways. Figure adapted from: (Yu and Cui 2016).

insulin signaling (Iovino, Burkart et al. 2014). These iPSCs maintained a phenotype of insulin resistance and presented reduced proliferation and altered gene expression demonstrating the importance of insulin signaling in pluripotency (Iovino, Burkart et al. 2014).

Chapter II – Research Aims

Research Aims

Aim 1

Chapter III – *NREP Bridges TGF-ß Signaling and Lipid Metabolism in the Epigenetic Reprogramming of NAFLD in the Offspring of Insulin-Resistant Parents*

The prevalence of non-alcoholic fatty liver disease (NAFLD) is increasing worldwide and few studies have linked parental diabetes and birth weights with increased risk for NAFLD. For our studies we used a unique non-dietary model, manifesting hyperglycemia, hyperinsulinemia and dyslipidemia – three hallmarks of gestational and type 2 diabetes. We aimed to determine the genetic and epigenetic effects of paternal versus maternal genetic insulin resistance on the developmental programming in the offspring of the liver-specific insulin receptor knockout (LIRKO) mice.

Aim 2

Chapter IV – *Insulin receptor-mediated signaling regulates pluripotency markers and lineage differentiation*

Insulin receptor (IR)-mediated signaling is involved in the regulation of pluripotency and differentiation of pluripotent stem cells. However, its direct effects on regulating the maintenance of pluripotency and lineage development are not fully understood. In this thesis, we aimed to investigate the significance of IR dependent and independent signaling pathways involved in mammalian stem cell pluripotency and differentiation.

Chapter III

NREP Bridges TGF-ß Signaling and Lipid Metabolism in the Epigenetic Reprogramming of NAFLD in the Offspring of Insulin-Resistant Parents

Chapter III

NREP Bridges TGF-ß Signaling and Lipid Metabolism in the Epigenetic Reprogramming of NAFLD in the Offspring of Insulin-Resistant Parents

3.1 Contribution

I contributed to the main body of work presented here. I was responsible for driving this project from its very beginning, including experimental design, experimental work, analysis, writing and the establishment of collaborations.

3.2 Publication

This work is under review in a scientific journal at this date. The unpublished manuscript is reproduced below in this Chapter III.

NREP bridges TGF-β Signaling and Lipid Metabolism in the Epigenetic Programming of NAFLD

Dario F. De Jesus[1,2], Kazuki Orime[1], Ercument Dirice[1], Dorota Kaminska[3], Chih-Hao Wang[4], Jiang Hu[1], Ville Männistö[5], Amélia M. Silva[6], Yu-Hua Tseng[4], Jussi Pihlajamaki[3,7], Rohit N. Kulkarni[1*]

[1] Islet Cell and Regenerative Biology, Joslin Diabetes Center, Department of Medicine, Brigham and Women's Hospital, Harvard Stem Cell Institute, Harvard Medical School, Boston, MA 02215, USA
[2] Graduate Program in Areas of Basic and Applied Biology (GABBA), Abel Salazar Biomedical Sciences Institute, University of Porto, 4050-313 Porto, Portugal
[3] Department of Public Health and Clinical Nutrition, University of Eastern Finland, Kuopio, Finland
[4] Integrative Physiology and Metabolism, Joslin Diabetes Center, Harvard Medical School, Boston, MA 02215, USA
[5] Department of Medicine, University of Eastern Finland and Kuopio University Hospital, Kuopio, Finland
[6] Department of Biology and Environment, Centre for the Research and Technology of Agro-Environmental and Biological Science, University of Tras-os-Montes and Alto Douro, 5000-801 Vila Real, Portugal
[7] Clinical Nutrition and Obesity Center, Kuopio University Hospital, Kuopio, Finland

*Correspondence and Lead contact:
Rohit N. Kulkarni, MD, PhD
Islet Cell and Regenerative Biology
Joslin Diabetes Center,
Harvard Medical School
One Joslin Place, Boston, MA 02215, USA.
Tel: +1-617-309-3460; Fax: +1-617-309-3476
E-mail: rohit.kulkarni@joslin.harvard.edu

ABSTRACT

The prevalence of Nonalcoholic fatty liver disease (NAFLD) is increasing worldwide in parallel with the obesity epidemic. Although gene-environment interactions have been implicated in the etiology of several disorders, including obesity and diabetes, the impact of paternal and/or maternal metabolic syndrome on the clinical phenotypes of their offspring and the underlying genetic and epigenetic contributors of NAFLD have not been fully explored. To this end, we used the liver-specific insulin receptor knockout (LIRKO) mouse, a unique non-dietary model manifesting three hallmarks that confer high risk for development of NAFLD, namely, hyperglycemia, insulin resistance and dyslipidemia. Here we report that parental metabolic syndrome epigenetically reprograms members of the TGF-β family including the neuronal regeneration-related protein (NREP). NREP modulates the expression of several genes involved in the regulation of hepatic lipid metabolism. In particular, NREP downregulation increases the protein abundance of HMG-CoA Reductase (HMGCR) and ATP-citrate lyase (ACLY) in a TGF-βR>PI3K>AKT dependent manner, to regulate hepatic acetyl-CoA and cholesterol synthesis. The reduced hepatic expression of NREP in patients with NAFLD, and significant correlations between the low serum NREP levels and the presence of steatosis and NASH highlight the clinical translational relevance of our findings in the context of recent preclinical trials implicating ATP-citrate lyase in NAFLD progression.

INTRODUCTION

The liver receives dietary lipids and fatty acids derived from adipose tissue and hepatocytes and generally retains no more than ~5% of its weight in lipids in the normal physiological condition in contrast to accumulating lipids in obesity (1-3). Non-alcoholic fatty liver disease (NAFLD) encompasses a heterogeneous set of conditions that are characterized by an increased hepatic lipid accumulation (steatosis), which may lead to inflammation and fibrosis resulting in non-alcoholic steatohepatitis (NASH), cirrhosis and end-stage liver disease (1-3).

The global prevalence of NAFLD is estimated to be 24% and represents a massive economic burden on the healthcare systems (3). Notably, NAFLD in the pediatric community has a prevalence of 3-12% and can affect up to 80% of the obese sub-population among children (2, 4). NAFLD has a strong genetic component and familial aggregation studies identified that siblings and parents of children with NAFLD were more likely to manifest fatty liver (5), and cross-sectional studies in twins also report a strong positive correlation between the presence of hepatic steatosis among monozygotic twins (6). The identification of several polymorphisms in genes such as *APOC3*, *PNPLA3*, *TM6SF2* and *PPP1R3B* that correlate with NAFLD in genome-wide association studies (GWAS) reflect the genetic architecture of the disease (7).

Nevertheless, several studies have underscored the importance of environmental factors in the development of NAFLD early in life via epigenetic mechanisms (2, 3). Such epigenetic factors may prime fetal livers thereby increasing their susceptibility to NAFLD and potentially explain the missing heritability and the increasing incidence of NAFLD over the last few decades (2). The importance of environmental factors for reprogramming in offspring is well documented in several animal models designed to study the effects of early-life exposures in the parents on the phenotypes of their offspring (2, 8-12). However, a vast majority of these models represent nutritional interventions that result in

gender specific phenotypes dependent on maternal or paternal transmission and lack human translation.

In humans dissecting the individual contributors to NAFLD such as lipids, glucose, hormones or diet is challenging. Thus, experimental models continue to provide excellent opportunities to dissect the factor(s) that impact NAFLD priming. In this study, we used a unique genetic model of tissue-specific-mediated insulin resistance – the LIRKO mouse (13, 14), to identify new genes that would contribute to prenatal developmental priming of NAFLD. At 2 months of age LIRKO mice present hyperglycemia and hyperinsulinemia. Furthermore, LIRKOs have increased levels of hepatic cholesterol (14). Indeed, many changes seen in cholesterol metabolism in LIRKOs are also observed in humans with metabolic syndrome (14). For example, both show decreased levels of HDL and increased secretion of apoB and VLDL. These findings make the LIRKO mouse a unique non-dietary model of insulin resistant, hyperglycemia, dyslipidemia and atherosclerosis and resembles several clinical features of human metabolic syndrome.

We report that members of the TGF-β family are differentially expressed in the offspring of parents with metabolic syndrome, including the neuronal regeneration-related protein (NREP). Here, for the first time to our knowledge, we report the role of NREP in mediating NAFLD development by controlling hepatic lipid metabolism. The clinical relevance of these findings is strengthened by the observation of low hepatic expression of NREP in human patients with NAFLD and the negative correlation between serum NREP levels and NAFL activity score in an independent cohort of well-characterized obese NAFLD patients.

RESULTS

Parental genetic insulin resistance impacts body weight trajectories and body composition in offspring

To determine the effects of parental metabolic syndrome (for breeding scheme see Supplementary Figure 1A) we compared the wild-type (WT) progeny obtained by breeding a) liver-specific insulin receptor KO (LIRKO) male mice with control females (FL – "*father LIRKO*"), or WT progeny from breeding b) LIRKO females with control males (ML – "*mother LIRKO*"), with offspring from c) breeding control male and female ("*control*") (for characteristics of animals used for breeding see Supplementary Figure 1B-M and Supplementary Table 1).

Since altered birth weights are risk factors for the development of NAFLD in children (15) we began by analyzing the body weight trajectories of the offspring. Consistent with our previous observation (10), offspring from insulin resistant parents at post-natal day 5 presented transient increased body weights compared to controls (Figure 1A). However, from 4 to 8 weeks of age FL and ML groups preserved low body weights compared to controls (Figure 1B). In fact, challenging FL and ML offspring with a high-fat diet increased the body weight trajectory in the latter at 12 weeks of age (Figure 1C) and a similar pattern was evident in aging (Figure 1D).

To further explore the body weight differences we subjected the offspring to dual energy X-ray absorptiometry (DEXA, Online methods). On chow diets, the FL and ML groups presented decreased total fat mass (Figure 1E), however, when challenged with a high-fat diet or subjected to aging both FL and ML offspring accumulated significantly more fat than controls (Figure 1F, G). We then manually measured different tissues and identified the liver and subcutaneous white adipose tissue to be the most altered among the groups (Figure 1 H-J). We next examined the differences in energy expenditure using comprehensive laboratory animal monitoring system (CLAMS, Online methods). Indeed, on a high-fat diet, FL and ML groups presented significantly decreased energy expenditure

(Figure 1K, L) and metabolic inflexibility in shifting from a fatty-acid to a carbohydrate energy source compared to controls (Figure 1M, N). These changes could not be explained by differences in food intake among groups either on the chow (Figure 1O) or high fat diets (Figure 1P).

Insulin sensitivity is altered in FL and ML offspring

We speculated that the impairments observed in energy expenditure would affect glucose metabolism and insulin sensitivity. Fasting blood glucose levels were increased in FL on chow (Figure 2A) and in FL and ML groups fed either a high-fat diet or as a consequence of aging (Figure 2B, C). On the other hand, fasted serum insulin levels remained unchanged among groups on chow diet, and were elevated especially in the ML offspring on the high-fat diet or during aging (Figure 2D, E, F and Supplementary Table 2). Both ML and FL groups presented a phenotype of insulin resistance both on chow and high-fat diets (Figure 2G, H). The insulin sensitivity phenotypes between groups in aging were not significantly different likely due to the control animals also developing insulin resistance (Figure 2I). Glucose tolerance was relatively normal in the ML group and mildly impaired in the FL group on chow (Figure 2J). On high-fat diet both FL and ML groups presented mildly impaired glucose tolerance (Figure 2K) which worsened significantly in both groups upon aging (Figure 2L). FL and ML offspring showed compensation for the insulin resistance by a significantly greater beta-cell secretory response to glucose in the chow fed group (Figure 2M), and this response was blunted in animals on a high-fat diet and with aging (Figure 2N, O). Female offspring shared many of the metabolic phenotypes with their male siblings (Supplementary Figure 2). Together these data indicate that parental insulin resistance, as in the LIRKO model, induces insulin resistance in offspring even without the mutation and potentially reprograms their metabolic response, as shown by an inability to adapt to a high calorie diet, leading to altered growth and adiposity.

FL and ML offspring are primed to develop HFD-induced hepatic steatosis

The observation that humans mostly adapt to excess nutrients by storing energy as triglycerides in adipose tissue and in "ectopic sites" such as liver (16), prompted us to focus on the liver and flank subcutaneous white adipose tissues to further investigate the cause of the metabolic impairments. On a chow diet, FL and ML offspring presented normal liver histological architecture (Figure 3A), without significant changes in hepatic triglycerides (Figure 3B) or cholesterol (Figure 3C). Notably, FL and ML offspring presented hepatic steatosis on the high-fat diet compared to controls (Figure 3D and Supplementary Figure 3A). Concordantly, the liver triglyceride (Figure 3E) and cholesterol (Figure 3F) content was increased and gene expression analyses revealed upregulation of master regulators of lipid metabolism such as *Pparγ* and *Srebp1c* (Supplementary Figure 3B, C and D) in the FL and ML groups. The alterations in hepatic gene expression patterns in FL and ML fed a high-fat diet were restricted to lipid metabolism without significantly impacting glycolysis, gluconeogenesis or glycogenesis (Supplementary Figure 3E, F). Finally, interrogation of the hepatic insulin signaling cascade in FL and ML groups revealed an impaired phospho-GSK3β response to insulin on chow consistent with liver insulin resistance (Supplementary Figure 3G, left and right panels). Flank-subcutaneous white adipose tissue presented normal morphology (Supplementary Figure 3H) and the gene expression patterns in adipocytes (Supplementary Figure 3I, J) were independent of the increase in fat mass seen in FL and ML challenged a high-fat diet.

Hepatic transcriptomic analyses in FL and ML offspring reveals several members of TGF-β family and identifies *Nrep*

To explore the presence of a gene signature that could define the metabolic changes we undertook RNA-sequencing in the liver mRNA of FL and ML groups and compared it to control offspring on chow diet (Figure 3G). An unbiased global analysis revealed several members of the TGF-β family

genes that were commonly altered between FL and ML compared to controls (Figure 3H) including *Nre*p and *Gdf15*. ConsensusPathDB over-representation pathway analysis of differentially expressed genes commonly altered between FL and ML revealed enrichment in the cholesterol synthesis, fatty-acyl-CoA synthesis, collagen synthesis, triglyceride synthesis and AKT signaling pathways (Figure 3I and Supplementary Figure 4A-D).

The NAFLD 'multiple hit hypothesis' posits that diverse factors act to trigger disease development on genetically susceptible individuals (17). We therefore proceeded to investigate the effects of a metabolic hit, such as a high calorie diet, on the behavior of metabolic genes reprogrammed by parental metabolic syndrome. First, we validated the RNA-sequencing experiment by analyzing the top candidate genes by RT-PCR in the chow-fed group (Supplementary Figure 5A – explored the changes in the gene expression patterns in the HFD group (Supplementary Figure 5B) and in other models such as a short-term high fat feeding (Supplementary Figure 5C) and in mouse models exhibiting hepatic steatosis and steatohepatitis, such as *ob/ob* (Supplementary Figure 5D), or in mice with hepatic steatosis such as *db/db* (Supplementary Figure 5E)). Among several candidates belonging to the TGF-β superfamily, the neuronal regeneration-related protein (NREP) and growth differentiation factor 15 (GDF15) emerged as the most significant and consistently altered genes. *Nrep* was upregulated in the insulin resistant FL and ML offspring compared to controls on chow (Figure 3J). However, challenging offspring with a high-fat diet resulted in a significant decrement in *Nrep* mRNA in the FL and ML groups (Figure 3K). Hepatic *Nrep* expression was not altered by a short-term high-fat diet (Figure 3L) but was consistently downregulated in *ob/ob* (Figure 3M) and *db/db* (Figure 3N) livers suggesting its involvement in the pathophysiology of NAFLD in rodent models. Interestingly, *Nrep* and *Gdf15*, despite belonging to the same family, presented an almost opposite pattern of expression among the different models (Supplementary Figure 5F-H).

Nrep is susceptible to DNA methylation modifications

To investigate a potential epigenetic layer of gene regulation, we performed genome-wide DNA methylation analyses by enhanced reduced representation bisulfite sequencing (ERRBS) and compared the controls with a combined (FL+ML) group on chow diet since the individual ML and FL groups showed largely similar phenotypes (Figure 4A and Online methods). ERRBS was enriched for promoter regions – 43% of all CpGs (Figure 4B), as previously reported (18), and these were highly unmethylated while the hypomethylated CpGs (10% of all CpGs) were more abundant compared to hypermethylated (8% of all CpGs) in FL/ML versus controls (Figure 4B). To determine if DNA methylation affected the same pathways which showed enrichment at the gene expression level we performed pathway analyses to confirm that genes with differential DNA methylation were also enriched for cholesterol synthesis, MAPK, AKT, insulin and TGF-β signaling (Figure 4C, D and Supplementary Table 4). An intersect of the gene expression and promoter DNA methylation datasets (Figure 4E) revealed Nrep among the few genes that were upregulated at the mRNA level and exhibited decreased promoter DNA methylation (Figure 4F). Consistently, despite the global hypomethylation state of promoter regions, one CpG at the *Nrep* promoter region (Figure 4G) and another at the gene body (Figure 4H) presented decreased methylation levels in the FL/ML group compared to controls.

NREP is downregulated by palmitate-induced steatosis and modulates fatty-acid and cholesterol synthesis

NREP, also known as P311, is a highly conserved 8kD protein belonging to the TGF-β superfamily (19) and has been associated with wound healing (20), nerve and lung regeneration (21, 22), and kidney fibrosis (19). TGF-β signaling is important in the development of fibrosis in advanced NAFLD and is upregulated in NASH (23, 24), and shown to reduce β-oxidation and promote fatty-acid synthesis in mouse primary hepatocytes in the presence of palmitate (23). Although the development of

steatosis and progression of NAFLD to NASH likely involve inflammation, fibrosis and fatty-acid metabolism the molecular mechanisms are not well understood. We speculated that NREP bridges TGF-β and lipid synthesis pathways to regulate steatosis development by controlling β-oxidation and/or fatty-acid and cholesterol synthesis.

To test this possibility, we first investigated the behavior of candidate genes in a human *in-vitro* model of hepatic steatosis (25-27) by examining human HepG2 cells treated either with fatty acid-free bovine serum albumin (BSA) or palmitate (Supplementary Figure 6A, B and Online methods). Treatment of HepG2 with palmitate and/or oleate has been used widely to mimic the effects of NAFLD *in vitro* (28-30). Treatment of HepG2 cells with fatty acids reproduces several clinical aspects of NAFLD including signaling, apoptosis, and mitochondrial dysfunction (28-30). Palmitate treatment of HepG2 mimicked several aspects of hepatic steatosis and the expression patterns of several candidate genes, including NREP, were similar to those observed in *ob/ob* and *db/db* liver samples or in the FL and ML groups on a high-fat diet (Supplementary Figure 6C, D). Consistently, treatment of HepG2 with palmitate induced a decrease in NREP protein levels compared to BSA treatment (Figure 5A, B).

Next, to determine the possible direct role of NREP in the development of hepatic steatosis, we contrasted the effects of knock-down versus over-expression of *NREP* in HepG2 cells (Online methods). *NREP* knock-down cells (Figure 5C) treated with palmitate displayed greater lipid-droplet accumulation (Figure 5D) that was consistent with increased triglycerides and cholesterol content compared to scramble (Figure 5E,F). To determine if triglyceride accumulation resulted from decreased β-oxidation, we analyzed fatty-acid oxidation (FAO) using the seahorse instrument (Online methods). Cells lacking *NREP* exhibited decreased basal and maximal respiration in the presence of a palmitate:BSA substrate (Supplementary Figure 7A, B). The impaired respiration and concomitant increase in triglyceride and cholesterol content in HepG2 cells lacking *NREP* was supported by a decrease in *PPARα* expression and increase in the transcriptional network of genes associated with

fatty-acid (*PPARγ, SREBP1c, FAS, ELOVL5*), glycerolipid (*LPIN1*), and cholesterol synthesis (*SREBP2, HMGCR and FDFT1*) in palmitate-induced steatosis (Supplementary Figure 7C).

To further evaluate the global transcriptomic changes induced by NREP downregulation we employed RNA-sequencing in HepG2 cells lacking NREP. Enriched pathway analyses of upregulated genes revealed pathways involved in cholesterol synthesis, fatty acid metabolism, NAFLD and PI3K-AKT signaling (Figure 5G). In contrast, enriched downregulated genes included those for membrane trafficking, non-sense mediated decay, glucagon signaling and cell-cycle (Figure 5H). Differently expressed genes included *HMGCR* (cholesterol synthesis) and *TGFBR1* (TGF-β signaling and fibrosis) (Figure 5I). These results are consistent with a previous study identifying *Nrep* as the most significant downregulated hepatic gene in response to an olive oil bolus and showing a negative correlation between *Nrep* mRNA and hepatic triglycerides and cholesterol content in rats (31). Together these data suggest a potential role for NREP in the development of steatosis in a human *in-vitro* model of hepatic steatosis.

NREP modulates HMGCR and ACLY protein levels via the non-canonical TGF-β pathway

The signaling pathways that orchestrate the development of NAFLD are not entirely known. TGF-β signaling is important in liver homeostasis, development, regeneration and is involved in molecular mechanisms that lead to liver fibrosis (32). The role of TGF-β signaling, and in particular, the non-canonical branch TGF-βR>PI3K>AKT is virtually not explored in the context of lipid metabolism and NAFLD priming. *NREP* knock-down increased the abundance of TGF-β1 and 2 receptor proteins and this was accompanied by the decrease in the regulatory subunit PI3K p85α (Figure 5J and Supplementary Figure 7D). Consistent with increased TGF-βR>PI3K signaling, NREP KD induced a robust increase in AKT phosphorylation (Figure 5J and Supplementary Figure 7D). Interestingly, *NREP* overexpression (Supplementary Figure 8A, B) virtually reversed all the effects of the knock-down. Thus,

HepG2 cells overexpressing *NREP* showed less lipid accumulation when stimulated with palmitate (Supplementary Figure 8C) and partially increased basal fatty-acid oxidation (Supplementary Figure 8D,E) which resulted in lower triglyceride and cholesterol content (Supplementary Figure 8F,G). *NREP* overexpression increased the gene transcriptional network associated with β-oxidation while reducing expression of genes related to fatty-acid and cholesterol synthesis (Supplementary Figure 8H). Finally, *NREP* overexpression caused a significant and notable decrease in phospho-AKT and phospho-mTOR (Supplementary Figure 8I). Together, these data prompted us to hypothesize that NREP regulates hepatic metabolism by acting on common nodes of cholesterol and fatty-acid synthesis via the non-canonical branch of the TGF-βR>AKT pathway.

ATP-citrate-lyase (ACLY) is a cytosolic enzyme responsible for the production of acetyl-CoA – a substrate for *de novo* cholesterol and fatty-acid synthesis (33-36). ACLY is regulated by AKT signaling and has been a focus of recent clinical trials to treat hypercholesterolemia and NAFLD (34, 36). On the other hand, 3-hydroxy-3-methylglutaryl-CoA reductase (HMGCR) a rate-limiting enzyme for cholesterol synthesis and a target of statins (37) is increased in NAFLD and correlates with the histologic severity of the disease (38). To investigate whether NREP is linked to ACLY and HMGCR via the AKT signaling, we challenged HepG2 cells knocked down for *NREP*, either with BSA or palmitate, in the presence or absence of an AKT inhibitor (MK-2206) or DMSO. Palmitate treatment increased ACLY expression but not HMGCR in HepG2 cells, while cells with a knock-down of *NREP* exhibited a further increase in ACLY and HMGCR protein levels that was partially blocked by an AKT inhibitor (Figure 5K and Supplementary Figure 8J). Overall, these data support a novel role for NREP in regulating hepatic TGF-βR>PI3K>AKT signaling to modulate ACLY and HMGCR in response to steatosis.

NREP is expressed in hepatocytes and its expression is decreased in NAFLD

To investigate the clinical translational relevance of these findings, we first validated the effects of *NREP* knock-down in human primary hepatocytes (Online methods). Concordant with previous results in HepG2 (Figure 5A,B), palmitate treatment decreased *NREP* mRNA levels by 30% (Figure 6A). While we achieved ~70-80% silencing of *NREP* expression in human primary hepatocytes in the absence of palmitate, treatment with the fatty acids likely induced toxicity in the hepatocytes as evidenced by a variation in the ability to knock-down *NREP* (~30%) (Figure 6A). Finally, *NREP* abrogation in human primary hepatocytes increased lipid-droplet accumulation in BSA and palmitate treated cells (Figure 6B, C). NREP KD in primary hepatocytes cultured in BSA increased expression of *PPARγ* , *SREBP1c* , *SREBP2*, *HMGCR* and *ACLY* mRNA (Figure 6D). Palmitate treatment further increased *HMGCR* and *ACLY* mRNA levels in primary hepatocytes bearing a NREP KD (Figure 6D) consistent with our findings in HepG2 cells. Next, we sought to analyze NREP expression in human liver samples from patients with histologically defined hepatic steatosis (sample information in Supplementary Table 5). Immunohistological analyses revealed virtually undetectable NREP protein in hepatocytes from patients with hepatic steatosis in contrast to the presence of NREP positive hepatocytes in the controls (Figure 6E). Consistent with our hypothesis hepatic *NREP* mRNA was decreased by 40% in patients manifesting hepatic steatosis (Figure 6F). Next, we sought to validate our results by re-analyzing public available datasets comparing the transcriptomic signatures of biopsy-obtained samples from controls, steatosis and NASH patients. Re-analyses of the GSE33814 dataset from a previous study comparing the gene expression signatures between steatohepatitis versus steatosis and controls (39) were congruent with our observations with *NREP* mRNA levels tending to be lower in steatosis and dramatically downregulated in steatohepatitis (Figure 6G). In the same study, re-examining the relationship between *NREP* and ATP-citrate lyase (*ACLY*) mRNA levels showed a strong opposite correlation between *NREP* and *ACLY* (Figure 6H).

NREP circulating levels are decreased in NAFLD and correlate with steatosis grade and NAFL activity score

The last decade has revealed the significance of TGF-β and TGF-β-related proteins, including cytokines and secreted growth factors in modulating diverse signaling pathways (40). Therefore, to explore whether NREP is secreted by hepatocytes we collected cell- and FBS-free culture media supernatants from HepG2 cells with a KD of NREP, scramble and NREP-overexpression. NREP was clearly and easily detected in the culture media from scramble and NREP overexpressing HepG2 cultured cells in contrast to HepG2 cells with a NREP KD (Figure 7A). Next, to examine whether plasma NREP levels reflect the changes in hepatic mRNA and protein levels in patients with NAFLD we analyzed NREP plasma levels in controls (n=106), simple steatosis (n=36) and NASH (n=28) patients in an extended and comprehensive obese liver biopsy-proven cohort (i.e. the Kuopio cohort, see Supplementary Table 6). Consistent with our hypothesis, NREP levels were significantly decreased in both steatosis and NASH compared to controls (Figure 7B). Indeed, several metabolic parameters had significant correlations with NREP (Figure 7C). For example, serum NREP levels correlated positively with HDL-cholesterol (r=0.27) and negatively with serum triglycerides (r=-0.21), reflecting its involvement in cholesterol and triglyceride metabolism. Furthermore, NREP correlated strongly with steatosis grade (Figure 7C) and NAFL activity score (Figure 7C, D). Estimation of AUROC as a diagnostic tool revealed a moderate sensitivity/specificity for NREP for the prediction of steatosis and NASH (AUC: 0.67; p=0.0001; Figure 7E).

DISCUSSION

There is increasing evidence that epigenetic mechanisms may contribute to the development of NAFLD (41). Contrary to simple steatosis which is generally benign, NASH is strongly associated with co-morbidities and reduced life-span. Follow-up studies have demonstrated that the progression of steatosis to NASH and consequently hepatic fibrosis is not simply linear and may be influenced by genetic and/or environmental mechanisms (3). This provides a strong rationale for the identification of new early responsive genes whose expression is triggered by the parental metabolic syndrome and to identify mechanisms underlying NAFLD progression that are translatable to clinical therapy.

While the association of obesity and diabetes with NAFLD development is well documented there is also global consensus regarding the roles of the preconception environment such as diet, body composition, metabolism, smoking and stress in modulating chronic disease risk (42). Models of maternal overnutrition, such as high fat diet-induced obesity are among the most extensively studied paradigm and have been reported to promote hepatic triglyceride accumulation and lead to NAFLD in non-human primates (43). However, adopting a diet-induced obesity paradigm to mimic the metabolic syndrome in humans is limited by the difficulty in distinguishing the contributions of diverse metabolic phenotypes, observed in obesity and type 2 diabetes from those directly linked to high fat consumption.

Previous studies have used genetic mouse models to modulate the effects of either paternal and maternal hyperglycemia (Akita mouse) (44) or maternal hyperinsulinemia (IRS1-heterozygous mouse) (45) in offspring; however, virtually none have investigated the combined contributions of hyperglycemia, hyperinsulinemia, and dyslipidemia. We used the LIRKO mouse, a unique model of genetic insulin resistance to study the effects of metabolic syndrome in NAFLD priming (13, 46). In the Akita model, paternal and maternal hyperglycemia resulted in decreased body weights, elevated fasted blood glucose levels and mild glucose intolerance in male offspring (44) however, no phenotype was described regarding the development of hepatic steatosis. On the other hand, the effects of maternal

hyperinsulinemia have been shown to induce hepatic steatosis in male offspring at 6 months of age despite an absence of changes in body composition, or energy expenditure suggesting that the development of steatosis may be driven by the increased circulating serum insulin levels (45). We employed an unbiased, transversal and original approach to identify new genes and mechanisms underlying NAFLD priming. We used a genetic model of metabolic syndrome and only used WT offspring, excluding any effects secondary to insulin-receptor ablation. We further focused on common genes and pathways affecting both genders and common to paternal and maternal effects that exclude confounding effects of *in-utero* exposures or lactation. Our results point to parental metabolic syndrome acting concomitantly to impact body weight trajectories and body composition in the offspring secondary to decreased energy expenditure and metabolic inflexibility leading to hepatic lipid accumulation and insulin resistance. Analyses of the hepatic transcriptomic datasets in the offspring allowed us to identify a subset of genes that are transversely affected by paternal and maternal metabolic syndrome.

We report that maternal and paternal genetic insulin resistance epigenetically reprograms NREP in hepatocytes that reflect a novel molecular bridge between TGF-β signaling and hepatic lipid metabolism that is highly susceptible to environmental triggers such as a high calorie diet. A notable observation is the reduced expression of NREP in hepatocytes in rodent models of steatosis and steatohepatitis, human *in-vitro* models of steatosis and in human liver samples from patients with hepatic steatosis. NREP belongs to the transforming growth factor beta superfamily which encompasses a group of regulatory proteins that control several aspects of cell biology (47). TGF-β1, a cytokine, was the first protein to be identified in this family (48) and is known to be involved in the fibrogenic response by stellate cell activation (23) and in the adaptive response seen in the F1 and F2 offspring of fathers with a history of liver damage (11). Although the canonical branch of TGF-β signaling modulates hepatic lipid metabolism by regulating lipogenesis and β-oxidation, its exact role in

NAFLD development and in particular the involvement of the non-canonical branch of TGF-β signaling has not been explored (23).

Our mechanistic data suggest that NREP can be epigenetically modified by DNA methylation and controls hepatic lipid content (e.g. cholesterol and triglycerides) by modulating fatty-acid oxidation and regulating the expression of master-regulators of fatty-acid synthesis such as PPARγ and SREBP1c while controlling ATP-citrate lyase and HMG-CoA reductase levels in an AKT-dependent manner. ATP-citrate lyase is an enzyme highly expressed in liver that is responsible for the production of acetyl-CoA necessary for the synthesis of cholesterol, fatty-acids, and in protein acetylation (34, 35). It is strategically positioned at the intersection of these pathways and may work as a nutrient sensor (34). Silencing of hepatic ATP-citrate lyase protects against NAFLD development in the *db/db* mouse (35) and recent studies performed in humans reported that ATP-citrate lyase expression is increased in NAFLD patients (49). While all these data point to ATP-citrate lyase as an attractive target a suitable pharmacological inhibitor is still lacking. On the other hand HMG-CoA reductase catalyzes the rate-limiting step in cholesterol biosynthesis and has been an attractive clinical target of lipid-lowering drugs – statins. HMGCR expression is increased in NAFLD and positively correlates with the severity of the disease, explaining in part, the increased cholesterol synthesis in NAFLD patients (38). Interestingly, our RNA-sequencing data revealed that NREP ablation induces the expression of several fibrotic genes and may explain the concomitant increase in lipid synthesis and fibrosis seen in human NAFLD progression.

Our data are consistent with previous studies involving AKT signaling in the regulation of ATP-citrate lyase (50). However, the precise role of PI3K>AKT pathway in the development of NAFLD is complex (51). Excessive AKT activation leads to NAFLD development by maturation of the transcription factor SREBP1c leading to increased transcription of several lipogenic enzymes (52, 53) . PTEN is a negative regulator of AKT and is frequently mutated in several cancers. PTEN deficient mice develop severe NAFLD as a result of increased phospho-AKT and lipid synthesis (51, 54). Recently, hippo

signaling was show to prevent NAFLD development by inhibiting IRS2/AKT signaling (55). Interestingly, in a recent study, the receptor-interacting protein kinase-3 (RIPK3) was shown to promote fibrinogenesis by an AKT-dependent activation of ATP-citrate lyase in response to TGF-β1 in fibroblasts (56). These results in the light of previous reports that NREP overexpression inhibits TGF1-β and TGF-β2 receptor levels (20) and that NREP can bind to the latency-associated protein (LAP) of TGF-β1 and TGF-β2 to decrease TGF-β autoinduction (57) indicate that NREP regulates AKT signaling and ATP-citrate lyase and HMG-CoA reductase levels via the non-canonical TGF-β pathway.

Three observations from our studies support the concept that NREP is regulating NAFLD development. First, re-analysis of a previously published dataset (39) demonstrated decreased hepatic *NREP* mRNA in patients with steatohepatitis and the presence of a strong negative correlation between hepatic *NREP* and ATP-citrate lyase mRNA levels. Second, plasma NREP levels are decreased in patients with simple steatosis and NASH. Finally, plasma NREP is strongly negatively correlated with steatosis grade and NAFL activity score in the Kuopio cohort.

In summary the present study identifies NREP as a novel molecular mediator of NAFLD development that further elucidates the role of TGF-β signaling in mediating hepatic lipid accumulation and fibrosis development. Further studies in diverse ethnic cohorts will strengthen the possible utility of NREP as a steatosis or NASH biomarker. Interestingly, several obese control patients presented decreased serum NREP levels. Future longitudinal studies will reveal if this heterogeneity seen in controls represents different NAFLD progression susceptibilities and if NREP is an early biomarker of NAFLD progression. We propose that recombinant NREP or gene-therapy mediated approaches targeting hepatic NREP gene expression can be harnessed as clinical therapeutic targets to improve NAFLD.

METHODS

Mice and Diets

Liver-specific insulin receptor KO mice - LIRKO (insulin receptor-IR$^{lox/lox}$; Albumin-Cre$^{+/-}$) mice were generated as previous described (13). In brief, control offspring group consisted in the F1 offspring from a control male and female (insulin receptor-IR$^{lox/lox}$; Albumin-Cre$^{-/-}$). Control parents were crossed for 4 generations for minimizing any epigenetic memory from the presence of Cre. Father LIRKO offspring (FL) resulted from the crossing of a male LIRKO (insulin receptor-IR$^{lox/lox}$; Albumin-Cre$^{+/-}$) with a control female. Mother LIRKO offspring (ML) resulted from the breeding of a control male with a LIRKO female. The animals were matched for age (8-9 weeks) and the determination of the pregnancy day was made accordantly the presence of a copulation plug (vaginal plug). After confirmation of pregnancy day the females were separated from males and single-caged. Litters sizes were normalized to 4-5 pups. Litters with less than 4 pups were excluded and litters with more than 5 pups, pups were randomly selected for sacrification. We only used virgin females and F1 offspring from different groups were weaned together to minimize any microbiome effects and were maintained in the same rack. Phenotypes between male and female offspring were similar (please see Fig1 and S3) so we focused on the male offspring to minimize any cofounding effects of female hormones. Mice were maintained on a chow diet (PicoLab® mouse diet 20 – 5058) or weaned at 3 weeks of age on a high-fat diet containing 60% fat (D12492 - Research diets Inc., USA) until 3 months of age. We purchased from Jackson laboratories 12 weeks old male C57BL/6 on a low-fat diet (10% fat) or a 60% high-fat diet since 6 weeks old. We also purchased controls male ob/+,db/+, and the obesogenic models C57BL/6 Lep$^{-/-}$ and Lepr$^{-/-}$ at 12 weeks of age. Mice were anesthetized using Avertin and blood was collected by heart puncture from all the animals used in our experiments unless else specified. Serum Insulin, c-peptide, leptin, resistin, GIP and MCP-1 were measured using the Luminex xMAP® technology (Luminex Corp.) according to manufacturer guidelines. Sample sizes for animal experiments were chosen on the basis of experience in previous in-house studies of metabolic phenotypes and to balance

the ability to detect significant differences with minimization of the number of animals used in accordance with NIH guidelines.

Study subjects

Present study contains data from the total of 170 obese individuals selected from an ongoing Kuopio Obesity Surgery study (KOBS) (58) (for clinical characteristics see Supplementary Table 6). All patients with alcohol consumption of more than two doses per day and patients with previously diagnosed liver diseases, not related to obesity, were excluded from the study. Clinical parameters were assessed prior to surgery, after 4 weeks of very low calorie diet (VLCD). Liver biopsies were collected as a wedge biopsy during the elective Roux-en-Y gastric bypass surgery at Kuopio University Hospital. The histological assessment of liver biopsy samples was performed by one pathologist according to the standard criteria (1). Subjects were divided into three categories, based on the liver phenotype: Normal, Simple steatosis or NASH (as described previously (59)).

Intraperitoneal glucose tolerance test (GTT), insulin tolerance test (ITT) and *in-vivo* glucose-stimulated insulin secretion (GSIS)

For the glucose-tolerance tests, animals were fasted for 16 hours O/N and 20% (v/v) dextrose (Hospira) was given through intraperitoneal injection in a 2g/kg body weight proportion. Blood glucose levels were measured using an automated glucose monitor (Glucometer Elite, Bayer) by tail punch immediately before and at 15, 30, 60 and 120 minutes after injection. For the *in-vivo* glucose-stimulated insulin secretion mice were fasted for 16 hours O/N and 20% (v/v) dextrose (Bioexpress) was given through intraperitoneal injection in a 2.5g/kg body. Serum was collected by tail vein at minutes 0, 2 and 5 after injection and insulin was assayed with an insulin ELISA kit (Crystal Chem) according to manufacture instructions. The insulin-tolerance test was performed after fasting the animals for 5h (10h-15h) and 0.5 U/kg insulin (Humalog) was administered by intraperitoneal injection. Glucose levels

were measured using an automated glucose monitor (Glucometer Elite, Bayer) by tail punch at time points 0, 15, 30 and 60 minutes after injection and were plotted to the initial glucose levels.

Comprehensive Laboratory Animal Monitoring System (CLAMS)

The OxyMax CLAMS system from Columbus Instruments was used to provide direct measurement of volumetric oxygen consumption (VO_2) and carbon dioxide (CO_2) production, respiratory exchange ratio (RER), food and drinking behavior, and activity level. Measurements were obtained during 24h at dark and light cycles and a fed state. Mice were housed individually in 12 chambers and were placed into individual acclimation chambers prior to the experiment. Sampling of the chambers occurred serially completing 1 cycle every 15 minutes and was controlled by OxyMax v5.02 software. Total body weight of each mouse was entered into the system at setup and the system was calibrated using a certified O2/CO2 gas mixture. Drierite was replaced prior to each run to eliminate moisture from the system and maintain constant humidity. Data analysis was provided by CLAX v2.2.10 software.

Dual Energy X-Ray Absorptiometry (DEXA)

The DEXA system uses x-ray absorbance to assess lean and fat mass composition, bone mineral density and bone length on mice up to 55 grams in weight. We used the Lunar Piximus II densitometer (GE Lunarcorp.) DEXA system which includes the scanner and software for display, analysis and database handling of images. Prior to a scanning session, the system was calibrated using a Phantom of known absorbance for fat and bone. Mice were anesthetized by 2% isoflurane inhalation administered using the EZ-1500 Isoflurane Anesthesia Machine (Euthanax Corporation PA, USA). Each mouse was initially placed in a priming chamber to induce anesthesia then moved to a nose cone for maintenance. Mice were placed on a Piximus scanning tray on the imaging platform prior to imaging. Mice were returned to their cages and monitored until emergence. Analysis for total and percent lean and fat mass was measured for total body and defined regions of interest.

Histology analyses

Mouse liver sections were fixed in 10% buffered formalin for 1h, paraffin embedded, sectioned and stained with hematoxylin and eosin according using standard methods. HepG2 cells and human primary hepatocytes were fixed with 10% buffered formalin for 30min stained in filtered Oil Red-O for 10 min. Sections were washed in distilled water, counterstained with hematoxylin for 2min and visualized on a microscope. For NREP immunohistochemistry, human liver sections were from controls and patients with steatosis were purchased from Xenotech Inc. (Supplementary Table 5). Formalin fixed paraffin embedded human liver sections were processed by standard immunohistochemistry protocol. After blocking endogenous peroxidase and biotin, 5% donkey serum was used to block non-specific protein binding. Anti-P311 (NREP) antibody (Abcam #167017) was applied and incubated at 4C overnight. Biotinylated conjugated antibody was used followed by streptavidin-peroxidase. Staining was completed by DAB chromogen.

Lipid Isolation and Measurements

Livers and HepG2 lysates were homogenized for 10min in an ice-cold chloroform-methanol (2:1). Neutral lipid extraction was performed overnight at room temperature. For phase separation, distilled water was added, samples were centrifuged, and the organic bottom layer was collected. The organic phase was dried using a Speed Vac® and re-dissolved in chloroform. Triglycerides and cholesterol content of each sample was measured after evaporation of the organic phase using colorimetric kits according manufacture protocol (Stanbio LiquiColor® Triglycerides and Stanbio Cholesterol LiquiColor®).

RNA isolation and RT-PCRs

High quality total RNA (>200nt) was extracted using standard Trizol reagent (Invitrogen) according manufacturer instructions and resultant aqueous phase was mixed (1:1) with 70% RNA-free ethanol and added to Qiagen Rneasy mini kit columns (Qiagen) and the kit protocol was followed. RNA

quality and quantity was analyzed using Nanodrop 1000 and used for reserve transcription step using the high-capacity cDNA synthesis kit (Applied Biosciences). cDNA was analyzed using the ABI 7900HT system (Applied Biosciences) and gene expression was calculated using the $^{\Delta\Delta}$Ct method. Data was normalized to β-Actin.

RNA-sequencing

High quality RNA was isolated as described above and the final elution was performed in 20µl of RNase-free sterile distilled water. The concentration and integrity of the extracted total RNA were estimated using the Qubit® 2.0 Fluorometer (Invitrogen) and Agilent 2100 Bioanalyzer (Applied Biosystems, USA), respectively. Five hundred nanograms of total RNA was required for downstream RNA-seq applications. Polyadenylated RNAs were isolated using NEBNext Magnetic Oligo d(T)25 Beads. Next, first strand synthesis was performed using NEBNext RNA first strand synthesis module (New England BioLabs Inc., USA). Immediately, directional second strand synthesis was performed using NEBNExt Ultra Directional second strand synthesis kit. The NEBNext® DNA Library Prep Master Mix Set for Illumina® was then used to prepare individually bar-coded next-generation sequencing expression libraries as per manufacturer's recommended protocol. Library quality was assessed using the Qubit 2.0 Fluorometer, and the library concentration was estimated by utilizing a DNA 1000 Chip on an Agilent 2100 Bioanalyzer. Accurate quantification for sequencing applications was determined using the qPCR-based KAPA Biosystems Library Quantification Kit (Kapa Biosystems, Inc., USA). Paired-end sequencing (100bp) was performed on an Illumina HiSeq2500 sequencer to obtain approximately 50 million reads per sample. Raw reads were de-multiplexed using bcl2fastq Conversion Software (Illumina, Inc.) with default settings.

Enhanced Reduced Representation Bisulphite Sequencing (ERRBS)

High molecular weight DNA was isolated from control, FL and ML offspring livers using the Gentra puregene tissue kit (Qiagen) according the manufacturer protocol. ERRBS library preparation,

sequencing and post-processing of the raw data was performed at the Epigenomics Core at Weill Cornell Medicine previously described (18). Briefly, 75 ng of DNA (>20kb in size) were digested with MspI. After phenol extraction and ethanol precipitation MspI ends were end-repaired, A-tailed and ligated to methylated TruSeq adapters (Illumina Inc. San Diego, CA). Samples were size selected in a 1.5% agarose gel and two size fragment lengths of 150–250 bp and 250–400 bp were gel isolated. These two fractions were subjected to overnight bisulfite conversion (55 cycles of 95 °C for 30 sec, 50 °C for 15 min) using EZ DNA methylation kit (Zymo Research, Irvine CA). Purified bisulfate converted DNA was PCR amplified using TruSeq primers (Illumina Inc. San Diego, CA) for 18 cycles of denaturing, annealing and extension/elongation steps: 94 °C for 20 secs, 65 °C for 30 secs, 72 °C for 1 min, followed by 72 °C for 3 min. The resulting libraries were normalized to 2nM and pooled at the same molar ratio. The final samples were pooled according to the desired plexity, clustered at 6.5pM on single read flow cell and sequenced for 50 cycles on an Illumina HiSeq 2500. Primary processing of sequencing images was done using Illumina's Real Time Analysis software (RTA) as suggested by the Illumina. Illumina's BCL2FASTQ version 2.17 software was then used to de-multiplex samples and generate raw reads and respective quality scores. For analysis of bisulfite treated sequence reads (with an average bisulfite conversion rate of >99% for all samples), reads were filtered for adapter sequences using the FLEXBAR software. Adapter sequence present in the 3' end of the reads was removed if it aligned with the adapter sequence at least 6 bps and had at most a 0.2 mismatch error rate. Reads were aligned to the whole genome using the Bismark alignment software with a maximum of two mismatches in a directional manner and only uniquely aligning reads were retained. In order to call a methylation score for a base position, read bases aligning to that position had at least a 20 phred quality score and that base position had at least 10x coverage. The percentage of bisulfite converted cytosines (representing unmethylated cytosines) and non-converted cytosines (representing methylated cytosines) were recorded for each cytosine position in CpG, CHG, and CHH contexts (with H corresponding to A, C, or T nucleotides).

Bioinformatics

RNA-sequencing data was aligned to the genome using STAR (60), mapped reads were assigned to genomic features using featureCounts (61), the counts were normalized using TMM (62), and the normalized counts were incorporated into linear modeling using limma voom (63). DNA methylation data were analyzed with methylKit (64). False discovery rates (FDRs) were calculated using the Benjamini-Hochberg method. Bioinformatic analyses were done in the R software. Pathway analyses were done in ConsensusPathDB (65).

Western blotting

Total proteins were harvested from tissue and cell lines lysates using RIPA buffer and M-PER protein extraction reagent (Thermo Fisher) respectively supplemented with proteinase and phosphatase inhibitors (Sigma) according to standard protocol. Protein concentrations were determined using the BCA standard protocol followed by standard western immunoblotting protocol of proteins. The blots were developed using chemiluminescent substrate ECL (ThermoFisher) and quantified using Image studio Lite Ver. 5.2 software (LICOR).

FAO by Seahorse

The Seahorse XFe96 (Agilent Technologies) was utilized for respirometry to measure Oxygen Consumption Rate (OCR) according to manufacturer's protocol. Cells were seeded into XFe 96 cell culture microplates at the density of 50 000 cells per well. To determine the Fatty Acid Oxidation (FAO), cells were incubated with substrate-limited medium one day before, then FAO running media plus palmitate-BSA substrate were added with or without etomoxir (ETO), an inhibitor of carnitine palmitoyltransferase-1 (CPT1) (Agilent Technologies). After measuring the basal FAO respiration, 1 mM oligomycin, 0.5 mM FCCP and 2 mM Antimycin was injected subsequently to determine ATP-coupled, maximal, non-mitochondrial FAO. FAO-contributed OCR was calculated by subtracting the total respiration (without ETO) with the non-FAO respiration (with ETO).

Cell Culture and Treatments

HepG2 cells were obtained from ATCC and were cultured in DMEM supplemented with 10% (v/v) fetal bovine serum and non-essential amino acids. For *in-vitro* modelling of hepatic steatosis in HepG2, cells were treated with fatty-acid free bovine serum albumin (BSA; Sigma) or 500µM of albumin-conjugated palmitate in 25mM glucose DMEM for 24h. Albumin-conjugated palmitate was prepared by dissolving sodium palmitate (Sigma) with distilled water and NaOH at 70ºC and then conjugated with fatty-acid free albumin (BSA; Sigma). Human palatable primary hepatocytes were cultured in William E media supplemented with primary hepatocyte supplements (Thermo Fisher) and HepExtend supplement (Thermo Fisher). For the analyses of HepG2 supernatant, 12ml of HepG2 FBS-free culture media was collected after 72h of knock-down or NREP overexpression and passed through a 0.22µm filter. Supernatant was further centrifuged at maximum speed for 10 minutes. A total of 10mL of cell-culture supernatant was purified and concentrated into 100µl using StrataResin (Agilent, USA) accordingly to manufacturer protocol. 40µl of resulted media was run on a 20% SDS-PAGE gel according to western-blot standard protocol.

siRNAs Gene Silencing

HepG2 cells were trypsinized at 70% of confluency and reverse transfection was performed using 30nM of genome smart-pool non-target siRNA (scramble), siNREP or siGDF15 targeting 4 different sequences (Dpharmacon). Lipofectamine RNAiMA reagent (Invitrogen) in Opti-MEM (Invitrogen) was used and media was exchanged after 8h of transfection. At 48h cells were treated with DMEM containing BSA or BSA:palmitate for 24h. Human palatable primary hepatocytes were seeded on collagen-treated plates containing William E media supplemented with primary hepatocyte supplements (Thermo Fisher) and HepExtend supplement (Thermo Fisher) let to attach for 6h. Cells were forward transfected with 100nM of non-target siRNA or siNREP and media was exchanged after 12h. At 24h cells were treated with William E supplemented with BSA or BSA:palmitate for 24h.

Plasmid transfections

70% confluent HepG2 cells were forward transfected with pCMV-empty, pCMV-Myc-NREP or pCMV-Myc-GDF15 (Origene) using Lipofectamine 3000 (Invitrogen) and Opti-MEM (Invitrogen) according to manufacturer protocols. Media was exchanged with fresh DMEM after 8h of transfection and at 48h cells were treated with DMEM containing BSA or BSA:palmitate for 24h.

Analytical methods used in human studies

Plasma glucose, insulin, serum lipids and lipoproteins were measured from fasting venous blood samples. Plasma glucose was measured by enzymatic hexokinase photometric assay (Konelab Systems Reagents, Thermo Fischer Scientific, Vantaa, Finland). Plasma insulin was determined by immunoassay (ADVIA Centaur Insulin IRI, no 02230141, Siemens Medical Solutions Diagnostics, Tarrytown, NY). Cholesterol, high-density lipoprotein (HDL) cholesterol and triglyceride concentrations were assayed by standard automated enzymatic methods (Roche Diagnostics, Mannheim, Germany). Plasma NREP levels were measured using a quantitative sandwich ELISA using a capture mouse monoclonal antibody which immunogen is recombinant partial protein corresponding to amino acids 1 to 68 of human NREP and a detection rabbit polyclonal which immunogen is a synthetic peptide corresponding to human NREP. Used standards consisted in recombinant full-length human NREP protein expressed by *E. coli* (#MBS9323406, MyBiosoure, San Diego, USA).

Statistical analysis

Data were analyzed for statistical significance using the unpaired two-tailed t-test, one-way ANOVA with Dunnet's post hoc test, one-way ANOVA with Sidak-Holm multi comparisons test or Kruskal-Wallis test with Dunn's multi comparisons test. Analyzes were performed with GraphPad prism. Normal distribution was calculated using the D'Agostino and Pearson omnibus normality test. Spearman's rank correlation was used for correlation analysis. Where applicable, the Bonferroni

adjustment for multiple comparisons was used. Correlation analyses were conducted with the SPSS version 25 program (IBM SPSS Statistics).

Study Approval

All animal experiments were conducted in accordance with the Association for Assessment and Accreditation of Laboratory Animal Care. All protocols were approved by the Institutional Animal Care and Use Committee of the Joslin Diabetes Center in accordance with NIH guidelines. Human liver lysates were purchased for Xenotech Inc. (Supplementary Figure 5). Human plateable primary hepatocytes from 5-donors were purchased from Gibco (Thermo Fisher). All human studies and protocols used were approved by the Joslin Diabetes Center's Committee on Human Studies (CHS#5-05). The study protocol of Kuopio cohort was approved by the Ethics Committee of Northern Savo Hospital District (54/2005, 104/2008 and 27/2010), and carried out in accordance with the Helsinki Declaration. Informed written consent was obtained from all participants.

AUTHOR CONTRIBUTIONS

DFDJ conceived the idea, designed and performed the experiments, analyzed the data and wrote the manuscript. KO assisted with overexpression experiments. CHW performed seahorse FAO. JH performed immunohistochemistry**.** ED assisted with *in-vivo* GSIS. AMS, YHT researched data, assisted with technical support and/or critical reading of the manuscript. DK, VM and JP assisted with human serum samples and correlation experiments. RNK contributed to conceptual discussions, designed the experiments, supervised the project and wrote the manuscript. All the authors have reviewed, commented and edited the manuscript.

ACKNOWLEDGMENTS

LIRKO mice were kindly provided by C. Ronald Kahn MD (Joslin Diabetes Center). We would like to thank Mary Elizabeth Patti MD (Joslin Diabetes Center) and Stephan Kissler PhD (Joslin Diabetes Center) for their critical advice. We thank the Joslin Specialized Assay Core, Joslin Physiology Core and Joslin Bioinformatics Core (P30 DK36836). We thank the Epigenomics Core at Weill Cornell Medicine for assistance with ERRBS. We thank the Genomic Services Laboratory (GSL) at HudsonAlpha Institute for Biotechnology for assistance with RNA-sequencing. DFDJ was supported by the Portuguese Foundation for Science and Technology – SFRH/BD/51699/2011, Albert Ronald Travel Fellowship 2015 and 2016 FLAD R&D@PhD Internship grant. RNK is supported by NIH grants R01 DK67536, R01 DK103215 and R01 DK055523.

REFERENCES

1. Brunt, E.M., and Tiniakos, D.G. 2010. Histopathology of nonalcoholic fatty liver disease. *World J Gastroenterol* 16:5286-5296.
2. Brumbaugh, D.E., and Friedman, J.E. 2013. Developmental origins of nonalcoholic fatty liver disease. *Pediatric Research* 75:140.
3. Younossi, Z., Anstee, Q.M., Marietti, M., Hardy, T., Henry, L., Eslam, M., George, J., and Bugianesi, E. 2018. Global burden of NAFLD and NASH: trends, predictions, risk factors and prevention. *Nat Rev Gastroenterol Hepatol* 15:11-20.
4. Bush, H., Golabi, P., and Younossi, Z.M. 2017. Pediatric Non-Alcoholic Fatty Liver Disease. *Children* 4:48.
5. Schwimmer, J.B., Celedon, M.A., Lavine, J.E., Salem, R., Campbell, N., Schork, N.J., Shiehmorteza, M., Yokoo, T., Chavez, A., Middleton, M.S., et al. 2009. Heritability of Nonalcoholic Fatty Liver Disease. *Gastroenterology* 136:1585-1592.
6. Loomba, R., Schork, N., Chen, C.-H., Bettencourt, R., Bhatt, A., Ang, B., Nguyen, P., Hernandez, C., Richards, L., Salotti, J., et al. 2015. Heritability of Hepatic Fibrosis and Steatosis Based on a Prospective Twin Study. *Gastroenterology* 149:1784-1793.
7. Wruck, W., Kashofer, K., Rehman, S., Daskalaki, A., Berg, D., Gralka, E., Jozefczuk, J., Drews, K., Pandey, V., Regenbrecht, C., et al. 2015. Multi-omic profiles of human non-alcoholic fatty liver disease tissue highlight heterogenic phenotypes. *Scientific Data* 2:150068.
8. De Jesus, D.F., and Kulkarni, R.N. 2014. Epigenetic modifiers of islet function and mass. *Trends Endocrinol Metab* 25:628-636.
9. Sales, V.M., Ferguson-Smith, A.C., and Patti, M.-E. 2017. Epigenetic Mechanisms of Transmission of Metabolic Disease across Generations. *Cell Metabolism* 25:559-571.
10. Kahraman, S., Dirice, E., De Jesus, D.F., Hu, J., and Kulkarni, R.N. 2014. Maternal insulin resistance and transient hyperglycemia impact the metabolic and endocrine phenotypes of offspring. *Am J Physiol Endocrinol Metab* 307:E906-918.
11. Zeybel, M., Hardy, T., Wong, Y.K., Mathers, J.C., Fox, C.R., Gackowska, A., Oakley, F., Burt, A.D., Wilson, C.L., Anstee, Q.M., et al. 2012. Multigenerational epigenetic adaptation of the hepatic wound-healing response. *Nature Medicine* 18:1369.
12. McCurdy, C.E., Bishop, J.M., Williams, S.M., Grayson, B.E., Smith, M.S., Friedman, J.E., and Grove, K.L. 2009. Maternal high-fat diet triggers lipotoxicity in the fetal livers of nonhuman primates. *The Journal of Clinical Investigation* 119:323-335.
13. Michael, M.D., Kulkarni, R.N., Postic, C., Previs, S.F., Shulman, G.I., Magnuson, M.A., and Kahn, C.R. 2000. Loss of Insulin Signaling in Hepatocytes Leads to Severe Insulin Resistance and Progressive Hepatic Dysfunction. *Molecular cell* 6:87-97.
14. Biddinger, S.B., Hernandez-Ono, A., Rask-Madsen, C., Haas, J.T., Alemán, J.O., Suzuki, R., Scapa, E.F., Agarwal, C., Carey, M.C., Stephanopoulos, G., et al. 2008. Hepatic Insulin Resistance Is Sufficient to Produce Dyslipidemia and Susceptibility to Atherosclerosis. *Cell Metabolism* 7:125-134.
15. Newton, K.P., Feldman, H.S., Chambers, C.D., Wilson, L., Behling, C., Clark, J.M., Molleston, J.P., Chalasani, N., Sanyal, A.J., Fishbein, M.H., et al. 2017. Low and High Birth Weights Are Risk Factors for Nonalcoholic Fatty Liver Disease in Children. *The Journal of Pediatrics* 187:141-146.e141.
16. Savage, D.B., Petersen, K.F., and Shulman, G.I. 2007. Disordered Lipid Metabolism and the Pathogenesis of Insulin Resistance. *Physiological Reviews* 87:507-520.
17. Buzzetti, E., Pinzani, M., and Tsochatzis, E.A. 2016. The multiple-hit pathogenesis of non-alcoholic fatty liver disease (NAFLD). *Metabolism - Clinical and Experimental* 65:1038-1048.

18. Garrett-Bakelman, F.E., Sheridan, C.K., Kacmarczyk, T.J., Ishii, J., Betel, D., Alonso, A., Mason, C.E., Figueroa, M.E., and Melnick, A.M. 2015. Enhanced Reduced Representation Bisulfite Sequencing for Assessment of DNA Methylation at Base Pair Resolution.e52246.
19. Yao, Z., Yang, S., He, W., Li, L., Xu, R., Zhang, X., Li, H., Zhan, R., Sun, W., Tan, J., et al. 2015. P311 promotes renal fibrosis via TGFβ1/Smad signaling. *Scientific Reports* 5:17032.
20. Pan, D., Zhe, X., Jakkaraju, S., Taylor, G.A., and Schuger, L. 2002. P311 induces a TGF-β1–independent, nonfibrogenic myofibroblast phenotype. *The Journal of Clinical Investigation* 110:1349-1358.
21. Fujitani, M., Yamagishi, S., Che, Y.H., Hata, K., Kubo, T., Ino, H., Tohyama, M., and Yamashita, T. 2004. P311 accelerates nerve regeneration of the axotomized facial nerve. *Journal of Neurochemistry* 91:737-744.
22. Zhao, L., Leung, J.K., Yamamoto, H., Goswami, S., Kheradmand, F., and Vu, T.H. 2006. Identification of P311 as a Potential Gene Regulating Alveolar Generation. *American Journal of Respiratory Cell and Molecular Biology* 35:48-54.
23. Yang, L., Roh, Y.S., Song, J., Zhang, B., Liu, C., Loomba, R., and Seki, E. 2013. Transforming growth factor beta signaling in hepatocytes participates in steatohepatitis through regulation of cell death and lipid metabolism in mice. *Hepatology* 59:483-495.
24. Seki, E., and Schwabe, R.F. 2015. Hepatic inflammation and fibrosis: Functional links and key pathways. *Hepatology* 61:1066-1079.
25. Yan, C., Chen, J., and Chen, N. 2016. Long noncoding RNA MALAT1 promotes hepatic steatosis and insulin resistance by increasing nuclear SREBP-1c protein stability. *Scientific Reports* 6:22640.
26. Joshi-Barve, S., Barve, S.S., Amancherla, K., Gobejishvili, L., Hill, D., Cave, M., Hote, P., and McClain, C.J. 2007. Palmitic acid induces production of proinflammatory cytokine interleukin-8 from hepatocytes. *Hepatology* 46:823-830.
27. Gao, D., Nong, S., Huang, X., Lu, Y., Zhao, H., Lin, Y., Man, Y., Wang, S., Yang, J., and Li, J. 2010. The Effects of Palmitate on Hepatic Insulin Resistance Are Mediated by NADPH Oxidase 3-derived Reactive Oxygen Species through JNK and p38MAPK Pathways. *Journal of Biological Chemistry* 285:29965-29973.
28. Garcia-Ruiz, I., Solis-Munoz, P., Fernandez-Moreira, D., Munoz-Yague, T., and Solis-Herruzo, J.A. 2015. In vitro treatment of HepG2 cells with saturated fatty acids reproduces mitochondrial dysfunction found in nonalcoholic steatohepatitis. *Dis Model Mech* 8:183-191.
29. Gao, D., Nong, S., Huang, X., Lu, Y., Zhao, H., Lin, Y., Man, Y., Wang, S., Yang, J., and Li, J. 2010. The effects of palmitate on hepatic insulin resistance are mediated by NADPH Oxidase 3-derived reactive oxygen species through JNK and p38MAPK pathways. *J Biol Chem* 285:29965-29973.
30. Harasim-Symbor, E., Konstantynowicz-Nowicka, K., and Chabowski, A. 2016. Additive effects of dexamethasone and palmitate on hepatic lipid accumulation and secretion. *J Mol Endocrinol* 57:261-273.
31. Martinez-Beamonte, R., Navarro, M.A., Guillen, N., Acin, S., Arnal, C., Guzman, M.A., and Osada, J. 2011. Postprandial transcriptome associated with virgin olive oil intake in rat liver. *Frontiers in Bioscience* E3.
32. Fabregat, I., Moreno-Càceres, J., Sánchez, A., Dooley, S., Dewidar, B., Giannelli, G., and ten Dijke, P. 2016. TGF-β signalling and liver disease. *The FEBS Journal* 283:2219-2232.
33. Pinkosky, S.L., Newton, R.S., Day, E.A., Ford, R.J., Lhotak, S., Austin, R.C., Birch, C.M., Smith, B.K., Filippov, S., Groot, P.H.E., et al. 2016. Liver-specific ATP-citrate lyase inhibition by bempedoic acid decreases LDL-C and attenuates atherosclerosis. *Nature Communications* 7:13457.
34. Pinkosky, S.L., Groot, P.H.E., Lalwani, N.D., and Steinberg, G.R. 2017. Targeting ATP-Citrate Lyase in Hyperlipidemia and Metabolic Disorders. *Trends in Molecular Medicine* 23:1047-1063.

35. Wang, Q., Jiang, L., Wang, J., Li, S., Yu, Y., You, J., Zeng, R., Gao, X., Rui, L., Li, W., et al. 2009. Abrogation of hepatic ATP-citrate lyase protects against fatty liver and ameliorates hyperglycemia in leptin receptor-deficient mice. *Hepatology* 49:1166-1175.
36. Burke, A.C., and Huff, M.W. 2017. ATP-citrate lyase: genetics, molecular biology and therapeutic target for dyslipidemia. *Curr Opin Lipidol* 28:193-200.
37. Sharpe, L.J., and Brown, A.J. 2013. Controlling Cholesterol Synthesis beyond 3-Hydroxy-3-methylglutaryl-CoA Reductase (HMGCR). *Journal of Biological Chemistry* 288:18707-18715.
38. Min, H.-K., Kapoor, A., Fuchs, M., Mirshahi, F., Zhou, H., Maher, J., Kellum, J., Warnick, R., Contos, Melissa J., and Sanyal, Arun J. 2012. Increased Hepatic Synthesis and Dysregulation of Cholesterol Metabolism Is Associated with the Severity of Nonalcoholic Fatty Liver Disease. *Cell Metabolism* 15:665-674.
39. Starmann, J., Fälth, M., Spindelböck, W., Lanz, K.-L., Lackner, C., Zatloukal, K., Trauner, M., and Sültmann, H. 2012. Gene Expression Profiling Unravels Cancer-Related Hepatic Molecular Signatures in Steatohepatitis but Not in Steatosis. *PLoS ONE* 7:e46584.
40. Robertson, I.B., and Rifkin, D.B. 2016. Regulation of the Bioavailability of TGF-β and TGF-β-Related Proteins. *Cold Spring Harbor Perspectives in Biology* 8.
41. Lee, J., Friso, S., and Choi, S.-W. 2014. Epigenetic Mechanisms Underlying the Link between Non-Alcoholic Fatty Liver Diseases and Nutrition. *Nutrients* 6:3303.
42. Fleming, T.P., Watkins, A.J., Velazquez, M.A., Mathers, J.C., Prentice, A.M., Stephenson, J., Barker, M., Saffery, R., Yajnik, C.S., Eckert, J.J., et al. 2018. Origins of lifetime health around the time of conception: causes and consequences. *Lancet*.
43. Thorn, S.R., Baquero, K.C., Newsom, S.A., El Kasmi, K.C., Bergman, B.C., Shulman, G.I., Grove, K.L., and Friedman, J.E. 2014. Early Life Exposure to Maternal Insulin Resistance Has Persistent Effects on Hepatic NAFLD in Juvenile Nonhuman Primates. *Diabetes* 63:2702-2713.
44. Grasemann, C., Devlin, M.J., Rzeczkowska, P.A., Herrmann, R., Horsthemke, B., Hauffa, B.P., Grynpas, M., Alm, C., Bouxsein, M.L., and Palmert, M.R. 2012. Parental Diabetes: The Akita Mouse as a Model of the Effects of Maternal and Paternal Hyperglycemia in Wildtype Offspring. *PLoS ONE* 7:e50210.
45. Isganaitis, E., Woo, M., Ma, H., Chen, M., Kong, W., Lytras, A., Sales, V., Decoste-Lopez, J., Lee, K.J., Leatherwood, C., et al. 2014. Developmental programming by maternal insulin resistance: hyperinsulinemia, glucose intolerance, and dysregulated lipid metabolism in male offspring of insulin-resistant mice. *Diabetes* 63:688-700.
46. Cohen, S.E., Kokkotou, E., Biddinger, S.B., Kondo, T., Gebhardt, R., Kratzsch, J., Mantzoros, C.S., and Kahn, C.R. 2007. High Circulating Leptin Receptors with Normal Leptin Sensitivity in Liver-specific Insulin Receptor Knock-out (LIRKO) Mice. *Journal of Biological Chemistry* 282:23672-23678.
47. Massagué, J. 2012. TGFβ signalling in context. *Nature Reviews Molecular Cell Biology* 13:616.
48. Assoian, R.K., Komoriya, A., Meyers, C.A., Miller, D.M., and Sporn, M.B. 1983. Transforming growth factor-beta in human platelets. Identification of a major storage site, purification, and characterization. *Journal of Biological Chemistry* 258:7155-7160.
49. Ahrens, M., Ammerpohl, O., von Schönfels, W., Kolarova, J., Bens, S., Itzel, T., Teufel, A., Herrmann, A., Brosch, M., Hinrichsen, H., et al. 2013. DNA Methylation Analysis in Nonalcoholic Fatty Liver Disease Suggests Distinct Disease-Specific and Remodeling Signatures after Bariatric Surgery. *Cell Metabolism* 18:296-302.
50. Berwick, D.C., Hers, I., Heesom, K.J., Moule, S.K., and Tavaré, J.M. 2002. The Identification of ATP-citrate Lyase as a Protein Kinase B (Akt) Substrate in Primary Adipocytes. *Journal of Biological Chemistry* 277:33895-33900.
51. Matsuda, S., Kobayashi, M., and Kitagishi, Y. 2013. Roles for PI3K/AKT/PTEN Pathway in Cell Signaling of Nonalcoholic Fatty Liver Disease. *ISRN Endocrinol* 2013:472432.

52. Porstmann, T., Santos, C.R., Griffiths, B., Cully, M., Wu, M., Leevers, S., Griffiths, J.R., Chung, Y.-L., and Schulze, A. 2008. SREBP Activity Is Regulated by mTORC1 and Contributes to Akt-Dependent Cell Growth. *Cell Metabolism* 8:224-236.
53. Krycer, J.R., Sharpe, L.J., Luu, W., and Brown, A.J. 2010. The Akt–SREBP nexus: cell signaling meets lipid metabolism. *Trends in Endocrinology & Metabolism* 21:268-276.
54. He, L., Hou, X., Kanel, G., Zeng, N., Galicia, V., Wang, Y., Yang, J., Wu, H., Birnbaum, M.J., and Stiles, B.L. 2010. The critical role of AKT2 in hepatic steatosis induced by PTEN loss. *Am J Pathol* 176:2302-2308.
55. Jeong, S.-H., Kim, H.-B., Kim, M.-C., Lee, J.-m., Lee, J.H., Kim, J.-H., Kim, J.-W., Park, W.-Y., Kim, S.-Y., Kim, J.B., et al. 2018. Hippo-mediated suppression of IRS2/AKT signaling prevents hepatic steatosis and liver cancer. *The Journal of Clinical Investigation* 128:1010-1025.
56. Imamura, M., Moon, J.S., Chung, K.P., Nakahira, K., Muthukumar, T., Shingarev, R., Ryter, S.W., Choi, A.M., and Choi, M.E. 2018. RIPK3 promotes kidney fibrosis via AKT-dependent ATP citrate lyase. *JCI Insight* 3.
57. Paliwal, S., Shi, J., Dhru, U., Zhou, Y., and Schuger, L. 2004. P311 binds to the latency associated protein and downregulates the expression of TGF-β1 and TGF-β2. *Biochemical and Biophysical Research Communications* 315:1104-1109.
58. Walle, P., Takkunen, M., Männistö, V., Vaittinen, M., Lankinen, M., Kärjä, V., Käkelä, P., Ågren, J., Tiainen, M., Schwab, U., et al. 2016. Fatty acid metabolism is altered in non-alcoholic steatohepatitis independent of obesity. *Metabolism - Clinical and Experimental* 65:655-666.
59. Männistö, V.T., Simonen, M., Hyysalo, J., Soininen, P., Kangas, A.J., Kaminska, D., Matte, A.K., Venesmaa, S., Käkelä, P., Kärjä, V., et al. 2015. Ketone body production is differentially altered in steatosis and non-alcoholic steatohepatitis in obese humans. *Liver International* 35:1853-1861.
60. Dobin, A., Davis, C., Schlesinger, F., Drenkow, J., Zaleski, C., Jha, S., Batut, P., Chaisson, M., and Gingeras, T. 2013. STAR: ultrafast universal RNA-seq aligner. *Bioinformatics* 29:15-21.
61. Liao, Y., Smyth, G., and Shi, W. 2014. featureCounts: an efficient general purpose program for assigning sequence reads to genomic features. *Bioinformatics (Oxford, England)* 30:923-930.
62. Robinson, M., and Oshlack, A. 2010. A scaling normalization method for differential expression analysis of RNA-seq data. *Genome Biology* 11:1-9.
63. Law, C., Chen, Y., Shi, W., and Smyth, G. 2014. voom: precision weights unlock linear model analysis tools for RNA-seq read counts. *Genome Biology* 15:R29.
64. Akalin, A., Kormaksson, M., Li, S., Bakelman, F., Figueroa, M., Melnick, A., and Mason, C. 2012. methylKit: a comprehensive R package for the analysis of genome-wide DNA methylation profiles. *Genome Biology* 13:R87.
65. Herwig, R., Hardt, C., Lienhard, M., and Kamburov, A. 2016. Analyzing and interpreting genome data at the network level with ConsensusPathDB. *Nature Protocols* 11:1889.

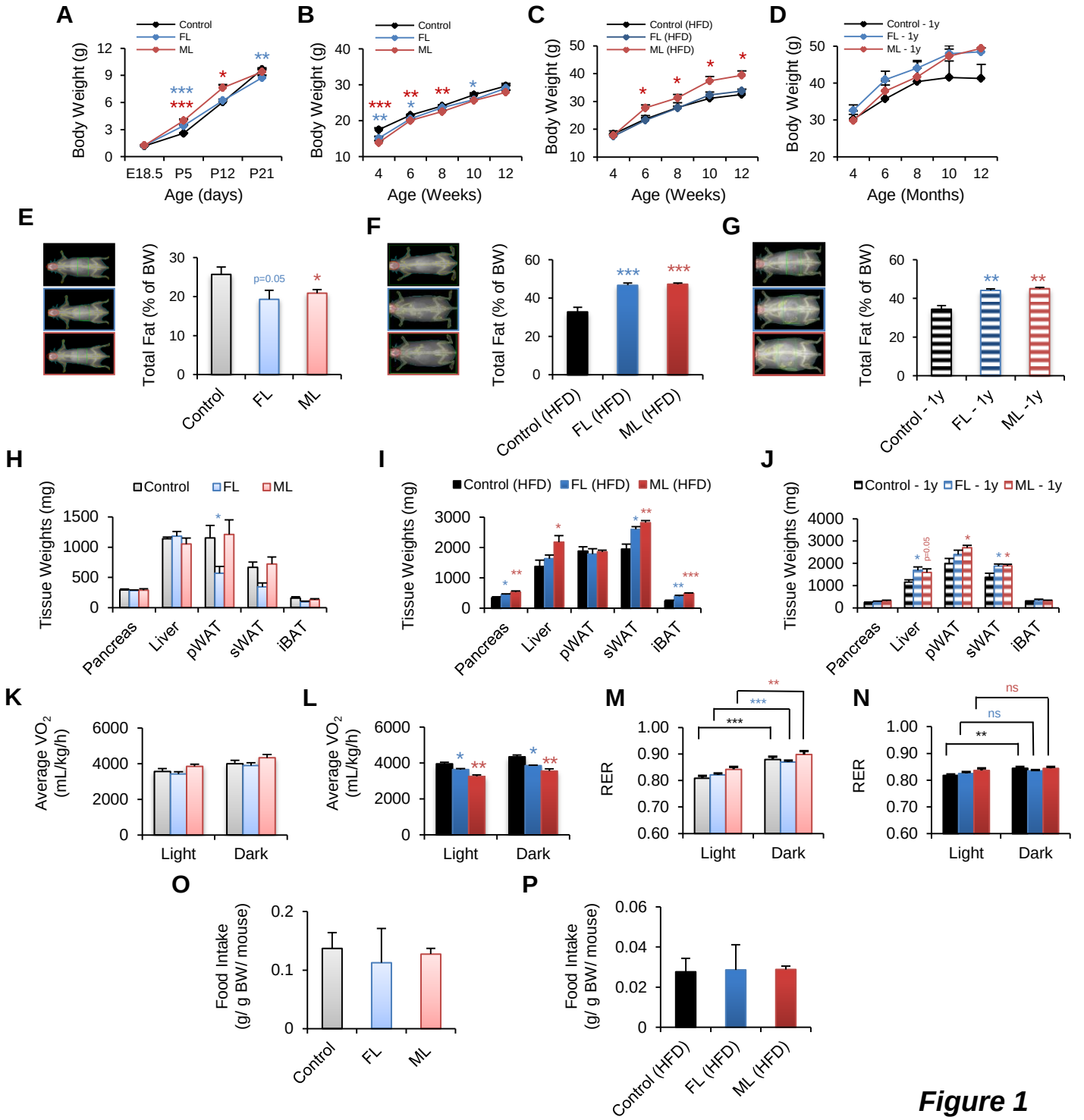

Figure 1: Body weight trajectories and body composition are altered in FL and ML offspring. (**A**) Body weight trajectories in the male offspring of parents who are both controls (black), or father is LIRKO (FL, in blue), or mother is LIRKO (ML, in red) from embryonic day 18.5 (E18.5) to postnatal day 21 (P21) (All groups reflect offsprings. Control, n=27-49, corresponding to 5-6 litters; FL, n=27-49, 5-6 litters; ML, n=17-21, 3-4 litters). (**B**) Body weight in control, FL and ML on chow diet from 4 to 12 weeks of age (control, n=9-24, 6 litters; FL, n=10-18, 5 litters; ML, n=13-20, 5 litters). (**C**) Body weight in control, FL and ML on high-fat diet (HFD) from 4 to 12 weeks of age (control, n=9-24, 5 litters; FL, n=6-10, 3 litters; ML, n=8-13, 3 litters). (**D**) Body weight of control, FL and ML on chow diet from 4 to 12 months of age (control, FL and ML N=5/group). (**E-G**) Total fat mass measured by DEXA in control, FL and ML on chow (**E**) and HFD (**F**) at 3 months of age, and 1 year-old offspring on chow (**G**) (Chow, control, n=7; FL, n=6; ML, n=8. HFD, control, n=5; FL, n=7; ML, n=8; Aging, n=5/group). (**H-J**) Body composition in control, FL or ML offspring on chow (**H**), or HFD (**I**) diets or in aged (**J**) mice. (**K-L**) Energy expenditure (VO2) in 24h light/dark cycle measured by CLAMS in chow (**K**) and HFD (**L**) groups at 3 months of age (Chow, control n=7, FL and ML, n=8; HFD, n=4/group). (**M-N**) Respiratory exchange ratio (RER) measured by CLAMS in control, FL or ML offspring on chow (**M**) or HFD (**N**) diets (Chow, control n=7, FL and ML, n=8; HFD, n=4/group). (**O-P**) Food intake in control (black), FL (blue) or ML (red) offspring on chow (**O**) or HFD (**P**) diets. Significance was determined by two-tailed unpaired t-test. All data are shown as mean ± SEM and represent 3 litters/group or as stated. *p<0.05; **p<0.01; ***p<0.001.

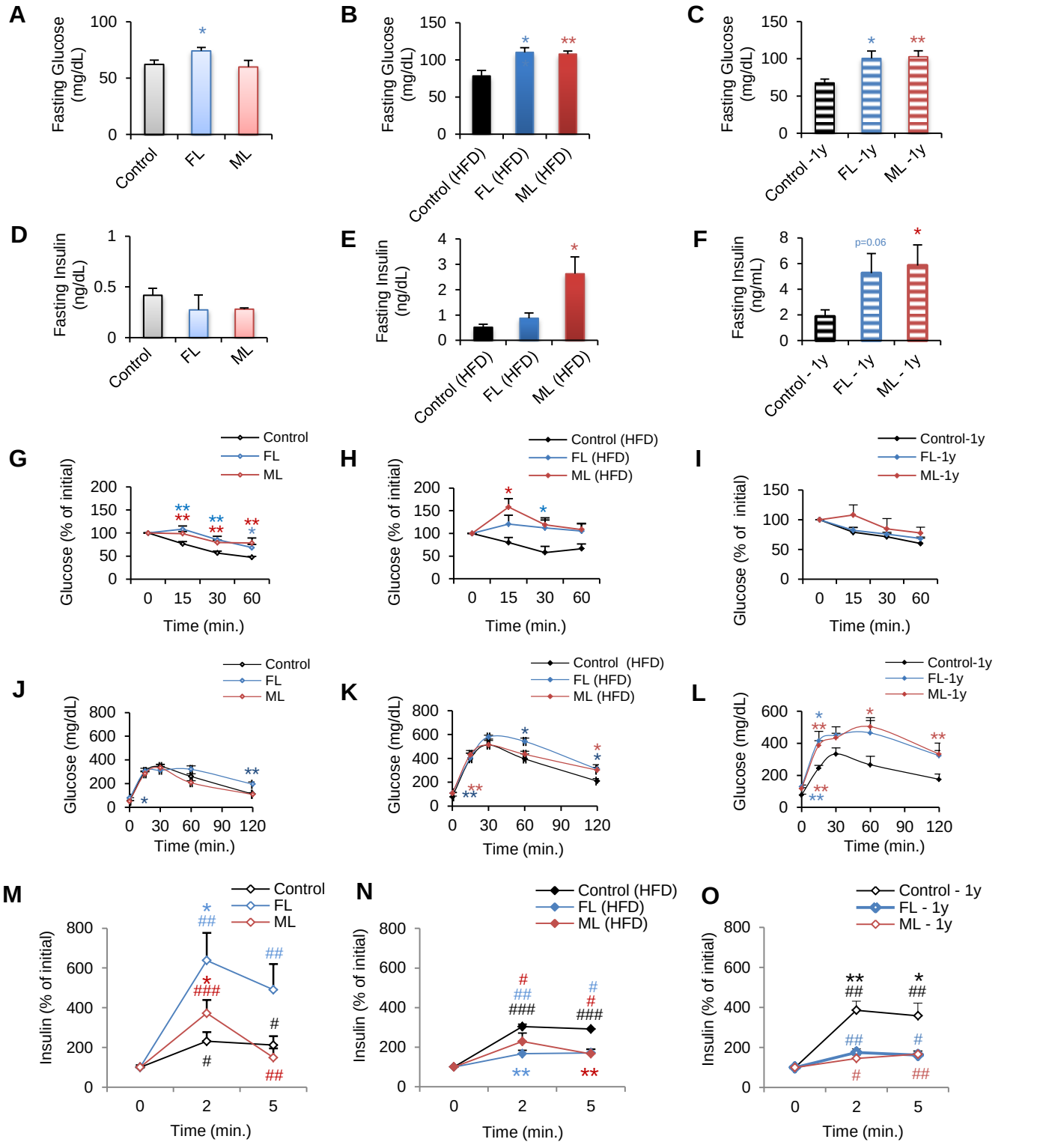

Figure 2

Figure 2: Altered insulin sensitivity in FL and ML offspring. (**A-C**) Fasted glucose levels in chow (**A**) and HFD (**B**) at 2 months of age, and aged offspring (**C**) (Chow, control, n=8, 3 litters; FL, n=11, 4 litters; ML, n=5, 3 litters; HFD, control, FL and ML, n=6, 3 litters/group). (**D-E**) Fasted serum insulin levels in chow (**D**), HFD (**E**) at 2 months of age and aged animals at 12 months of age (**F**) (Chow and HFD, n=4, 4 litters/group, Aged, n=5, 3 litters/group). (**G-I**) Insulin tolerance tests in chow (**G**), HFD (**H**) and aged (**I**) (Chow, control, n=10, 4 litters; FL, n=11, 4 litters; ML, n=6, 3 litters; HFD, control, n=3, FL, n=4, ML, n=3; 3 litters/group, 2 months of age; Aged, n=5/group, 1 year old). (**J-L**) Blood glucose values following an intraperitoneal glucose tolerance test in aged control, FL, or ML offspring. (**M-O**) Insulin levels plotted as % of basal levels after an intraperitoneal glucose injection on chow (**M**), or HFD (**N**) diets or in aged offspring (**O**). All data are based on n=3-11/group representing a minimum of 3 independent litters/group and analyzed using the one-way ANOVA with Dunnett's post hoc test. * P < 0.05, ** P < 0.01 and ***P < 0.001. In M, N and O # represent the statistical comparisons between time points 0 versus 2 or 5 min. RNA-Seq. data was based on control (n=4 mice/litters), FL (n=3 mice/litters) and ML (n=3 mice/litters). Data are expressed as means ± SEM. #p<0.05, ##p<0.01, ###p<0.001. pWAT: perigonadal white adipose tissue; sWAT: flank subcutaneous white adipose tissue; iBAT: intrascapular brown adipose tissue.

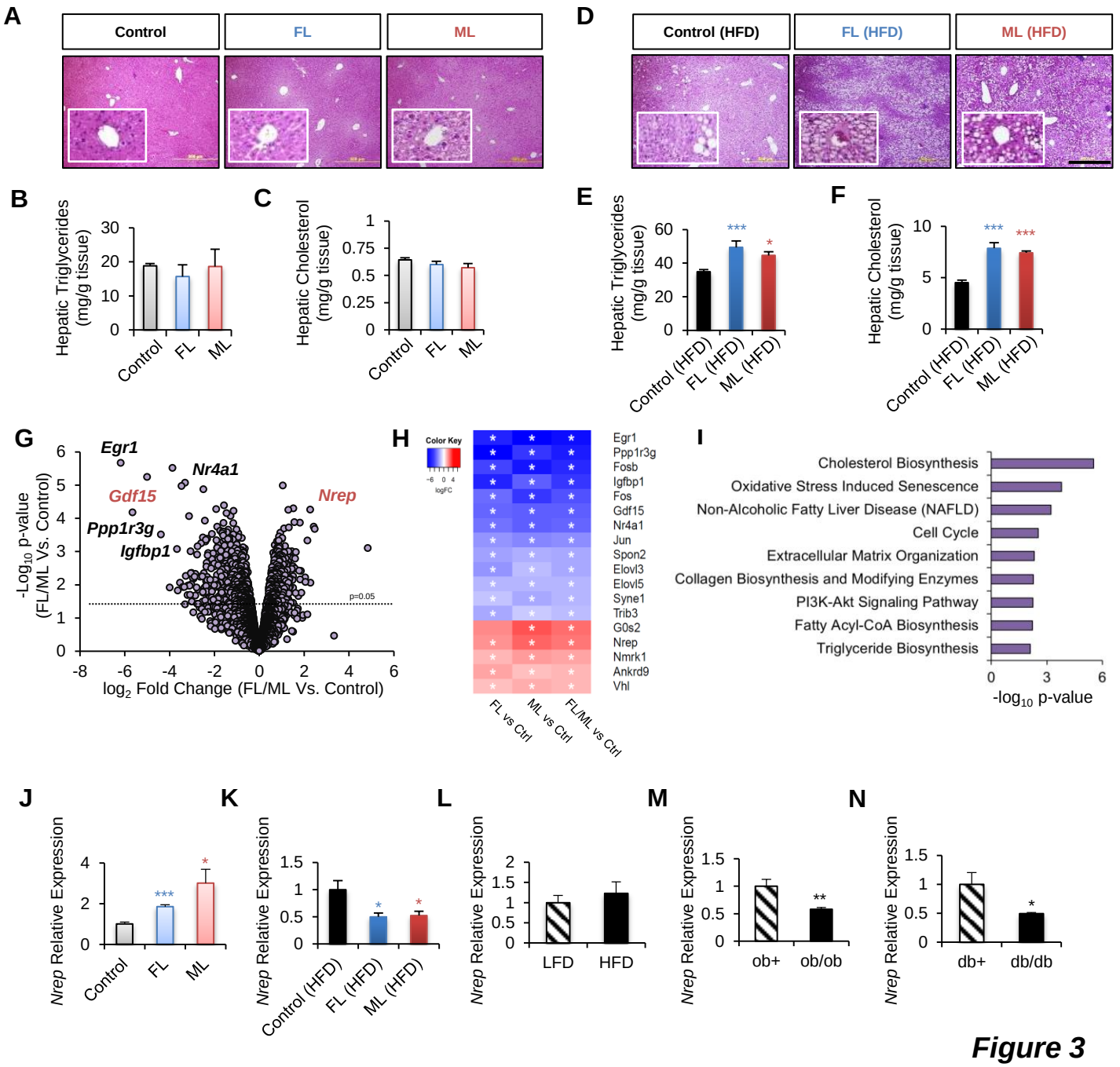

Figure 3

Figure 3: Hepatic transcriptome of NAFLD primed offspring reveals *Nrep* and *Gdf15*. (**A**) Hematoxylin and Eosin-stained liver sections from control, FL or ML offspring in chow diet (Magnification 200x, scale bar = 200µm). (**B**) Hepatic triglycerides content in chow diet offspring. (**C**) Hepatic cholesterol content in chow diet offspring. Selected-pathway analyses of differentially expressed genes. (**D**) Hematoxylin and Eosin-stained liver sections from control, FL or ML offspring in HFD (Magnification 200x, scale bar = 200µm). (**E**) Hepatic triglycerides content in HFDt offspring. (**F**) Hepatic cholesterol content HFD offspring. (**G**) Volcano-plot RNA-sequencing representation of differently expressed genes (Chow diet; Control, n=4; FL, n=3; ML, n=3). (**H**) Heat map representation of most significantly altered genes including Nrep and Gdf15. (**I**) Selected pathways analyses of altered genes in FL and ML compared to controls. (**J-K**) Hepatic Nrep gene expression analyses by qPCR in FL, ML and controls on chow (**J**) and HFD (**K**) (Chow and HFD; n=4, 4 litters/group). **(L**) Hepatic Nrep mRNA by qPCR in mice challenged with a 6 week-long low-fat diet (LFD) and high-fat diet HFD. (LFD and HFD, n=5/group, diet intervention of 6 weeks). (**M-N**) Hepatic Nrep mRNA levels by qPCR in ob/ob (**M**) and db/db mice (**N**) at 12 weeks of age (n=5/group). Unless otherwise stated, Chow, control, n=8, 3 litters; FL, n=11, 4 litters; ML, n=5, 3 litters; HFD, control, FL and ML, n=6, 3 litters/group. One-way ANOVA with the Dunnett's post hoc test in E, F, J, and K.. Two-tailed unpaired t-test in L, M and N. *p<0.05; **p<0.01; ***p<0.001. In H *represents FDR<0.25 in FL and FDR<0.10 in ML and FL/ML comparisons.

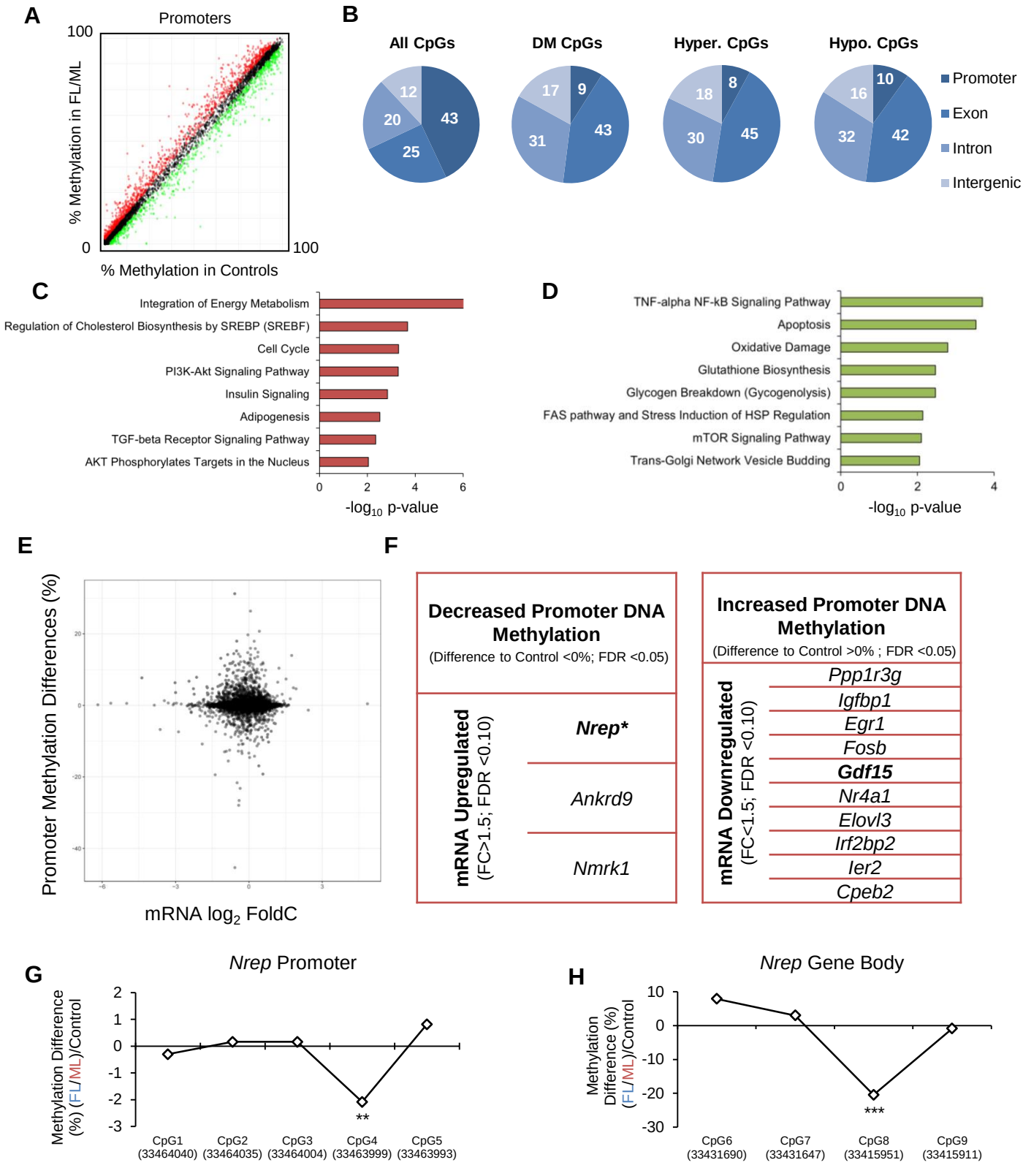

Figure 4

Figure 4: Hepatic global DNA methylation analyses by enhanced reduced representation bisulfite sequencing. (**A**) Scatter-plot representation of global promoter DNA methylation analyses by ERRBS (n=4, 4 litters/group). (**B**) Genomic features of hepatic DNA methylation (All CpGs–all detected cytosine's; DM CpGs–differently methylated cytosine's; Hyper. CpGs–hypermethylated cytosines; hypo. CpGs–hypomethylated cytosines). (**C**) Selected pathways of genes with increased promoter DNA methylation. (**D**) Selected pathways of genes with decreased promoter DNA methylation. (**E**) Scatter-plot representation of RNA-Seq. and RRBS datasets intersection. (**F**) Genes showing differential transcription regulation (mRNA FL/ML versus Control [FC>1.5]) and differential promoter methylation (FDR<0.05). (**G**) Nrep promoter DNA methylation in covered CpGs. (**H**) Nrep gene body DNA methylation in covered CpGs. Significance was determined by Benjamini-Hochberg method (see methods).

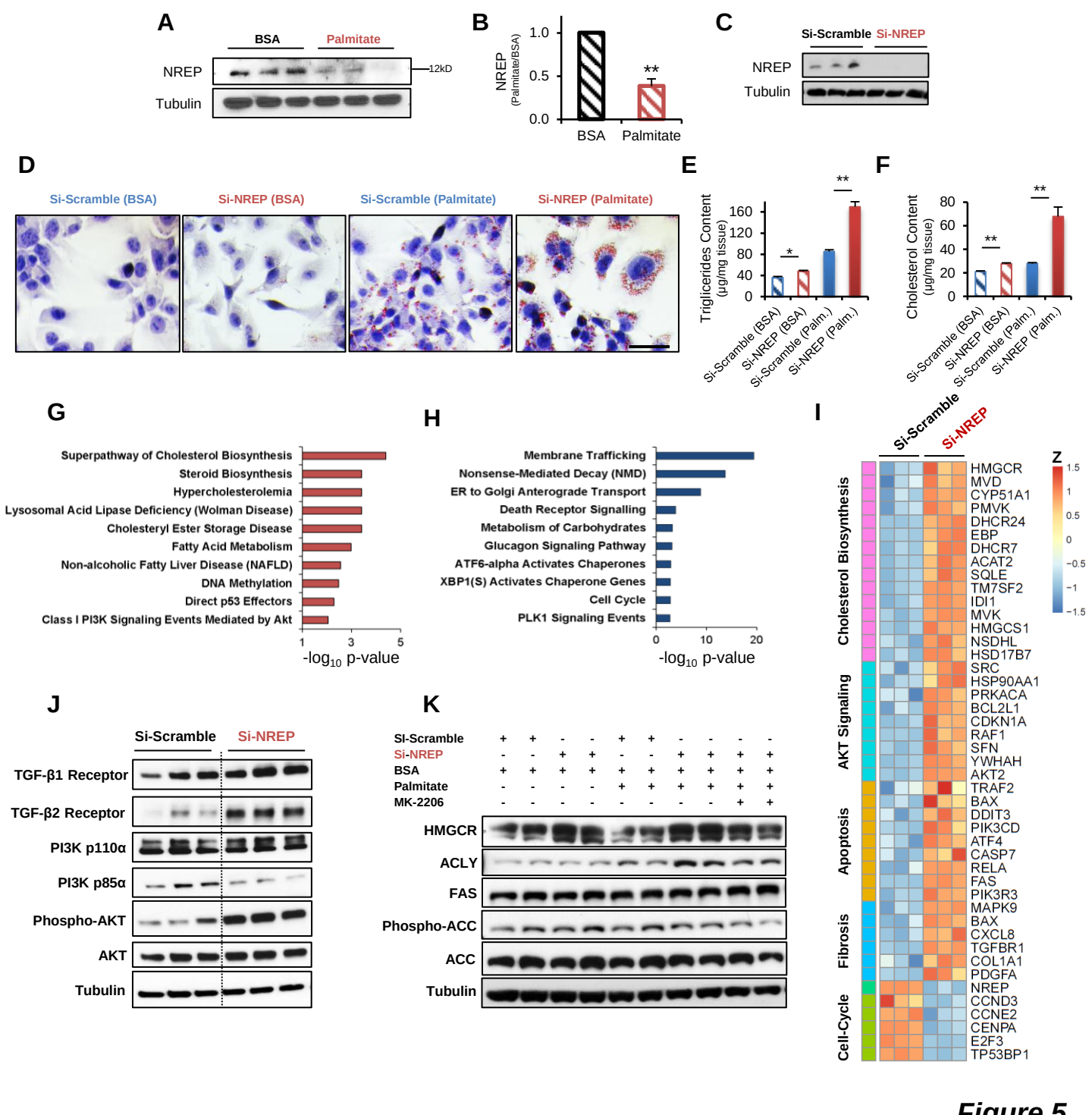

Figure 5

Figure 5: NREP is downregulated by palmitate-induced steatosis in HepG2. *NREP* regulates hepatic β-oxidation and lipid metabolism. (**A**) NREP protein levels in HepG2 cells treated with BSA (blue hatch) or palmitate (red hatch) for 24h (n=3 independent experiments). (**B**) Quantification of NREP protein levels. (**C**) *NREP* knock-down (KD) in HepG2 cells at protein levels (n=3). (**D**) Representative oil-red staining in HepG2 cells with NREP KD challenged with palmitate for 24h (n=3 independent experiments, magnification 400x, scale bar = 50µm). (**E-F**) Triglyceride (**E**) and cholesterol (**F**) content quantification in HepG2 cells lysates after stimulation for 24h with 500µM palmitate (n=3 independent experiments. (**G-H**) RNA sequencing selected enriched pathways analyses of upregulated (**G**) and downregulated genes (**H**) in HepG2 with NREP KD compared to scramble (n=3/group). (**I**) Heat-map representation of differently expressed genes involved in cholesterol biosynthesis, AKT signaling, apoptosis, fibrosis, and cell-cycle. (**J**) Basal signaling analyses in lysates from HepG2 cells treated with scramble (left panel) or NREP KD (right panel) (n=3 independent experiments). (**K**) Protein levels of indicated proteins in HepG2-scramble and *NREP* KD treated with BSA or palmitate for 24h in the presence of AKT inhibitor (MK-2206) or DMSO. n=2 independent experiments. Significance was determined by two-tailed unpaired t-test. * P < 0.05, ** P < 0.01 and ***P < 0.001. Data are expressed as means ± SEM.

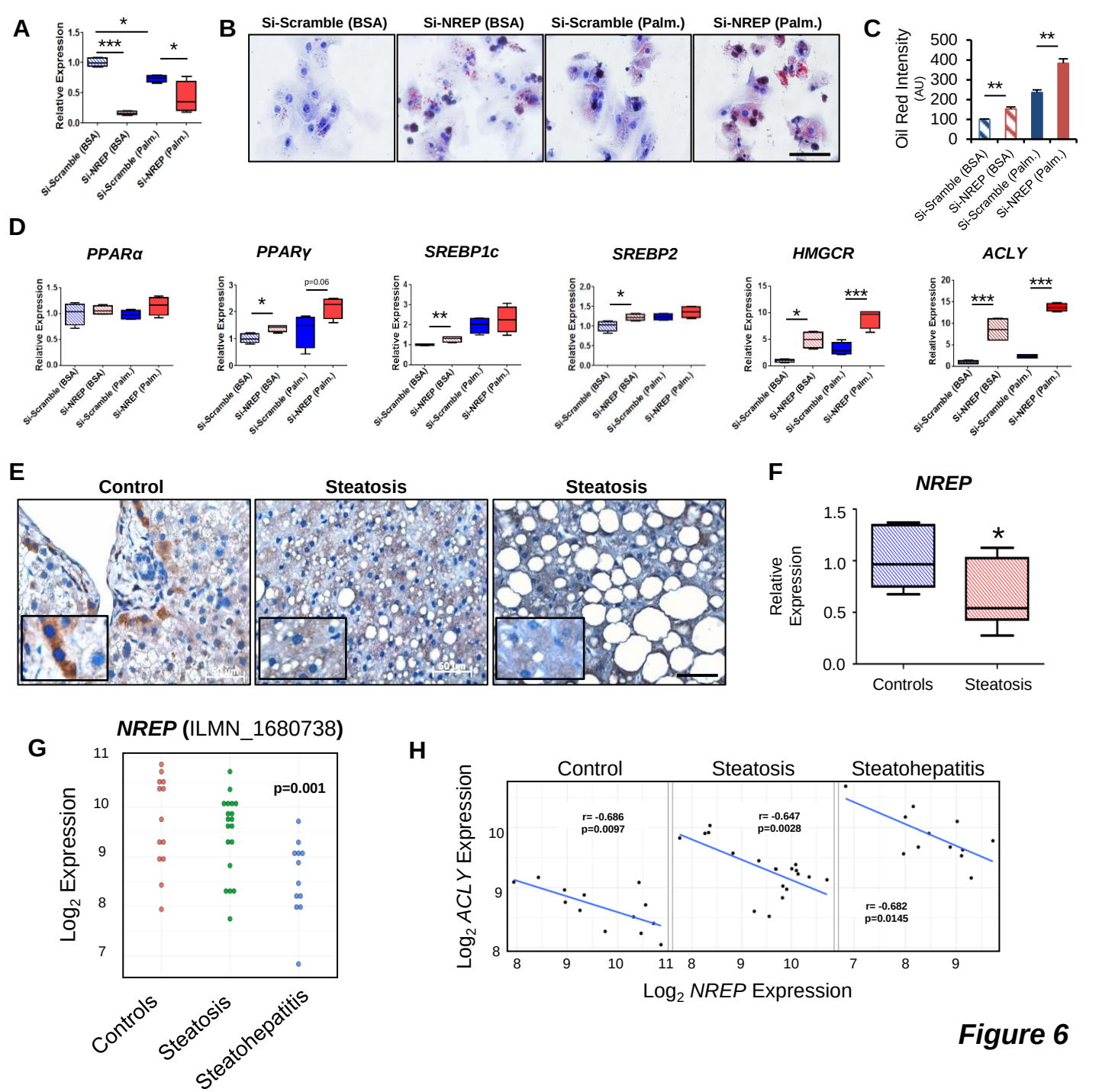

Figure 6

Figure 6: NREP relevance in human hepatic steatosis. *NREP* correlates negatively with ATP-citrate lyase. (**A**) *NREP* knock-down in human primary hepatocytes (n=3 independent experiments, hepatocytes from 5 pooled healthy donors). (**B**) Representative oil-red staining showing lipid droplets in human primary hepatocytes treated with BSA or challenged with palmitate for 24h (n=3 independent experiments; magnification 400x, scale bar = 50µm). (**D**) RT-PCR analyses of genes involved in β-oxidation (*PPARα*), transcriptional regulation of fatty-acid (*PPARγ, SREBP1c*) and cholesterol (*SREBP2*) metabolism, Acyl-CoA (*ACLY*) and cholesterol synthesis (*HMGCR*) (n=3 independent experiments, hepatocytes from 5 pooled healthy donors). (**E-F**) NREP protein (**E**) and mRNA (**F**) levels in human liver samples from controls and patients with steatosis (control, n=7; steatosis, n=8; Supplementary Table 6). (**G**) Hepatic mRNAs levels in controls, steatosis and steatohepatitis patients by microarrays (GSE33814). (**G**) Heat-map representation of *NREP* and *ACLY* mRNA levels (GSE33814). (**H**) Pearson's correlations between *NREP* and *ACLY* mRNA levels in all groups in controls, steatosis and steatohepatitis (**I**). Significance between 2 group comparisons was determined by One-way ANOVA with the Dunnett's post hoc test. Benjamini-Hochberg method was used (see methods) in G. Pearson's correlations in H. *p<0.05; **p<0.01; ***p<0.001. All data are shown as mean ± SEM.

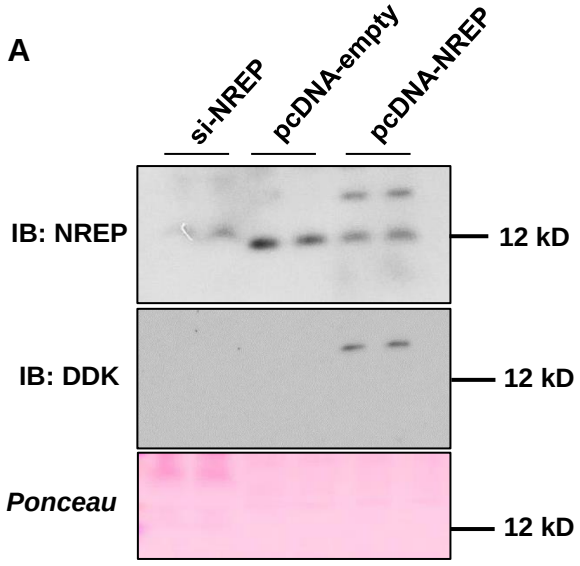

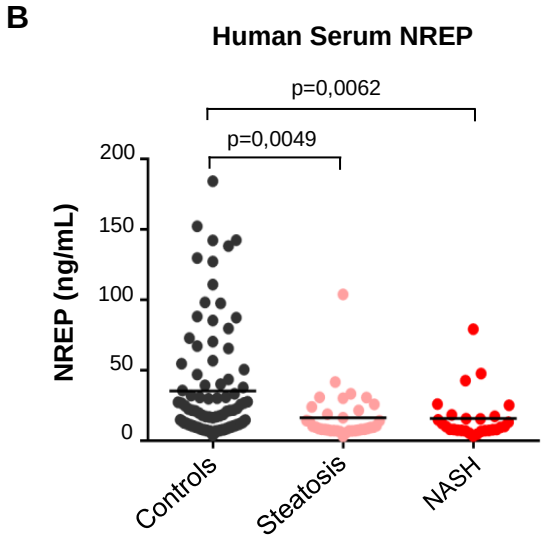

C

Correlations Between Plasma NREP and Clinical Features

	Correlation		Adj. Correlation (Sex, Age & BMI)		Adj. Correlation (Sex, Age, BMI and T2D)	
Parameter	rho	p	rho	p	rho	p
HDL-C	.269	0.0005	.227	0.0037	.216	0.0059
Triglycerides	-.206	0.0083	-.173	0.0286	-.151	0.0571
Fasting Insulin	-.181	0.0206	-.131	0.0979	-.101	0.2042
Steatosis Grade Baseline	-.286	0.0002	-.261	0.0007	-.234	0.0024
Lobular Inflammation Baseline	-.182	0.0174	-.154	0.0465	-.128	0.1010
NAS (NAFL Activity Score)	-.287	0.0001	-.259	0.0007	-.232	0.0027

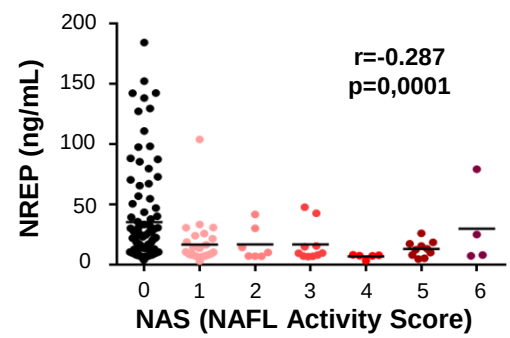

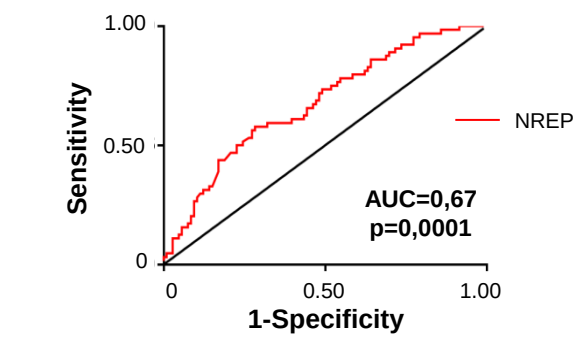

Figure 7

Figure 7: NREP is secreted by hepatocytes and its plasma levels reflect the changes in hepatic NREP mRNA seen in NAFLD. (**A**) NREP protein levels in the supernatant of HepG2 cells knock-down for NREP, Scramble or NREP Overexpression, cultured for 48h in FBS-free and 0.22µM filtered media. (**B**) NREP plasma levels in obese control, steatosis and NASH patients (control, n=106; steatosis, n=36; NASH, n=28). (**C**) Plasma NREP correlations with clinical parameters. (**D**) Correlation between plasma NREP with NAFL activity score. (**E**) ROC curves of NREP in controls versus steatosis plus NASH. Significance was determined by one-way ANOVA with Kruskal-Wallis test with Dunn's multi comparisons test in B. Adjusted spearman correlations in C and D. Data are expressed as means ± SEM. * p< 0.05, ** p< 0.01 and ***p< 0.001.

Supplementary Material

NREP bridges TGF-β Signaling and Lipid Metabolism in the Epigenetic Programming of NAFLD

Dario F. De Jesus[1,2], Kazuki Orime[1], Ercument Dirice[1], Dorota Kaminska[3], Chih-Hao Wang[4], Jiang Hu[1], Ville Männistö[5], Amelia M. Silva[6], Yu-Hua Tseng[4], Jussi Pihlajamaki[3,7], Rohit N. Kulkarni[1*]

[1] Islet Cell and Regenerative Biology, Joslin Diabetes Center, Department of Medicine, Brigham and Women's Hospital, Harvard Stem Cell Institute, Harvard Medical School, Boston, MA 02215, USA
[2] Graduate Program in Areas of Basic and Applied Biology (GABBA), Abel Salazar Biomedical Sciences Institute, University of Porto, 4050-313 Porto, Portugal
[3] Department of Public Health and Clinical Nutrition, University of Eastern Finland, Kuopio, Finland
[4] Integrative Physiology and Metabolism, Joslin Diabetes Center, Harvard Medical School, Boston, MA 02215, USA
[5] Department of Medicine, University of Eastern Finland and Kuopio University Hospital, Kuopio, Finland
[6] Department of Biology and Environment, Centre for the Research and Technology of Agro-Environmental and Biological Science, University of Tras-os-Montes and Alto Douro, 5000-801 Vila Real, Portugal
[7] Clinical Nutrition and Obesity Center, Kuopio University Hospital, Kuopio, Finland

*Correspondence to:
Rohit N. Kulkarni, MD, PhD
Islet Cell and Regenerative Biology
Joslin Diabetes Center
Harvard Medical School
One Joslin Place, Boston, MA 02215, USA.
Tel: +1-617-309-3460; Fax: +1-617-309-3476
E-mail: rohit.kulkarni@joslin.harvard.edu

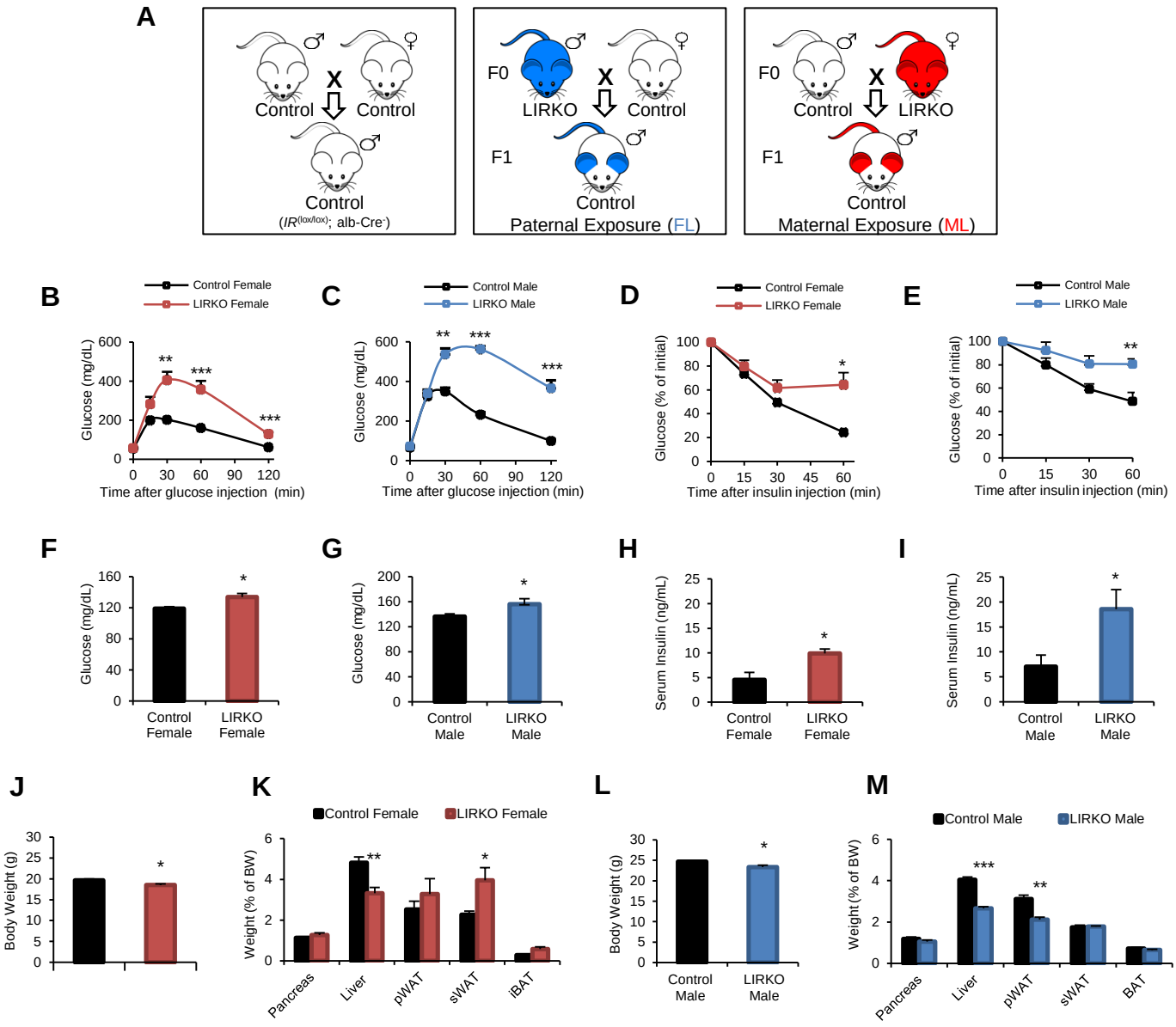

Supplementary Figure 1 (related to Figures 1 and 2): Schematic to study the metabolic phenotypes in offspring (F1) obtained from insulin resistant parents (F0). (**A**) Breeding scheme. In brief, control offspring were derived by breeding a control male and female (insulin receptor $^{lox/lox}$; Albumin-Cre$^{-/-}$). FL offspring were derived by breeding a male LIRKO (insulin receptor $^{lox/lox}$; Albumin-Cre$^{+/-}$) with a control female. ML offspring were derived by breeding a control male with a LIRKO female. (**B-C**) Blood glucose values following an intraperitoneal glucose tolerance test in control (black) or LIRKO (red) females (**B**) and control (black) or LIRKO (blue) males (**C**). Glucose levels plotted as % of basal values, following intraperitoneal injection of insulin in control or LIRKO females (**D**) and control or LIRKO males (**E**). (**F**) Random-fed blood glucose levels in control or LIRKO females. (**G**) Random-fed blood glucose levels in control or LIRKO males. (**H**) Random-fed serum insulin levels in control or LIRKO females. (**I**) Random-fed serum insulin levels in control or LIRKO males. (**J**) Body weight of controls or LIRKO females at 2 months of age. (**K**) Body composition in controls and LIRKO females at 2 months of age. (**L**) Body weight of controls and LIRKO males at 2 months of age. (**M**) Body composition of controls and LIRKO males at 2 months of age. All data from n=4-9/group and analyzed using the unpaired two-tailed Student's t-test. *p < 0.05, **p< 0.01 and ***p < 0.001. Data are expressed as means ± SEM.

Supplementary Figure 1 (related to Figure 1 and 2)

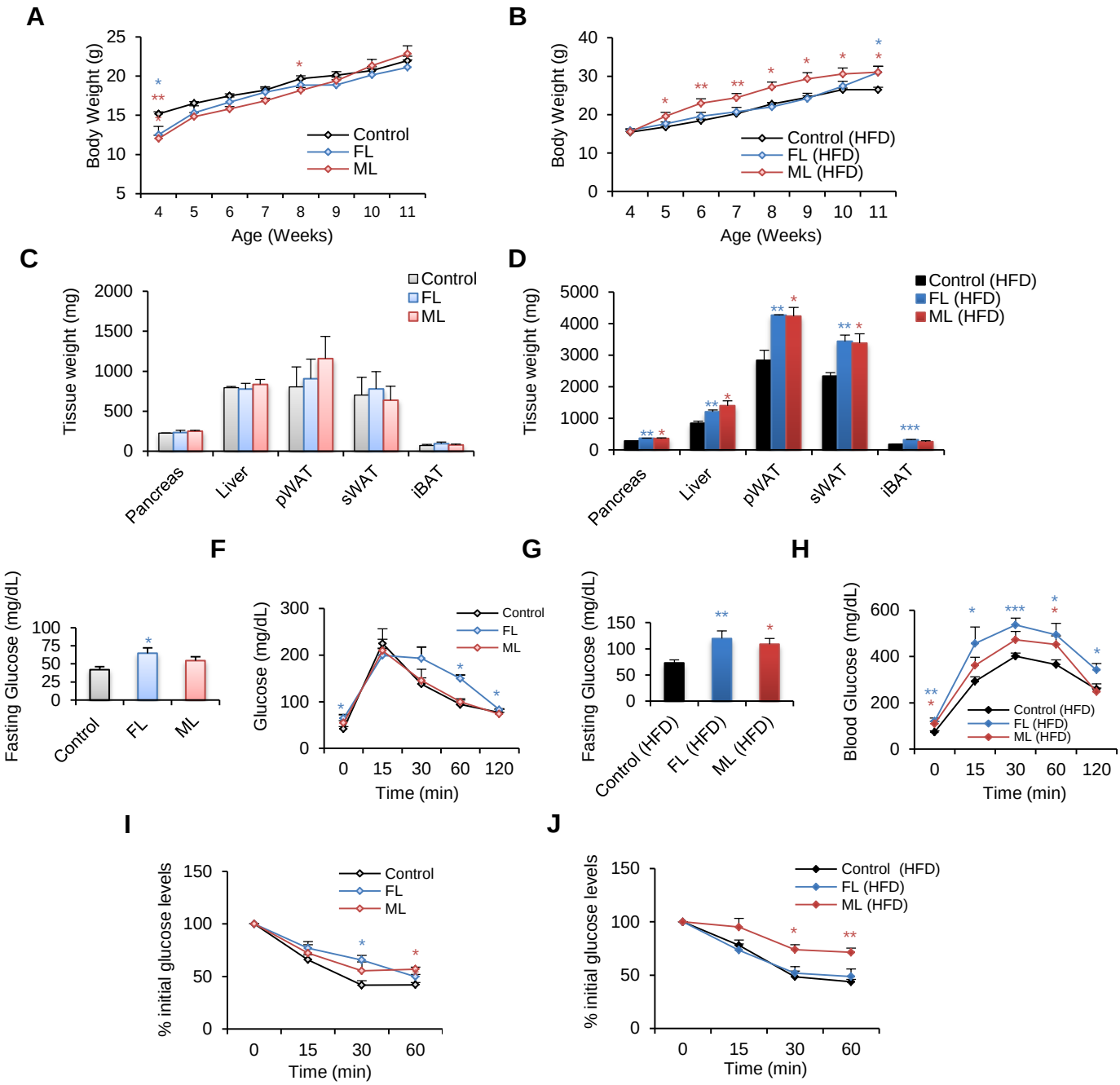

Supplementary Figure 2 (related to figure 1 and 2): Females F1 offspring from insulin resistant parents present metabolic abnormalities similar to male siblings. (**A-B**) Body weight trajectories in control (black), FL (blue) or ML (red) female offspring on chow (**A**) or HFD (**B**) diets. (**C-D**) Body weight composition in mice on chow (**C**) or HFD (**D**) diets at 3 months of age. (**E**) Fasted blood glucose levels in control, FL or ML offspring on chow diet at 2 months of age. (**F**) Blood glucose values following an intraperitoneal glucose tolerance test in control, FL, and ML in chow. (**G**) Fasted blood glucose levels in control, FL or ML on HFD diet at 2 months of age. (**H**) Blood glucose values following an intraperitoneal glucose tolerance test in control, FL, or ML on HFD diets. (**I-J**) Insulin tolerance test with glucose levels plotted as % of basal values, following intraperitoneal injection of insulin in control, FL, or ML on chow (**I**) or HFD (**J**) diets. All data are based on n=4-8/group representing a minimum of 3 independent litters/group and analyzed using the one-way ANOVA with Dunnett's post hoc test. * P < 0.05, ** P < 0.01 and ***P < 0.001. Data are expressed as means ± SEM.

Supplementary Figure 2 (related to Figure 1 and 2)

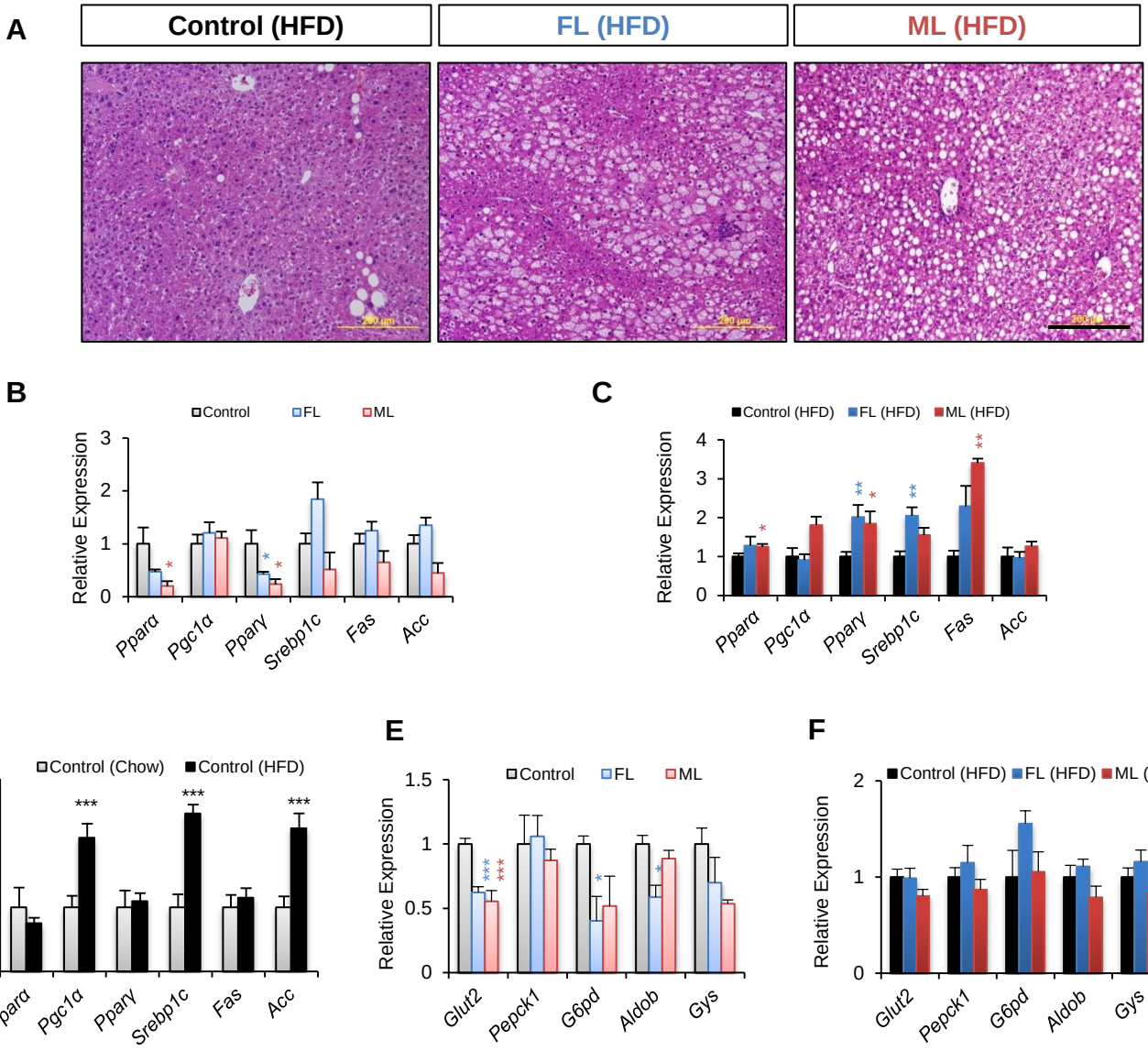

Supplementary Figure 3 (related to Figure 2 and 3)

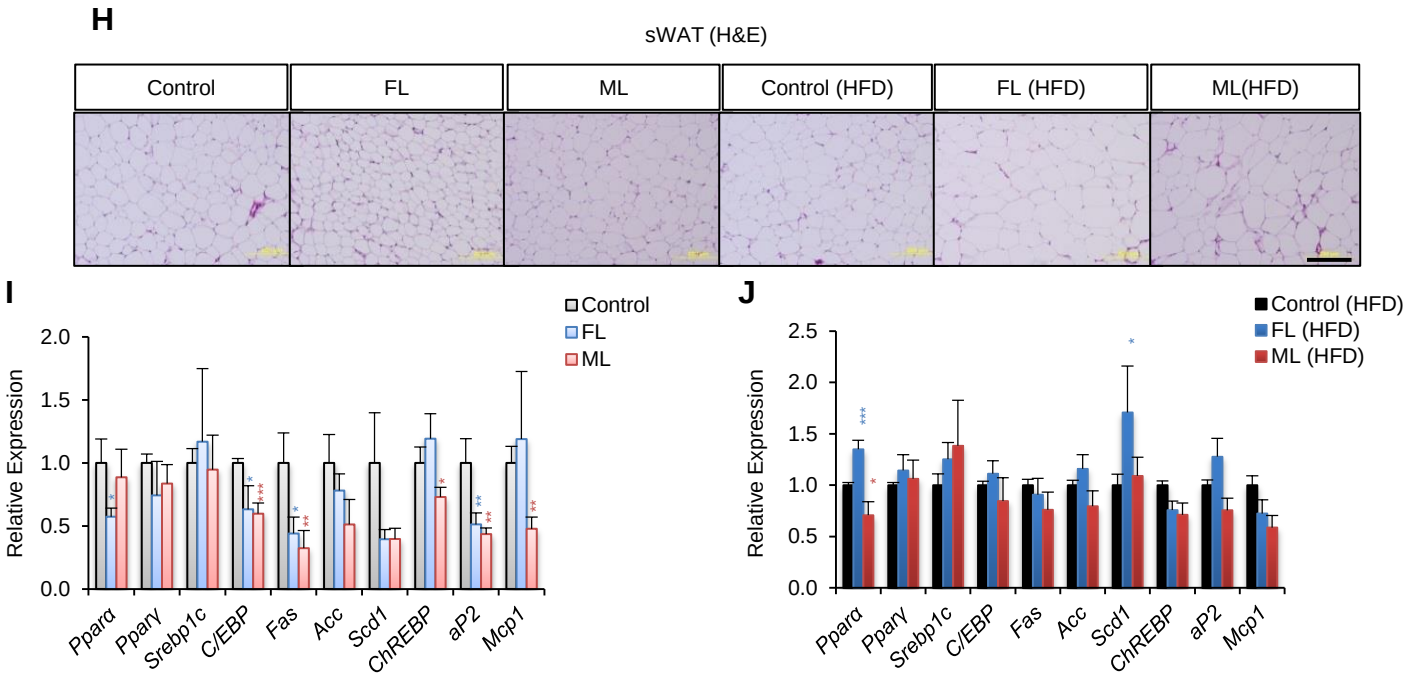

Supplementary Figure 3 (related to figure 2 and 3): Extended phenotypic characterization in F1 male offspring. (**A**) High magnification Hematoxylin and Eosin-stained (H and E) liver sections from control, FL or ML offspring (Magnification 200x, scale bar = 200µm). (**B-C**) qPCR analysis of genes involved in lipid β-oidation and fatty acid synthesis in chow (**B**) and HFD (**C**).(**D**) qPCR comparison of gene expression between control on chow versus HFD diets. (**E-F**). Further hepatic expression analysis of genes involved in glucose transport, glycolysis, gluconeogenesis and glycogenesis on chow (**E**) or HFD (**F**) diets. (**G**) Signaling analysis in liver lysates from control, FL or ML offspring in chow following *vena-cava* infusion of insulin. (**H**) Representative H and E stained flank subcutaneous white adipose tissue (sWAT) sections in control, FL or ML on chow or HFD diets (Magnification 200x, scale bar = 200µm). (**I-J**) qPCR analyses of genes involved in lipid biology and inflammation on chow (**I**) or (**J**) HFD diets. All data are based on n=3-9/group representing a minimum of 3 independent litters/group and analyzed using the unpaired two-tailed Student's t-test. * P < 0.05, ** P < 0.01 and ***P < 0.001. Data are expressed as means ± SEM.

Supplementary Figure 3 (Cont.)

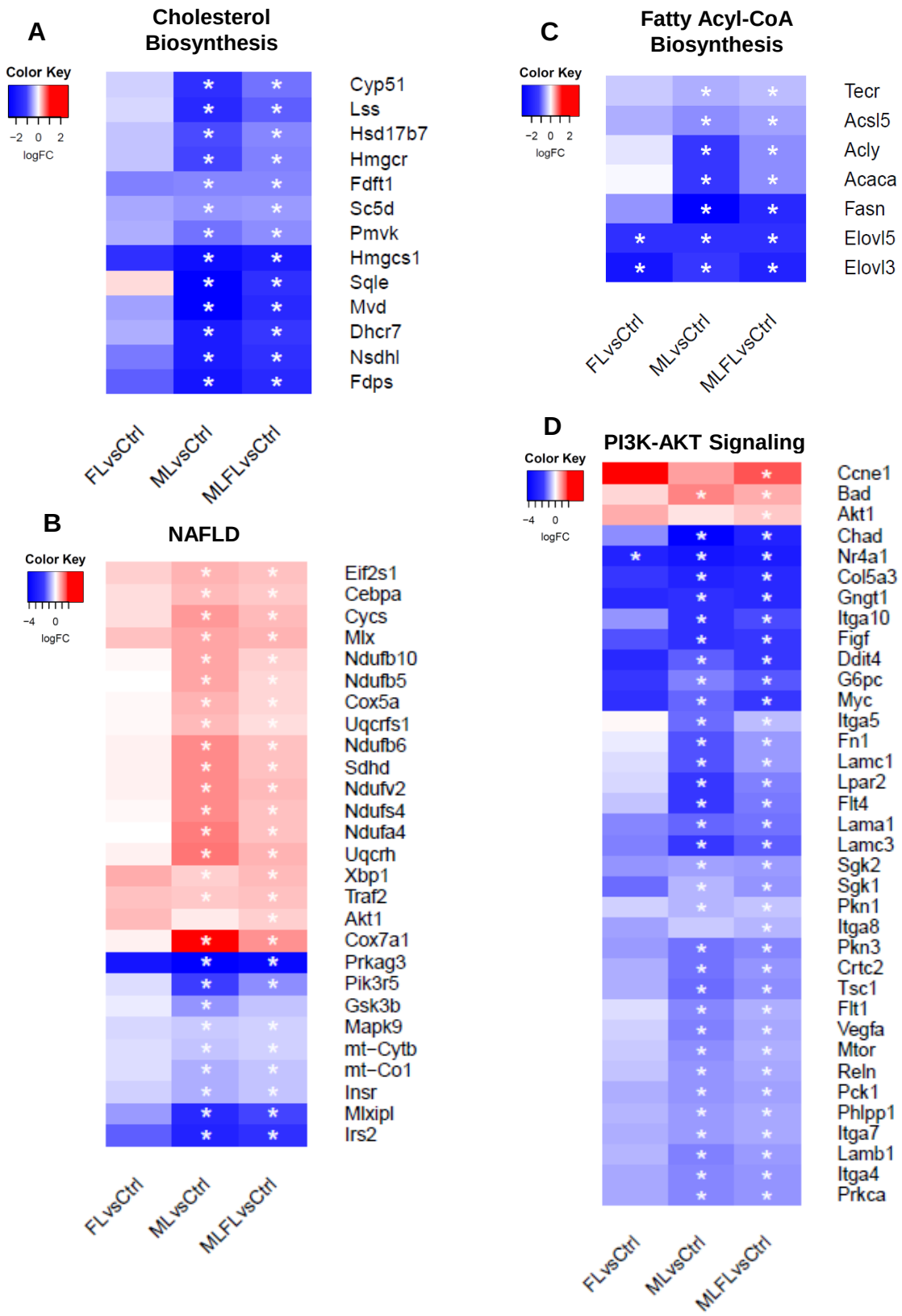

Supplementary Figure 4 (related to figure 2 and 3): (A-D) Heat-map representation of differently expressed genes related to cholesterol biosynthesis (**A**), NAFLD (**B**), fatty Acyl-CoA biosynthesis (**C**), and PI3K-AKT signaling (**D**) in FL and ML offspring compared to controls. *represent FDR<0.10.

Supplementary Figure 4 (related to Figure 3)

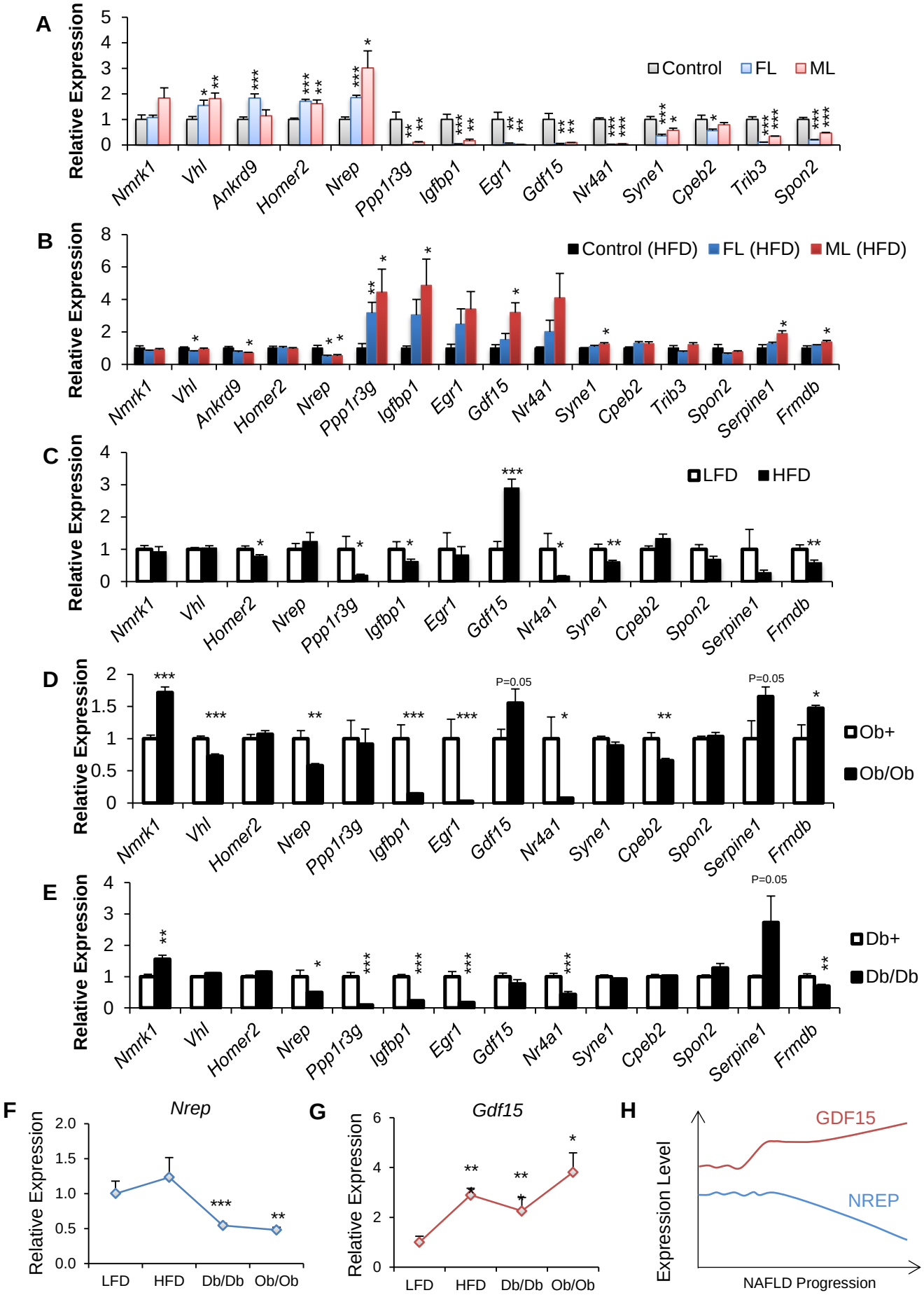

Supplementary Figure 5 (related to Figure 3)

Supplementary Figure 5 (related to figure 3). (**A**) qPCR analyses of selected-candidate genes in FL or ML on chow diet. (**B**) qPCR analyses of selected-candidate genes in FL or ML on HFD. (**C**) qPCR analyses of candidate genes on a 6-week low-fat –LFD (white bars) versus HFD diets (black bars). (**D**) qPCR analyses of candidate genes in leptin-deficient ob/ob mice (black bars) versus ob+ (white bars). (**E**) qPCR analyses of candidate genes in leptin receptor-deficient db/db mice (black bars) versus db+ (white bars). (**F**) Hepatic *Nrep* mRNA levels plotted in different models of steatosis. (**G**) Hepatic *Gdf15* mRNA plotted in different models of steatosis.(**G**) Proposed model of GDF15 and NREP expression during the development of steatosis. (**O**) qPCR in FL, ML and control (n=4 mice/litters). qPCR in other models (n=5 mice). All data are means ± SEM and analyzed using an unpaired two-tailed Student's t-test. * $P < 0.05$, ** $P < 0.01$ and ***$P < 0.001$.

Supplementary Figure 5 (cont.)

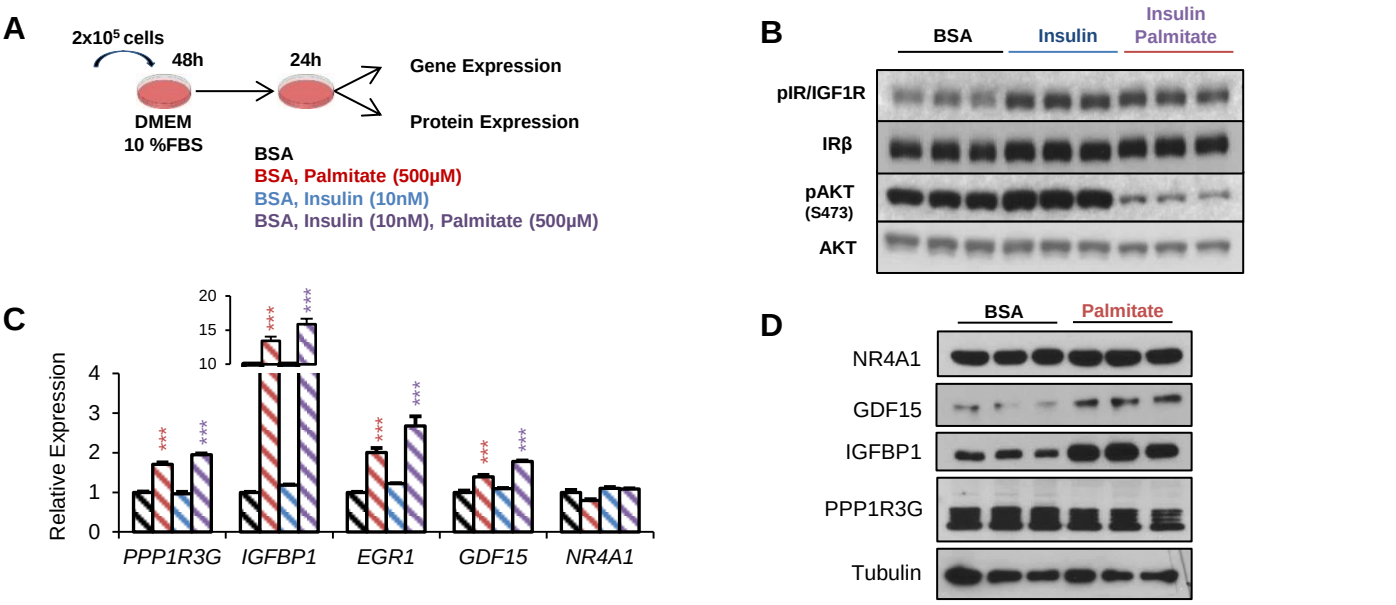

Supplementary Figure 6 (related to figure 5): (**A**) Schematic for the *in-vitro* modulation of hepatic steatosis. (**B**) Signaling analysis of lysates from HepG2 cells treated with insulin (blue) or insulin+palmitate, (purple). (**C**) qPCR analyses of candidate genes in cells challenged with BSA (black), palmitate (red), insulin (blue) or insulin+palmitate (purple). Insert shows values for *IGFBP1* on a higher scale. (**D**) Protein analyses of candidate genes in lysates from HepG2 cells challenged with BSA or palmitate. All data are based on 3 independent experiments (n=3) and 2-group comparisons analyzed using an unpaired two-tailed Student's T-test. * P < 0.05, ** P < 0.01 and ***P < 0.001. Data are expressed as means ± SEM.

Supplementary Figure 6 (related to Figure 5)

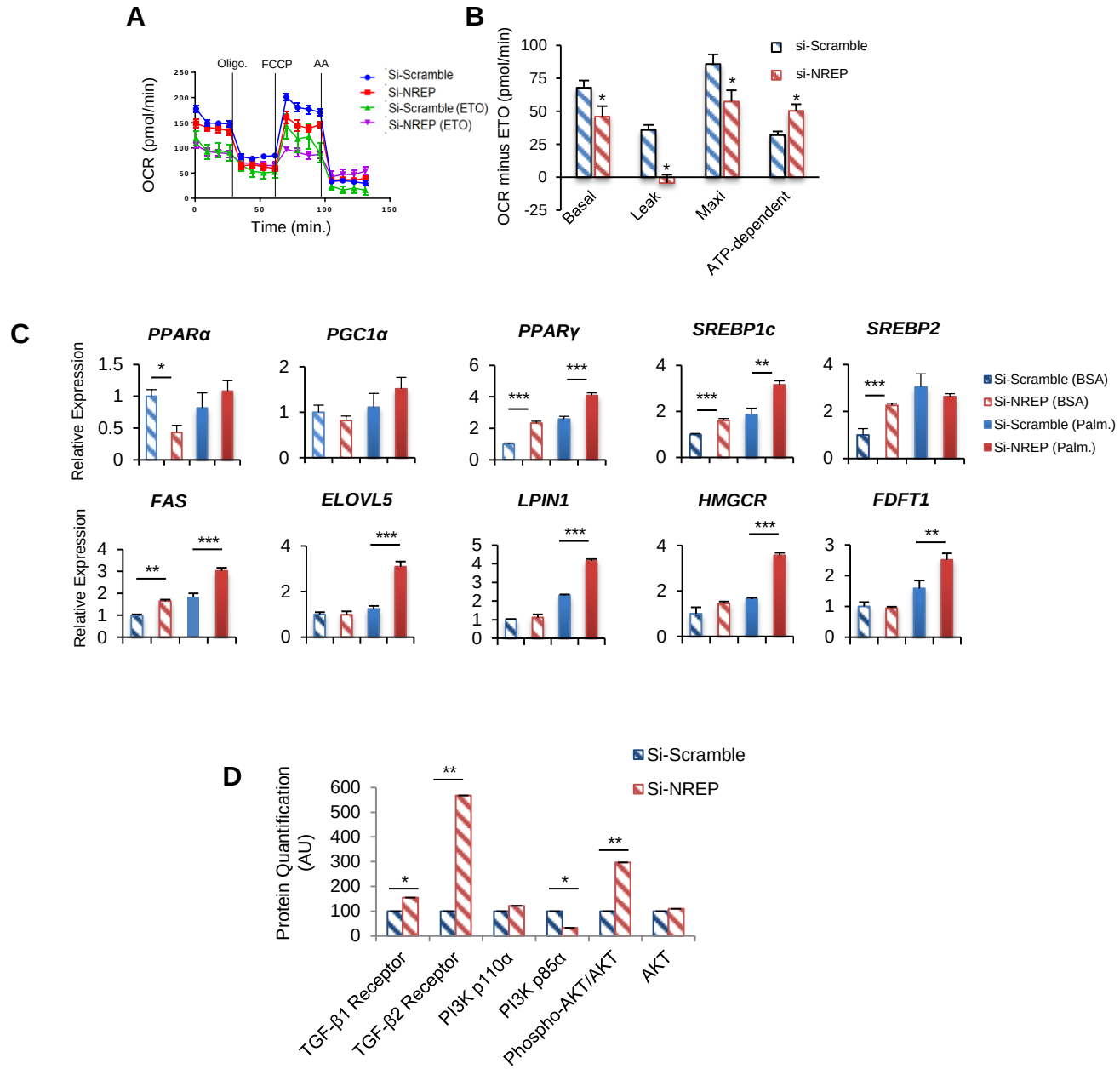

Supplementary Figure 7 (related to figure 5) (**A**) Oxygen-consumption ratio (OCR) from seahorse analyses of fatty-acid oxidation (FAO) in scramble and *NREP* KD treated with a BSA:palmitate substrate (n=6 experiments). (**B**) Quantification of seahorse results. (**C**) RT-PCR analyses of genes involved in β-oxidation (*PPARα*), mitochondrial bioge–nesis (*PGC1α*), transcriptional regulation of fatty-acid (*PPARγ, SREBP1c,*) and cholesterol metabolism transcriptional regulation (*SREBP2*), *de-novo* fatty-acid synthesis (*FAS*), fatty-acid elongation (*ELOVL5*), glycerolipid synthesis (*LPIN1*), and cholesterol synthesis (*HMCGR, FDFT1*) in HepG2-scramble or NREP KD challenged with BSA or Palmitate for 24h (n=3 independent experiments). (**D**) Protein quantification of indicated proteins related to Figure 5J. Statistical analyses using One-way ANOVA with the Dunnett's post hoc test.

Supplementary Figure 7 (related to Figure 5)

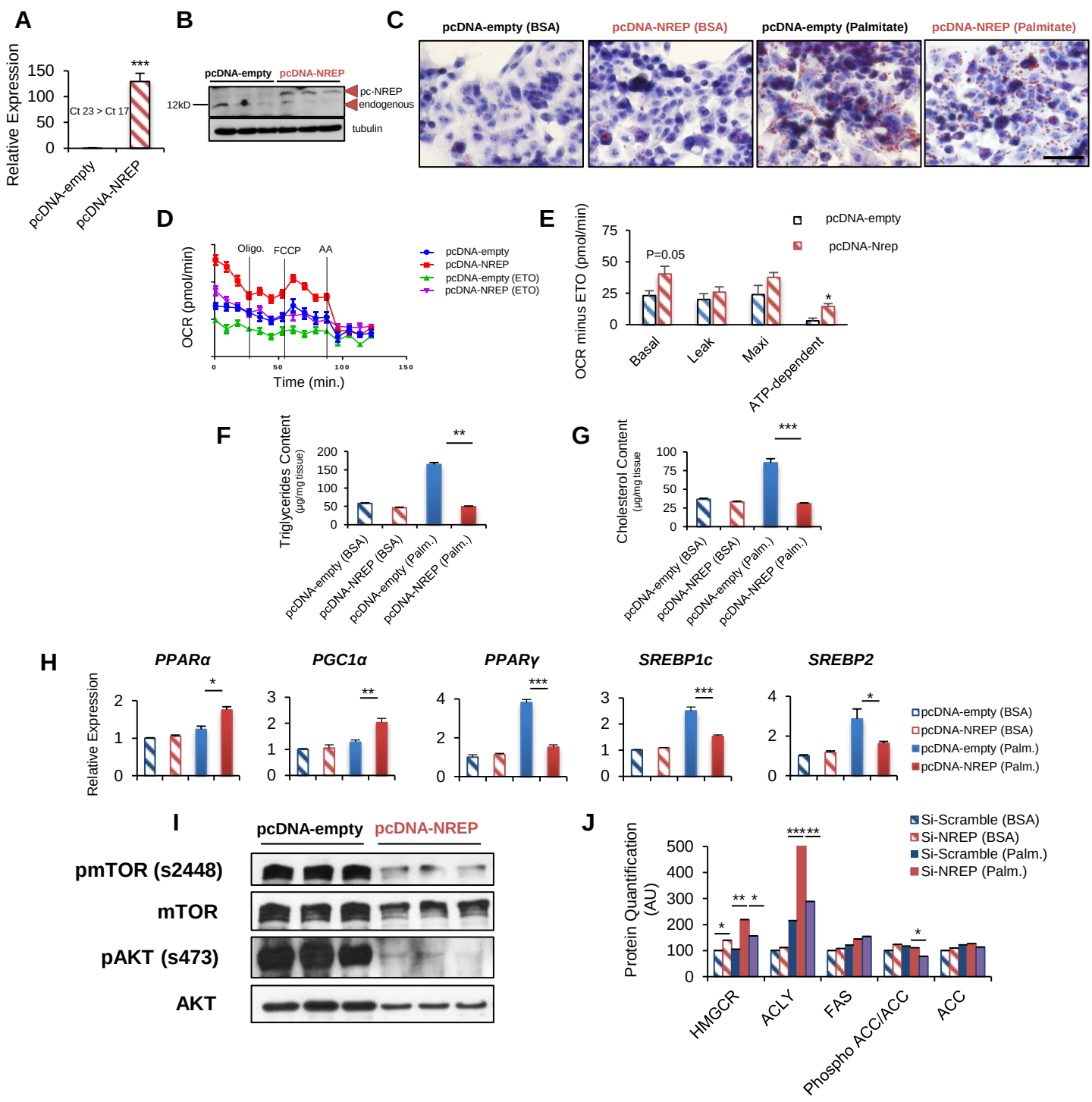

Supplementary Figure 8 (related to figure 5): NREP overexpression in HepG2 cells increases the expression of master regulators of beta-oxidation, mitochondrial biogenesis and dramatically blocks the increment of fatty-acid synthesis-related genes in response to palmitate. (**A-B**) HepG2 cells with NREP overexpression (OE) evaluated by qPCR (**A**) or western blot (**B**). (**C**) Representative oil-red staining in NREP OE HepG2 cells challenged with palmitate for 24h (magnification 400x, Scale bar = 50µm). (**D-E**) Fatty-acid oxidation (FAO) analysis by Seahorse (**D**) and quantification (**E**) in NREP OE HepG2 cells. (**F-G**) Triglycerides (**F**) and cholesterol (**G**) content quantification in lysates from HepG2 cells stimulated for 24h with 500uM of Palmitate. (**H**) qPCR analyses of genes involved in beta-oxidation, mitochondrial biogenesis and fatty-acid synthesis in HepG2 cells (scramble or NREP OE) challenged with BSA or Palmitate for 24h. (**I**) Basal signaling analyses in lysates from HepG2 cells (scramble or NREP OE). (**J**) Protein quantification of indicated proteins related to Figure 5K. All data are based on 3 independent experiments (n=3) Statistical analyses using One-way ANOVA with the Dunnett's post hoc test. . * P < 0.05, ** P < 0.01 and ***P < 0.001. Data are expressed as means ± SEM.

Supplementary Figure 8 (related to Figure 5)

Table 1: Random-fed serum metabolites from F0 parents

	Control (n=3-4)	LIRKO (n=3-4)
F0 Mothers (ML)		
C-peptide (ng/mL)	2.2 ± 0.8	1.4 ± 0.1
Leptin (ng/mL)	5.6 ± 1.6	3.9 ± 0.6
MCP-1 (pg/mL)	38.2 ± 9.3	10.7 ± 3.2
Resistin (pg/mL)	7353.4 ± 606.4	6214 ± 658.8
F0 Fathers (FL)		
C-peptide (ng/mL)	1.7 ± 0.3	2.4 ± 0.4
Leptin (ng/mL)	8.5 ± 1.5	5.4 ± 1.4
MCP-1 (pg/mL)	307 ± 112.3	14.4 ± 2.1
Resistin (pg/mL)	6318.8 ± 313.2	6701.8 ± 662.6

Table 2: Random-fed serum metabolites in male F1 offspring at 3 months of age

F1 Offspring	Control	FL	ML	Control (HFD)	FL (HFD)	ML (HFD)
Insulin (ng/mL)	5.0 ± 0.4	3.6 ± 1.3	**3.5 ± 0.3**[a]	13 ± 6.3	14.6 ± 4.1	14.9 ± 4.1
C-peptide (ng/mL)	3.2 ± 0.8	1.6 ± 0.5	1.8 ± 0.6	2.7 ± 1.6	2.6 ± 1.4	1.8 ± 0.6
Leptin (ng/mL)	9.6 ± 2.9	5.9 ± 1.7	9.8 ± 3.1	22.9 ± 1.8	**33.2 ± 3.7**[c]	28.8 ± 2.6
GIP (pg/mL)	77.6 ± 34.7	126.9 ± 45.6	76.5 ± 24.7	338.9 ± 179.3	199.1 ± 91.9	131 ± 42
MCP-1 (pg/mL)	16 ± 7.9	**57.2 ± 6.4**[b]	23.7 ± 5.2	203.7 ± 44.8	**50 ± 7.1**[c]	**70.9 ± 9.8**[d]
Resistin (pg/mL)	5224.8 ± 2248.1	5902.5 ± 856.3	3933.8 ± 1168	8411.8 ± 1637.5	5740.2 ± 1444	**4914.8 ± 789.4**[d]

[a] $p<0.05$ (Control Vs. ML)
[b] $p<0.01$ (Control Vs. FL)
[c] $p<0.05$ (Control HFD Vs. FL HFD)
[d] $p<0.05$ (Control HFD Vs. ML HFD)

Table 3: Pathway analyses of RNA-SEQ dataset

select allnone	pathway name	set size	candidates contained	p-value	q-value	pathway source
	TGF Beta Signaling Pathway	52(40)	3 (7.5%)	0.000124	0.00449	Wikipathways
	Amphetamine addiction - Mus musculus (mouse)	68(41)	3 (7.3%)	0.000133	0.00449	KEGG
	spermine biosynthesis II	9(8)	2 (25.0%)	0.000166	0.00449	MouseCyc
	Fc epsilon receptor (FCERI) signaling	155(119)	4 (3.4%)	0.000182	0.00449	Reactome
	Activation of the AP-1 family of transcription factors	10(9)	2 (22.2%)	0.000214	0.00449	Reactome
	Synthesis of very long-chain fatty acyl-CoAs	13(10)	2 (20.0%)	0.000267	0.00467	Reactome
	Insulin Signaling	157(138)	4 (2.9%)	0.000322	0.00483	Wikipathways
	Spinal Cord Injury	103(62)	3 (4.8%)	0.000458	0.00602	Wikipathways
	Fatty Acyl-CoA Biosynthesis	17(14)	2 (14.3%)	0.000536	0.00626	Reactome
	Metabolism of polyamines	16(15)	2 (13.3%)	0.000618	0.00649	Reactome
	Urea cycle and metabolism of amino groups	20(17)	2 (11.8%)	0.000798	0.00702	Wikipathways
	Chagas disease (American trypanosomiasis) - Mus musculus (mouse)	104(75)	3 (4.0%)	0.000802	0.00702	KEGG
	Fatty acid elongation - Mus musculus (mouse)	24(21)	2 (9.5%)	0.00122	0.00989	KEGG
	Osteoclast differentiation - Mus musculus (mouse)	126(100)	3 (3.0%)	0.00185	0.0139	KEGG
	MAPK targets/ Nuclear events mediated by MAP kinases	29(27)	2 (7.4%)	0.00203	0.0139	Reactome
	Myometrial Relaxation and Contraction Pathways	157(106)	3 (2.8%)	0.00218	0.0139	Wikipathways
	Cellular responses to stress	127(107)	3 (2.8%)	0.00224	0.0139	Reactome
	Cocaine addiction - Mus musculus (mouse)	50(31)	2 (6.5%)	0.00267	0.0148	KEGG
	Triglyceride Biosynthesis	36(31)	2 (6.5%)	0.00267	0.0148	Reactome
	Signaling of Hepatocyte Growth Factor Receptor	34(33)	2 (6.1%)	0.00303	0.0151	Wikipathways
	FCERI mediated MAPK activation	38(33)	2 (6.1%)	0.00303	0.0151	Reactome
	MAPK signaling pathway	158(133)	3 (2.3%)	0.00416	0.0199	Wikipathways
	TGF-beta Receptor Signaling Pathway	150(136)	3 (2.2%)	0.00443	0.0202	Wikipathways
	Selenium metabolism-Selenoproteins	47(42)	2 (4.8%)	0.00487	0.0213	Wikipathways
	Arginine and proline metabolism - Mus musculus (mouse)	57(44)	2 (4.5%)	0.00533	0.0224	KEGG
	MAP kinase activation in TLR cascade	48(45)	2 (4.4%)	0.00557	0.0225	Reactome
	Glutathione metabolism - Mus musculus (mouse)	55(46)	2 (4.3%)	0.00582	0.0226	KEGG
	Leishmaniasis - Mus musculus (mouse)	66(53)	2 (3.8%)	0.00767	0.0226	KEGG
	Rheumatoid arthritis - Mus musculus (mouse)	84(54)	2 (3.7%)	0.00795	0.0226	KEGG
	Oxidative Stress Induced Senescence	71(55)	2 (3.6%)	0.00824	0.0226	Reactome
	Colorectal cancer - Mus musculus (mouse)	64(56)	2 (3.6%)	0.00853	0.0226	KEGG
	Pertussis - Mus musculus (mouse)	74(57)	2 (3.5%)	0.00883	0.0226	KEGG
	TRAF6 Mediated Induction of proinflammatory cytokines	63(58)	2 (3.4%)	0.00913	0.0226	Reactome
	MAPK signaling pathway - Mus musculus (mouse)	257(180)	3 (1.7%)	0.00965	0.0226	KEGG
	PI3K/AKT Signaling in Cancer	86(60)	2 (3.3%)	0.00975	0.0226	Reactome
	PIP3 activates AKT signaling	86(60)	2 (3.3%)	0.00975	0.0226	Reactome
	PI-3K cascade	86(60)	2 (3.3%)	0.00975	0.0226	Reactome
	PI3K events in ERBB2 signaling	86(60)	2 (3.3%)	0.00975	0.0226	Reactome
	PI3K events in ERBB4 signaling	86(60)	2 (3.3%)	0.00975	0.0226	Reactome

Supplementary Table 4: Pathway Analyses RNA SEQ

Pathway- Increased Me FDR=5%	set size	candidates contained	p-value	q-value	pathway source
XPodNet - protein-protein interactions in the podocyte expanded by STRING	831	280 (33.9%)	1.25E-13	1.97E-10	Wikipathways
PluriNetWork	291	114 (39.3%)	2.74E-10	2.16E-07	Wikipathways
PodNet- protein-protein interactions in the podocyte	315	115 (36.5%)	3.42E-08	1.74E-05	Wikipathways
Developmental Biology	307	112 (36.6%)	4.42E-08	1.74E-05	Reactome
Regulation of Insulin Secretion	69	35 (52.2%)	1.94E-07	6.11E-05	Reactome
Integration of energy metabolism	90	42 (47.7%)	3.24E-07	8.49E-05	Reactome
Insulin secretion - Mus musculus (mouse)	88	40 (46.0%)	2.05E-06	0.00046	KEGG
IL-3 Signaling Pathway	100	44 (44.0%)	2.80E-06	0.000551	Wikipathways
Signalling by NGF	275	95 (34.7%)	6.99E-06	0.00122	Reactome
EGFR1 Signaling Pathway	176	66 (37.5%)	1.03E-05	0.00154	Wikipathways
Axon guidance	225	80 (35.7%)	1.07E-05	0.00154	Reactome
Signaling by FGFR in disease	155	59 (38.3%)	1.42E-05	0.00186	Reactome
MAPK signaling pathway - Mus musculus (mouse)	257	86 (33.9%)	5.08E-05	0.00609	KEGG
Pathways in cancer - Mus musculus (mouse)	326	105 (32.5%)	5.42E-05	0.00609	KEGG
Integrin-mediated Cell Adhesion	98	40 (40.8%)	6.50E-05	0.00624	Wikipathways
Oocyte meiosis - Mus musculus (mouse)	113	44 (39.6%)	6.62E-05	0.00624	KEGG
Dopaminergic synapse - Mus musculus (mouse)	135	50 (38.2%)	6.98E-05	0.00624	KEGG
NGF signalling via TRKA from the plasma membrane	184	65 (35.5%)	8.44E-05	0.00624	Reactome
Disease	608	179 (29.6%)	8.46E-05	0.00624	Reactome
Vasopressin-regulated water reabsorption - Mus musculus (mouse)	44	22 (50.0%)	8.64E-05	0.00624	KEGG
Ubiquitin mediated proteolysis - Mus musculus (mouse)	143	52 (37.4%)	9.32E-05	0.00624	KEGG
Progesterone-mediated oocyte maturation - Mus musculus (mouse)	89	36 (41.4%)	0.000106	0.00624	KEGG
mRNA processing	465	138 (30.6%)	0.000107	0.00624	Wikipathways
Regulation of actin cytoskeleton - Mus musculus (mouse)	218	74 (34.3%)	0.000109	0.00624	KEGG
T Cell Receptor Signaling Pathway	133	50 (37.6%)	0.000109	0.00624	Wikipathways
Neurotrophin signaling pathway - Mus musculus (mouse)	123	47 (38.2%)	0.00011	0.00624	KEGG
Calcium Regulation in the Cardiac Cell	150	55 (36.7%)	0.000111	0.00624	Wikipathways
Neuronal System	254	84 (33.3%)	0.000114	0.00624	Reactome
Ras signaling pathway - Mus musculus (mouse)	230	77 (33.9%)	0.000115	0.00624	KEGG
Cell Cycle, Mitotic	337	107 (31.8%)	0.000133	0.0069	Reactome
Signaling by SCF-KIT	125	47 (37.9%)	0.000138	0.0069	Reactome
Fc gamma R-mediated phagocytosis - Mus musculus (mouse)	89	36 (40.9%)	0.00014	0.0069	KEGG
Regulation of Cholesterol Biosynthesis by SREBP (SREBF)	12	9 (75.0%)	0.000203	0.00945	Reactome
Hedgehog signaling pathway - Mus musculus (mouse)	49	23 (46.9%)	0.000204	0.00945	KEGG
Downstream signal transduction	142	51 (36.2%)	0.000285	0.0128	Reactome
Signaling by PDGF	160	56 (35.2%)	0.000325	0.014	Reactome
GABAergic synapse - Mus musculus (mouse)	90	35 (39.8%)	0.00033	0.014	KEGG
Wnt Signaling Pathway NetPath	109	41 (38.0%)	0.000346	0.0143	Wikipathways
Metabolism	1386	366 (26.8%)	0.000374	0.0145	Reactome
Platelet Aggregation (Plug Formation)	36	18 (50.0%)	0.000377	0.0145	Reactome
Signaling by EGFR	161	56 (35.0%)	0.000389	0.0145	Reactome
Wnt Signaling Pathway	60	26 (43.3%)	0.000396	0.0145	Wikipathways
Signaling by FGFR1 fusion mutants	15	10 (66.7%)	0.000397	0.0145	Reactome
Signaling by FGFR	144	51 (35.7%)	0.00042	0.015	Reactome
Platelet activation, signaling and aggregation	190	64 (33.9%)	0.000442	0.0155	Reactome
Wnt Signaling Pathway and Pluripotency	96	37 (38.5%)	0.000469	0.016	Wikipathways
Cell Cycle	408	123 (30.1%)	0.000484	0.0162	Reactome
Amphetamine addiction - Mus musculus (mouse)	68	28 (41.8%)	0.000495	0.0162	KEGG
PI3K-Akt signaling pathway - Mus musculus (mouse)	356	107 (30.7%)	0.000509	0.0164	KEGG
Downregulation of SMAD2/3:SMAD4 transcriptional activity	23	13 (56.5%)	0.000546	0.0171	Reactome
Signaling by EGFR in Cancer	163	56 (34.6%)	0.000554	0.0171	Reactome
Transcriptional activity of SMAD2/SMAD3:SMAD4 heterotrimer	37	18 (48.6%)	0.000577	0.0173	Reactome
ErbB signaling pathway - Mus musculus (mouse)	87	34 (39.1%)	0.000584	0.0173	KEGG
Cocaine addiction - Mus musculus (mouse)	50	22 (44.9%)	0.000604	0.0176	KEGG
Focal adhesion - Mus musculus (mouse)	206	68 (33.0%)	0.000666	0.0191	KEGG
DAP12 signaling	147	51 (34.9%)	0.00073	0.0205	Reactome
Mitotic G2-G2/M phases	105	39 (37.1%)	0.000786	0.0206	Reactome
Axon guidance - Mus musculus (mouse)	129	46 (35.7%)	0.000789	0.0206	KEGG
Wnt signaling pathway - Mus musculus (mouse)	144	50 (35.0%)	0.000799	0.0206	KEGG
Signaling by ERBB2	144	50 (35.0%)	0.000799	0.0206	Reactome
Calcium signaling pathway - Mus musculus (mouse)	183	61 (33.5%)	0.000799	0.0206	KEGG
Regulation of Insulin Secretion by Glucagon-like Peptide-1	40	18 (47.4%)	0.000863	0.0219	Reactome
Regulation of PLK1 Activity at G2/M Transition	79	31 (39.2%)	0.000924	0.0228	Reactome
MAPK signaling pathway	158	54 (34.2%)	0.000934	0.0228	Wikipathways
SHC1 events in ERBB2 signaling	24	13 (54.2%)	0.000941	0.0228	Reactome
Glutamatergic synapse - Mus musculus (mouse)	115	41 (36.3%)	0.001	0.024	KEGG
Leukocyte transendothelial migration - Mus musculus (mouse)	121	43 (35.8%)	0.00103	0.0241	KEGG
G2/M Transition	103	38 (36.9%)	0.00106	0.0243	Reactome
Integrin alphaIIb beta3 signaling	27	14 (51.9%)	0.00106	0.0243	Reactome

Nucleotide Metabolism	19	11 (57.9%)	0.00113	0.0254	Wikipathways
Arrhythmogenic right ventricular cardiomyopathy (ARVC) - Mus musculus (mouse)	74	29 (39.2%)	0.00136	0.0299	KEGG
Hedgehog Signaling Pathway	22	12 (54.5%)	0.00137	0.0299	Wikipathways
Insulin Signaling	157	53 (33.8%)	0.00142	0.0307	Wikipathways
Senescence and Autophagy	98	36 (36.7%)	0.00154	0.0328	Wikipathways
Downregulation of ERBB2:ERBB3 signaling	12	8 (66.7%)	0.0016	0.0335	Reactome
Generic Transcription Pathway	123	43 (35.0%)	0.0018	0.0364	Reactome
p38 MAPK Signaling Pathway	34	16 (47.1%)	0.00181	0.0364	Wikipathways
Glycogen Metabolism	34	16 (47.1%)	0.00181	0.0364	Wikipathways
IL-6 signaling Pathway	99	36 (36.4%)	0.00189	0.0377	Wikipathways
Dilated cardiomyopathy - Mus musculus (mouse)	90	33 (37.1%)	0.00199	0.0391	KEGG
Cytoplasmic Ribosomal Proteins	79	30 (38.0%)	0.00204	0.0393	Wikipathways
Hemostasis	412	120 (29.2%)	0.00205	0.0393	Reactome
Post-translational protein modification	164	54 (33.1%)	0.00207	0.0393	Reactome
MASTL Facilitates Mitotic Progression	10	7 (70.0%)	0.00213	0.0395	Reactome
Role of DCC in regulating apoptosis	10	7 (70.0%)	0.00213	0.0395	Reactome
Long-term potentiation - Mus musculus (mouse)	66	26 (39.4%)	0.00217	0.0397	KEGG
Rap1 signalling	15	9 (60.0%)	0.00232	0.042	Reactome
Myometrial Relaxation and Contraction Pathways	157	52 (33.1%)	0.0025	0.0446	Wikipathways
G alpha (z) signalling events	29	14 (48.3%)	0.00256	0.0453	Reactome
Signalling to ERKs	35	16 (45.7%)	0.00262	0.0456	Reactome
Adrenoceptors	8	6 (75.0%)	0.00273	0.0456	Reactome
VEGF binds to VEGFR leading to receptor dimerization	8	6 (75.0%)	0.00273	0.0456	Reactome
Fc epsilon receptor (FCERI) signaling	155	51 (33.1%)	0.00274	0.0456	Reactome
Downstream signaling of activated FGFR	130	44 (34.1%)	0.00277	0.0456	Reactome
Kit Receptor Signaling Pathway	67	26 (38.8%)	0.00278	0.0456	Wikipathways
Transmission across Chemical Synapses	178	57 (32.4%)	0.00283	0.0456	Reactome
NCAM signaling for neurite out-growth	55	22 (40.7%)	0.00283	0.0456	Reactome
superoxide radicals degradation	4	4 (100.0%)	0.00284	0.0456	MouseCyc
Adipogenesis	133	45 (33.8%)	0.00298	0.047	Wikipathways
Id Signaling Pathway	51	21 (41.2%)	0.003	0.047	Wikipathways
Morphine addiction - Mus musculus (mouse)	93	33 (36.3%)	0.00301	0.047	KEGG
IL-4 signaling Pathway	61	24 (39.3%)	0.00322	0.0497	Wikipathways
heparan sulfate biosynthesis (late stages)	21	11 (52.4%)	0.00331	0.0505	MouseCyc
Role of LAT2/NTAL/LAB on calcium mobilization	96	34 (35.8%)	0.00336	0.0509	Reactome
IL-5 Signaling Pathway	68	26 (38.2%)	0.00353	0.0529	Wikipathways
Interleukin-2 signaling	39	17 (43.6%)	0.00362	0.0537	Reactome
B Cell Receptor Signaling Pathway	156	51 (32.7%)	0.00369	0.0543	Wikipathways
Gene Expression	720	192 (27.3%)	0.00389	0.0562	Reactome
Amyotrophic lateral sclerosis (ALS) - Mus musculus (mouse)	52	21 (40.4%)	0.00395	0.0562	KEGG
HTLV-I infection - Mus musculus (mouse)	285	82 (30.1%)	0.00396	0.0562	KEGG
Adaptive Immune System	457	127 (28.5%)	0.00406	0.0562	Reactome
Proteoglycans in cancer - Mus musculus (mouse)	229	70 (30.8%)	0.00408	0.0562	KEGG
Endocytosis - Mus musculus (mouse)	224	67 (31.0%)	0.0042	0.0562	KEGG
Signaling by Wnt	49	20 (40.8%)	0.00421	0.0562	Reactome
Regulation of KIT signaling	16	9 (56.2%)	0.00422	0.0562	Reactome
DAP12 interactions	158	51 (32.5%)	0.00426	0.0562	Reactome
TGF-beta Receptor Signaling Pathway	150	49 (32.7%)	0.00444	0.0562	Wikipathways
Melanogenesis - Mus musculus (mouse)	100	35 (35.0%)	0.00448	0.0562	KEGG
IL-2 Signaling Pathway	76	28 (36.8%)	0.00466	0.0562	Wikipathways
Regulation of Apoptosis	11	7 (63.6%)	0.00469	0.0562	Reactome
Mitotic M-M/G1 phases	202	63 (31.2%)	0.0047	0.0562	Reactome
Fcgamma receptor (FCGR) dependent phagocytosis	66	25 (37.9%)	0.00482	0.0562	Reactome
Signaling by TGF-beta Receptor Complex	66	25 (37.9%)	0.00482	0.0562	Reactome
SMAD4 MH2 Domain Mutants in Cancer	66	25 (37.9%)	0.00482	0.0562	Reactome
Loss of Function of SMAD4 in Cancer	66	25 (37.9%)	0.00482	0.0562	Reactome
SMAD2/3 Phosphorylation Motif Mutants in Cancer	66	25 (37.9%)	0.00482	0.0562	Reactome
SMAD2/3 MH2 Domain Mutants in Cancer	66	25 (37.9%)	0.00482	0.0562	Reactome
Loss of Function of SMAD2/3 in Cancer	66	25 (37.9%)	0.00482	0.0562	Reactome
TGFBR2 MSI Frameshift Mutants in Cancer	66	25 (37.9%)	0.00482	0.0562	Reactome
TGFBR2 Kinase Domain Mutants in Cancer	66	25 (37.9%)	0.00482	0.0562	Reactome
Loss of Function of TGFBR2 in Cancer	66	25 (37.9%)	0.00482	0.0562	Reactome
TGFBR1 LBD Mutants in Cancer	66	25 (37.9%)	0.00482	0.0562	Reactome
TGFBR1 KD Mutants in Cancer	66	25 (37.9%)	0.00482	0.0562	Reactome
Loss of Function of TGFBR1 in Cancer	66	25 (37.9%)	0.00482	0.0562	Reactome
Signaling by TGF-beta Receptor Complex in Cancer	66	25 (37.9%)	0.00482	0.0562	Reactome
SHC1 events in ERBB4 signaling	19	10 (52.6%)	0.00485	0.0562	Reactome
Circadian entrainment - Mus musculus (mouse)	99	34 (35.1%)	0.00491	0.0564	KEGG
TNF-alpha NF-kB Signaling Pathway	184	58 (31.5%)	0.00506	0.0575	Wikipathways
Chronic myeloid leukemia - Mus musculus (mouse)	74	27 (37.0%)	0.00508	0.0575	KEGG
Regulation of Actin Cytoskeleton	151	49 (32.5%)	0.00513	0.0575	Wikipathways
Regulation of actin dynamics for phagocytic cup formation	53	21 (39.6%)	0.00515	0.0575	Reactome
Cyclin A/B1 associated events during G2/M transition	22	11 (50.0%)	0.00525	0.0578	Reactome

Gastrin-CREB signalling pathway via PKC and MAPK	188	59 (31.4%)	0.00525	0.0578	Reactome
Oxidative Stress	28	13 (46.4%)	0.00552	0.0603	Wikipathways
VEGF signaling pathway - Mus musculus (mouse)	60	23 (38.3%)	0.00566	0.0615	KEGG
DCC mediated attractive signaling	14	8 (57.1%)	0.00617	0.0661	Reactome
Activation of Rac	14	8 (57.1%)	0.00617	0.0661	Reactome
Signaling by NOTCH	81	29 (35.8%)	0.00642	0.0683	Reactome
ADP signalling through P2Y purinoceptor 1	9	6 (66.7%)	0.00658	0.0695	Reactome
Toll Like Receptor 4 (TLR4) Cascade	106	36 (34.0%)	0.00689	0.0723	Reactome
FCERI mediated MAPK activation	38	16 (42.1%)	0.00705	0.0735	Reactome
Thrombin signalling through proteinase activated receptors (PARs)	17	9 (52.9%)	0.00715	0.074	Reactome
Glucagon signaling in metabolic regulation	37	15 (42.9%)	0.00739	0.0761	Reactome
RNA Polymerase I Transcription Termination	20	10 (50.0%)	0.00772	0.0785	Reactome
GnRH signaling pathway - Mus musculus (mouse)	89	31 (34.8%)	0.00778	0.0785	KEGG
GAB1 signalosome	90	31 (34.8%)	0.00778	0.0785	Reactome
Signaling by FGFR1 mutants	26	12 (46.2%)	0.00803	0.08	Reactome
EPO Receptor Signaling	26	12 (46.2%)	0.00803	0.08	Wikipathways
Tight junction - Mus musculus (mouse)	138	44 (32.4%)	0.00818	0.081	KEGG
G alpha (12/13) signalling events	55	21 (38.2%)	0.00843	0.0823	Reactome
Glycerolipid metabolism - Mus musculus (mouse)	56	21 (38.2%)	0.00843	0.0823	KEGG
Antigen processing: Ubiquitination & Proteasome degradation	129	42 (32.6%)	0.00854	0.0823	Reactome
Androgen Receptor Signaling Pathway	111	37 (33.3%)	0.00868	0.0823	Wikipathways
Signaling by NOTCH1	62	23 (37.1%)	0.00893	0.0823	Reactome
Signaling by NOTCH1 t(7;9)(NOTCH1:M1580_K2555) Translocation Mutant	62	23 (37.1%)	0.00893	0.0823	Reactome
Signaling by NOTCH1 HD Domain Mutants in Cancer	62	23 (37.1%)	0.00893	0.0823	Reactome
Signaling by NOTCH1 PEST Domain Mutants in Cancer	62	23 (37.1%)	0.00893	0.0823	Reactome
Signaling by NOTCH1 HD+PEST Domain Mutants in Cancer	62	23 (37.1%)	0.00893	0.0823	Reactome
FBXW7 Mutants and NOTCH1 in Cancer	62	23 (37.1%)	0.00893	0.0823	Reactome
Signaling by NOTCH1 in Cancer	62	23 (37.1%)	0.00893	0.0823	Reactome
AKT phosphorylates targets in the nucleus	7	5 (71.4%)	0.00899	0.0823	Reactome
CREB phosphorylation	7	5 (71.4%)	0.00899	0.0823	Reactome
NF-kappa B signaling pathway - Mus musculus (mouse)	103	33 (34.0%)	0.00915	0.0832	KEGG
APC/C-mediated degradation of cell cycle proteins	39	16 (41.0%)	0.00944	0.0849	Reactome
Regulation of mitotic cell cycle	39	16 (41.0%)	0.00944	0.0849	Reactome
Focal Adhesion	182	56 (30.8%)	0.00994	0.0889	Wikipathways

Pathway- Decreased Me FDR=5%	set size	candidates contained	p-value	q-value	pathway source
Wnt Signaling Pathway NetPath	109	35 (32.4%)	3.37E-06	0.00454	Wikipathways
ISG15 antiviral mechanism	25	13 (52.0%)	1.52E-05	0.00681	Reactome
Antiviral mechanism by IFN-stimulated genes	25	13 (52.0%)	1.52E-05	0.00681	Reactome
Rho GTPase cycle	118	35 (29.7%)	2.96E-05	0.007	Reactome
Signaling by Rho GTPases	118	35 (29.7%)	2.96E-05	0.007	Reactome
p75 NTR receptor-mediated signalling	87	28 (32.2%)	3.62E-05	0.007	Reactome
XPodNet - protein-protein interactions in the podocyte expanded by STRING	831	164 (19.8%)	3.64E-05	0.007	Wikipathways
eNOS activation	9	7 (77.8%)	4.39E-05	0.00738	Reactome
Hepatitis B - Mus musculus (mouse)	148	40 (27.4%)	6.23E-05	0.00862	KEGG
Hippo signaling pathway - Mus musculus (mouse)	156	42 (26.9%)	6.41E-05	0.00862	KEGG
G Protein Signaling Pathways	91	28 (30.8%)	8.90E-05	0.0109	Wikipathways
Signalling by NGF	275	64 (23.4%)	0.000115	0.0117	Reactome
eNOS activation and regulation	19	10 (52.6%)	0.000133	0.0117	Reactome
Metabolism of nitric oxide	19	10 (52.6%)	0.000133	0.0117	Reactome
Exercise-induced Circadian Regulation	49	18 (36.7%)	0.000135	0.0117	Wikipathways
B Cell Receptor Signaling Pathway	156	41 (26.3%)	0.000139	0.0117	Wikipathways
Activation of Kainate Receptors upon glutamate binding	16	9 (56.2%)	0.000149	0.0118	Reactome
TNF-alpha NF-kB Signaling Pathway	184	46 (25.0%)	0.000202	0.0151	Wikipathways
Membrane Trafficking	148	38 (26.2%)	0.000256	0.0181	Reactome
Apoptosis	83	25 (30.1%)	0.000301	0.0187	Wikipathways
Activation of Ca-permeable Kainate Receptor	11	7 (63.6%)	0.000305	0.0187	Reactome
Ionotropic activity of Kainate Receptors	11	7 (63.6%)	0.000305	0.0187	Reactome
Myometrial Relaxation and Contraction Pathways	157	40 (25.5%)	0.000337	0.0197	Wikipathways
RIG-I/MDA5 mediated induction of IFN-alpha/beta pathways	45	16 (35.6%)	0.000482	0.027	Reactome
Pathways in cancer - Mus musculus (mouse)	326	70 (21.7%)	0.000591	0.0318	KEGG
Colorectal cancer - Mus musculus (mouse)	64	20 (31.2%)	0.000699	0.0361	KEGG
Pentose phosphate pathway - Mus musculus (mouse)	30	12 (40.0%)	0.000725	0.0361	KEGG
Wnt signaling pathway - Mus musculus (mouse)	144	36 (25.2%)	0.000829	0.0399	KEGG
Huntington,s disease - Mus musculus (mouse)	189	42 (24.0%)	0.00092	0.0418	KEGG
Trafficking of AMPA receptors	27	11 (40.7%)	0.001	0.0418	Reactome
Glutamate Binding, Activation of AMPA Receptors and Synaptic Plasticity	27	11 (40.7%)	0.001	0.0418	Reactome
Viral carcinogenesis - Mus musculus (mouse)	236	51 (22.8%)	0.00101	0.0418	KEGG
Antigen Activates B Cell Receptor Leading to Generation of Second Messengers	31	12 (38.7%)	0.00102	0.0418	Reactome
Pancreatic cancer - Mus musculus (mouse)	67	20 (30.3%)	0.00108	0.0427	KEGG
Phosphatidylinositol signaling system - Mus musculus (mouse)	81	23 (28.4%)	0.00128	0.0491	KEGG
Dopaminergic synapse - Mus musculus (mouse)	135	33 (25.2%)	0.00132	0.0495	KEGG

Bacterial invasion of epithelial cells - Mus musculus (mouse)	77	22 (28.6%)	0.00147	0.053	KEGG
Apoptosis - Mus musculus (mouse)	82	23 (28.0%)	0.00153	0.053	KEGG
G-protein mediated events	45	15 (33.3%)	0.00154	0.053	Reactome
Protein processing in endoplasmic reticulum - Mus musculus (mouse)	169	40 (23.7%)	0.00159	0.0535	KEGG
Oxidative Damage	17	8 (47.1%)	0.00164	0.054	Wikipathways
Toxoplasmosis - Mus musculus (mouse)	113	29 (25.7%)	0.00186	0.0577	KEGG
Estrogen signaling pathway - Mus musculus (mouse)	99	26 (26.5%)	0.00189	0.0577	KEGG
Lysosome Vesicle Biogenesis	23	9 (42.9%)	0.0019	0.0577	Reactome
Inositol phosphate metabolism	46	15 (32.6%)	0.00197	0.0577	Reactome
NRAGE signals death through JNK	46	15 (32.6%)	0.00197	0.0577	Reactome
Calcium Regulation in the Cardiac Cell	150	36 (24.0%)	0.00206	0.059	Wikipathways
NOSTRIN mediated eNOS trafficking	5	4 (80.0%)	0.00216	0.0606	Reactome
Cell death signalling via NRAGE, NRIF and NADE	65	19 (29.2%)	0.00227	0.0623	Reactome
Proteoglycans in cancer - Mus musculus (mouse)	229	50 (22.0%)	0.00238	0.0642	KEGG
Recruitment of NuMA to mitotic centrosomes	11	6 (54.5%)	0.00255	0.0657	Reactome
Apoptosis Modulation by HSP70	18	8 (44.4%)	0.00258	0.0657	Wikipathways
EGFR interacts with phospholipase C-gamma	34	12 (35.3%)	0.00259	0.0657	Reactome
mRNA Processing	163	38 (23.3%)	0.00273	0.066	Reactome
ZBP1(DAI) mediated induction of type I IFNs	31	11 (36.7%)	0.00274	0.066	Reactome
Opioid Signalling	66	19 (28.8%)	0.00275	0.066	Reactome
Cellular Senescence	111	28 (25.2%)	0.0029	0.0684	Reactome
Cytosolic sensors of pathogen-associated DNA	58	17 (29.8%)	0.003	0.0695	Reactome
Intrinsic Pathway for Apoptosis	39	13 (33.3%)	0.00311	0.0706	Reactome
Diurnally Regulated Genes with Circadian Orthologs	48	15 (31.2%)	0.00315	0.0706	Wikipathways
PodNet- protein-protein interactions in the podocyte	315	65 (20.6%)	0.00326	0.0717	Wikipathways
glutathione biosynthesis	3	3 (100.0%)	0.0033	0.0717	MouseCyc
PLCG1 events in ERBB2 signaling	35	12 (34.3%)	0.00341	0.0723	Reactome
Glycogen breakdown (glycogenolysis)	15	7 (46.7%)	0.00344	0.0723	Reactome
PLC beta mediated events	44	14 (31.8%)	0.00355	0.0736	Reactome
Glutathione and one carbon metabolism	31	11 (35.5%)	0.00369	0.0752	Wikipathways
Glutathione metabolism	19	8 (42.1%)	0.00387	0.0765	Wikipathways
Synthesis of IP3 and IP4 in the cytosol	27	10 (37.0%)	0.0039	0.0765	Reactome
One carbon metabolism and related pathways	49	15 (30.6%)	0.00392	0.0765	Wikipathways
Regulation of actin cytoskeleton - Mus musculus (mouse)	218	47 (21.8%)	0.00406	0.0781	KEGG
Phospholipase C-mediated cascade	54	16 (29.6%)	0.00422	0.08	Reactome
Tetrahydrobiopterin (BH4) synthesis, recycling, salvage and regulation	12	6 (50.0%)	0.00445	0.0833	Reactome
Primary Focal Segmental Glomerulosclerosis FSGS	71	19 (27.5%)	0.00473	0.0872	Wikipathways
DAG and IP3 signaling	32	11 (34.4%)	0.00487	0.0887	Reactome
Neuronal System	254	53 (21.0%)	0.005	0.0897	Reactome
Gene Expression	720	129 (18.3%)	0.00537	0.095	Reactome
Elevation of cytosolic Ca2+ levels	9	5 (55.6%)	0.00544	0.095	Reactome
Small cell lung cancer - Mus musculus (mouse)	86	22 (25.9%)	0.00561	0.0962	KEGG
Glutathione synthesis and recycling	6	4 (66.7%)	0.00572	0.0962	Reactome
Cam-PDE 1 activation	6	4 (66.7%)	0.00572	0.0962	Reactome
Cellular responses to stress	127	30 (23.6%)	0.00593	0.0985	Reactome
Apoptosis	101	25 (24.8%)	0.00613	0.101	Reactome
Processing of Capped Intron-Containing Pre-mRNA	144	33 (22.9%)	0.00658	0.104	Reactome
mRNA Splicing - Major Pathway	112	27 (24.1%)	0.00659	0.104	Reactome
mRNA Splicing	112	27 (24.1%)	0.00659	0.104	Reactome
PluriNetWork	291	59 (20.3%)	0.00672	0.104	Wikipathways
Alzheimer,s disease - Mus musculus (mouse)	181	37 (22.3%)	0.00673	0.104	KEGG
FAS pathway and Stress induction of HSP regulation	38	12 (31.6%)	0.00721	0.11	Wikipathways
TRAF3-dependent IRF activation pathway	13	6 (46.2%)	0.00724	0.11	Reactome
DARPP-32 events	25	9 (36.0%)	0.00755	0.112	Reactome
Synaptic vesicle cycle - Mus musculus (mouse)	62	17 (27.4%)	0.00765	0.112	KEGG
mTOR signaling pathway - Mus musculus (mouse)	62	17 (27.4%)	0.00765	0.112	KEGG
Regulation of Actin Cytoskeleton	151	34 (22.5%)	0.00778	0.112	Wikipathways
TRAF6 mediated IRF7 activation	17	7 (41.2%)	0.00792	0.112	Reactome
Laminin interactions	21	8 (38.1%)	0.00792	0.112	Reactome
PLC-gamma1 signalling	34	11 (32.4%)	0.00814	0.114	Reactome
Integrin-mediated Cell Adhesion	98	24 (24.5%)	0.00821	0.114	Wikipathways
TNF signaling pathway - Mus musculus (mouse)	111	26 (23.9%)	0.00874	0.118	KEGG
MicroRNAs in Cardiomyocyte Hypertrophy	83	21 (25.3%)	0.00882	0.118	Wikipathways
Hepatitis C - Mus musculus (mouse)	136	31 (22.8%)	0.00895	0.118	KEGG
Clathrin derived vesicle budding	61	16 (27.6%)	0.00895	0.118	Reactome
trans-Golgi Network Vesicle Budding	61	16 (27.6%)	0.00895	0.118	Reactome
Spliceosome - Mus musculus (mouse)	137	30 (22.9%)	0.00936	0.122	KEGG
ESC Pluripotency Pathways	110	26 (23.6%)	0.00987	0.125	Wikipathways
TRIF-mediated TLR3/TLR4 signaling	89	22 (24.7%)	0.00991	0.125	Reactome
MyD88-independent cascade	89	22 (24.7%)	0.00991	0.125	Reactome
Toll Like Receptor 3 (TLR3) Cascade	89	22 (24.7%)	0.00991	0.125	Reactome

Supplementary Table 5: Patient information of human liver samples

Xenotech ID	Group	% Macro Fat	AGE	Gender	Ethnicity	BMI	Alcohol Use
H1299	Control 1	0	17	F	Caucasian	20.6	Occasional
H1283	Control 2	0	64	F	Caucasian	29.1	Occasional
H1336	Control 3	0	60	F	African American	24.1	Occasional
H1262	Control 4	0	26	M	Caucasian	22.9	Occasional
H1290	Control 5	0	51	M	Hispanic	30	Occasional
H1307	Control 6	0	50	M	Asian	26.4	No
H1288	Control 7	0	59	F	Caucasian	31.4	Occasional
H1235	Steatosis 1	30-40	38	M	Caucasian	31.9	Occasional
H1237	Steatosis 2	20	58	M	Caucasian	32.09	Occasional
H1243	Steatosis 3	75	41	M	Caucasian	23.5	Heavy
H1278	Steatosis 4	20	41	M	Caucasian	32	No
H0820	Steatosis 5	60	65	F	Caucasian	49.9	No
H0851	Steatosis 6	50	47	F	Caucasian	47.4	No
H1082	Steatosis 7	40	66	F	Caucasian	24	No
H0818	Steatosis 8	40	48	M	Hispanic	32.5	No

Supplementary Table 6: Clinical characteristics of the Kuopio Obesity Surgery (KOBS) study

	KOBS n=170
Male/Female	37/133
Age (years)	48.06 ± 9.23
BMI	41.80 ± 4.59
Glucose (mmol/l)	6.07 ± 1.42
Insulin (pmol/l)	113.04 ± 65.73
Cholesterol (mmol/l)	4.29 ± 0.91
HDL cholesterol (mmol/l)	1.21 ± 0.31
LDL cholesterol (mmol/l)	2.47 ± 0.82
Triglycerides (mmol/l)	1.39 ± 0.69
Type 2 diabetes (%)	22.35 %
Histology (normal / simple steatosis / NASH)	106/36/28

Mouse Primers RT-PCR	Forward	Reverse
β-actin	CGTGAAAAGATGACCCAGATCA	CACAGCCTGGATGGCTACGT
Pparα	GTACCACTACGGAGTTCACGCAT	CGCCGAAAGAAGCCCTTAC
Pgc-1α	GAGAATGAGGCAAACTTGCTAGCG	TGCATGGTTCTGAGTGCTAAGACC
Pparγ	TGGCCACCTCTTTGCTCTGCTC	AGGCCGAGAAGGAGAAGCTGTTG
Srebp1c	ACGACGGAGCCATGGATTGCAC	CCGGAAGGCAGGCTTGAGTACC
Fas	TGCAACTGTGCGTTAGCCACC	TGTTTCAGGGGAGAAGAGACC
Acc	GACAGACTGATCGCAGAGAAAG	TGGAGAGCCCCACACACA
Glut2	GGCTAATTTCAGGACTGGTT	TTTCTTTGCCCTGACTTCCT
Pepck1	GTGGGAGTGACACCTCACAGC	AGGACAGGGCTGGCCGGGACG
mG6pd	ATGAACATTCTCCATGACTTTGGG	GACAGGGAACTGCTTTATTATAGG
Aldob	AGCCTTCTGAGAAGGATGCTC	GTCCAGCATGAAGCAGTTGAC
Gys	ACTGCTTGGGCGTTATCTCTGTG	ATGCCCGCTCCATGCGTA
C/EBPα	TGGACAAGAACAGCAACGAG	TCACTGGTCAACTCCAGCAC
Scd1	AGATCTCCAGTTCTTACACGACCAC	GTGGACCTTCTTCTGTAGGCAG
ChREBP	CTGGGGACCTAAACAGGAGC	GAAGCCACCCTATAGCTCCC
aP2	CACCGCAGACGACAGGAAG	GCACCTGCACCAGGGC
Mcp1	AGCACCAGCCAACTCTCAC	TCTGGACCCATTCCTTCTTG
Nrep	GGTGTCGGTACTTTGTTTCCTGG	CTCACACTCTTGGTAGCATCCAC
Nmrk1	AGAGCTTGCAGAAGCACCTTCC	CATCCAACAGGAAACTGCTGACA
Vhl	GTTTGTGCCATCCCTCAATGTCG	ACCTGACGATGTCCAGTCTCCT
Ankrd9	GCAGTGGCTTTACACCATTGGAG	TCCTCAGACGAAGTGGTGTTGG
Homer2	TCCAGGAGGTAAGAGAAGCTGC	GTCTGTGCCATTGACGCTGGAT
Ppp1r3g	CTTTCACGGAGTGGCGTACCTT	AGGCACAGCGAGAAGTGGAAAC
Igfbp1	GCCCAACAGAAAGCAGGAGATG	GTAGACACACCAGCAGAGTCCA
Egr1	AGCGAACAACCCTATGAGCACC	ATGGGAGGCAACCGAGTCGTTT
Gdf15	AGCCGAGAGGACTCGAACTCAG	GGTTGACGCGGAGTAGCAGCT
Nr4a1	GTGCAGTCTGTGGTGACAATGC	CAGGCAGATGTACTTGGCGCTT
Syne1	CAGCCATTCAGTGTGAGCAGCT	CACCATCCAGACCTCTAAGGCT
Cpeb2	GAGATCACTGCCAGCTTCCGAA	CAATGAGTGCCTGGACTGAGCT
Trib3	CTGCGTCGCTTTGTCTTCAGCA	CTGAGTATCTCTGGTCCCACGT
Spon2	CGACAGTGGTTTCACCTTCTCC	AGGACTTGAGGCGTGGGTAGTA
Serpine1	CCTCTTCCACAAGTCTGATGGC	GCAGTTCCACAACGTCATACTCG
Frmd4b	CAGTTCATGGACACCAGGCATTC	TGCTGTAGGCATTCCGAGTCAG

Chapter IV

Insulin receptor-mediated signaling regulates pluripotency markers and lineage differentiation

Chapter IV

Insulin receptor-mediated signaling regulates pluripotency markers and lineage differentiation

3.1 Contribution

I contributed to a main body of work presented here. I was responsible for culturing of stem cells, assessing gene and protein expression, experiments related to teratoma formation *in vivo* in mice, performing differentiation, analyzing phosphoproteomics data and writing.

3.2 Publication

This work resulted in a co-first author publication reprinted in full:

Gupta, MK*, De Jesus DF*, Kahraman S, Valdez IA, Shamsi F, Yi L, Swensen, AC, Tseng, YH, Qian, WJ, Kulkarni RN. Insulin receptor-mediated signaling regulates pluripotency markers and lineage differentiation. Molecular Metabolism. doi:org/10.1016/j.molmet.2018.09.003, 2018.

Brief Communication

MOLECULAR METABOLISM

Insulin receptor-mediated signaling regulates pluripotency markers and lineage differentiation

Manoj K. Gupta [1,5], Dario F. De Jesus [1,2,5], Sevim Kahraman [1], Ivan A. Valdez [1], Farnaz Shamsi [3], Lian Yi [4], Adam C. Swensen [4], Yu-Hua Tseng [3], Wei-Jun Qian [4], Rohit N. Kulkarni [1,*]

ABSTRACT

Objectives: Insulin receptor (IR)-mediated signaling is involved in the regulation of pluripotent stem cells; however, its direct effects on regulating the maintenance of pluripotency and lineage development are not fully understood. The main objective of this study is to understand the role of IR signaling in pluripotency and lineage development.

Methods: To explore the role of IR signaling, we generated IR knock-out (IRKO) mouse induced pluripotent stem cells (miPSCs) from E14.5 mouse embryonic fibroblasts (MEFs) of global IRKO mice using a cocktail of four reprogramming factors: Oct4, Sox2, Klf4, cMyc. We performed pluripotency characterization and directed the differentiation of control and IRKO iPSCs into neural progenitors (ectoderm), adipocyte progenitors (mesoderm), and pancreatic beta-like cells (endoderm). We mechanistically confirmed these findings via phosphoproteomics analyses of control and IRKO iPSCs.

Results: Interestingly, expression of pluripotency markers including *Klf4*, *Lin28a*, *Tbx3*, and *cMyc* were upregulated, while abundance of Oct4 and Nanog were enhanced by 4-fold and 3-fold, respectively, in IRKO iPSCs. Analyses of signaling pathways demonstrated downregulation of phospho-STAT3, p-mTor and p-Erk and an increase in the total mTor and Erk proteins in IRKO iPSCs in the basal unstimulated state. Stimulation with leukemia inhibitory factor (LIF) showed a ~33% decrease of phospho-ERK in IRKO iPSCs. On the contrary, Erk phosphorylation was increased during *in vitro* spontaneous differentiation of iPSCs lacking IRs. Lineage-specific directed differentiation of the iPSCs revealed that cells lacking IR showed enhanced expression of neuronal lineage markers (*Pax6, Tubb3, Ascl1 and Oligo2*) while exhibiting a decrease in adipocyte (*Fas, Acc, Pparγ, Fabp4, C/ebpα, and Fsp27*) and pancreatic beta cell markers (*Ngn3, Isl1, and Sox9*). Further molecular characterization by phosphoproteomics confirmed the novel IR-mediated regulation of the global pluripotency network including several key proteins involved in diverse aspects of growth and embryonic development.

Conclusion: We report, for the first time to our knowledge, the phosphoproteome of insulin, IGF1, and LIF stimulation in mouse iPSCs to reveal the importance of insulin receptor signaling for the maintenance of pluripotency and lineage determination.

Keywords Insulin receptor signaling; Pluripotency; Lineage differentiation; Adipocyte; Beta cells; Neurons; Stem cells; Phosphoproteomics; Reprogramming

1. INTRODUCTION

The insulin/insulin-like growth factor (IGF) family regulates the pre- and post-natal development and maintenance of optimum metabolic functioning of virtually all mammalian cells [1–5]. Previous studies demonstrated the importance of IGFII/IGF1R and ERBB2 receptor signaling in the maintenance of self-renewal of human embryonic stem cells (ESCs) [6,7]. During lineage differentiation of human pluripotent stem cells, insulin has been shown to interact with Wnt/beta-catenin pathways redirecting mesoderm and endoderm towards neuroectoderm while inhibiting cardiac mesoderm [8,9]. Reprogramming of somatic cells into pluripotent stem cells was also demonstrated to be negatively regulated by insulin growth factor pathways [10]. In mouse ESCs, the PI3K/Akt signaling pathway promotes self-renewal via IGF1R, and, while IGF signaling regulates embryonic cardiac proliferation, insulin signaling plays a role in development and metanephrogenesis [8,11–15]. Finally, IGFs have been reported to regulate vasculogenesis in pluripotent stem cells by predisposing their differentiation into mesodermal lineages [16].

In this study, we explored the direct role of insulin receptor-mediated signaling in pluripotency maintenance and in lineage development by reprogramming insulin receptor global knockout (IRKO) mouse

[1]Islet Cell and Regenerative Biology, Joslin Diabetes Center, Department of Medicine, Brigham and Women's Hospital, Harvard Stem Cell Institute, Harvard Medical School, Boston, MA 02215, USA [2]Graduate Program in Areas of Basic and Applied Biology (GABBA), Abel Salazar Biomedical Sciences Institute, University of Porto, 5000 Porto, Portugal [3]Section of Integrative Physiology and Metabolism, Joslin Diabetes Center, Harvard Medical School, Boston, MA 02215, USA [4]Biological Sciences Division, Pacific Northwest National Laboratory, Richland, WA 99352, USA

[5] These authors contributed equally to this work.

*Corresponding author. Islet Cell and Regenerative Biology, Joslin Diabetes Center, One Joslin Place, Boston, MA 02215, USA. Fax: +1 617 309 3476. E-mail: rohit.kulkarni@joslin.harvard.edu (R.N. Kulkarni).

Received July 6, 2018 • Revision received September 7, 2018 • Accepted September 11, 2018 • Available online 19 September 2018

https://doi.org/10.1016/j.molmet.2018.09.003

embryonic fibroblasts into iPSCs [17]. IRKO iPSCs demonstrated upregulation of pluripotency markers including Oct4 and Nanog. Simultaneously, key signaling pathways including Stat3/mTor/Erk were downregulated in the basal state while Erk signaling was upregulated during spontaneous differentiation into embryoid bodies. Directed differentiation analysis revealed that neuronal markers (ectoderm) were upregulated while adipocyte (mesoderm) and pancreatic beta-cell (endoderm) differentiation markers were downregulated in IRKOs. Finally, unbiased phosphoproteomics analyses revealed an involvement of insulin signaling in pluripotency, growth and development. Together, these studies underscore the importance of insulin-mediated signaling for maintenance of pluripotency and lineage development.

2. MATERIAL AND METHODS

2.1. Mice and mouse embryonic fibroblasts (MEFs)

All studies involving mice were approved by the Institutional Review Board of the Joslin Diabetes Center and were in accordance with National Institute of Health (NIH) guidelines. Embryonic day 14.5 wild type control and insulin receptor (IR) knockout (IRKO) MEFs were derived from breeding IR heterozygous mice (Jackson Laboratory Inc.). All fibroblasts were maintained up to a maximum passage ~#10 in Dulbecco Modified Eagle's Media (DMEM) supplemented with Glutamax, 10% Fetal Bovine Serum (FBS), and 1% non-essential amino acids.

2.2. Lentiviral-mediated reprogramming and iPSC generation and characterization

Generation of mouse iPSCs involved infection of primary MEFs with mouse STEMCCA lentivirus vector expressing the reprogramming factors *Oct4, Sox2, Klf4*, and *cMyc.* iPSC characterization involved teratoma formation, H&E staining, and immunostaining for the three lineage markers performed according to previous reports [18–20]. Briefly, MEFs (5×10^4) were plated in six well plates and virally transduced with the lentiviral particles in the presence of 5 μg/ml Polybrene® (EMD Millipore) after 8–24 h. The fibroblasts were washed three times with PBS and fed fresh 15% mouse embryonic stem cell (ESC) media supplemented with leukemia inhibitory factor (LIF) (EMD millipore). On days 7–14, ESC-like colonies were individually picked, cultured, expanded, frozen and subsequently characterized in a 2i-media feeder-free system for pluripotency markers. Sex determination of iPSCs was performed by using primers RO5 and RO3 which exclusively amplify sex-determining region of the 326 base pair of Chr Y (Sry). IRS1 amplification of the 480 base pair was used as internal control.

2.3. Gene expression analyses using quantitative RT-PCR and western immunoblotting

RNA extraction was performed using standard Trizol reagent (Invitrogen) according to the manufacturer's instructions; the resultant aqueous phase was mixed (1:1) with 70% RNA-free ethanol and added to Qiagen Rneasy mini kit columns (Qiagen), and the manufacturer's protocol was followed. RNA quality and quantity were analyzed using Nanodrop 1000. One microgram of RNA was used for reserve transcription step using the high-capacity cDNA synthesis kit (Applied Biosciences) according to manufacturer instructions. cDNA was analyzed using the ABI 7900HT system (Applied Biosciences), and gene expression was calculated using the ΔΔCt method. Each RT-PCR was run in triplicate samples, and data was normalized to β-actin according to previous reports [21]. In parallel experiments, total cellular proteins were harvested using M-PER mammalian protein extraction reagent (Thermo Scientific) followed by western immunoblotting of proteins including Oct4 (Santa Cruz #Bio.sc-5279), Nanog (Cell Signaling, #8785s), Stat3 (Santa Cruz Bio. #sc-482), β-actin (Santa Cruz Bio. #sc-1616), pStat3 (Cell Signaling, #9145s), IR-β (Cell Signaling, #3025s), IGF1R-β (Cell Signaling, #9750s), pErk1/2 (Cell Signaling, #9101s), Erk1/2 (Cell Signaling, #9102s), pmTor (Cell Signaling, #5536s), mTor (Cell Signaling, #2972s), pMek (Cell Signaling, #9121s), Mek (Cell Signaling, #9122s), pIRS-1 (Cell Signaling, #2381s), IRS-1 (Cell Signaling, #2390s), PI3K85 (Millipore, # 06-496), PDK1 (Cell Signaling, #3062s), α-tubulin (Abcam, #ab7291). The blots were developed using chemiluminescent substrate (ECL, ThermoFisher, MA).

2.4. Embryoid body formation

Control and IRKO iPSCs grown in a 2i system were collected using accutase (Invitrogen), and two million control or IRKO iPSCs were seeded in 10 cm petri-dishes containing high glucose DMEM supplemented with 20% FBS without LIF. Media were replaced every 24h, and cells started to form EBs at day 2 of differentiation. On days 5 and 10, EBs were harvested for transcript and signaling analyses.

2.5. Neuronal differentiation

Control and IRKO iPSCs grown in a 2i system were collected using accutase (Invitrogen). Fifty thousand control and IRKO iPSCs were plated into gelatin-coated 6-well plates and treated with differentiation media and followed for 10 days in Ndiff 227® media (Clontech) [22]. Cells were harvested on day 10 for transcript analyses of neuronal markers.

2.6. Adipocyte differentiation

Control and IRKO iPSCs were differentiated into adipocytes using a slightly modified protocol from Cuaranta-Monroy et al. [23]. The protocol allows iPSCs to differentiate into adipocytes in 27 days in response to a combination of cocktails at various steps (Fig. S3C). The adipocytes were subjected to oil-red O staining for confirmation of lipid droplets. Furthermore, total RNA was isolated for transcript analyses of adipocyte markers. We used a spontaneous method of EB production rather than the hanging drop method to enable a larger yield of EBs.

2.7. Pancreatic beta cell differentiation

Control and IRKO iPSCs were differentiated into pancreatic beta-like cells using a protocol from Szu-Hsui Liu et al. [24]. Pancreatic beta-like cells were obtained on day 8. Total RNA was isolated from day 8 differentiated cells for transcript analyses of beta cell developmental markers. The differentiated beta-like cells were immunostained for chromogranin A (ab15160, abcam) and Ngn3 (F25A1B3, Developmental studies Hybridoma Bank, DSHB) proteins.

2.8. Phosphoproteomics

2.8.1. Phosphoproteomics – Phosphopeptide enrichment

Control and IRKO iPSCs (n = 3/group) were pelleted, washed with cold PBS, and lysed with ice-cold lysis buffer (8 M urea, 50 mM Tris pH 8.0, 1 mM ethylenediaminetetraacetic acid (EDTA)), 10 mM NaF, 1:100 phosphatase inhibitors (Sigma)). Proteins were reduced and alkylated with 5 mM dithiothreitol (DTT) and 10 mM iodoacetamide followed by trypsin (Promega) digestion for 3 h at 37 °C.

Peptides were subjected to clean-up via a C18 solid phase extraction column (SepPak). Phosphopeptides were enriched using Fe3+-NTA Agarose Beads (Qiagen) as previously described [25]. Enriched phosphopeptides were lyophilized and stored at −80 °C until analyses.

2.8.2. Global liquid chromatography tandem-mass spectrometry

Phosphopeptide samples were dissolved in 2% acetonitrile and 0.1% formic acid immediately before being injected onto a liquid chromatography-mass spectrometry (LC-MS) system consisting of a nanoACQUITY UPLC® system with a 75 μm × 20 cm C18 LC column and an Orbitrap Q-Exactive HF mass spectrometer (Thermo). A 110-minute gradient was applied for LC separation. The MS was operated at a resolution of 60,000 for MS scans and 30,000 for HCD MS/MS scans.

2.8.3. Phosphoproteomics data analysis

Data were analyzed at the peptide level using MaxQuant software (version 1.5.3.30) using match between runs with a false discovery rate of 0.01. We filtered out phosphosites that had missing values in more than 80% of samples, imputed missing values with half of the minimum intensity of the phosphosites, and normalized all samples to have the same median intensity followed by $\log_2$-transformation. Since principal component analysis showed sample heterogeneity, we accounted for batch effects and estimated weights per sample using an unbiased algorithm that assesses how well each sample's intensity matches those of its group [26]. We compared phosphosite intensities between groups with the linear modeling package limma [27]. We also used limma to plot Venn diagrams of significant phosphosites. We plotted the heat map with the heatmap.2 function from the gplots package. We compared pathways using the limma package roast method [28]. Pathway barplots were plotted with the ggplot2 package [29]. Bioinformatics analysis was done using R software [30].

3. RESULTS

3.1. Loss of insulin receptor (IR) in pluripotent stem cells upregulates pluripotency network

We generated control and IRKO MEFs from day 14.5 mouse embryos of mixed genders and reprogrammed them into iPSCs using the STEMCCA plasmid (Figure S1A,B) [18]. Real-time PCR and western blot analysis confirmed almost complete absence of IR in IRKO iPSCs, while expression of IGF1R remained unchanged compared to control iPSCs (Figure 1A,B). Cell counting analyses and Ki67-staining of control and IRKO iPSCs by flow cytometry showed similar proliferation profiles and did not reveal differences between groups (Figure S1C,D). Both groups of iPSCs were morphologically similar, as shown by bright field images and alkaline phosphatase staining (Figure S1E, F). Transcript expression of pluripotency markers including *Klf4*, *Lin28a*, *Tbx3*, and *c-Myc* were upregulated in IRKO iPSCs (Figure 1C). Western blot and immunohistochemistry demonstrated upregulation of Oct4 and Nanog proteins, while flow cytometry showed upregulated SSEA-1, a surface pluripotency marker, in IRKO iPSCs (Figure 1D,E and S1G). Interestingly, IRKO iPSCs presented a molecular memory of increased stemness with increased *Oct4*, *Sox2*, and *Klf4* mRNA after removal of LIF for 24 h (Figure 1F). Western blot for Oct4 and Nanog proteins showed abundance of their expression in IRKO iPSCs (Figure 1G,H). Injection of control and IRKO iPSCs into NOD SCID mice led to formation of similar sized teratomas indicating an ability to differentiate into the three lineages (Figure S1H,I and J). Interestingly, we observed significant downregulation of IGF1R in differentiating IRKO iPSCs in the absence of LIF for 24 h indicating a link between IR and IGF1R during differentiation (Figure S1K and L). These data suggest an association between loss of IR with enhanced stemness in the pluripotent stage and that IR removal is associated with a decrease in IGF1R expression during differentiation of iPSCs.

3.2. Insulin receptor ablation impacts key pluripotency pathways

To explore the crosstalk between proteins in the insulin signaling and pluripotency pathways, we examined iPSCs in the basal (unstimulated) versus stimulated states. In the unstimulated state, phosphorylation of Stat3 (y705), mTor (s2448), and Erk (thr202/y204) proteins were significantly decreased while total mTor and Erk proteins were upregulated in IRKO iPSCs (Figure 2A,B). Among other proteins in the insulin signaling cascade, IRS1 and the 85 kDa subunit of PI3K were not significantly altered while PDK1 was upregulated in IRKO iPSCs (Figure S2A,B). Next, we starved iPSCs overnight followed by stimulation with insulin (100 nM), IGF1 (100 nM) or LIF (100 units/ml) for 15 min. As expected, the phosphorylation of Akt was virtually absent or significantly reduced after insulin or IGF1 stimulation in IRKO iPSCs (Figure 2C,D).

3.3. Erk pathway is upregulated during differentiation of IRKO iPSCs

To examine the relevance of insulin signaling in differentiation, we undertook *in vitro* experiments to generate embryoid bodies (EBs) from control and IRKO iPSCs. Morphological evaluation on day 10 revealed larger EBs differentiating from IRKO iPSCs (Figure 2E,F). Furthermore, western blot analyses of unstimulated day 10 EBs revealed significant upregulation of phospho-Erk in the IRKO group. The phosphorylation of Mek was also upregulated in IRKOs but did not reach statistical significance (Figure 2G,H). Overnight starved day 10 EBs continued to exhibit significantly elevated phospho-Erk. Upon stimulation with insulin (100 nM) a significant increase in p-Akt, p-Erk and p-Stat3 was evident in both groups, but no significant differences were observed between groups (Figure S2C and D).

3.4. iPSCs lacking IR exhibit enhanced expression of neuronal differentiation markers

We next undertook differentiation of the iPSCs to generate tissues from the three germ layers. To investigate the role of insulin signaling in tissues originating from the ectoderm, we directed their differentiation towards the neuronal lineage (Figure S3A, B). While the neuronal progenitor marker (Tubb3) was evident on day 10 of differentiation in both groups (Figure 3A), we observed relatively prominent neural rosettes and enhanced intensity of class III tubulin neurons in the IRKO-iPSCs compared to control iPSCs (Figure 3A). Consistently, transcript levels of multiple neuronal markers including *Pax6*, *Tubb3*, *Ascl1*, and *Oligo2* were significantly upregulated in neuronal progenitors differentiated from IRKO iPSCs as compared to controls, indicating their role in neurogenesis (Figure 3B). These results indicate that lack of IR mediated signaling prompts mouse iPSCs to differentiate towards the ectodermal lineage differentiation.

3.5. Absence of IR in iPSCs limits differentiation towards adipocytes and pancreatic beta cells

Next, we chose to direct the differentiation of the iPSCs towards the mesodermal lineage to address the significance of insulin signaling in adipogenesis. The iPSCs were differentiated into pre-adipocytes over 27 days using a modified protocol from Curanat-Monroy et al. [23] (Figure S3C). Morphological analyses of differentiated adipocytes at

MOLECULAR METABOLISM 18 (2018) 153–163

www.molecularmetabolism.com

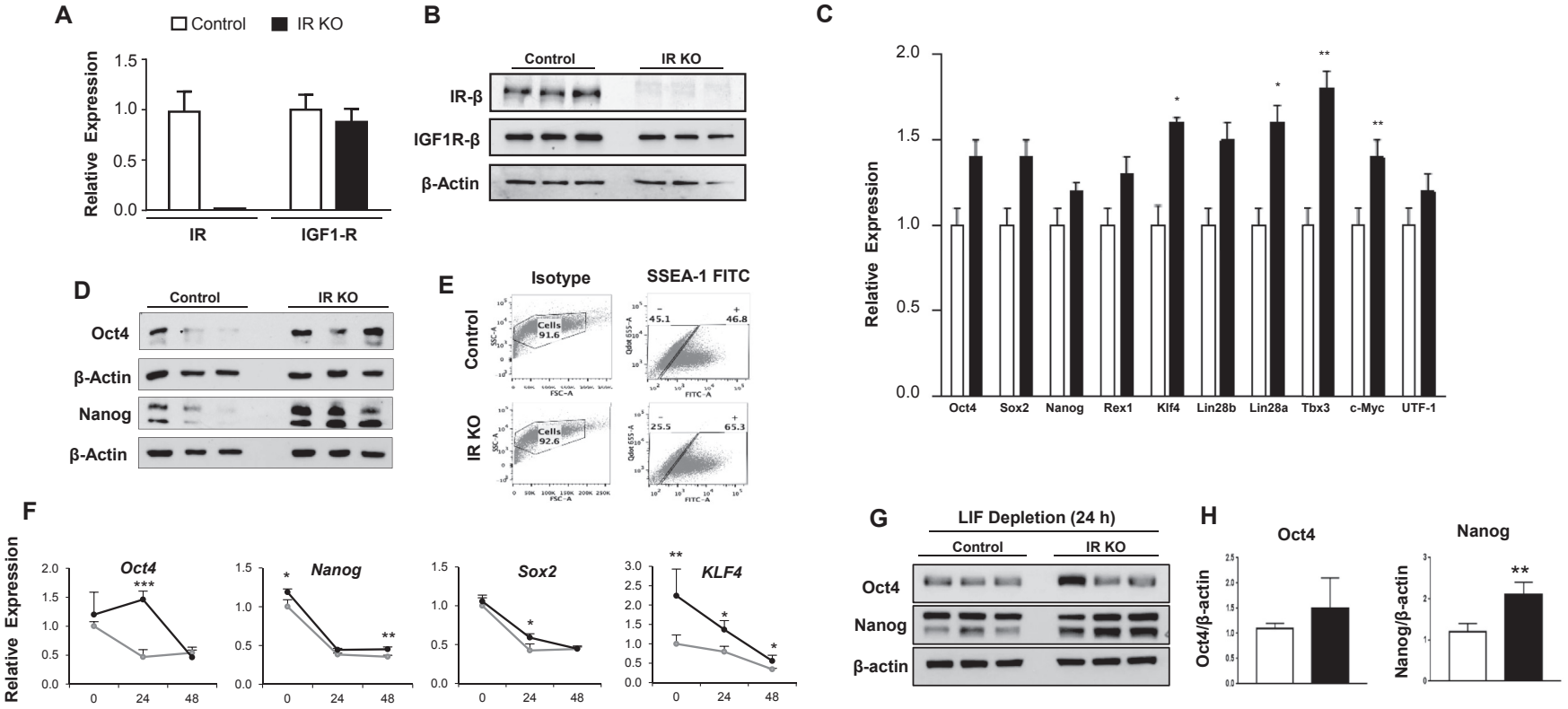

Figure 1: Mouse insulin receptor knockout (IRKO) induced pluripotent stem cells (iPSCs) revealed enhanced pluripotency network. **A**. Real-time PCR analysis, and **B**. Western blot analysis showed complete reduction of IR while IGF1-R levels were unchanged. **C**. Real time PCR analyses demonstrated the upregulation of core pluripotency markers in IR KO iPSCs as compared to control iPSCs. **D**. Western blot analysis demonstrated the significant increase of key pluripotency proteins Oct4 and Nanog in IRKO iPSCs as compared to controls. **E**. Flow cytometry analysis described higher expression of pluripotency surface marker, SSEA-1, in IRKO iPSCs. **F.** RT-PCR analysis demonstrated that key pluripotency markers *Oct4*, *Nanog*, *Sox2*, and *Klf4* have higher expression level in IRKO iPSCs compared to Control iPSCs at 24 h and 48 h after leukemia Inhibitory factor (LIF) removal during differentiation. **G.** Western blot analysis showed an upregulation of Oct4 and Nanog proteins in IRKO iPSCs after 24 h of LIF removal. **H.** Quantification analysis of Oct4 and Nanog. β-actin was used as a housekeeping control. All experiments represent 3 independent experiments using 3 independent biological clones/groups. Data are shown as mean ± SEM. Statistical significance was determined by unpaired two-tailed student's t-test. (*$p < 0.05$, **$p < 0.01$, ***$p < 0.001$).

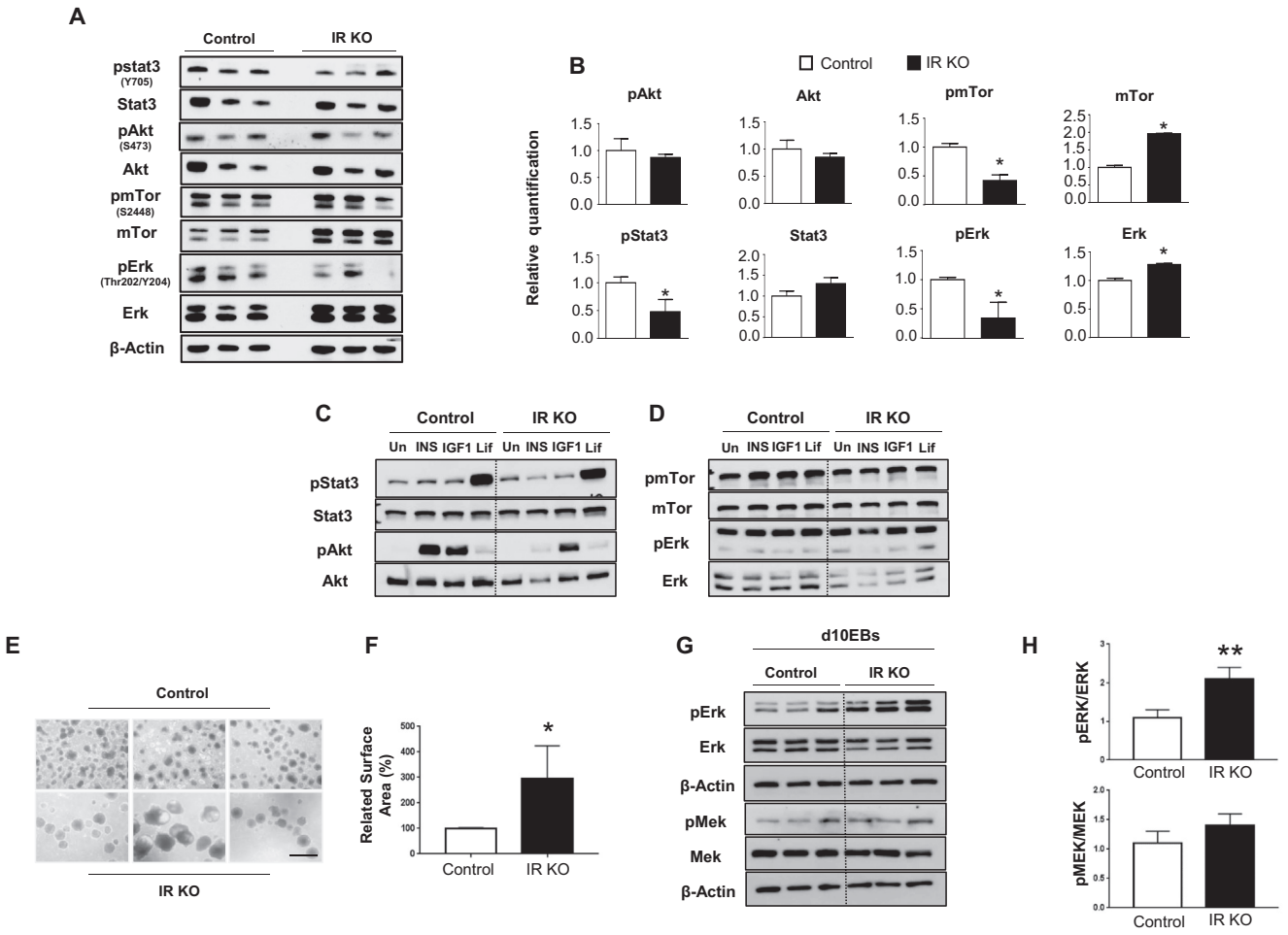

Figure 2: Signaling pathway analysis demonstrated the differential regulation of growth pathways between Control and IRKO iPSCs at basal and starved conditions. **A** and **B.** Basal signaling pathways analysis revealed no change in pAkt, Akt, and Stat3 and a decrease in pStat3, pmTor, and pErk in IRKO iPSCs. However, total proteins of mTOR and Erk were upregulated in IRKO iPSCs as compared to control iPSCs. **C** and **D**. In overnight starved conditions, IRKO iPSCs showed complete loss of pAkt and significant reduction in pmTor and pErk after insulin stimulation (100 nM). IGF1 stimulation (100 nM) revealed reduction in pAkt, pmTor and pErk in IRKO iPSCs. Differentiation analyses of IRKO and Control iPSCs showed differential regulation of growth pathways. **E.** Control and IRKO day 10 differentiated embryoid bodies (EBs). **F.** Quantification of cell size of embryoid bodies (N = 10 images per group quantified). **G.** Western blot demonstrated upregulated phosphorylation of Erk/Mek pathways in differentiated day 10 embryoid bodies of IRKO iPSCs. **H.** Quantification of Erk/Mek phosphorylation. β-actin was used a housekeeping control. All experiments represent 3 independent experiments using 3 independent biological clones/groups. Data are shown as mean ± SEM. Statistical significance was determined by unpaired two-tailed student's t-test. (*$p < 0.05$, **$p < 0.01$, ***$p < 0.001$).

MOLECULAR METABOLISM

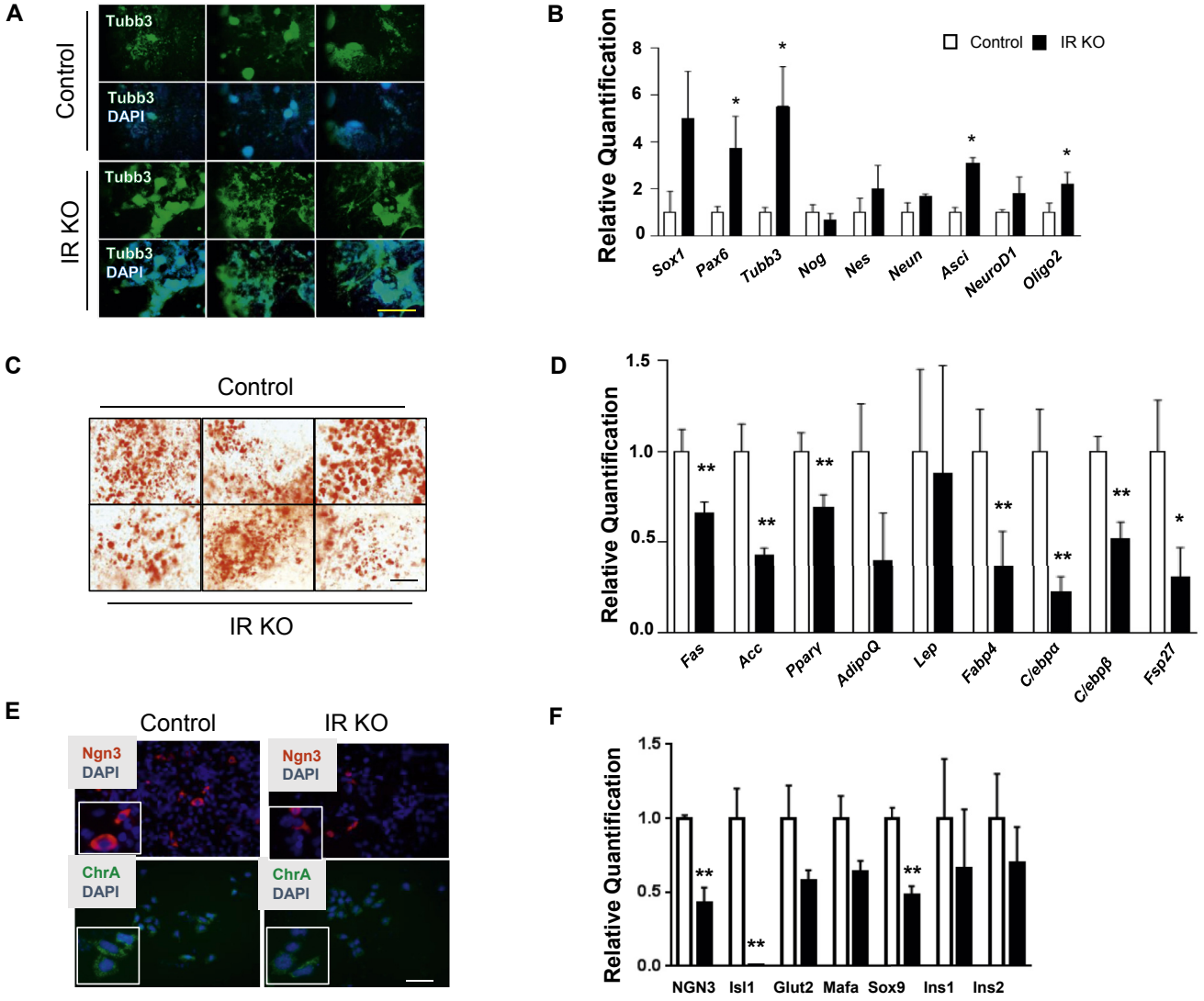

Figure 3: Upregulated neuronal and downregulated adipocyte differentiation in IRKO iPSCs. **A.** Beta III-tubulin immunofluorescent staining of day 10 differentiated neurons from control and IRKO iPSCs. **B.** RT-PCR analysis revealed that expression of neuronal markers, sex determining region Y-1 *(Sox1)*, Paired box protein 6 *(Pax6)*, Tubulin beta 3 class III protein (*Tubb3*), acid sensing ion channel (*Asic*), neuronal differentiation 1 (*NeuroD1*) and oligodendrocyte transcription factor 2 (*Oligo 2*) in day 10 differentiated neurons from IRKO iPSCs, while expression of other neuronal markers, noggin (*Nog*), Nestin (*Nes*) and neuronal nuclei (*Neun*) did not change as compared to controls. Downregulated adipocyte differentiation in IRKO iPSCs. **C.** Oil-red O staining images of day 28 adipocyte differentiation of control and IRKO iPSCs (scale bar-200um). **D**. RT-PCR analysis revealed downregulation of key adipocyte markers including fatty acid synthase (*Fas*), acetyl-coA carboxylase (*Acc*), fatty acid binding protein 4 (*Fabp4*), CCAAT/Enhancer binding protein alpha C/ebp α, CCAAT/Enhancer binding protein beta (*C/ebpβ*), peroxisome proliferator activated receptor gamma (*Pparγ*), fat-specific protein 27 (*Fsp27*), while the marker of mature adipocytes leptin (*Lep*) did not change in IRKO iPSCs. **E.** Immunostaining of chromogranin A (ChrA) and neurogenein3 (Ngn3) markers in differentiated pancreatic beta cells from control and IRKO iPSCs. **F.** RT-PCR analyses showed downregulation of early and late beta cell differentiation markers including *Ngn3, Isl1, Glut2, Mafa, Sox9, Ins1,* and *Ins2* in IRKO iPSCs. All experiments represent 3 independent experiments using 3 independent biological clones/groups. Data are shown as mean $\pm$ SEM. Statistical significance was determined by unpaired two-tailed student's t-test. (*p $<$ 0.05, **p $<$ 0.01, ***p $<$ 0.001).

day 27 showed poor differentiation in adipocytes derived from IRKO iPSCs as compared to control iPSCs (Figure S3D). The limited ability to differentiate along the adipocyte lineage was supported by a reduced number of oil droplets observed in adipocytes derived from IRKO iPSCs as shown by oil-red O staining (Figure 3C). Consistently, the expression of *Fas*, *Acc*, *Pparγ*, *Fabp4*, *Cebpα*, *Cebpβ*, and *Fsp27* were significantly downregulated in adipocytes differentiated from IRKO iPSCs, while the expression of *AdipoQ* and *Leptin (Lep)* was not significantly altered, probably due to the early stage of differentiation (Figure 3D). These findings are consistent with the report from *Boucher* et al. reporting that absence of IR is detrimental for the development of adipose tissue [14].

Finally, we directed the differentiation of control and IRKO iPSCs towards the endocrine lineage (Figure S3E) using a previously published protocol [24]. Control iPSCs differentiated into endoderm-like cells at day 14, as evidenced by bright field images of differentiated cells (Figure S3F). Immunohistochemical analyses revealed a reduction in chromogranin A+ cells and Ngn3+ cells in differentiated iPSCs deficient in IR (Figure 3E). The expression of endodermal progenitor transcripts *Ngn3*, *Isl1*, and *Sox9* were decreased significantly in IRKO iPSCs compared to controls, and genes that are typically highly expressed in mature pancreatic beta-cells, such as *Glut2*, *Mafa*, *Ins1,* and *Ins2,* presented a trend to be reduced in IRKO iPSCs (Figure 3F).

3.6. Phosphoproteomics data reveal differentially regulated pluripotency and development-associated proteins between control and IRKO iPSCs

We performed global phophoproteomics analyses between control and IRKO iPSCs with or without stimulation (insulin, IGF1 or LIF) and identified several differentially regulated phosphosites (Figure 4A). In the unstimulated basal state, phosphosites of several pluripotency-related proteins were upregulated in IRKO iPSCs compared to controls [e.g. Rif1. (S1029/2296), Kdm5b.(S1169), Slc2a3.(S482), Tfcp2l1.(S37), Zic3.(S203), Utf.(S99) and Tbx3.(S432)]. Similarly, phosphosites of proteins involved in embryonic development (Pwp2 (S895), Npat (T205), Kmt2d (S1562), Zscan4d (S312), Lig1 (S94)), neural development (Fxr2 (S452), Sema4b (S482)) cancer (Tmx2 (S211), Npat (T205)), and DNA damage (Mdc1 (T1113)) were all upregulated in iPSCs devoid of IR. A decreased phosphorylation was associated with proteins involved in development (Smg9(S53), Sec61b (S13), Thrap3 (S243)), mRNA splicing (Cpsf1(S754), Srm2 (S2638)), and cancer (Sash1 (S831), Prkd3 (S41), Hdac1(S410)) in IRKO iPSCs (Figure 4B and S4A). Notably, proteins presenting increased phosphorylation in the unstimulated state in IRKO compared to control iPSCs were enriched for GO terms associated with histone methylation, development, and telomere maintenance (Figure 4C) while downregulated phosphosites were enriched for GOs related to development, stem cell division, and autophagy (Figure 4D).

To further explore the differential regulation of proteins when insulin receptor signaling is compromised, we challenged control and IRKO iPSCs independently with insulin (100 nM), IGF1 (100 nM), or LIF (100 units/ml). Exogenous insulin regulated phosphoproteins such as Sema4b (S816), Med19 (S226), Hdac1 (S409), Gtf2f1 (T384) and Smg9 (S53). IGF1 stimulation altered Tbc1d10b (642), Ubr4 (S2715), Glis2 (S54), and Mdc1 (S1052). And, finally, LIF regulated phosphoproteins including Pias2 (S499), Fam193a (S293), Yap1 (S112), Zc3h13 (S207), Znf513 (S253), and Plekha7 (S116) (Figure 4B and S4B,C,D). Insulin regulated pathways between two groups involved in receptor binding, nutrient sensing, proliferation, development and differentiation (Figure 4E,F), while IGF1 regulated pathways related to metabolic processes, transduction, transport, membrane biology, transcription, and proteolysis (Figure 4G,H, S4C,E). Phosphoproteomics analysis between control and IRKO iPSCs revealed proteins in the LIF regulated pathways which are involved in metabolism, development, differentiation, histone methylation, kinase activity, cell maturation and tissue development (Figure 4I,J, S4D,E). Finally, all stimuli (e.g. insulin, IGF1 or LIF) regulated phosphoproteins related to DNA damage, gene expression, cell growth, development and cancer. Interestingly, the phosphosites Thrap3 (S243), Arhgef7 (S228), Hdac1 (S410), Cpsf1 (S754), and Zgpat (S64) were regulated by all three stimuli.

To exclude the possibility that the observed changes are due to differences in total proteins, we first re-analyzed the datasets by plotting the delta delta changes (e.g. for insulin stimulation: KO vs WT with insulin and KO vs WT with no stimulation) in each of the different stimulation conditions (Figure 4B). Second, we measured the total protein levels of three candidates showing decreased phosphorylation in the unstimulated state, namely, Trim28 (Figure 4B), Sec61B (Figure S4A) and Thrap3 (Figue. 4B and S4A), in an aliquot of the lysates also submitted for phosphoproteomics. The increased total protein expression patterns for all 3 candidates in IRKO iPSCs compared to controls suggested that alterations at the phosphorylation level was independent of changes in total protein levels (Figure S4G, H). The present study uncovers previously unidentified roles for insulin receptor-mediated signaling in the regulation of proteins involved in pluripotency and lineage development. Mechanistic studies to examine the function of these novel phosphosites require further investigation.

4. DISCUSSION

The proteins in the insulin/IGF-1 signaling family regulate the growth and function of most mammalian cells. The role of IGFII/IGF1R in pluripotency and differentiation has been reported previously. For example, Bendall et al. reported that blocking of IGFII or loss of IGF1R cause differentiation of human pluripotent stem cells [6]. Similarly, Wang et al. also revealed that blocking of IGF1R by an antibody or lentivirus shRNA prompts human pluripotent stem cells to apoptosis and begin to differentiate [7]. Delta40p53, a transactivation deficient isoform of tumor suppressor p53, has been reported to control switching between pluripotency and differentiation by regulating the level of IGF1R/PI3K in mouse pluripotent stem cells [31].

To address the direct role of IR in the maintenance of pluripotency and lineage determination, we undertook directed differentiation of control and IRKO iPSCs obtained from day 14.5 MEFs. In the present study, we report, for the first time to our knowledge, that loss of IR leads to upregulation of key pluripotency genes involved in self-renewal and differentiation such as *Oct4*, *Nanog*, along with other markers *such as Sox2*, *Lin28*b, *UTF1*, *Tbx3* and *Rex1. Oct4*, *Sox2*, and *Nanog*, all of which are key pluripotency genes involved in reprogramming, self-renewal and differentiation [17,32]. Oct4 overexpression triggers primitive endoderm or mesoderm while Oct4 reduction leads to trophectoderm differentiation in mouse pluripotent stem cells [33]. Wang et al. reported that Nanog represses an ectoderm differentiation program while Sox2 and Sox3 are redundant and block meso-endoderm differentiation [34]. Considering that *Lin28a* has been reported to control insulin/PI3K signaling via the repression of let-7 [35], it is possible that increased expression of the pluripotency network counteracts loss of IR to maintain pluripotency and self-renewal of the stem cells. Interestingly, pluripotency markers remain upregulated both at the transcript and protein levels even after removal of LIF, a key mouse pluripotency cytokine, for 24 h and 48 h in IRKO iPSCs. These findings provide new insights linking IR with regulation of pluripotency markers and differentiation.

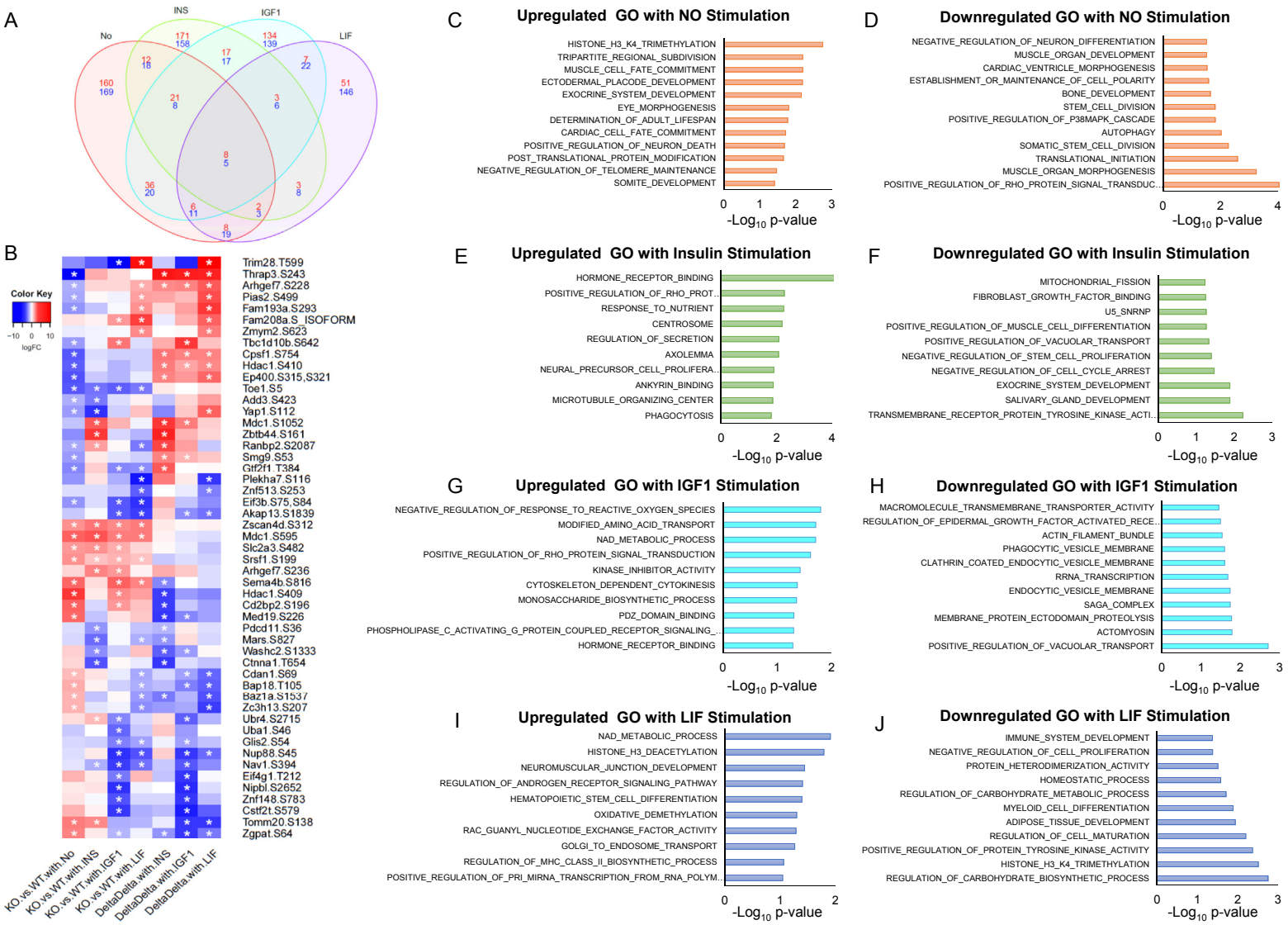

Figure 4: Phosphoproteomics analyses of control and IRKO iPSCs at basal and stimulated conditions. **A.** Venn diagram representation of phosphoproteins differentially regulated between control and IRKO iPSCs at basal state and after 15 min stimulation with insulin (100 nM), IGF1 (100 nm) or LIF (100 units/ml). Red color denotes basal condition regulated phosphoproteins while green, blue and purple colors represent insulin, IGF1 or LIF regulated phosphoproteins. **B.** Heat map representation of phosphoproteins differentially regulated between control and IRKO iPSCs at basal condition and various simulated conditions including INS, IGF1 or LIF. Heat map is in centered log2 value. Red color denotes upregulated while blue color defines downregulated phosphoproteins. Delta delta changes (KO vs. WT at stimulated condition and KO vs. WT at basal) represents the unique phosphoproteins differentially regulated by stimulation with insulin, IGF1, or LIF. **C** and **D**. GO pathway analyses showing the differentially regulated pathways in red color bar graphs between IRKO vs control iPSCs at basal condition. **E** and **F.** GO pathways analyses showing differentially regulated pathways in green color bar graphs between two groups in response to insulin stimulation **G** and **H.** GO pathways analyses showing differentially regulated pathways in blue color bar graphs between two groups in response to IGF1 stimulation. **I** and **J.** GO pathways analyses showing differentially regulated pathways in purple color bar graphs between IR KO vs Control iPSCs in response to LIF stimulation. In all bar graphs, the Y-axis denotes regulated pathways, while the X-axis represents their log10 p-value. All experiments represent 3 independent experiments using 3 independent biological clones/groups.

Next, we explored the signaling pathways involved in pluripotency and differentiation of stem cells. Stat3 and Akt pathways, along with Erk and mTor signaling, are reported to maintain growth, differentiation, and pluripotency of human and mouse pluripotent cells [36,37]. Interestingly, in our study, we observed a reduction in the Stat3/Erk/mTor pathways in IRKO iPSCs at basal state while the Akt pathway was virtually completely blunted after starved cells were stimulated with insulin, thus confirming the relevance of IR-mediated Akt signaling in normal pluripotent stem cells. These findings also suggest that insulin mediated Akt signaling is unlikely a critical element and can be compensated for by other pluripotency pathways. Erk pathway is involved in differentiation and was recently reported to be linked to self-renewal of mouse pluripotent stem cells [38]. Observations of decreased phosphorylation of Stat3, Akt and Erk in IRKO iPSCs led us to speculate that unidentified signaling pathways independent of IR are involved in upregulation of the pluripotency network.

While the Erk pathway has various functions involved in pluripotency of human pluripotent stem cells, in mice, Erk signaling has been linked to both pluripotency and differentiation of stem cells [38]. Trappmann et al. reported that enhanced phospho-Erk signaling reduces stem cell differentiation [39]. We observed an upregulation of Erk pathways in differentiating embryoid bodies developed from IRKO iPSCs that may have contributed to the larger EBs in this group. A more detailed study is required to investigate the role of the Erk pathway during differentiation. While genetic insulin resistance has been reported as a modulator of gene expression in human pluripotent stem cells [40], the role of insulin receptor-mediated signaling in lineage development has been studied in different contexts. For example, insulin receptor substrate 1 (IRS-1) has been reported to play a role in maintaining mouse pluripotency [41]. It has been previously described that insulin-mediated signaling favors differentiation of human pluripotent stem cells into the neuroectodermal lineage at the expense of mesendodermal lineages [8]. Lian et al. reported that exogenous insulin inhibits cardiac mesoderm which can be rescued by modulation of the canonical Wnt signaling pathway [9].

To investigate the role of increased Erk pathway and loss of IR during differentiation, we directly differentiated control and IRKO iPSCs into neuronal cells (ectoderm), adipocytes (mesodermal) or beta-like cell (endoderm). IRKO iPSCs showed an upregulation of neuronal markers including early neural progenitor markers such as *Pax6, Tubb3, Oligo2* and *Ascl1*. This is consistent with the report that the insulin receptor is involved in development of the peripheral nervous system in drosophila [42]. On the contrary, adipocytes differentiated from IRKO iPSCs presented features of reduced adipogenesis. Thus, we observed significantly reduced expression of adipocyte and lipogenesis markers, such as *Fas*, *Acc*, *Fsp27*, *Fabp4*, *Cebp*α, and *Cebp*β. Fas and Acc are lipogenic enzymes, while Fabp4 is a lipid transporter, which is highly expressed in mature white adipocytes. Fsp27 is involved in unilocular lipid droplet and adipocyte formation [43]. Furthermore, Cebp is reported to play a developmental role in adipogenesis [44]. These data are supported by an earlier report that adipocyte-specific IRKO mice exhibit a significant ($\sim$90%) reduction in white adipocytes [14].

Finally, we explored the ability of IRKO iPSCs to differentiate towards the endocrine lineage. Among the markers that are known to contribute to pancreatic cell development, it was notable that *Ngn3, Sox9*, and *Isl1* were all significantly downregulated, while insulin1 (*Ins1*) and insulin2 (*Ins2*) were unaltered in differentiated cells from IRKO iPSCs. These results suggest that insulin receptor-mediated signaling regulates a specific set of pancreatic cell developmental markers and warrants further investigation of the pathway during early developmental stages in mammals.

The lack of previous reports on detailed phosphoprotemics analyses underscores the importance of our observations that insulin receptor signaling regulates the pluripotency network in iPSCs and provides several novel and uncharacterized post-translational modifications in proteins involved in diverse aspects of growth, pluripotency, cell cycle and life span regulation. For instance, among the significantly altered proteins, Rif1 is reported to maintain telomere length homeostasis in pluripotent stem cells by mediating heterochromatin silencing [45]; and Kdm5b regulates self-renewal of embryonic stem cells and opposes cryptic intragenic transcription [46]. Tfcp2l1 is a transcription factor acting at the intersection of LIF and 2i-mediated self-renewal pathways to maintain ESC identity by promoting Nanog expression [47]. UTF1, Tbx3 and Zic3 which were identified in our phosphoproteomics analyses are known to be involved in pluripotency of iPSCs.

Phosphoproteomics data also provided mechanistic insights into the differentiation properties of IRKO IPSCs. Thus, phosphoproteins involved in neuronal development, such as Fxr2 and Sema4b, were among those upregulated in IRKO iPSCs, confirming our findings of upregulation of neuronal differentiation markers in IRKO iPSCs. Among the several proteins involved in development and differentiation is Pwp2, which is upregulated in IRKO iPSCs. Pwp1, a family member of Pwp2, is required for the differentiation of mouse pluripotent stem cells [48]. On the contrary, Sec61b which is required for the development of drosophila, Smg9, involved in the development of brain, heart and eye, and Thrap3, reported to play a role in bone and adipocyte development, are downregulated in IRKO iPSCs [49–51]. Taken together, our studies on directed differentiation and phophoproteomics analyses support our hypothesis that insulin receptor signaling is a key regulator of stemness and is important for the regulation of pluripotency markers and normal embryonic development. It would be interesting to contrast these data with a iPS model lacking IGF-1 receptors or both.

5. CONCLUSION

In summary, the present study provides a novel role for IR-mediated signaling in the global regulation of the pluripotency network and differentiation potential of ectoderm, mesoderm and endoderm lineages by upregulating the Erk pathway. The identification of several previously uncharacterized phosphosites provides a unique opportunity to further examine their significance as pluripotency regulators and development mediators.

AUTHOR CONTRIBUTIONS

Conceptualization, M.K.G., R.N.K., D.F.J.; Validation and Investigation, M.K.G., D.F.J., I.A.V.,F.S., and S.K.; Phosphoproteomics analyses, L.Y., A.C.W., W.Q.; Writing-original draft, review and editing, M.K.G., D.F.J., and R.N.K.; Supervision, R.N.K.; Funding acquisition and final approval, R.N.K. All authors have reviewed the manuscript.

ACKNOWLEDGMENTS

We thank G. Mostoslavsky PhD (Boston University) for the kind gift of STEMCCA lentiviral plasmids. We thank J.Hu for technical assistance. Authors acknowledge Joslin Diabetes Center iPS Core Facility (DRC, NIH DK036836). MKG is supported by JDRF advanced postdoctoral fellowship grant 3-APF-2017-393-A-N. DFJ was supported by the Portuguese Foundation for Science and Technology – FCT (SFRH/BD/51699/2011), Albert Ronald Travel Fellowship 2015, 2016 FLAD R&D@PhD Internship Grant. RNK is supported by the HSCI and NIH grants R01 DK67536 and R01 DK103215. WQ is

supported by NIH grants UC4 DK104167 and DP3 DK110844. Y-HT is supported by NIH grants R01DK077097 and R01DK102898. FS is supported by American Diabetes Association Fellowship #1-18-PDF-169. Part of the experimental work was performed in the Environmental Molecular Sciences Laboratory, a national scientific user facility sponsored by the DOE and located at Pacific Northwest National Laboratory, which is operated by Battelle Memorial Institute for the DOE under Contract DE-AC05-76RL0 1830. All authors declare no financial conflict of interest.

CONFLICT OF INTEREST

All authors declare no conflict of interest.

APPENDIX A. SUPPLEMENTARY DATA

Supplementary data to this article can be found online at https://doi.org/10.1016/j.molmet.2018.09.003.

REFERENCES

[1] Michael, M.D., Kulkarni, R.N., Postic, C., Previs, S.F., Shulman, G.I., Magnuson, M.A., et al., 2000. Loss of insulin signaling in hepatocytes leads to severe insulin resistance and progressive hepatic dysfunction. Molecular Cell 6(1):87–97.

[2] Kulkarni, R.N., Brüning, J.C., Winnay, J.N., Postic, C., Magnuson, M.A., Kahn, C.R., 1999. Tissue-specific knockout of the insulin receptor in pancreatic B cells creates an insulin secretory defect similar to that in type 2 diabetes. Cell 96(3):329–339.

[3] Kulkarni, R.N., 2002. Receptors for insulin and insulin-like growth factor-1 and insulin receptor substrate-1 mediate pathways that regulate islet function. Biochemical Society Transactions 30:317–322.

[4] Nakae, J., Kido, Y., Accili, D., 2001. Distinct and overlapping functions of insulin and IGF-I receptors. Endocrine Reviews 22(6):818–835.

[5] Taniguchi, C.M., Emanuelli, B., Kahn, C.R., 2006. Critical nodes in signalling pathways: insights into insulin action. Nature Reviews Molecular Cell Biology 7(2):85–96.

[6] Bendall, S.C., Stewart, M.H., Menendez, P., George, D., Vijayaragavan, K., Werbowetski-Ogilvie, T., et al., 2007. IGF and FGF cooperatively establish the regulatory stem cell niche of pluripotent human cells in vitro. Nature 448(7157):1015–1021.

[7] Wang, L., Schulz, T.C., Sherrer, E.S., Dauphin, D.S., Shin, S., Nelson, A.M., et al., 2007. Self-renewal of human embryonic stem cells requires insulin-like growth factor-1 receptor and ERBB2 receptor signaling. Blood 110(12):4111–4119.

[8] Freund, C., Ward-van Oostwaard, D., Monshouwer-Kloots, J., van den Brink, S., van Rooijen, M., Xu, X., et al., 2008. Insulin redirects differentiation from cardiogenic mesoderm and endoderm to neuroectoderm in differentiating human embryonic stem cells. Stem Cells 26(3):724–733.

[9] Lian, X., Zhang, J., Zhu, K., Kamp, T.J., Palecek, S.P., 2013. Insulin inhibits cardiac mesoderm, not mesendoderm, formation during cardiac differentiation of human pluripotent stem cells and modulation of canonical Wnt signaling can rescue this inhibition. Stem Cells 31(3):447–457.

[10] Tran, K.A., Jackson, S.A., Olufs, Z.P., Zaidan, N.Z., Leng, N., Kendziorski, C., et al., 2015. Collaborative rewiring of the pluripotency network by chromatin and signalling modulating pathways. Nature Communications 6:6188.

[11] Liu, Z.Z., Kumar, A., Ota, K., Wallner, E.I., Kanwar, Y.S., 1997. Developmental regulation and the role of insulin and insulin receptor in metanephrogenesis. Proceedings of the National Academy of Sciences of the U S A 94(13):6758–6763.

[12] Li, Y., Geng, Y.J., 2010. A potential role for insulin-like growth factor signaling in induction of pluripotent stem cell formation. Growth Hormone & IGF Research 20(6):391–398.

[13] Li, P., Cavallero, S., Gu, Y., Chen, T.H., Hughes, J., Hassan, A.B., et al., 2011. IGF signaling directs ventricular cardiomyocyte proliferation during embryonic heart development. Development 138(9):1795–1805.

[14] Boucher, J., Mori, M.A., Lee, K.Y., Smyth, G., Liew, C.W., Macotela, Y., et al., 2012. Impaired thermogenesis and adipose tissue development in mice with fat-specific disruption of insulin and IGF-1 signalling. Nature Communications 3:902.

[15] Magner, N.L., Jung, Y., Wu, J., Nolta, J.A., Zern, M.A., Zhou, P., 2013. Insulin and IGFs enhance hepatocyte differentiation from human embryonic stem cells via the PI3K/AKT pathway. Stem Cells 31(10):2095–2103.

[16] Piecewicz, S.M., Pandey, A., Roy, B., Xiang, S.H., Zetter, B.R., Sengupta, S., 2012. Insulin-like growth factors promote vasculogenesis in embryonic stem cells. PLoS One 7(2) e32191.

[17] Takahashi, K., Yamanaka, S., 2006. Induction of pluripotent stem cells from mouse embryonic and adult fibroblast cultures by defined factors. Cell 126(4):663–676.

[18] Sommer, C.A., Stadtfeld, M., Murphy, G.J., Hochedlinger, K., Kotton, D.N., Mostoslavsky, G., 2009. Induced pluripotent stem cell generation using a single lentiviral stem cell cassette. Stem Cells 27(3):543–549.

[19] Bhatt, S., Gupta, M.K., Khamaisi, M., Martinez, R., Gritsenko, M.A., Wagner, B.K., et al., 2015. Preserved DNA damage checkpoint pathway protects against complications in long-standing type 1 diabetes. Cell Metabolism 22(2):239–252.

[20] Teo, A.K., Windmueller, R., Johansson, B.B., Dirice, E., Njolstad, P.R., Tjora, E., et al., 2013. Derivation of human induced pluripotent stem cells from patients with maturity onset diabetes of the young. Journal of Biological Chemistry 288(8):5353–5356.

[21] Gupta, M.K., Teo, A.K., Rao, T.N., Bhatt, S., Kleinridders, A., Shirakawa, J., et al., 2015. Excessive cellular proliferation negatively impacts reprogramming efficiency of human fibroblasts. Stem Cells Translational Medicine 4(10):1101–1108.

[22] Ying, Q.L., Stavridis, M., Griffiths, D., Li, M., Smith, A., 2003. Conversion of embryonic stem cells into neuroectodermal precursors in adherent monoculture. Nature Biotechnology 21(2):183–186.

[23] Cuaranta-Monroy, I., Simandi, Z., Kolostyak, Z., Doan-Xuan, Q.M., Poliska, S., Horvath, A., et al., 2014. Highly efficient differentiation of embryonic stem cells into adipocytes by ascorbic acid. Stem Cell Research 13(1):88–97.

[24] Liu, S.H., Lee, L.T., 2012. Efficient differentiation of mouse embryonic stem cells into insulin-producing cells. Experimental Diabetes Research 2012:201295.

[25] Mertins, P., Yang, F., Liu, T., Mani, D.R., Petyuk, V.A., Gillette, M.A., et al., 2014. Ischemia in tumors induces early and sustained phosphorylation changes in stress kinase pathways but does not affect global protein levels. Molecular & Cellular Proteomics 13(7):1690–1704.

[26] Ritchie, M.E., Diyagama, D., Neilson, J., van Laar, R., Dobrovic, A., Holloway, A., et al., 2006. Empirical array quality weights in the analysis of microarray data. BMC Bioinformatics 7(1).

[27] Ritchie, M.E., Phipson, B., Wu, D., Hu, Y., Law, C.W., Shi, W., et al., 2015. Limma powers differential expression analyses for RNA-sequencing and microarray studies. Nucleic Acids Research 43(7) gkv007-e47.

[28] Wu, D., Lim, E., Vaillant, F., Asselin-Labat, M.L., Visvader, J.E., Smyth, G.K., 2010. ROAST: rotation gene set tests for complex microarray experiments. Bioinformatics (Oxford, England) 26(17):2176–2182.

[29] Wickham, H., 2010. A layered grammar of graphics. Journal of Computational & Graphical Statistics 19(1):3–28.

[30] Gentleman, R.C., Carey, V.J., Bates, D.M., Bolstad, B., Dettling, M., Dudoit, S., et al., 2004. Bioconductor: open software development for computational biology and bioinformatics. Genome Biology 5(10):1–16.

[31] Ungewitter, E., Scrable, H., 2010. Delta40p53 controls the switch from pluripotency to differentiation by regulating IGF signaling in ESCs. Genes & Development 24(21):2408–2419.

[32] Wernig, M., Meissner, A., Foreman, R., Brambrink, T., Ku, M., Hochedlinger, K., et al., 2007. In vitro reprogramming of fibroblasts into a pluripotent ES-cell-like state. Nature 448(7151):318–324.

[33] Niwa, H., Miyazaki, J., Smith, A.G., 2000. Quantitative expression of Oct-3/4 defines differentiation, dedifferentiation or self-renewal of ES cells. Nature Genetics 24(4):372—376.

[34] Wang, Z., Oron, E., Nelson, B., Razis, S., Ivanova, N., 2012. Distinct lineage specification roles for NANOG, OCT4, and SOX2 in human embryonic stem cells. Cell Stem Cell 10(4):440—454.

[35] Zhu, H., Shyh-Chang, N., Segrè, A.V., Shinoda, G., Shah, S.P., Einhorn, W.S., et al., 2011. The Lin28/let-7 axis regulates glucose metabolism. Cell 147(1):81—94.

[36] Li, J., Wang, G., Wang, C., Zhao, Y., Zhang, H., Tan, Z., et al., 2007. MEK/ERK signaling contributes to the maintenance of human embryonic stem cell self-renewal. Differentiation 75(4):299—307.

[37] Cherepkova, M.Y., Sineva, G.S., Pospelov, V.A., 2016. Leukemia inhibitory factor (LIF) withdrawal activates mTOR signaling pathway in mouse embryonic stem cells through the MEK/ERK/TSC2 pathway. Cell Death & Disease 7:e2050.

[38] Chen, H., Guo, R., Zhang, Q., Guo, H., Yang, M., Wu, Z., et al., 2015. Erk signaling is indispensable for genomic stability and self-renewal of mouse embryonic stem cells. Proceedings of the National Academy of Sciences of the U S A 112(44):E5936—E5943.

[39] Trappmann, B., Gautrot, J.E., Connelly, J.T., Strange, D.G., Li, Y., Oyen, M.L., et al., 2012. Extracellular-matrix tethering regulates stem-cell fate. Nature Materials 11(7):642—649.

[40] Iovino, S., Burkart, A.M., Kriauciunas, K., Warren, L., Hughes, K.J., Molla, M., et al., 2014. Genetic insulin resistance is a potent regulator of gene expression and proliferation in human iPS cells. Diabetes 63(12):4130—4142.

[41] Rubin, R., Arzumanyan, A., Soliera, A.R., Ross, B., Peruzzi, F., Prisco, M., 2007. Insulin receptor substrate (IRS)-1 regulates murine embryonic stem (mES) cells self-renewal. Journal of Cellular Physiology 213(2):445—453.

[42] Dutriaux, A., Godart, A., Brachet, A., Silber, J., 2013. The insulin receptor is required for the development of the Drosophila peripheral nervous system. PLoS One 8(9) e71857.

[43] Zhou, L., Park, S.Y., Xu, L., Xia, X., Ye, J., Su, L., et al., 2015. Insulin resistance and white adipose tissue inflammation are uncoupled in energetically challenged Fsp27-deficient mice. Nature Communications 6:5949.

[44] Darlington, G.J., Ross, S.E., MacDougald, O.A., 1998. The role of C/EBP genes in adipocyte differentiation. Journal of Biological Chemistry 273(46):30057—30060.

[45] Dan, J., Liu, Y., Liu, N., Chiourea, M., Okuka, M., Wu, T., et al., 2014. Rif1 maintains telomere length homeostasis of ESCs by mediating heterochromatin silencing. Developmental Cell 29(1):7—19.

[46] Xie, L., Pelz, C., Wang, W., Bashar, A., Varlamova, O., Shadle, S., et al., 2011. KDM5B regulates embryonic stem cell self-renewal and represses cryptic intragenic transcription. The EMBO Journal 30(8):1473—1484.

[47] Ye, S., Li, P., Tong, C., Ying, Q.L., 2013. Embryonic stem cell self-renewal pathways converge on the transcription factor Tfcp2l1. The EMBO Journal 32(19):2548—2560.

[48] Shen, J., Jia, W., Yu, Y., Chen, J., Cao, X., Du, Y., et al., 2015. Pwp1 is required for the differentiation potential of mouse embryonic stem cells through regulating Stat3 signaling. Stem Cells 33(3):661—673.

[49] Valcárcel, R., Weber, U., Jackson, D.B., Benes, V., Ansorge, W., Bohmann, D., et al., 1999. Sec61beta, a subunit of the protein translocation channel, is required during Drosophila development. Journal of Cell Science 112(Pt 23): 4389—4396.

[50] Shaheen, R., Anazi, S., Ben-Omran, T., Seidahmed, M.Z., Caddle, L.B., Palmer, K., et al., 2016. Mutations in SMG9, encoding an essential component of nonsense-mediated decay machinery, cause a multiple congenital anomaly syndrome in humans and mice. The American Journal of Human Genetics 98(4):643—652.

[51] Katano-Toki, A., Satoh, T., Tomaru, T., Yoshino, S., Ishizuka, T., Ishii, S., et al., 2013. THRAP3 interacts with HELZ2 and plays a novel role in adipocyte differentiation. Molecular Endocrinology 27(5):769—780.

Supplemental Figure 1

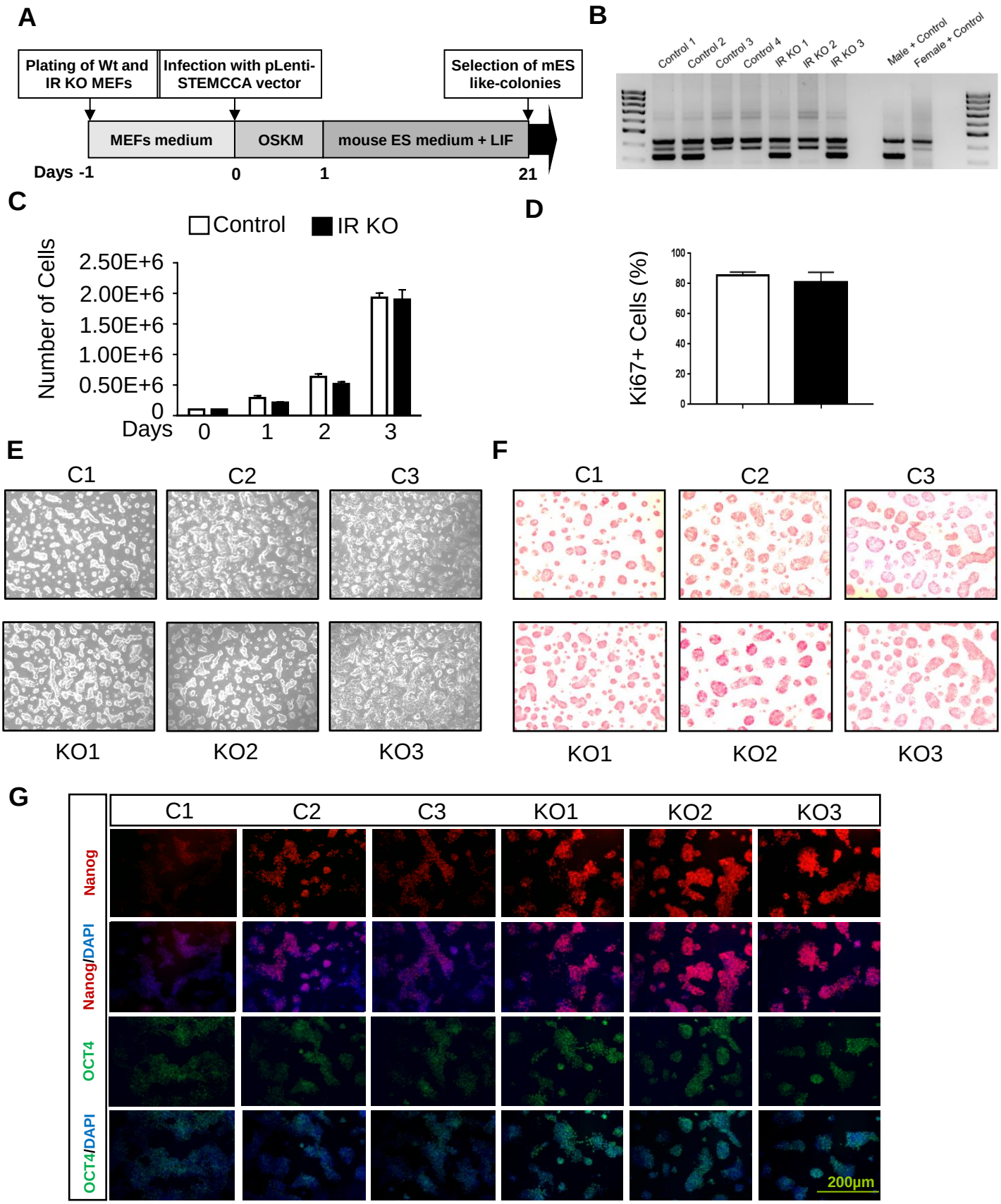

Supplemental Figure S1 : Generation and characterization of Control and IRKO iPSCs : **A**. Schematic reprogramming of mouse embryonic fibroblasts (MEFs) into induced-pluripotent stem cells (iPSCs) **B.** Sex determination of iPSCs by PCR. **C** and **D**. Cell proliferation determined by cellometer (left) and by Ki67 staining flow cytometry analysis (right); N=3. **E-F**. Morphological images of iPSCs in 2i media (left), alkaline phosphatase stainings (right). **G**. Immunostainings of Nanog (in red) and Oct4 (in green) proteins in Control and IRKO iPSCs. DAPI is stained in blue. Scale bar-200µm, N=3 (Related to Figure 1).

Supplemental Figure 1 (Continued)

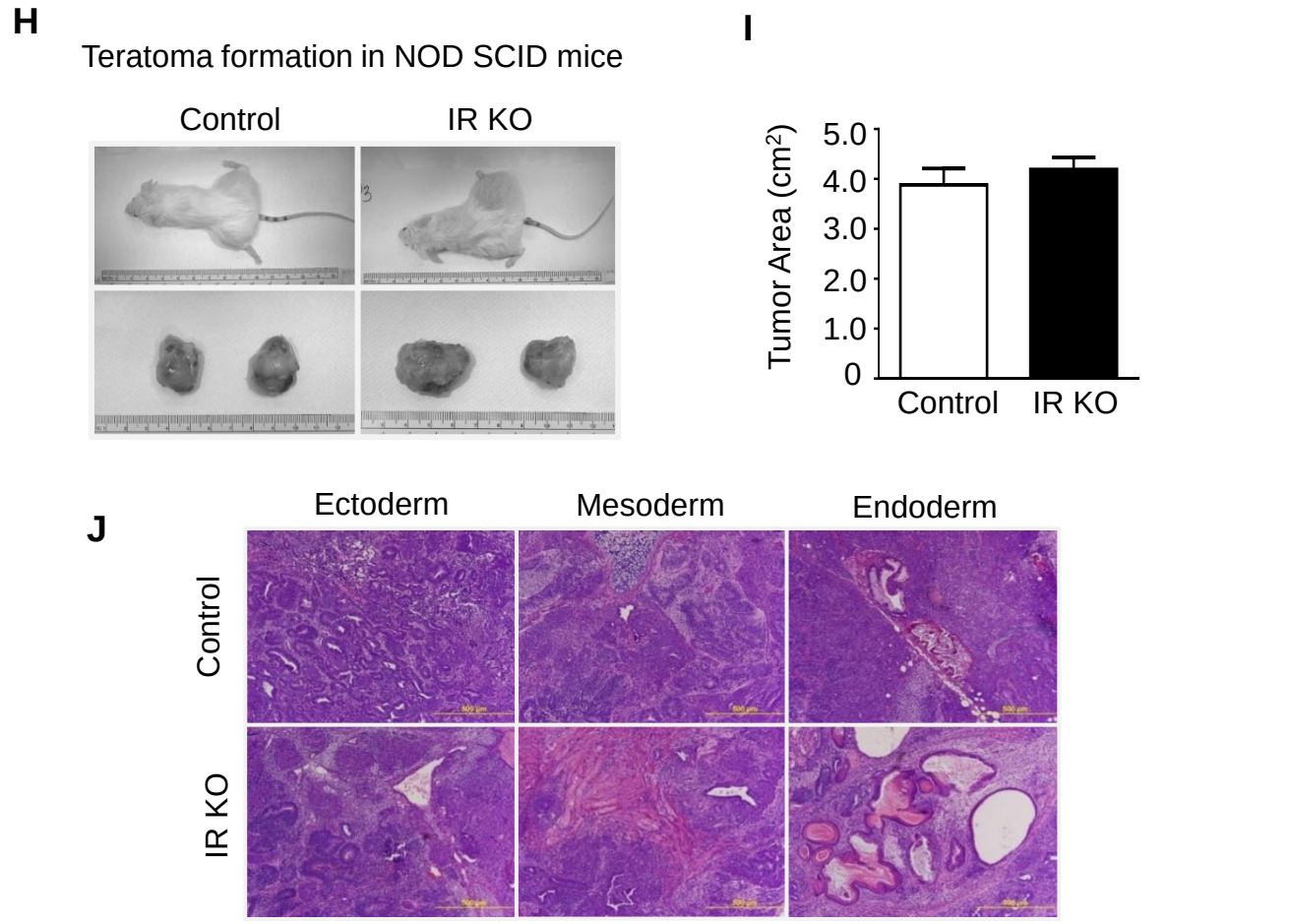

Supplemental Figure S1 (Continued) : *In vivo* differential potential of Control and IRKO iPSCs: **H**. Control and IRKO iPSCs were injected into NOD SCID and teratomas harvested after 4 weeks for analysis. **I**. Teratoma volume obtained from Control and IR KO iPSCs. **J**. H&E stainings of teratoma sections obtained from control and IRKO iPSCs. **K.** Western blot analyses of insulin receptor and IGF1 receptor in Control and IRKO iPSCs devoid of LIF for 24 hours. **L**. Western blot quantifications. (Related to Figure 1). Scale bar-200μm and N=3.

Supplemental Figure 2

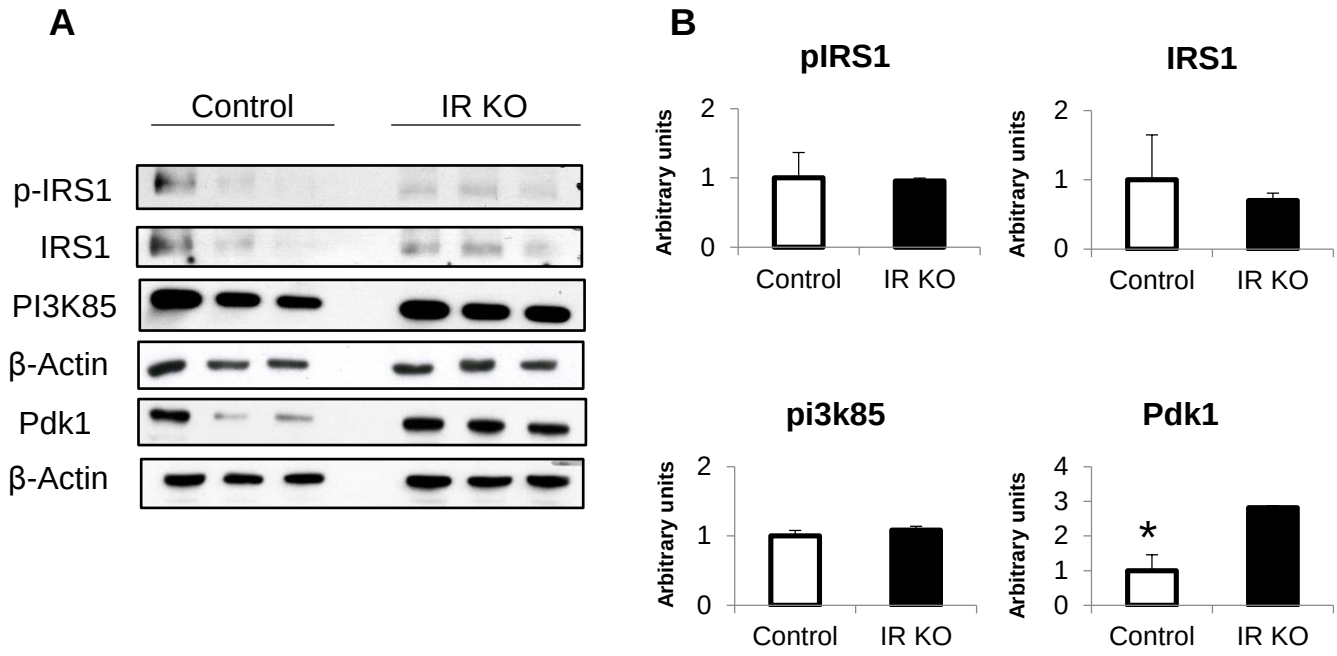

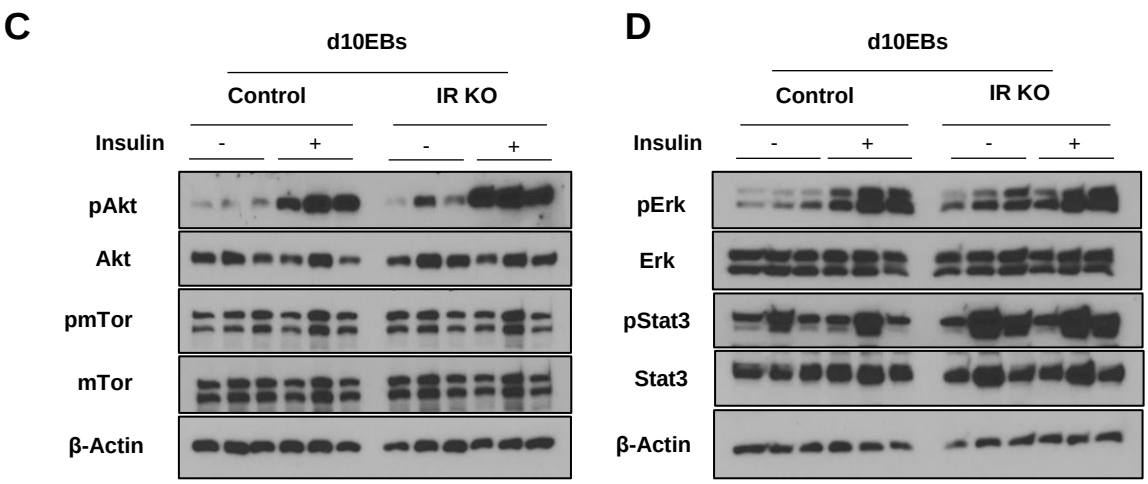

Supplemental Figure S2 : Insulin receptor mediated signaling analyses in control and IRKO iPSCs. **A**. Phosphorylation of IRS1 and total IRS1, PI3K85 do not change in IRKO iPSCs. However, PDK1 is upregulated in IRKO iPSCs **B.** Western blot quantifications. **C. and D**. Day 10 embryoid bodies from control and IRKO iPSCs were starved overnight and stimulated with insulin (100nM). Western blot analyses showed basal level upregulation of Erk pathway in IR KO day 10 EBs while Akt, mTor and Stat3 pathways remain unchanged. N=3. (Related to Figure 2).

Supplemental Figure 3

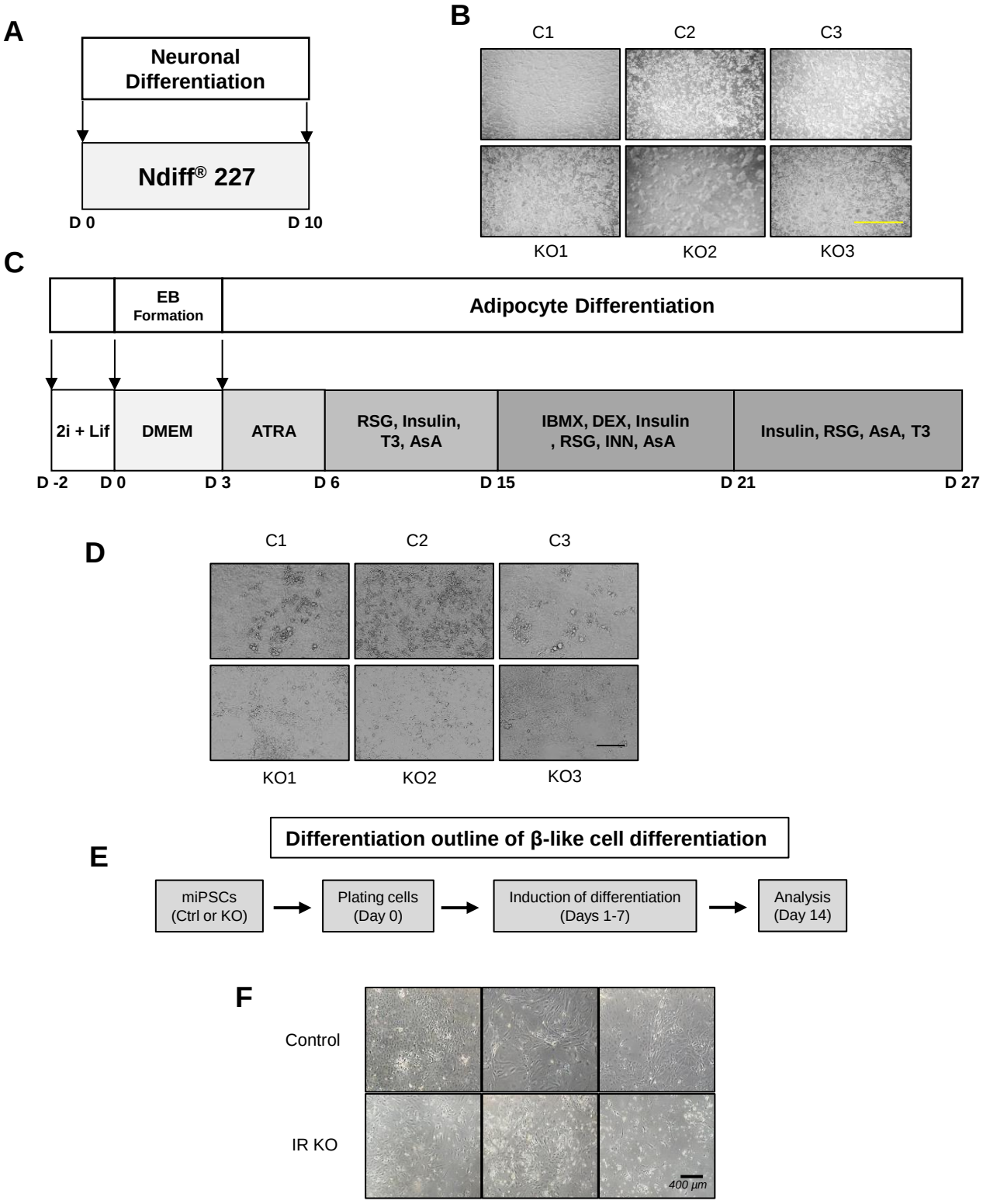

Supplemental Figure S3 : Insulin receptor mediated signaling in lineage development : **A.** Schematic diagram showing of neuronal differentiation protocol. **B.** Morphological images of day 10 differentiated neurons from control and IRKO iPSCs (scale bar-200um). **C.** Schematic diagram of adipocyte differentiation adapted-protocol. **D.** Morphological images of day 28 adipocyte differentiation of control and IR KO iPSCs (left panel, scale bar-200um). **E**. Schematic diagram showing of pancreatic beta-cell differentiation protocol. **F**. Bright field images of pancreatic beta cells at day 14 in both the groups (Related to Figure 3).

Supplemental Figure 4

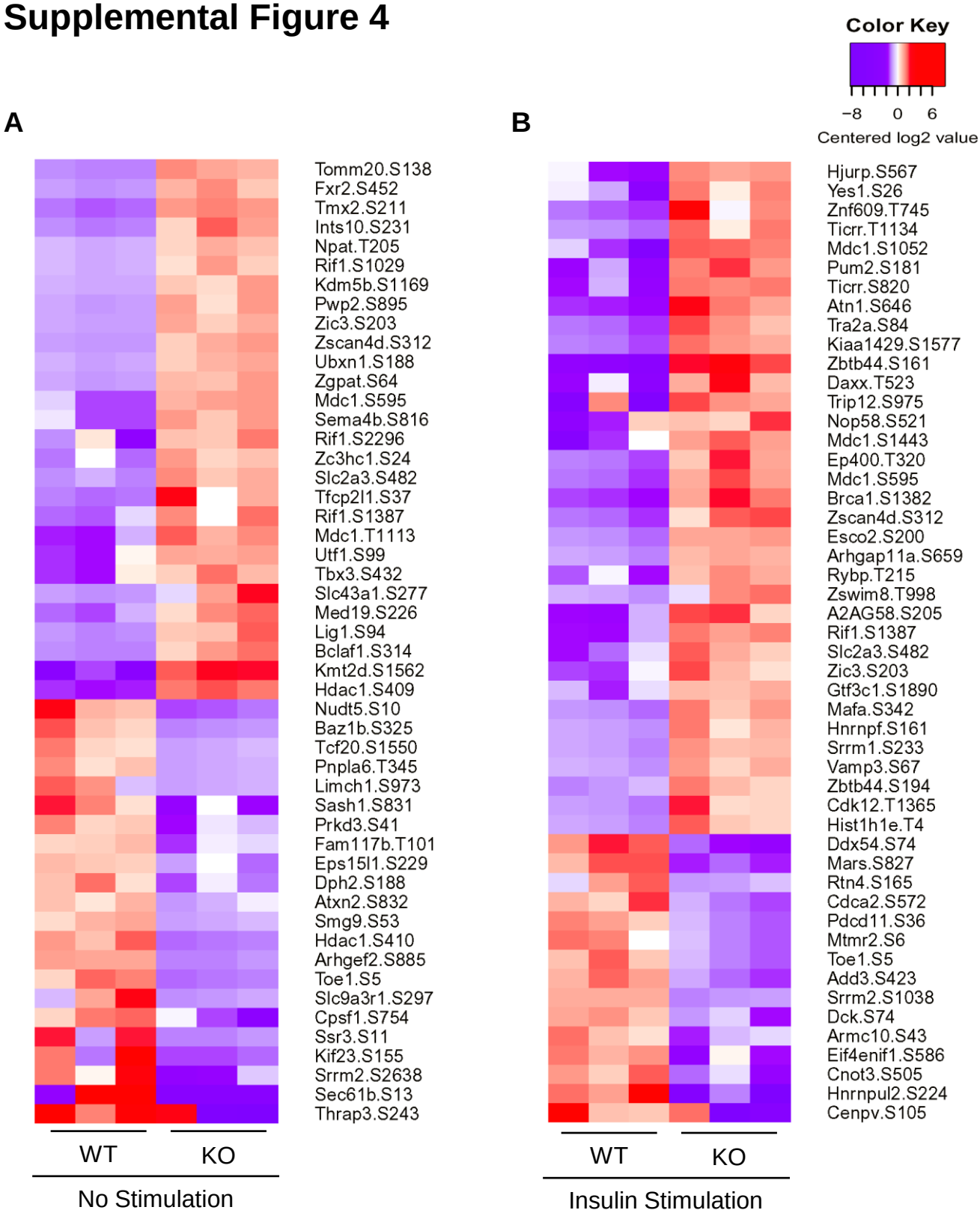

Supplemental Figure S4 : Phosphoproteomics analyses of control and IR KO iPSCs in the basal unstimulated state (A) or following insulin treatment (**B**). Red color denotes upregulation while blue color defines downregulation of phosphoproteins (Related to Figure 4). N=3.

Supplemental Figure 4

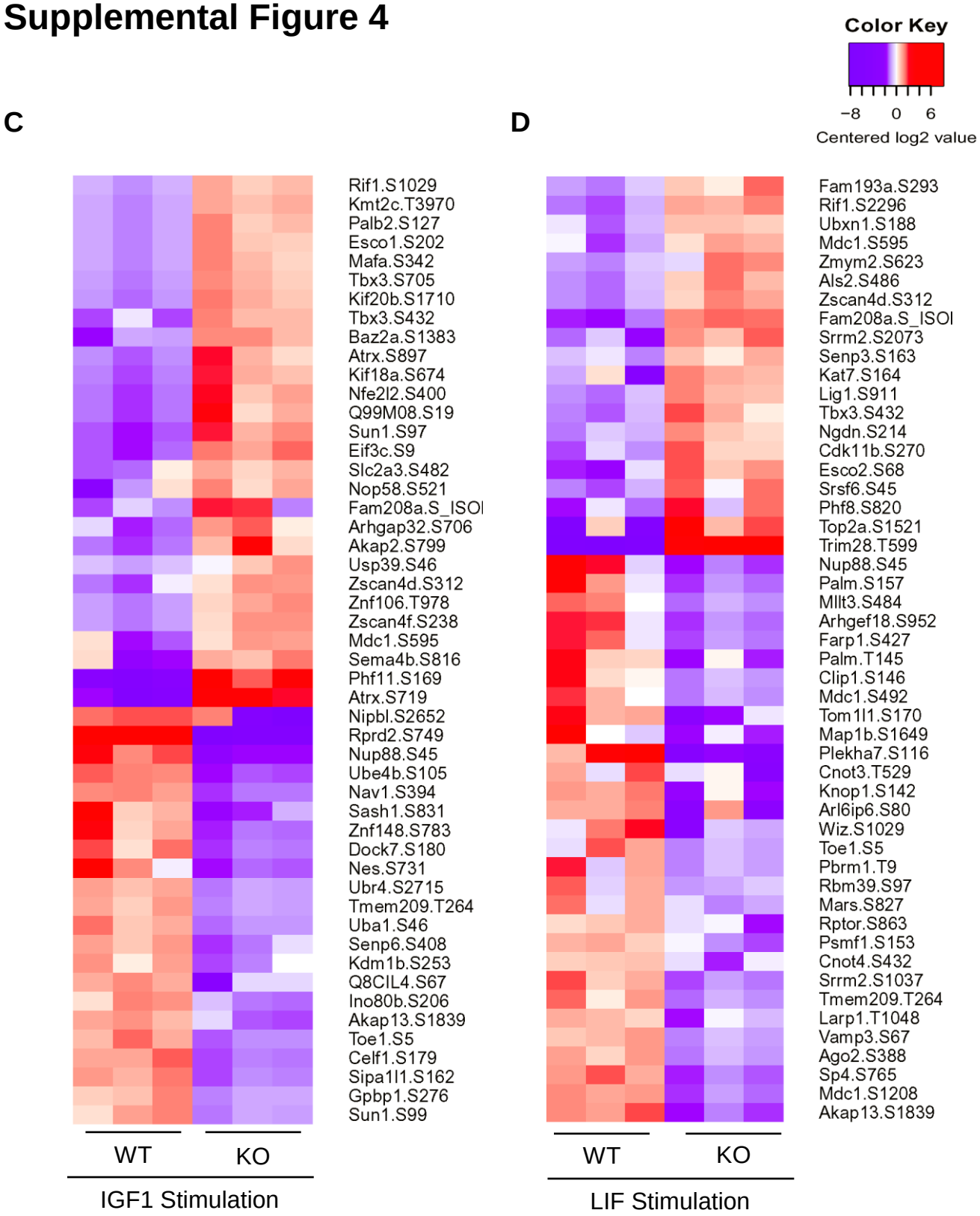

Supplemental Figure S4 : Phosphoproteomics analyses of control and IR KO iPSCs stimulated with IGF1 (**C**) or LIF (**D**). Red color denotes upregulated while blue color defines downregulated phosphoproteins (Related to Figure 4). N=3.

Supplemental Figure 4 (Continued)

E

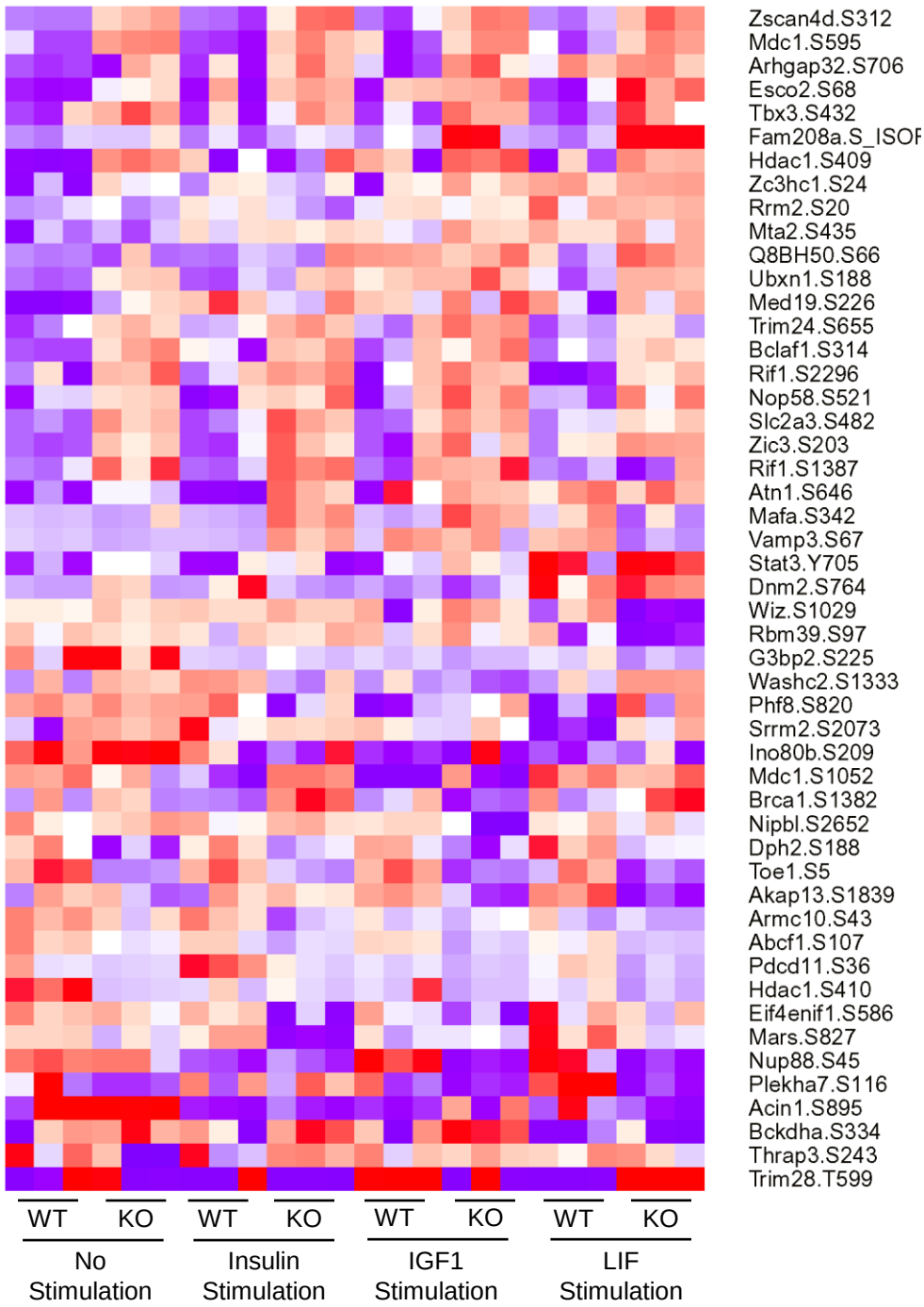

Supplemental Figure S4 : E. Individual samples phosphoproteomics analyses of control and IR KO iPSCs at basal and stimulated conditions. Red color denotes upregulated while blue color defines downregulated phosphoproteins (Related to Figure 4). N=3.

Supplemental Figure 4 (Continued)

F

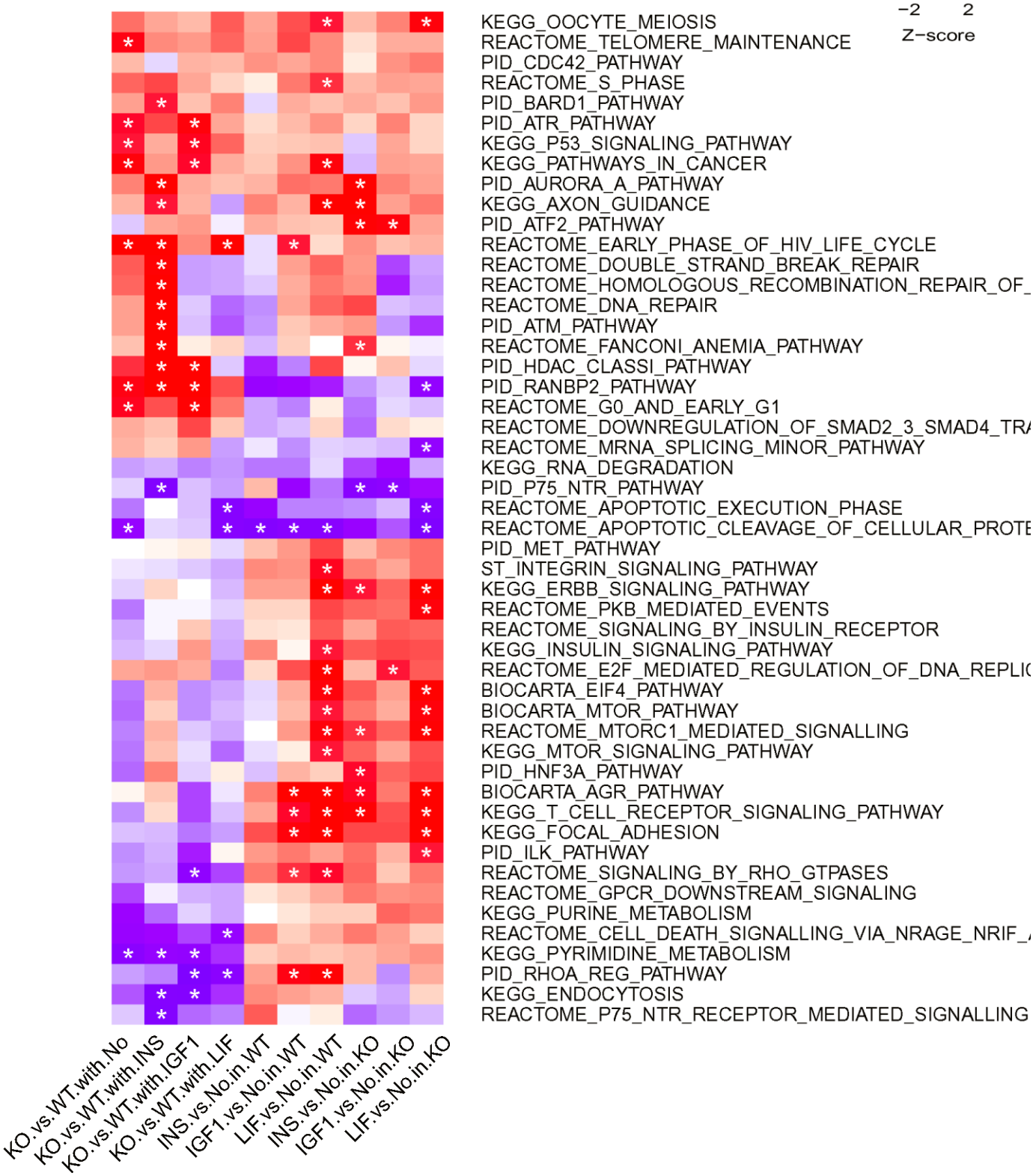

Supplemental Figure S4 : F. Pathway analyses of altered phosphosites in control and IR KO iPSCs at basal and stimulated conditions (Related to Figure 4). N=3.

Supplemental Figure 4 (Continued)

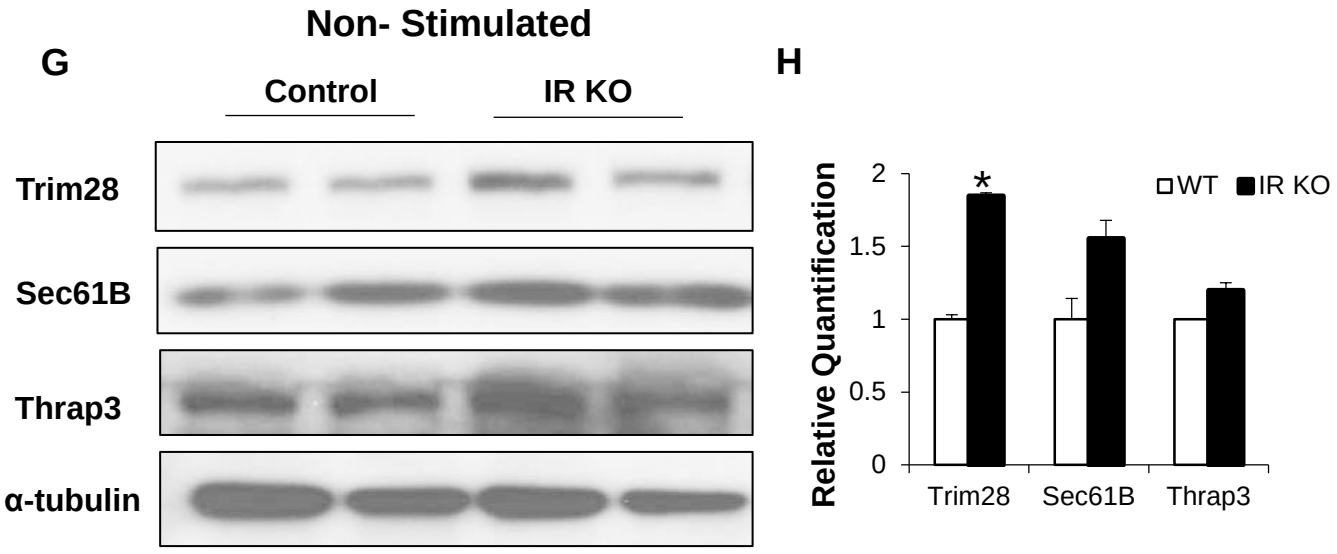

Supplemental Figure S4 G and H: . G. Protein analysis of candidates by western blotting showing decreased phosphorylation in the unstimulated state. **H**. Density quantification of western blots. α-tubulin was used as internal control (Related to Figure 4). (n=4; *, $p<0.05$).

Chapter V – Conclusion

5. Conclusion

5.1 NREP Bridges TGF-ß Signaling and Lipid Metabolism in the Epigenetic Reprogramming of NAFLD in the Offspring of Insulin-Resistant Parents

This work, for the first time to our knowledge, links the TGF-β pathway and lipid metabolism in the context of NAFLD epigenetic priming using a unique non-dietary model of insulin resistance and dyslipidemia. The work presented here points to the role of paternal genetic insulin resistance in epigenetic reprograming of NREP in hepatocytes. The findings indicate a novel molecular bridge between TGF-β signaling and hepatic lipid metabolism that is highly susceptible to environmental triggers such as a high calorie diet. Our mechanistic data suggests that NREP controls hepatic lipid content (e.g. cholesterol and triglycerides) in an AKT dependent manner and identifies NREP as a possible novel molecular mediator of the development of NAFLD. NAFLD is characterized by severe hepatic lipid accumulation which frequently progresses to liver cancer. The precise role of PI3K>AKT>GSK3 pathway in the development of NAFLD is controversial and remains largely unexplored. Our findings are significant in the context of a role for AKT in the progression of NAFLD. However, to fully elucidate the role of NREP we propose to further characterize the signaling events mediating AKT phosphorylation including the involvement of PTEN. Currently, we are conducting additional studies to determine the physiological role of NREP by using the AAV8 system to overexpress NREP *in vivo* and by treating mouse models of NAFLD with recombinant NREP. We are also dissecting the signaling pathways that mediate the effects of NREP effects in regulating hepatic lipid metabolism by comparing phosphoproteomics in samples of human primary hepatocytes with or without a knock-down of NREP.

5.2 Insulin receptor-mediated signaling regulates pluripotency markers and lineage differentiation

In this thesis, we reveal a novel role for IR-mediated signaling in the global regulation of the pluripotency network and differentiation potential. We report that stem cells with a knockout of the insulin receptor display a shift towards ectodermal differentiation due to increased pErk. The intriguing observation that IR KO cells show enhanced Erk phosphorylation suggests that IR inhibits the Erk pathway during normal

differentiation. This novel observation warrants further investigation to explore the link between IR mediated signaling and Erk pathways during development. We report several new phosphosites downstream of insulin, IGF1 and LIF that are a great resource for the scientific community and provide a unique opportunity to further examine their significance as pluripotency regulators and development mediators. Finally, to further elucidate the transcriptional pluripotency network altered by IR ablation we are currently employing RNA-sequencing experiments in iPSCs devoid of IR.

Chapter VI – Bibliography

6. Bibliography

Belfiore, A., F. Frasca, et al. (2009). "Insulin Receptor Isoforms and Insulin Receptor/Insulin-Like Growth Factor Receptor Hybrids in Physiology and Disease." Endocr Rev 30(6): 586-623.

Bendall, S. C., M. H. Stewart, et al. (2007). "IGF and FGF cooperatively establish the regulatory stem cell niche of pluripotent human cells in vitro." Nature 448: 1015.

Bhutani, N., David M. Burns, et al. (2011). "DNA Demethylation Dynamics." Cell 146(6): 866-872.

Blüher, M., M. D. Michael, et al. (2002). "Adipose Tissue Selective Insulin Receptor Knockout Protects against Obesity and Obesity-Related Glucose Intolerance." Developmental Cell 3(1): 25-38.

Brumbaugh, D. E. and J. E. Friedman (2013). "Developmental origins of nonalcoholic fatty liver disease." Pediatric Research 75: 140.

Brüning, J. C., D. Gautam, et al. (2000). "Role of Brain Insulin Receptor in Control of Body Weight and Reproduction." Science 289(5487): 2122-2125.

Burgueño, A. L., R. Cabrerizo, et al. (2013). "Maternal high-fat intake during pregnancy programs metabolic-syndrome-related phenotypes through liver mitochondrial DNA copy number and transcriptional activity of liver PPARGC1A." The Journal of Nutritional Biochemistry 24(1): 6-13.

Bush, H., P. Golabi, et al. (2017). "Pediatric Non-Alcoholic Fatty Liver Disease." Children 4(6): 48.

Buzzetti, E., M. Pinzani, et al. (2016). "The multiple-hit pathogenesis of non-alcoholic fatty liver disease (NAFLD)." Metabolism - Clinical and Experimental 65(8): 1038-1048.

Carone, B. R., L. Fauquier, et al. (2010). "Paternally Induced Transgenerational Environmental Reprogramming of Metabolic Gene Expression in Mammals." Cell 143(7): 1084-1096.

Chen, C.-Y., Y.-Y. Cheng, et al. (2017). "Mechanisms of pluripotency maintenance in mouse embryonic stem cells." Cellular and Molecular Life Sciences 74(10): 1805-1817.

Chen, H., R. Guo, et al. (2015). "Erk signaling is indispensable for genomic stability and self-renewal of mouse embryonic stem cells." Proceedings of the National Academy of Sciences 112(44): E5936-E5943.

Costanza, B., I. Umelo, et al. (2017). "Stromal Modulators of TGF-β in Cancer." Journal of Clinical Medicine 6(1): 7.

De Meyts, P. and J. Whittaker (2002). "Structural biology of insulin and IGF1 receptors: implications for drug design." Nat Rev Drug Discov 1(10): 769-783.

Donnelly, K. L., C. I. Smith, et al. (2005). "Sources of fatty acids stored in liver and secreted via lipoproteins in patients with nonalcoholic fatty liver disease." The Journal of Clinical Investigation 115(5): 1343-1351.

Eslam, M., L. Valenti, et al. (2018). "Genetics and epigenetics of NAFLD and NASH: Clinical impact." J Hepatol 68(2): 268-279.

Evans, M. J. and M. H. Kaufman (1981). "Establishment in culture of pluripotential cells from mouse embryos." Nature 292: 154.

Hall, J., G. Guo, et al. (2009). "Oct4 and LIF/Stat3 Additively Induce Krüppel Factors to Sustain Embryonic Stem Cell Self-Renewal." Cell Stem Cell 5(6): 597-609.

Iovino, S., A. M. Burkart, et al. (2014). "Genetic Insulin Resistance Is a Potent Regulator of Gene Expression and Proliferation in Human iPS Cells." Diabetes 63(12): 4130-4142.

Kulkarni, R. N., J. C. Brüning, et al. (1999). "Tissue-Specific Knockout of the Insulin Receptor in Pancreatic β Cells Creates an Insulin Secretory Defect Similar to that in Type 2 Diabetes." Cell 96(3): 329-339.

Li, M., C. M. Reynolds, et al. (2015). "Developmental Programming of Nonalcoholic Fatty Liver Disease: The Effect of Early Life Nutrition on Susceptibility and Disease Severity in Later Life." BioMed Research International 2015: 12.

Lin, J., C. Handschin, et al. (2005). "Metabolic control through the PGC-1 family of transcription coactivators." Cell Metabolism 1(6): 361-370.

Liu, Z. Z., A. Kumar, et al. (1997). "Developmental regulation and the role of insulin and insulin receptor in metanephrogenesis." Proceedings of the National Academy of Sciences 94(13): 6758-6763.

Loh, Y.-H., Q. Wu, et al. (2006). "The Oct4 and Nanog transcription network regulates pluripotency in mouse embryonic stem cells." Nature Genetics 38: 431.

Loomba, R., N. Schork, et al. (2015). "Heritability of Hepatic Fibrosis and Steatosis Based on a Prospective Twin Study." Gastroenterology 149(7): 1784-1793.

Magner, N. L., Y. Jung, et al. (2013). "Insulin and igfs enhance hepatocyte differentiation from human embryonic stem cells via the PI3K/AKT pathway." STEM CELLS 31(10): 2095-2103.

Mazzio, E. A. and K. F. A. Soliman (2012). "Basic concepts of epigenetics: Impact of environmental signals on gene expression." Epigenetics 7(2): 119-130.

Michael, M. D., R. N. Kulkarni, et al. (2000). "Loss of Insulin Signaling in Hepatocytes Leads to Severe Insulin Resistance and Progressive Hepatic Dysfunction." Molecular cell 6(1): 87-97.

Navarro, P., N. Festuccia, et al. (2012). "OCT4/SOX2-independent Nanog autorepression modulates heterogeneous Nanog gene expression in mouse ES cells." EMBO J 31(24): 4547-4562.

Niwa, H., J.-i. Miyazaki, et al. (2000). "Quantitative expression of Oct-3/4 defines differentiation, dedifferentiation or self-renewal of ES cells." Nature Genetics 24: 372.

Paliwal, S., J. Shi, et al. (2004). "P311 binds to the latency associated protein and downregulates the expression of TGF-β1 and TGF-β2." Biochemical and Biophysical Research Communications 315(4): 1104-1109.

Pan, D., X. Zhe, et al. (2002). "P311 induces a TGF-β1–independent, nonfibrogenic myofibroblast phenotype." The Journal of Clinical Investigation 110(9): 1349-1358.

Pruis, M. G. M., Á. Lendvai, et al. (2014). "Maternal western diet primes non-alcoholic fatty liver disease in adult mouse offspring." Acta Physiologica 210(1): 215-227.

Saltiel, A. R. and C. R. Kahn (2001). "Insulin signalling and the regulation of glucose and lipid metabolism." Nature 414(6865): 799-806.

Samuel, W., C. N. Nagineni, et al. (2002). "Transforming Growth Factor-β Regulates Stearoyl Coenzyme A Desaturase Expression through a Smad Signaling Pathway." Journal of Biological Chemistry 277(1): 59-66.

Schwarz, Benjamin A., O. Bar-Nur, et al. (2014). "Nanog Is Dispensable for the Generation of Induced Pluripotent Stem Cells." Current Biology 24(3): 347-350.
Schwimmer, J. B., M. A. Celedon, et al. (2009). "Heritability of Nonalcoholic Fatty Liver Disease." Gastroenterology 136(5): 1585-1592.

Sookoian, S., M. S. Rosselli, et al. (2010). "Epigenetic regulation of insulin resistance in nonalcoholic fatty liver disease: Impact of liver methylation of the peroxisome proliferator–activated receptor γ coactivator 1α promoter." Hepatology 52(6): 1992-2000.

Sterneckert, J., S. Höing, et al. (2012). "Concise Review: Oct4 and More: The Reprogramming Expressway." STEM CELLS 30(1): 15-21.

Stradiot, L., I. Mannaerts, et al. (2018). "P311, Friend, or Foe of Tissue Fibrosis?" Frontiers in Pharmacology 9(1151).

Studler, J.-M., J. Glowinski, et al. (1993). "An Abundant mRNA of the Embryonic Brain Persists at a High Level in Cerebellum, Hippocampus and Olfactory Bulb During Adulthood." European Journal of Neuroscience 5(6): 614-623.

Suzuki, M. M. and A. Bird (2008). "DNA methylation landscapes: provocative insights from epigenomics." Nat Rev Genet 9(6): 465-476.

Taguchi, A. and M. F. White (2008). "Insulin-Like Signaling, Nutrient Homeostasis, and Life Span." Annual Review of Physiology 70(1): 191-212.

Takahashi, K. and S. Yamanaka (2006). "Induction of Pluripotent Stem Cells from Mouse Embryonic and Adult Fibroblast Cultures by Defined Factors." Cell 126(4): 663-676.

Takahashi, K. and S. Yamanaka (2016). "A decade of transcription factor-mediated reprogramming to pluripotency." Nature Reviews Molecular Cell Biology 17: 183.

Taylor, G. A., E. Hudson, et al. (2000). "Regulation of P311 Expression by Met-Hepatocyte Growth Factor/Scatter Factor and the Ubiquitin/Proteasome System." Journal of Biological Chemistry 275(6): 4215-4219.

Wang, L., T. C. Schulz, et al. (2007). "Self-renewal of human embryonic stem cells requires insulin-like growth factor-1 receptor and ERBB2 receptor signaling." Blood 110(12): 4111-4119.

Williams, K., J. Christensen, et al. (2012). "DNA methylation: TET proteins[mdash]guardians of CpG islands?" EMBO Rep 13(1): 28-35.

Yang, L., Y. S. Roh, et al. (2014). "Transforming growth factor beta signaling in hepatocytes participates in steatohepatitis through regulation of cell death and lipid metabolism in mice." Hepatology 59(2): 483-495.

Ye, S., D. Liu, et al. (2014). "Signaling pathways in induced naïve pluripotency." Curr Opin Genet Dev 28: 10-15.

Younossi, Z., Q. M. Anstee, et al. (2018). "Global burden of NAFLD and NASH: trends, predictions, risk factors and prevention." Nat Rev Gastroenterol Hepatol 15(1): 11-20.

Yu, J. S. L. and W. Cui (2016). "Proliferation, survival and metabolism: the role of PI3K/AKT/mTOR signalling in pluripotency and cell fate determination." Development 143(17): 3050-3060.

Zeybel, M., T. Hardy, et al. (2015). "Differential DNA methylation of genes involved in fibrosis progression in non-alcoholic fatty liver disease and alcoholic liver disease." Clinical Epigenetics 7(1): 25.

Zhang, S. and W. Cui (2014). "Sox2, a key factor in the regulation of pluripotency and neural differentiation." World J Stem Cells 6(3): 305-311.

Zhao, H. and Y. Jin (2017). "Signaling networks in the control of pluripotency." Curr Opin Genet Dev 46: 141-148.

Zhu, J.-K. (2009). "Active DNA Demethylation Mediated by DNA Glycosylases." Annual Review of Genetics 43(1): 143-166.

Appendix

Appendix A1

Publication

Dirice E, Kahraman S, Jiang W, El Ouaamari A, **De Jesus DF**, Teo A, Hu J, Kawamori D, Gaglia J, Mathis D, Kulkarni RN. Soluble factors secreted by T-cells promote β-cell proliferation. Diabetes 63:188-202, 2014.

Contribution

I contributed by performing genotyping, animal phenotyping, histochemistry, and assisting in islet isolation.

Ercument Dirice,[1] Sevim Kahraman,[1] Wenyu Jiang,[2] Abdelfattah El Ouaamari,[1] Dario F. De Jesus,[1] Adrian K.K. Teo,[1] Jiang Hu,[1] Dan Kawamori,[1] Jason L. Gaglia,[3] Diane Mathis,[4] and Rohit N. Kulkarni[1]

Soluble Factors Secreted by T Cells Promote β-Cell Proliferation

Type 1 diabetes is characterized by infiltration of pancreatic islets with immune cells, leading to insulin deficiency. Although infiltrating immune cells are traditionally considered to negatively impact β-cells by promoting their death, their contribution to proliferation is not fully understood. Here we report that islets exhibiting insulitis also manifested proliferation of β-cells that positively correlated with the extent of lymphocyte infiltration. Adoptive transfer of diabetogenic $CD4^+$ and $CD8^+$ T cells, but not B cells, selectively promoted β-cell proliferation in vivo independent from the effects of blood glucose or circulating insulin or by modulating apoptosis. Complementary to our in vivo approach, coculture of diabetogenic $CD4^+$ and $CD8^+$ T cells with NOD.RAG1$^{-/-}$ islets in an in vitro transwell system led to a dose-dependent secretion of candidate cytokines/chemokines (interleukin-2 [IL-2], IL-6, IL-10, MIP-1α, and RANTES) that together enhanced β-cell proliferation. These data suggest that soluble factors secreted from T cells are potential therapeutic candidates to enhance β-cell proliferation in efforts to prevent and/or delay the onset of type 1 diabetes.

Diabetes 2014;63:188–202 | DOI: 10.2337/db13-0204

ISLET STUDIES

Type 1 diabetes (T1D) is a chronic T-cell–mediated autoimmune disease characterized by selective destruction of β-cells, resulting in hyperglycemia (1). A major limitation to successful therapy has been a lack of complete understanding of the precise pathways and mechanisms that trigger T1D compounded by the polygenic nature of the disease and the influence of environmental and/or stochastic factors (2).

Studies using the nonobese diabetic (NOD) mice have identified roles for $CD4^+$ and $CD8^+$ T cells and macrophages in β-cell destruction. Other cell types, including B cells, natural killer (NK) cells, NKT cells, and the dendritic cell subsets, have also been detected in the pancreatic infiltrate and draining lymph nodes and could contribute to β-cell death (3).

Although immune cells are generally considered to promote β-cell death, some studies argue that they also enhance their replication. For example, Sreenan et al. (4) have reported increased β-cell proliferation in NOD mice that exhibit infiltration of pancreatic islets prior to the onset of diabetes. In addition, von Herrath et al. (5) reported that nondiabetic RIP-LCMV x SV129 mice, where the numbers and effector functions of autoaggressive $CD4^+$ and $CD8^+$ lymphocytes were not decreased, have increased β-cell regeneration compared with nondiabetic C57BL/6 controls. In other studies, Sherry et al. (6) suggested the increased β-cell proliferation that occurs after arresting the autoimmune process is secondary to effects of the inflammatory infiltrate. The latter study also showed that reversal of infiltration by anti-CD3

[1]Section of Islet Cell Biology and Regenerative Medicine, Joslin Diabetes Center and Harvard Medical School, Boston, MA
[2]Department of Pathology, Brigham and Women's Hospital, Boston, MA
[3]Section of Immunobiology, Joslin Diabetes Center and Harvard Medical School, Boston, MA
[4]Division of Immunology, Department of Microbiology and Immunobiology, Harvard Medical School, Boston, MA

Corresponding author: Rohit N. Kulkarni, rohit.kulkarni@joslin.harvard.edu.

Received 5 February 2013 and accepted 15 September 2013.

This article contains Supplementary Data online at http://diabetes.diabetesjournals.org/lookup/suppl/doi:10.2337/db13-0204/-/DC1.

S.K. and W.J. contributed equally to this study.

monoclonal antibody (mAb) or regulatory T-cell therapy was associated with reduced β-cell proliferation. A notable study that partially addressed the mechanism is that by Dor and colleagues (7), who reported that the use of standard immunosuppression drugs abolished β-cell proliferation and recovery from diabetes. Recent studies have also reported that humans with T1D exhibit persistent mature β-cells in the pancreas that may be secondary to protective factors that prevent their destruction (8,9). An understanding of how these β-cells survive and/or regenerate is an exciting and timely area of interest.

Notwithstanding the scant information on the ability of human β-cells to replicate (10,11), studies in rodent models indicate that β-cell proliferation is increased in physiologic conditions, pathophysiologic states, and injury models (7,12–15). In these models, glucose, insulin, IGFs, growth hormone, glucagon-like peptide 1, adipokines such as leptin, hepatocyte growth factor, and lactogens such as prolactin have all been implicated in regulating β-cell proliferation (16).

In addition to the factors noted above, cytokines derived from the inflammatory response itself have been reported to stimulate islet cell replication (17,18), and treatment with interleukin-4 (IL-4) or IL-10 has been reported to inhibit the development and prevent the recurrence of T1D in NOD mice (19,20).

In this study, we tested the hypothesis that one or more lymphocytes, or their secretions, promote β-cell regeneration in vivo. We report, for the first time to our knowledge, that $CD4^+$ and $CD8^+$ T-cell subsets, but not B cells, secrete soluble factors and are potential novel targets that can be harnessed to promote β-cell proliferation to counter the progression of T1D.

RESEARCH DESIGN AND METHODS

Mice

Female NOD/shiLTJ mice, 20 weeks of age, were used as splenocyte donors, and NOD.RAG1$^{-/-}$ mice, 5–6 weeks of age, were used as recipients for adoptive transfer studies and islet donors for splenocyte-islet coculture experiments. Male C57BL/6J (B6) mouse islets, 5–6 weeks of age, were used for recombinant protein treatments. Blood glucose was measured under ad libidum conditions, and mice were considered diabetic when two consecutive measurements of blood glucose exceeded 200 mg/dL.

Adoptive Transfer of Diabetes and Depletion of Splenocytes

A total of 10^7 splenocytes were purified from NOD mice with diabetes and injected intravenously into a single NOD.RAG1$^{-/-}$ mouse. To obtain splenocyte preparations devoid of B cells and $CD4^+$ and $CD8^+$ T cells, they were incubated with anti–B220-PE, anti–CD4-PE, and anti–CD8a-PE (BioLegend), respectively. The cells were washed in PBS and resuspended in magnetic-activated cell sorter (MACS) buffer and anti-PE Microbeads and run on the autoMACS system (Miltenyi Biotec). Samples from the B-cell–, $CD4^+$-, and $CD8^+$-depleted splenocyte aliquots were stained with anti-mouse CD19-PE, anti–CD4-Pacific Blue, and anti–CD8a-FITC (BioLegend), respectively, analyzed with a FACSAria (BD Biosciences), and determined to be >98% depleted (data not shown). For $CD4^+$ and $CD8^+$ double depletion, fractionated depleted cells were injected into NOD.RAG1$^{-/-}$ mice. We also used in vivo depletion by injecting 0.5 mg of anti-CD4, anti-CD8, or both mAbs into NOD.RAG1$^{-/-}$ mice every 3 days after depleted splenocyte transfer. Three weeks postinjection of total or depleted splenocytes, pancreas was harvested and prepared for β-cell morphometry. To track lymphocyte homing to host pancreatic islets in adoptively transferred mice, we used NOD.Raspberry splenocytes from mice generated by microinjection of a β-actin/mRaspberry construct in the pronucleus of fertilized NOD mouse eggs.

Streptozotocin Injection and Insulitis Scoring

Eighteen female NOD mice 6 weeks of age were injected intraperitoneally with streptozotocin (STZ) (Sigma-Aldrich) at a concentration of 75 or 100 mg/kg/body weight (BW). Day 0 was defined as the first day of injection, and pancreas was harvested from three mice every other day starting at day 1 until day 7. Insulitis was evaluated as reported (21).

Immunohistochemistry

Pancreata were harvested, fixed, and embedded in paraffin 6 h postinjection with BrdU (100 mg/kg/BW). Sections were stained using antibodies to BrdU, Ki67, phosphohistone H3, or insulin and appropriate secondary antibodies and counterstained with DAPI. At least 1,000–2,000 β-cell nuclei were counted per animal, and data were expressed as percentage of $BrdU^+$, $Ki67^+$, or $pHH3^+$ β-cells. Cell death was detected by TUNEL assay (ApopTag S7100; Chemicon). Frozen sections were coimmunostained for insulin and a DSRed polyclonal antibody (Clontech) to detect mRaspberry protein followed by appropriate secondary antibodies.

Islet Isolation and Mixed Lymphocyte-Islet Cell Culture

Islets were isolated from 5–6-week-old NOD.RAG1$^{-/-}$ or B6 mice and cultured as described previously (22). In parallel, we prepared depleted or total lymphocyte cell suspensions from 20-week-old diabetic (DM) or 7–8-week-old prediabetic (pre-DM) female NOD mice (23). After starvation, 150 size-matched islets were cocultured with splenocytes or treated with recombinant proteins in 5 mmol/L glucose. Contact between islets and splenocytes placed above the transwell membrane was prevented by using a 0.4-μm transwell insert (Corning Life Sciences). Forty-eight hours after coculture, medium was collected for Luminex assay and islets were embedded in agar for β-cell morphometry. At least 1,000–2,000 β-cell nuclei were counted for quantifying proliferation and apoptosis.

Islet Dispersion and Cell Sorting

Overnight cultured islets were dispersed and β-cells were sorted as described previously (24). Sorted β-cells were washed and stained with anti-CD45 (eBioscience) followed by fixation, permeabilization, and staining with anti-BrdU (BrdU Staining Kit-APC; eBioscience). Cells were analyzed with BD LSR II analyzer.

Recombinant Protein Treatment

One hundred fifty handpicked islets isolated from B6 mice were cultured in the absence or presence of IL-2 (5 or 500 pg/mL), IL-6 (200 pg/mL or 200 ng/mL), IL-10 (4 or 400 pg/mL), macrophage inflammatory protein 1α (MIP-1α) (10 pg/mL or 10 ng/mL), RANTES (5 or 500 pg/mL), a low-dose combination of all the cytokines/chemokines, or 15% FBS (positive control). Low doses were selected from our Luminex assay results, and high doses were based on manufacturer recommendations (R&D Systems). To determine whether the proliferative effects are direct, islets treated with either recombinant proteins or total DM splenocytes were cultured in the presence of specific inhibitors/neutralizing molecules: Ro 26-4550 (IC_{50} = 3 μmol/L), anti–IL-6 (ND_{50} = 0.005 μg/mL), anti–IL-10 (ND_{50} = 0.045 μg/mL), maraviroc (IC_{50} = 3.3 nmol/L), and maraviroc (IC_{50} = 5.2 nmol/L) to block IL-2, IL-6, IL-10, MIP-1α, and RANTES, respectively

Statistics

Data are expressed as means ± SEM after a two-tailed Student *t* test and considered significant at *P* value ≤0.05.

Study Approval

All animal experiments were conducted after approval by the Institutional Animal Care and Use Committee of the Joslin Diabetes Center in accordance with National Institutes of Health (NIH) guidelines.

RESULTS

Adoptive Transfer of Diabetogenic Splenocytes Promotes β-Cell Replication in NOD.RAG1$^{-/-}$ Mice

To directly examine whether splenocytes induce proliferation of β-cells, we performed adoptive transfer experiments (6,25). We used 20-week-old hyperglycemic (DM) or 7–8-week-old normoglycemic NOD mice (pre-DM) as splenocyte donors. Since the kinetics of disease transfer are dependent on the age of the mice when the splenocytes are transferred (26) and most islets in prediabetic animals have only peri-insulitis (Supplementary Fig. 1*A*), we considered pre-DM as the control cohort. To confirm that splenocytes after adoptive transfer target host pancreatic islets, we injected splenocytes derived from hyperglycemic NOD.Raspberry mice congenically marked with mRaspberry fluorescent protein, a far red protein that is generally preferred for in vivo imaging, into female NOD mice. We visualized that marked cells accumulate and infiltrate into host islets (Supplementary Fig. 1*B*). Intravenous injection of freshly isolated total DM splenocytes or control pre-DM splenocytes into 5–6-week-old immune-deficient NOD.RAG1$^{-/-}$ mice (Fig. 1*A*) showed a significant increase in β-cell mitosis in the group injected with DM splenocytes compared with controls. To ascertain that we were counting only proliferating β-cells and not overlapping immune cells, we used confocal microscopy z-stack, three-dimensional (3D), and orthographic imaging and double staining for insulin and CD3, a T-cell receptor marker, or F4/80, a common macrophage marker (Fig. 2*A–N*). A fivefold increase in BrdU incorporation indicated β-cells in the S phase of the cell cycle (Fig. 1*B* and *C*), whereas an augmentation in pHH3 immunostaining suggested progression into the G2 or M phases (Fig. 1*B* and *D*). The enhanced mitosis was confirmed using Ki67 (Fig. 1*B* and *E*). To confirm our immunohistological findings, we performed fluorescence-activated cell sorter analysis of dispersed islets for β-cell sorting according to autofluorescence and size (Fig. 2*O* and *P*). We used CD45 staining to gate out immune cells and quantified BrdU^{+} β-cells (Fig. 2*Q*). We examined BrdU immunostaining in the CD45^{+} cell population as an internal control (Supplementary Fig. 1*C–F*). The increase in proliferating β-cells was consistent with the immunohistological data (Fig. 2*R–T*). In addition, coimmunostaining for BrdU and insulin or GLUT2 (β-cell membrane marker) confirmed the identity of the cells (Supplementary Fig. 2*A* and *B*). TUNEL immunostaining did not reveal significant differences in β-cell apoptosis between groups (Fig. 1*F* and *G*). Together these data indicate that injection of splenocytes isolated from DM promotes β-cell replication in vivo.

T Cells, but Not B Cells, Are the Dominant Players in β-Cell Proliferation

Previous studies have reported that T1D is primarily a T-cell–mediated autoimmune disease (27–29). To evaluate the effect of B cells on β-cell proliferation, we injected total (10^7) or B-cell–depleted (6.4×10^6) cell populations intravenously into female NOD.RAG1$^{-/-}$ mice (Fig. 1*A*) followed, 3 weeks later, by harvesting of pancreas, liver, and epididymal fat. Coimmunostaining of BrdU and insulin in pancreas sections from animals receiving total splenocytes from diabetic animals and animals administered B-cell–depleted splenocytes showed no significant difference in β-cell replication (Fig. 3*A* and *B*). Furthermore, coimmunostaining of pancreas sections for PDX1 (pancreatic and duodenal homebox-1), a β-cell transcription factor, and BrdU did not reveal differences between groups (Supplementary Fig. 2*C*). The β-cell specificity of the effects on proliferation was confirmed by a virtual lack of proliferation in hepatocytes or adipocytes (Supplementary Fig. 2*D* and *E*). These data demonstrate that B cells are unlikely to contribute to β-cell proliferation in this model.

We next evaluated the relative importance of T cells for β-cell proliferation using a similar approach. We

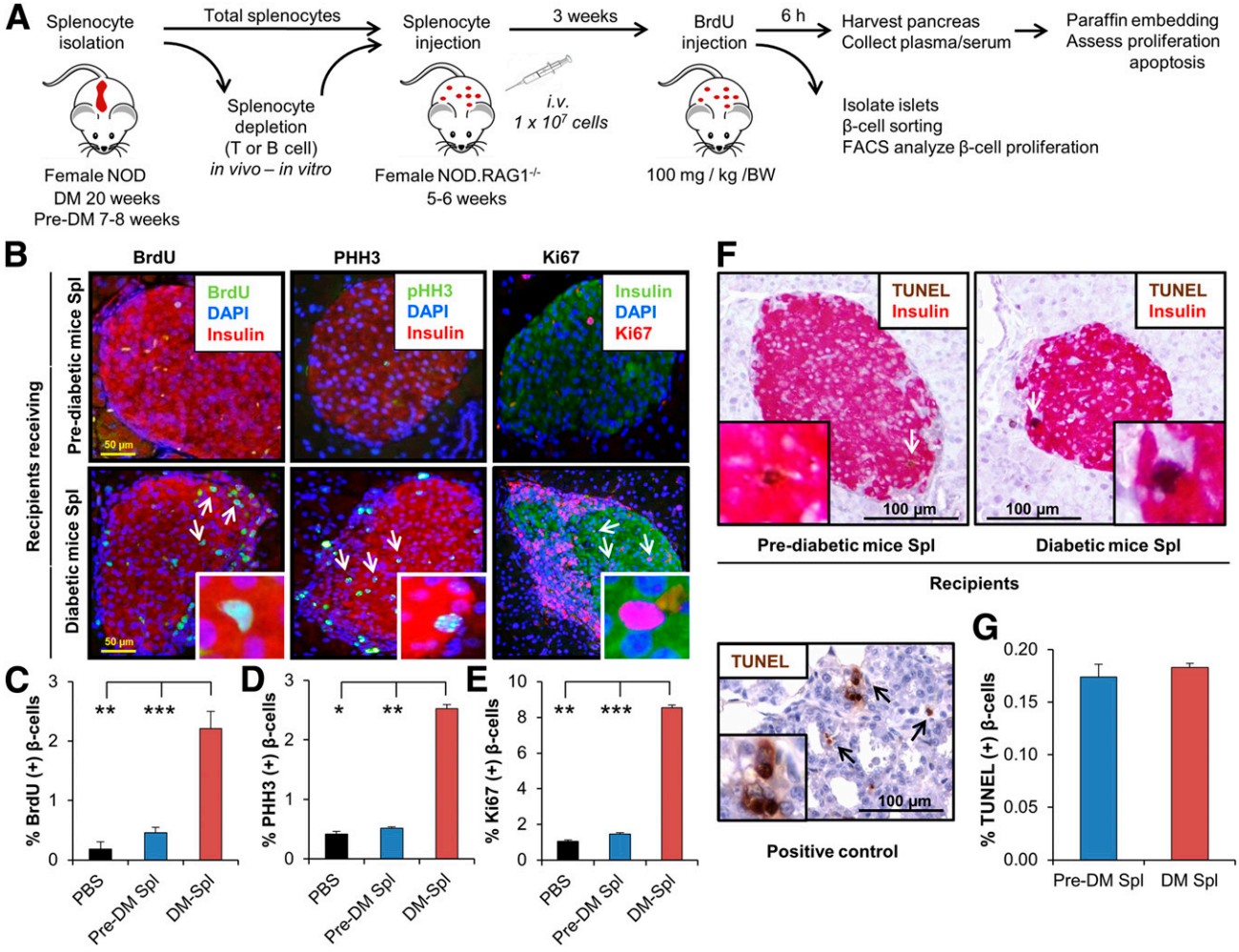

Figure 1—Adoptive transfer of diabetes stimulates β-cell proliferation in NOD.RAG1$^{-/-}$ recipients. *A*: Experimental strategy showing total splenocyte (DM or pre-DM) or depleted splenocyte (diabetic mice) transfer (1×10^7 cells) into NOD.RAG1$^{-/-}$ mice. BrdU (100 mg/kg/BW) was injected 3 weeks post-transfer, and 6 h later, the pancreases were harvested for immunohistochemical analyses. *B*: Paraffin-embedded sections of pancreas from mice receiving DM or pre-DM splenocytes, costained with proliferation markers BrdU, pHH3, or Ki67 with insulin and DAPI. Scale bar, 50 μm. Arrows indicate proliferating β-cells (BrdU$^+$/insulin$^+$). Insets show magnified view of representative proliferating β-cells. Quantification of data shown in *B* for BrdU (*C*), pHH3 (*D*), and Ki67 (*E*) (n = 4–16 mice in each group). *$P < 0.05$; **$P < 0.01$; ***$P < 0.001$ (Student t test). *F*: TUNEL staining of paraffin-embedded sections of pancreatic tissues obtained from recipient mice receiving DM or pre-DM splenocytes for apoptosis detection. Scale bar, 100 μm. Arrows indicate TUNEL$^+$/β-cell$^+$ cells undergoing apoptosis. Inset shows a magnified representative image of TUNEL$^+$ β-cell. Lower image represents positive control of TUNEL staining in rat tumor tissue. *G*: Quantification of data in *F*. n = 4–6 mice in each group. Data are expressed as means ± SEM. FACS, fluorescence-activated cell sorting; Spl, splenocyte.

considered CD4$^+$ and CD8$^+$ T cells to be likely candidate(s) because they are the major T-cell subsets infiltrating in or around the islets and are the final executors of β-cell destruction (30). In addition to in vitro depletion, we injected NOD.RAG1$^{-/-}$ mice receiving in vitro depleted splenocytes with anti-CD4, anti-CD8, or both mAbs to promote in vivo depletion. The groups receiving the individual CD4$^+$- and CD8$^+$-depleted splenocytes as well as the CD4/CD8–double-depleted splenocytes exhibited dramatically decreased β-cell proliferation compared with the groups injected either with whole splenocytes from diabetic animals or B-cell–depleted splenocytes. Moreover, mice that received CD8$^+$-depleted splenocytes showed a slightly greater β-cell proliferation compared with animals administered CD4$^+$ or double-depleted splenocytes ($P < 0.05$) (Fig. 3*B*). Apoptosis tended to be higher in the total DM splenocyte– and B-cell–depleted splenocyte–administered animals but did not reach statistical significance (Supplementary Fig. 5*A*). These results suggest that CD4$^+$ and CD8$^+$ T cells act together to stimulate β-cell replication in animals injected with diabetogenic splenocytes.

β-Cell Proliferation Is Positively Correlated With Islet Infiltration

Infiltration in the pancreatic islets with mononuclear inflammatory cells is a key feature in T1D in NOD mice. An interesting observation during the analyses of

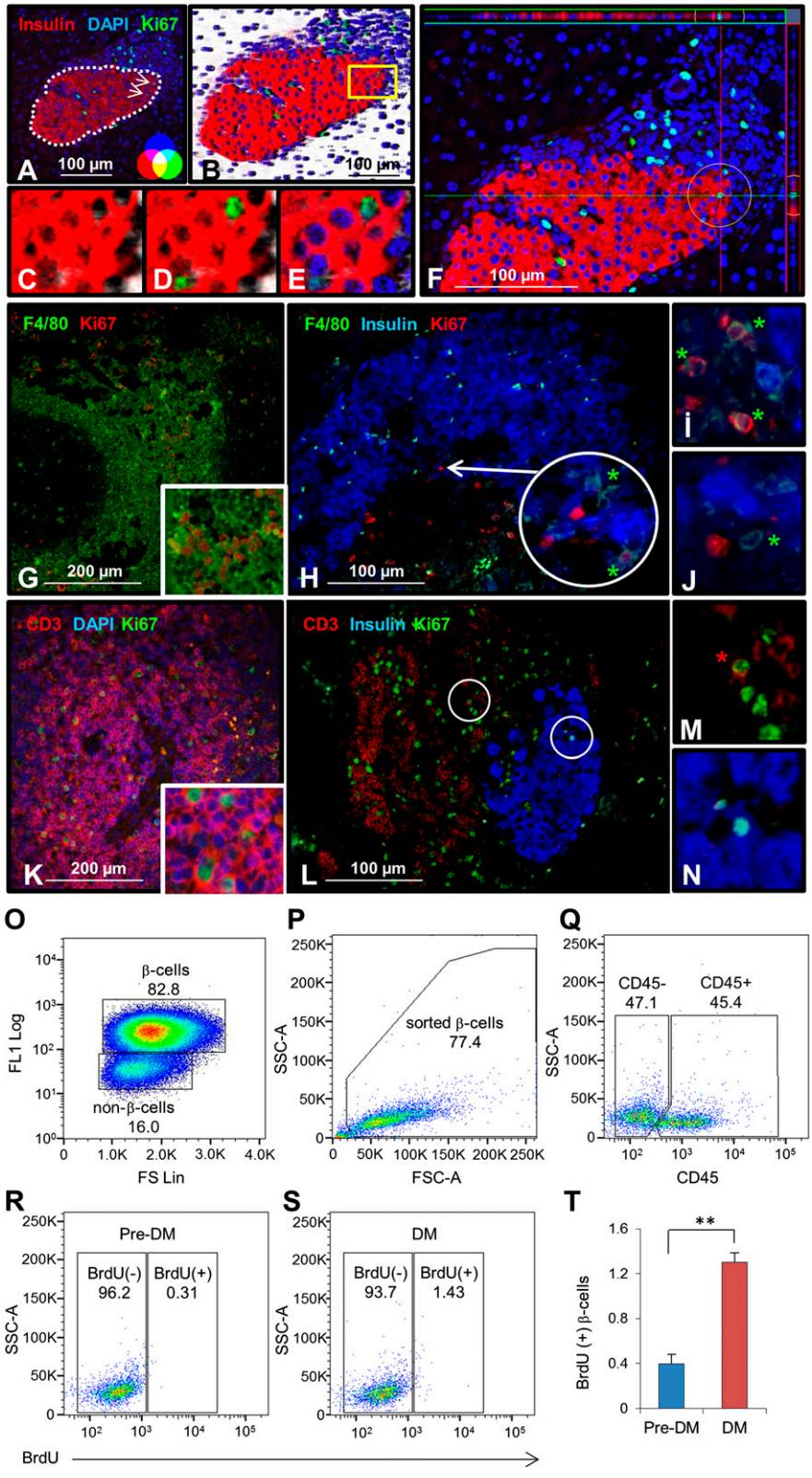

Figure 2—Confirmation of proliferating β-cells. Two-dimensional (*A*) and three-dimensional (*B*) confocal microscopy view of pancreatic section derived from total diabetic NOD mouse splenocyte–injected animal. Dotted line in *A* represents the border between islet and immune cells. Magnified area highlighted from *B* shows three-dimensional imaging of insulin (red) (*C*), Ki67 (green) (*D*), and DAPI (blue) (*E*). Scale bar, 100 μm. Arrows indicate proliferating β-cells. *F*: Orthographic image of the same pancreatic section in *A* shows the horizontal and vertical view of a proliferating β-cell in a circle (ZEN-2009). *G*: Mouse spleen section stained as positive control for F4/80 (green), common macrophage marker, and Ki67 (red). *H*: Total diabetic splenocyte–injected NOD.RAG1$^{-/-}$ pancreatic section stained for F4/80 (green), insulin (blue), and Ki67 (red). Scale bar, 100 μm. Arrow indicates proliferating β-cells. Magnified view of proliferating (*I*) and

sections for β-cell proliferation in the different groups discussed above was a striking difference in the percentage of infiltrated cells (Fig. 4*A*). Scoring for insulitis revealed that whereas the animals receiving total DM splenocytes and B-cell–depleted DM splenocytes contained islets with moderate to severe insulitis, the number of affected islets was significantly reduced in animals receiving pre-DM splenocytes. In contrast, all the groups that received T-cell subtype(s)–depleted splenocytes were virtually free of insulitis, with a few scattered islets exhibiting minimal infiltration (Fig. 4*A* and *B*). We observed a linear and significant correlation between the islets manifesting insulitis and β-cell proliferation ($r = 0.71$; $P = 0.004$) (Fig. 4*C*). To confirm this finding, we used an alternative model that promotes infiltration in islets, namely the STZ-induced diabetic NOD mouse. Examination of pancreas sections in mice that receive intraperitoneal injection of a single dose (75 or 100 mg/kg/BW) of STZ again revealed a positive correlation between β-cell proliferation and mononuclear cell infiltration beginning on day 1 and peaking on day 5 or day 3 after injection (Fig. 4*D* and *E*). The lack of significant alterations in blood glucose and insulin levels at the peak of the proliferation effect suggested that the proliferation was independent of the effects of glycemia or insulin (Supplementary Fig. 3*A* and *B*). The mice that were subjected to the adoptive transfer experiments over the 3-week period after splenocyte injection were also normoglycemic (Supplementary Fig. 3*C*). The virtual absence of mononuclear immune cell infiltration in liver and adipose confirmed the β-cell specificity (Supplementary Fig. 3*D*). Together these results suggest that β-cell proliferation occurs soon after immune cell infiltration, prior to the onset of diabetes, and is independent of the effects of glucose and insulin.

Soluble Factors Secreted by Lymphocytes Promote β-Cell Proliferation

Our in vivo data indicated that increasing numbers of infiltrating lymphocytes positively correlated with β-cell proliferation. To determine whether this direct effect is observed in vitro, we designed mixed lymphocyte-islet culture experiments to examine whether splenocytes (total or T-cell depleted) from diabetic NOD mice promoted β-cell proliferation. In brief, islets were isolated from NOD.RAG1$^{-/-}$ mice and cultured overnight; in parallel, we isolated aliquots of diabetogenic total or T-cell–depleted splenocytes (Fig. 5*A*).

Prior to coculture of lymphocytes with islets, we hypothesized that a specific ratio of islet cells to lymphocytes is critical to promote proliferation of β-cells and that soluble factors mediate the proliferation. Analyses of β-cell proliferation in single islets showed a positive correlation with lymphocyte infiltration (Fig. 5*B*) that was similar to the in vivo studies (Fig. 4*C*). To determine the ratio between infiltrating immune cells versus insulin$^+$ β-cells, pancreas sections from total splenocyte– or STZ-injected mice were examined for both cell types; the infiltrating cells were between 4 and 10 times greater than β-cells in the islets that exhibited proliferation (Fig. 5*C*). Therefore, we cocultured freshly isolated splenocytes with 150 islets in varying ratios for 48 h followed by embedding the islets in agar for immunohistochemical analyses (Fig. 5*A*). To address whether the effects are mediated by soluble factors or by direct contact, we cocultured the lymphocytes with the islets either in the presence or absence of microporous transwell inserts, which prevent direct splenocyte-islet contact while allowing soluble factors to diffuse across (Fig. 5*D*). We first assessed the capacity of total DM and pre-DM splenocytes to stimulate β-cell proliferation at an increasing islet cell to splenocyte ratio (1:1, 1:2, 1:5, and 1:10). Forty-eight hours after coculture, we observed that total splenocytes from diabetic mice, at a ratio of 1:5 and 1:10, significantly induced β-cell proliferation in a dose-dependent manner compared with islets cocultured with pre-DM splenocytes in transwell conditions, suggesting a role for soluble factors secreted from lymphocytes isolated from DM in β-cell proliferation (Fig. 5*D*). On the other hand, nontranswell conditions that permitted cell-cell contact also revealed an effect on β-cell proliferation that was slightly higher compared with the transwell studies likely due to the increased cell-cell contact (Fig. 5*E*).

Next, we performed a second set of coculture experiments to examine the effects of selected T-cell subtype(s) on β-cell proliferation in vitro (Fig. 5*F*). A 1:1 and 1:10 islet cell to splenocyte ratio in the transwell system revealed that islets cocultured with total DM splenocytes promoted a 3–10-fold higher β-cell proliferation at the 1:10 ratio compared with pre-DM splenocytes or splenocytes that are depleted for T-cell subtype(s). The proliferation was either very low or undetectable (ND) at the 1:1 ratio. Among the groups treated with splenocytes that are depleted of the T-cell subtype(s), the CD8$^+$-depleted group revealed statistically significant higher β-cell proliferation compared with CD4$^+$ only or

nonproliferating (*J*) macrophages from *H*. *K*: Mouse spleen section stained as positive control for CD3 (red), T-cell marker, and Ki67 (green). *L*: Total diabetic splenocyte–injected NOD.RAG1$^{-/-}$ pancreatic section stained for CD3 (red), insulin (blue), and Ki67 (green). Scale bar, 100 μm. Magnified view of proliferating T cell (*M*) and β-cell (*N*) from *L*. *O*: Sorting of β- and non–β-cells from dispersed islets from mice after adoptive transfer of pre-DM or DM splenocytes by flow cytometry based on size (FS Lin) and autofluorescence (FL1). *P*: Sorted β-cells stained for CD45 and BrdU. Dot plot showing gated-out CD45$^+$ cells (*Q*) and BrdU$^+$ β-cells from pre-DM (*R*) or DM (*S*) splenocyte-transferred mice. *T*: Quantification of data in *R* and *S*. $n = 3$ each group. *Proliferating macrophages or T cells. **$P < 0.01$. Experiment was performed in triplicate. Data are expressed as means ± SEM. FSC-A, forward scatter detector A; SSC-A, side scatter detector A.

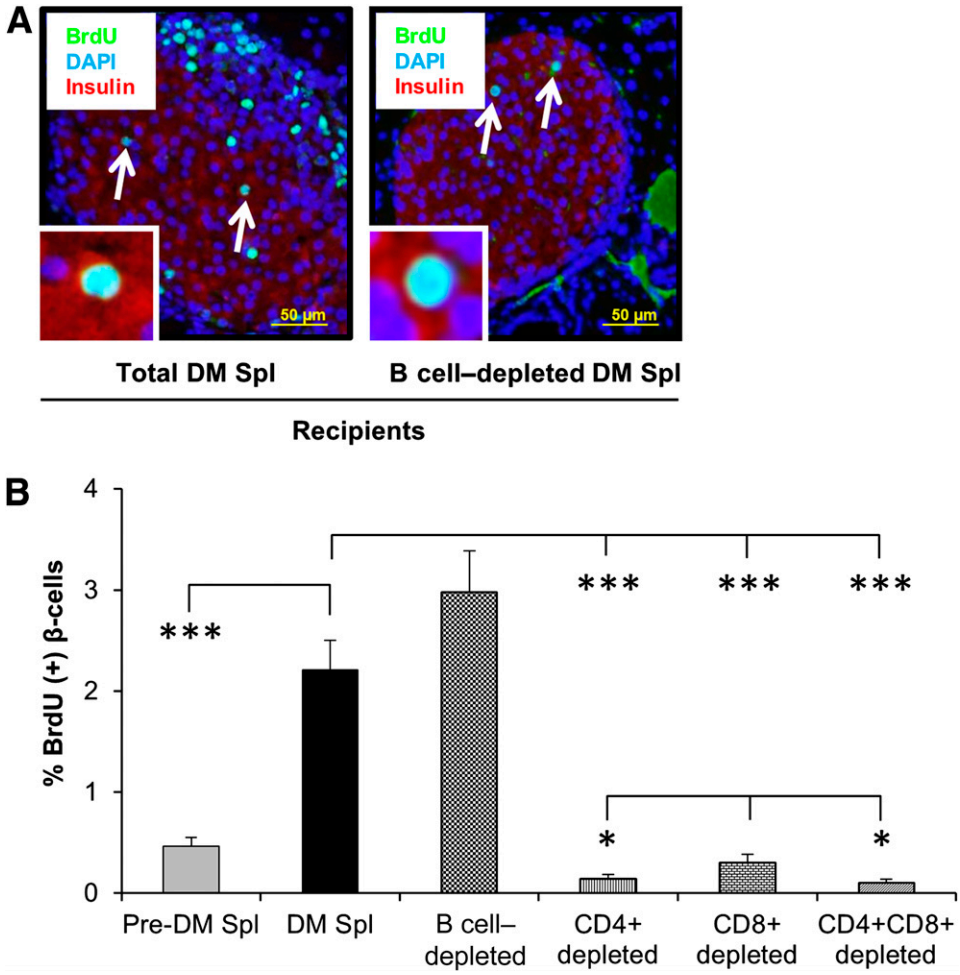

Figure 3—T-cell subsets play a major role in β-cell proliferation. *A*: Paraffin-embedded sections of pancreatic tissues derived from recipient mice receiving total diabetic or B-cell–depleted diabetic NOD mouse splenocytes, costained for the proliferation marker BrdU (green) with insulin (red) and DAPI (blue). Scale bar, 50 μm. Arrows indicate proliferating β-cells ($BrdU^+$/$insulin^+$). Insets show a magnified representative image of a proliferating β-cell. *B*: Quantification of proliferating β-cells in pancreatic sections obtained from mice receiving total (DM or pre-DM) or B-cell–, $CD4^+$-, $CD8^+$-, and $CD4^+$/$CD8^+$–double-depleted diabetic NOD splenocytes. n = 4–6 mice each group. *$P < 0.05$; ***$P < 0.001$ (Student t test). Data are expressed as means ± SEM. Spl, splenocyte.

$CD4^+$/$CD8^+$–double-depleted ($P < 0.05$) groups. Moreover, in positive selection experiments, islets cultured with only $CD4^+$ cells (1:10 ratio of islet cells to $CD4^+$ cells) showed higher ($P = 0.07$) β-cell proliferation compared with $CD8^+$-only cocultured groups (Fig. 5*F*) and was consistent with our negative selection experiments exhibiting low proliferation in the $CD4^+$-depleted group. Evaluation of β-cell death by TUNEL assay did not reveal significant differences between groups (Supplementary Fig. 5*B*). These results support our in vivo findings that $CD4^+$ and $CD8^+$ T cells act together and that $CD4^+$ T cells are likely more effective in stimulating β-cell proliferation by secreting soluble factors independent of cell-cell contact.

Effects of Cytokines on β-Cell Proliferation

To identify the soluble factor(s) that drive β-cell proliferation in pancreatic islets, we analyzed media in the coculture experiments to detect potential cytokines/chemokines/growth factors released by the splenocytes. We ranked the cytokines/chemokines from 1 to 4 according to their significant differences between DM and pre-DM splenocyte treatments in the two transwell conditions (Supplementary Table 1). Among them, group 1 cytokines/chemokines included candidate molecules (IL-2, IL-6, IL-10, MIP-1α, and RANTES) that showed a dose-dependent higher concentration in the group treated with splenocytes from DM compared with mice treated with splenocytes from pre-DM in both coculture conditions (Fig. 6*A*–*E*). We ruled out IP-10 as a candidate since it is not expressed on lymphocytes, is a known chemoattractant for immune cells, and has been shown to be produced by the β-cells. The candidate molecules in the other groups (groups 2–4) were not significantly increased between DM and pre-DM splenocyte–treated mice at least in one or both coculture conditions and were therefore not studied in detail. Whereas some of the candidates (IL-2

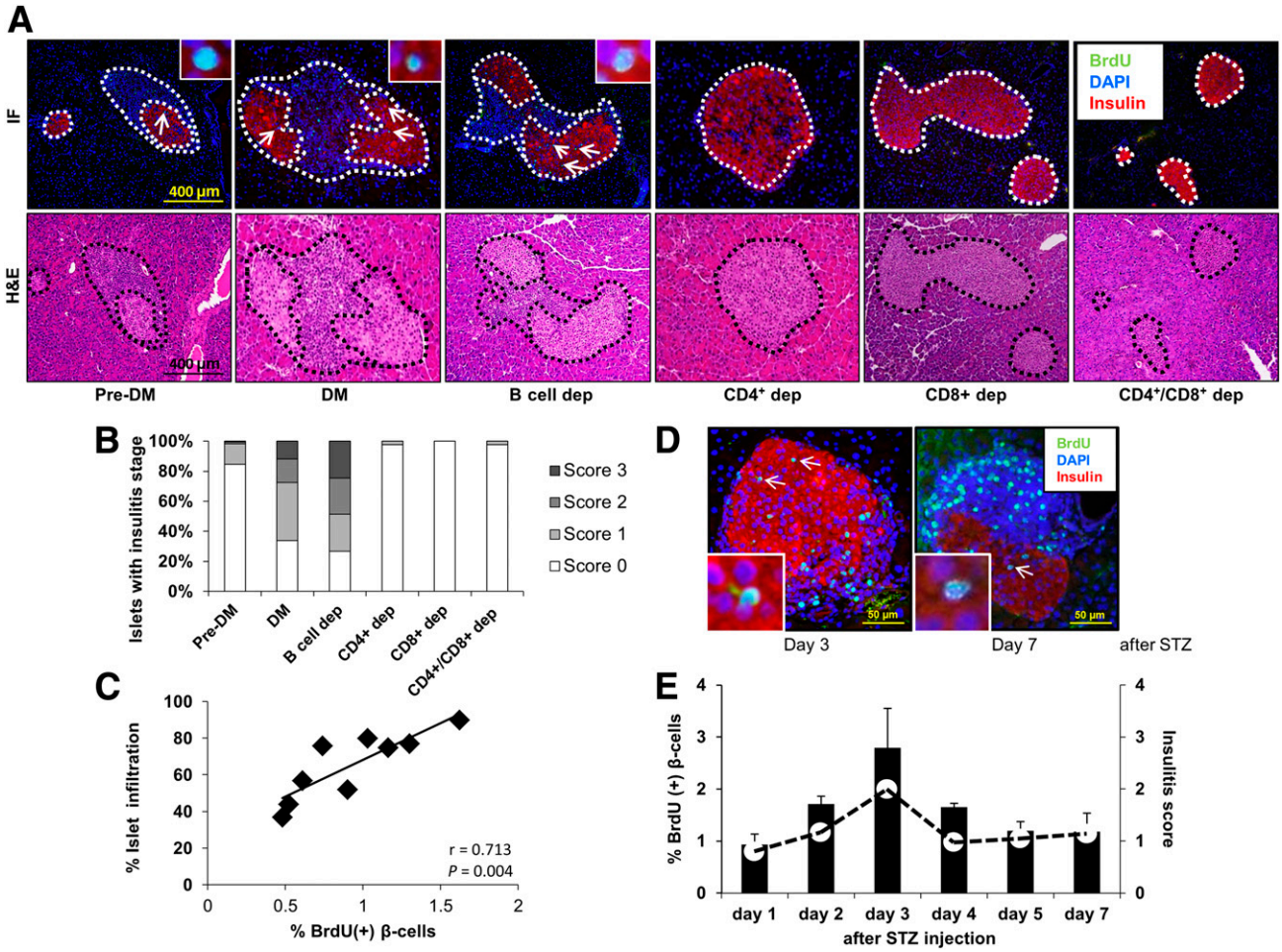

Figure 4—Pancreatic islet infiltration positively correlates with β-cell proliferation. *A*: Immunofluorescence (IF) and hematoxylin and eosin (H&E) staining of consecutive pancreatic sections harvested from NOD.RAG1$^{-/-}$ mice 3 weeks after receiving total (DM or pre-DM) or B-cell–, CD4$^+$-, CD8$^+$-, and CD4$^+$/CD8$^+$–double-depleted diabetic NOD splenocytes. Scale bar, 400 μm. Pancreatic islets are outlined with dotted lines for ease of comprehension. *B*: Pancreatic islets showing insulitis expressed as a percentage in the treated groups in *A*. *C*: Linear regression of islet infiltration and BrdU$^+$ β-cells in pancreas sections harvested from NOD.RAG1$^{-/-}$ mice transferred with total diabetic splenocytes. Each square represents a mouse (n = 9) scored for insulitis in at least 20 islets (n = 9). r = 0.713; P = 0.004. *D*: Pancreatic sections harvested from STZ-induced diabetic NOD mice at day 3 and day 7, costained for the proliferation marker BrdU (green), with insulin (red) and DAPI (blue). Scale bar, 50 μm. Arrows indicate proliferating β-cells (BrdU$^+$/insulin$^+$). Insets show a magnified view of a representative proliferating β-cell. *E*: Quantification of β-cell proliferation (bars) and insulitis scores (red dots) in the pancreatic islets in STZ-injected NOD mice at 1–7 days post-STZ administration (n = 3 mice for each time point). Data are expressed as means ± SEM. dep, depleted.

and IL-6) were increased in both "with" and "without" transwell conditions, others (IL-10, MIP-1α, and RANTES) were higher in the "without" transwell condition probably due to direct cell-cell contact, which potentially allows immune cells to respond rapidly via multiple pathways. In support of a potential proliferative role for each of the five cytokines/chemokines on β-cells, we first confirmed expression of their receptors on sorted β-cells. (Fig. 7*A*). Second, we investigated the effects of the individual cytokines/chemokines on pancreatic islets isolated from B6 mice in the presence or absence of specific inhibitors and/or neutralizing antibodies over a range of concentrations (18,31,32). Low doses of IL-6 (200 pg/mL) strongly induced β-cell proliferation and increased up to 10-fold at the higher dose (200 ng/mL) ($P < 0.05$) (Supplementary Fig. 4*B*). Moreover, IL-2, IL-10, and MIP-1α demonstrated significantly higher proliferation even at low levels, with eight-, four-, and threefold increases, respectively ($P < 0.05$) (Supplementary Fig. 4*A*, *C*, and *D*). On the other hand, treatment with RANTES resulted in β-cell proliferation at lower doses (5 and 500 pg/mL), but the effect was surprisingly reduced at 50 ng/mL (Supplementary Fig. 4*E*). To determine specificity, we examined the effects of specific inhibitors or neutralizing antibodies in islets treated with low-dose cytokines/chemokines. In all cases, we observed neutralization of the proliferative effects of the respective cytokine/chemokine (Fig. 7*B*–*F*). In some cases (IL-2 inhibitor and maraviroc 3.3 nmol/L), the neutralization was not complete and is likely due to variable IC_{50}s of the compounds (Fig. 7*G*). Cytokines

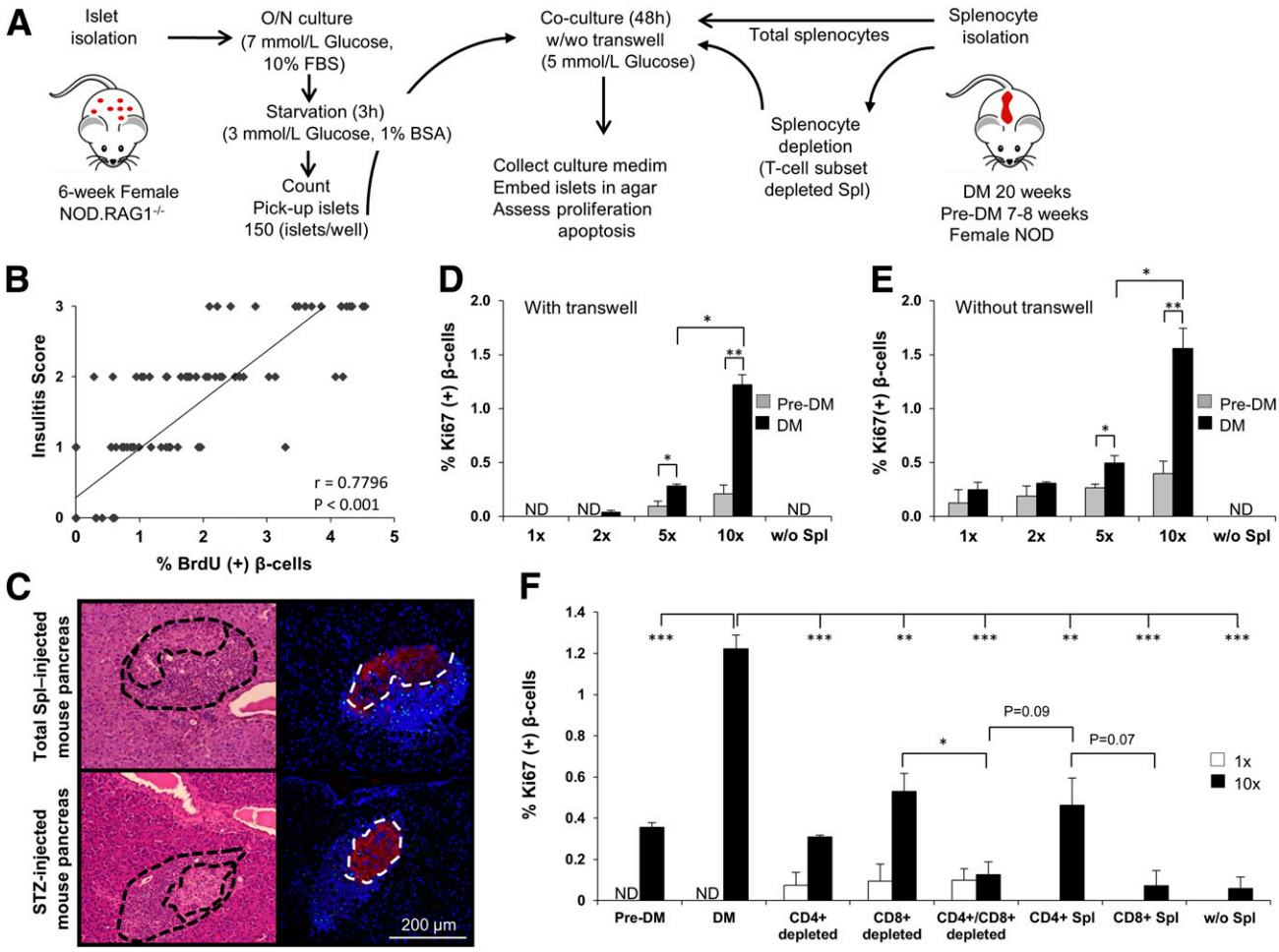

Figure 5—β-cell proliferation is stimulated by infiltrating lymphocytes via soluble factors. *A*: Experimental strategy showing total splenocytes (DM or pre-DM) or depleted splenocytes (diabetic mice), cocultured with 5–6-week-old NOD.RAG1$^{-/-}$ mouse islets (150 islets/condition) for 48 h in 5 mmol/L glucose in the presence or absence of transwell inserts. *B*: Linear regression of insulitis score and BrdU^{+} β-cells in single pancreatic islets harvested from NOD.RAG1$^{-/-}$ mice transferred with total diabetic splenocytes. Each square represents a single islet out of 120 analyzed islets. $r = 0.80$; $P < 0.001$. *C*: Representing pancreatic sections derived from total splenocyte– or STZ-injected mice used for determining the ratio between infiltrating immune cells vs. insulin^{+} β-cells. Islets are indicated by dotted lines in the *right panel*. The area of infiltration is shown around the islet in the *left panels*. β-cell proliferation in agar-embedded NOD.RAG1$^{-/-}$ islets cocultured with total splenocytes from DM or pre-DM at a ratio of 1:1, 1:2, 1:5, or 1:10 or without splenocytes in the presence (*D*) or absence (*E*) of transwell inserts ($n = 3$–4). *$P < 0.05$; **$P < 0.01$ (Student *t* test). *F*: Quantification of proliferating β-cells in pancreatic islets cocultured with total (DM or pre-DM), negatively, or positively selected DM splenocytes at 1:1 or 1:10 ratio with transwell conditions (n = 3–6 for each condition). *$P < 0.05$; **$P < 0.01$; ***$P < 0.001$ (Student *t* test). Data are expressed as means ± SEM. ND, not detected; O/N, overnight; Spl, splenocyte.

and/or chemokines are known to be secreted by macrophages or dendritic cells to impact T-cell function, and, conversely, secretions from T cells can also impact macrophages (27,33). To examine whether the cytokines/chemokines act synergistically to enhance β-cell proliferation, we compared the individual effects versus a combination (Supplementary Fig. 4*F*). In addition to their significant individual effects on proliferation, a combination of the cytokines/chemokines, at doses used in the individual treatments, showed a significant increase ($P <$ 0.001) but was not dramatically different from the individual effects likely because some of the cytokines share common downstream pathways to stimulate proliferation. Finally, to confirm the recombinant protein treatment findings, we undertook an independent experiment wherein total DM splenocytes served as the source of cytokines/chemokines. Islet cells and splenocytes were cultured in a 1:10 ratio in a transwell system in the presence or absence of inhibitory/neutralizing antibodies against the candidate factors. Whereas splenocytes alone significantly increased β-cell proliferation compared with untreated islets (Fig. 8*A* and *B*), adding the inhibitory/neutralizing molecule reversed this effect. Consistent with our previous observations, these data suggested that each candidate has a potential to induce β-cell regeneration (Fig. 8*C*–*H*). In summary, cytokines/chemokines that are secreted from lymphocytes in close proximity to islet cells promote detectable β-cell proliferation.

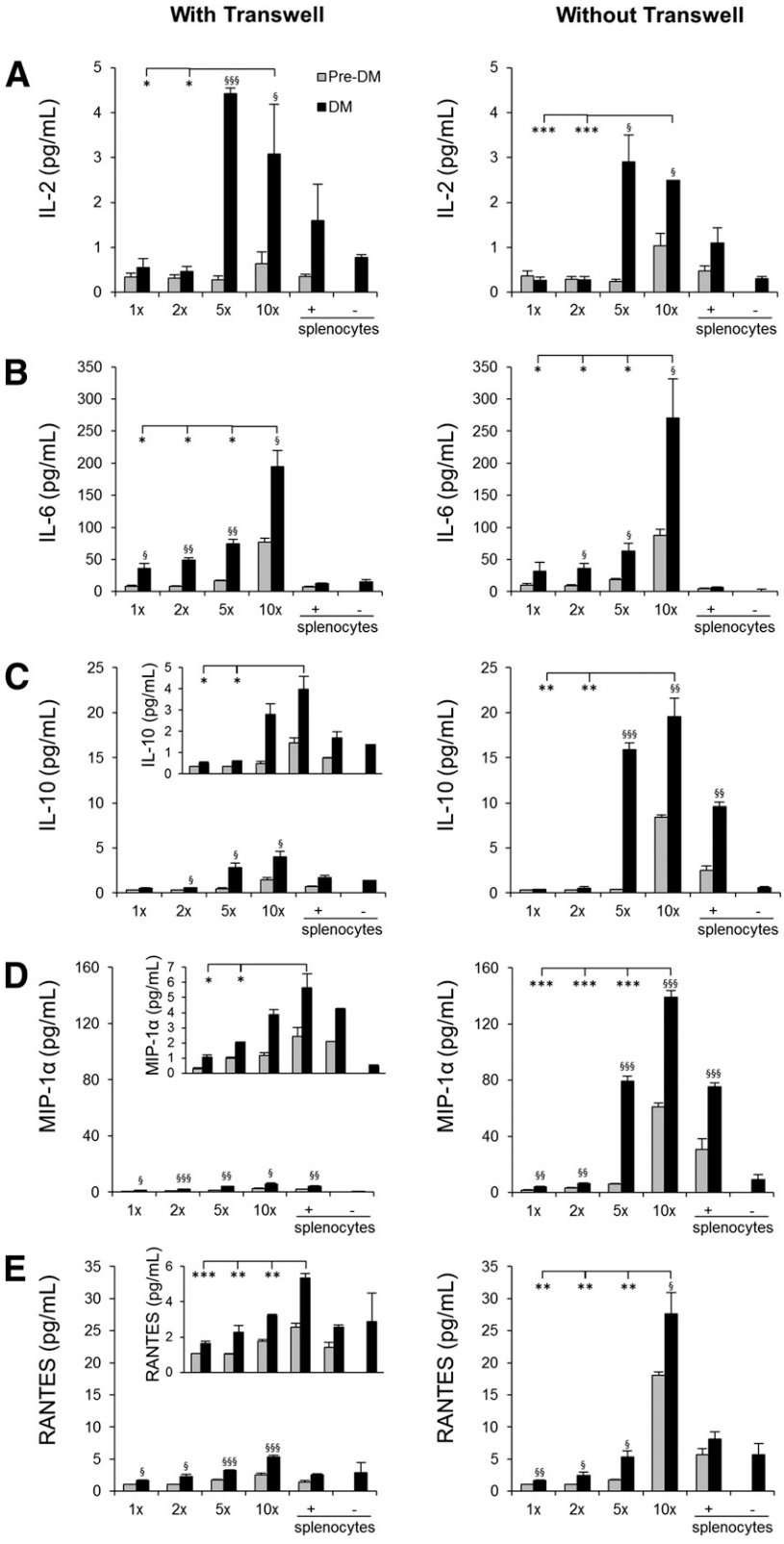

Figure 6—Lymphocyte-secreted soluble factors that drive β-cell proliferation. Luminex assay results from culture medium obtained 48 h after coculturing NOD.RAG1$^{-/-}$ islets with NOD splenocytes (DM or pre-DM) at a ratio of 1:1, 1:2, 1:5, or 1:10 or only splenocytes at 10× in the presence or absence of transwell for IL-2 (*A*), IL-6 (*B*), IL-10 (*C*), MIP-1α (*D*), and RANTES (*E*) (n = 3–4 for each condition). *, §P < 0.05; **, §§P < 0.01; ***, §§§P < 0.001 (Student t test). *, diabetic vs. diabetic; §, diabetic vs. prediabetic. Data are expressed as means ± SEM.

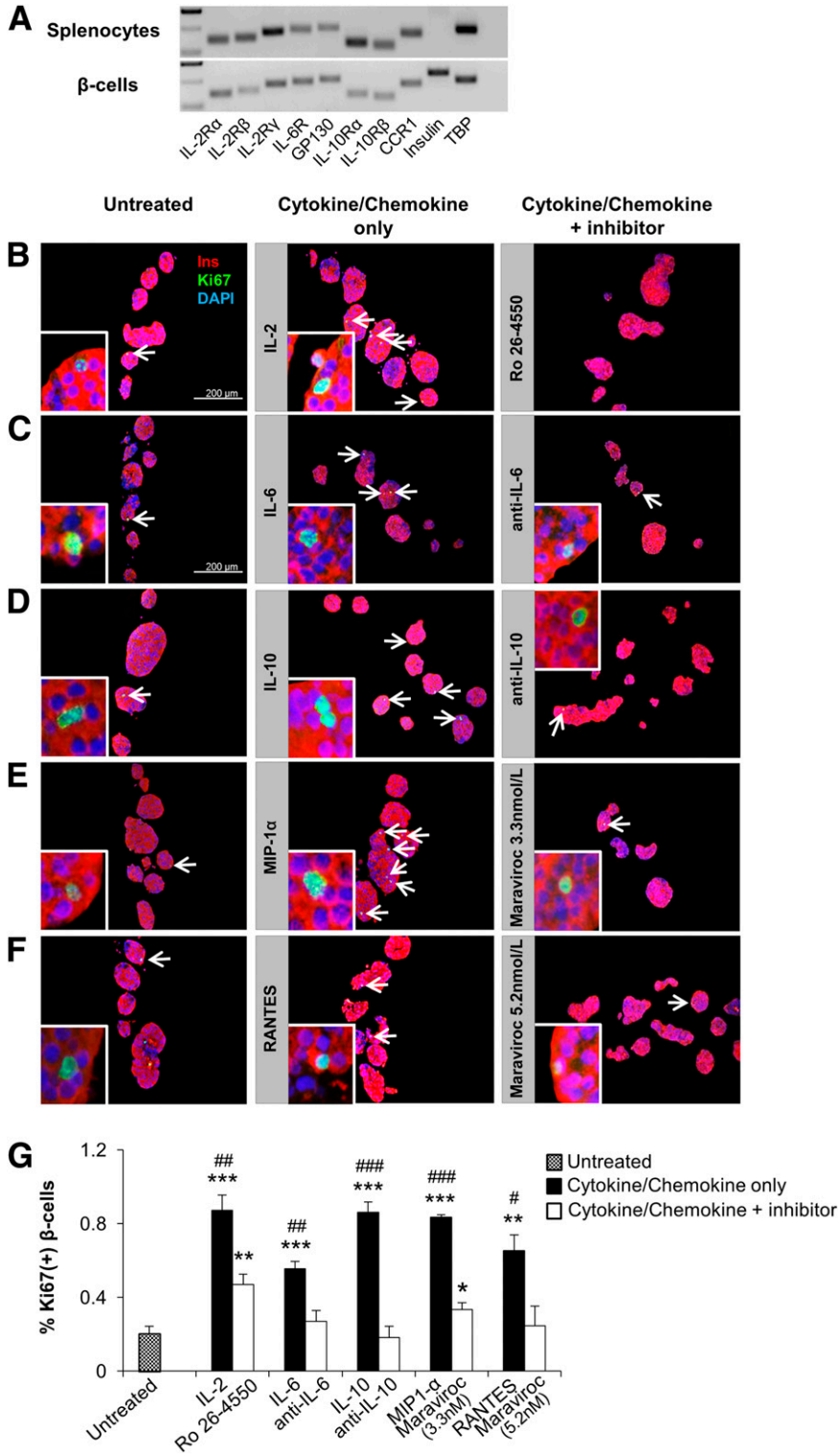

Figure 7—Effect of soluble factors on β-cell proliferation is reversed by inhibitory/neutralizing antibody treatment in vitro. *A*: Detection of the cytokine/chemokine receptor subunit mRNAs by real-time PCR from sorted β-cells and splenocytes harvested from C57BL/6 mice. Tata-box-binding protein (TBP) was used as reference. *B–F*: Agar-embedded pancreatic islets from C57BL/BJ mouse treated in the absence (control) or presence of low-dose recombinant proteins with or without inhibitory/neutralizing molecules (as described in RESEARCH DESIGN AND METHODS) for 48 h (150 islets/condition, three to four replicates). Representative sections are shown. Islets were costained for the proliferation marker Ki67 (green) with insulin (red) and DAPI (blue). Arrows indicate proliferating β-cells (Ki67$^+$/insulin$^+$). Scale bar, 200 μm. Insets show a magnified image of a representative proliferating β-cell. *G*: Quantification of data in *B–F* (n = 3–4 in each group). *, #P < 0.05; **, ##P < 0.01; ***, ###P < 0.001 (Student t test). *, untreated vs. cytokine/chemokine or inhibitory/neutralizing antibody treated; #, cytokine/chemokine treated vs. inhibitory/neutralizing antibody treated. Data are expressed as means ± SEM. CCR1, C-C chemokine receptor type 1; GP130, glycoprotein 130; IL-2R, IL-2 receptor.

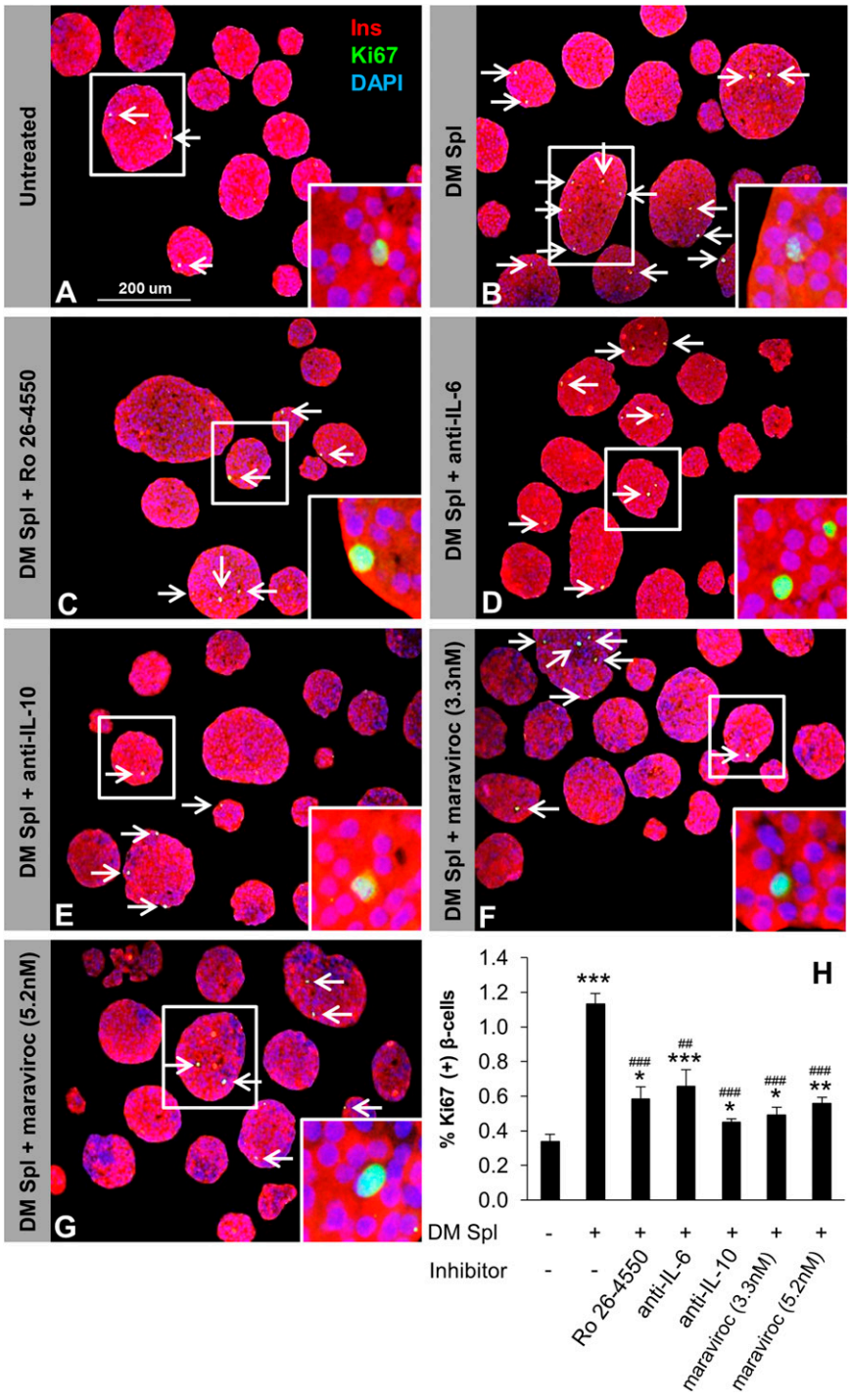

Figure 8—Lymphocyte-secreted soluble factors enhance β-cell proliferation in vitro. One hundred fifty agar-embedded islets harvested from C57BL/6 mice cocultured without (untreated control) (*A*) or with total DM splenocytes in the absence (treated control) (*B*) or presence of inhibitory/neutralizing molecule Ro 26-4550 (*C*), anti–IL-6 (*D*), anti–IL-10 (*E*), maraviroc 3.3 nmol/L (*F*), or maraviroc 5.2 nmol/L (*G*). Islets were costained for the proliferation marker Ki67 (green), insulin (red), and DAPI (blue). Arrows indicate proliferating β-cells (Ki67$^+$/insulin$^+$). Scale bar, 200 μm. Insets show magnified image of a representative proliferating β-cell. *H*: Quantification of proliferating β-cells in *A–G* (n = 3–4 in each group). *P < 0.05; **, ##P < 0.01; ***, ###P < 0.001 (Student t test). *, untreated vs. DM splenocyte treated; #, DM splenocyte treated vs. inhibitory/neutralizing antibody treated. Data are expressed as means ± SEM. Ins, insulin; Spl, splenocyte.

DISCUSSION

Although immune cells have been implicated in the proliferation of β-cells during the progression of T1D (4,6), the cell type(s) and mechanisms that control β-cell regeneration remain unknown. Here we report that soluble factors secreted from CD4$^+$ and CD8$^+$ T cells directly stimulate β-cell proliferation.

NOD.RAG1$^{-/-}$ mice injected with DM splenocytes exhibited a significant elevation in all markers of β-cell proliferation compared with controls. Adoptive transfer of diabetes to immunocompromised syngenic recipients can be achieved only when a combination of splenic CD4$^+$ and CD8$^+$ T cells from donor NOD mice is used and not by either T-cell subsets alone (34). Injecting CD4$^+$-, CD8$^+$-, or CD4$^+$/CD8$^+$–double-depleted splenocytes into NOD.RAG1$^{-/-}$ animals resulted in a dramatic decrease in β-cell proliferation compared with the animals that received total DM splenocytes. In addition, we also observed that animals with depleted T-cell subtype(s) exhibited minimal pancreatic islet infiltration compared with animals receiving total splenocytes or B-cell–depleted splenocytes. Considering that the development of T1D requires the presence of both CD4$^+$ and CD8$^+$ T cells, depleting one or both of these cells would impact the inflammatory response and alter β-cell replication. This possibility was supported by a linear and significant correlation between β-cell proliferation and immune cell infiltration in our studies. Among the T-cell subtypes, both CD8$^+$ T-cell–depleted splenocyte injection (in vivo) and islet coculture (in vitro) studies demonstrated higher proliferation compared with CD4$^+$-depleted or CD4$^+$/CD8$^+$–double-depleted cohorts. Similar results were observed when islets were cultured with CD4$^+$ T-cell subset alone, signifying their role in β-cell proliferation. We did not detect a significant difference in β-cell apoptosis between the groups because the duration after injection of splenocytes is not sufficient to promote significant apoptosis and/or because it is often difficult to detect dead β-cells due to their rapid engulfment and disposal (35).

Although our studies point to CD4$^+$ and CD8$^+$ T cells as critical for β-cell proliferation during T1D progression, we cannot exclude the potential contribution of macrophages or dendritic cells and their secreted products (36). Our data suggest that B cells are unlikely to play a role in β-cell replication. Depletion of macrophages prevents T1D development (37), and macrophages have been reported to impact β-cells by producing proinflammatory cytokines (38). One possible role for macrophages in β-cell proliferation is that T-cell subtypes, especially CD4$^+$, recruit additional CD4$^+$, CD8$^+$, or granulocytes into the infiltrate and contribute to local secretion of cytokines and chemokines. Indeed, T cells secrete soluble factors such as granulocyte macrophage–colony-stimulating factor (39) to influence leukocytes and recruit them to inflammatory sites during inflammation (40,41). Thus, in addition to their direct effect on β-cell proliferation by cytokine secretion, it is possible that T cells act indirectly by triggering mononuclear cells to secrete soluble factors, via the classical or nonclassical pathways, that can in turn enhance β-cell proliferation.

Although earlier studies implicate a T-cell–dependent proliferative effect on aortic smooth muscle (42) and orbital fibroblasts (43), the mechanism(s) remains unclear. Careful analyses of our data from the transwell experiments indicate that CD4$^+$ and CD8$^+$ lymphocytes secrete IL-2, IL-6, IL-10, MIP-1α, and RANTES, each of which showed a dose-dependent effect on β-cell proliferation. Some of these factors have been associated with proliferation of other cell types. For example, IL-2 regulates the growth and function of T cells (44), and IL-6 stimulates α- and β-cell proliferation in vitro (18) and is known to reinforce the effects of IL-2 in promoting the differentiation of CD4$^+$ cells into type 2 T-helper cells (45). RANTES acts with IL-2 to induce the proliferation and activation of NK cells to form chemokine-activated killer cells (46). Since β-cells themselves have been reported to produce inflammatory cytokines such as IL-1β (47), we do not exclude the β-cell as a source of some of these molecules. Cytokines, such as IL-1β and interferon-γ, when used in combination, can induce de-differentiation of newly generated β-cells mediated by re-expression of the Notch-Delta pathway (48). Whether the soluble factors detected in our experiments are also involved in similar pathways to modulate β-cell mass warrants further investigation.

Although the capacity to proliferate is strikingly different between rodents and humans, the observations that β-cells can regenerate in humans have prompted studies to investigate safe approaches to enhance their functional mass. Whether the candidate molecules identified in our study can be used either individually or in combination with an appropriate immunosuppressive regimen to preserve β-cell mass requires further research. In the context of cytokines, IL-6 has been reported to stimulate human islet proliferation (18). Although attempts at expansion ex vivo resulted in a change in the β-cell phenotype, lineage-tracing studies suggest that de-differentiated human β-cells are able to survive and replicate in vitro (49). Thus, testing the candidates we have identified in ex vivo conditions can be a first step to evaluate their ability to expand human β-cells. However, a role for these molecules as "therapeutic" agents has to be viewed with caution due to their well-established roles in the immune network. For example, rapamycin, an immunosuppressant drug used to protect rejection in organ transplantations, inhibits lymphocyte proliferation by inhibiting their response to IL-2 (50). Despite IL-2 being important in lymphocyte activation, it also contributes to the development and expansion of CD4$^+$ CD25$^+$ regulatory T cells, which promote self-tolerance by suppressing T-cell responses in vivo. Thus, extensive and careful dosing studies are necessary to examine the potential of the candidate cytokines/chemokines for β-cell expansion.

We propose that some of the pro- and anti-inflammatory cytokines/chemokines secreted in the islet microenvironment during insulitis have the potential to promote proliferation by activating diverse signaling

cascades (e.g., JAK/STAT, mitogen-activated protein kinase, or phosphatidylinositol 3-kinase/AKT). This potential beneficial effect triggers the islets to secrete chemoattractant molecules (e.g., eotaxin [CCL11], IP-10 [CXCL-10], and MCP-1 [CCL2]), which in turn amplify the recruitment of mononuclear cells and the release of multiple cytokines/chemokines. The detection of increased levels of chemotactic molecules in our experiments, especially IP-10 and eotaxin, likely amplifies the number of immune cells that secrete soluble factors in the inflamed area to further promote β-cell proliferation and prevent progression of diabetes.

In summary, we report that $CD4^+$ and $CD8^+$ T cells secrete soluble factors that promote β-cell replication in the NOD model of T1D. Therapeutic targeting of one or a combination of these soluble factors may prove useful to delay and/or counter the progression of T1D by enhancing functional β-cell mass.

Acknowledgments. The authors thank G.C. Weir (Joslin Diabetes Center and Harvard Medical School) and F. Urano (Washington University School of Medicine, St. Louis, MO) for discussions and advice, O. Lovegreen (Joslin Diabetes Center) for editorial assistance, and the Specialized Assay Core (Joslin Diabetes Center) for hormone and metabolite analyses.

Funding. This work was supported by a Juvenile Diabetes Research Foundation Fellowship (3-2010-474) and Turkish Diabetes, Obesity and Nutrition Association Novartis Science Award to E.D. Some of the reagents were supported by NIH Grant RO1-DK-67536 to R.N.K., and the Joslin Diabetes Center Flow Cytometry Cores were supported by Diabetes Research Center Grant NIH P30-DK-036836 and NIH PO1-AI-054904 to D.M.

Duality of Interest. No potential conflicts of interest relevant to this article were reported.

Author Contributions. E.D. conceived the idea, designed the experiments, performed all experiments, analyzed the data, and wrote the manuscript. S.K. contributed to animal maintenance and assisted in islet isolation. W.J. assisted in the adoptive transfer experiments. A.E.O. assisted in islet isolation. D.F.D.J. contributed to animal maintenance. A.K.K.T. assisted in the real-time PCR experiments. J.H. and D.K. assisted in the immunohistochemical experiments. J.L.G. contributed to the flow cytometry analysis and NOD.Raspberry studies. D.M. contributed to designing the experiments, troubleshooting, and the NOD.Raspberry studies. R.N.K. conceived the idea, designed the experiments, supervised the project, and wrote the manuscript. R.N.K. and E.D. are the guarantors of this work and, as such, had full access to all the data in the study and take responsibility for the integrity of the data and the accuracy of the data analysis.

Prior Presentation. This study was presented at the 73rd Scientific Sessions of the American Diabetes Association, Chicago, Illinois, 21–25 June 2013.

References

1. Mathis D, Vence L, Benoist C. beta-Cell death during progression to diabetes. Nature 2001;414:792–798
2. Redondo MJ, Fain PR, Eisenbarth GS. Genetics of type 1A diabetes. Recent Prog Horm Res 2001;56:69–89
3. Turley S, Poirot L, Hattori M, Benoist C, Mathis D. Physiological beta cell death triggers priming of self-reactive T cells by dendritic cells in a type-1 diabetes model. J Exp Med 2003;198:1527–1537
4. Sreenan S, Pick AJ, Levisetti M, Baldwin AC, Pugh W, Polonsky KS. Increased beta-cell proliferation and reduced mass before diabetes onset in the nonobese diabetic mouse. Diabetes 1999;48: 989–996
5. von Herrath MG, Wolfe T, Möhrle U, Coon B, Hughes A. Protection from type 1 diabetes in the face of high levels of activated autoaggressive lymphocytes in a viral transgenic mouse model crossed to the SV129 strain. Diabetes 2001;50:2700–2708
6. Sherry NA, Kushner JA, Glandt M, Kitamura T, Brillantes AM, Herold KC. Effects of autoimmunity and immune therapy on beta-cell turnover in type 1 diabetes. Diabetes 2006;55:3238–3245
7. Nir T, Melton DA, Dor Y. Recovery from diabetes in mice by beta cell regeneration. J Clin Invest 2007;117:2553–2561
8. Keenan HA, Sun JK, Levine J, et al. Residual insulin production and pancreatic β-cell turnover after 50 years of diabetes: Joslin Medalist Study. Diabetes 2010;59:2846–2853
9. Meier JJ, Bhushan A, Butler AE, Rizza RA, Butler PC. Sustained beta cell apoptosis in patients with long-standing type 1 diabetes: indirect evidence for islet regeneration? Diabetologia 2005;48:2221–2228
10. Lee YC, Nielsen JH. Regulation of beta cell replication. Mol Cell Endocrinol 2009;297:18–27
11. Meier JJ, Butler AE, Saisho Y, et al. Beta-cell replication is the primary mechanism subserving the postnatal expansion of beta-cell mass in humans. Diabetes 2008;57:1584–1594
12. Finegood DT, Scaglia L, Bonner-Weir S. Dynamics of beta-cell mass in the growing rat pancreas. Estimation with a simple mathematical model. Diabetes 1995;44:249–256
13. Karnik SK, Chen H, McLean GW, et al. Menin controls growth of pancreatic beta-cells in pregnant mice and promotes gestational diabetes mellitus. Science 2007;318:806–809
14. Michael MD, Kulkarni RN, Postic C, et al. Loss of insulin signaling in hepatocytes leads to severe insulin resistance and progressive hepatic dysfunction. Mol Cell 2000;6:87–97
15. Peshavaria M, Larmie BL, Lausier J, et al. Regulation of pancreatic beta-cell regeneration in the normoglycemic 60% partial-pancreatectomy mouse. Diabetes 2006;55:3289–3298
16. Dirice E, Kulkarni RN. Pathways underlying β-cell regeneration in type 1, type 2 and gestational diabetes. In *Islet Cell Growth Factors*. Kulkarni RN, Ed. Texas, Landies Bioscience, 2011, p. 1–15
17. Maedler K, Schumann DM, Sauter N, et al. Low concentration of interleukin-1beta induces FLICE-inhibitory protein-mediated beta-cell proliferation in human pancreatic islets. Diabetes 2006;55:2713–2722
18. Ellingsgaard H, Ehses JA, Hammar EB, et al. Interleukin-6 regulates pancreatic alpha-cell mass expansion. Proc Natl Acad Sci USA 2008;105: 13163–13168
19. Cameron MJ, Strathdee CA, Holmes KD, Arreaza GA, Dekaban GA, Delovitch TL. Biolistic-mediated interleukin 4 gene transfer prevents the onset of type 1 diabetes. Hum Gene Ther 2000;11:1647–1656
20. Pennline KJ, Roque-Gaffney E, Monahan M. Recombinant human IL-10 prevents the onset of diabetes in the nonobese diabetic mouse. Clin Immunol Immunopathol 1994;71:169–175
21. Flodström-Tullberg M, Yadav D, Hägerkvist R, et al. Target cell expression of suppressor of cytokine signaling-1 prevents diabetes in the NOD mouse. Diabetes 2003;52:2696–2700
22. Kulkarni RN, Winnay JN, Daniels M, et al. Altered function of insulin receptor substrate-1-deficient mouse islets and cultured beta-cell lines. J Clin Invest 1999;104:R69–R75

23. Haxhinasto S, Mathis D, Benoist C. The AKT-mTOR axis regulates de novo differentiation of CD4+Foxp3+ cells. J Exp Med 2008;205:565–574
24. King AJ, Fernandes JR, Hollister-Lock J, Nienaber CE, Bonner-Weir S, Weir GC. Normal relationship of beta- and non-beta-cells not needed for successful islet transplantation. Diabetes 2007;56:2312–2318
25. Gonzalez A, Andre-Schmutz I, Carnaud C, Mathis D, Benoist C. Damage control, rather than unresponsiveness, effected by protective DX5+ T cells in autoimmune diabetes. Nat Immunol 2001;2:1117–1125
26. Fuchtenbusch M, Larger E, Thebault K, Boitard C: Transfer of diabetes from prediabetic NOD mice to NOD-SCID/SCID mice: association with pancreatic insulin content. Horm Metab Res 2005;37:63–67
27. Lehuen A, Diana J, Zaccone P, Cooke A. Immune cell crosstalk in type 1 diabetes. Nat Rev Immunol 2010;10:501–513
28. Adorini L, Gregori S, Harrison LC. Understanding autoimmune diabetes: insights from mouse models. Trends Mol Med 2002;8:31–38
29. Bluestone JA, Herold K, Eisenbarth G. Genetics, pathogenesis and clinical interventions in type 1 diabetes. Nature 2010;464:1293–1300
30. van Belle TL, Coppieters KT, von Herrath MG. Type 1 diabetes: etiology, immunology, and therapeutic strategies. Physiol Rev 2011;91:79–118
31. Crawley JB, Rawlinson L, Lali FV, Page TH, Saklatvala J, Foxwell BM. T cell proliferation in response to interleukins 2 and 7 requires p38MAP kinase activation. J Biol Chem 1997;272:15023–15027
32. Hanifi-Moghaddam P, Kappler S, Seissler J, et al. Altered chemokine levels in individuals at risk of type 1 diabetes mellitus. Diabet Med 2006; 23:156–163
33. Eizirik DL, Colli ML, Ortis F. The role of inflammation in insulitis and beta-cell loss in type 1 diabetes. Nat Rev Endocrinol 2009;5:219–226
34. Phillips JM, Parish NM, Raine T, et al. Type 1 diabetes development requires both CD4+ and CD8+ T cells and can be reversed by non-depleting antibodies targeting both T cell populations. Rev Diabet Stud 2009;6:97–103
35. Scaglia L, Cahill CJ, Finegood DT, Bonner-Weir S. Apoptosis participates in the remodeling of the endocrine pancreas in the neonatal rat. Endocrinology 1997;138:1736–1741
36. Hu CY, Rodriguez-Pinto D, Du W, et al. Treatment with CD20-specific antibody prevents and reverses autoimmune diabetes in mice. J Clin Invest 2007;117:3857–3867
37. Jun HS, Yoon CS, Zbytnuik L, van Rooijen N, Yoon JW. The role of macrophages in T cell-mediated autoimmune diabetes in nonobese diabetic mice. J Exp Med 1999;189:347–358
38. Dahlén E, Dawe K, Ohlsson L, Hedlund G. Dendritic cells and macrophages are the first and major producers of TNF-alpha in pancreatic islets in the nonobese diabetic mouse. J Immunol 1998;160: 3585–3593
39. Khajah M, Millen B, Cara DC, Waterhouse C, McCafferty DM. Granulocyte-macrophage colony-stimulating factor (GM-CSF): a chemoattractive agent for murine leukocytes in vivo. J Leukoc Biol 2011;89: 945–953
40. Codarri L, Gyülvészi G, Tosevski V, et al. RORγt drives production of the cytokine GM-CSF in helper T cells, which is essential for the effector phase of autoimmune neuroinflammation. Nat Immunol 2011;12:560–567
41. Huffnagle GB, Lipscomb MF, Lovchik JA, Hoag KA, Street NE. The role of CD4+ and CD8+ T cells in the protective inflammatory response to a pulmonary cryptococcal infection. J Leukoc Biol 1994;55:35–42
42. Rolfe BE, Campbell JH, Smith NJ, Cheong MW, Campbell GR. T lymphocytes affect smooth muscle cell phenotype and proliferation. Arterioscler Thromb Vasc Biol 1995;15:1204–1210
43. Feldon SE, Park DJ, O'Loughlin CW, et al. Autologous T-lymphocytes stimulate proliferation of orbital fibroblasts derived from patients with Graves' ophthalmopathy. Invest Ophthalmol Vis Sci 2005;46:3913–3921
44. Liou HC, Smith KA. The roles of c-rel and interleukin-2 in tolerance: a molecular explanation of self-nonself discrimination. Immunol Cell Biol 2011;89:27–32
45. Diehl S, Rincón M. The two faces of IL-6 on Th1/Th2 differentiation. Mol Immunol 2002;39:531–536
46. Maghazachi AA, Al-Aoukaty A, Schall TJ. CC chemokines induce the generation of killer cells from CD56+ cells. Eur J Immunol 1996;26:315–319
47. Maedler K, Sergeev P, Ris F, et al. Glucose-induced beta cell production of IL-1beta contributes to glucotoxicity in human pancreatic islets. J Clin Invest 2002;110:851–860
48. Darville MI, Eizirik DL. Notch signaling: a mediator of beta-cell dedifferentiation in diabetes? Biochem Biophys Res Commun 2006;339: 1063–1068
49. Russ HA, Bar Y, Ravassard P, Efrat S. In vitro proliferation of cells derived from adult human beta-cells revealed by cell-lineage tracing. Diabetes 2008; 57:1575–1583
50. Kay JE, Kromwel L, Doe SE, Denyer M. Inhibition of T and B lymphocyte proliferation by rapamycin. Immunology 1991;72:544–549

Appendix A2

Publication

Kahraman S*, Dirice E*, **De Jesus DF**, Hu J, Kulkarni RN. Maternal insulin resistance and transient hyperglycemia impacts the metabolic and endocrine phenotypes of offspring. APJ - Endocrinology and Metabolism DOI: 10.1152/ajpendo.00210.2014, 2014. (*co-first authors).

Contribution

I contributed by performing genotyping, animal phenotyping, histochemistry, tissue harvesting, and assisting in islet isolation.

Am J Physiol Endocrinol Metab 307: E906–E918, 2014.
First published September 23, 2014; doi:10.1152/ajpendo.00210.2014.

Maternal insulin resistance and transient hyperglycemia impact the metabolic and endocrine phenotypes of offspring

Sevim Kahraman,* Ercument Dirice,* Dario F. De Jesus, Jiang Hu, and Rohit N. Kulkarni

Section of Islet Cell and Regenerative Biology, Joslin Diabetes Center and Department of Medicine, Harvard Medical School, Boston, Massachusetts

Submitted 7 May 2014; accepted in final form 9 September 2014

Kahraman S, Dirice E, De Jesus DF, Hu J, Kulkarni RN. Maternal insulin resistance and transient hyperglycemia impact the metabolic and endocrine phenotypes of offspring. *Am J Physiol Endocrinol Metab* 307: E906–E918, 2014. First published September 23, 2014; doi:10.1152/ajpendo.00210.2014.—Studies in both humans and rodents suggest that maternal diabetes leads to a higher risk of the fetus developing impaired glucose tolerance and obesity during adulthood. However, the impact of hyperinsulinemia in the mother on glucose homeostasis in the offspring has not been fully explored. We aimed to determine the consequences of maternal insulin resistance on offspring metabolism and endocrine pancreas development using the LIRKO mouse model, which exhibits sustained hyperinsulinemia and transient increase in blood glucose concentrations during pregnancy. We examined control offspring born to either LIRKO or control mothers on embryonic days 13.5, 15.5, and 17.5 and postpartum days 0, 4, and 10. Control offspring born to LIRKO mothers displayed low birth weights and subsequently rapidly gained weight, and their blood glucose and plasma insulin concentrations were higher than offspring born to control mothers in early postnatal life. In addition, concentrations of plasma leptin, glucagon, and active GLP-1 were higher in control pups from LIRKO mothers. Analyses of the endocrine pancreas revealed significantly reduced β-cell area in control offspring of LIRKO mothers shortly after birth. β-Cell proliferation and total islet number were also lower in control offspring of LIRKO mothers during early postnatal days. Together, these data indicate that maternal hyperinsulinemia and the transient hyperglycemia impair endocrine pancreas development in the control offspring and induce multiple metabolic alterations in early postnatal life. The relatively smaller β-cell mass/area and β-cell proliferation in these control offspring suggest cell-autonomous epigenetic mechanisms in the regulation of islet growth and development.

maternal insulin resistance; intrauterine environment; offspring metabolism; endocrine pancreas development; hyperinsulinemia

MATERNAL METABOLIC STATUS DURING PREGNANCY is important for fetal growth and development, since the fetus is completely dependent upon its mother for nutrition. Studies have reported that adverse experiences during fetal life can impair fetal development and cause permanent metabolic adaptations in the offspring that would influence their long-term health by increasing the risk for developing insulin resistance, type 2 diabetes, obesity, and/or cardiovascular disease in adulthood (8). To understand the role of intrauterine environment on fetal growth and development, investigators have used various animal models of maternal overnutrition [obesity (29), high-fat diet (15)] and maternal malnutrition (low-protein diet, low-energy diet) (11) and have also investigated other conditions affecting mothers during pregnancy [e.g., gestational diabetes (34), hyperglycemia (16), hypoxia (46), anemia (24), and glucocorticoid exposure (23)] (2). However, the effects of insulin resistance on a background of transient hyperglycemia in the mother on alterations in metabolism and pancreas development in the offspring remain unclear.

Insulin resistance contributes to a range of serious health problems ranging from diabetes to heart disease and cancer (4), and its increasing prevalence in adults, including women of childbearing age, makes this syndrome a growing concern worldwide. Since insulin resistance alters the metabolic status in the affected individuals, its presence in women during pregnancy has the potential to be detrimental to growth and metabolism in the offspring. Thus, insulin resistance directly impacts pregnant women and also their offspring.

In this study, we used a mouse model of insulin resistance to determine how maternal insulin resistance affects metabolism and endocrine pancreas development in the offspring. To this end, we investigated the liver-specific insulin receptor knockout (LIRKO) mouse, in which the insulin receptor gene is deleted specifically in the liver by Cre-loxP-mediated recombination (27). LIRKO females were hyperinsulinemic with normal random blood glucose levels before the onset of pregnancy and displayed a transient increase in blood glucose levels and glucose intolerance. They became more insulin resistant compared with the pregestational state and developed pronounced diabetic phenotypes as a result of pregnancy. These results indicate that LIRKO females exhibit significant metabolic alterations during pregnancy and can be used as a potential model to study the effects of hyperinsulinemia and transient hyperglycemia on fetal growth and development. Our data using this unique model indicated that offspring born to LIRKO mothers have multiple metabolic alterations and are characterized by a reduction in β-cell reserves during early postnatal life.

MATERIALS AND METHODS

Animals

Control ($IR^{lox/lox}$:alb-$Cre^{-/-}$) and LIRKO ($IR^{lox/lox}$:alb-$Cre^{+/-}$) mice were maintained on the C57BL/6 background after back-crossing to 12 generations and bred at the Joslin Animal Facility on a 12:12-h light-dark cycle with ad libitum water and food. Female mice were caged with males, and mating was confirmed by the presence of vaginal plaque checked in the morning. The presence of vaginal plaques was considered to represent pregnancy day 0.5. Fetuses or neonates were euthanized together with their mothers at key stages during normal mouse pancreatic development {embryonic day [E]13.5, E15.5, and E17.5, newborn [postnatal day 0 (P0)], P4, and P10}. Fetuses/neonates were counted, weighed, and euthanized by decapitation, and blood was collected from cervical vessels. Pancreata were rapidly dissected, weighed, and fixed in Z-fix or 4% parafor-

* S. Kahraman and E. Dirice contributed equally to this article.

Address for reprint requests and other correspondence: R. N. Kulkarni, Joslin Diabetes Center and Harvard Medical School Boston, MA 02215 (e-mail: Rohit.Kulkarni@joslin.harvard.edu).

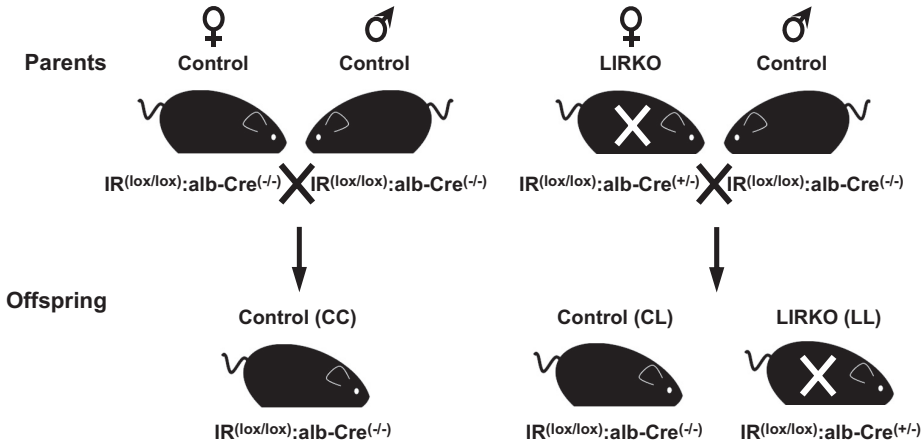

Fig. 1. Breeding scheme. Female control mice were crossed to male control mice to produce control offspring exposed to a normal intrauterine environment (CC, control offspring from control mother). Female liver-specific insulin receptor knockout (LIRKO) mice were crossed to male control mice to produce control offspring exposed to an insulin-resistant intrauterine environment (CL, control offspring from LIRKO mother; LL, LIRKO offspring from LIRKO mother). All studies were focused on comparing control pups (CC vs. CL). IR, insulin receptor; alb, albumin.

maldehyde solution. Perigonadal white adipose tissues from 10-day-old offspring were dissected, divided into two parts, and either rapidly frozen in liquid nitrogen or fixed in Z-fix overnight at 4°C. Sexes and genotypes were determined by PCR analysis of genomic DNA obtained from tail snip (22). All procedures were approved by the Joslin Diabetes Center Institutional Animal Care and Use Committee and performed in accordance with National Institutes of Health (NIH) guidelines.

Oral Glucose Tolerance Tests

All mice were subjected to oral glucose tolerance tests (OGTT) on day 15.5 of pregnancy. Mice were fasted overnight for 14 h, followed by glucose administration (2.5 g/kg body wt) using oral gavage. Blood glucose was measured using an automatic glucometer (Glucometer Elite; Bayer) immediately before (*time 0*) and 15, 30, 60, and 120 min after the injection.

Insulin Tolerance Test

An insulin tolerance test was performed on control and LIRKO females before pregnancy, on day 15.5 of pregnancy, and after delivery (L0 and L4). The mice were fasted for 3 h (between 7 and 10 AM) and were injected intraperitoneally with 1 U/kg body wt insulin (Humulin R, U-100; Eli Lilly). Blood glucose concentrations were measured from the tail vein using an automatic glucometer before (*time 0*) and 15, 30, 45, and 60 min after insulin injection.

Pregnancy Hormone Concentrations

The levels of progesterone (Cusabio Biotech), prolactin (Calbiotech), and estradiol (Calbiotech) were measured by ELISA in the Joslin Specialized Assay Core.

Blood Glucose, Plasma Insulin, Leptin, Glucagon, Glucagon-Like Peptide-1, and C-peptide Concentrations

Ad libitum glucose levels were measured by a glucometer using tail vein blood. Plasma insulin, leptin, glucagon, glucagon-like peptide-1 (GLP-1), and C-peptide concentrations were measured in the Joslin Specialized Assay Core.

Measurement of Adipocyte Size

Five-micrometer sections of paraffin-embedded perigonadal white adipose tissues from 10-day-old pups were stained with hematoxylin and eosin. Five digital images from nonoverlapping fields were obtained at ×20 magnification from each section from four different animals per group. Pictures were analyzed using Cell Profiler image analysis software, and adipocyte pixel area was converted to adipocyte diameter (3, 6). A total of 2,000 cells (CC group) or 1,250 cells (CL group) were analyzed per section.

RNA Extraction and Quantitative RT-PCR

Perigonadal white adipose tissue from 10-day-old pups was homogenized in Trizol (Life Technologies) using Bullet Blender (Next Advance, Averill Park, NY) at speed 9 for 5 min at 4°C. Total RNA was extracted using the Direct-zol RNA MiniPrep Kit (Zymo Research, Irvine, CA) according to the manufacturer's instructions. Complementary DNA (cDNA) was generated from total RNA with the High Capacity cDNA Reverse Transcription Kits (Applied Biosystems, Foster City, CA) and used for quantitative RT-PCR with i*Taq* Universal SYBR Green (Bio-Rad Laboratories). Expression was normalized to TATA box-binding protein. Primer sequences are listed in Table 6.

Table 1. *Measurements of body weight, blood glucose, and serum insulin in control and LIRKO dams*

	Body Weight, g		Weight Gain/Pup, g		Blood Glucose, mg/dl		Serum Insulin, ng/ml	
	Control (n = 7–10)	LIRKO (n = 6–9)	Control (n = 7)	LIRKO (n = 7)	Control (n = 4)	LIRKO (n = 4)	Control (n = 3–6)	LIRKO (n = 3–6)
G0	20.4 ± 0.7	21.4 ± 1.1			123.8 ± 3.7	137.0 ± 16.5	0.38 ± 0.12	4.54 ± 1.12‡
G13.5	27.0 ± 1.0***	27.7 ± 1.1**	0.88 ± 0.06	0.91 ± 0.07	125.8 ± 9.0	131.3 ± 23.1	ND	ND
G15.5	30.5 ± 1.0***	30.0 ± 1.0***	1.25 ± 0.07†	1.32 ± 0.11§	109.4 ± 9.0	196.3 ± 55.3‡	1.43 ± 0.12*	8.08 ± 1.05*‡
G17.5	34.8 ± 1.2***	33.2 ± 1.4***	1.77 ± 0.08†	1.70 ± 0.06§	97.3 ± 8.3*	121.6 ± 9.3‡	1.21 ± 0.80	6.30 ± 1.74‡
L0	26.4 ± 0.8***	27.6 ± 1.6**			109.7 ± 6.2*	147.5 ± 17.2	1.79 ± 0.50*	3.21 ± 0.35‡
L4	25.3 ± 0.7***	26.9 ± 0.7***			113.0 ± 12.3	127.0 ± 1.7	2.20 ± 0.68**	4.07 ± 0.82
L10	25.7 ± 1.7***	26.9 ± 0.6**			121.7 ± 4.1	148.0 ± 25.5	ND	ND

Values are means ± SE. LIRKO, liver-specific insulin receptor knockout; G, gestational days; L, lactation days (L0 is first day of lactation); ND, not determined. ***$P < 0.001$ vs. G0; **$P < 0.01$ vs. G0; †$P < 0.001$ vs. G13.5; §$P < 0.05$ vs. G13.5; *$P < 0.05$ vs. G0; ‡$P < 0.05$ vs. control.

Table 2. *Measurements of OGTT in control and LIRKO dams on day 15.5 of pregnancy*

	Blood Glucose, mg/dl	
	Control (n = 6)	LIRKO (n = 6)
Time, min		
0	84.8 ± 4.8	80.1 ± 5.3
15	269.3 ± 11.0	319.9 ± 17.4*
30	326.0 ± 9.4	394.0 ± 12.9**
60	255.2 ± 32.9	362.3 ± 36.5*
120	111.8 ± 23.6	272.9 ± 24.1***
Glucose AUC, mg·min·dl^{-1}	26,848.8 ± 1,722.0	38,752.5 ± 1,902.6***

Values are means ± SE. OGTT, oral glucose tolerance test; AUC, area under the curve. *$P < 0.05$, **$P < 0.01$, and ***$P < 0.001$ vs. control.

Immunohistochemistry

Five-micrometer sections of paraffin-embedded pancreas were dewaxed using xylene and rehydrated through serial dilutions of ethyl alcohol. Deparraffinized sections were subjected to heat-induced antigen retrieval using 10 mM citrate (pH 6.1). The sections were washed, blocked with 5% donkey serum for 1 h, and incubated overnight at 4°C with the primary antibodies guinea pig anti-insulin (1:200; Abcam), mouse anti-glucagon (1:50; Sigma-Aldrich), rabbit anti-somatostatin (1:50; Abcam), or mouse anti-Ki-67 (1:50; BD Bioscience). Slides were washed in PBS and incubated for 1 h at room temperature with the secondary antibodies Texas Red-conjugated anti-guinea pig, AMCA-conjugated anti-mouse, Cy2-conjugated anti-rabbit, and DyLight-488-conjugated anti-mouse (1:200; Jackson ImmunoResearch Laboratories) and counterstained with DAPI for 5 min.

Morphometric Analysis of Pancreas

Two representative sections from three to four animals per group per stage were viewed and photographed using a fluorescent microscope (Olympus BX-61; Olympus America, Melville, NY) equipped with a DP72 digital camera. The total area of pancreatic tissue for each section and the area of insulin immunoreactivity for each islet were measured by using ImageJ software (http:/rsb.info.nih.gov/ij/). β-Cell area was determined by dividing insulin positive area over the total pancreas area, and β-cell mass was estimated by morphometric analysis, as described previously (27). An islet cluster was defined as containing eight (~800 μm^2) endocrine cells, as reported previously (47). Islet number per square millimeter total pancreatic area was determined by dividing the total number of islets over total pancreas area. The percentage of Ki-67-expressing β-cells at different stages was calculated by proportion of insulin plus Ki-67+ over total insulin+ cells. At least 1,000–2,000 β-cell nuclei per pancreas were counted, and data were expressed as the percent of Ki-67+ β-cells.

Statistical Analysis

Statistical analysis was performed by Student's t-test. All values are means ± SE, and statistical significance was set at $P < 0.05$.

RESULTS

Breeding Insulin-Resistant Dams

Eight- to 10-week-old control females (IR$^{lox/lox}$:alb-Cre$^{-/-}$) and LIRKO females (IR$^{lox/lox}$:alb-Cre$^{+/-}$) were bred with aged matched control males (IR$^{lox/lox}$:alb-Cre$^{-/-}$). Three types of progeny resulted from these crosses: *1*) control offspring (IR$^{lox/lox}$:alb-Cre$^{-/-}$) from control mothers (CC), *2*) control offspring (IR$^{lox/lox}$:alb-Cre$^{-/-}$) from LIRKO mothers (CL), and *3*) LIRKO offspring (IR$^{lox/lox}$:alb-Cre$^{+/-}$) from LIRKO mothers (LL) (Fig. 1). To study the contributions of genetically imposed insulin resistance in the mother per se to metabolic and endocrine phenotypes in the offspring, we compared the differences in phenotypes between control offspring born to insulin-resistant or control mothers (CL vs. CC).

Effects in the Mother

Changes in maternal body weight, blood glucose concentrations, and serum insulin concentrations. To assess the effects of genetic insulin resistance on weight gain patterns of dams during and after pregnancy, body weight was monitored from conception until lactation. All dams gained weight significantly during pregnancy, and body weight changes were comparable between control and LIRKO dams. Body weight gain of dams per pup was not significantly different between control and LIRKO dams (Table 1).

Control dams revealed lower blood glucose concentrations on gestational day 17.5 (G17.5) compared with the nongravid state ($P < 0.05$), whereas LIRKO dams did not. On the other hand, LIRKO dams exhibited elevated concentrations of blood glucose on G15.5 and G17.5 compared with the control group (Table 1).

Serum insulin concentrations were persistently high in LIRKO mothers compared with the control group throughout the entire study. In addition, both LIRKO and control dams displayed elevated concentrations of serum insulin on G15.5 compared with the nongravid state ($P < 0.05$) due to increased insulin demand during pregnancy (Table 1).

Development of gestational diabetes in pregnant LIRKO females. To determine whether LIRKO females could maintain glucose homeostasis during pregnancy, OGTT were performed

Table 3. *Measurements of insulin tolerance test in control and LIRKO dams at different time points (G0, G15.5, L0, and L4)*

	Initial Blood Glucose, %							
	G0		G15.5		L0		L4	
Time, min	Control (n = 6)	LIRKO (n = 5)	Control (n = 3)	LIRKO (n = 4)	Control (n = 3)	LIRKO (n = 3)	Control (n = 3)	LIRKO (n = 3)
0	100.0 ± 0.0	100.0 ± 0.0	100.0 ± 0.0	100.0 ± 0.0	100.0 ± 0.0	100.0 ± 0.0	100.0 ± 0.0	100.0 ± 0.0
15	77.8 ± 4.6	79.2 ± 4.1	66.0 ± 7.7	96.3 ± 2.5*	63.8 ± 9.7	68.5 ± 7.6	69.8 ± 1.0	73.1 ± 4.8
30	57.7 ± 4.7	65.2 ± 5.2	50.2 ± 4.4	86.0 ± 10.1*	41.3 ± 7.2	51.1 ± 5.9	52.7 ± 2.1	56.4 ± 3.9
45	38.9 ± 4.3	59.8 ± 6.1	35.7 ± 3.3	78.4 ± 11.2*	31.2 ± 3.9	45.1 ± 7.9	38.4 ± 6.9	51.1 ± 2.9
60	34.1 ± 4.8	69.4 ± 12.9*	29.5 ± 7.6	76.1 ± 4.8**	27.8 ± 2.8	57.8 ± 5.9*	33.4 ± 2.2	60.1 ± 4.9*
AUC	3,647.2 ± 265.2	4,333.6 ± 244.8	3,249.9 ± 239.8	5,231.1 ± 349.0**	3,002.4 ± 302.1	3,655.5 ± 270.0	3,413.5 ± 125.3	3,910.1 ± 192.5

Values are means ± SE. *$P < 0.05$ and **$P < 0.01$ vs. control.

Table 4. *Measurements of hormone levels in control and LIRKO dams during pregnancy*

	Plasma Prolactin, ng/ml (n = 7)		Plasma Progesterone, ng/ml (n = 7)		Plasma Estradiol, pg/ml (n = 7)		Plasma Leptin, pg/ml (n = 7–8)	
	Control	LIRKO	Control	LIRKO	Control	LIRKO	Control	LIRKO
G0	81.3 ± 24.1	33.1 ± 12.7	2.98 ± 0.6	2.20 ± 0.3	102.3 ± 5.0	121.8 ± 6.2†	157.4 ± 24.8	252.8 ± 14.5‡
G15.5	143.8 ± 39.3	11.9 ± 3.4†	22.62 ± 4.7**	9.90 ± 1.1***†	110.2 ± 6.5	170.3 ± 17.8*†	229.0 ± 33.8	272.3 ± 33.9
G17.5	187.4 ± 24.9*	45.0 ± 15.0†	9.75 ± 2.7*	5.43 ± 1.1*	227.2 ± 59.0*	155.4 ± 8.9*	162.2 ± 19.0	427.2 ± 71.2*†
L0	83.0 ± 25.8	15.2 ± 6.6†	3.07 ± 0.6	2.89 ± 1.4	120.6 ± 16.7	108.6 ± 12.8	203.9 ± 46.4	149.5 ± 20.4**
L4	33.3 ± 10.5	17.8 ± 13.0	3.61 ± 0.5	2.13 ± 0.1	100.4 ± 16.8	94.3 ± 9.6*	197.9 ± 51.0	170.1 ± 23.9*

Values are means ± SE. *$P < 0.05$ vs. G0; **$P < 0.01$ vs. G0; ***$P < 0.001$ vs. G0; †$P < 0.05$ vs. control; ‡$P < 0.01$ vs. control.

on G15.5. LIRKO females displayed impaired glucose tolerance at G15.5 compared with control females. In humans, gestational diabetes mellitus is diagnosed if two or more values are abnormal on a 2-h, 75-g OGTT. The normal cutoff values of the OGTT are <95 mg/dl at fasting, 180 mg/dl at 1 h, and 155 mg/dl at 2 h (35). According to our results, blood glucose levels of both control and LIRKO dams were <95 mg/dl at fasting but then increased 1 h after glucose challenge in both control and LIRKO females >180 mg/dl (362 ± 37 mg/dl in LIRKO vs. 255 ± 33 mg/dl in control, $P < 0.05$; Table 2). Although the blood glucose concentrations were within the normal range in control females 2 h after glucose challenge, they remained significantly high in LIRKO females (273 ± 24 mg/dl in LIRKO vs. 112 ± 24 mg/dl in control, $P < 0.001$), indicating glucose intolerance in the latter LIRKO females during pregnancy. The presence of impaired glucose tolerance and transient increase in blood glucose levels in LIRKO females during pregnancy suggests that this is a model of gestational diabetes (34).

Exacerbation of insulin resistance in pregnant LIRKO females. Insulin tolerance tests revealed that LIRKO dams were mildly resistant to the blood glucose-lowering effects of exogenous insulin before pregnancy and are severely resistant on day 15.5 of pregnancy (Table 3). One interpretation of these data is that pregnancy exacerbates the preexisting insulin resistance in LIRKO dams.

Changes in hormone concentrations. To determine the changes in pregnancy hormones in our model, plasma levels of prolactin, progesterone, estradiol, and leptin were measured in LIRKO and control dams. The production of prolactin, progesterone, and estrogens increases exponentially in normal pregnancy and declines during lactation (14). Interestingly, plasma prolactin levels remained low in LIRKO females throughout gestation, whereas they increased in control females. The levels of prolactin observed in our experiments are consistent with a previous study in mice (28). Plasma progesterone levels were elevated at G15.5 in both control and LIRKO females but were significantly lower in LIRKO compared with control females. In contrast, plasma estradiol levels on G15.5 and leptin levels on G17.5 were significantly higher in LIRKO compared with control females (Table 4).

Table 5. *Litter size and newborn death*

	Newborn No.		Newborns That Died After Birth	
Group (n)	Total no.	No./litter	Total no.	No./litter
Control (13)	87	6.69 ± 0.46	12	0.92 ± 0.47
LIRKO (13)	76	5.85 ± 0.63	22	1.69 ± 0.52
P value		0.09		0.14

Values are means ± SE.

Effects in the Offspring

Effects of maternal insulin resistance on litter size and neonatal death. The mean litter sizes for the control (6.69 ± 0.46 pups/litter) and the LIRKO groups (5.85 ± 0.63 pups/litter) was not significantly different ($P = 0.09$). The newborn deaths in litters from either group were also not significantly different (control, 0.92 ± 0.47 pups/litter vs. LIRKO, 1.69 ± 0.52 pups/litter), although there was a tendency to increase in the latter group ($P = 0.14$) (Table 5). These results suggest that maternal insulin resistance was not obviously detrimental to fetal life in this model.

Low birth weight and rapid catchup growth in offspring born to insulin-resistant mothers. To investigate whether maternal insulin resistance affects growth of the progeny, we monitored body weights of offspring from E13.5 to P10 (Fig. 2, *A* and *B*). Offspring in both groups and both sexes gained body weight significantly over the period from E13.5 to P10. The birth weights of male offspring born to insulin-resistant mothers were below the mean value of the birth weights of the male control group, and these offspring recovered their lower body weight shortly after birth by gaining more weight compared with CC group. The CL offspring not only recovered their body weight deficiency but in fact exhibited faster weight gain and outpaced the controls in absolute weight gain in the postnatal period. Similarly, female pups from LIRKO mothers exhibited reduced birth weight and catchup growth at P10. Together, these data indicated that maternal insulin resistance results in low birth weight followed by catchup growth in offspring in both sexes.

Higher blood glucose and insulin concentrations in offspring born to insulin-resistant mothers shortly after birth. To evaluate the effects of maternal insulin resistance on glucose homeostasis in the offspring, blood glucose and plasma insulin concentrations were analyzed. As expected, blood glucose increased gradually in all offspring as they aged and gained weight. No significant difference in blood glucose levels was observed between groups either before or at the time of birth in either sex (Fig. 2, *C* and *D*). However, fluctuations in the concentrations of plasma insulin were observed in both CL and CC groups before birth due to the alterations in the islet cell population in the late fetal period. Plasma insulin concentrations of CC fetuses peaked at E17.5 ($P < 0.05$, E17.5 vs. E15.5), followed by a decrease at birth ($P < 0.05$, E17.5 vs. P0) in both sexes (Fig. 2, *E* and *F*). Similarly, plasma insulin concentrations of CL fetuses increased at E17.5 ($P < 0.05$, E17.5 vs. E15.5), but this increase remained lower compared

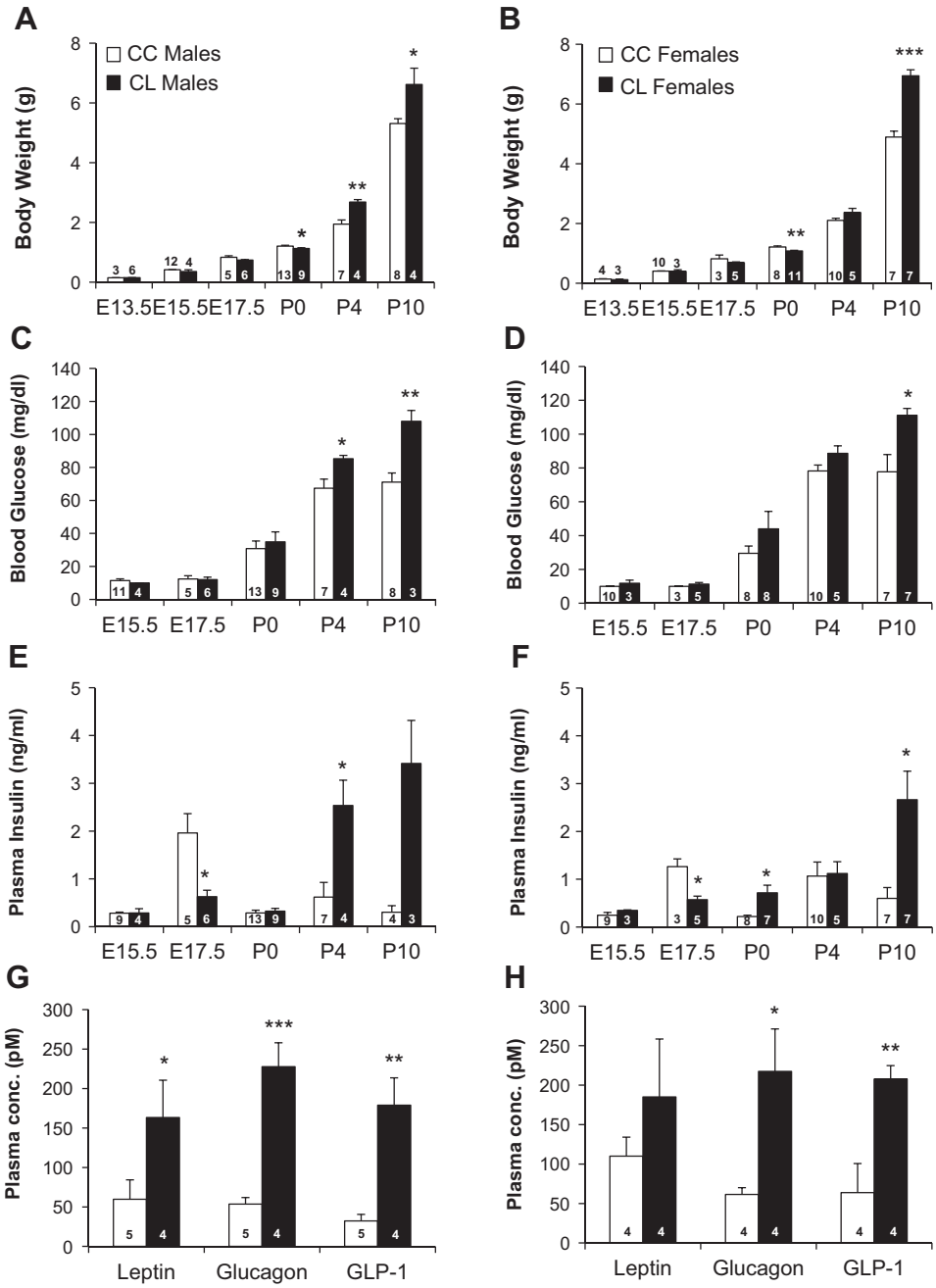

Fig. 2. Changes in body weight and metabolic and hormonal parameters in offspring. Changes in body weight (*A* and *B*), blood glucose concentrations (*C* and *D*), and plasma insulin concentrations (*E* and *F*) with age for male (*A*, *C*, and *E*) and female (*B*, *D*, *F*) offspring. Changes in plasma leptin, glucagon, and glucagon-like peptide-1 (GLP-1) concentrations of 4-day-old male (*G*) and female (*H*) offspring. Open bars, CC; black bars, CL. $*P < 0.05$, $**P < 0.01$, and $***P < 0.001$ vs. CC (Student's *t*-test). Data are expressed as means ± SE. Numbers (*n*) are included within each bar. E13.5, E15.5, and E17.5, embryonic days 13.5, 15.5, and 17.5, respectively; P0, newborn (postnatal day 0); P4 and P10, postnatal days 4 and 10, respectively.

with the CC group. Low levels of insulin at E17.5 might indicate abnormalities in the development of fetal β-cells in offspring born to insulin-resistant mothers. Shortly after birth, male offspring born to LIRKO mothers showed significant increases in both blood glucose and plasma insulin concentrations compared with male CC offspring. These effects were more prominent at P10 in the female CL offspring.

C-peptide analysis in CL males. To determine whether the increased plasma insulin levels in 4-day-old and 10-day-old CL males were a consequence of increased secretion from β-cells, we also measured plasma C-peptide levels. C-peptide, which is cosecreted with insulin from β-cells at a 1:1 molar ratio, is a reliable measurement of secretion (44). Although C-peptide levels tended to increase in 4-day-old CL males compared with CC, the difference did not reach statistical significance (Fig. 3*A*). To differentiate insulin secretion vs. insulin resistance, the mean for C-peptide/insulin (C/I) ratio was calculated as individual C-peptide concentration divided by the insulin concentration (39). Although there were no significant differences in the C-peptide levels between the CL and CC pups on either P4 (Fig. 3*A*) or P10 (Fig. 3*B*), the C/I ratio tended to decrease in 4-day-old CL males compared with controls. These results suggested that the altered insulin levels are likely due to development of insulin resistance in CL pups (Fig. 3*C*).

Higher plasma leptin, glucagon, and GLP-1 concentrations in offspring born to insulin-resistant mothers shortly after birth. To further determine changes in metabolism of offspring, metabolic markers (leptin, glucagon, and active GLP-1) were

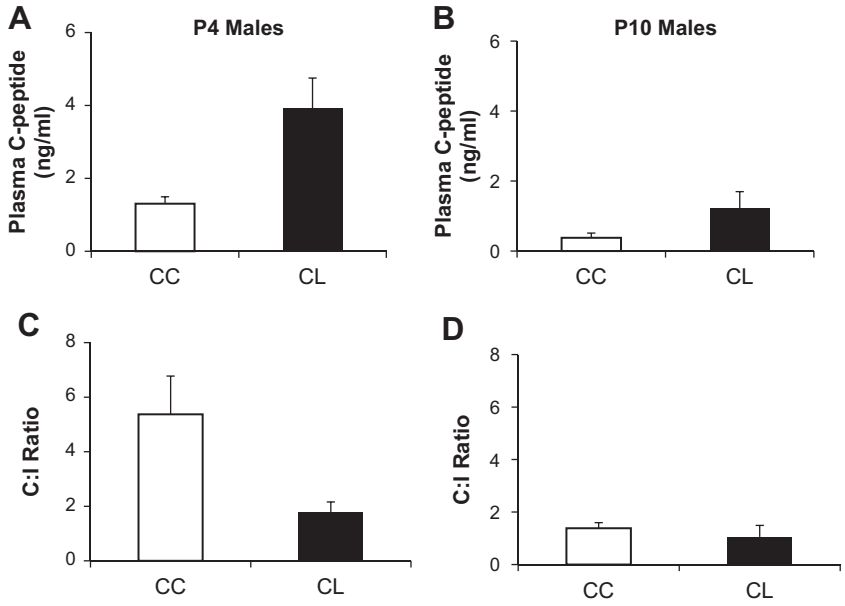

Fig. 3. Plasma C-peptide concentrations and C-peptide/insulin (C/I) ratios in the male offspring. Changes in plasma C-peptide concentrations of 4- (*A*) and 10-day-old male offspring (*B*). The C/I ratio was calculated as the C-peptide concentration divided by the insulin concentration for each individual pup. C/I ratios were given for 4- (*C*) and 10-day-old males (*D*). Open bars, CC; black bars, CL. Data are expressed as means ± SE; $n = 3$/group.

measured in plasma samples obtained from 4-day-old pups, when catch up growth was detected in the LIRKO group (Fig. 2, *G* and *H*). Plasma leptin concentrations were elevated more than twofold in male CL compared with male CC offspring. Similarly, female pups from LIRKO mothers had elevated levels of leptin compared with female CC pups, but this did not reach statistical significance. An increase in leptin concentrations, which is an adiposity marker (32), in offspring born to insulin-resistant mothers might indicate an increase in adipose mass. CL pups exhibited significantly higher levels of plasma glucagon and GLP-1 than CC pups in both sexes. Together, these results suggest that maternal insulin resistance induces multiple metabolic alterations in the offspring, as shown by elevated levels of leptin, glucagon, and GLP-1.

Adipocyte size is increased in 10-day-old CL pups. To examine whether the increased plasma leptin levels in CL males were due to an increase in adipose tissue, adipocyte size was measured. Hematoxylin and eosin staining revealed that mean adipocyte diameters were similar in CL and in CC pups in both sexes (Fig. 4, *C* and *D*). When adipocytes were plotted according to their size, we noted a marked decrease in the number of small adipocytes (20–30 and 30–40 μm) and an increase in adipocytes >50 μm in CL compared with CC offspring, indicating a rightward shift in the CL group (Fig. 4, *E* and *F*). Thus, the increase in adipocyte size might be one factor that contributes to higher body weights and metabolic phenotypes in CL mice.

To determine whether the increase in adipocyte size was accompanied by alterations in gene expression in adipocyte differentiation processes, we performed quantitative RT-PCR of RNA from adipose tissue of 10-day-old CL offspring. As shown in Fig. 5, a significant increase in expression of the adipogenic transcription factor C/EBPα was observed in both sexes. PPARα gene expression was significantly increased in CL females and tended to be higher in CL males ($P = 0.08$). Expression of genes involved in lipogenesis (*Fasn*, *Acc*, and *Chrebp*) or the differentiated adipocyte marker *aP2* tended to be higher in the CL group but did not reach statistical significance, and the expression of *Srebf1* did not show a change (primer sets are listed in Table 6).

Reduced β-cell area and islet number in CL offspring. To elucidate how insulin resistance in the mother could affect the development of fetal endocrine pancreas, pancreatic sections were analyzed for β-cell morphology both before and after birth. Although morphologically similar islets were observed in both CL and CC offspring (Fig. 6*A*), the β-cell mass tended to decrease in CL compared with CC throughout the study in male offspring (Fig. 6*B*). In females, β-cell mass was comparable between CC and CL offspring throughout the study and tended to decrease when they were 10 days old. The percentage of β-cell area in CL offspring was significantly lower in males at P4 and P10 (Fig. 6*C*) and relatively small in CL females at P10 ($P = 0.09$). The total number of islets was fewer in both CL males and females than CC at P10 (Fig. 6*D*).

Diminished β-cell proliferation in CL offspring during early postnatal life. To determine the contribution of β-cell proliferation to the observed changes in β-cell mass and β-cell area in offspring, pancreatic sections were coimmunostained with the Ki-67 antibody, a marker for proliferating cells (Fig. 6*E*) and insulin. The percentage of Ki-67+ β-cells tended to decrease in CL offspring during the perinatal period and exhibited a significant reduction on P10 compared with CC pups (Fig. 6*F*). This suggests that a low β-cell proliferation capacity contributes in part to the significantly reduced β-cell area in the CL group. Despite reduction in their β-cell area, offspring born to insulin-resistant mothers were mildly hyperinsulinemic. This may indicate a higher insulin content per β-cell. Hypersecretion of insulin of islets observed in offspring of undernutrition pregnancies (18) and neonatal β-cell hyperactivity observed in nonobese diabetic mice neonates (43) indicate that maternal environment might affect β-cell secretory function in offspring.

To determine whether formation of new islets could contribute to the observed changes in β-cell mass and β-cell area in offspring, the number of small islet clusters was evaluated (Fig. 7*A*). Reduction in the number of small islet clusters of 10-day-

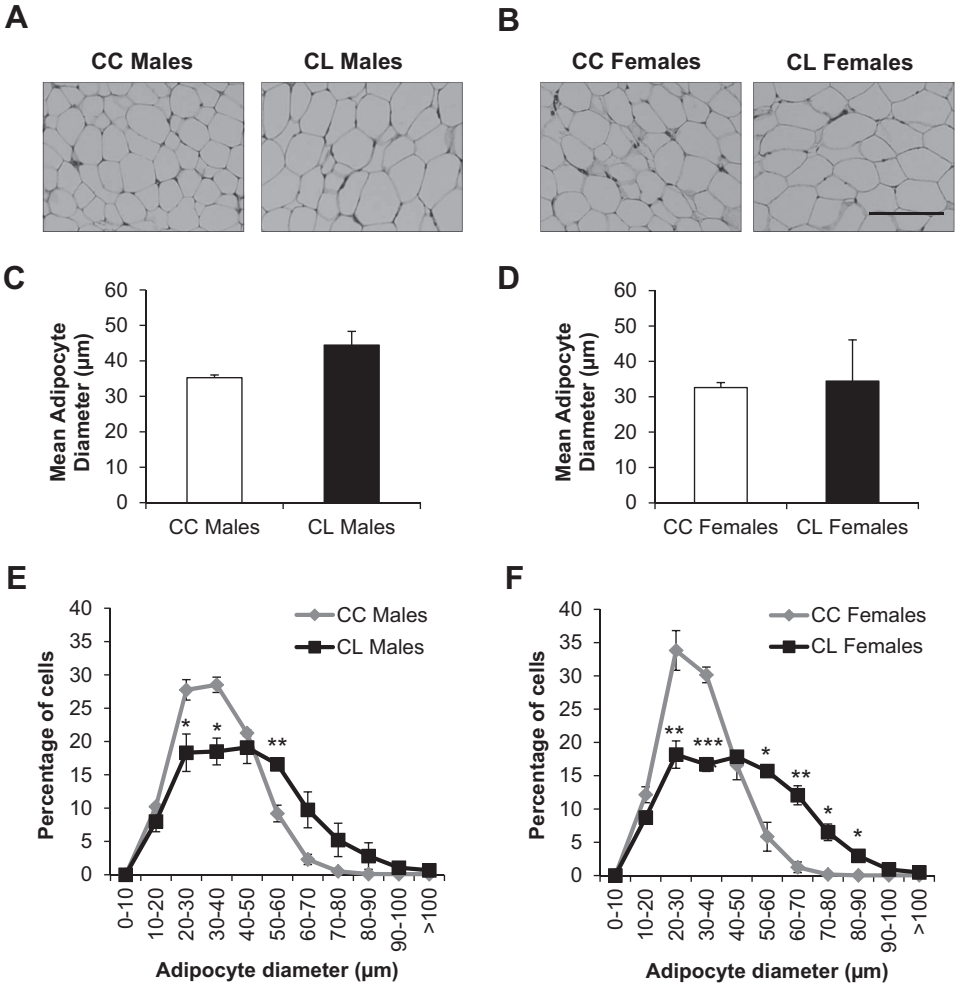

Fig. 4. Representative hematoxylin and eosin staining of subcutaneous adipose tissue of 10-day-old male (*A*) and female (*B*) offspring. Scale bar, 100 μm. Mean adipocyte diameter (μm) for males (*C*) and females (*D*). Adipocyte cell size distribution for males (*E*) and females (*F*). $*P < 0.05$, $**P < 0.01$, and $***P < 0.001$ vs. CC (Student's *t*-test). Data are expressed as means ± SE; $n = 4$/group.

old CL pups vs. CC was observed (Fig. 7*B*). This suggests that the appearance of small islet cell clusters contributes in part to the significantly reduced β-cell area in the CL group.

To determine the effect of maternal insulin resistance on the development of endocrine cells other than β-cells, we measured α-cell area and α-cell mass of the offspring. α-Cell area tended to decrease in the CL group after birth, and the difference between CL and CC group became significant in males on P10 (Fig. 7*C*). Similarly, α-cell mass was significantly smaller in CL compared with the CC pups on P0 and was slightly smaller, albeit insignificant, on P4 and P10 (Fig. 7*D*).

DISCUSSION

The impairment of maternal glucose homeostasis has clearly defined effects on the development of the fetus, and especially on the development and function of its endocrine pancreas (45). However, the effects of maternal insulin resistance on fetal metabolism and the consequences on fetal pancreas development have not been fully explored. To examine the hypothesis that an insulin-resistant intrauterine environment influences metabolism in the offspring and development of the endocrine pancreas, we used LIRKO females as an insulin-resistant mouse model.

Human pregnancy is characterized by a series of metabolic changes to meet the demands of the growing fetus. For example, an increase in serum insulin levels, a slight decrease in blood glucose levels, and development of peripheral insulin resistance all occur during pregnancy, and these changes trigger adaptive responses in β-cells to increase both insulin secretion and mass (41). Similarly, in our study, control mothers exhibited enhanced serum insulin and reduced blood glucose during late gestation, whereas LIRKO females, who already exhibit hyperinsulinemia (27), showed a further increase in insulin levels and an increase in blood glucose during pregnancy. Glucose and insulin tolerance tests on G15.5 showed a decrease in insulin sensitivity in LIRKO mice compared with controls. LIRKO females developed pronounced diabetic phenotypes during pregnancy and returned to pregestational levels after parturition in terms of blood glucose concentrations and insulin sensitivity. Considering that normal pregnancy itself induces a physiological insulin-resistant state (1), especially during late gestation, it is conceivable that LIRKO dams were more glucose intolerant and displayed a transient increase in blood glucose levels on G15.5 compared with control dams. These phenotypic changes observed in LIRKO females prompted us to use them as a potential model for studying the effects of gestational diabetes and insulin resistance in the mother on progeny.

Control offspring born to insulin-resistant mothers had reduced birth weight compared with offspring born to control

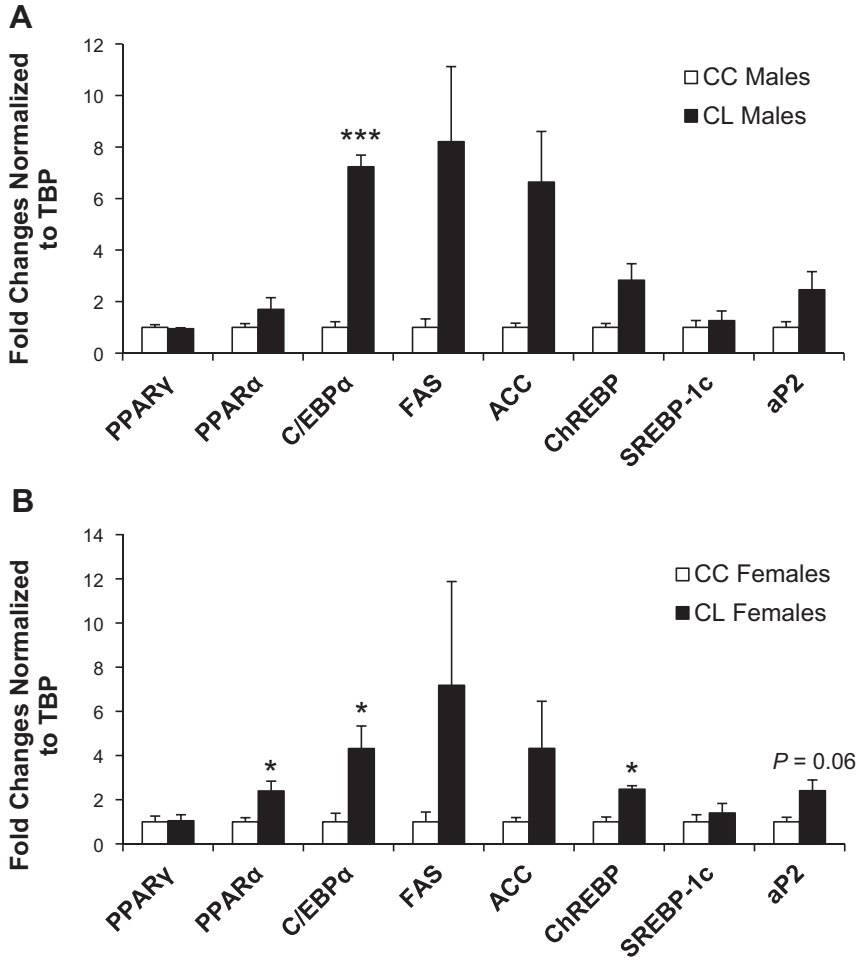

Fig. 5. Expression of genes related to adipocyte differentiation by quantitative RT-PCR of RNA from white adipose tissue of 10-day-old males (*A*) and females (*B*). $*P < 0.05$ and $***P < 0.001$ vs. CC (Student's *t*-test). Data are expressed as means ± SE; $n = 4$/group. Data are normalized to expression of TATA box-binding protein (TBP).

mothers, and this is consistent with the results from studies using hyperinsulinemic pregnant rats created by exogenous insulin treatment (without causing hypoglycemia) (5, 38). In the latter studies, fetuses of hyperinsulinemic rats were smaller than those of control mothers. Although maternal insulin has been reported not to cross the placental barrier to reach the fetus, excessive amounts of insulin in maternal circulation can alter placental gene expression to affect growth and function of placenta (9). Khamaisi et al. (21) and Skarzinski et al. (40) reported altered expression of endothelin-converting enzyme-1 and nitric oxide synthase expression in the placenta of hyperinsulinemic dams compared with normal pregnant dams and found an association between these alterations in the placental gene expression and intrauterine growth restriction in rats with maternal hyperinsulinemia. In accord with these findings, elevated insulin concentrations in LIRKO dams could result in various alterations in the placenta to influence fetal growth and development. However, the presence of transient hyperglycemia along with hyperinsulinemia in our model indicates that both elevated blood glucose and insulin levels potentially contribute to the fetal phenotype.

Consistent with previous reports, we observed that loss of insulin signaling in the liver of LIRKO mouse leads to an increase in serum leptin concentrations (7) and reduction in serum triacylglycerol and free fatty acid concentrations (27). Furthermore, during pregnancy, plasma levels of prolactin,

Table 6. *Primer sequences used for quantitative RT-PCR*

Gene Name	Sequence
PPARγ	
Forward	5′-GAC ATC AAG CCC TTT ACC AC-3′
Reverse	5′-CAC TTC TGA AAC CGA CAG TAC-3′
PPARα	
Forward	5′-GCG TAC GGC AAT GGC TTT AT-3′
Reverse	5′-GAA CGG CTT CCT CAG GTT CTT-3′
C/EBPα	
Forward	5′-GCG CAA GAG CCG AGA TAA A-3′
Reverse	5′-GGT GAG GAC ACA GAC TCA AAT C-3′
FASN	
Forward	5′-CTC TGA TCA GTG GCC TCC TC-3′
Reverse	5′-TGC TGC AGT TTG GTC TGA AC-3′
ACC	
Forward	5′-TGA CAG ACT GAT CGC AGA GAA AG-3′
Reverse	5′-TGG AGA GCC CCA CAC ACA-3′
ChREBP	
Forward	5′-CTG GGG ACC TAA ACA GGA GC-3′
Reverse	5′-GAA GCC ACC CTA TAG CTC CC-3′
SREBF1	
Forward	5′-ACG ACG GAG CCA TGG ATT GCA C-3′
Reverse	5′-CCG GAA GGC AGG CTT GAG TAC C-3′
AP2	
Forward	5′-CTG GGC GTG GAA TTC GAT-3′
Reverse	5′-GCT CTT CAC CTT CCT GTC GTC T-3′

PPARα and -γ, peroxisome proliferator-activated receptor-α and -γ, respectively; C/EBPα, CCAAT enhancer-binding protein-α; FASN, fatty acid synthase; ACC, acetyl-CoA carboxylase; ChREBP, carbohydrate response element-binding protein; SREBF1, sterol regulatory element-binding transcription factor 1; AP2, activator protein 2.

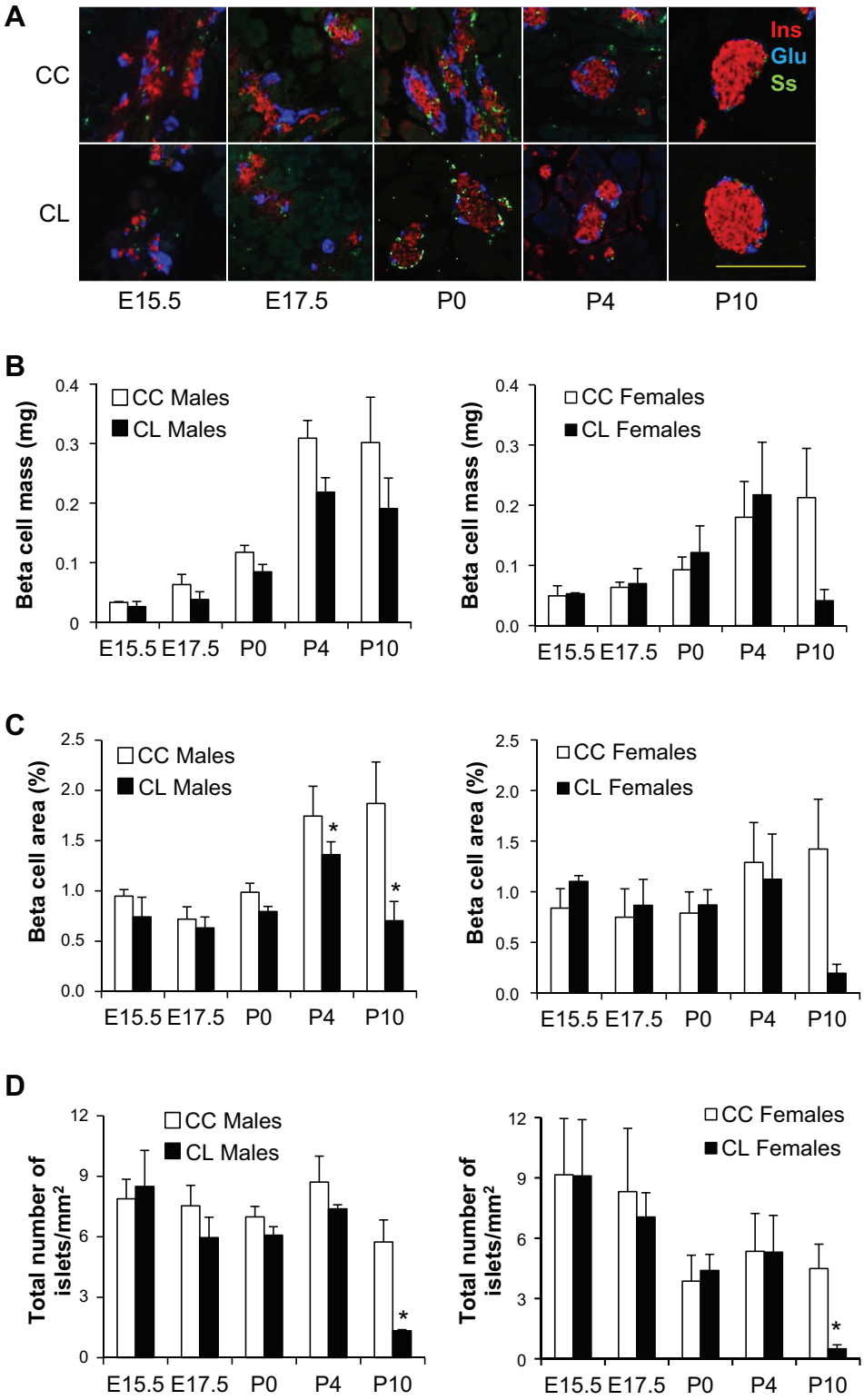

Fig. 6. Changes in islet morphology and β-cell proliferation in the offspring. *A*: representative immunofluorescent images of islets from male offspring at different ages coimmunostained for insulin (red), glucagon (blue), and somatostatin (green). *Top*: CC. *Bottom*: CL. Scale bar, 200 μm. *B* and C: alterations in β-cell mass (*B*) and %β-cell area (*C*) with age in the male and female offspring. *D*: alterations in total no. of islets in the male and female offspring. *E*: coimmunostaining of pancreas sections for the proliferation marker Ki-67 (green) with insulin (red) and DAPI (blue). Arrows indicate proliferating β-cells. *Top*: CC. *Bottom*: CL. Scale bar, 200 μm. *F*: changes in %β-cell proliferation in the male and female offspring. Open bars, control offspring from control mother; black bars, control offspring from LIRKO mother. *$P < 0.05$ vs. CC (Student's *t*-test). Data are expressed as means ± SE; $n = 3–4$/group (2 sections per pancreas).

progesterone, estradiol, and leptin were also altered in LIRKO dams compared with control dams. Although changes in placental hormone levels are known to occur during maternal adaptation to pregnancy to allow for optimal fetal growth, the roles of placental hormone expression in regulating fetal growth remain poorly understood (14). Thus, we cannot rule out the possibility that changes in one or more of these hormones and/or metabolites contribute to reduced birth weight or other abnormalities in control offspring born to LIRKO mothers (13).

Offspring born with low birth weight displayed a rapid catchup growth after birth and surpassed the weight of the

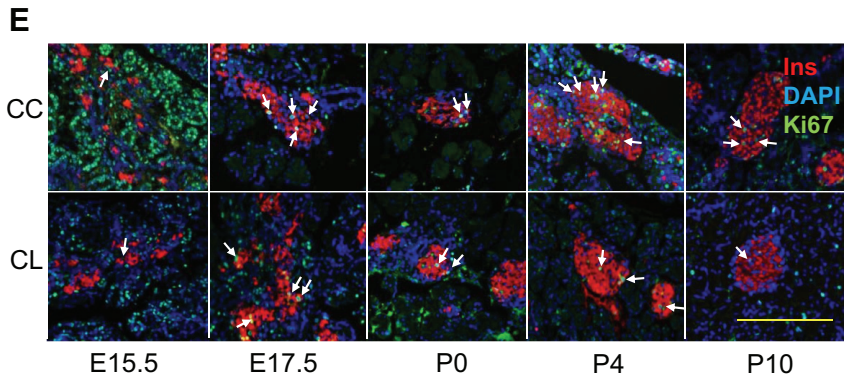

Fig. 6—*Continued*

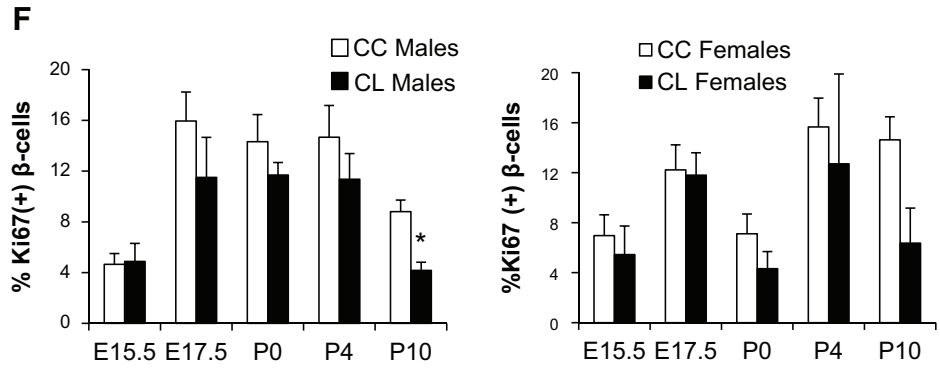

controls in early postnatal days. The finding of an association between accelerated catchup growth and increased adiposity (17) suggested that these offspring showed overgrowth due to the increase in their adipose mass. The elevated levels of plasma leptin, a marker of adiposity, and enlarged adipocytes associated with altered expression patterns of genes involved in adipocyte differentiation and lipogenesis supported these data. The finding of an association between accelerated catchup growth in early postnatal days and increased risk for insulin resistance and obesity in later life (33) could indicate an increased susceptibility to development of metabolic disease in the CL offspring during adulthood.

Shortly after birth, control offspring born to LIRKO mothers displayed higher plasma concentrations of both glucose and insulin than offspring born to control mothers, indicating early development of insulin resistance. In humans, early development of adiposity and insulin resistance after catchup growth supports this concept (17). Together with hyperinsulinemia and hyperglycemia, we observed higher plasma glucagon concentrations in CL pups. It is possible that α-cells of CL pups were insulin resistant, and therefore, they were poorly responsive to the suppressive effects of insulin (20) and glucose (31, 48). A similar explanation could underlie the higher concentrations of glucagon in CL males on day 4 after birth, even though their α-cell mass was similar to CC pups. Four-day-old CL pups also had elevated levels of GLP-1 that might be upregulated in response to the hyperglycemia. Further studies are warranted to identify mechanisms underlying hyperglucagonemia and elevated levels of GLP-1 observed in control pups of LIRKO mothers.

Normally, plasma insulin concentrations increase rapidly during the late fetal period, followed by a decrease immediately after birth (26, 30) due to the alterations in fetal β-cell mass in rats (19, 25). The lower insulin concentrations and relatively small β-cell mass in the control fetuses of LIRKO mothers compared with those of control mothers on E17.5 might indicate that maternal insulin resistance impairs the development of fetal β-cells. Following birth, CL pups exhibited reduced β-cell area and islet number and relatively reduced β-cell mass; however, they completely recovered their low body weights, supporting the possibility of a selective impairment in pancreas development by maternal insulin resistance. Reduced β-cell proliferation at P10 in CL pups compared with CC pups makes it likely that maternal insulin resistance affected β-cell proliferation and consequent reduction in β-cell mass in CL offspring. Consistent with our findings, previous studies have reported that abnormal intrauterine milieu could affect the development of the fetal endocrine pancreas by inducing gene expression modification permanently in pancreatic β-cells, leading to the development of diabetes in adulthood. Epigenetic alterations involved in the reduced β-cell mass could be one underlying molecular mechanism (10, 36, 37, 42).

The most profound differences in metabolic parameters between control offspring born to control and insulin-resistant mothers were evident during the early postnatal days, a stage that is approximately equivalent to postnatal human infancy or human childhood in mice. These results have potential implications for humans if maternal insulin resistance increases the risk of insulin resistance and obesity in children.

Early nutrition both in utero and after birth is known to be critical for the development of the offspring. Breast milk composition has been shown to influence infant growth and accrual of fat and lean body mass (12). Therefore, postnatal

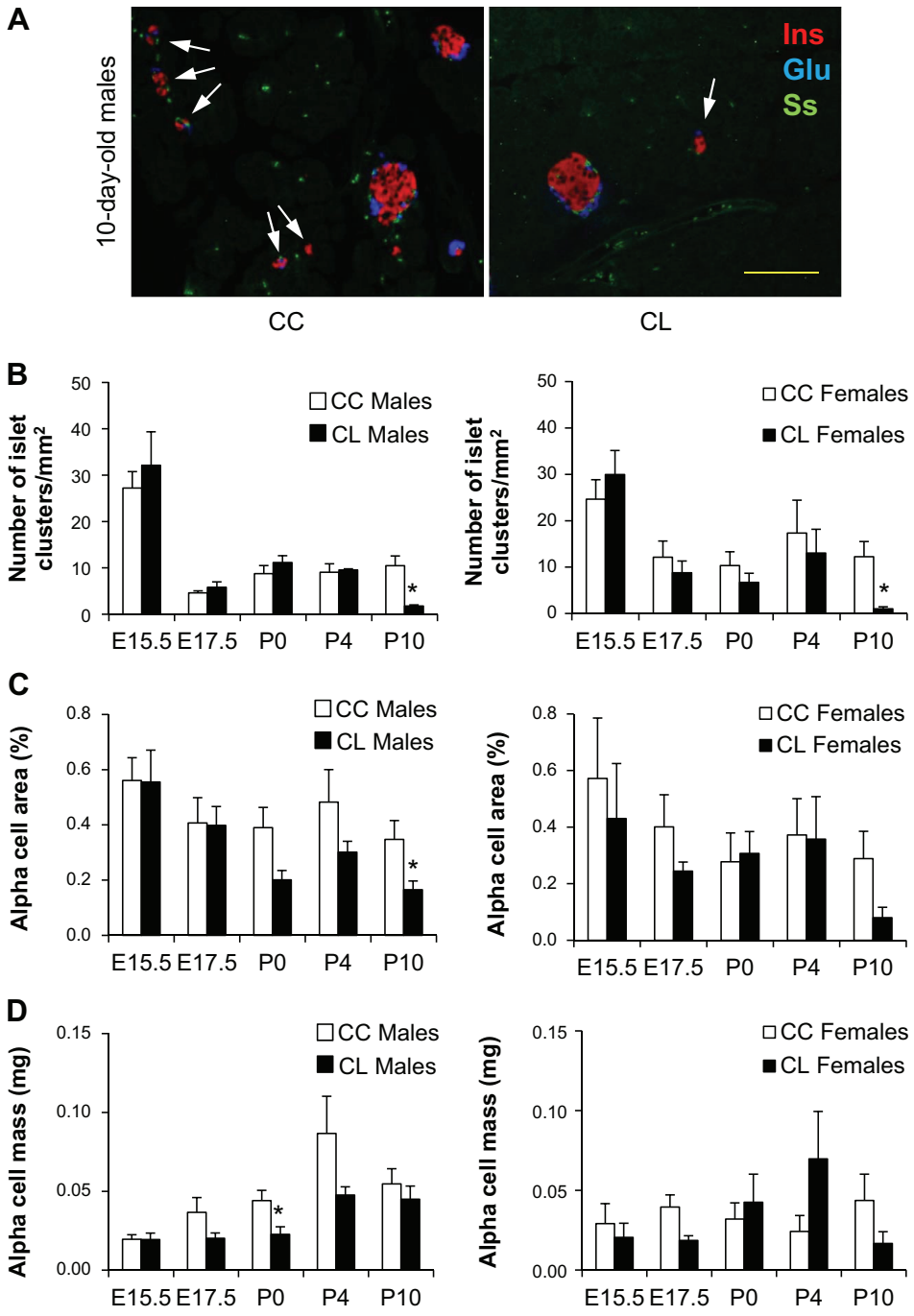

Fig. 7. Changes in the number of islet clusters and α-cell area in the offspring. *A*: representative immunofluorescent images of newly formed islets from 10-day-old male offspring coimmunostained for insulin (Ins; red), glucagon (Glu; blue), and somatostatin (Ss; green). Arrows indicate small islet clusters. *Left*: CC. *Right*: CL. Scale bar, 100 μm. *B*: the number of small islet clusters was decreased significantly in 10-day-old CL vs. CC in both sexes. *C* and *D*: alterations in α-cell area (*C*) and α-cell mass (*D*) of male and female offspring at different ages. $^*P < 0.05$ vs. CC (Student's *t*-test). Data are expressed as means ± SE; n = 3–4/group (2 sections per pancreas).

consumption of breast milk produced by LIRKO mothers might be a contributor to the metabolic phenotype observed in CL offspring. The impact of lactational nutrition on offspring by cross-fostering pups onto control mothers or insulin-resistant mothers warrants further investigation.

In the present study, we specifically assessed the effects of maternal insulin resistance on metabolic and endocrine phenotypes of offspring independently from the effects of maternal obesity. Since obesity is associated with a multitude of metabolic impairments, the exact cause of abnormalities in the metabolism of offspring and endocrine pancreas development would be confounding when studying obese models. In utero exposure to an insulin-resistant environment impairs adequate development of the endocrine pancreas, which fails to recuperate after birth, leading to decreased β-cell reserve and a potential predisposition to type 2 diabetes. Further studies are necessary to investigate the underlying mechanisms of reduced β-cell mass and β-cell proliferation in the progeny of insulin-resistant mothers.

ACKNOWLEDGMENTS

We thank Dr. C. Ronald Kahn (Joslin Diabetes Center and Harvard Medical School, Boston, MA) for the LIRKO mice and the Specialized Assay Core (Joslin Diabetes Center, Boston, MA) for hormone analyses.

GRANTS

R. N. Kulkarni acknowledges support from National Institute of Diabetes and Digestive and Kidney Diseases Grants RO1-DK-67536 and R01-DK-103215.

DISCLOSURES

All authors disclosed no potential conflicts of interest, financial or otherwise, that are relevant to this article.

AUTHOR CONTRIBUTIONS

S.K., E.D., and R.N.K. conception and design of research; S.K., E.D., D.F.D.J., and J.H. performed experiments; S.K., E.D., and R.N.K. analyzed data; S.K., E.D., and R.N.K. interpreted results of experiments; S.K. prepared figures; S.K. and R.N.K. drafted manuscript; S.K., E.D., and R.N.K. edited and revised manuscript; S.K., E.D., D.F.D.J., J.H., and R.N.K. approved final version of manuscript.

REFERENCES

1. **Barbour LA, McCurdy CE, Hernandez TL, Kirwan JP, Catalano PM, Friedman JE.** Cellular mechanisms for insulin resistance in normal pregnancy and gestational diabetes. *Diabetes Care* 30, *Suppl* 2: S112–S119, 2007.
2. **Barnes SK, Ozanne SE.** Pathways linking the early environment to long-term health and lifespan. *Prog Biophys Mol Biol* 106: 323–336, 2011.
3. **Berry R, Church CD, Gericke MT, Jeffery E, Colman L, Rodeheffer MS.** Imaging of adipose tissue. *Methods Enzymol* 537: 47–73, 2014.
4. **Biddinger SB, Kahn CR.** From mice to men: insights into the insulin resistance syndromes. *Annu Rev Physiol* 68: 123–158, 2006.
5. **Bursztyn M, Gross ML, Goltser-Dubner T, Koleganova N, Birman T, Smith Y, Ariel I.** Adult hypertension in intrauterine growth-restricted offspring of hyperinsulinemic rats: evidence of subtle renal damage. *Hypertension* 48: 717–723, 2006.
6. **Carpenter AE, Jones TR, Lamprecht MR, Clarke C, Kang IH, Friman O, Guertin DA, Chang JH, Lindquist RA, Moffat J, Golland P, Sabatini DM.** CellProfiler: image analysis software for identifying and quantifying cell phenotypes. *Genome Biol* 7: R100, 2006.
7. **Cohen SE, Kokkotou E, Biddinger SB, Kondo T, Gebhardt R, Kratzsch J, Mantzoros CS, Kahn CR.** High circulating leptin receptors with normal leptin sensitivity in liver-specific insulin receptor knock-out (LIRKO) mice. *J Biol Chem* 282: 23672–23678, 2007.
8. **Dabelea D, Crume T.** Maternal environment and the transgenerational cycle of obesity and diabetes. *Diabetes* 60: 1849–1855, 2011.
9. **Desoye G, Hauguel-de Mouzon S.** The human placenta in gestational diabetes mellitus. The insulin and cytokine network. *Diabetes Care* 30, *Suppl* 2: S120–S126, 2007.
10. **Ding GL, Wang FF, Shu J, Tian S, Jiang Y, Zhang D, Wang N, Luo Q, Zhang Y, Jin F, Leung PC, Sheng JZ, Huang HF.** Transgenerational glucose intolerance with Igf2/H19 epigenetic alterations in mouse islet induced by intrauterine hyperglycemia. *Diabetes* 61: 1133–1142, 2012.
11. **Dumortier O, Blondeau B, Duvillie B, Reusens B, Breant B, Remacle C.** Different mechanisms operating during different critical time-windows reduce rat fetal beta cell mass due to a maternal low-protein or low-energy diet. *Diabetologia* 50: 2495–2503, 2007.
12. **Fields DA, Demerath EW.** Relationship of insulin, glucose, leptin, IL-6 and TNF-alpha in human breast milk with infant growth and body composition. *Pediatr Obes* 7: 304–312, 2012.
13. **Freemark M.** Placental hormones and the control of fetal growth. *J Clin Endocrinol Metab* 95: 2054–2057, 2010.
14. **Freemark M.** Regulation of maternal metabolism by pituitary and placental hormones: roles in fetal development and metabolic programming. *Horm Res* 65, *Suppl* 3: 41–49, 2006.
15. **Gniuli D, Calcagno A, Caristo ME, Mancuso A, Macchi V, Mingrone G, Vettor R.** Effects of high-fat diet exposure during fetal life on type 2 diabetes development in the progeny. *J Lipid Res* 49: 1936–1945, 2008.
16. **Han J, Xu J, Long YS, Epstein PN, Liu YQ.** Rat maternal diabetes impairs pancreatic β-cell function in the offspring. *Am J Physiol Endocrinol Metab* 293: E228–E236, 2007.
17. **Ibanez L, Ong K, Dunger DB, de Zegher F.** Early development of adiposity and insulin resistance after catch-up weight gain in small-for-gestational-age children. *J Clin Endocrinol Metab* 91: 2153–2158, 2006.
18. **Jimenez-Chillaron JC, Hernandez-Valencia M, Reamer C, Fisher S, Joszi A, Hirshman M, Oge A, Walrond S, Przybyla R, Boozer C, Goodyear LJ, Patti ME.** Beta-cell secretory dysfunction in the pathogenesis of low birth weight-associated diabetes: a murine model. *Diabetes* 54: 702–711, 2005.
19. **Kaung HL.** Growth dynamics of pancreatic islet cell populations during fetal and neonatal development of the rat. *Dev Dyn* 200: 163–175, 1994.
20. **Kawamori D, Kurpad AJ, Hu J, Liew CW, Shih JL, Ford EL, Herrera PL, Polonsky KS, McGuinness OP, Kulkarni RN.** Insulin signaling in alpha cells modulates glucagon secretion in vivo. *Cell Metab* 9: 350–361, 2009.
21. **Khamaisi M, Skarzinski G, Mekler J, Zreik F, Damouni R, Ariel I, Bursztyn M.** Hyperinsulinemia increases placenta endothelin-converting enzyme-1 expression in trophoblasts. *Am J Hypertens* 25: 109–114, 2012.
22. **Kulkarni RN, Bruning JC, Winnay JN, Postic C, Magnuson MA, Kahn CR.** Tissue-specific knockout of the insulin receptor in pancreatic beta cells creates an insulin secretory defect similar to that in type 2 diabetes. *Cell* 96: 329–339, 1999.
23. **Lindsay RS, Lindsay RM, Waddell BJ, Seckl JR.** Prenatal glucocorticoid exposure leads to offspring hyperglycaemia in the rat: studies with the 11 beta-hydroxysteroid dehydrogenase inhibitor carbenoxolone. *Diabetologia* 39: 1299–1305, 1996.
24. **Lisle SJ, Lewis RM, Petry CJ, Ozanne SE, Hales CN, Forhead AJ.** Effect of maternal iron restriction during pregnancy on renal morphology in the adult rat offspring. *Br J Nutr* 90: 33–39, 2003.
25. **McEvoy RC, Madson KL.** Pancreatic insulikn-, glucagon-, and somatostatin-positive islet cell populatins during the perinatal development of the rat. I. Morphometric quantitation. *Biol Neonate* 38: 248–254, 1980.
26. **McEvoy RC, Madson KL.** Pancreatic insulin-, glucagon-, and somatostatin-positive islet cell populations during the perinatal development of the rat. II. Changes in hormone content and concentration. *Biol Neonate* 38: 255–259, 1980.
27. **Michael MD, Kulkarni RN, Postic C, Previs SF, Shulman GI, Magnuson MA, Kahn CR.** Loss of insulin signaling in hepatocytes leads to severe insulin resistance and progressive hepatic dysfunction. *Mol Cell* 6: 87–97, 2000.
28. **Murr SM, Bradford GE, Geschwind II.** Plasma luteinizing hormone, follicle-stimulating hormone and prolactin during pregnancy in the mouse. *Endocrinology* 94: 112–116, 1974.
29. **Nivoit P, Morens C, Van Assche FA, Jansen E, Poston L, Remacle C, Reusens B.** Established diet-induced obesity in female rats leads to offspring hyperphagia, adiposity and insulin resistance. *Diabetologia* 52: 1133–1142, 2009.
30. **Noda K.** [Studies on developmental changes in rat pancreatic endocrine system during perinatal period]. *Nihon Sanka Fujinka Gakkai Zasshi* 41: 441–448, 1989.
31. **Ohneda A, Watanabe K, Horigome K, Sakai T, Kai Y, Oikawa S.** Abnormal response of pancreatic glucagon to glycemic changes in diabetes mellitus. *J Clin Endocrinol Metab* 46: 504–510, 1978.
32. **Okereke NC, Uvena-Celebrezze J, Hutson-Presley L, Amini SB, Catalano PM.** The effect of gender and gestational diabetes mellitus on cord leptin concentration. *Am J Obstet Gynecol* 187: 798–803, 2002.
33. **Ong KK, Loos RJ.** Rapid infancy weight gain and subsequent obesity: systematic reviews and hopeful suggestions. *Acta Paediatr* 95: 904–908, 2006.
34. **Pasek RC, Gannon M.** Advancements and challenges in generating accurate animal models of gestational diabetes mellitus. *Am J Physiol Endocrinol Metab* 305: E1327–E1338, 2013.
35. **Perkins JM, Jagasia SM.** Perspectives in Gestational Diabetes Mellitus: A Review of Screening, Diagnosis, and Treatment. *Clin Diabetes* 25: 57–62, 2007.
36. **Pinney SE, Jaeckle Santos LJ, Han Y, Stoffers DA, Simmons RA.** Exendin-4 increases histone acetylase activity and reverses epigenetic modifications that silence Pdx1 in the intrauterine growth retarded rat. *Diabetologia* 54: 2606–2614, 2011.
37. **Pinney SE, Simmons RA.** Epigenetic mechanisms in the development of type 2 diabetes. *Trends Endocrinol Metab* 21: 223–229, 2010.
38. **Podjarny E, Bursztyn M, Rashed G, Benchetrit S, Katz B, Green J, Karmeli F, Peleg E, Bernheim J.** Chronic exogenous hyperinsulinaemia-induced hypertension in pregnant rats: effect of chronic treatment with l-arginine. *Clin Sci (Lond)* 100: 667–671, 2001.
39. **Polonsky KS, Rubenstein AH.** C-peptide as a measure of the secretion and hepatic extraction of insulin. Pitfalls and limitations. *Diabetes* 33: 486–494, 1984.
40. **Skarzinski G, Khamaisi M, Bursztyn M, Mekler J, Lan D, Evdokimov P, Ariel I.** Intrauterine growth restriction and shallower implantation site

in rats with maternal hyperinsulinemia are associated with altered NOS expression. *Placenta* 30: 898–906, 2009.
41. **Sorenson RL, Brelje TC.** Adaptation of islets of Langerhans to pregnancy: beta-cell growth, enhanced insulin secretion and the role of lactogenic hormones. *Horm Metab Res* 29: 301–307, 1997.
42. **Thompson RF, Fazzari MJ, Niu H, Barzilai N, Simmons RA, Greally JM.** Experimental intrauterine growth restriction induces alterations in DNA methylation and gene expression in pancreatic islets of rats. *J Biol Chem* 285: 15111–15118, 2010.
43. **Throsby M, Coulaud J, Durant S, Homo-Delarche F.** Increased transcriptional preproinsulin II beta-cell activity in neonatal nonobese diabetic mice: in situ hybridization analysis. *Rev Diabet Stud* 2: 75–83, 2005.
44. **Tura A, Ludvik B, Nolan JJ, Pacini G, Thomaseth K.** Insulin and C-peptide secretion and kinetics in humans: direct and model-based measurements during OGTT. *Am J Physiol Endocrinol Metab* 281: E966–E974, 2001.
45. **Van Assche FA, Holemans K, Aerts L.** Long-term consequences for offspring of diabetes during pregnancy. *Br Med Bull* 60: 173–182, 2001.
46. **Wang Z, Huang Z, Lu G, Lin L, Ferrari M.** Hypoxia during pregnancy in rats leads to early morphological changes of atherosclerosis in adult offspring. *Am J Physiol Heart Circ Physiol* 296: H1321–H1328, 2009.
47. **Zhang H, Zhang J, Pope CF, Crawford LA, Vasavada RC, Jagasia SM, Gannon M.** Gestational diabetes mellitus resulting from impaired beta-cell compensation in the absence of FoxM1, a novel downstream effector of placental lactogen. *Diabetes* 59: 143–152, 2010.
48. **Zhang Q, Ramracheya R, Lahmann C, Tarasov A, Bengtsson M, Braha O, Braun M, Brereton M, Collins S, Galvanovskis J, Gonzalez A, Groschner LN, Rorsman NJ, Salehi A, Travers ME, Walker JN, Gloyn AL, Gribble F, Johnson PR, Reimann F, Ashcroft FM, Rorsman P.** Role of KATP channels in glucose-regulated glucagon secretion and impaired counterregulation in type 2 diabetes. *Cell Metab* 18: 871–882, 2013.

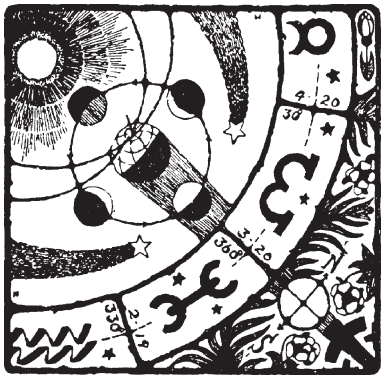

Appendix A3

Publication

De Jesus DF, Kulkarni RN. Epigenetic modifiers of islet function and mass. TEM 25(12): 628-636, 2015.

Contribution

I am the first author of this review article.

Review

CellPress

Epigenetic modifiers of islet function and mass

Dario F. De Jesus[1,2] and Rohit N. Kulkarni[1,3]

[1] Section of Islet Cell and Regenerative Biology, Joslin Diabetes Center, Harvard Medical School, Boston, MA 02215, USA
[2] Graduate Program in Areas of Basic and Applied Biology (GABBA), Abdel Salazar Biomedical Sciences Institute, University of Porto, 5000 Porto, Portugal
[3] Department of Medicine, Brigham and Women's Hospital, Harvard Medical School, Boston, MA 02215, USA

Type 2 diabetes (T2D) is associated with insulin resistance in target tissues including the β-cell, leading to significant β-cell loss and secretory dysfunction. T2D is also associated with aging, and the underlying mechanisms that increase susceptibility of an individual to develop the disease implicate epigenetics: interactions between susceptible loci and the environment. In this review, we discuss the effects of aging on β-cell function and adaptation, besides the significance of mitochondria in islet bioenergetics and epigenome. We highlight three important modulators of the islet epigenome, namely: metabolites, hormones, and the nutritional state. Unraveling the signaling pathways that regulate the islet epigenome during aging will help to better understand the development of disease progression and to design novel therapies for diabetes prevention.

Diabetes – an environmental and genetic multifactorial disease

Diabetes mellitus is increasing worldwide with a global prevalence of 6.4% in the adult population (aged 20–79 years), and new cases of diabetes are predicted to be higher in developing countries (69%), compared with developed nations (20%) [1]. It is a metabolic disease that affects virtually all tissues in the body, and is characterized by uncontrolled hyperglycemia and tissue-specific complications in the untreated state. Type 1 diabetes (T1D) is caused by an autoimmune attack targeting the insulin-producing pancreatic β-cells, while type 2 diabetes (T2D) is associated with aging, early development of insulin resistance, and a deteriorating β-cell function [2]. The underlying mechanisms responsible for changes in β-cell function, glucose tolerance, and insulin sensitivity are areas of intensive investigation. Among the diverse factors that impact the disease, environmental stimuli have been reported to shape epigenetic signatures of different tissue types, and contribute to the disease process [3]. In this review, we will briefly outline the basic epigenetic principles and focus on their relevance in the aging-associated β-cell dysfunction in T2D. We will also discuss the importance of epigenetic regulation of β-cell adaptation and the importance of metabolic, hormonal and nutritional factors that contribute to the β-cell epigenome.

Epigenetics and aging

Common to virtually all living organisms, aging is broadly defined as a time-dependent loss of homeostatic structure and function [4]. Although genomic instability is an important hallmark of aging and is characterized by increased accumulation of nuclear and mitochondrial DNA mutations [5], there are no functional studies reporting a direct effect of a mutation on the life-span of an organism [4]. Thus, an important question in the field has been to determine how the accumulation of mutations contribute to a phenotype associated with aging. Beyond the genome, epigenetics emerges as a complementary and dynamic mechanism by which the environment can directly affect the life-span of an organism.

First coined by Conrad H. Waddington, epigenetics is defined as 'the structural adaptation of chromosomal regions so as to register, signal or perpetuate altered activity states' [6]. Epigenetics is also defined as the science that studies the changes in gene expression, without an alteration in the nucleotide sequence. Epigenetic alterations can be further transmitted in a cell-to-cell manner (mitosis) or through generations (meiosis). The most widely studied epigenetic modifications include: DNA methylation (Box 1), chromatin modification (Box 2), and non-coding RNA expression (Box 2).

Epigenetics changes associated with diabetes

Diabetes is a multifactorial and complex disease influenced by both genetic and environmental factors (Box 3). The concordance rate in adult-onset of T1D is low (<20%), suggesting that factors other than genetics are implicated in the development of this complex autoimmune disease [7]. Indeed, epigenome-wide association studies (EWAS) are beginning to identify differently methylated cytosine–phosphate–guanine (CpG) dinucleotides that precede the onset of T1D and implicate a role for epigenetics [8]. While insulin resistance is strongly associated with obesity and aging, the overt development of T2D in both states is triggered by an inability of the β-cells to compensate by increasing insulin secretion and/or enhancing cell mass. Notably, a majority of the genes associated with T2D are related to β-cell function [9], and new rare monogenic forms of diabetes and individual loci conferring risk for

Corresponding author: Kulkarni, R.N. (Rohit.Kulkarni@joslin.harvard.edu).

1043-2760/
 http://dx.doi.org/10.1016/j.tem.2014.08.006

Box 1. DNA methylation

DNA methylation is an evolutionary conserved mechanism, that is absent in some species in a lineage-restricted manner [96], and implies the addition of a methyl group to the 5′ position of the cytosine pyrimidine ring (5-mC). Approximately 70% of all CpG dinucleotides (CpGs) are methylated, and most of the unmethylated CpGs are clustered in 'CpG islands' [97]. CpG islands are CG enriched segments often situated close to the promoter regions of the genes, and can influence the affinity of transcription factors to the DNA binding sites [97]. DNA methylation is established and maintained by DNA methyltransferase enzymes (DNMTs). There are different classes of DNMTs with different molecular functions, for example, the role of DNMT1 is to maintain the DNA methylation pattern, while DNMT3a and 3b generate new methylation patterns (*de novo* methylation) [98]. DNA hypermethylation is generally associated with gene silencing, in a process that recruits DNA-binding proteins (e.g., MeCP2, MBD1, MBD2, MBD3, and MBD4), histone deacetylases, and other co-repressors, all of which affect the affinity of transcription factors [98]. While DNA demethylation was thought to occur due to a lack or reduction of DNMTs, recent studies report three families of enzymes that were associated with active and dynamic DNA demethylation, namely Tet methylcytosine dioxygenase 1 (TET), activation-induced deaminase/apolipoprotein B (AID/APOBEC), and base-excision repair glycosylases (BER) [99,100]. Furthermore, the proposal that DNA can be demethylated and remethylated by the cooperation between these enzymes, with hydroxymethylation being an intermediate state [99], was confirmed by Hackett *et al.* [101] who demonstrated that genome-wide germline demethylation occurs via conversion to hydroxymethylation.

T2D have been recently identified [10]. Although the number of genes associated with T2D surpassed the barrier of 100, together they account for a small portion of the disease risk [11]. Many common and age-related diseases, including T1D and T2D are characterized by altered methyl metabolism, and are consequently associated with alterations in DNA methylation [12].

Aging and β-cell function

Data from complementary studies in humans and rodents, including hyperglycemic clamps, and glucose or arginine challenges, indicate that aging is associated with decreased insulin secretion [13]. For example, a study analyzing both the first and second phase of insulin secretion using hyperglycemic clamps in 130 individuals (aged 20–70 years) with normal glucose tolerance, concluded that there is a decrease in the ability to secrete insulin at a rate of approximately 0.7% per year [14]. In an independent study in a large European cohort (n=957), basal insulin secretion was assessed in individuals aged 18–85 years. The authors developed a multivariate model to determine the age-dependent effect on basal β-cell function, and after normalizing for BMI, fasting plasma glucose, and waist-to-hip ratio, they concluded that, independent of gender, Caucasians exhibited decreased basal insulin release and insulin clearance with aging [15]. Using a different approach, Ihm *et al.* [16] analyzed human islets isolated from cadaveric humans that were transplanted into male athymic nude mice. The glucose stimulated insulin release (GSIR) and islet ATP content was higher in younger versus older donors.

Modulation of insulin release by the mitochondrial machinery is essential for normoglycemia. *PPARGC1A* mRNA expression, a determinant gene for mitochondrial biogenesis and function, was demonstrated to be reduced up to 90% in islets from T2D patients, and this correlated with decreased insulin secretion. Furthermore, the *PPARGC1A* gene promoter was shown to have a two-fold increase in methylation in T2D islets as compared with controls [17].

Insulin gene (*INS*) expression is regulated by DNA methylation and histone modifications. Studies demonstrate that the *Pdx-1*-mediated insulin gene activation in response to glucose is mediated by the recruitment of the histone acetyltransferase (HAT) p300 and histone methyltransferase (HMT) Set9 to the insulin promoter [18]. Through bisulfite treatment and sequencing, it was possible to determine in genomic DNA isolated from

Box 2. Histone modifications and non-coding RNAs

Each of the 147 bp of DNA is wrapped around a histone octamer, which in turn is composed of two copies of the core histones H2A, H2B, H3, and H4 [102]. Repeated histone units give rise to nucleosomes, and nucleosomes constitute the chromatin [98]. Histones are known to regulate gene expression and are also important for DNA repair, replication, and recombination [103]. Amino acid residues present in the N terminal of histones can be exposed to a variety of epigenetic modifications, namely: lysine acetylation, arginine and lysine methylation, threonine and serine phosphorylation, and lysine sumoylation and ubiquitination [104]. The combination of these alterations in the different histone tails form the 'histone code' [105]. These covalent modifications promote alterations in the chromatin conformation, and consequently, its affinity to DNA, either inducing expression by disrupting the association between DNA and histones, or inducing silencing through constricting the nucleosomes to methylated CpGs in DNA [98]. The most widely studied histone modifications involve methylation and acetylation. Histone acetylation is mediated by histone acetyl transferase enzymes (HATs) which utilize acetyl-CoA as a co-factor to dynamically catalyze the transfer of an acetyl group to lysine residues which can be reversed by histones deacetylases (HDACs) [106]. Histone methylation involves the transfer of a methyl group to either a lysine or an arginine residue, and the process is catalyzed by histone methyltransferases (HMTs). The opposite process, histone demethylation, depends upon histone demethylases (HKDMs) [107]. Contrary to acetylation, which is associated with gene transcription, the effect of histone methylation depends on the residue that is methylated and extension of the methylation [107].

A small percentage of the mammalian genome corresponds to protein coding genes, and most of the genome is transcribed. In addition to biochemical modifications of DNA and histones, gene expression is regulated by small non-coding RNA (ncRNA; 20–30 bp) and long non-coding RNA (lncRNA; >200 bp). Mammalian ncRNAs act predominantly to decrease the mRNA by acting on the poly(A) tails, resulting in decay and repression of translation [108]. Using *Drosophila*, at least three different pathways of ncRNA-mediated gene silencing have been identified to address mechanisms underlying inhibition of protein synthesis [109]. Notably, ncRNAs act together with histone-modifying enzymatic complexes to epigenetically silence transcription [107].

Box 3. Environment versus epigenome

The environment can modulate genomes and consequently reshape phenotypes. For example, at birth, identical monozygotic twins present a general identical pattern of global and locus-specific DNA methylation and histone acetylation. However, aging has been shown to cause a substantial discordance in these epigenetic marks [110]. Another example is in adults exposed to famine during the 'Dutch Hunger Winter' in the late period of World War II. The offspring of these individuals presented a low-birth weight, as well as an increase in the incidence of obesity, T2D, and dyslipidemia [111]. A key question arising from these observations is the ability of how epigenetic information being transmitted via gametes, evidence for which is accumulating (reviewed in [112]).

β-cells, that human *INS* promoters are naturally demethylated and their methylation reduced their expression by up to 90% [19]. Consistently, T2D β-cells displayed increased DNA methylation in the *INS* promoter, inversely correlating with *INS* gene expression [20]. Interestingly, the *INS* gene region is the second most important locus commonly associated with T1D, and it is susceptible to DNA methylation modifications in T1D patients [21]. Finally, DNA methylation analysis of islets collected from five T2D and 11 non-diabetic patients revealed that a total of 276 CpGs, corresponding to the promoter regions of 254 genes involved in a very broad category of biological functions, were differently methylated [22]. Furthermore, these changes did not affect blood cells, and, through *in vitro* experiments, it was possible to rule out the transient effect of high glucose [22].

Aging and β-cell adaptation

β-cell mass is maintained by a balance between cell gain (i.e., replication, neogenesis, transdifferentiation, and hypertrophy) and cell loss (i.e., apoptosis, autophagy) [2,23]. During periods of intense metabolic demand, such as pregnancy or obesity, proper β-cell function and mass are essential for glucose homeostasis (Figure 1). Epigenetic mechanisms are known to be important, not only in cell-fate decisions and differentiation, but also in maintaining

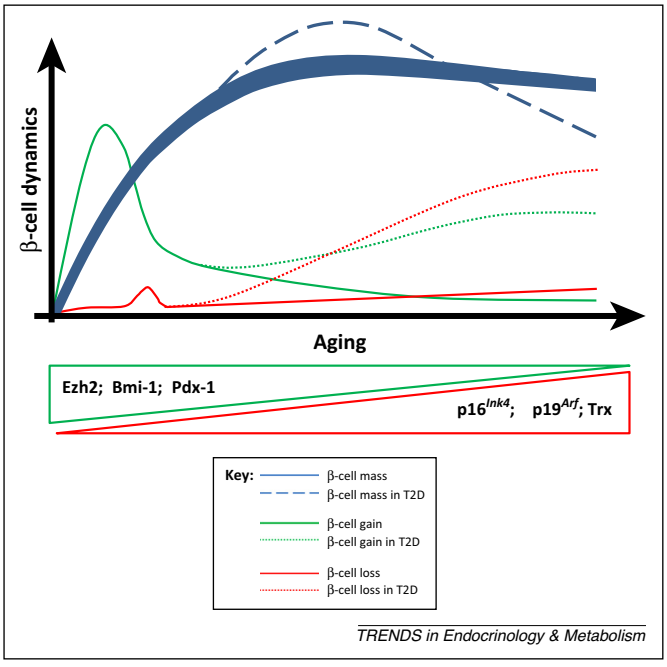

Figure 1. β-cell adaptation during aging in normal (unbroken lines) or type 2 diabetes (T2D) individuals (broken lines). Blue lines represent chronobiology of β-cell mass, green lines represent mechanisms of cell gain (replication, neogenesis, hypertrophy, transdifferentiation), and red lines represent mechanisms of cell loss (apoptosis, autophagy, dedifferentiation). The thickness of the unbroken blue line represents the spectrum of the β-cell mass in normal individuals. The rise in the broken blue line represents the β-cell mass compensation observed during the early stages of T2D. In normal individuals β-cell gain mechanisms increase exponentially prenatally and decrease with aging, while in T2D as a result of the intense metabolic demand, β-cell gain mechanisms increase until saturation of β-cell sources. In normal individuals, a brief increase in loss of β-cells in the postnatal period is followed by a slow and gradual loss with aging. This loss is accelerated in T2D. During aging, there is diminishing expression of the polycomb complex proteins Enhancer of Zeste Homolog 2 (Ezh2) and B Lymphoma Mo-MLV insertion Region 1 Homolog (Bmi-1) that leads to poor inhibition of the cell cycle inhibitors (e.g., $p16^{Ink4a}$ and $p19^{Arf}$), leading to age-associated decline in β-cell proliferation.

differentiated cell states of the endocrine pancreas [24], and epigenetic modulators of islet-specific genes continue to be areas of current research.

Aristaless-related homeobox (*Arx*) is a transcription factor specifically expressed in α-cells, but not in β-cells. Using the β-cell-specific knockout (KO) model of DNA-methyltransferase 1 (*Dnmt1*), it was possible to define the importance of DNA methylation in the maintenance of β-cell identity through a mechanism involving the silencing of the *Arx* gene [25]. In β-cells, the *Arx* locus is methylated and bound to a complex integrating methyl CpG binding protein 2 (MeCP2) and the protein arginine *N*-methyltransferase 6 (PRMT6), and removal of DNA methylation results in conversion of β-cells to α-cells [25]. Further analysis revealed that DNMT3, GASA-like protein (Geg3), and histone deacetylase 1 (HDAC1) form a large repressing complex modulating the β-cell identity [26]. Histone deacetylases (HDACs) have an important role in the developmental regulation of the pancreas. Lenoir *et al.* [27] created mutant rats lacking HDAC4, 5, and 9, and performed immunohistochemical analysis of pancreatic sections from embryonic day 15.5 (E15.5), postnatal day 1 (P1) and postnatal day 7 (P7) animals. Rats lacking *Hdac 5* and *9* had an increasing number of β-cells, and animals lacking *Hdac4* and *5* revealed a greater pool of δ-cells [27]. These results suggest that different HDACs operate in the control of the pancreatic β/δ lineage.

The homeodomain-containing transcription factor pancreatic and duodenal homeobox 1 (*Pdx-1*) is crucial for β-cell development, function, and for β-cell compensation in response to insulin resistance [28]. Yang *et al.* [29] isolated islets from 55 non-diabetic and nine diabetic donors and reported a decrease in the expression of *Pdx-1* mRNA in the latter. Additionally, 10 CpG sites in the distal *Pdx-1* promoter and enhancer regions were observed to be highly methylated in T2D islets [29]. *Pdx-1* has been reported to interact with Set7/9 – an islet-specific methyltransferase responsible for the methylation of H3K4 [24], and experiments targeting Set7/9 in insulinoma cells and mouse islets showed repression of genes such as *Ins1*, *Ins2*, glucose transporter 2 (*Glut2*), and *MafA*, which are known to be important for β-cell function [30].

The expression of *INK4a/ARF* locus, which encodes for the tumor suppressor proteins $p16^{Ink4a}$ and $p19^{Arf}$ has been reported to be associated with mechanisms limiting β-cell proliferation. The histone methyltransferase Enhancer of Zeste Homolog 2 (*Ezh2*; component of the PRC1 Polycomb group protein complex) represses *INK4a/ARF* in β-cells through H3 trimethylation, regulating the levels of $p16^{Ink4a}$, $p19^{Arf}$ and, consequently, β-cell proliferation and mass. Conditional KO of *Ezh2* in β-cells results in reduced proliferation, mass, and hypoinsulinemia. Experiments using streptozotocin (STZ)-induced diabetic mice, revealed an increased *Ezh2* expression, together with higher β-cell proliferation [31]. Recently, *Ezh2* was shown to be involved in the chromatin pattern formation in the pancreas, and is, therefore, essential in the modulation of cell fate decision during development [32]. B Lymphoma Mo-MLV Insertion Region 1 Homolog (*Bmi-1*: a member of PRC1 Polycomb complex) has a regulatory function at the *INK4a/ARF* locus, and

also controls β-cell proliferation [33]. The age-associated repression of β-cell proliferation through the activation of *INK4a/ARF* locus is complex and involves other histone regulatory complexes. While the transgenic expression of *Ezh2* in β-cells from young mice is sufficient to increase replication, this response is abrogated in old animals. Older mice exhibit an enrichment of trithorax (Trx) complex proteins at the *Ink4a* locus [34], and increased β-cell proliferation is potentially achieved by targeting *Trx* and inducing expression of *Ezh2* [34].

Endocrine neoplasia type 1 (MEN1) results from the mutation of *Men1* gene which encodes the protein menin, a HMT protein member of the Trx complex that promotes H3K4 methylation. The expression of *Men1* prevents islet expansion by maintaining the expression of $p16^{INK4a}$, $p27^{Kip1}$ and $p18^{INK4}$ [35]. Consistently, β-cell specific deletion of *Men1*, induces β-cell hyperplasia leading to insulinomas, hyperinsulinemia, and hypoglycemia [36]. In a recent report, Chamberlain *et al.* [37] analyzed the importance of K-RAS in the proliferation of pancreatic endocrine cells by examining the molecular differences between pancreatic ductal adenocarcinomas (PDAC) and pancreatic endocrine tumors (PETs). Although K-RAS acts through the RAF-mitogen-activated protein kinase (RAF/MAPK) pathway to induce proliferation in different types of cancer and has not been linked to PETs, mice heterozygous for *Kras* developed β-cell hyperplasia with increased neogenesis. To explore the role of menin in the K-RAS-induced β-cell proliferation, the authors derived mice heterozygous for *Men1* deletion and expressing constitutively active K-RAS, and again observed increased β-cell proliferation [35,37]. Investigating how menin controls K-RAS-mediated β-cell proliferation during aging may help design strategies to overcome the refractory phenotype of human β-cells.

The importance of microRNAs (miRNAs) in the regulation of multiple biological processes has become evident recently [38]. This class of noncoding RNA is implicated in gene expression alterations, and consequently, β-cell dysfunction associated with T2D [39]. Aging and environmental factors, such as obesity, can shape the human pancreatic islets miRNA repertoire [40]. The importance of miRNAs is evident early during the development of the pancreas. For instance, deletion of *Dicer1*, a gene responsible for an enzyme involved in the miRNA processing, in mouse pancreas, causes impaired pancreatic islet development [41]. Furthermore, *miR-375* and *miR-7a* are highly expressed during human pancreatic islet differentiation [42], and are the most abundant miRNAs in mouse and human islets [43]. *miR-7a* acts by targeting components of the mammalian target of rapamycin (mTOR) and MAPK pathways controlling β-cell proliferation. Indeed, a 30-fold increase in Ki67+ β-cells is observed following the inhibition of *miR-7a*, in dispersed human β-cells [44].

Therefore, the β-cell epigenome is only partially explored, and while functional characterization is still necessary to fully understand the adaptive mechanisms underlying the maintenance of β-cell mass, major efforts are being devoted to identify modulators of the islet epigenome.

Epigenetic modifiers of islet cells

Metabolic

Adipocytes produce a spectrum of biological metabolites important for the regulation of several types of cells, including β-cells [45]. Increased adipocyte mass is associated with obesity and impaired lipid metabolism. Consequently, the high levels of circulating free fatty acids (FFA) and glucose are potent inducers of cellular reactive oxygen species (ROS) [46]. β-cells possess a highly developed endoplasmic reticulum (ER), necessary for the folding of high amounts of insulin and other peptides secreted by the cell, rendering them highly susceptible to FFA-induced ER stress (Figure 2) [47].

Lipotoxicity, a concept that is defined as the impairment of cell function and viability due to chronic exposure to FFA, induces β-cell ER stress depending on the length and saturated state of the FFAs [48]. This affects glucose utilization by insulin-sensitive tissues, and especially induces β-cell dysfunction and apoptosis [49]. ER stress signal transduction induces the unfolded protein response (UPR) [50], which acts mainly through three ER membrane transducers: PKR-like endoplasmic reticulum (ER) kinase (PERK; antioxidant response), inositol-requiring 1 (IRE1; inflammatory response), and activating transcription factor 6 (AT6; chaperone and lipid biosynthesis response) (reviewed in: [51]). The effects of ROS on the epigenetic status of genomic DNA could result from hydroxyl radicals inducing DNA damage and impairing the ability of DNMTs to bind DNA. It is also possible that the replacement of guanine by 8-hydroxy-2-deoxyguanosine within CpG dinucleotides impairs the adjacent cytosine methylation leading to a state of hypomethylation [52]. These changes are well documented in several cells types [52–54] and research is warranted in β-cells.

Mitochondria are essential in ER stress-mediated apoptosis and mitochondrial DNA (mtDNA) can be modified by methylation and hydroxymethylation. DNMT1 is catalytically active in the mitochondria and is regulated by peroxisome proliferator-activated receptor γ-coactivator 1α (PGC-1α) and nuclear respiratory factor 1 (NFR-1) transcription factors [55]. Moreover, co-factors, such as flavin adenine dinucleotide (FAD), acetyl-coenzyme A (acetyl-CoA), or α-ketoglutarate (α-KG), which are utilized in the process of methylation or deacetylation, are synthesized in mitochondria [56]. In high oxygen conditions, the Jumonji-family (JmdC) histone demethylases and the ten–eleven translocation (TET) protein family members, responsible for the hydroxymethylation (5-hmC) of cytosines [57,58], are activated by the mitochondrial-derived α-KG [59].

In addition to elevated FFAs, there is evidence that elevated glucose levels can also contribute to β-cell dysfunction [60]. Chronic hyperglycemia, and in particular, fasting glucose levels above 100 mg/dl have been reported to impair GSIS [60]. Similar to the effects of lipotoxicity, hyperglycemia induces ER stress and consequently β-cell dysfunction [61,62], and it has been suggested that glucotoxicity and lipotoxicity act together to induce β-cell dysfunction [61]. One of the mechanisms involved in the glucose-mediated ER stress is the formation of advanced glycation end products (AGE) which accumulate during

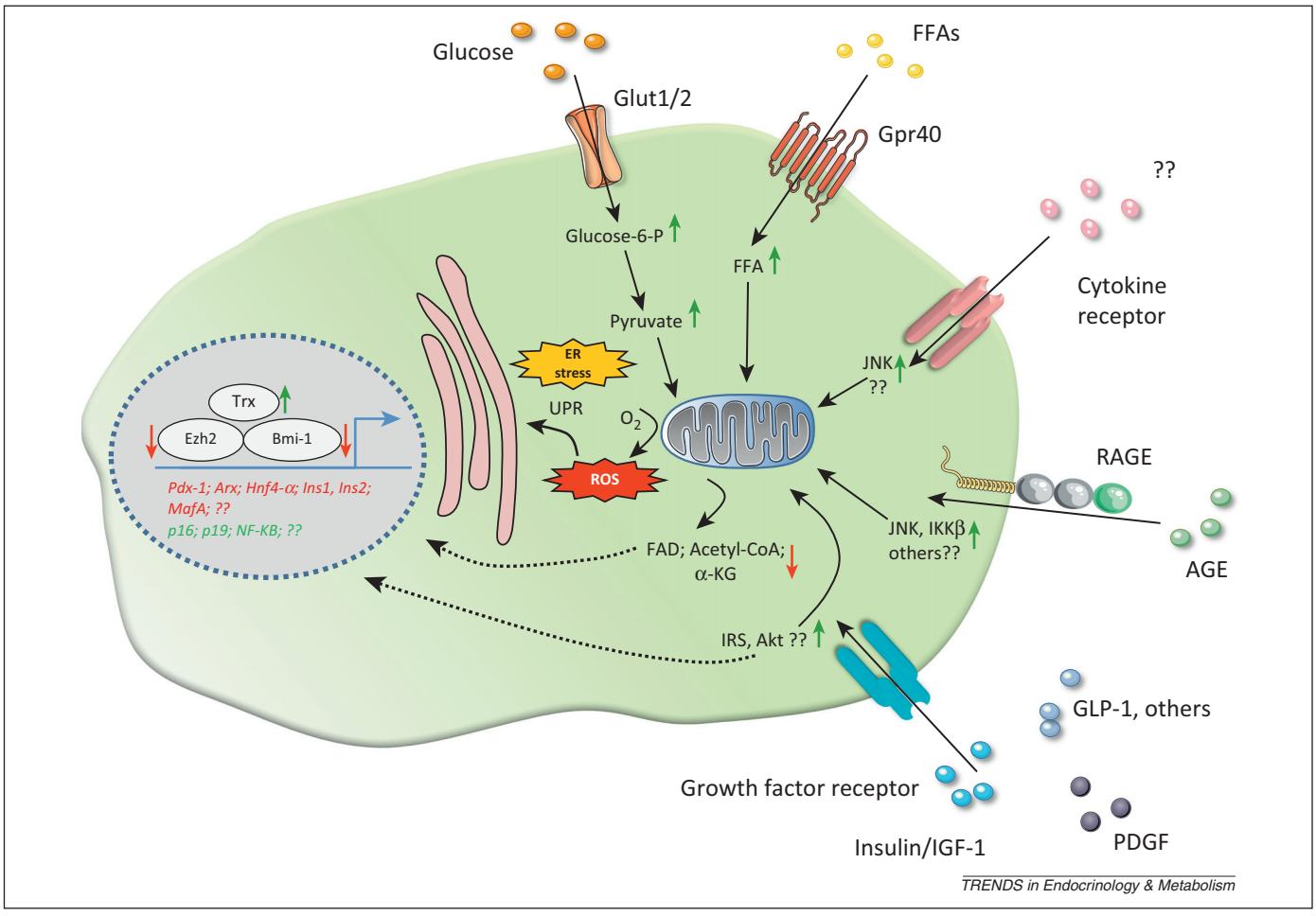

Figure 2. Schematic depicting the metabolic, hormonal and nutritional modulators of the aging pancreatic β-cell epigenome. Pancreatic β-cells possess well-developed endoplasmic reticulum (ER), and therefore, are highly susceptible to ER-stress. Type 2 diabetes (T2D) is characterized by high levels of glucose, insulin, advanced glycated end products (AGE), inflammatory cytokines, and free fatty acids (FFAs), among others. These factors, and potentially others associated with aging, lead to the mitochondrial production of reactive oxygen species (ROS) that ultimately induces ER-stress and cellular dysfunction. Mitochondria are essential for the β-cell bioenergetics and are also responsible for the production of a broad group of co-factors such as flavin adenine dinucleotide (FAD), alpha ketoglutaric acid (α-KG) or acetyl coenzyme A (Acetyl-CoA), involved in methylation and deacetylation reactions. By contrast, hormonal signals including insulin, glucagon-like peptide 1 (GLP-1) analogues and platelet-derived growth factor (PDGF), modulate the expression of critical epigenetic regulatory complexes such as Enhancer of Zeste Homolog 2 (Ezh2), B Lymphoma Mo-MLV insertion Region 1 Homolog (Bmi-1), or trithorax-group proteins (Trx) involved in regulating β-cell compensation. Together, these signals regulate the expression of genes crucial for β-cell function and identity, by repressing *Pdx-1*, Arx, *Ins1*, *Ins2*, *HNF4-α* and *MafA*, or activating the *INK4a/ARK* locus, and consequently, $p16^{Ink4a}$ and $p19^{Arf}$. Abbreviations: '??', indicates potential mediators not yet linked to epigenetics; Glut1/2, glucose transporters 1 and 2; Gpr40, free fatty acid receptor 1; FFA, free fatty acids; RAGE, receptor for advanced end products; AGE, advanced glycated end products; GLP-1, glucagon-like peptide 1; IGF-1, insulin-like growth factor; PDGF, platelet-derived growth factor; Glucose-6-p, glucose-6-phosphate; JNK, c-Jun N terminal kinases; IKK-β, IkB kinase; IRS, insulin receptor substrate; Akt, protein kinase B; FAD, flavin adenine dinucleotide; Acetyl-CoA, acetyl coenzyme A; α-KG, alpha ketoglutaric acid; ROS, reactive oxygen species; ER, endoplasmatic reticulum; UPR, unfolded protein response; Ezh2, Enhancer of Zeste homolog 2; Bmi-1, B lymphoma Mo-MLV insertion region 1 homolog; Trx, trithorax-group proteins; *Pdx-1*, pancreatic and duodenal homebox 1; *Arx*, aristaless-related homeobox; *Hnf4-α*, hepatocyte nuclear factor 4 alpha; *MafA*, transcription factor MafA; *Ins1/2*, insulin gene 1 and insulin gene 2; p16, cyclin-dependent kinase inhibitor 2A; p19, *Arf* tumor supressor; NF-KB, factor nuclear kappa B. Several elements in this illustration are courtesy of "Servier Medical Art".

aging, and can increase exponentially under chronic hyperglycemic conditions [63]. Among the effects of hyperglycemia, the ROS-mediated activation of the inflammatory nuclear factor-kappaB gene *NF-kB* has received considerable attention. Transient high levels of glucose increase the expression of the NF-kB subunit p65 in vascular cells, even 6 days after attaining normoglycemia [64]. Enhanced H3K4 and reduced H3K9 methylation of the *NF-kB–p65* promoter appears to mediate the glucose-induced gene expression changes [65]. The effect of glucose restriction on lifespan is mediated by the class III histone deacetylase sirtuin 1 (SIRT1) [66]. In fact, SIRT1 regulates various biological processes such as apoptosis, cell cycle progression, ROS levels, and inflammatory responses [67]. *Sirt1* expression decreases in bovine retinal capillary endothelial cells (BRECs) after exposure to high levels of glucose, while expression of *NF-kB–p65* and the pro-apoptotic gene *Bax* increases [68].

In human pancreatic islets, the levels of glycosylated hemoglobin (HbA1c) correlate positively with DNA methylation of insulin [20] and the *Pdx1* promoter genes [29]. Culturing rat clonal β-cells (INS 832/13) in RPMI 1640 medium with high glucose, leads to a decrease in *Pdx-1*, while DNA methylation of *Pdx-1* promoter increases. Hyperglycemia increased the expression of the DNA methyltransferase *Dnmt1* [29]. In addition to its effects on histone modifications and DNA methylation, glucose also regulates miRNAs [69,70]. Glucolipotoxicity-induced mitochondrial dysfunction can be one potential explanation for the gene expression changes observed in β-cells from T2D patients.

Hormonal

Insulin is important for the maintenance of normoglycemia and β-cell mass [71]. While multiple studies have reported the significance of insulin and insulin-like-growth factor 1 (IGF-1) receptors and their signaling proteins in the regulation of islet cell mass and function [72], functional studies analyzing the direct effect of insulin on the β-cell epigenome are lacking. Nevertheless, insulin has been shown to modulate lifespan by regulating the expression of H3K27 demethylase UTX-1 through the insulin–FoxO signaling pathway [73] and in the recruitment of BAF60, a member of the BAF-related chromatin complex, to induce the expression of lipogenic enzymes [74]. Treatment of L6 skeletal muscle myoblasts with low (5 mM) or higher (25 mM) glucose concentrations, in the absence or presence of insulin (100 nM), revealed increased production of ROS and multiple histone modifications only in the group treated with insulin. Given that H3K4me is associated with gene activation, while H3K9me is associated with gene repression, the authors performed microarray experiments and concluded that insulin in the presence of high glucose concentrations acts by epigenetically downregulating the expression of different genes involved in diverse pathways, such as signal transduction, transcription, metabolism, protein transport, cell adhesion, and ion transport [75].

The platelet-derived growth factor (PDGF), common to many tyrosine kinase receptor ligands, promotes survival and proliferation in different tissues. The effects of PDGF on proliferation of β-cells was demonstrated by a landmark paper wherein the authors [76] used purified β-cells from 2–week-old or 5-month-old mice and reported a decrease in the mRNA expression of PDGF receptor (*PDGF-R*) and *Ezh2* with aging. Treating juvenile or adult mouse islets with physiological concentrations of recombinant PDGF-AA, led to increased β-cell proliferation only in younger animals. Using complementary KO models, the authors concluded that *Ezh2* is essential for the β-cell expansion in response to PDGF-R activation. Importantly, the proliferative effect of PDGF was also evident in juvenile human islets [76].

The development of T2D following intrauterine growth retardation (IUGR) in rats is partially explained by the epigenetic silencing of *Pdx-1* in islet cells [77]. Pinney *et al.* [78] administered exendin-4 to newborn offspring of IUGR rats for a period of 6 days, and were able to reverse the IUGR-associated increase in DNA methylation at the *Pdx-1* promoter. Exendin-4 appears to act by increasing HAT activity by recruiting the transcription factor upstream stimulatory factor 1 (USF1) and the co-activator P300/CBP-associated factor PCAF to the proximal promoter of *Pdx-1* [78].

Organ crosstalk is a necessary yet complex system involved in the regulation of metabolic homeostasis. El Ouaamari *et al.* [79] used elegant *in vivo* parabiosis and transplantation assays on liver-specific insulin receptor KO (LIRKO) mice to demonstrate that hepatocyte-derived factors drive mammalian β-cell replication. This initial observation prompted several other groups to identify potential circulating islet cell growth factors. For example, a chemical insulin receptor antagonist (S961) was used to induce systemic insulin resistance and expression of betatrophin (*ANGPL8*) in liver and fat, which in turn, induced β-cell proliferation in mice [80]. More recently, the adipokine adipsin has been reported to boost pancreatic β-cell function [81]. Follow-up work is necessary to address whether the beneficial effects of one or more of these circulating factors persists across generations by acting via epigenetic mechanisms. Together, these findings reinforce the notion that chronic hormonal exposure can induce epigenetic alterations and gene expression changes in diverse cell types including pancreatic islet cells (Figure 2). Further work is necessary to decipher the relative hormonal axes specifically involved in modulating epigenetic changes, and to design experiments to differentiate the confounding effects of metabolites.

Nutritional

Several models illustrate the early effects of metabolic reprogramming in offspring during different times of development, including low protein diets (LPD), maternal undernutrition (UN), IUGR, high fat diets (HFD), as well as models of T2D or obesity.

Among the models, maternal protein restriction experiments are the most widely studied and demonstrate the importance of appropriate metabolic regulation during gestation. For example, 15-day-old and 21-day-old offspring from pregnant Wistar rats fed a LPD in the last week of gestation revealed a lower β-cell mass due to 50% lower β-cell proliferation compared with controls. Interestingly, feeding the animals with a LPD throughout gestation resulted in an ~33% reduction in β-cell mass [82]. One possible mechanism promoting β-cell loss is the induction of oxidative stress, which is based on the findings that islets from rats fed a LPD revealed a decrease in the antioxidative enzymes catalase and glutathione peroxidase. Consistent with a detrimental effect on β-cells, islets from these animals revealed lower insulin mRNA and higher *c-Myc* expression [83].

HNF4-α is a transcription factor essential for β-cell development and function, and has been shown to be downregulated in islets from patients with T2D [84]. In an elegant study, Sandovici *et al.* [85] fed female rats a LPD during pregnancy and lactation, and assessed the epigenetic effects on islets. They observed reduced expression of *HNF4-α*, which was caused by an increase in methylation of the *HNF4-α* promoter, together with depletion of the histone active marks H3 acetylation and H3K3me that complemented the enhanced repressive marks H3K9me2 [85]. Using a mouse model of caloric undernutrition (UN), Jimenez-Chillaron *et al.* [86] reported the transmission of a phenotype of glucose intolerance, reduced birth weight, and obesity through F1 and F2 generations [86]. The mechanism involved in the F1-to-F2 paternal transmission of the *in utero* nutritional perturbation present in the UN model was recently deciphered [87,88]. Radford *et al.* [87] performed methylated DNA immunoprecipitation followed by next-generation sequencing (MeDIP-seq) on the germline of F1 offspring males from UN-subject mothers, and identified differently methylated regions resistant to early embryo epigenetic erasure. Interestingly, the methylation patterns identified in the males F1 germline were not present in the adult tissues of F2; however, locus-specific

gene expression changes were identified [87]. Mechanistically, maternal undernutrition can affect β-cell mass by modulating the proliferation/apoptosis balance through changes in the expression of *IGF-2* [89] and *Pdx-1* [90]. Pdx-1, a transcription factor crucial for β-cell adaptation to insulin resistant states [28], was downregulated in islets of IUGR rats and correlated with the development of T2D [91]. Using chromatin immunoprecipitation (ChIP) experiments on IUGR rat islets, Park *et al.* [92] demonstrated a recruitment of HDAC1 and the co-repressor Sin3A to the proximal promoter of *Pdx-1*, while the binding of USF-1 was observed to be impaired. These studies revealed neonatal epigenetic regulation of *Pdx-1*, which could be reversed by using HDAC inhibitors [77].

While the maternal contribution to epigenetics is established, two independent groups used two different rodent models to address 'paternal' metabolic reprogramming. Carone *et al.* [93] crossed male mice fed a LPD with control animals, and observed that the offspring of both sexes revealed altered liver gene expression. The gene expression changes were particularly related to lipid metabolism, and occurred due to altered DNA methylation on multiple sites [93]. By contrast, Ng *et al.* [94] fed male rats a HFD and crossed them with control females. Female offspring from the HFD-fed male rats revealed a phenotype of β-cell impairment, and 642 genes were differentially expressed in pancreatic islets, when compared to controls. Among these, interleukin-13 receptor-α2 (*IL13rα2*) had the highest fold change and a cytosine close to the transcription start site (TSS) exhibited reduced DNA methylation [94]. While these studies clearly suggest that altered nutrition in either parent can cause stable epigenetic changes in a tissue specific-manner, functional characterization is necessary to uncover the specific causal mechanisms in each metabolic reprogramming models.

Concluding remarks and future perspectives

T2D is a complex disease characterized by uncontrolled hyperglycemia, insulin resistance, and dyslipidemia. The pathophysiology of T2D is known to be associated with numerous genetic factors, as well as alterations in the environment that can impact gene expression. The pancreatic β-cells are unique among the primary cells contributing to the pathogenesis of the disease, given their susceptibility to ER stress, and the detrimental effects of hyperglycemia and hyperinsulinemia, as well as alterations secondary to mitochondrial dysfunction. The recent surge in epigenetic studies provides an opportunity to specifically address the significance of maternal, paternal, and environmental influences in regulating β-cell function and mass. Although it is generally accepted that epigenetic mechanisms impact islet function and adaptation in rodents, investigators are faced with the daunting challenge of validating the findings in humans. The major limitation continues to be access to islets and longitudinal investigation of islet function and mass in living humans. Notwithstanding, the collective data generated in rodents regarding the effects of nutrition during gestation are being used to design nutritional intervention strategies to prevent metabolic syndrome in the offspring (reviewed in [95]). Continuing to gain a better understanding of the mechanisms underlying the molecular communication between metabolism, epigenetics and gene expression is likely to provide opportunities to identify epigenetic markers that can potentially predict disease-risk, with the long-term goal of therapeutic interventions targeting islet bioenergetics.

Acknowledgments

We thank Amélia M. Silva, Carmén Jerónimo, Inês S. Lima, and the Kulkarni lab members Anders Molven and Ivan Valdez for their helpful discussions and critical reading of the manuscript. We regret that several reports could not be cited due to space constraints. D.F.DJ. is supported by the Portuguese Foundation for Science and Technology – FCT (SFRH/BD/51699/2011), and R.N.K. is supported by NIH R01 DK 67536.

References

1 Shaw, J.E. *et al.* (2010) Global estimates of the prevalence of diabetes for 2010 and 2030. *Diabetes Res. Clin. Pract.* 87, 4–14
2 Dirice, E. and Kulkarni, R.N. (2011) Pathways underlying β-cell regeneration in type 1, type 2 and gestational diabetes. In *Islet Cell Growth Factors* (Kulkarni, R.N., ed.), p. 142, Landies Bioscience
3 Horvath, S. (2013) DNA methylation age of human tissues and cell types. *Genome Biol.* 14, R115
4 López-Otín, C. *et al.* (2013) The hallmarks of aging. *Cell* 153, 1194–1217
5 Vijg, J. and Suh, Y. (2013) Genome instability and aging. *Annu. Rev. Physiol.* 75, 645–668
6 Bird, A. (2007) Perceptions of epigenetics. *Nature* 447, 396–398
7 Dang, M.N. *et al.* (2013) Epigenetics in autoimmune diseases with focus on type 1 diabetes. *Diabetes Metab. Res. Rev.* 29, 8–18
8 Rakyan, V.K. *et al.* (2011) Identification of type 1 diabetes – associated DNA methylation variable positions that precede disease diagnosis. *PLoS Genet.* 7, e1002300
9 Gilbert, E.R. and Liu, D. (2012) Epigenetics: the missing link to understanding beta-cell dysfunction in the pathogenesis of type 2 diabetes. *Epigenetics* 7, 841–852
10 Pal, A. and McCarthy, M.I. (2013) The genetics of type 2 diabetes and its clinical relevance. *Clin. Genet.* 83, 297–306
11 Kluth, O. *et al.* (2014) Differential transcriptome analysis of diabetes resistant and sensitive mouse islets reveals significant overlap with human diabetes susceptibility genes. *Diabetes* http://dx.doi.org/10.2337/db14-0425
12 Calvanese, V. *et al.* (2009) The role of epigenetics in aging and age-related diseases. *Ageing Res. Rev.* 8, 268–276
13 Gunasekaran, U. and Gannon, M. (2011) Type 2 diabetes and the aging pancreatic beta cell. *Aging (Albany N.Y.)* 3, 565–575
14 Szoke, E. *et al.* (2008) Effect of aging on glucose homeostasis: accelerated deterioration of β-cell function in individuals with impaired glucose tolerance. *Diabetes Care* 31, 539–543
15 Iozzo, P. *et al.* (1999) Independent influence of age on basal insulin secretion in nondiabetic humans. *J. Clin. Endocrinol. Metab.* 84, 863–868
16 Ihm, S-H. *et al.* (2006) Effect of donor age on function of isolated human islets. *Diabetes* 55, 1361–1368
17 Ling, C. *et al.* (2008) Epigenetic regulation of *PPARGC1A* in human type 2 diabetic islets and effect on insulin secretion. *Diabetologia* 51, 615–622
18 Andrali, S.S. *et al.* (2008) Glucose regulation of insulin gene expression in pancreatic β-cells. *Biochem. J.* 415, 1–10
19 Kuroda, A. *et al.* (2009) Insulin gene expression is regulated by DNA methylation. *PLoS ONE* 4, e6953
20 Yang, B.T. *et al.* (2011) Insulin promoter DNA methylation correlates negatively with insulin gene expression and positively with HbA1c levels in human pancreatic islets. *Diabetologia* 54, 360–367
21 Fradin, D. *et al.* (2012) Association of the CpG methylation pattern of the proximal insulin gene promoter with type 1 diabetes. *PLoS ONE* 7, e36278
22 Volkmar, M. *et al.* (2012) DNA methylation profiling identifies epigenetic dysregulation in pancreatic islets from type 2 diabetic patients. *EMBO J.* 31, 1405–1426

23 Rieck, S. and Kaestner, K.H. (2010) Expansion of β-cell mass in response to pregnancy. *Trends Endocrinol. Metab.* 21, 151–158
24 Sandovici, I. *et al.* (2013) Developmental and environmental epigenetic programming of the endocrine pancreas: consequences for type 2 diabetes. *Cell. Mol. Life Sci.* 70, 1575–1595
25 Dhawan, S. *et al.* (2011) Pancreatic β cell identity is maintained by DNA methylation-mediated repression of *Arx*. *Dev. Cell* 20, 419–429
26 Papizan, J.B. *et al.* (2011) *Nkx2.2* repressor complex regulates islet beta-cell specification and prevents beta-to-alpha-cell reprogramming. *Genes Dev.* 25, 2291–2305
27 Lenoir, O. *et al.* (2011) Specific control of pancreatic endocrine β- and δ-cell mass by class IIa histone deacetylases HDAC4, HDAC5, and HDAC9. *Diabetes* 60, 2861–2871
28 Kulkarni, R.N. *et al.* (2004) *PDX-1* haploinsufficiency limits the compensatory islet hyperplasia that occurs in response to insulin resistance. *J. Clin. Invest.* 114, 828–836
29 Yang, B.T. *et al.* (2012) Increased DNA methylation and decreased expression of *PDX-1* in pancreatic islets from patients with type 2 diabetes. *Mol. Endocrinol.* 26, 1203–1212
30 Deering, T.G. *et al.* (2009) Methyltransferase set7/9 maintains transcription and euchromatin structure at islet-enriched genes. *Diabetes* 58, 185–193
31 Chen, H. *et al.* (2009) Polycomb protein Ezh2 regulates pancreatic β-cell *Ink4a/Arf* expression and regeneration in diabetes mellitus. *Genes Dev.* 23, 975–985
32 Xu, C-R. *et al.* (2011) Chromatin 'prepattern' and histone modifiers in a fate choice for liver and pancreas. *Science* 332, 963–966
33 Dhawan, S. *et al.* (2009) *Bmi-1* regulates the *Ink4a/Arf* locus to control pancreatic β-cell proliferation. *Genes Dev.* 23, 906–911
34 Zhou, J.X. *et al.* (2013) Combined modulation of polycomb and trithorax genes rejuvenates β cell replication. *J. Clin. Invest.* 123, 4849–4858
35 Garcia-Ocana, A. and Stewart, A.F. (2014) 'RAS'ling beta cells to proliferate for diabetes: why do we need MEN? *J. Clin. Invest.* 124, 3698–3700
36 Karnik, S.K. *et al.* (2007) Menin controls growth of pancreatic beta-cells in pregnant mice and promotes gestational diabetes mellitus. *Science* 318, 806–809
37 Chamberlain, C.E. *et al.* (2014) Menin determines K-RAS proliferative outputs in endocrine cells. *J. Clin. Invest.* 124, 4093–4101
38 Ameres, S.L. and Zamore, P.D. (2013) Diversifying microRNA sequence and function. *Nat. Rev. Mol. Cell Biol.* 14, 475–488
39 Guay, C. *et al.* (2011) Diabetes mellitus, a microRNA-related disease? *Transl. Res.* 157, 253–264
40 Zhao, E. *et al.* (2009) Obesity and genetics regulate microRNAs in islets, liver, and adipose of diabetic mice. *Mamm. Genome* 20, 476–485
41 Morita, S. *et al.* (2009) *Dicer* is required for maintaining adult pancreas. *PLoS ONE* 4, e4212
42 Joglekar, M.V. *et al.* (2009) Expression of islet-specific microRNAs during human pancreatic development. *Gene Expr. Patterns* 9, 109–113
43 Vetere, A. *et al.* (2014) Targeting the pancreatic beta-cell to treat diabetes. *Nat. Rev. Drug Discov.* 13, 278–289
44 Wang, Y. *et al.* (2013) *MicroRNA-7* regulates the mTOR pathway and proliferation in adult pancreatic beta-cells. *Diabetes* 62, 887–895
45 Dunmore, S.J. and Brown, J.E.P. (2013) The role of adipokines in β-cell failure of type 2 diabetes. *J. Endocrinol.* 216, T37–T45
46 Weaver, J.R. *et al.* (2012) Integration of pro-inflammatory cytokines, 12-lipoxygenase and NOX-1 in pancreatic islet beta cell dysfunction. *Mol. Cell. Endocrinol.* 358, 88–95
47 Qi, Y. and Xia, P. (2012) Cellular inhibitor of apoptosis protein-1 (cIAP1) plays a critical role in β-cell survival under endoplasmic reticulum stress: promoting ubiquitination and degradation of C/EBP homologous protein (CHOP). *J. Biol. Chem.* 287, 32236–32245
48 Supale, S. *et al.* (2012) Mitochondrial dysfunction in pancreatic β cells. *Trends Endocrinol. Metab.* 23, 477–487
49 Tang, C. *et al.* (2013) Susceptibility to fatty acid-induced β-cell dysfunction is enhanced in prediabetic diabetes-prone biobreeding rats: a potential link between β-cell lipotoxicity and islet inflammation. *Endocrinology* 154, 89–101
50 Eizirik, D.L. *et al.* (2013) Signalling danger: endoplasmic reticulum stress and the unfolded protein response in pancreatic islet inflammation. *Diabetologia* 56, 234–241
51 Cnop, M. *et al.* (2012) Endoplasmic reticulum stress, obesity and diabetes. *Trends Mol. Med.* 18, 59–68
52 Franco, R. *et al.* (2008) Oxidative stress, DNA methylation and carcinogenesis. *Cancer Lett.* 266, 6–11
53 Quan, X. *et al.* (2011) Reactive oxygen species downregulate catalase expression via methylation of a CpG island in the *Oct-1* promoter. *FEBS Lett.* 585, 3436–3441
54 Bernal, A.J. *et al.* (2013) Adaptive radiation-induced epigenetic alterations mitigated by antioxidants. *FASEB J.* 27, 665–671
55 Shock, L.S. *et al.* (2011) DNA methyltransferase 1, cytosine methylation, and cytosine hydroxymethylation in mammalian mitochondria. *Proc. Natl. Acad. Sci. U.S.A.* 108, 3630–3635
56 Minocherhomji, S. *et al.* (2012) Mitochondrial regulation of epigenetics and its role in human diseases. *Epigenetics* 7, 326–334
57 Kriaucionis, S. and Heintz, N. (2009) The nuclear DNA base 5-hydroxymethylcytosine is present in Purkinje neurons and the brain. *Science* 324, 929–930
58 Tahiliani, M. *et al.* (2009) Conversion of 5-methylcytosine to 5-hydroxymethylcytosine in mammalian DNA by MLL partner TET1. *Science* 324, 930–935
59 Chia, N. *et al.* (2011) Hypothesis: environmental regulation of 5-hydroxymethylcytosine by oxidative stress. *Epigenetics* 6, 853–856
60 Weir, G.C. *et al.* (2009) Towards better understanding of the contributions of overwork and glucotoxicity to the beta-cell inadequacy of type 2 diabetes. *Diabetes Obes. Metab.* 11 (Suppl 4), 82–90
61 Poitout, V. and Robertson, R.P. (2008) Glucolipotoxicity: fuel excess and beta-cell dysfunction. *Endocr. Rev.* 29, 351–366
62 Tang, C. *et al.* (2012) Glucose-induced beta cell dysfunction *in vivo* in rats: link between oxidative stress and endoplasmic reticulum stress. *Diabetologia* 55, 1366–1379
63 Coughlan, M.T. *et al.* (2011) Advanced glycation end products are direct modulators of β-cell function. *Diabetes* 60, 2523–2532
64 El-Osta, A. *et al.* (2008) Transient high glucose causes persistent epigenetic changes and altered gene expression during subsequent normoglycemia. *J. Exp. Med.* 205, 2409–2417
65 Brasacchio, D. *et al.* (2009) Hyperglycemia induces a dynamic cooperativity of histone methylase and demethylase enzymes associated with gene-activating epigenetic marks that coexist on the lysine tail. *Diabetes* 58, 1229–1236
66 Li, Y. and Tollefsbol, T.O. (2011) $p16^{INK4a}$ suppression by glucose restriction contributes to human cellular lifespan extension through SIRT1-mediated epigenetic and genetic mechanisms. *PLoS ONE* 6, e17421
67 Houtkooper, R.H. *et al.* (2012) Sirtuins as regulators of metabolism and healthspan. *Nat. Rev. Mol. Cell Biol.* 13, 225–238
68 Zheng, Z. *et al.* (2012) *S*irtuin 1-mediated cellular metabolic memory of high glucose via the LKB1/AMPK/ROS pathway and therapeutic effects of metformin. *Diabetes* 61, 217–228
69 Tang, X. *et al.* (2009) Identification of glucose-regulated miRNAs from pancreatic β cells reveals a role for *miR-30d* in insulin transcription. *RNA* 15, 287–293
70 Esguerra, J.L.S. *et al.* (2011) Differential glucose-regulation of microRNAs in pancreatic islets of non-obese type 2 diabetes model Goto–Kakizaki rat. *PLoS ONE* 6, e18613
71 Goldfine, A.B. and Kulkarni, R.N. (2012) Modulation of β-cell function: a translational journey from the bench to the bedside. *Diabetes Obes. Metab.* 14, 152–160
72 Mezza, T. and Kulkarni, R. (2014) The regulation of pre- and post-maturational plasticity of mammalian islet cell mass. *Diabetologia* 57, 1291–1303
73 Maures, T.J. *et al.* (2011) The H3K27 demethylase UTX-1 regulates *C. elegans* lifespan in a germline-independent, insulin-dependent manner. *Aging Cell* 10, 980–990
74 Wang, Y. *et al.* (2013) Phosphorylation and recruitment of BAF60c in chromatin remodeling for lipogenesis in response to insulin. *Mol. Cell* 49, 283–297
75 Kabra, D.G. *et al.* (2009) Insulin induced alteration in post-translational modifications of histone H3 under a hyperglycemic condition in L6 skeletal muscle myoblasts. *Biochim. Biophys. Acta* 1792, 574–583
76 Chen, H. *et al.* (2011) PDGF signalling controls age-dependent proliferation in pancreatic beta-cells. *Nature* 478, 349–355

77 Park, J.H. *et al.* (2008) Development of type 2 diabetes following intrauterine growth retardation in rats is associated with progressive epigenetic silencing of *Pdx1*. *J. Clin. Invest.* 118, 2316–2324
78 Pinney, S.E. *et al.* (2011) Exendin-4 increases histone acetylase activity and reverses epigenetic modifications that silence *Pdx1* in the intrauterine growth retarded rat. *Diabetologia* 54, 2606–2614
79 El Ouaamari, A. *et al.* (2013) Liver-derived systemic factors drive β cell hyperplasia in insulin-resistant states. *Cell Rep.* 3, 401–410
80 Yi, P. *et al.* (2013) Betatrophin: a hormone that controls pancreatic β cell proliferation. *Cell* 153, 747–758
81 Lo, J.C. *et al.* (2014) Adipsin is an adipokine that improves β cell function in diabetes. *Cell* 158, 41–53
82 Dumortier, O. *et al.* (2007) Different mechanisms operating during different critical time-windows reduce rat fetal beta cell mass due to a maternal low-protein or low-energy diet. *Diabetologia* 50, 2495–2503
83 Theys, N. *et al.* (2009) Early low protein diet aggravates unbalance between antioxidant enzymes leading to islet dysfunction. *PLoS ONE* 4, e6110
84 Gunton, J.E. *et al.* (2005) Loss of *ARNT*/*HIF1*^{2} mediates altered gene expression and pancreatic-islet dysfunction in human type 2 diabetes. *Cell* 122, 337–349
85 Sandovici, I. *et al.* (2011) Maternal diet and aging alter the epigenetic control of a promoter–enhancer interaction at the *Hnf4a* gene in rat pancreatic islets. *Proc. Natl. Acad. Sci. U.S.A.* 108, 5449–5454
86 Jimenez-Chillaron, J.C. *et al.* (2009) Intergenerational transmission of glucose intolerance and obesity by *in utero* undernutrition in mice. *Diabetes* 58, 460–468
87 Radford, E.J. *et al.* (2014) *In utero* undernourishment perturbs the adult sperm methylome and intergenerational metabolism. *Science* 345, 1255903
88 Martínez, D. *et al.* (2014) *In utero* undernutrition in male mice programs liver lipid metabolism in the second-generation offspring involving altered *Lxra* DNA methylation. *Cell Metab.* 19, 941–951
89 de Miguel-Santos, L. *et al.* (2010) Maternal undernutrition increases pancreatic IGF-2 and partially suppresses the physiological wave of β-cell apoptosis during the neonatal period. *J. Mol. Endocrinol.* 44, 25–36
90 Xu, Y-P. *et al.* (2011) The levels of *Pdx1*/insulin, *Cacna1c* and *Cacna1d*, and β-cell mass in a rat model of intrauterine undernutrition. *J. Mater. Fetal Neonatal Med.* 24, 437–443
91 Simmons, R. (2007) Role of metabolic programming in the pathogenesis of β-cell failure in postnatal life. *Rev. Endocr. Metab. Disord.* 8, 95–104
92 Park, I-H. *et al.* (2008) Reprogramming of human somatic cells to pluripotency with defined factors. *Nature* 451, 141–146
93 Carone, B.R. *et al.* (2010) Paternally induced transgenerational environmental reprogramming of metabolic gene expression in mammals. *Cell* 143, 1084–1096
94 Ng, S-F. *et al.* (2010) Chronic high-fat diet in fathers programs β-cell dysfunction in female rat offspring. *Nature* 467, 963–966
95 Duque-Guimarães, D.E. and Ozanne, S.E. (2013) Nutritional programming of insulin resistance: causes and consequences. *Trends Endocrinol. Metab.* 24, 525–535
96 Yi, S. (2012) Birds do it, bees do it, worms and ciliates do it too: DNA methylation from unexpected corners of the tree of life. *Genome Biol.* 13, 174
97 Suzuki, M.M. and Bird, A. (2008) DNA methylation landscapes: provocative insights from epigenomics. *Nat. Rev. Genet.* 9, 465–476
98 Mazzio, E.A. and Soliman, K.F.A. (2012) Basic concepts of epigenetics: impact of environmental signals on gene expression. *Epigenetics* 7, 119–130
99 Bhutani, N. *et al.* (2011) DNA demethylation dynamics. *Cell* 146, 866–872
100 Williams, K. *et al.* (2012) DNA methylation: TET proteins – guardians of CpG islands? *EMBO Rep.* 13, 28–35
101 Hackett, J.A. *et al.* (2013) Germline DNA demethylation dynamics and imprint erasure through 5-hydroxymethylcytosine. *Science* 339, 448–452
102 Waki, H. *et al.* (2012) The epigenome and its role in diabetes. *Curr. Diab. Rep.* 12, 673–685
103 Xu, Y. *et al.* (2012) Histone H2A.Z. controls a critical chromatin remodeling step required for DNA double-strand break repair. *Mol. Cell* 48, 723–733
104 Bramswig, N.C. and Kaestner, K.H. (2012) Epigenetics and diabetes treatment: an unrealized promise? *Trends Endocrinol. Metab.* 23, 286–291
105 Rando, O.J. (2012) Combinatorial complexity in chromatin structure and function: revisiting the histone code. *Curr. Opin. Genet. Dev.* 22, 148–155
106 Verdone, L. *et al.* (2005) Role of histone acetylation in the control of gene expression. *Biochem. Cell Biol.* 83, 344–353
107 Suganuma, T. and Workman, J.L. (2011) Signals and combinatorial functions of histone modifications. *Annu. Rev. Biochem.* 80, 473–499
108 Guo, H. *et al.* (2010) Mammalian microRNAs predominantly act to decrease target mRNA levels. *Nature* 466, 835–840
109 Fukaya, T. and Tomari, Y. (2012) MicroRNAs mediate gene silencing via multiple different pathways in *Drosophila*. *Mol. Cell* 48, 825–836
110 Fraga, M.F. *et al.* (2005) Epigenetic differences arise during the lifetime of monozygotic twins. *Proc. Natl. Acad. Sci. U.S.A.* 102, 10604–10609
111 Heijmans, B.T. *et al.* (2008) Persistent epigenetic differences associated with prenatal exposure to famine in humans. *Proc. Natl. Acad. Sci. U.S.A.* 105, 17046–17049
112 Daxinger, L. and Whitelaw, E. (2012) Understanding transgenerational epigenetic inheritance via the gametes in mammals. *Nat. Rev. Genet.* 13, 153–162

Appendix A4

Publication

El Ouaamari A, Zhou J, Liew CW, Shirakawa J, Dirice E, Gedeon N, Kahraman S, **De Jesus DF**, Bhatt S, Kim JS, Clauss TRW, Camp DG, Smith RD, Qian WJ and Kulkarni RN. Compensatory Islet Response to Insulin Resistance Revealed by Quantitative Proteomics. J. Proteome Res 14(8):3111-22, 2015.

Contribution

I contributed by assisting in tissue harvesting and islet isolation.

HHS Public Access

Author manuscript

J Proteome Res. Author manuscript; available in PMC 2016 May 07.

Published in final edited form as:

J Proteome Res. 2015 August 7; 14(8): 3111–3122. doi:10.1021/acs.jproteome.5b00587.

Compensatory Islet Response to Insulin Resistance Revealed by Quantitative Proteomics

Abdelfattah El Ouaamari[#1], **Jian-Ying Zhou**[#2], **Chong Wee Liew**[#3], **Jun Shirakawa**[#1], **Ercument Dirice**[#1], **Nicholas Gedeon**[1], **Sevim Kahraman**[1], **Dario F. De Jesus**[1], **Shweta Bhatt**[1], **Jong-Seo Kim**[2], **Therese RW Clauss**[2], **David G. Camp II**[2], **Richard D. Smith**[2], **Wei-Jun Qian**[2,*], and **Rohit N. Kulkarni**[1,*]

[1]Islet Cell & Regenerative Biology, Joslin Diabetes Center, Department of Medicine, Brigham and Women's Hospital, Harvard Medical School, Boston, Massachusetts 02215

[2]Biological Sciences Division and Environmental Molecular Sciences Laboratory, Pacific Northwest National Laboratory, Richland, Washington 99352

[3]Department of Physiology and Biophysics, University of Illinois at Chicago, Chicago, IL 60612, USA.

[#] These authors contributed equally to this work.

Abstract

Compensatory islet response is a distinct feature of the pre-diabetic insulin resistant state in humans and rodents. To identify alterations in the islet proteome that characterize the adaptive response, we analyzed islets from five-month-old male control, high-fat diet fed (HFD) or obese ob/ob mice by LC-MS(/MS) and quantified ~1,100 islet proteins (at least two peptides) with a false discovery rate <1%. Significant alterations in abundance were observed for ~350 proteins between groups. A majority of alterations were common to both models, and the changes of a subset of ~40 proteins and 12 proteins were verified by targeted quantification using selected reaction monitoring and Western blots, respectively. The insulin resistant islets in both groups exhibited reduced expression of proteins controlling energy metabolism, oxidative phosphorylation, hormone processing, and secretory pathways. Conversely, an increased expression of molecules involved in protein synthesis and folding suggested effects in endoplasmic reticulum stress response, cell survival, and proliferation in both insulin resistant

[*]Correspondence to: Rohit N. Kulkarni: Rohit.Kulkarni@joslin.harvard.edu and Tel: (617) 309-3460, Wei-Jun Qian: Weijun.qian@pnnl.gov and Tel: (509) 371-6572.

ASSOCIATED CONTENT

Supporting Information Available

Supplemental tables and figures are available free of charge via the Internet at http://pubs.acs.org.

Table S1: List of all quantified proteins. All values in each sample are log2 of peptide intensities after normalization.
Table S2: List of proteins showing significant change. All ratios are in log2 scale.
Table S3: SRM validation of candidate proteins.
Table S4: Protein candidates only showing significant change in HFD model.
Table S5: Protein candidates only showing significant change in ob/ob model.
Table S6: List of all identified peptides.
Table S7: List of all SRM peptides and associated transitions
Figure S1: Histograms of the extent of changes for altered proteins.
Figure S2: Examples of extracted ion chromatograms of SRM measurements.

models. In summary, we report a unique comparison of the islet proteome that is focused on the compensatory response in two insulin resistant rodent models that are not overtly diabetic. These data provide a valuable resource of candidate proteins to the scientific community to undertake further studies aimed at enhancing β-cell mass in patients with diabetes. The data are available via the MassIVE repository, with accession MSV000079093.

Keywords

insulin resistance; pancreatic islets; proteome; proliferation; metabolism; function

INTRODUCTION

Type 2 diabetes has reached epidemic proportions worldwide and impacts multiple organ systems. Following the development of insulin resistance the onset of the disease is triggered when the residual functional β-cells fail to compensate for the increased metabolic needs of the individual[1]. Despite available insulin-based and oral hypoglycemic medications, the disease continues to spread worldwide and is predicted to affect over 360 million individuals globally by 2030[2]. Genome wide association studies revealed that type 2 diabetes-linked genes are involved in regulating β-cell mass as well as function[3] suggesting the relevance of targeting β-cells as a therapeutic strategy for type 2 diabetes. Although islet transplantation has achieved success in reversing the disease and limiting its complications[4], the shortage of islets from donors has prompted a reconsideration of designing alternative therapies.

While it is still debatable whether therapies should target enhancing insulin secretion from residual β-cells or increasing the number of functional insulin-producing cells[5], insights to design efficient therapeutics might emerge from an understanding of the processes by which β-cells compensate to chronic increased demands for insulin. Indeed, obese non-diabetic individuals develop compensatory islet β-cell response to adjust the levels of insulin to counteract insulin resistance and therefore maintaining normoglycemia. Generally speaking, humans with insulin resistance (e.g. impaired fasting glucose or pregnancy) exhibit increased insulin secretion as compared to controls[6]. However, whether this compensatory response is attributed to structural or functional adaptation of islet β-cells is incompletely understood. Although increased β-cell proliferation in metabolically challenged rodents is known as a major structural adaptive response within islets[7], the proportional contribution of functional changes in islet cells is unclear. Most studies which investigated islet-cell function in the context of insulin resistance were performed *in vivo*[1a] where the islet-cell mass is a considerable confounder – and fewer *in vitro* metabolic studies have been undertaken in rat islets[8]. Several proteomics studies were performed on islets derived from insulin resistant diabetic mice[9]. However, these studies did not address adaptive functional molecular changes in islet-cells in response to insulin resistance but rather dysfunction of islet β-cells in diabetes. In one study, the diabetic MKR (a transgenic mouse with a dominant-negative IGF-1R in skeletal muscle) mouse was used to investigate deleterious effects of insulin resistance on β-cell function[9c]. The same group reported a combined proteomic and microarray screen to assess defects occurring in insulin resistance-induced β-

cell failure[9b]. Interestingly, a proteomics screen was used to address the transition from obesity to diabetes in the Zucker Fatty (ZF) and Zucker Diabetic Fatty (ZDF) rat models[9a]. Finally, a two-dimensional gel electrophoresis approach was applied to identify proteomic changes in the entire pancreas derived from db/db or C57BL/6J mice challenged with high fat diet (HFD); however, a major limitation in these studies was a lack of distinction between acinar and islet cells[9d, 10].

Herein we used a comparative proteomics approach to characterize changes in the islet proteome in two commonly used insulin resistant pre-diabetic models, the ob/ob (small or large islets) and HFD mice. Ingenuity pathway analysis of the significantly altered proteins revealed an intriguing down-regulation of major proteins involved in pathways critical for hormone secretion including glucose and amino acid metabolism, Krebs cycle, mitochondrial oxidative phosphorylation, hormone biosynthesis and the final steps of exocytosis, suggesting functional maladaptation of islet-cells in insulin resistance states. Moreover, an increased protein synthesis and vesicular transport was observed indicating endoplasmic reticulum (ER) stress in insulin resistant islets. Interestingly, several proteins known to control cell proliferation and survival were upregulated in both HFD and ob/ob islets as compared to controls. Finally, it is notable that most proteomic changes were observed in both models of insulin resistance, and in both small and large islets. These data provide a comprehensive view of proteomic changes occurring during obesity induced islet hyperplasia and provide potential opportunities for therapeutic strategies to address β-cell decline in diabetic states.

EXPERIMENTAL PROCEDURES

Islet isolation

Islets from 5-month old C57/Bl6 male high-fat diet (HFD) fed mouse and obese ob/ob mice (n=6) manifesting insulin-resistance and age-matched control C57/Bl6 males were isolated by the intraductal enzyme injection technique using liberase[11]. Briefly, the pancreas was inflated with collagenase and islets were isolated as reported previously[12]. All islets were cultured overnight at physiological glucose levels (7 mM glucose, 10% FBS) to allow the islets to recover from the effects of liberase digestion. Islets were then transferred to nuclease- and pyrogen-free tubes and washed with phosphate buffer. Following removal of the buffer, pellets were frozen at – 80°C prior to proteomic analyses.

Protein digestion

Islet samples were homogenized and digested using a 2,2,2-trifluoroethanol (TFE)-based protocol[13]. Briefly, islets were dissolved in 30 ul of 50% TFE / 50% 25 mM NH_4HCO_3 by 3 min sonication in 5510 Branson ultrasonic water bath (Branson Ultrasonics, Danbury, CT) with ice cold water bath. Protein concentration was determined by BCA assay. About 40 μg islet proteins from each mouse were denatured in 50% TFE for 105 min at 60 °C, reduced by 2 mM DTT for 60 min at 37 °C, diluted by 5 fold with 50mM NH_4HCO_3, and digested by 0.8 μg trypsin (1:50 w/w trypsin-to-protein ratio) for 3 hours at 37°C. The digestion was stopped by 0.1% TFA. All peptide samples were dried down in Speed Vac remove TFE, and resuspended in 25 mM NH_4HCO3 for LC-MS/MS analysis.

LC-MS/MS analysis

LC-MS/MS analyses were performed on a custom-built automated LC system coupled on-line to an LTQ-Orbitrap mass spectrometer (Thermo Scientific, San Jose, CA) via a nanoelectrospray ionization interface as previously described[14]. Briefly, 0.75 μg of peptides were loaded onto a home-made 65-cm-long reversed-phase capillary column with 75-μm-inner diameter packed using 3 μm Jupiter C18 particles (Phenomenex, Torrance, CA). The mobile phase was held at 100% A (0.1% formic acid) for 20 min, followed by a linear gradient from 0 to 60% buffer B (0.1% formic acid in 90% acetonitrile) over 85 min. The instrument was operated in data-dependent mode with an m/z range of 400–2000, in which a full MS scan with a resolution of 100K was followed by 6 MS/MS scans. The 6 most intensive precursor ions were dynamically selected in the order of highest intensity to lowest intensity and subjected to collision-induced dissociation using a normalized collision energy setting of 35% and a dynamic exclusion duration of 1 min. The heated capillary was maintained at 200 °C, while the ESI voltage was kept at 2.2 kV.

MS/MS data analysis

LC-MS/MS raw data were converted into .dta files using Extract_MSn (version 3.0) in Bioworks Cluster 3.2 (Thermo Fisher Scientific, Cambridge, MA), and the SEQUEST algorithm (version 27, revision 12) was used to search all MS/MS spectra against a mouse protein FASTA file that contains 16, 244 entries (Uniprot, released on April 20, 2010). The search parameters used were: dynamic oxidation of methionine, 3 Da tolerances for precursor ion masses, and 1 Da for fragment ion masses. The search parameter file did not include any enzyme cleavage restraints on the termini of the identified peptides, which means that both tryptic peptides and non-tryptic peptides were identified during database searching and tryptic rules were only applied during data filtering steps. Moreover, the search parameter file allowed a maximum of three trypsin miscleavage sites for any given peptide identification. MS Generating-Function (MSGF) scores were generated for each identified spectrum as described previously by computing rigorous p-values (spectral probabilities)[15]. Fully tryptic peptides with MSGF score <5E-10 and mass measurement errors <3 ppm were accepted as identifications. All peptides that passed the filtering criteria were input into the ProteinProphet program[16] to generate a final non-redundant list of proteins. The decoy-database searching methodology[13,17] was used to control the FDR at the unique peptide level to <0.5%. The LC-MS/MS raw data along with Sequest output files have been deposited into the MassIVE repository, with accession MSV000079093. It was also shared with ProteomeXchange, and assigned dataset identifier PXD002009.

Label-free quantification

Label-free MS intensity-based quantification was performed using the accurate mass and time (AMT) tag approach as previously described[18]. Briefly, the islet AMT tag database were populated based on all the confident peptide identifications from the MS/MS data and the theoretical masses and observed normalized elution time (NET) values for each identified peptide were included in the database. The AMT tag database essentially serves as a “look-up” table for LC-MS feature identifications. LC-MS datasets were automatically analyzed using an in-house-developed software package that included Decon2LS and

VIPER informatics software tools[19]. Initial analysis of the raw LC-MS data involved the use of Decon2LS to perform a de-isotoping step, which generated a text file report for the detected masses and their corresponding intensities. Each dataset was then processed by using the feature-matching tool VIPER to identify and quantify peptides. LC-MS feature identification was achieved by matching the accurately measured masses and NET values of each detected feature to the islet AMT tag database. Only when the measured mass and NET for each given feature matched the calculated mass and NET of a peptide in the AMT tag database within a 2 ppm mass error and 2% NET error, the features were considered confidently identified as peptides.

The obtained abundance data (MS intensities) for all identified peptides from different dataset were further processed by statistical data analysis software tool DAnTE[20]. The peptide abundance data were initially log2 transformed, normalized using the central tendency approach. Protein abundance profiles across different conditions were generated by taking a rescaling procedure for peptide profiles for each protein against a reference peptide[18a]. Statistical analysis using nested ANOVA was applied to identify proteins with significant abundance changes between different biological conditions by considering both biological replicates (n=5) and technical replicates (n=2). Proteins with significant abundance changes across the biological groups were identified by requiring a p-value of <0.01 and log2 ratio (over control) >0.58 (corresponding to 50% change) in at least one of the conditions.

Preparation of ^{18}O-labeled peptide reference sample

The ^{18}O-labeled peptide reference sample was generated by trypsin-catalyzed ^{18}O labeling at the peptide level was performed using a recently improved protocol[21]. Briefly, the reference sample pooled from all biological replicates was lyophilized to dryness and reconstituted in 100 µl of 50 mM NH_4HCO_3 in H $^{18}_2$O (97%; ISOTEC, Miamisburg, OH), pH 7.8. One µl of 1 M $CaCl_2$ and solution phase trypsin dissolved in H $^{18}_2$O at a 1:50 trypsin/peptide ratio (w/w) were added to the samples. The tubes were wrapped in parafilm and mixed continuously for 5 h at 37 °C. The reaction was stopped by boiling the sample in a water bath for 10 min. After snap-freezing the sample in liquid nitrogen, the samples were acidified by adding 5 µl of formic acid, and final peptide concentrations were measured using a BCA assay.

Targeted quantification using selected reaction monitoring (SRM)

SRM-based targeted quantification using ^{18}O-based reference[22] was performed for 39 selected proteins. The peptides and SRM transitions was selected and screened as previously described[22], and were listed in Supplemental Table 7. At least 6 transitions of each peptide were monitored in initial screening to ensure the confident identification and detection of the targeted peptides. The best two transitions (without interference) for each peptide were selected for final quantification. The predicted collision energies from Skyline were used for all peptides. Prior to LC-SRM analyses, the ^{18}O-labeled reference sample was spiked into each peptide sample in 1:1 mixing ratio. All peptide samples were analyzed on a Waters nanoACQUITY UPLC system (Waters Corporation, Milford MA) directly coupled to coupled on-line to a triple quadrupole mass spectrometer (TSQ Vantage; Thermo Fisher

Scientific) using a 25-cm-long, 75-μm-inner diameter fused silica capillary column. 1 μl aliquots of each sample containing ~ 0.5 μg/μl peptides were injected onto the analytical column with a 40-min linear gradient of 10–50% acetonitrile and 0.1% formic acid. A fixed dwell time of 10 ms and a scan window of 0.002 *m*/*z* were employed. All datasets were analyzed by Skyline software. The peak area ratios were used for the evaluation of protein abundance changes.

Western blot and antibodies

For western blotting, more than 150 isolated islets from six-month old male C57/Bl6 and age-matched male ob/ob mice were lysed in ice-cold M-PER buffer (Thermo Fisher Scientific) with protease inhibitor cocktail and phosphatase inhibitor cocktail (Sigma). After centrifugation, the extracts were subjected to western blotting with antibodies to CDK5Rap3 (Santa Cruz, sc-134627), Sel1I (Abcam, ab78298), Nucb2 (Abcam, ab30945), PCSK1 (Thermo Fisher, PA1-057), PCSK2 (Thermo Fisher, PA1-058), SYTL4 (Santa Cruz, sc-34446), UCN3 (Bioss, bs-2786R), VAMP2 (Thermo Fisher, PA1-766), COX7A2 (Life technologies, A21367), COX4I1 (Cell Signaling, #4850), MAOB (Abcam, ab125010), SDHB (Life technologies, A21345), or β-actin (Cell Signaling, #4697). Densitometry was performed using Image J software.

RESULTS

To examine islet proteome changes occurring during islet-cell adaptation in the course of insulin resistance, we performed comprehensive LC-MS-based quantitative proteomic profiling using freshly isolated islets from 5 month-old wild type, age matched leptin-deficient obese (ob/ob), or mice challenged for 12 weeks with 60% kcal High Fat Diet (HFD) beginning at age 8-weeks. Moreover, to elucidate whether insulin resistance-induced islet compensatory response is distinct in populations of islets with variable size, we also compared the proteome of small (S, ~50 microns) and large (L, 200 microns) islets from ob/ob mice where the variability in islet size was greater compared to the HFD model. Mice in both models exhibited increased body weight, and mild hyperglycemia (200 mg/dl), hyperinsulinemia in the fed state, and manifested islet hyperplasia as compared to controls **(Fig. 1A-D)**.

LC-MS based label-free quantification of samples isolated from control, ob/ob small, ob/ob large, or HFD islets (n=5 for each group) resulted in confident identification and quantification of ~6,900 unique peptides and ~1,100 proteins with at least two peptides per protein applying the accurate mass and time (AMT) tag approach[18b] (Supplementary Table 1 and Table 6). **Fig. 2A and 2B** illustrates the data analysis process where the raw peptide abundance profiles for a given protein obtained by the AMT tag approach was displayed in 2A using the data analysis tool DAnTE[20]. In Fig. 2B, a protein abundance profile was obtained for the protein (blank curve) after rescaling and rolling up to protein level. The high reproducibility of the quantitative approach was illustrated in the comparison of two technical replicates (**Fig. 2C)**, while the comparison between control and ob/ob (small islets) conditions shows more biological variation (**Fig. 2D)**. After subjecting the data to statistical analysis, approximately ~350 proteins were revealed to be significantly altered in either

ob/ob or HFD mouse islets (**Fig. 2E**, and Supplemental Table 2). Among the ~350 proteins, the majority displayed a relative small changes (log2 ratio <1) for any given biological conditions (HFD, ob/ob small, or ob/ob large) and only ~100 proteins exhibited more than 2-fold changes (Supplemental Figure 1). Since we did not observe significant difference between small and large islets from ob/ob mice, only the data from the small islets from ob/ob mice are presented here.

To further validate the global quantitative data, targeted quantification using selected reaction monitoring (SRM), a multiplexed quantitative technology providing similar quality as western blot or immunoassays[23], was applied to validate a select list of 39 proteins from different functional categories (Supplemental Table 3). Selected examples of extracted ion chromatograms (XICs) for targeted peptides from SRM measurements are shown in Supplemental Figure S2. **Fig.2F** shows that SRM measured abundance ratios (HF or ob/ob divided by control) for the 39 proteins correlate well with the abundance ratio data obtained from AMT tag-based global profiling, supporting the overall high quality of the global quantitative profiling.

Among the altered proteins, most of the changes were common between HFD and ob/ob models (**Fig. 2E**). The subcellular components, molecular functions, and canonical pathways of the altered proteins were analyzed by Ingenuity Pathway Analysis (IPA) as shown in **Fig. 3**. The distribution of altered proteins in subcellular components indicated that the majority of protein alterations occurred in the cytoplasm, which consisted of nearly a third of total quantified protein in the category (**Fig. 3A**). The observation that enzymes are the most altered category in molecular function (**Fig. 3B**) corroborates well with cytoplasm as the main component of protein alterations. The canonical pathway analysis (**Fig. 3C**) clearly indicated down-regulation in mitochondrial function and metabolism, and up-regulation in translational regulation and stress-related signaling. Selected regulated proteins implicated in different functional categories (**Table 1**) were further examined in detail.

Metabolic and mitochondrial dysfunction

IPA analysis of the altered proteins revealed significant changes in glycolysis, gluconeogenesis and Krebs cycle pathways (**Table 1**). Although Aldo-Keto Reductase family 1, member A1 (AKR1A1), lactate dehydrogenase A (LDHA) and phosphoglucomutase 2 (PGM2) were found upregulated in insulin resistance-derived islets, proteins regulating glycolysis/gluconeogenesis were observed to be down-regulated. The down-regulated proteins including aldehyde dehydrogenase 3 family, member A2 (ALDH3A2), aldolase A (ALDOA), dihydrolipoamide S-acetyltransferase (DLAT), dihydrolipoamide dehydrogenase (DLD), enolase 2 (ENO2) and phosphofructokinase, liver (PFKL). Moreover, several enzymes regulating citrate cycle were affected. Proteins belonging to isocitrate dehydrogenase family (IDH1, IDH2 and IDH3A), pyruvate carboxylase (PC), phosphoenolpyruvate carboxykinase 2 (PCK2), and succinate dehydrogenase complex, subunit B (SDHB) were down-regulated in islets derived from both HFD and ob/ob models. Down-regulation in mitochondrial function was detected in islets derived from HFD and ob/ob animals since the expression levels of several components of ATP synthase machinery, including ATP5I, ATP6V1D, ATP5J2, ATP6V1A, ATP6V1B2,

ATP6V1F, and ATP6V1H were lower compared to control animals (**Table 1 and Supplemental Table 2**). Furthermore, members of cyclooxygenase family were also affected. Thus, expression of COX4I1, COX5A, COX6A1 and COX7A2, cytochrome C1 (CYC1) and components of ubiquinol-cytochrome c reductase complex (UQCRC1, UQCRC2, UQCRFS1 and UQCRQ) were decreased in hyperplastic islets (**Table 1 and Supplemental Table 2**). Notably, we found SOD2, a major enzyme of defense against oxidative damage, to be down-regulated in all insulin resistant islets

Protein synthesis and transport and endoplasmic reticulum stress

A remarkable feature observed in this study is the up-regulation of key components of the translational machinery (**Table 1 and Supplemental Table 2**). Eukaryotic translation initiation factors (eIFs) such as eIF3C, eIF3E, eIF3F, eIF3G, eIF3H, eIF2S1 and subsets of ribosomal proteins including RPL5, RPL7 and RPS19 were up-regulated and several proteins implicated in biogenesis of ribosomal and/or transfer RNAs such as keratin 7 (KRT7), nucleophosmin (NMP1), ribosomal binding protein 1 (RRBP1), Aspartyl-tRNA synthetase (DARS) and phenylalanyl-tRNA synthetase beta subunit (FARSB) were found to be over-expressed in islets from HFD and ob/ob as compared to control islets. ER stress proteins, including endoplasmic proteins 29 and 44 (ERP29 and ER44), lectin mannose-binding 1 (LMAN1), mannosyl-oligosaccharide glucosidase (MOGS), protein disulfide isomerase family A, member 3 and 6 (PDIA3 and PDIA6) and selenoprotein 15 (SEP15) were up-regulated in insulin resistant islets. Significant upregulation of key proteins implicated in facilitating intracellular protein transport were also observed, including endoplasmic reticulum protein 29 (ERP29), eukaryotic initiation factor 5A (EIF5A), melanoma inhibitory activity 3 (MIA3), new molecular entity 2 (NME2), nucleophosmin (NPM1), protein disulfide isomerase 3 (PDIA3) and SEC23-interacting protein (SEC23IP). Additionally, several members of clathrin-ordered proteins family (COP) involved in protein transport and cell membrane organization manifested substantial increases in their protein levels in insulin resistant islets.

Insulin processing and exocytosis

In contrast to the marked increase in the machinery of protein biosynthesis, folding and transport, a substantial down-regulation of proteins involved in hormone processing PCSK1 and PCSK2[24] was observed in both models of insulin resistance models although more pronounced in HFD islets. Consistent with the latter observation, glucagon and somatostatin were down-regulated in islets derived from HFD and ob/ob mice. Finally, several proteins implicated in vesicular transport and exocytosis of hormone granules such as VAMP2[25], RAB5C , RAB7A, STYL4 and UCN3[26] were also down-regulated **(Table 1 and Supplemental Table 2)**.

Apoptosis and proliferation

Increased β-cell mass in rodents is a major structural compensation to insulin resistance that involves both an enhancement of cell proliferation and inhibition of cell death[7a, 27]. However, the downstream intracellular targets mediating these effects have not been fully identified. Using IPA analysis, we focused on identifying factors that are relevant to cell

survival and proliferation. We observed that several anti-apoptotic factors, including TXNDC5, TPT1, HSPA5, HSP90B1, TXM1 and ANXA4 were found to be commonly up-regulated while pro-apoptotic factors such as HSPDA1, HSPA9 and RTN4 are down-regulated in islets derived from either HFD or ob/ob models. On the other hand, and in agreement with the compensatory role of cell proliferation in insulin resistant islets, we found that several proliferation-linked proteins were up-regulated in insulin resistant islets including, isoform 1 of protein SEL-1 homolog1 (Sel1I), previously reported for its mitogenic action on β-cells[28]. We also found Nucleobindin-2 (Nucb2)[29], CDK5 regulatory subunit associated protein 3 (CDK5rap3)[30] and Peroxiredoxin 6 (PRDX6)[31] up-regulated in both HFD and ob/ob suggesting their potential in promoting proliferation of insulin resistant islet cells. Moreover, a notable increase was observed in SEPT5 and SEPT7, members of septin family known to control cell division[32] and Nucleophosmin-1 (NPM), a protein described to promote c-Myc-mediated proliferation[33] **(Table 1)**.

Western blot validation of selected protein targets

Considering that most islet proteome changes occur in both HFD and ob/ob models and in both small and large islets, we focused on the ob/ob mouse model to validate key regulated proteins in various biological processes in insulin resistant states. To this end, we isolated islets from five month-old wild type or age matched ob/ob mice and subjected the extracted proteins to Western blotting and quantification (**Fig 4A and 4B**). Consistent with proteomics data, we observed that expression of CDK5rap3, Sel1I and Nucb2, proteins reported to be linked to proliferation, are increased in ob/ob islets as compared to the control group. Moreover, expression of PCSK1 and PCSK2, involved in hormone biosynthesis were down-regulated, in insulin resistant ob/ob islets, in Western blot experiments, similar to the proteomics data. Additionally, a decrease in expression of SYTL4, UCN3 and VAMP2 exocytosis-regulating proteins was validated in ob/ob islets. A subset of proteins involved in mitochondrial function and oxidative phosphorylation, including COX4I1 and COX7A2 were also decreased consistent with the proteomics data. Finally, we confirmed by Western blot approach that two metabolic enzymes, MAOB and SDHB, are down-regulated in ob/ob islets as compared to controls **(Fig. 4)**.

Discussion

This study was designed to interrogate changes occurring in the islet proteome of insulin resistant models prior to the development of overt diabetes. We used a genetic leptin deficient (ob/ob) and dietary-induced insulin resistance (HFD) mouse models to elucidate whether compensatory islet-cell response to insulin resistance is mediated by morphological or functional adaptation. Furthermore, we used small and large islets to uncover potentially distinct signatures in the adaptation of islet subpopulations to insulin resistance.

Surprisingly, most of the changes noted in our proteomic study were common between HFD and ob/ob and only a subset of proteins appeared to be differentially regulated. One possibility for the observed similarities in the proteome phenotypes is that HFD mice develop leptin resistance in insulin resistant settings[34], and become blind to the leptin as naturally occurring in ob/ob mice. The alterations in proteins specific to HFD model were

mainly involved in protein processing, translation, regulation of secretion and exocytosis; while those specific to the ob/ob were associated to processes such as sugar metabolism, oxidation and reduction processes, chromatin and nucleosome assembly (**Supplemental Table 4 and 5**). These observations are intriguing and require further investigation.

A unique feature of our approach is the comparison between small and large islets in the ob/ob model. Although several previous studies have suggested functional differences in islet subpopulations in different species[35] that may occur in normal states, we observed that in the case of insulin resistance nearly all the changes observed in proteins involved in hormone processing and secretory pathways, energy metabolism, mitochondrial function, protein synthesis and ER stress were affected to a similar extent in both small and large islets in the ob/ob model. One interpretation of these data is that impairment of β-cell function likely precedes the proliferation, and that alterations in proliferation are unlikely to promote β-cell dysfunction. The cause of β-cell secretory dysfunction is likely due to a combination of the deleterious effects of hyperglycemia and hyperlipidemia and/or pro-inflammatory cytokines[36]. Consistently, several studies have reported alterations in function following chronic *in vitro* treatment of β-cells with glucose, FFA or cytokines[37].

In the global context, our data suggest that insulin resistant conditions limit islet-cell energy metabolism and shut down the ability of cells to produce sufficient amounts of key metabolic intermediates. This is illustrated by a decline in the abundances of proteins controlling various metabolic pathways, including glycolysis, Krebs cycle, amino acid metabolism, and mitochondrial oxidative phosphorylation. Moreover, several mitochondrial proteins were down-regulated suggesting mitochondrial dysfunction in islet-cells derived from obese insulin resistant animals. The reduction of anti-oxidant proteins such as PRDX3 and SOD2 is suggestive of oxidative stress consistent with the protective role of these proteins is islet-cells, particularly in β-cells where the levels of these molecules are low, to mitigate oxidative stress[38]. However, islet cells showed increased PRDX6, another antioxidant member of the Peroxiredoxin family known (as for PRDX3) to be down-regulated by inflammation[38b,39]. It is possible that PRDX6 is upregulated by other stimulatory molecules to restore a mitochondrial redox state and protect the mice from developing overt diabetes[40].

Several components of protein synthetic machinery, including proteins facilitating rRNA/tRNA biogenesis, initiation of translation factors, and regulators of protein transport and cell membrane organization were found to be activated and potentially participating in enhancing the biosynthetic capacity of insulin and other hormones. Consistent with the latter possibility, ER overloading by newly synthesized proteins increased protein expression of ER stress-induced chaperones in an attempt to limit ER stress.

It is of interest that several proteins involved in oxidative metabolism that were decreased in islets from HFD or ob/ob were also reported to be down-regulated in islets derived from 10-week old diabetic MKR mice[9b]. Commonly decreased proteins in HFD, ob/ob and MKR models include PFKL, DLD, IDH1, COX5A, GPD2 and MAOB. The alterations in expression of proteins in islets from models of “pre-diabetes” (e.g. HFD and ob/ob) that is also detectable in islets from diabetic MKR mice suggests their causal role in defective β-

cell metabolism. We also observed that UCN3, a marker of β-cell maturation[26, 41], was decreased in HFD, ob/ob and MKR models and is consistent with its previously reported role in impaired GSIS[42].

A previous study used differential islet proteome analyses of Zucker Fatty (ZF) and Zucker Diabetic Fatty (ZDF) rats to reveal changes in the expression of proteins involved in insulin secretion, mitochondrial dysfunction, extracellular matrix proteins, or microvascular ischemia[9a]. Similar to the HFD or ob/ob models, islets derived from obese ZF rats, also exhibited increased protein levels of ATP5l, COPB, NME2, or PGM2, and decreased levels of GCG, GOT2, IDH2, or PCSK1[9a]. This cross-species observation provides a valuable set of proteins associated with the transition from insulin resistance to type 2 diabetes in the context of islets. It is important, however, to note that some changes in the expression of secretory proteins such as SCG2, RAB5C and RAB7A, were commonly found in ZF or ZDF rats but not in HFD or ob/ob[9a], suggesting that the regulation of expression of proteins involved in hormone secretion is not conserved in the mouse and rat.

As expected several proteins involved in cell proliferation were increased in insulin resistant islets[43]. We observed that the ER membrane protein Suppressor of lin-12-like protein 1 (Sel1l) is upregulated in insulin resistant islets. Sel1l is the ortholog of C. elegans gene sel-1, which is a negative regulator of LIN-12/NOTCH receptor proteins, previously implicated in β-cell growth and function. Heterozygote Sel1l (+/-) mice exhibit decreased β-cell mass due to reduced β-cell proliferation, and are predisposed to hyperglycemia upon a high-fat diet[28, 44]. Our observation of a substantial increase in the amounts of CDK5rap3 in the hyperplastic islets is interesting in the context of recent findings that over-expression of CDK5rap3 is positively correlated with cell proliferation of hepatocytes[30] and lung cells[45] both of which along with pancreatic cells share a common endodermal origin. The increased expression of Nucb2, a protein reported to be expressed in human and rodent islet β-cells and shown to be decreased in islets derived from type 2 diabetic patients[29b] is relevant because Nucb2 was reported to enhance cell proliferation via EGF-stimulated MAPK kinase/Erk signaling[46]. The decreased islet levels of Nucb2 are decreased in patients with type 2 diabetes[29b] warrants studies to explore a role for this protein to enhance pancreatic β-cell proliferation. The increased amounts of EIF5A in insulin resistant compared to control islets in our studies suggests that this protein which was initially described as an “initiator” of translation may be also relevant in proliferation. For example, EGF stimulates proliferation of corneal epithelial cells through PI3K-Akt-EIF5A signaling pathway[47] and knockdown of EIF5A by small interfering RNAs abolishes the stimulatory action of EGF on cell proliferation[47].

In summary, during the progression of insulin resistance, the secretory capacity of islet-cells tend to decline upon down-regulation of key proteins controlling multiple steps of insulin synthesis and release, including energy metabolism, mitochondrial function and hormone biosynthesis/exocytosis. Increased cell survival and proliferation of the endocrine pancreas appear to be central features that enable islet cells to meet chronic elevated demands of insulin and potentially other hormones **(Fig. 5)**. The candidates identified and validated in this report could be considered for strategies aimed at developing new anti-diabetic therapeutics to enhance β-cell mass in efforts to counter diabetes.

Supplementary Material

Refer to Web version on PubMed Central for supplementary material.

ACKNOWLEDGMENTS

This work was supported by NIH grants R01 DK074795, R01 DK067536, R01 DK103215, K99 DK090210, Société Francophone du Diabète (to A.E.), Association Française des Diabétiques (to A.E.), American Diabetes Association (to A.E.) and JDRF advanced postdoctoral fellowship (to A.E.). Samples were analyzed using capabilities developed under the support of the NIH Biomedical Technology Research Resource for integrative biology (P41 GM103493). Significant portions of the work were performed in the Environmental Molecular Science Laboratory, a DOE/BER national scientific user facility at Pacific Northwest National Laboratory (PNNL) in Richland, Washington. PNNL is operated for the DOE by Battelle under contract DE-AC05-76RLO-1830.

REFERENCES

1. a Assmann A, Hinault C, Kulkarni RN. Growth factor control of pancreatic islet regeneration and function. Pediatr Diabetes. 2009; 10(1):14–32. [PubMed: 18828795] b Weir GC, Bonner-Weir S. Five stages of evolving beta-cell dysfunction during progression to diabetes. Diabetes. 2004; 53(Suppl 3):S16–21. [PubMed: 15561905]
2. Wild S, Roglic G, Green A, Sicree R, King H. Global prevalence of diabetes: estimates for the year 2000 and projections for 2030. Diabetes Care. 2004; 27(5):1047–53. [PubMed: 15111519]
3. Doria A, Patti ME, Kahn CR. The emerging genetic architecture of type 2 diabetes. Cell Metab. 2008; 8(3):186–200. [PubMed: 18762020]
4. a Shapiro AM, Ricordi C, Hering BJ, Auchincloss H, Lindblad R, Robertson RP, Secchi A, Brendel MD, Berney T, Brennan DC, Cagliero E, Alejandro R, Ryan EA, DiMercurio B, Morel P, Polonsky KS, Reems JA, Bretzel RG, Bertuzzi F, Froud T, Kandaswamy R, Sutherland DE, Eisenbarth G, Segal M, Preiksaitis J, Korbutt GS, Barton FB, Viviano L, Seyfert-Margolis V, Bluestone J, Lakey JR. International trial of the Edmonton protocol for islet transplantation. The New England journal of medicine. 2006; 355(13):1318–30. [PubMed: 17005949] b Thompson DM, Meloche M, Ao Z, Paty B, Keown P, Shapiro RJ, Ho S, Worsley D, Fung M, Meneilly G, Begg I, Al Mehthel M, Kondi J, Harris C, Fensom B, Kozak SE, Tong SO, Trinh M, Warnock GL. Reduced progression of diabetic microvascular complications with islet cell transplantation compared with intensive medical therapy. Transplantation. 2011; 91(3):373–8. [PubMed: 21258272]
5. a Buteau J, Shlien A, Foisy S, Accili D. Metabolic diapause in pancreatic beta-cells expressing a gain-of-function mutant of the forkhead protein Foxo1. J Biol Chem. 2007; 282(1):287–93. [PubMed: 17107961] b de Koning EJ, Bonner-Weir S, Rabelink TJ. Preservation of beta-cell function by targeting beta-cell mass. Trends Pharmacol Sci. 2008; 29(4):218–27. [PubMed: 18359095] c Hansen JB, Arkhammar PO, Bodvarsdottir TB, Wahl P. Inhibition of insulin secretion as a new drug target in the treatment of metabolic disorders. Curr Med Chem. 2004; 11(12):1595–615. [PubMed: 15180566] d Talchai C, Xuan S, Lin HV, Sussel L, Accili D. Pancreatic beta cell dedifferentiation as a mechanism of diabetic beta cell failure. Cell. 2012; 150(6):1223–34. [PubMed: 22980982]
6. a Jones CN, Pei D, Staris P, Polonsky KS, Chen YD, Reaven GM. Alterations in the glucose-stimulated insulin secretory dose-response curve and in insulin clearance in nondiabetic insulin-resistant individuals. J Clin Endocrinol Metab. 1997; 82(6):1834–8. [PubMed: 9177392] b Parsons JA, Brelje TC, Sorenson RL. Adaptation of islets of Langerhans to pregnancy: increased islet cell proliferation and insulin secretion correlates with the onset of placental lactogen secretion. Endocrinology. 1992; 130(3):1459–66. [PubMed: 1537300] c Polonsky KS, Given BD, Hirsch L, Shapiro ET, Tillil H, Beebe C, Galloway JA, Frank BH, Karrison T, Van Cauter E. Quantitative study of insulin secretion and clearance in normal and obese subjects. J Clin Invest. 1988; 81(2): 435–41. [PubMed: 3276729]
7. a Bruning JC, Winnay J, Bonner-Weir S, Taylor SI, Accili D, Kahn CR. Development of a novel polygenic model of NIDDM in mice heterozygous for IR and IRS-1 null alleles. Cell. 1997; 88(4): 561–72. [PubMed: 9038347] b Michael MD, Kulkarni RN, Postic C, Previs SF, Shulman GI,

Magnuson MA, Kahn CR. Loss of insulin signaling in hepatocytes leads to severe insulin resistance and progressive hepatic dysfunction. Mol Cell. 2000; 6(1):87–97. [PubMed: 10949030]

8. a Chen C, Hosokawa H, Bumbalo LM, Leahy JL. Mechanism of compensatory hyperinsulinemia in normoglycemic insulin-resistant spontaneously hypertensive rats. Augmented enzymatic activity of glucokinase in beta-cells. J Clin Invest. 1994; 94(1):399–404. [PubMed: 8040280] b Liu YQ, Jetton TL, Leahy JL. beta-Cell adaptation to insulin resistance. Increased pyruvate carboxylase and malate-pyruvate shuttle activity in islets of nondiabetic Zucker fatty rats. J Biol Chem. 2002; 277(42):39163–8. [PubMed: 12147706]
9. a Han D, Moon S, Kim H, Choi SE, Lee SJ, Park KS, Jun H, Kang Y, Kim Y. Detection of differential proteomes associated with the development of type 2 diabetes in the Zucker rat model using the iTRAQ technique. J Proteome Res. 2011; 10(2):564–77. [PubMed: 21117707] b Lu H, Koshkin V, Allister EM, Gyulkhandanyan AV, Wheeler MB. Molecular and metabolic evidence for mitochondrial defects associated with beta-cell dysfunction in a mouse model of type 2 diabetes. Diabetes. 2010; 59(2):448–59. [PubMed: 19903739] c Lu H, Yang Y, Allister EM, Wijesekara N, Wheeler MB. The identification of potential factors associated with the development of type 2 diabetes: a quantitative proteomics approach. Mol Cell Proteomics. 2008; 7(8):1434–51. [PubMed: 18448419] d Qiu L, List EO, Kopchick JJ. Differentially expressed proteins in the pancreas of diet-induced diabetic mice. Mol Cell Proteomics. 2005; 4(9):1311–8. [PubMed: 15961380]
10. Perez-Vazquez V, Guzman-Flores JM, Mares-Alvarez D, Hernandez-Ortiz M, Macias-Cervantes MH, Ramirez-Emiliano J, Encarnacion-Guevara S. Differential proteomic analysis of the pancreas of diabetic db/db mice reveals the proteins involved in the development of complications of diabetes mellitus. International journal of molecular sciences. 2014; 15(6):9579–93. [PubMed: 24886809]
11. Kulkarni RN, Bruning JC, Winnay JN, Postic C, Magnuson MA, Kahn CR. Tissue-specific knockout of the insulin receptor in pancreatic beta cells creates an insulin secretory defect similar to that in type 2 diabetes. Cell. 1999; 96(3):329–39. [PubMed: 10025399]
12. Kulkarni RN, Winnay JN, Daniels M, Bruning JC, Flier SN, Hanahan D, Kahn CR. Altered function of insulin receptor substrate-1-deficient mouse islets and cultured beta-cell lines. J Clin Invest. 1999; 104(12):R69–75. [PubMed: 10606633]
13. Wang H, Qian WJ, Mottaz HM, Clauss TR, Anderson DJ, Moore RJ, Camp DG 2nd, Khan AH, Sforza DM, Pallavicini M, Smith DJ, Smith RD. Development and evaluation of a micro- and nanoscale proteomic sample preparation method. J Proteome Res. 2005; 4(6):2397–403. [PubMed: 16335993]
14. Zhou JY, Schepmoes AA, Zhang X, Moore RJ, Monroe ME, Lee JH, Camp DG, Smith RD, Qian WJ. Improved LC-MS/MS spectral counting statistics by recovering low-scoring spectra matched to confidently identified peptide sequences. J Proteome Res. 2010; 9(11):5698–704. [PubMed: 20812748]
15. Kim S, Gupta N, Pevzner PA. Spectral probabilities and generating functions of tandem mass spectra: a strike against decoy databases. J Proteome Res. 2008; 7(8):3354–63. [PubMed: 18597511]
16. Nesvizhskii AI, Keller A, Kolker E, Aebersold R. A statistical model for identifying proteins by tandem mass spectrometry. Anal Chem. 2003; 75(17):4646–58. [PubMed: 14632076]
17. Elias JE, Gygi SP. Target-decoy search strategy for increased confidence in large-scale protein identifications by mass spectrometry. Nat Methods. 2007; 4(3):207–14. [PubMed: 17327847]
18. a Qian WJ, Liu T, Petyuk VA, Gritsenko MA, Petritis BO, Polpitiya AD, Kaushal A, Xiao W, Finnerty CC, Jeschke MG, Jaitly N, Monroe ME, Moore RJ, Moldawer LL, Davis RW, Tompkins RG, Herndon DN, Camp DG, Smith RD. Large-scale multiplexed quantitative discovery proteomics enabled by the use of an (18)O-labeled “universal” reference sample. J Proteome Res. 2009; 8(1):290–9. [PubMed: 19053531] b Zimmer JS, Monroe ME, Qian WJ, Smith RD. Advances in proteomics data analysis and display using an accurate mass and time tag approach. Mass Spectrom Rev. 2006; 25(3):450–82. [PubMed: 16429408]
19. Monroe ME, Tolic N, Jaitly N, Shaw JL, Adkins JN, Smith RD. VIPER: an advanced software package to support high-throughput LC-MS peptide identification. Bioinformatics. 2007; 23(15): 2021–3. [PubMed: 17545182]

20. Polpitiya AD, Qian WJ, Jaitly N, Petyuk VA, Adkins JN, Camp DG, Anderson GA, Smith RD. DAnTE: a statistical tool for quantitative analysis of -omics data. Bioinformatics. 2008; 24(13): 1556–1558. [PubMed: 18453552]

21. Petritis BO, Qian WJ, Camp DG 2nd, Smith RD. A simple procedure for effective quenching of trypsin activity and prevention of 18O-labeling back-exchange. J Proteome Res. 2009; 8(5):2157–63. [PubMed: 19222237]

22. Kim JS, Fillmore TL, Liu T, Robinson E, Hossain M, Champion BL, Moore RJ, Camp DG 2nd, Smith RD, Qian WJ. 18O-labeled proteome reference as global internal standards for targeted quantification by selected reaction monitoring-mass spectrometry. Mol Cell Proteomics. 2011; 10(12):M110 007302.

23. a Shi T, Fillmore TL, Sun X, Zhao R, Schepmoes AA, Hossain M, Xie F, Wu S, Kim JS, Jones N, Moore RJ, Pasa-Tolic L, Kagan J, Rodland KD, Liu T, Tang K, Camp DG 2nd, Smith RD, Qian WJ. Antibody-free, targeted mass-spectrometric approach for quantification of proteins at low picogram per milliliter levels in human plasma/serum. Proc Natl Acad Sci U S A. 2012; 109(38): 15395–400. [PubMed: 22949669] b Shi T, Qian WJ. Antibody-free PRISM-SRM for multiplexed protein quantification: is this the new competition for immunoassays in bioanalysis? Bioanalysis. 2013; 5(3):267–9. [PubMed: 23394691]

24. Neerman-Arbez M, Cirulli V, Halban PA. Levels of the conversion endoproteases PC1 (PC3) and PC2 distinguish between insulin-producing pancreatic islet beta cells and non-beta cells. The Biochemical journal. 1994; 300(Pt 1):57–61. [PubMed: 8198551]

25. Regazzi R, Sadoul K, Meda P, Kelly RB, Halban PA, Wollheim CB. Mutational analysis of VAMP domains implicated in Ca2+-induced insulin exocytosis. The EMBO journal. 1996; 15(24): 6951–9. [PubMed: 9003771]

26. Blum B, Hrvatin SS, Schuetz C, Bonal C, Rezania A, Melton DA. Functional beta-cell maturation is marked by an increased glucose threshold and by expression of urocortin 3. Nature biotechnology. 2012; 30(3):261–4.

27. a Chen Z, Morris DL, Jiang L, Liu Y, Rui L. SH2B1 in beta cells regulates glucose metabolism by promoting beta cell survival and islet expansion. Diabetes. 2013b Jetton TL, Lausier J, LaRock K, Trotman WE, Larmie B, Habibovic A, Peshavaria M, Leahy JL. Mechanisms of compensatory beta-cell growth in insulin-resistant rats: roles of Akt kinase. Diabetes. 2005; 54(8):2294–304. [PubMed: 16046294] c Okada T, Liew CW, Hu J, Hinault C, Michael MD, Krtzfeldt J, Yin C, Holzenberger M, Stoffel M, Kulkarni RN. Insulin receptors in beta-cells are critical for islet compensatory growth response to insulin resistance. Proc Natl Acad Sci U S A. 2007; 104(21): 8977–82. [PubMed: 17416680]

28. Francisco AB, Singh R, Sha H, Yan X, Qi L, Lei X, Long Q. Haploid insufficiency of suppressor enhancer Lin12 1-like (SEL1L) protein predisposes mice to high fat diet-induced hyperglycemia. The Journal of biological chemistry. 2011; 286(25):22275–82. [PubMed: 21536682]

29. a Oh IS, Shimizu H, Satoh T, Okada S, Adachi S, Inoue K, Eguchi H, Yamamoto M, Imaki T, Hashimoto K, Tsuchiya T, Monden T, Horiguchi K, Yamada M, Mori M. Identification of nesfatin-1 as a satiety molecule in the hypothalamus. Nature. 2006; 443(7112):709–12. [PubMed: 17036007] b Riva M, Nitert MD, Voss U, Sathanoori R, Lindqvist A, Ling C, Wierup N. Nesfatin-1 stimulates glucagon and insulin secretion and beta cell NUCB2 is reduced in human type 2 diabetic subjects. Cell and tissue research. 2011; 346(3):393–405. [PubMed: 22108805]

30. Mak GW, Chan MM, Leong VY, Lee JM, Yau TO, Ng IO, Ching YP. Overexpression of a novel activator of PAK4, the CDK5 kinase-associated protein CDK5RAP3, promotes hepatocellular carcinoma metastasis. Cancer research. 2011; 71(8):2949–58. [PubMed: 21385901]

31. Chang XZ, Li DQ, Hou YF, Wu J, Lu JS, Di GH, Jin W, Ou ZL, Shen ZZ, Shao ZM. Identification of the functional role of peroxiredoxin 6 in the progression of breast cancer. Breast cancer research : BCR. 2007; 9(6):R76. [PubMed: 17980029]

32. Mostowy S, Cossart P. Septins: the fourth component of the cytoskeleton. Nature reviews. Molecular cell biology. 2012; 13(3):183–94. [PubMed: 22314400]

33. Li Z, Hann SR. Nucleophosmin is essential for c-Myc nucleolar localization and c-Myc-mediated rDNA transcription. Oncogene. 2012

34. Enriori PJ, Evans AE, Sinnayah P, Jobst EE, Tonelli-Lemos L, Billes SK, Glavas MM, Grayson BE, Perello M, Nillni EA, Grove KL, Cowley MA. Diet-induced obesity causes severe but

reversible leptin resistance in arcuate melanocortin neurons. Cell Metab. 2007; 5(3):181–94. [PubMed: 17339026]

35. a Bonner-Weir S, Like AA. A dual population of islets of Langerhans in bovine pancreas. Cell and tissue research. 1980; 206(1):157–70. [PubMed: 6986987] b Farhat B, Almelkar A, Ramachandran K, Williams SJ, Huang HH, Zamierowksi D, Novikova L, Stehno-Bittel L. Small human islets comprised of more beta-cells with higher insulin content than large islets. Islets. 2013; 5(2):87–94. [PubMed: 23648896] c Huang HH, Novikova L, Williams SJ, Smirnova IV, Stehno-Bittel L. Low insulin content of large islet population is present in situ and in isolated islets. Islets. 2011; 3(1):6–13. [PubMed: 21325888]
36. Robertson RP. Beta-cell deterioration during diabetes: what's in the gun? Trends in endocrinology and metabolism: TEM. 2009; 20(8):388–93. [PubMed: 19748794]
37. a Chen X, Cui Z, Wei S, Hou J, Xie Z, Peng X, Li J, Cai T, Hang H, Yang F. Chronic high glucose induced INS-1beta cell mitochondrial dysfunction: a comparative mitochondrial proteome with SILAC. Proteomics. 2013; 13(20):3030–9. [PubMed: 23956156] b D'Hertog W, Overbergh L, Lage K, Ferreira GB, Maris M, Gysemans C, Flamez D, Cardozo AK, Van den Bergh G, Schoofs L, Arckens L, Moreau Y, Hansen DA, Eizirik DL, Waelkens E, Mathieu C. Proteomics analysis of cytokine-induced dysfunction and death in insulin-producing INS-1E cells: new insights into the pathways involved. Mol Cell Proteomics. 2007; 6(12):2180–99. [PubMed: 17921177] c Maris M, Ferreira GB, D'Hertog W, Cnop M, Waelkens E, Overbergh L, Mathieu C. High glucose induces dysfunction in insulin secretory cells by different pathways: a proteomic approach. J Proteome Res. 2010; 9(12):6274–87. [PubMed: 20942503] d Maris M, Robert S, Waelkens E, Derua R, Hernangomez MH, D'Hertog W, Cnop M, Mathieu C, Overbergh L. Role of the saturated nonesterified fatty acid palmitate in beta cell dysfunction. J Proteome Res. 2013; 12(1):347–62. [PubMed: 23170928]
38. a Kang L, Dai C, Lustig ME, Bonner JS, Mayes WH, Mokshagundam S, James FD, Thompson CS, Lin CT, Perry CG, Anderson EJ, Neufer PD, Wasserman DH, Powers AC. Heterozygous SOD2 deletion impairs glucose-stimulated insulin secretion, but not insulin action, in high-fat-fed mice. Diabetes. 2014; 63(11):3699–710. [PubMed: 24947366] b Wolf G, Aumann N, Michalska M, Bast A, Sonnemann J, Beck JF, Lendeckel U, Newsholme P, Walther R. Peroxiredoxin III protects pancreatic ss cells from apoptosis. The Journal of endocrinology. 2010; 207(2):163–75. [PubMed: 20807727]
39. Paula FM, Ferreira SM, Boschero AC, Souza KL. Modulation of the peroxiredoxin system by cytokines in insulin-producing RINm5F cells: down-regulation of PRDX6 increases susceptibility of beta cells to oxidative stress. Molecular and cellular endocrinology. 2013; 374(1-2):56–64. [PubMed: 23623867]
40. Pacifici F, Arriga R, Sorice GP, Capuani B, Scioli MG, Pastore D, Donadel G, Bellia A, Caratelli S, Coppola A, Ferrelli F, Federici M, Sconocchia G, Tesauro M, Sbraccia P, Della-Morte D, Giaccari A, Orlandi A, Lauro D. Peroxiredoxin 6, a novel player in the pathogenesis of diabetes. Diabetes. 2014; 63(10):3210–20. [PubMed: 24947358]
41. van der Meulen T, Xie R, Kelly OG, Vale WW, Sander M, Huising MO. Urocortin 3 marks mature human primary and embryonic stem cell-derived pancreatic alpha and beta cells. PloS one. 2012; 7(12):e52181. [PubMed: 23251699]
42. Li C, Chen P, Vaughan J, Lee KF, Vale W. Urocortin 3 regulates glucose-stimulated insulin secretion and energy homeostasis. Proc Natl Acad Sci U S A. 2007; 104(10):4206–11. [PubMed: 17360501]
43. a Bock T, Pakkenberg B, Buschard K. Increased islet volume but unchanged islet number in ob/ob mice. Diabetes. 2003; 52(7):1716–22. [PubMed: 12829638] b Hull RL, Kodama K, Utzschneider KM, Carr DB, Prigeon RL, Kahn SE. Dietary-fat-induced obesity in mice results in beta cell hyperplasia but not increased insulin release: evidence for specificity of impaired beta cell adaptation. Diabetologia. 2005; 48(7):1350–8. [PubMed: 15937671] c Stamateris RE, Sharma RB, Hollern DA, Alonso LC. Adaptive beta-cell proliferation increases early in high-fat feeding in mice, concurrent with metabolic changes, with induction of islet cyclin D2 expression. Am J Physiol Endocrinol Metab. 2013; 305(1):E149–59. [PubMed: 23673159]
44. Sun S, Shi G, Han X, Francisco AB, Ji Y, Mendonca N, Liu X, Locasale JW, Simpson KW, Duhamel GE, Kersten S, Yates JR 3rd, Long Q, Qi L. Sel1L is indispensable for mammalian

endoplasmic reticulum-associated degradation, endoplasmic reticulum homeostasis, and survival. Proc Natl Acad Sci U S A. 2014; 111(5):E582–91. [PubMed: 24453213]

45. Stav D, Bar I, Sandbank J. Usefulness of CDK5RAP3, CCNB2, and RAGE genes for the diagnosis of lung adenocarcinoma. The International journal of biological markers. 2007; 22(2):108–13. [PubMed: 17549666]
46. Tagaya Y, Miura A, Okada S, Ohshima K, Mori M. Nucleobindin-2 is a positive modulator of EGF-dependent signals leading to enhancement of cell growth and suppression of adipocyte differentiation. Endocrinology. 2012; 153(7):3308–19. [PubMed: 22514047]
47. Ding L, Gao LJ, Gu PQ, Guo SY, Cai YQ, Zhou XT. The role of eIF5A in epidermal growth factor-induced proliferation of corneal epithelial cell association with PI3-k/Akt activation. Molecular vision. 2011; 17:16–22. [PubMed: 21224998]

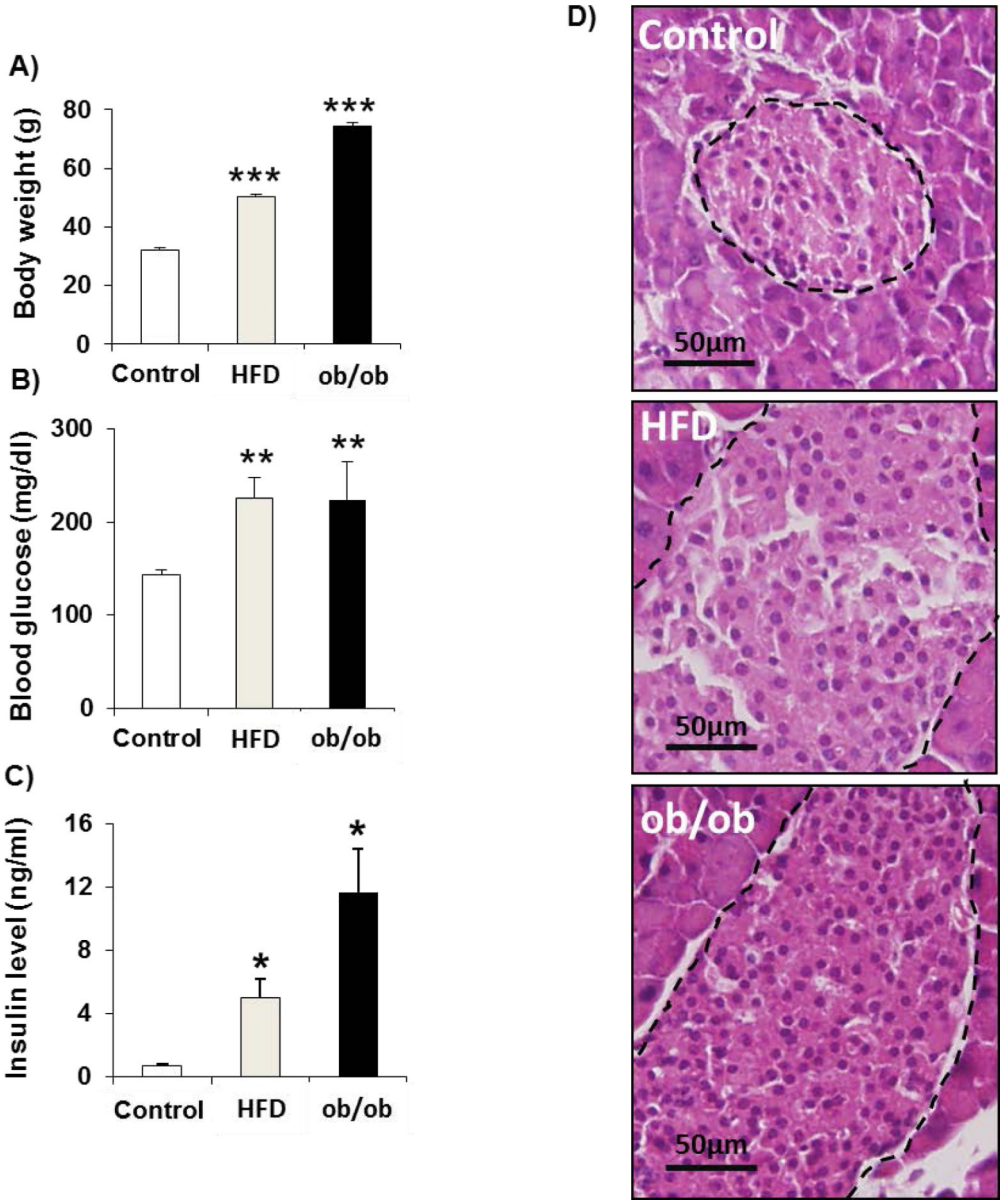

Fig.1. Characteristics of HFD and ob/ob mice

A. body weights. **B.** random fed blood glucose. **C.** random fed insulin levels. **D.** Hematoxylin and Eosin staining of pancreatic sections. Data represent mean ± SEM, * $p < 0.05$ based on Student's t-test, (n= 5-6 per group). HFD: high fat diet mice, ob/ob: leptin-deficient mice. The black dashed lines in Figure 1D indicate the islet contour, which shows the larger sizes of islets in HFD and ob/ob compared to the Control.

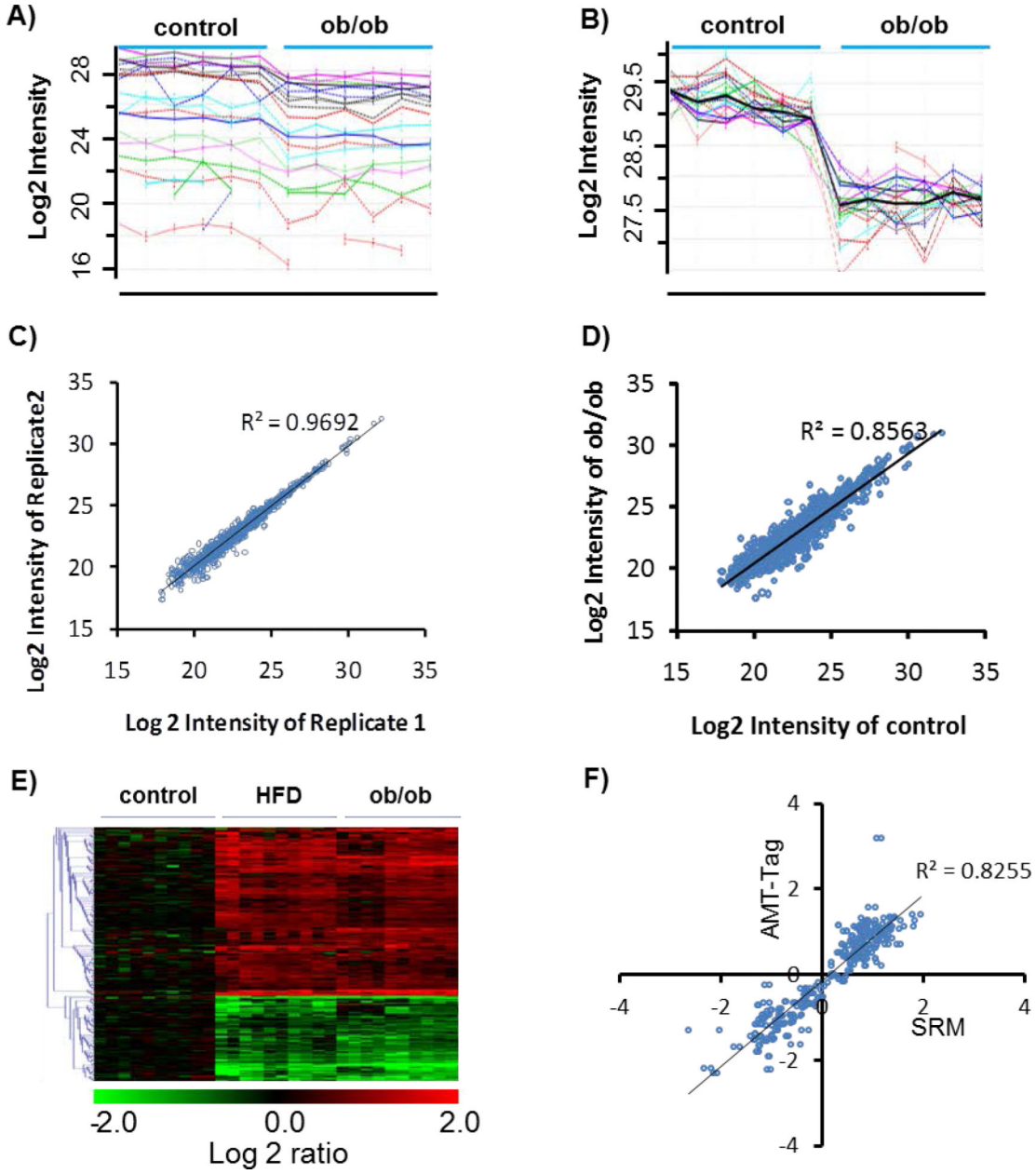

Fig.2. Quantitative analysis strategy for the islet proteome

A, Raw peptide intensity profile data (log2 transformed) of all peptides identified from glucagon. Each line profile represents a peptide from glucagon. 3 Control and 3 ob/ob (small islets) samples are presented with each sample analyzed in duplicated. **B**, Rescaled peptide intensity profile data. Dark line represents the protein abundance profile by averaging the intensity of all peptides after the rescaling process. **C**, Reproducibility of protein abundance quantification between technical replicates. **D**, Comparison of protein abundances between control and ob/ob (small islets). **E**, Heatmap of all proteins with significant changes. Each condition has 5 biological replicates, each replicate has duplicated runs. Values are normalized to the average of control. Only data from small islets from ob/ob mice were presented here. **F**, Validation of label-free quantitative data for selected proteins by selected

reaction monitoring (SRM). Values are the log2 ratios to control. Each data represents one protein in one condition summarized from 5 biological replicates. Data points from both HFD and ob/ob mice were included here.

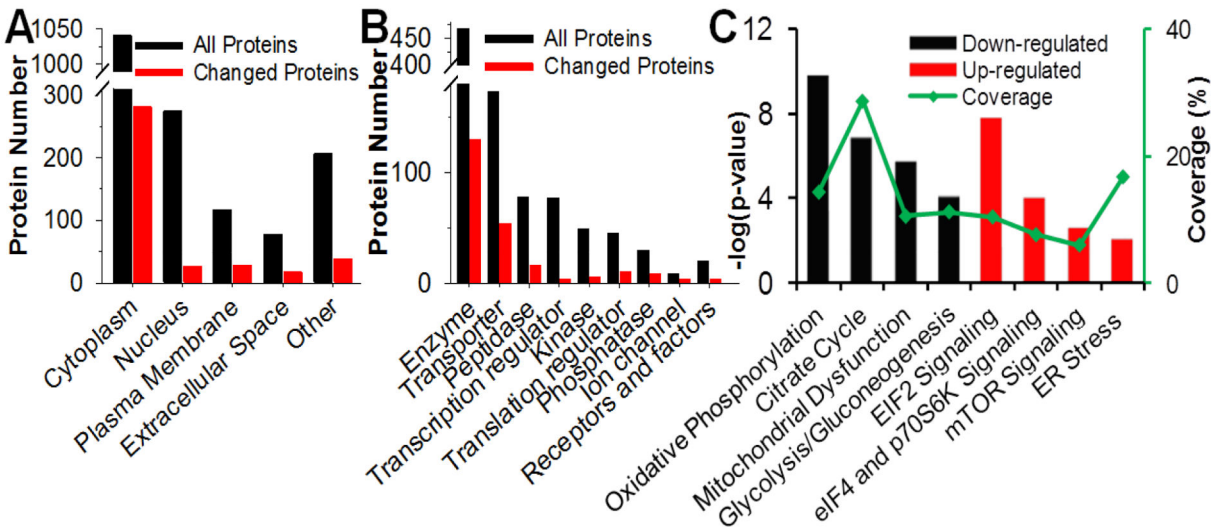

Fig.3. Functional analysis of quantified proteins

All quantified proteins were submitted to Ingenuity Pathway Analysis (IPA) to evaluate the biological function. Proteins were grouped based on subcellular location (**A**) or molecular functions (**B**). The major significantly down-regulated (black) and up-regulated (red) canonical pathways are presented in **C**. Green line in C is the proteome coverage of each canonical pathway.

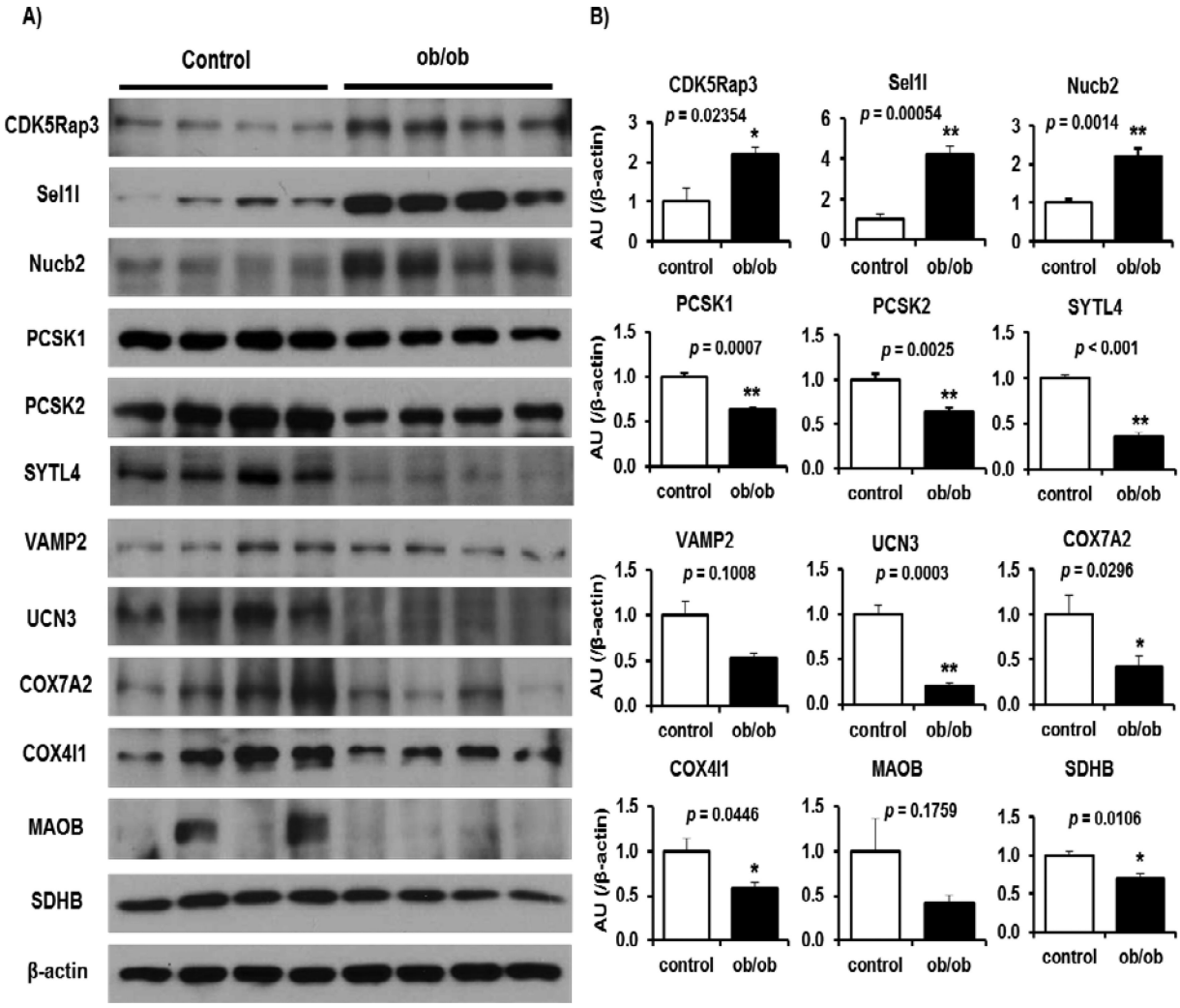

Fig.4. Validation of key regulated proteins in ob/ob mice

A, The total cell extracts from the islets were subjected to immunoblotting as indicated. **B**, Intensity of the signals quantified by densitometry (image J) (n = 4-6). Data are normalized to actin. Individual *p* values from Student's t-test for each quantification are indicated in Figure 4B.

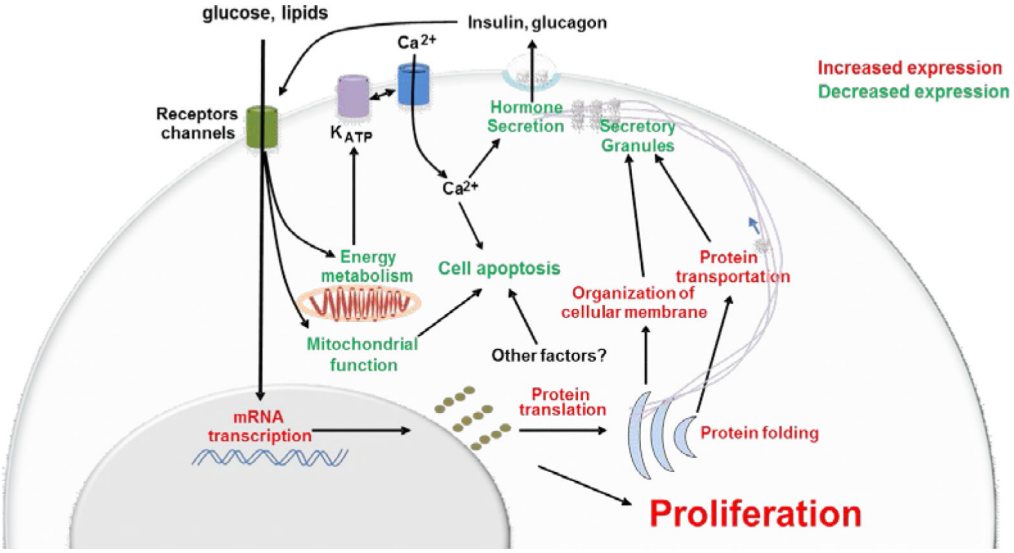

Fig.5. Islet compensatory response in insulin resistance

Schematic illustrating major regulated pathways in insulin resistant islets. Down- and upregulated biological processes are shown in green and red, respectively.

Table 1

List of selected altered proteins involved in different functional categories.

Gene symbol	Protein name	Log2 ratio ± SEM		
		HFD vs. Control	ob/ob (S) vs. Control	ob/ob (L) vs. Control
Glycolysis/Gluconeogenesis				
AKR1A1	Alcohol dehydrogenase [NADP+]	0.17±0.08	0.47±0.11	0.64±0.04
LDHA	L-lactate dehydrogenase A chain	0.12±0.26	1.70±0.15	2.10±0.13
PGM2	Phosphoglucomutase-2	0.90±0.06	0.77±0.21	1.32±0.05
ALDH3A2	Fatty aldehyde dehydrogenase	−0.03±0.11	−0.28±0.12	−0.6±0.06
ALDOA	Fructose-bisphosphate aldolase A	−0.41±0.07	−0.65±0.08	−0.45±0.03
ENO2	Gamma-enolase	−0.45±0.10	−1.01±0.10	−0.82±0.16
PFKL	6-phosphofructokinase, liver type	−0.65±0.09	−0.72±0.06	−0.73±0.06
Citrate cycle				
DLD	Dihydrolipoyl dehydrogenase	−0.39±0.11	−0.78±0.08	−0.70±0.08
IDH1	Isocitrate dehydrogenase	−0.66±0.10	−0.67±0.13	−0.23±0.13
IDH2	Isocitrate dehydrogenase	−0.81±0.15	−1.25±0.09	−1.20±0.09
PC	Pyruvate carboxylase, mitochondrial	−0.8±0.12	−1.10±0.19	−1.42±0.15
PCK2	Phosphoenolpyruvate carboxykinase	−0.65±0.11	−0.52±0.11	−0.87±0.10
SDHB	Succinate dehydrogenase	−0.34±0.08	−0.45±0.05	−0.66±0.08
Oxidative phosphorylation and mitochondrial dysfunction				
ATP5I	ATP synthase subunit e, mitochondrial	−0.35±0.12	−0.61±0.13	−0.34±0.02
ATP5J2	ATP synthase subunit f, mitochondrial	−0.02±0.07	−0.13±0.13	−0.60±0.09
ATP6V1A	V-type proton ATPase catalytic	−0.32±0.09	−0.54±0.05	−0.62±0.03
COX5A	Cytochrome c oxidase subunit 5A	−0.34±0.18	−0.59±0.07	−0.58±0.10
COX7A2	Cytochrome c oxidase subunit 7A2	−0.45±0.16	−0.87±0.14	−0.56±0.07
UQCRFS1	Cytochrome b-c1 subunit Rieske	−0.26±0.23	−0.99±0.16	−0.60±0.08
UQCRQ	Cytochrome b-c1 complex subunit 8	−0.78±0.17	−1.12±0.12	−1.65±0.28
GPD2	Glycerol-3-phosphate dehydrogenase	−1.06±0.17	−1.36±0.14	−1.76±0.08
MAOB	Amine oxidase [flavin-containing] B	−1.38±0.16	−2.10±0.22	−2.55±0.14
NDUFB3	NADH dehydrogenase 1 beta subunit 3	−0.22±0.06	−0.28±0.09	−0.59±0.05
PRDX3	Peroxide reductase	−0.06±0.09	−0.74±0.10	−0.52±0.13
SOD2	Superoxide dismutase [Mn]	−0.59±0.05	−0.80±0.06	−0.65±0.05
Protein synthesis				
EIF3C	EIF 3 subunit C	0.63±0.04	0.46±0.03	0.44±0.05
EIF3E	EIF 3 subunit E	0.60±0.06	0.56±0.05	0.60±0.07
KHSRP	Far upstream element-binding protein 2	0.16±0.12	0.53±0.05	0.59±0.07
RPL5	60S ribosomal protein L5	0.60±0.11	0.29±0.06	0.43±0.06
RRBP1	Ribosome-binding protein 1	1.06±0.12	1.03±0.11	0.78±0.09
RPS19	40S ribosomal protein S19	0.60±0.05	0.27±0.05	0.39±0.08
DARS	Aspartyl-tRNA synthetase, cytoplasmic	0.62±0.02	0.45±0.10	0.55±0.09

Gene symbol	Protein name	Log2 ratio ± SEM		
		HFD vs. Control	ob/ob (S) vs. Control	ob/ob (L) vs. Control
Protein folding and transport				
ERP29	ER resident protein 29	0.82±0.04	0.32±0.05	0.20±0.06
LMAN1	Protein ERGIC-53	0.75±0.07	0.62±0.04	0.65±0.03
MOGS	Mannosyl-oligosaccharide glucosidase	1.15±0.05	1.16±0.10	0.80±0.14
PDIA6	Protein disulfide-isomerase A6	1.04±0.09	0.61±0.09	0.48±0.11
MIA3	Melanoma inhibitory activity protein 3	1.13±0.08	0.97±0.08	0.90±0.12
NME2	Nucleoside diphosphate kinase B	0.64±0.05	0.19±0.16	0.50±0.06
ARCN1	Coatomer subunit delta	0.81±0.006	0.65±0.04	0.56±0.05
COPA	Coatomer subunit alpha	0.76±0.03	0.70±0.04	0.56±0.05
SEC23A	Protein transport protein Sec23A	0.57±0.08	0.66±0.05	0.64±0.02
Processing and hormone secretion				
GCG	Glucagon	−1.14±0.29	−1.50±0.06	−1.23±0.07
PCSK1	Neuroendocrine convertase 1	−1.03±0.20	−0.74±0.24	−0.35±0.14
PCSK2	Neuroendocrine convertase 2	−1.11±0.15	−0.21±0.28	−0.16±0.17
PYY	Peptide YY	−1.35±0.37	−1.30±0.07	−0.93±0.1
RTN4	Reticulon-4	−1.05±0.12	−1.27±0.13	−1.23±0.09
SST	Somatostatin	−1.58±0.30	−2.32±0.07	−2.42±0.09
STXBP1	Syntaxin-binding protein 1	−0.47±0.06	−0.83±0.12	−0.91±0.08
UCN3	Urocortin-3	−2.40±0.14	−1.47±0.32	−1.19±0.27
VAMP2	Vesicle-associated membrane protein 2	−0.91±0.14	−0.28±0.14	−0.05±0.1
Anti-apoptosis				
TXNDC5	Thioredoxin domain-containing protein 5	1.23±0.08	0.95±0.10	0.75±0.11
TPT1	Translationally-controlled tumor protein	0.85±0.06	0.82±0.07	0.60±0.12
HSPA5	78 kDa glucose-regulated protein	0.82±0.06	0.57±0.09	0.55±0.08
HSP90B1	Endoplasmin	0.67±0.08	0.18±0.08	0.06±0.11
TMX1	Thioredoxin-related membrane protein 1	0.85±0.08	0.52±0.15	0.25±0.16
ANXA4	Annexin A4	0.15±0.03	0.53±0.06	0.70±0.05
Pro-apoptosis				
HSPD1	60 kDa heat shock protein, mitochondrial	−0.46±0.06	−0.56±0.07	−0.69±0.03
HSPA9	Stress-70 protein, mitochondrial	−0.63±0.10	−0.66±0.06	−0.84±0.03
RTN4	Reticulon-4	−1.05±0.12	−1.27±0.13	−1.23±0.09
Proliferation				
CDK5rap3	CDK5 regulatory subunit-associated protein	0.83±0.14	0.65±0.09	0.60±0.09
PRDX6	Peroxiredoxin-6	0.43±0.04	0.65±0.05	0.74±0.02
Sel1I	Protein sel-1 homolog 1	1.35±0.10	1.55±0.18	1.61±0.16
Nucb2	Nucleobindin-2	1.13±0.11	1.14±0.08	1.18±0.08
SEPT5	Septin-5	1.34±0.12	1.75±0.07	1.54±0.08
SEPT7	Septin-7	0.34±0.06	0.44±0.06	0.71±0.05

Gene symbol	Protein name	Log2 ratio ± SEM		
		HFD vs. Control	ob/ob (S) vs. Control	ob/ob (L) vs. Control
NPM	Nucleophosmin	0.40±0.07	0.68±0.10	0.45±0.07

All changes are presented as log2 ratio between HFD or ob/ob versus control. Standard errors of the mean (SEM) for log2ratio were also included. Proteins are grouped by functional analysis results using Ingenuity Pathway Analysis (IPA).

Appendix A5

Publication

Gupta MK, Teo AKK, Rao TN, Bhatt S, Kleinridders A, Shirakawa, J, Takatani T, **De Jesus DF**, Windmueller R, Wagers AJ, Kulkarni RN. Excessive cellular proliferation negatively impacts reprogramming efficiency of human fibroblasts. Stem Cells Trans Med DOI: 10.5966/sctm.2014-0217.

Contribution

I contributed by assisting in iPSCs cell culture.

STEM CELLS TRANSLATIONAL MEDICINE®

PLURIPOTENT STEM CELLS

Excessive Cellular Proliferation Negatively Impacts Reprogramming Efficiency of Human Fibroblasts

MANOJ K. GUPTA,[a,b] ADRIAN KEE KEONG TEO,[a,b] TATA NAGESWARA RAO,[a,c] SHWETA BHATT,[a,b] ANDRE KLEINRIDDERS,[b,d] JUN SHIRAKAWA,[a,b] TOMOZUMI TAKATANI,[a,b] JIANG HU,[a,b] DARIO F. DE JESUS,[a,b] REBECCA WINDMUELLER,[a,b] AMY J. WAGERS,[a,c] ROHIT N. KULKARNI[a,b]

Key Words. Reprogramming • Insulin signaling • Cell proliferation • Human pluripotency

Sections of [a]Islet Cell and Regenerative Biology and [d]Integrative Physiology and Metabolism, Joslin Diabetes Center, and [b]Department of Medicine, Brigham and Women's Hospital, Harvard Medical School, Boston, Massachusetts, USA; [c]Howard Hughes Medical Institute, Department of Stem Cell and Regenerative Biology, Harvard Stem Cell Institute, Harvard University, Cambridge, Massachusetts, USA

Correspondence: Rohit N. Kulkarni, M.D., Ph.D., Section of Islet Cell and Regenerative Biology, Joslin Diabetes Center, Harvard Medical School, Boston, Massachusetts 02215, USA. Telephone: 617-309-3460; E-Mail: rohit.kulkarni@joslin.harvard.edu

Received September 29, 2014; accepted for publication June 22, 2015; published Online First on August 7, 2015.

1066-5099/2015/$20.00/0

http://dx.doi.org/10.5966/sctm.2014-0217

ABSTRACT

The impact of somatic cell proliferation rate on induction of pluripotent stem cells remains controversial. Herein, we report that rapid proliferation of human somatic fibroblasts is detrimental to reprogramming efficiency when reprogrammed using a lentiviral vector expressing *OCT4*, *SOX2*, *KLF4*, and *cMYC* in insulin-rich defined medium. Human fibroblasts grown in this medium showed higher proliferation, enhanced expression of insulin signaling and cell cycle genes, and a switch from glycolytic to oxidative phosphorylation metabolism, but they displayed poor reprogramming efficiency compared with cells grown in normal medium. Thus, in contrast to previous studies, our work reveals an inverse correlation between the proliferation rate of somatic cells and reprogramming efficiency, and also suggests that upregulation of proteins in the growth factor signaling pathway limits the ability to induce pluripotency in human somatic fibroblasts. STEM CELLS TRANSLATIONAL MEDICINE *2015;4:1101–1108*

SIGNIFICANCE

The efficiency with which human cells can be reprogrammed is of interest to stem cell biology. In this study, human fibroblasts cultured in media containing different concentrations of growth factors such as insulin and insulin-like growth factor-1 exhibited variable abilities to proliferate, with consequences on pluripotency. This occurred in part because of changes in the expression of proteins involved in the growth factor signaling pathway, glycolysis, and oxidative phosphorylation. These findings have implications for efficient reprogramming of human cells.

INTRODUCTION

Breakthrough discoveries from the Yamanaka laboratory [1, 2] and the establishment of human induced pluripotent stem cells (hiPSCs) have opened new avenues for generating patient-specific stem cell derivatives that can be used for in vitro modeling of human disease, drug development, and cell replacement therapy. However, current methodologies of induced pluripotent stem cell (iPSC) generation continue to face technical challenges, in part because of relatively poor reprogramming efficiencies. As efforts to make iPSCs more useful in human transplantation studies continue, many groups have contributed to significant progress in this field, including the use of reduced numbers of reprogramming factors, and adopting nonintegrating methods of their delivery, cell permeable proteins, and stand-alone small molecules or direct reprogramming [3–7]. Despite these efforts, reprogramming efficiency and its relationship with cell proliferation continues to remain poorly understood in the iPSC field. For example, vitamin C has been suggested to promote reprogramming by limiting cell senescence and indirectly promoting proliferation [8], and mitochondrial regression has been reported to be associated with a pluripotent state [9]. Other studies suggest that a high proliferation rate of human somatic fibroblasts is essential for efficient reprogramming by decreasing apoptosis rates and limiting reprogramming barriers, including senescence [10, 11]. In contrast, Xu et al. [12] reported that the slow proliferation of mouse somatic cells is beneficial for reprogramming. Consistently, several small molecule inhibitors of cell proliferation have also been reported to enhance somatic cell reprogramming [13–15].

To directly address the significance of proliferation for reprogramming, we cultured primary human fibroblasts in either defined insulin-rich AmnioMAX (Ax) medium or in normal, conventional Dulbecco's modified Eagle's medium (N) (both from Thermo Fisher Scientific Inc., Waltham, MA, http://www.thermofisher.com). AmnioMAX,

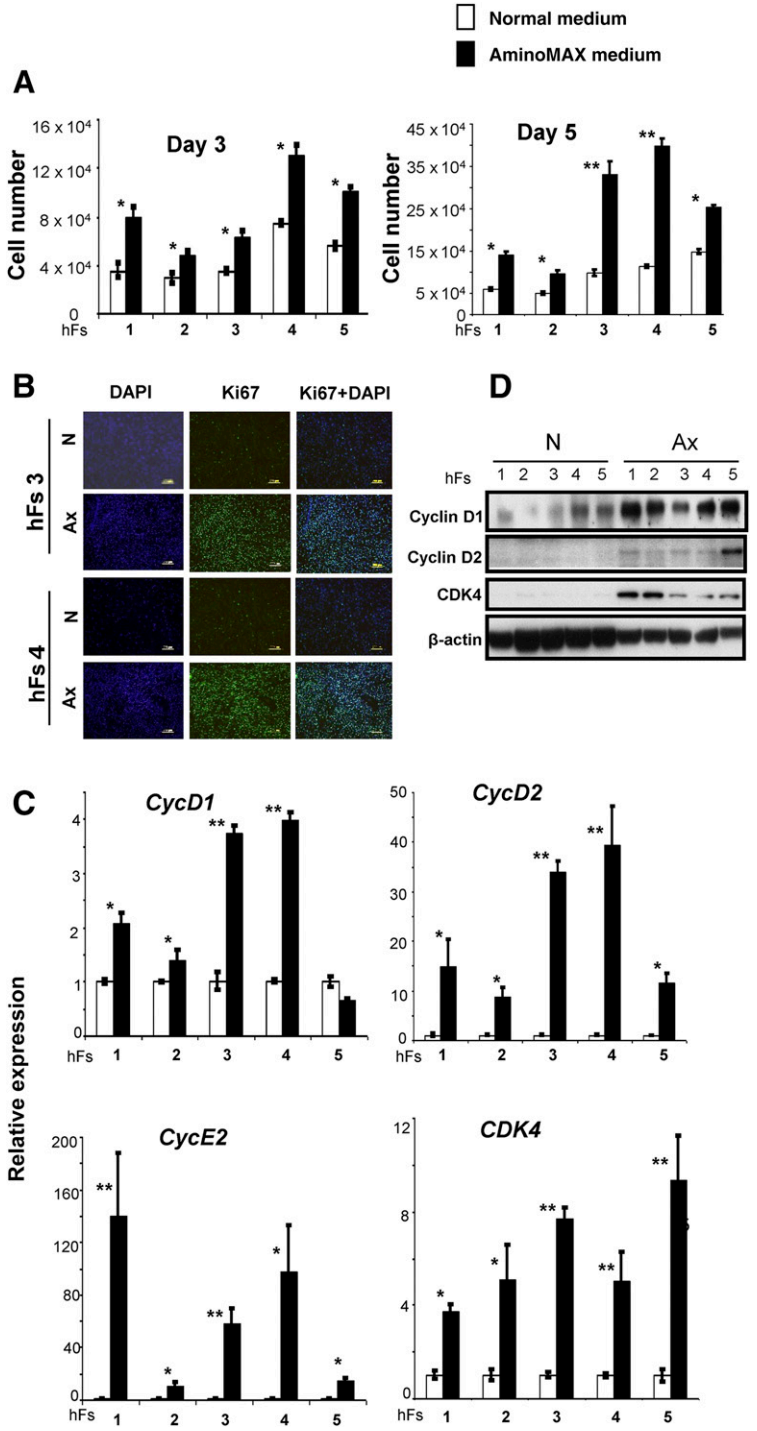

Figure 1. The growth medium determines growth kinetics of human somatic fibroblasts. **(A)**: The cell numbers of 5 primary hFs—AG16104 (hFs 1), AG16086 (hFs 2), 120111 (hFs 3), 120116 (hFs 4), and AG16102 (hFs 5)—were measured by a hemocytometer on day 3 and day 5 after excluding dead cells by trypan blue staining. (White boxes represent cell numbers in N and black boxes indicate cell numbers in defined Ax.) The cells were seeded at equal densities (30,000 cells per well) on day 0 and counted on day 3 and day 5 in triplicate wells. The *x*-axis denotes the hFs. **(B)**: hFs 3 and hFs 4 were seeded at equal densities (30,000 cells per well) and cultured in N or Ax medium. Cells were harvested on day 3 and subjected to Ki67 immunostaining to identify cycling cells. DAPI was used to stain nuclei. Scale bars = 200 μm. **(C)**: The relative expression of cell cycle genes *CycD1, CycD2, CDK4*, and *CycE2* in hFs grown in N (white bars) or Ax medium (black bars). Expression was normalized to the *β-actin* gene and is shown relative to the average N medium level. The *x*-axis denotes the number of hFs. **(D)**: Expression of CycD1, CycD2, and CDK4 proteins was demonstrated by Western immunoblot analysis. β-actin was used as an internal control. All experiments were performed three times. Data are shown as mean $\pm$ SD. Statistical significance was determined by Student's *t* test. $*$, $p < .05$; $**$, $p < .01$ for Ax versus N. Abbreviations: Ax, AminoMAX medium; DAPI, 4,6-diamidino-2-phenylindole; hF, human fibroblast; N, Dulbecco's Modified Eagle's medium.

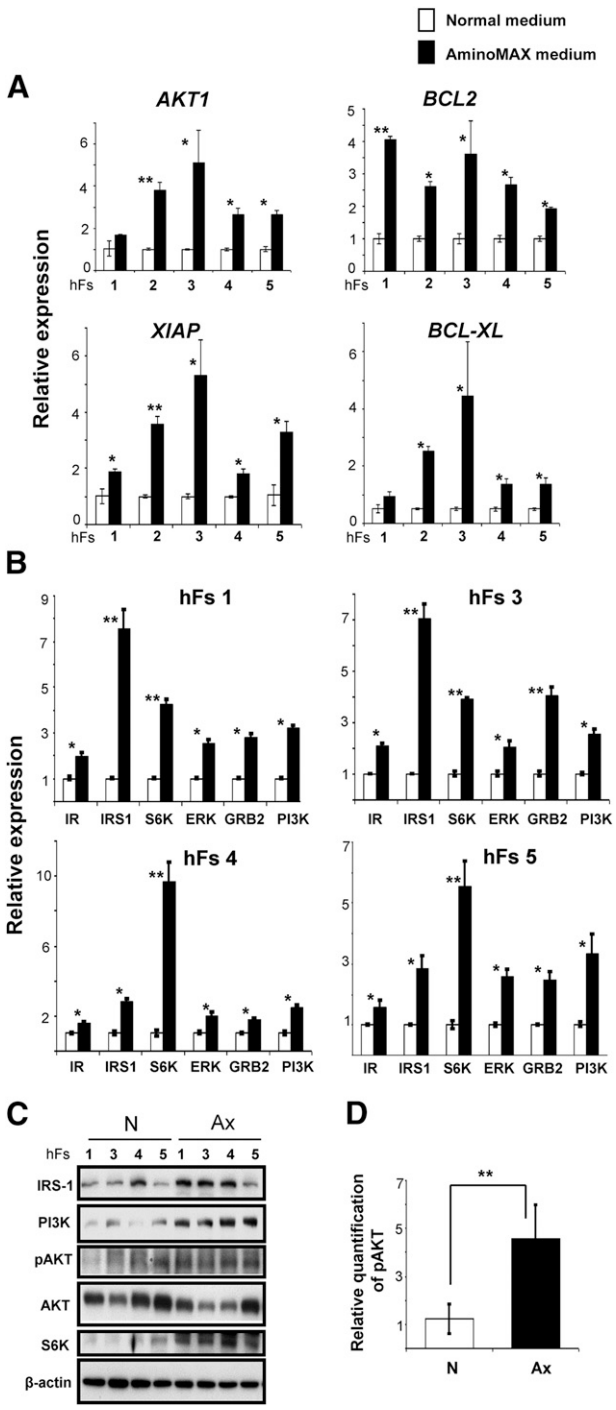

Figure 2. Fibroblasts cultured in Ax growth medium exhibit altered expression of genes in cell survival and growth factor (insulin/insulin-like growth factor-1 [IGF-1]) signaling pathways. **(A):** The relative expression of *AKT1, BCL2, XIAP*, and *BCL-XL* genes by real-time polymerase chain reaction in human fibroblasts (hFs 1, 2, 3, 4, and 5) cultured in N (white bars) or Ax (black bars) medium. The *x*-axis denotes the hFs. **(B):** Gene expression analysis of proteins in the growth factor (insulin/IGF-1) signaling pathway, including IR, IRS1, S6K, ERK, GRB2, and PI3K, in four hFs (hFs 1, hFs 3, hFs 4, and hFs 5) grown in N or Ax medium. In both **(A)** and **(B)**, expression was normalized to the *β-actin* gene and is shown relative to the average N medium level. The *x*-axis denotes the number of hFs. **(C):** Western blot analysis of IRS1, PI3K, S6K, pAKT, and AKT proteins in hFs 1, hFs 3, hFs 4, and hFs 5 cultured in N or Ax medium. *β*-Actin was used as an internal control. **(D):** Graph representing the relative quantity of phosphorylation of AKT normalized to total AKT band density by ImageJ software (US National Institutes of Health, Bethesda, MD, http://imagej.nih.gov/ij). All experiments were performed three times, represented as mean ± SD. Statistical significance was determined by Student's *t* test. ∗, $p < .05$; ∗∗, $p < .01$ for Ax versus N. Abbreviations: Ax, AminoMAX medium; D, day; ERK, extracellular signal-regulated kinase; GRB2, growth factor receptor-bound protein; IR, insulin receptor; IRS1, insulin receptor substrate-1; N, Dulbecco's modified Eagle's medium; PI3K, phosphatidylinositol 3-kinase; S6K, S6 kinase.

a well-defined medium, has been used for culturing human amniotic fluid cells and fibroblasts [16, 17]. Our study demonstrates a direct inverse correlation of high cell proliferation and reprogramming efficiency for human somatic cells in Ax medium. These results have important implications for utility of these cells for translational studies in humans.

Results and Discussion

AmnioMAX Medium Accelerates the Growth Kinetics of Somatic Fibroblasts

Human fibroblasts (hFs) obtained from healthy individuals—AG16104 (hFs 1), AG16086 (hFs 2), 120111 (hFs 3), 120116 (hFs 4), and AG16102 (hFs 5)—were either grown in conventional normal growth medium (N) or Ax medium. Strikingly, fibroblasts grew faster when grown in Ax medium compared with cells grown in N medium (supplemental online Fig. 1A). To quantify proliferation, we seeded an equal number of fibroblasts (2×10^4) on day 0 and counted the fibroblasts at days 3 and 5. We observed a 1.5- to 2-fold increase at day 3 and a 2- to 3-fold increase in number of cells at day 5, when cultured in Ax medium compared with N medium (Fig. 1A). An increased rate of proliferation in Ax medium was confirmed by Ki67/4′,6-diamidino-2-phenylindole immunostaining in hFs 3 and hFs 4 (Fig. 1B). Further quantification by flow cytometry analysis of hFs 3, hFs 4, and hFs 5 at day 5 revealed an average 2- to 3-fold increase in Ki67-positive cells grown in Ax medium (supplemental online Fig. 1B, 1C). We also observed an increase in expression of cell cycle genes *CycD1* (2- to 5-fold), *CycD2* (2- to 10-fold), *CycE2* (20- to 40-fold), and *CDK4* (2- to 6-fold) in human fibroblasts grown in Ax medium compared with fibroblasts cultured in N medium (Fig. 1C). Detection of increased CycD1, CycD2, and CDK4 proteins by Western immunoblotting confirmed enhanced cell cycle progression in fibroblasts cultured in Ax medium (Fig. 1D). Attempts to culture human fibroblasts in mTeSR human medium were not successful and the cells failed to grow in contrast to robust growth when cultured in N or Ax medium (supplemental online Fig. 1D). Together, these data suggest that growth of human fibroblasts in Ax medium leads to a greater rate of proliferation and the enhanced expression of cell cycle proteins.

Enhanced Growth Factor (Insulin) Signaling Contributes to Higher Proliferation of Fibroblasts Cultured in Ax Medium

The more rapid proliferation of somatic fibroblasts in defined Ax medium led us to investigate the expression of genes associated with cell survival and growth factor (insulin/insulin-like growth factor-1 [IGF-1]) signaling pathways. We observed a

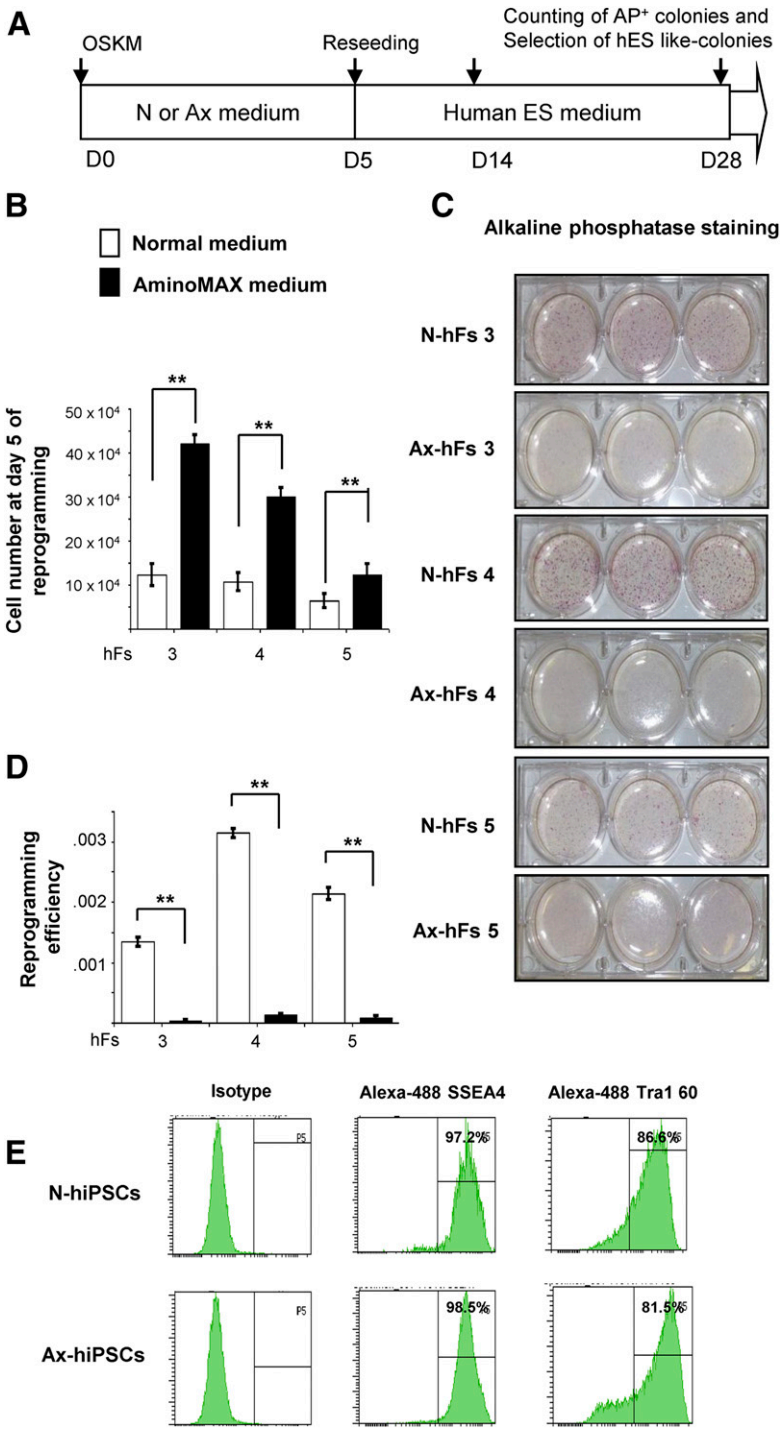

Figure 3. Cellular state of fibroblast growth affects cellular reprogramming. **(A)**: Scheme of reprogramming of human somatic fibroblasts into hiPSCs using a cocktail of a Cre-excisable STEMCCA lentivirus vector expressing OSKM. **(B)**: Human fibroblasts 120111 (hFs 3), 120116 (hFs 4), and AG16102 (hFs 5) were subjected to reprogramming by STEMCCA lentiviral vector. On day 5, at the time of further splitting during reprogramming process, cells were counted growing in N or Ax medium. **(C)**: On day 5 of reprogramming, hFs 3, hFs 4, and hFs 5, grown in N or Ax medium, were seeded at a density of 3×10^4 fibroblasts in triplicate in 6-well plates. AP staining was performed using a Stemgent kit (Stemgent Inc., Cambridge, MA, https://www.stemgent.com/products/227) between days 21 and 28 after iPSC colonies were visualized in reprogramming culture. **(D)**: Reprogramming efficiencies from hFs 3, hFs 4, and hFs 5 grown in N or Ax medium were determined by dividing the number of AP-positive colonies by the number of fibroblasts that were initially seeded and transduced (5×10^4 cells). **(E)**: hiPSCs from both the groups were subjected to flow cytometry analysis to evaluate the surface pluripotency markers SSEA4 and Tra-1 60, using Alexa Fluor 488 antibodies. All experiments were performed three times, represented as mean ± SD. Statistical significance by Student's *t* test. *, $p < .05$; **, $p < .01$ for Ax versus N. Abbreviations: AP, alkaline phosphatase; Ax, AminoMAX medium; ES, embryonic stem cell; hF, human fibroblast; hiPSC, human induced pluripotent stem cell; N, Dulbecco's modified Eagle's medium; OSKM, OCT4, SOX2, KLF4, and cMYC.

Table 1. Small molecules that suppress cellular proliferation increase reprogramming efficiency

Small molecules	Effect on reprogramming	Molecular targets	Effects on cell proliferation
Valproic acid [25]	Promotes reprogramming	HDAC inhibitor	Suppresses cell proliferation in various cell types
Tricostatin A [23]	Promotes reprogramming	HDAC inhibitor	Inhibits cell proliferation in various cancer cells
5-Azacytidine [26]	Increases reprogramming	DNA methyltransferase inhibitor	Inhibits cell proliferation
Kenpaullone [24]	Promotes reprogramming	Inhibitor of GSK-3β and cell cyclins	Suppresses cell cycle progression
BIX-01294 [26]	Improves reprogramming	G9a histone methytransferase inhibitor	Decreases cancer cell proliferation
CHIR99021 [24]	Promotes reprogramming	GSK3 inhibitor	Suppresses proliferation of various cancers
PD0325901 [24]	NA	MEK inhibitor	Antiproliferative against various cancer lines
Butyrate [23]	Improves reprogramming	Small-chain fatty acids	Suppresses proliferation in various cancers

Abbreviations: GSK, glycogen synthase kinase; HDAC, histone deacetylase; MEK, mitogen-activated protein kinase; NA, not available.

2- to 6-fold upregulation of genes involved in blocking apoptosis, including *AKT1, BCL2, XIAP*, and *BCL-XL* in human fibroblasts grown in Ax medium (Fig. 2A). Furthermore, growth factor (insulin/IGF-1) signaling pathway-related genes, including *IR, IRS1, S6K, ERK, GRB2*, and *PI3K*, were also significantly upregulated (2- to 3-fold) in fibroblasts grown in Ax medium (Fig. 2B). Western immunoblot analysis confirmed an increased phosphorylation of AKT (approximately 2.5-fold) and higher protein expression of phosphatidylinositol 3-kinase (PI3K), IRS-1, and S6K (approximately 5-fold) in human fibroblasts grown in defined Ax medium (Fig. 2C, 2D; supplemental online 2A). However, we did not observe any significant change in the protein levels of GRB2 or ERK (supplemental online Fig. 2B), suggesting Ax medium has a more prominent effect on the PI-3 kinase pathway than the MAP kinase pathway.

Our findings are consistent with previous studies [18] reporting increased expression of cell survival genes (*AKT1, BCL2, XIAP*, and *BCL-XL*) during increased proliferation. Consistent with the observation that insulin is a potent inducer of cell proliferation during development [19], we detected an upregulation of phosphorylated AKT and of proteins in the insulin/IGF-1 signaling pathway, including PI3K, IRS1, and S6K, in fibroblasts grown in defined Ax medium.

Our focus on examining the insulin signaling pathway and cell proliferation in the context of reprogramming of human somatic fibroblasts gains significance given several opposing reports in this field. Ruiz et al. [11] reported that high proliferation of somatic cells is beneficial to reprogramming by providing evidence that expression of CycD1, CycD2, and CycE2, but not CDK1, CDK2, and CDK4, increased the reprogramming efficiency of human keratinocytes by more than 2-fold. On the contrary, Xu et al. [12] reported that low proliferation of somatic cells is helpful to induce pluripotency. They demonstrated that removing cMyc from among the four reprogramming factors led to a 10-fold increase in reprogramming efficiency of mouse fibroblasts, whereas forced expression of cMyc led to hyperproliferation and correlated negatively with overall reprogramming efficiency. In contrast to these two studies, our observations implicate increased cell cycle markers and an upregulation of proteins in the insulin/IGF-1 signaling pathway in the reprogramming process.

High Proliferation Rate and Upregulation of Insulin Signaling in Somatic Fibroblasts Correlates With Lower Reprogramming Efficiency

Next, to examine whether cell cycle progression and increased growth determine somatic cell reprogramming, we subjected fibroblasts individually cultured in N or Ax medium to reprogramming into iPSCs, using a protocol reported previously [20] (Fig. 3A). As expected, even after human lentiviral transduction, we observed a 2- to 3-fold increase in viable cell numbers of both transduced and nontransduced fibroblasts in Ax medium (Fig. 3B). However, surprisingly, this increase in cell numbers was associated with a significant reduction in reprogramming efficiency of cells cultured in Ax medium compared with those cultured in N medium, as demonstrated by alkaline phosphatase staining. A similar outcome in three independent samples (hFs 3, hFs 4, and hFs 5) confirmed a uniform effect (Fig. 3C, 3D; supplemental online Fig. 2C). Real-time polymerase chain reaction analysis showed no difference in the expression levels of *OCT4* or *NANOG* between N-hiPSCs and Ax-hiPSCs, and there was no detection of *OCT4* and *NANOG* in their respective parental fibroblasts (supplemental online Fig 2D). Furthermore, we observed a similar level of expression of SSEA4 ($>$90%) and TRA1 60 ($>$80%) pluripotent surface markers by flow cytometry (Fig. 3E) and OCT4 expression by immunohistochemistry (supplemental online Fig. 2E) in hiPSCs derived from the fibroblasts cultured in either medium. The hiPSCs from both groups were able to form embryoid bodies as well as develop teratomas that included cells from the three lineages, as shown by immunostaining (supplemental online Fig. 2F, 2G). These results indicate that a higher proliferation and an upregulation in expression of proteins in the growth factor (insulin/IGF-1) signaling pathway does not impact pluripotency of the derived hiPSCs that are successfully reprogrammed, but does influence the frequency of cells that undergo reprogramming. Consistent with our results, Xu et al. [12] reported that low proliferation of mouse fibroblasts is beneficial for reprogramming. Although these authors did not explain the precise mechanism, their data reveal that different small molecules that are antiproliferative agents (e.g., amphidicolin, cisplatin, aloisine A, CDK9 inhibitor II) enhanced the reprogramming efficiency of mouse somatic fibroblasts. One possible explanation for the altered reprogramming is that higher proliferation rates affect some epigenetic markers and/or influence the heterochromatin stage of the cells to eventually limit cellular reprogramming.

Vitamin C, a small molecule, was reported to improve somatic cell reprogramming by enhancing cell proliferation. In contrast, valproic acid has been shown to increase reprogramming efficiency and to induce pluripotency in human amniotic-fluid cells alone, without ectopic expression of reprogramming factors [15, 21, 22]. Indeed, several small molecules, such as kenpaullone,

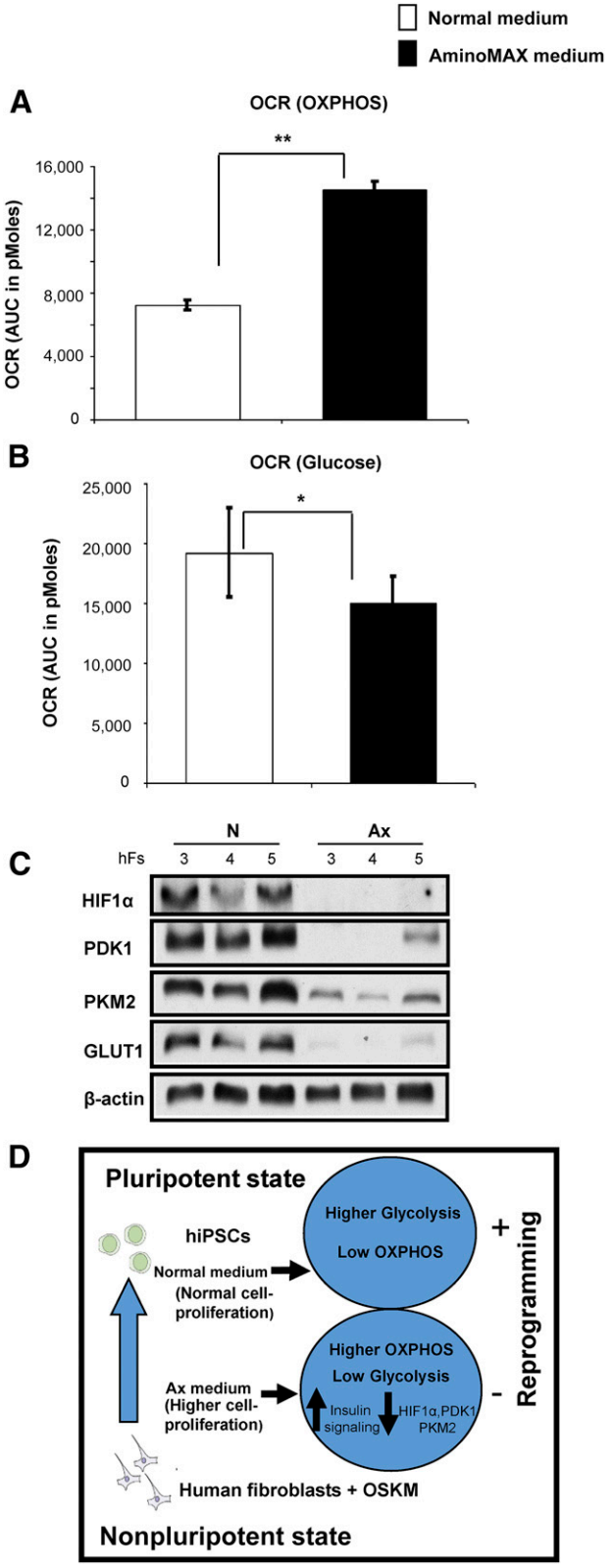

Figure 4. Metabolic shift and the expression of genes regulating reprogramming in fibroblasts grown in N or Ax medium. **(A)**: OCR during basal respiration, displayed as AUC, of human hFs 3 and hFs 4 grown in N or Ax medium **(B)**: OCR in the presence of glucose as sole energy substrate, displayed as AUC, of human somatic fibroblasts hFs 3 and hFs 4 grown in N or Ax medium. **(C)**: Western blot analysis of HIF1α, PDK1, PKM2, and GLUT1 in hFs 3, hFs 4, and hFs 5 cultured in N or Ax medium. β-Actin was used as an internal control. **(D)**: A proposed model for the effects of high cell proliferation and insulin signaling on reprogramming of human fibroblasts. In fibroblasts with normal proliferation, cells maintain higher glycolysis and low OXPHOS. Cells cultured in Ax medium, with higher cell proliferation, exhibit increased growth factor (insulin/IGF-1) signaling and a higher OXPHOS by downregulating the expression of HIF1a, PDK1, PKM2, and GLUT1 proteins, leading to a significant decrease in the efficiency of induction of pluripotency (hiPSCs). All experiments were performed three times, represented as mean $\pm$ SD. Statistical significance was determined by Student's *t* test. $*$, $p < .05$; $**$, $p < .01$ for Ax versus N. Abbreviations: AUC, area under the curve; GLUT1, glucose transporter-1; Ax, AminoMAX medium; HIF1α, hypoxia inducible factor-1 α; hiPSC, human induced pluripotent stem cell; N, Dulbecco's modified Eagle's medium; OCR, oxygen consumption rate; OSKM, OCT4, SOX2, KLF4, and cMYC; OXPHOS, oxidative phosphorylation; PDK1, phosphoinositide dependent kinase-1; PKM2, pyruvate kinase M2 isoform.

trichostatin A, 5-azacytidine, and CHIR99021, have all been identified as antiproliferative agents in various cell types [23–26] that also promote reprogramming of fibroblasts [13, 15] (Table 1; supplemental online data).

To further validate the role of IGF-1 and insulin signaling, we reprogrammed hFs 3, 4, and 5 cultured in N medium with or without supplementation with IGF-1 (100 nM) or insulin (43 ng/ml). We used the same concentration of insulin as that present in Ax medium. Interestingly, we observed a significant decrease in reprogramming efficiency in the presence of either IGF-1 or insulin (supplemental online Fig. 3A–3C). This supplementation experiment further supported a potential role for insulin or IGF-1 signaling in reprogramming of human fibroblasts.

Activation of Metabolic Switch From Glycolysis to Oxidative Phosphorylation Leads to Significant Decrease in Reprogramming Efficiency of Somatic Fibroblasts

Previous reports indicating that cell-fate conversion is associated with a transition between oxidative phosphorylation and glycolytic metabolism [9], coupled with the observation that insulin/IGF-1 is known to regulate mitochondrial function [27, 28], prompted us to explore whether a similar switch appears in the phenotype of human fibroblasts that show altered insulin/IGF-1 signaling. To this end, we undertook metabolic profiling by investigating cellular metabolism in the context of reprogramming, using the Seahorse Bioflux Analyzer (Seahorse Bioscience, Billerica, MA ,http://www.seahorsebio.com). This analysis revealed that human fibroblasts cultured in defined Ax medium exhibit increased basal respiration, as shown by a 2-fold higher oxygen consumption rate (OCR) compared with fibroblasts grown in conventional N medium (Fig. 4A; supplemental online Fig. 4A). Interestingly, fibroblasts cultured in N medium displayed increased glycolytic capacity compared with fibroblasts grown in Ax medium. Thus, in response to glucose stimulation, fibroblasts grown in N medium showed a higher OCR and extracellular acidification rate than fibroblasts grown in Ax medium (Fig. 4B; supplemental online Fig. 4B). Consistent with a role for altered glycolysis and hypoxia in the regulation of reprogramming [29], we observed a significantly reduced protein expression of HIF1α (93%), PDK1 (77.1%), PKM2 (91.6%), and GLUT1 (95.9%) in total cell extracts

of fibroblasts grown in Ax medium (Fig. 4C; supplemental online Fig. 4C).

HIF1α signaling enhances reprogramming efficiency via metabolic switch toward glycolysis by upregulating expression of PDK1. Therefore, activation of HIF1α regulates Oct4 expression and augments the induction of human stemness signature in various tumor cell lines [29, 30]. Consistent with this notion, our findings demonstrate that reduction in HIF1α protein in highly proliferating somatic fibroblasts grown in Ax medium promotes refractoriness to reprogramming. Previous reports implicated an upregulation of PDK1 by small molecules in an increase in reprogramming [3]. Similarly, PKM2 may be involved in positive regulation of OCT4 and GLUT1 in glycolysis [31]. In our study, we noted that key regulators of glycolysis (e.g., PDK1, PKM2, and GLUT1) are all decreased in human fibroblasts that are rapidly proliferating when cultured in Ax medium and, consequently, exhibit a significant loss of reprogramming efficiency (Fig. 4D).

To further validate the role of PDK1 in reprogramming, a central regulator of glycolysis, we knocked down PDK1 in hFs 3, hFs 4, and hFs 5 using scrambled or PDK1-specific siRNAs (supplemental online Fig. 5A). Knocked-down PDK1 human fibroblasts showed significantly reduced reprogramming efficiency as compared with fibroblasts cultured in scrambled control small interfering RNA (supplemental online Fig. 5B, 5C). This loss-of-function study further validated our findings in regard to a potential role of PDK1 and glycolysis in reprogramming of human fibroblasts.

Conclusion

We report that stimulation of cell proliferation limits human somatic cell reprogramming via upregulation of proteins in the insulin/IGF-1 signaling pathway and by promoting a metabolic switch from glycolysis to oxidative phosphorylation. These data provide a previously unidentified perspective on the roles of cell proliferation and growth factor signaling in induction of pluripotency and have implications for studies aimed at reprogramming of cells derived from humans with pathological states associated with impaired metabolism and/or cell proliferation, such as diabetes or cancer.

Acknowledgments

We thank Dr. G. Mostoslavsky (Boston University) for the kind gift of lentiviral plasmids and R. Martinez for technical assistance. We thank Dr. C.R. Kahn (Joslin Diabetes Center) for allowing access to the Seahorse instrument. The Joslin DRC iPS Core is supported by NIH Grant 5 P30 DK036836-27. A.K.K.T. is supported by a Juvenile Diabetes Research Foundation Postdoctoral Fellowship. A.K. was supported by Deutsche Forschungsgemeinschaft projects KL2399/1-1 and KL2399/3-1. R.N.K. is supported by NIH Grant R01 DK67536 and a grant from AstraZeneca.

Author Contributions

M.K.G.: conception and design, collection and assembly of data, data analysis and interpretation, manuscript writing, final approval of manuscript; A.K.K.T. and T.N.R.: collection and assembly of data, data analysis and interpretation, final approval of manuscript; S.B., J.S., T.T., J.H., D.F.D.J., and R.W.: collection and assembly of data, final approval of manuscript; A.K.: collection and assembly of data of metabolic study, data analysis and interpretation, final approval of manuscript; A.J.W.: provision of suggestions, manuscript editing, final approval of manuscript; R.N.K.: conception and design, manuscript writing, financial support, final approval of manuscript.

Disclosure of Potential Conflicts of Interest

A.J.W. is on the scientific advisory board of FATE Therapeutics. R.N.K. has compensated research funding from AstraZeneca. The other authors indicated no potential conflicts of interest.

References

1 Takahashi K, Tanabe K, Ohnuki M et al. Induction of pluripotent stem cells from adult human fibroblasts by defined factors. Cell 2007;131:861–872.

2 Daley GQ. Stem cells: Roadmap to the clinic. J Clin Invest 2010;120:8–10.

3 Zhu S, Li W, Zhou H et al. Reprogramming of human primary somatic cells by OCT4 and chemical compounds. Cell Stem Cell 2010;7: 651–655.

4 Hou P, Li Y, Zhang X et al. Pluripotent stem cells induced from mouse somatic cells by small-molecule compounds. Science 2013;341:651–654.

5 Kim JB, Greber B, Arauzo-Bravo MJ et al. Direct reprogramming of human neural stem cells by OCT4. Nature 2009;461:649–643.

6 Park IH, Zhao R, West JA et al. Reprogramming of human somatic cells to pluripotency with defined factors. Nature 2008;451:141–146.

7 Hanna J, Markoulaki S, Schorderet P et al. Direct reprogramming of terminally differentiated mature B lymphocytes to pluripotency. Cell 2008;133:250–264.

8 Esteban MA, Wang T, Qin B et al. Vitamin C enhances the generation of mouse and human induced pluripotent stem cells. Cell Stem Cell 2010;6:71–79.

9 Folmes CD, Nelson TJ, Martinez-Fernandez A et al. Somatic oxidative bioenergetics transitions into pluripotency-dependent glycolysis to facilitate nuclear reprogramming. Cell Metab 2011;14:264–271.

10 Son MJ, Son MY, Seol B et al. Nicotinamide overcomes pluripotency deficits and reprogramming barriers. Stem Cells 2013;31: 1121–1135.

11 Ruiz S, Panopoulos AD, Herrerias A et al. A high proliferation rate is required for cell reprogramming and maintenance of human embryonic stem cell identity. Curr Biol 2011; 21:45–52.

12 Xu Y, Wei X, Wang M et al. Proliferation rate of somatic cells affects reprogramming efficiency. J Biol Chem 2013;288:9767–9778.

13 Li W, Zhou H, Abujarour R et al. Generation of human-induced pluripotent stem cells in the absence of exogenous Sox2. Stem Cells 2009;27:2992–3000.

14 Lyssiotis CA, Foreman RK, Staerk J et al. Reprogramming of murine fibroblasts to induced pluripotent stem cells with chemical complementation of Klf4. Proc Natl Acad Sci USA 2009;106:8912–8917.

15 Huangfu D, Maehr R, Guo W et al. Induction of pluripotent stem cells by defined factors is greatly improved by small-molecule compounds. Nat Biotechnol 2008;26:795–797.

16 Ye L, Chang JC, Lin C et al. Induced pluripotent stem cells offer new approach to therapy in thalassemia and sickle cell anemia and option in prenatal diagnosis in genetic diseases. Proc Natl Acad Sci USA 2009;106:9826–9830.

17 Staunstrup NH, Madsen J, Primo MN et al. Development of transgenic cloned pig models of skin inflammation by DNA transposon-directed ectopic expression of human beta1 and alpha2 integrin. PloS One 2012;7: e36658.

18 Yu X, Zhang X, Dhakal IB et al. Induction of cell proliferation and survival genes by estradiol-repressed microRNAs in breast cancer cells. BMC Cancer 2012;12:29.

19 Strassburger K, Tiebe M, Pinna F et al. Insulin/IGF signaling drives cell proliferation in part via Yorkie/YAP. Dev Biol 2012;367:187–196.

20 Teo AK, Windmueller R, Johansson BB et al. Derivation of human induced pluripotent stem cells from patients with maturity onset

diabetes of the young. J Biol Chem 2013;288: 5353–5356.

21 Moschidou D, Mukherjee S, Blundell MP et al. Valproic acid confers functional pluripotency to human amniotic fluid stem cells in a transgene-free approach. Mol Ther 2012;20: 1953–1967.

22 Moschidou D, Mukherjee S, Blundell MP et al. Human mid-trimester amniotic fluid stem cells cultured under embryonic stem cell conditions with valproic acid acquire pluripotent characteristics. Stem Cells Dev 2013;22:444–458.

23 Medina V, Edmonds B, Young GP et al. Induction of caspase-3 protease activity and apoptosis by butyrate and trichostatin A (inhibitors of histone deacetylase): Dependence on protein synthesis and synergy with a mitochondrial/cytochrome c-dependent pathway. Cancer Res 1997;57:3697–3707.

24 Tighe A, Ray-Sinha A, Staples OD et al. GSK-3 inhibitors induce chromosome instability. BMC Cell Biol 2007;8:34.

25 Xia Q, Sung J, Chowdhury W et al. Chronic administration of valproic acid inhibits prostate cancer cell growth in vitro and in vivo. Cancer Res 2006;66:7237–7244.

26 Weller EM, Poot M, Hoehn H. Induction of replicative senescence by 5-azacytidine: fundamental cell kinetic differences between human diploid fibroblasts and NIH-3T3 cells. Cell Prolif 1993;26:45–54.

27 Liu S, Okada T, Assmann A et al. Insulin signaling regulates mitochondrial function in pancreatic beta-cells. PloS One 2009;4: e7983.

28 Zarse K, Schmeisser S, Groth M et al. Impaired insulin/IGF1 signaling extends life span by promoting mitochondrial L-proline catabolism to induce a transient ROS signal. Cell Metab 2012;15:451–465.

29 Yoshida Y, Takahashi K, Okita K et al. Hypoxia enhances the generation of induced pluripotent stem cells. Cell Stem Cell 2009;5: 237–241.

30 Prigione A, Rohwer N, Hoffman S et al. HIF1α modulates reprogramming through early glycolytic shift and upregulation of PDK1-3 and PKM2. STEM CELLS 2014;32:364–376.

31 Lee J, Kim HK, Han YM et al. Pyruvate kinase isozyme type M2 (PKM2) interacts and cooperates with Oct-4 in regulating transcription. Int J Biochem Cell Biol 2008;40:1043–1054.

See www.StemCellsTM.com for supporting information available online.

Appendix A6

Publication

El Ouaamari A, Dirice E, Gedeon N, Hu J, Zhou JY, Shirakawa J, Hou L, Goodman J, Karampelias C, Qiang G, Boucher J, Martinez R,Gritsenko MA, **De Jesus DF**, Kahraman S, Bhatt S, Smith RD, Beer H, Jungtrakoon P, Gong Y, Goldfine AB, Liew CW, Doria A, Andersson O, Qian WJ, Remold-O'Donnell E, and Kulkarni RN. SerpinB1 Promotes Pancreatic β-Cell Proliferation. Cell Metabolism 23:1-12, 2016.

Contribution

I contributed by assisting in islet isolation and gene expression analyses by RT-PCR.

Article

Cell Metabolism

SerpinB1 Promotes Pancreatic β Cell Proliferation

Graphical Abstract

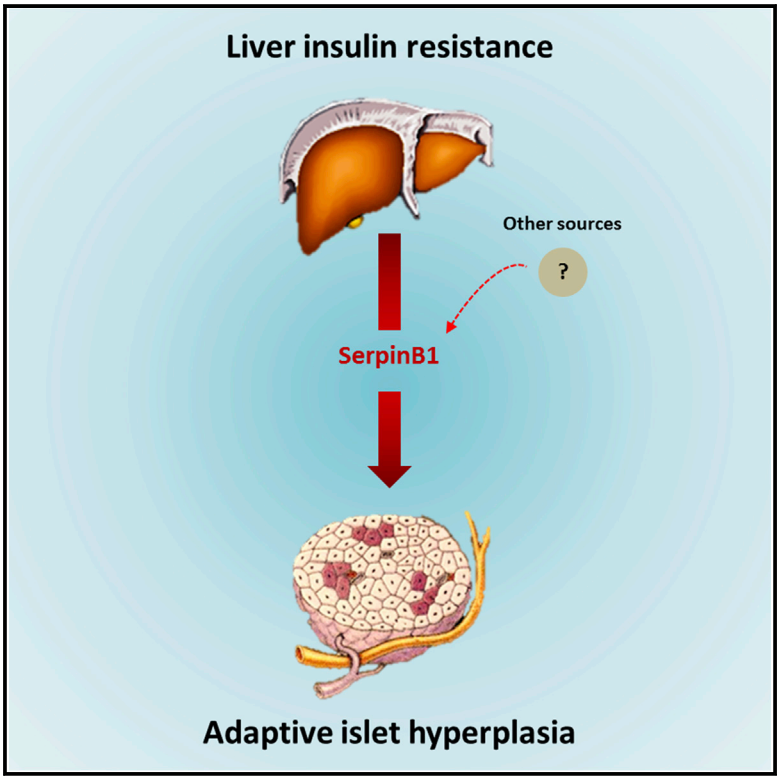

Highlights

- Elevated serpinB1 correlates with β cell proliferation in insulin resistance
- SerpinB1 promotes β cell proliferation in multiple species
- SerpinB1 deficiency leads to maladaptive β cell proliferation in insulin resistance
- SerpinB1 inhibits elastase and activates growth/survival factor signaling pathways

Authors

Abdelfattah El Ouaamari, Ercument Dirice, Nicholas Gedeon, ..., Wei-Jun Qian, Eileen Remold-O'Donnell, Rohit N. Kulkarni

Correspondence

rohit.kulkarni@joslin.harvard.edu

In Brief

Factors that promote compensatory β cell response to insulin resistance, a common feature in mammals, have been elusive. El Ouaamari et al. identify SerpinB1 as a hepatocyte-secretory protease inhibitor regulating β cell proliferation in humans, mice, and zebrafish. SerpinB1 acts by modulating canonical growth and survival signaling pathways.

Accession Numbers

PXD003182

El Ouaamari et al., 2016, Cell Metabolism *23*, 194–205
January 12, 2016
http://dx.doi.org/10.1016/j.cmet.2015.12.001

CellPress

Cell Metabolism
Article

SerpinB1 Promotes Pancreatic β Cell Proliferation

Abdelfattah El Ouaamari,[1] Ercument Dirice,[1] Nicholas Gedeon,[1] Jiang Hu,[1] Jian-Ying Zhou,[2] Jun Shirakawa,[1] Lifei Hou,[3,4] Jessica Goodman,[3] Christos Karampelias,[5] Guifeng Qiang,[6] Jeremie Boucher,[7,12] Rachael Martinez,[1] Marina A. Gritsenko,[2] Dario F. De Jesus,[1] Sevim Kahraman,[1] Shweta Bhatt,[1] Richard D. Smith,[2] Hans-Dietmar Beer,[8] Prapaporn Jungtrakoon,[9] Yanping Gong,[3] Allison B. Goldfine,[10] Chong Wee Liew,[6] Alessandro Doria,[9] Olov Andersson,[5] Wei-Jun Qian,[2] Eileen Remold-O'Donnell,[3,4,11] and Rohit N. Kulkarni[1,*]

[1]Islet Cell and Regenerative Medicine, Joslin Diabetes Center, Department of Medicine, Harvard Medical School, Harvard Stem Cell Institute, Boston, MA 02215, USA
[2]Biological Sciences Division and Environmental Molecular Sciences Laboratory, Pacific Northwest National Laboratory, Richland, WA 99352, USA
[3]Program in Cellular and Molecular Medicine at Boston Children's Hospital, 3 Blackfan Circle, Boston, MA 02215, USA
[4]Department of Pediatrics, Harvard Medical School, Boston, MA 02215, USA
[5]Department of Cell and Molecular Biology, Karolinska Institutet, von Eulers väg 3, 17177 Stockholm, Sweden
[6]Department of Physiology and Biophysics, University of Illinois at Chicago, Chicago, IL 60612, USA
[7]Section on Integrative Physiology and Metabolism, Joslin Diabetes Center, Harvard Medical School, Boston, MA 02215, USA
[8]University Hospital Zurich, Department of Dermatology, 8006 Zurich, Switzerland
[9]Section on Genetics and Epidemiology, Joslin Diabetes Center and Harvard Medical School, Boston, MA 02215, USA
[10]Section on Clinical Research, Joslin Diabetes Center and Department of Medicine, Brigham and Women's Hospital, Harvard Medical School, Boston, MA 02215, USA
[11]Division of Hematology/Oncology, Boston Children's Hospital, Boston, MA 02215, USA
[12]Cardiovascular and Metabolic Diseases iMed, AstraZeneca R&D, 431 83 Mölndal, Sweden
*Correspondence: rohit.kulkarni@joslin.harvard.edu
http://dx.doi.org/10.1016/j.cmet.2015.12.001

SUMMARY

Although compensatory islet hyperplasia in response to insulin resistance is a recognized feature in diabetes, the factor(s) that promote β cell proliferation have been elusive. We previously reported that the liver is a source for such factors in the liver insulin receptor knockout (LIRKO) mouse, an insulin resistance model that manifests islet hyperplasia. Using proteomics we show that serpinB1, a protease inhibitor, which is abundant in the hepatocyte secretome and sera derived from LIRKO mice, is the liver-derived secretory protein that regulates β cell proliferation in humans, mice, and zebrafish. Small-molecule compounds, that partially mimic serpinB1 effects of inhibiting elastase activity, enhanced proliferation of β cells, and mice lacking serpinB1 exhibit attenuated β cell compensation in response to insulin resistance. Finally, SerpinB1 treatment of islets modulated proteins in growth/survival pathways. Together, these data implicate serpinB1 as an endogenous protein that can potentially be harnessed to enhance functional β cell mass in patients with diabetes.

INTRODUCTION

While the etiopathogenesis of type 1 and type 2 diabetes is different (Boitard, 2012; Muoio and Newgard, 2008), a paucity of functional β cell mass is a central feature in both diseases (Butler et al., 2003; Henquin and Rahier, 2011; Lysy et al., 2013). Currently there is considerable interest in developing safe approaches to replenish bioactive insulin in patients with diabetes by deriving insulin-producing cells from pluripotent cells (D'Amour et al., 2006; Kroon et al., 2008; Pagliuca et al., 2014; Rezania et al., 2014) or promoting proliferation of pre-existing β cells (Dor et al., 2004; El Ouaamari et al., 2013; Yi et al., 2013). While the former approach continues to evolve, several groups have focused on identifying growth factors, hormones, and/or signaling proteins to promote β cell proliferation (cited in El Ouaamari et al., 2013 and Dirice et al., 2014). Compared to rodents, adult human β cells are contumacious to proliferation and have been suggested to turnover very slowly, with the β cell mass reaching a peak by early adulthood (Butler et al., 2003; Gregg et al., 2012; Kassem et al., 2000). Attempts to enhance human β cell proliferation have also been hampered by poor knowledge of the signaling pathways that promote cell-cycle progression (Bernal-Mizrachi et al., 2014; Kulkarni et al., 2012; Stewart et al., 2015). While two recent studies have reported the identification of a small molecule, harmine (Wang et al., 2015), and denosumab, a drug approved for the treatment of osteoporosis (Kondegowda et al., 2015) to increase human β cell proliferation, the identification of endogenous circulating factors that have the ability to replenish insulin-secreting cells is attractive for therapeutic purposes. We previously reported (Flier et al., 2001) that compensatory β cell growth in response to insulin resistance is mediated, in part, by liver-derived circulating factors in the liver-specific insulin receptor knockout (LIRKO) mouse, a model that exhibits significant hyperplasia of islets without compromising β cell secretory responses to metabolic or hormonal stimuli (El Ouaamari et al., 2013). Here we report the identification of serpinB1 as a liver-derived secretory protein that promotes proliferation of human, mouse, and zebrafish β cells.

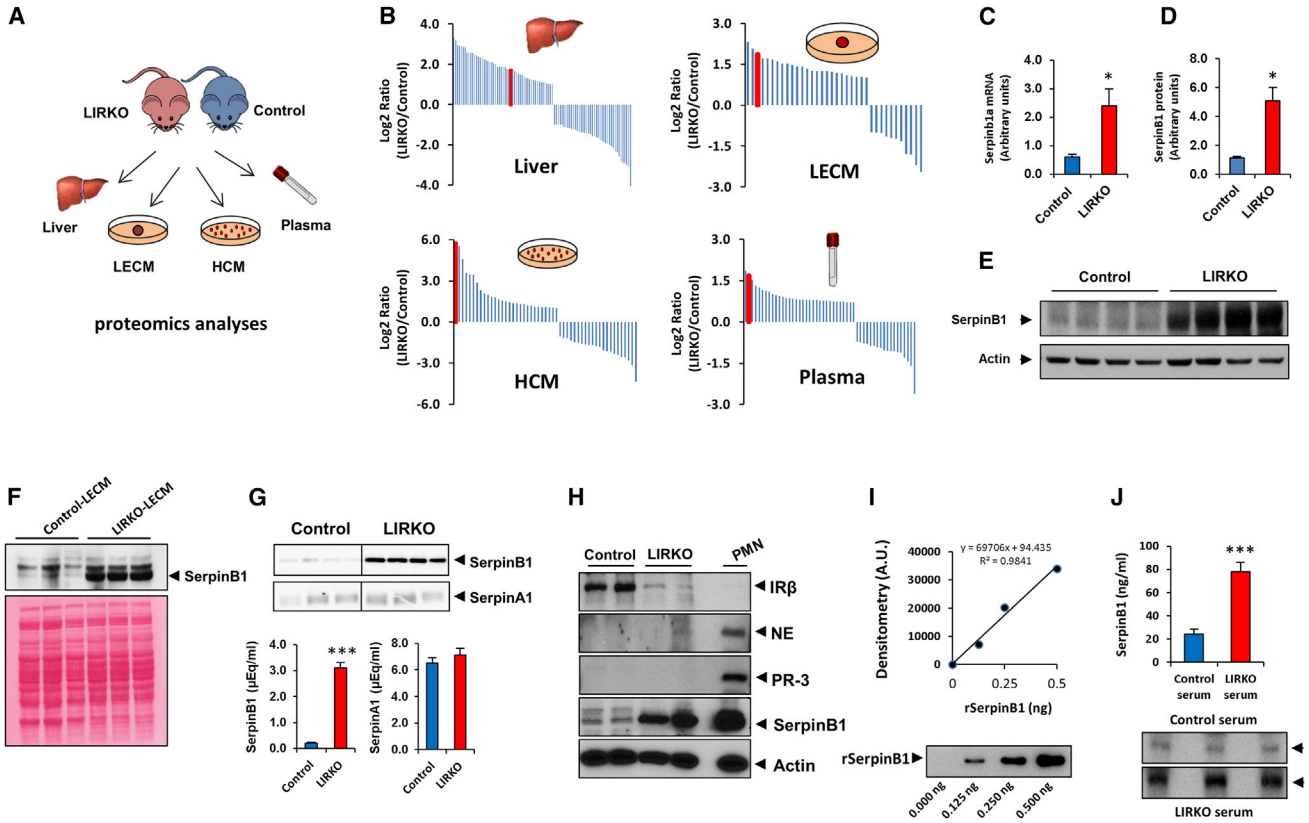

Figure 1. Identification of SerpinB1 in the LIRKO Model

(A) Experimental workflow for analysis of proteins from liver, liver explant-conditioned media (LECM), hepatocyte-conditioned media (HCM), and plasma.

(B) Identification of serpinB1 by LC-MS/MS proteomics. Protein abundances were quantified based on spectral counts, and top differentially expressed proteins were plotted as $\log_2$ ratio of LIRKO versus control. Red bars correspond to serpinB1.

(C) Relative quantification of liver *serpinb1a* mRNA by qRT-PCR (normalized to TBP). Data represent mean ± SEM; *p ≤ 0.05 (n = 6 per group).

(D) Quantification of serpinB1 protein (in E) in 12-week-old male control and LIRKO mice.

(E) Western blot of serpinB1 in liver. SerpinB1 protein was normalized to actin, and data represent mean ± SEM; *p ≤ 0.05 (n = 4–5 per group).

(F) Western blot (top panel) of serpinB1 in LECM from 12-week-old male control and LIRKO mice. Bottom panel shows Ponceau S staining of protein.

(G) Western blot of serpinB1 and serpinA1 (α1-antitrypsin) in LECM from control or LIRKO mice (10-week-old males). The bands (top panel) were quantified (bottom panel) relative to human SerpinB1 and human SerpinA1 run in parallel as standards. Data represent mean ± SEM; ***p ≤ 0.001 (n = 3–4 per group).

(H) Western blot of insulin receptor, serpinB1, neutrophil elastase (NE), and proteinase-3 (PR-3) in hepatocytes from 12-week-old male control or LIRKO mice. IR-β, insulin receptor beta subunit; NE, neutrophil elastase; PR-3, proteinase-3; PMN; polymorphonuclear leukocytes.

(I and J) Analysis of serpinB1 by western blot in serum derived from 12-week-old male control or LIRKO mice. Quantification of serpinB1 bands in (J) is based on parallel standard curve of recombinant human SerpinB1 shown in (I). Data represent mean ± SEM; ***p ≤ 0.01 (n = 10–12 per group).

RESULTS

Identification of SerpinB1 as a Hepatocyte-Derived Circulating Protein in LIRKO Mice

To identify the putative β cell trophic factor in the LIRKO model, we performed mass spectrometry (MS)-based proteomics analyses of liver, liver explant-conditioned media (LECM), hepatocyte-conditioned media (HCM), and plasma from control or LIRKO animals (Figure 1A). Data analysis pointed to serpinB1 as the top significantly upregulated protein in all samples with substantial increases in liver (~3.3-fold), LECM (~3.7-fold), HCM (~54-fold), and plasma (~3.3-fold) (Figure 1B; red bars indicate serpinB1). To validate the proteomics data, we examined liver expression and circulating levels of serpinB1 in the LIRKO mouse. RT-PCR and western blotting experiments using cross-reactive antibody to human SerpinB1 revealed that serpinB1 mRNA (LIRKO 2.4 ± 0.6 versus control 0.6 ± 0.1, $p < 0.05$, $n = 6$) and protein levels (LIRKO 5.1 ± 0.9 versus control 1.1 ± 0.06, $p < 0.05$, $n = 4–5$) were elevated by 5-fold in 12-week-old LIRKO mice compared to age-matched controls (Figures 1C–1E). Western blot analyses showed increased levels of serpinB1 in LIRKO-LECM (Figure 1F). SerpinA1 (also called α1-antitrypsin), which has partially overlapping biochemical activity, was not increased in LECM of LIRKO mice (Figure 1G). Importantly, we observed that serpinB1 is increased in LIRKO hepatocyte lysates where neutrophil markers such as proteinase-3 (PR-3) and neutrophil elastase (NE) were not detected, therefore excluding contaminating blood cells as a significant source of serpinB1 (Figure 1H). We used recombinant human SerpinB1 (rSerpinB1) to introduce a standard curve in western blotting experiments to provide a semiquantitative measure of serpinB1 in serum samples (Figure 1I). Circulating serpinB1

was elevated in sera from 6-month-old LIRKO mice (78 ± 7.9 versus control 24.2 ± 4.2 ng equivalents/ml, $p < 0.01$, $n = 10–12$) (Figure 1J).

Serpins are a highly conserved superfamily of ~45 kDa proteins, which are classified in 16 clades from A to P, and 36 members have been identified in humans (Silverman et al., 2001) and are known to regulate important proteolytic events. SerpinB1 is an evolutionarily conserved member of serpin clade B (Benarafa and Remold-O'Donnell, 2005) and inhibits the activity of several proteases including neutrophil elastase, cathepsin G, and proteinase-3 (Cooley et al., 2001). While serpinB1 lacks the hydrophobic signal peptide commonly harbored by secretory proteins (Remold-O'Donnell, 1993), the protein is detectable in hepatic-conditioned media and serum, suggesting that its release is mediated by an unconventional pathway (Nickel, 2010). Since previous studies reported a caspase-1-dependent mechanism of unconventional secretion (Becker et al., 2009; Chakraborty et al., 2013; Keller et al., 2008), we used human primary keratinocytes to investigate whether SerpinB1 secretion requires intact caspase-1. Consistent with previous reports (Chakraborty et al., 2013; Feldmeyer et al., 2007), irradiation of human keratinocytes with UVB light activated the inflammasome and induced release of several pro-inflammatory cytokines including IL-1β and IL-18, concomitant with caspase-1 activation. SerpinB1 is released in culture media when keratinocytes were UVB-irradiated; when caspase-1 was downregulated by a siRNA approach the SerpinB1 secretion was abolished, as was secretion of IL-1β and IL-18 (Figure S1A). Similar observations were evident when cells were treated with the caspase-1 inhibitor YVAD or pan-caspase inhibitor VAD prior to UVB treatment (Figure S1B). We also detected SerpinB1 in supernatants from cultured HepG2 cells and observed that several inflammatory molecules stimulate its release upon short-term (5 hr) or long-term (24 hr) treatment (Figure S1C). Consistent with increased levels of serpinB1 in LECM and serum from LIRKO mice, we found that caspase-1 mRNA and protein levels are increased in liver derived from LIRKO versus control groups (Figure S1D). Active caspase-1 (p20) was also highly abundant in LIRKO-LECM when compared to control conditions (Figure S1E).

To explore the clinical significance of SerpinB1 in humans, we developed an ELISA to measure plasma levels of SerpinB1 and observed that its concentration in healthy individuals ranges between 10 and 20 ng/ml (Figure S2A). Furthermore, a multivariate analysis in a cohort of 49 individuals with risk factor(s) for type 2 diabetes revealed that the range in concentration was greater, generally 4–56 ng/ml; however, interestingly, one individual with morbid obesity without diabetes (BMI = 59) exhibited extremely high levels (299 ng/ml) of circulating serpinB1. In a multivariate analysis, excluding this outlier, a positive correlation between circulating serpinB1 and insulin resistance ($R^2 = 0.15$, $p = 0.026$) was observed, using BMI and the composite insulin sensitivity index (CISI, Matsuda index) (Matsuda and DeFronzo, 1999) as covariates for measures of insulin sensitivity (Figure S2B). Furthermore, a search for missense variants of the corresponding gene in whole-exome sequencing data generated for 52 Joslin families with autosomal dominant diabetes showed that one of the families (for individual characteristics, see Table S1) carried a previously described variant (rs114597282, c.A269G, p.N90S) having a frequency of 1.7% among African Americans and 0.01% among Europeans in the NHLBI Exome Sequencing Project (ESP) database. The variant segregated with diabetes in this family, with all four diabetic members being heterozygous for this substitution (transmission disequilibrium test p value = 0.046) and only one non-penetrant individual being present in the youngest generation (Figure S2C). This variant is conserved among species (GERP score = 5.44) and is predicted as "probably damaging" by Polyphen (score = 0.98) and other prediction algorithms. Taken together, the significantly elevated serpinB1 in serum and hepatocyte secretome (HCM) in the LIRKO model, its presence in human sera, and its elevation in insulin-resistant states in humans, as well as the segregation of a genetic variant of *serpinb1* with human diabetes prompted us to focus on this protein as a potential β cell growth factor.

SerpinB1 and Its Partial Mimics Promote Proliferation of Pancreatic β Cells in Multiple Species

To address whether serpinB1 promotes β cell proliferation, we cultured mouse islets in the presence of recombinant human serpinB1 or ovalbumin and evaluated proliferation by Ki67 immunofluorescence staining. Ovalbumin, encoded by *serpinb14*, was chosen as control because it is a serpin closely related in structure to serpinB1 but lacks protease inhibitory activity (Benarafa and Remold-O'Donnell, 2005). Ovalbumin-treated mouse islets displayed low β cell proliferation comparable to non-treated islets; rSerpinB1-treated islets exhibited a dose-dependent effect, and a 2-fold increase in the percentage of $Ki67^+$ $insulin^+$ cells was observed at the dose of 1 μg/ml (Figures 2A and 2B). We next tested whether small-molecule pharmacological agents that inhibit elastinolytic proteases, and thus partially mimic serpinB1 activity, GW311616A (Macdonald et al., 2001), and sivelestat (Kawabata et al., 1991), would affect β cell proliferation. Treatment of islets freshly isolated from male C57Bl/6 mice with GW311616A or sivelestat increased β cell proliferation (Figures 2C and 2D). To further explore the role of serpinB1 in vivo, we administered 7- to 8-week-old C57Bl/6 male mice with GW311616A, a partial mimic of serpinB1, by oral gavage (2 mg/kg/day for 2 weeks). Morphometric analyses showed that GW311616A treatment enhanced β cell mass (Figures 2E and 2F) by increasing β cell, but not α cell, proliferation as assessed by BrdU incorporation (Figures 2G and 2H). The lack of proliferation in extra-pancreatic tissues including liver, skeletal muscle, visceral and subcutaneous adipose tissues, spleen, and kidney (Figures S3A and S3B) suggests that GW311616A promotes selective β cell proliferation. The proliferative action of SerpinB1 was also evident in human β cells using islets obtained from 7 cadaveric organ donors (for donor characteristics, see Table S2). Quantification of $Ki67^+$ $insulin^+$ cells revealed that the number of proliferating β cells increased in islets cultured in serpinB1-containing media (Figures 2I and 2J). The percent of proliferating human β cells is in a range similar to those reported previously (El Ouaamari et al., 2013; Jiao et al., 2014; Rieck et al., 2012; Rutti et al., 2012; Walpita et al., 2012). Similar to its effect on mouse islets, sivelestat also increased proliferation of human β cells (Figures 2K–2M; for donor characteristics, see Table S3). To test whether sivelestat induces human β cell proliferation in vivo, we transplanted human islets (obtained from the Integrated Islet Distribution Program, IIDP) under the kidney capsule of 10-week-old male

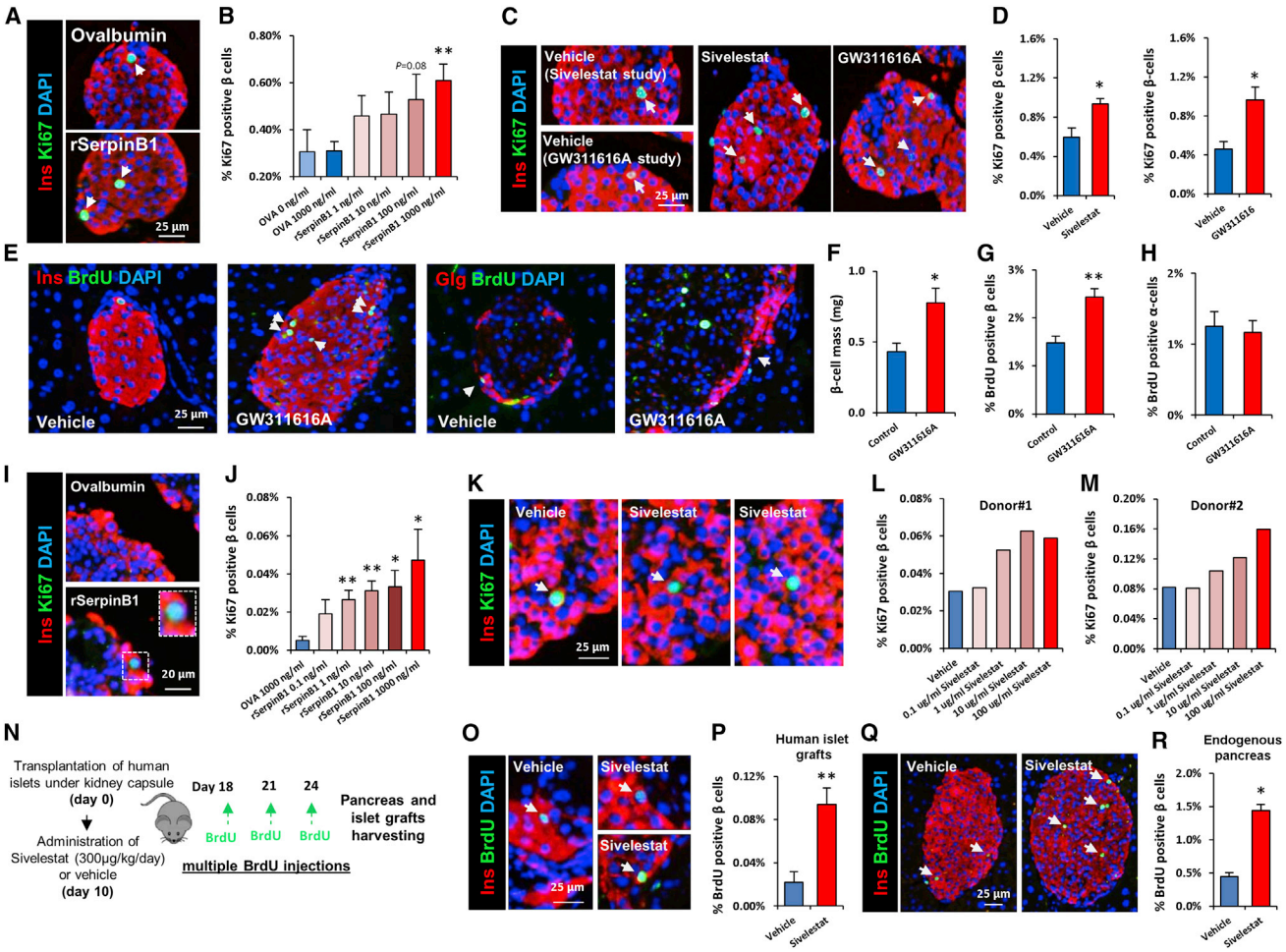

Figure 2. SerpinB1 and Its Partial Mimics Promote Proliferation of Mouse and Human Pancreatic β Cells

(A) Representative images of mouse islets treated with ovalbumin or SerpinB1 and co-immunostained for Ki67, insulin, and DAPI.

(B) Quantification of Ki67$^+$ insulin$^+$ cells (in A). Data represent mean ± SEM; **p ≤ 0.01 (n = 6–12 per group).

(C) Representative images and quantitation of insulin$^+$ Ki67$^+$ cells of islets isolated from wild-type male mice and cultured for 48 hr in the presence of 100 μg/ml of either sivelestat or GW311616A.

(D) Quantification of insulin$^+$ Ki67$^+$ cells of sivelestat-treated islets (in C). Data represent mean ± SEM; *p ≤ 0.05 (n = 3 per group for GW311616A studies and n = 6 per group for sivelestat studies). 5- to 6-week-old wild-type male mice were treated with GW311616A for 2 weeks. Islet β cell and α cell proliferation was assessed by immunostaining.

(E) Pancreatic sections co-immunostained for BrdU and insulin and DAPI (two left panels) or co-immunostained for glucagon and BrdU and DAPI (two right panels).

(F) Quantification of β cell mass (in E). Data represent mean ± SEM; *p ≤ 0.05 (n = 4–5 per group).

(G) Quantification of insulin$^+$ BrdU$^+$ cells (in E). Data represent mean ± SEM; **p ≤ 0.01 (n = 4–5 per group).

(H) Quantification of glucagon$^+$ BrdU$^+$ cells (in E). Data represent mean ± SEM; **p ≤ 0.01 (n = 4–5 per group).

(I) Representative images of human islets treated with ovalbumin or SerpinB1 and co-immunostained for Ki67, insulin, and DAPI.

(J) Quantification of Ki67$^+$ insulin$^+$ cells (in I). Data represent mean ± SEM; *p ≤ 0.05, **p ≤ 0.01 (n = 7 per group). For details of the human donors please see Table S2.

(K) Representative images of human islets treated with vehicle or sivelestat and co-immunostained for Ki67, insulin, and DAPI.

(L and M) Quantification of Ki67$^+$ insulin$^+$ cells (in K). For details of human donors (Donor #1, L; Donor #2, M) please see Table S3.

(N) Experimental workflow for transplantation studies to explore the effects of sivelestat on human β cell proliferation in vivo.

(O) Representative images of human islet grafts retrieved from mice treated with sivelestat or vehicle and co-immunostained for BrdU, insulin, and DAPI.

(P) Quantification of BrdU$^+$ insulin$^+$ cells (in O).

(Q) Representative images of endogenous pancreases harvested from mice treated with sivelestat or vehicle and co-immunostained for BrdU, insulin, and DAPI.

(R) Quantification of BrdU$^+$ insulin$^+$ cells (in Q). For details of human donors please see Table S3. Data represent mean ± SEM; *p ≤ 0.05, **p ≤ 0.01 (n = 5–6 per group for retrieved human islet grafts and n = 3 for endogenous pancreas). Arrows indicate proliferating cells.

non-obese diabetic-severe combined immunodeficiency-IL2rγ^{null} (NSG) mice (Greiner et al., 2011). At 10 days post-transplantation, osmotic pumps loaded with sivelestat (300 μg/kg/day) or vehicle were implanted into the mice and allowed to infuse for 14 days. Mice were provided BrdU in drinking water (80 mg/ml) during the 14-day treatment period and received intraperitoneal injections of BrdU (100 mg/kg body weight) on days 8, 11, and 14 post-transplantation. At 5 hr after the last

BrdU injection islet grafts and endogenous pancreases were harvested to assess β cell proliferation (Figure 2N). As assessed by co-immunostaining with anti-insulin and anti-BrdU antibodies, human islet grafts retrieved from mice treated with sivelestat exhibited higher β cell proliferation compared to vehicle-treated controls (Figures 2O and 2P). In parallel, islet β cell proliferation was also increased in endogenous pancreases harvested from NSG mice infused with sivelestat (Figures 2Q and 2R). The in vivo effect of sivelestat on β cell proliferation was also evident in C57Bl/6 mice (Figures S4A and S4B).

Next, to determine whether the potentiation of β cell proliferation by *serpinb1* is conserved across species, we examined *serpinb1*-overexpressing zebrafish larvae (Figure 3A). Whereas the human clade B serpin loci encode 13 proteins (serpinB1–13) with distinct functions, the corresponding locus in zebrafish is substantially simpler: it includes a distinct serpinb1 orthologous gene with a strikingly conserved reactive center loop, suggesting conserved function (Benarafa and Remold-O'Donnell, 2005). The overexpressing larvae were generated by cloning *serpinb1* downstream of a ubiquitous promoter (*beta-actin*), i.e., generating widespread mosaic overexpression of *serpinb1* (see details in Supplemental Experimental Procedures). The same cloning procedure was performed for the controls H2A-mCherry and *serpina7* (another member of the zebrafish Serpin family). We started by determining serpinb1's effect on β cell regeneration using different transgenic zebrafish larvae expressing nitroreductase (NTR)—an enzyme that converts metronidazole to a cytotoxic product—under the control of the insulin promoter; incubating these larvae in metronidazole results in the specific ablation of their β cells (Andersson et al., 2012). Each construct was injected, together with mRNA encoding transposase, into 1-cell-stage *Tg(ins:CFP-NTR);Tg(ins:Kaede)* embryos, giving rise to zebrafish larvae in which the β cells are visualized by the GFP Kaede. From 3 to 4 days post fertilization (dpf), we used metronidazole to ablate the β cells of mosaically overexpressing larvae and control larvae, and at 6 dpf we examined whether overexpression of any of the proteins had increased β cell regeneration. Overexpression of *serpinb1* strikingly increased regeneration of the β cell mass by 50%, whereas none of the controls had a significant effect (Figures 3B–3F). To determine serpinb1's effect on β cell proliferation, we examined the incorporation of EdU as an indicator of DNA replication. We exposed *Tg(ins:-flag-NTR);Tg(ins:H2B-GFP)* larvae to metronidazole from 3 to 4 dpf to ablate the β cells and then incubated control and *bactin:serpinb1*-overexpressing larvae with EdU from 4 to 6 dpf (Figures 3G and 3H). Overexpression of *serpinb1* significantly increased the total number of β cells, as well as doubled the number of β cells incorporating EdU, when compared to control larvae (Figures 3I and 3J). We next assessed the effect of serpinb1 on β cell formation during development, rather than regeneration, of the pancreas. To examine the total number of β cells, as well as their proliferation, we exposed *Tg(ins:H2B-GFP)* control and *bactin:serpinb1*-overexpressing larvae to EdU from 4 to 6 dpf (Figures 3K and 3L). Serpinb1 did not significantly increase the total number of β cells, but it significantly increased the number of β cells that incorporated EdU (Figures 3M and 3N). Together, these data provide evidence for serpinB1 as a phylogenetically conserved protein that stimulates β cell proliferation in multiple species including zebrafish, mouse, and man.

SerpinB1 Deficiency Leads to Maladaptive β Cell Proliferation in Insulin-Resistant States

To assess the in vivo relevance of serpinB1 in the adaptive β cell response to insulin-resistant states, we challenged control or *serpinb1a*-deficient (serpinB1KO) mice with stimuli that caused acute or chronic insulin resistance. To evaluate the response to acute insulin resistance, we adopted two approaches: first, we treated 16-week-old control male mice with the insulin receptor antagonist S961 (10 nmoles/week) for 2 weeks (Figure S5A) and observed progressive hyperglycemia in the mice (Figure S5B) as previously described (Yi et al., 2013). SerpinB1KO mice treated with S961 peptide showed elevated random-fed blood glucose that was higher when compared to S961-treated controls. No differences were observed in blood glucose levels between PBS-treated control and serpinB1KO mice (Figure S5B). Quantitation of proliferation by co-immunostaining $BrdU^+$ $insulin^+$ cells revealed an ~10-fold increase in S961-infused mice when compared to respective PBS-treated controls (Figures S5C and S5D). Importantly, while PBS-infused serpinB1KO mice showed a low level of proliferating β cells similar to PBS-infused controls, S961-treated serpinB1KO mice showed a detectable, but attenuated, response; the number of $BrdU^+$ $insulin^+$ cells was ~40% fewer compared with S961-treated control mice (Figures S5C and S5D). The reduction in adaptive β cell proliferation was supported by an attenuated increase in the number of β cells that co-stained positive for phospho-histone H3 (pHH3), an additional marker of cell proliferation (Figure S5E). In a second model, we fed 16-week-old control and serpinB1KO mice with 60% kcal high-fat diet (HFD) for 10 weeks and analyzed β cell proliferation by BrdU incorporation and immunofluorescence staining. An ~50% reduction in the number of $BrdU^+$ $insulin^+$ cells in serpinB1KO-HFD mice compared to age-matched control-HFD mice (Figures S5F and S5G) suggested impaired compensatory β cell proliferation; this was confirmed by staining for two additional proliferation markers including pHH3 (Figures S5H and S5I) and Ki67 (Figures S5J and S5K). However, we did not observe significant alterations in β cell mass in serpinB1KO as compared to control mice in either the S961 or the short-term HFD models, suggesting that additional factors likely contribute to increasing the β cell mass in these short-term insulin resistance models. In a third model, we explored whether *serpinb1* is critical for long-term β cell response by subjecting 8-week-old control and serpinB1KO mice to low- or high-fat diets (LFD or HFD) for 30 weeks, which led to chronic insulin resistance as shown by hyperinsulinemia in both groups (control, LFD: 1.5 ± 0.2 versus HFD: 9.6 ± 1.5 ng/ml; $p < 0.05$; serpinB1KO, LFD: 1.8 ± 0.2 versus HFD: 3.7 ± 0.7 ng/ml; $p < 0.05$, $n = 4–5$). As expected, control mice challenged with HFD, compared to the corresponding LFD cohort, showed enhanced β cell proliferation and mass. In contrast, mice lacking *serpinb1* challenged with a similar HFD showed significantly lower increases in β cell proliferation and mass (Figures 4A–4E). Taken together, these data suggest that the effects of serpinb1 for β cell compensatory hyperplasia are more apparent in chronic insulin resistance.

SerpinB1 Activates Proteins in the Growth Factor Signaling Pathway

To demonstrate whether protease inhibitory activity is critical for enhancement of β cell proliferation by SerpinB1, we tested

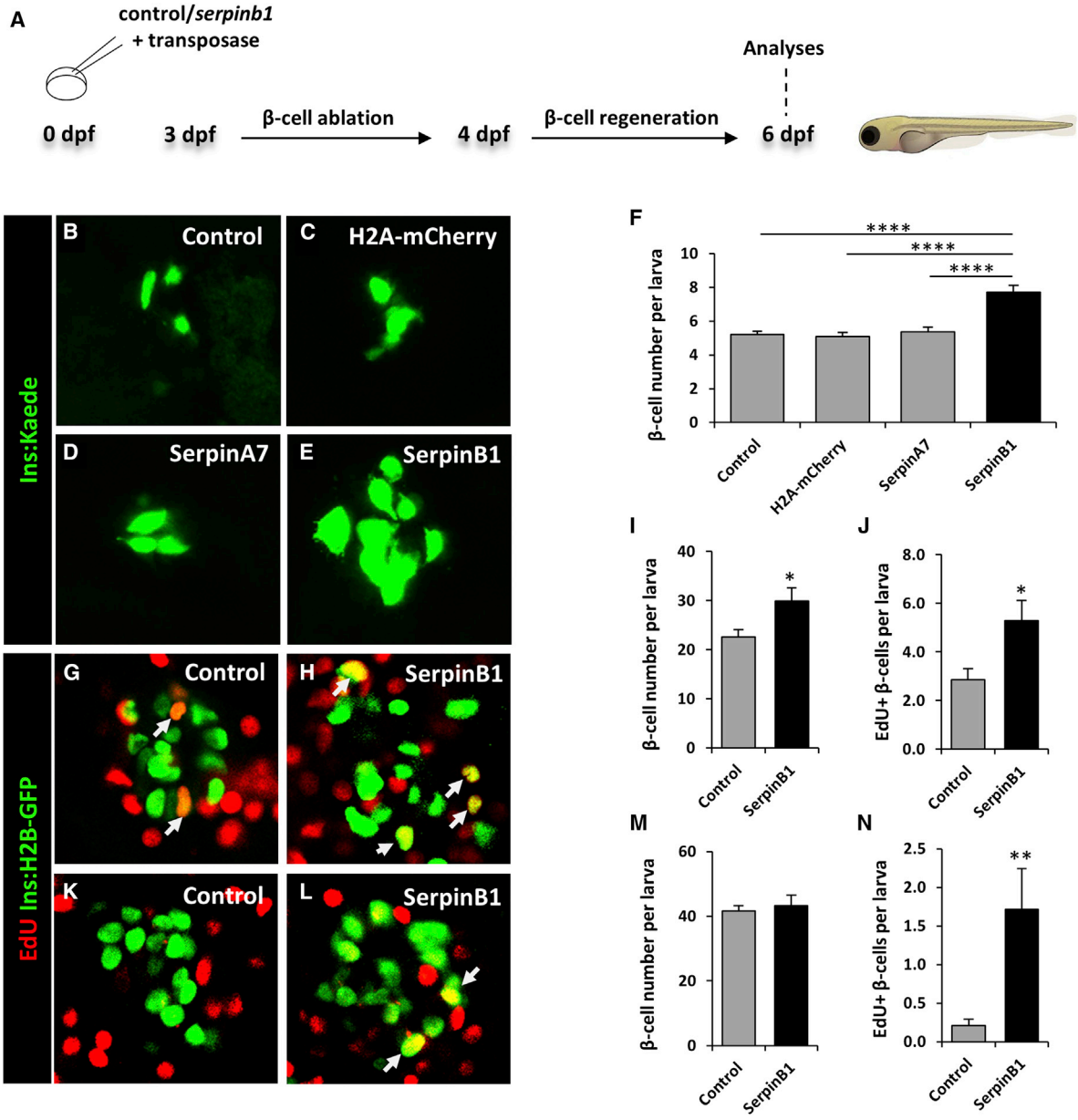

Figure 3. Overexpression of Serpinb1 in Zebrafish Enhances β Cell Regeneration and Proliferation

(A) Schematic of experimental plan.

(B–E) Representative images at 6 dpf of *Tg(ins:kaede);Tg(ins:CFP-NTR)* transgenic larvae that had not been injected (control), or were injected at the 1-cell stage with transposase mRNA + *bactin*:H2A-mCherry, *bactin:serpina7*, or *bactin:serpinb1*; were subjected to β cell ablation by metronidazole during 3–4 dpf; and were subsequently allowed to regenerate for 2 days.

(F) Quantification of β cell regeneration at 6 dpf in control (n = 87), *bactin:H2A-mCherry*-overexpressing (n = 61), *bactin:serpina7*-overexpressing (n = 46), and *bactin:serpinb1*-overexpressing (n = 36) *Tg(ins:kaede);Tg(ins:CFP-NTR)* larvae.

(G–J) Control (n = 27) and *bactin:serpinb1*-overexpressing (n = 18) *Tg(ins:H2B-GFP);Tg(ins:Flag-NTR)* transgenics were treated with metronidazole from 3 to 4 dpf to ablate the β cells and subsequently incubated with EdU during regeneration from 4 to 6 dpf. Representative confocal images at 6 dpf of control (G) and *bactin:serpinb1*-overexpressing (H) larvae showing β cells in green and the β cells that had incorporated EdU in yellow (green and red overlap; arrowheads). (I) Quantification of the total number of β cells at 6 dpf. (J) Quantification of β cells that incorporated EdU during β cell regeneration from 4 to 6 dpf.

(K–N) To determine whether Serpinb1 affects β cell proliferation during regular development, we treated control (n = 25) and *bactin:serpinb1*-overexpressing *Tg(ins:H2B-GFP)* (n = 21) transgenic larvae with EdU from 4 to 6 dpf. Representative confocal images at 6 dpf of control (K) and *bactin:serpinb1*-overexpressing (L) larvae showing β cells in green and the β cells that had incorporated EdU in yellow (green and red overlap; arrowhead). (M) Quantification of the total number of β cells at 6 dpf. (N) Quantification of β cells that incorporated EdU from 4 to 6 dpf. Data shown are the mean ± SEM; ****$p < 0.0001$, **$p < 0.01$, *$p < 0.05$. Arrows indicate proliferating cells.

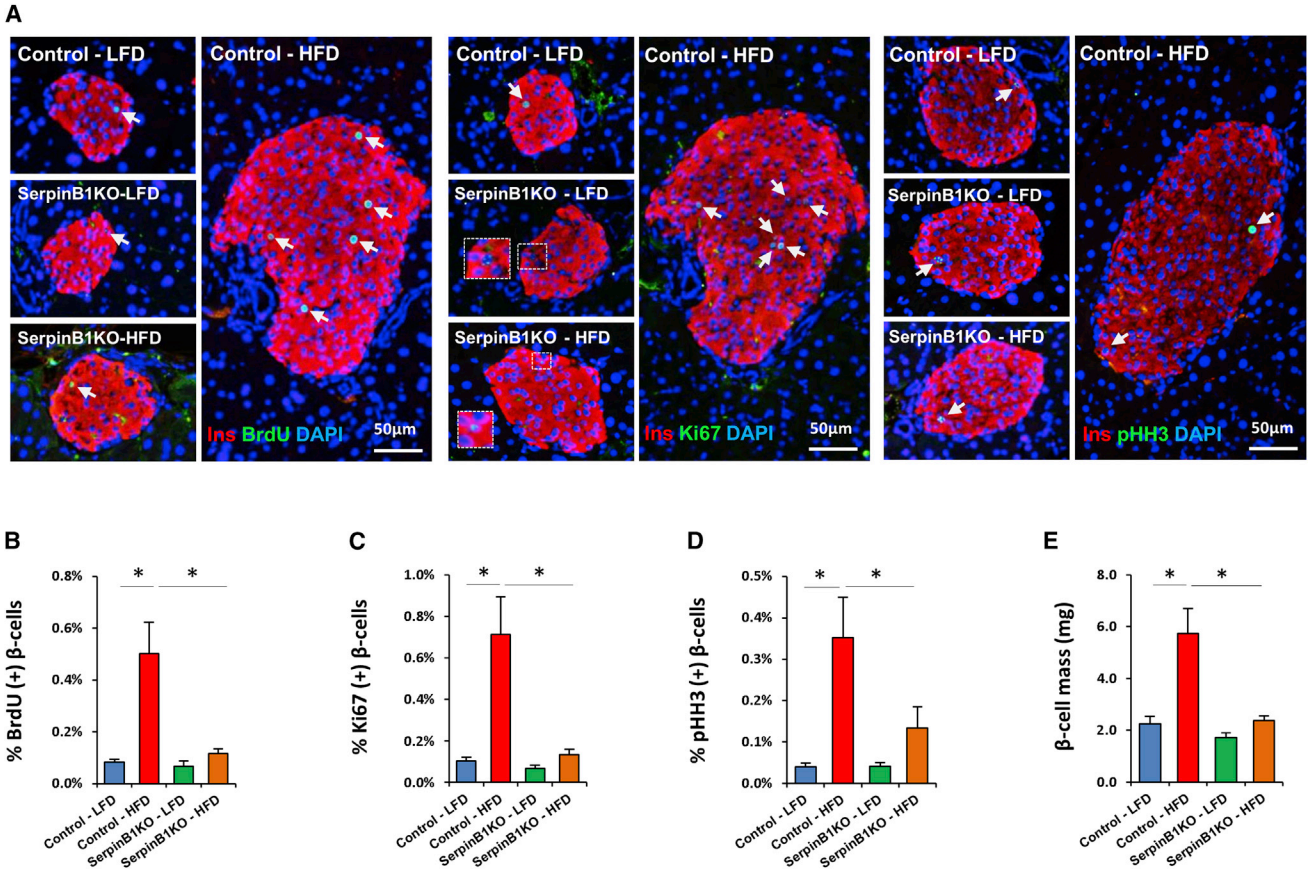

Figure 4. SerpinB1 Deficiency Leads to Maladaptive β Cell Proliferation in Insulin-Resistant States

8-week-old control or *serpinb1a*$^{-/-}$ (serpinB1KO) male mice were challenged with low-fat diet (LFD) or HFD for 30 weeks. 5 hr before sacrificing, mice were injected with BrdU (100 mg/kg body weight).

(A) Representative images of pancreases co-immunostained for BrdU and insulin and DAPI (left panel). Representative images of pancreases co-immunostained for Ki67 and insulin and DAPI (middle panel). Representative images of pancreases co-immunostained for pHH3 and insulin and DAPI (right panel).

(B) Quantification of BrdU^{+} insulin^{+} cells (in A).

(C) Quantification of Ki67^{+} insulin^{+} cells (in A).

(D) Quantification of pHH3^{+} insulin^{+} cells (in A).

(E) Measurement of β cell mass. Data represent mean ± SEM; *p $\leq$ 0.05 (n = 4–6 per group). Immunostaining for BrdU and Ki67 markers, shown in (A), were performed on consecutive sections. Arrows indicate proliferating cells.

different commercially available SerpinB1 recombinant proteins that bear a tag sequence at the N or C terminus. As reported previously, insect cell-derived SerpinB1, which is identical to the native protein (Cooley et al., 1998), forms a covalent complex (approximately 66 kD) with each of its target proteases (Cooley et al., 2001); this is shown for human neutrophil elastase (NE) and porcine pancreatic elastase (PE) (Figure 5A). Second, peptidase assays demonstrated that insect cell-derived untagged SerpinB1 from two independent preparations dose-dependently decreased activity of these proteases (shown for NE); however, the commercial proteins that are tagged at the N terminus (GeneCopoeia or OriGene) or C terminus (OriGene) only minimally inhibited peptidase activity of NE (Figure 5B). GeneCopoeia N-tagged SerpinB1 and OriGene C-tagged serpinB1 formed small amounts of complex, which was maximal with <0.1 or 0.3 molar equivalents NE, respectively, consistent with low inhibition in the peptidase assay; the OriGene C-tagged serpinB1 was also partially degraded (Figure 5C). For OriGene N-tagged serpinB1, no complex was detected on incubation with 0.3 molar equivalents of NE, and the recombinant serpin was completely degraded by NE; proteolytic degradation of the serpin by NE was confirmed by inactivating NE with DFP (diisopropyl fluorophosphate) (Amrein and Stossel, 1980) before use (Figure 5C). Insect cell-derived untagged serpinB1 was nearly quantitatively converted to complex or was further converted to the post-complex species, and importantly, no active 26 kDa NE band remained (Figure 5C). GeneCopoeia serpinB1, which lacks the ability to form a complex with neutrophil elastase and is unable to reduce peptidase activity, did not stimulate β cell proliferation as opposed to untagged serpinB1 (Figure 5D). These findings suggest that the ability to inhibit protease is a requirement that is necessary for the β cell proliferation-enhancing action of SerpinB1.

To gain initial insights into the signaling pathways mediating β cell proliferation in response to SerpinB1, we considered a phosphoproteomics approach. Protein phosphorylation has been

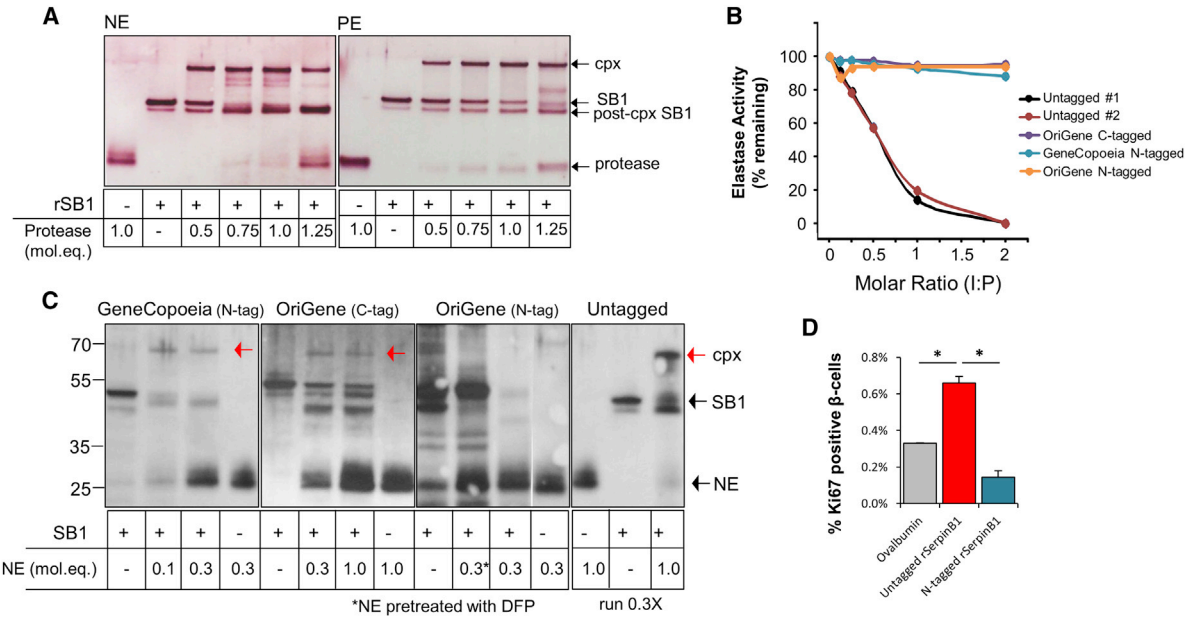

Figure 5. Protease Inhibitory Activity Is Involved in SerpinB1 Enhancement of β Cell Proliferation

(A) Activity of recombinant human SerpinB1 demonstrated by covalent complex formation with protease as previously described (Cooley et al., 2001). SerpinB1 (160 ng), generated in insect cells (see Experimental Procedures), was incubated with the indicated molar equivalents (mol.eq.) of human neutrophil elastase (NE) or porcine pancreatic elastase (PE) in 20 μl for 5 min at 37°C. Shown are reduced SDS gels gold-stained for total protein. Arrows indicate active SerpinB1 (42 kDa), NE or PE (26 kDa), complex (cpx, 66 kDa), and post-cpx (inactive) SerpinB1 (38 kDa).

(B) Activities of commercial recombinant SerpinB1 preparations and two preparations of insect cell-derived untagged SerpinB1 examined by peptidase inhibition. NE (500 ng) was combined with the indicated molar equivalents of SerpinB1 preparations in 150 μl, and the mixtures were incubated at 37°C for 3 min. The substrate Ala-Ala-Pro-Val-*p*-nitroanilide was added, and the change of OD_{405} nm was measured over 5 min. The *abscissa* shows the molar inhibitor:proteinase (I:P) ratio during the 3 min reaction.

(C) Activities of preparations of recombinant human serpinB1 examined by complex formation with NE. Equal amounts of SerpinB1 preparation (160 ng based on suppliers' information) was incubated with the indicated molar equivalents of NE for 5 min at 37°C. Shown are gold-stained reduced SDS gels. The three commercial products were examined on separate gels; insect cell-derived untagged SerpinB1 was examined on the same gel as the GeneCopoeia preparation, but only one-third of the reaction was run to avoid overloading. The NE control lane is shown twice (lanes 4 and 13) in lane 10; NE was inactivated with DFP (diisopropyl fluorophosphate) prior to incubation with the serpin. Red arrows in lanes 3, 7, and 15 indicate the covalent SerpinB1-NE complex. The lane, indicated by SB (-) and NE (0.3), in the experiment for Origene (N-tag) was spliced to follow the same order of samples in lanes shown in the experiments for GeneCopoeia (N-tag) and Origene (C-tag).

(D) Isolated islets of naive wild-type mice were stimulated with ovalbumin, insect cell-derived untagged SerpinB1, or N-tagged SerpinB1 from GeneCopoeia (1 μg/ml). Islets were embedded in agarose and immunostained for insulin and Ki67, and the nuclei were stained with DAPI. Quantification of $Ki67^+$ $insulin^+$ cells. Data represent mean ± SEM; *p < 0.05 (n = 3 per group).

long accepted as a major currency in signal transduction pathways, and cell proliferation is known to be regulated by signaling modules that include the MAP kinase pathways. Further, measurement of phosphorylation dynamics represents a more direct way to identify potential pathways and regulatory targets compared to other techniques, such as gene expression profiling. Briefly, isolated islets from C57Bl/6 male mice were cultured for 10, 30, or 120 min in the presence of 1 μg/ml of ovalbumin or SerpinB1. Subsequently, islets were subjected to phosphopeptide enrichment and LC-MS/MS analysis (Mertins et al., 2014) (Figure 6A). As shown by the heatmap (Figure 6B), a 10 min treatment with SerpinB1 had a minimal effect on the islet phosphoproteome. However, islets incubated with SerpinB1 for 30 or 120 min exhibited an enhanced phosphorylation of ~250 proteins with at least 2-fold change when compared to islets cultured with ovalbumin (for additional details, see data submitted to ProteomXchange with accession number PXD003182). The modulation of several phosphoproteins identified at 30 min was sustained 2 hr after SerpinB1 treatment. Ingenuity pathway analysis (IPA) revealed that SerpinB1 activated key proteins in the growth factor (insulin/IGF-1) signaling cascade. In early events (within 10 min), SerpinB1 stimulated MAPK3 phosphorylation, a kinase previously implicated in the proliferation of β cells (Hayes et al., 2013). Treatment for 30 or 120 min was characterized by activation of several proteins in the insulin/IGF-1 signaling cascade including IRS-2 (Kubota et al., 2004; Withers et al., 1998) and GSK3 (Liu et al., 2010). Finally, phosphoproteomics analyses also revealed increased phosphorylation of several proteins regulating cell survival and function, including protein kinase cAMP-dependent regulatory subunits (PRKAR1A, PRKAR1B, and PRKAR2B) (Hussain et al., 2006; Jhala et al., 2003) and phosphodiesterase 3B (PDE3B) (Härndahl et al., 2002). In independent experiments, we confirmed, by western blots, the altered phosphorylation of MAPK, PRKAR2B, and GSK3 subunits in response to treatment with SerpinB1 (Figures 6C–6E; lower panels show quantification). Incubation of freshly isolated islets with serpinB1 did not significantly affect glucose-stimulated secretion compared to

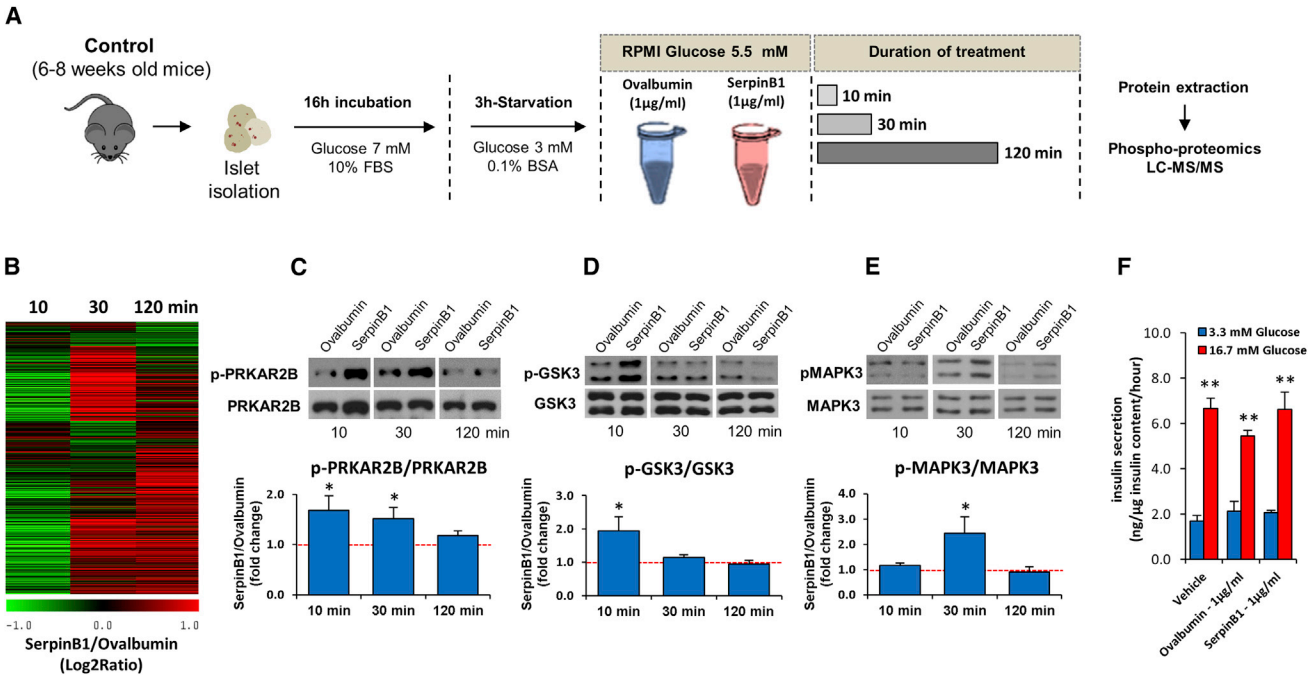

Figure 6. SerpinB1 Activates Proteins in the Growth Factor Signaling Pathway

(A) Schematic of experimental plan. Islets (100) isolated from male C57Bl/6 mice were treated for 10, 30, or 120 min (n = 3) with (1 μg/ml) ovalbumin or rSerpinB1 (insect cell derived), and islet lysates were analyzed by LC-MS/MS phosphoproteomics.

(B) Heatmap of the relative abundances of ~1,100 phosphopeptides in islets stimulated with SerpinB1 versus ovalbumin. The relative abundances were displayed as Log_2 Ratio (serpinB1/ovalbumin).

(C) Western blots (upper panel) and quantification (lower panel) of p-PRKAR2B/PRKAR2B in response to SerpinB1. Data represent mean ± SEM; *p < 0.05 (n = 5 per group).

(D) Western blots (upper panel) and quantification (lower panel) of p-GSK3/GSK3 in response to SerpinB1. Data represent mean ± SEM; *p < 0.05 (n = 5 per group).

(E) Western blots (upper panel) and quantification (lower panel) of p-MAPK3/MAPK3 in response to SerpinB1. Data represent mean ± SEM; *p < 0.05 (n = 5 per group).

(F) Glucose-stimulated insulin secretion (GSIS) in the presence of vehicle, ovalbumin (1 μg/ml), or rSerpinB1 (1 μg/ml). Data represent mean ± SEM; **p < 0.01 (n = 4 per group).

controls, suggesting that effects of serpinB1 on islet β cell proliferation do not adversely impact insulin secretion under the conditions tested (Figure 6F). Together, these data suggest that SerpinB1 enhances proliferation/survival by modulating proteins in the growth factor signaling pathway.

DISCUSSION

Identification of molecules that have the ability to enhance proliferation of terminally differentiated cells is a desirable goal in regenerative medicine, particularly in diabetes where β cell numbers are reduced. Here, we identified serpinB1 as an endogenous liver-derived secretory protein that stimulates human, mouse, and zebrafish β cell proliferation.

One interesting aspect of serpinB1 viewed as a secretory molecule is its lack of the classical hydrophobic signal peptide. Our data indicate that inflammation stimulates unconventional secretion of serpinB1 in a caspase-1-dependent manner. It is important to note, however, that the levels of several circulating cytokines in the LIRKO model are comparable to those observed in age-matched controls (El Ouaamari et al., 2013) and hence excludes systemic inflammation as a physiological factor triggering serpinB1 release in vivo. It is possible that the absence of insulin signaling in the liver interferes with caspase-1 activation and thus serpinB1 release. This notion is compatible with a previous report suggesting the suppressive role of insulin/IGF-1 in caspase-1 processing (Jung et al., 1996) and is consistent with increased levels of active caspase-1 in LIRKO-derived hepatocytes that are blind to insulin.

Since inhibition of proteases is SerpinB1's reported biochemical function to date (Cooley et al., 2001), we postulated that the enhancing effect of SerpinB1 on β cell proliferation involves the intermediacy of a protease. Indeed, recombinant SerpinB1 proteins lacking the ability to inhibit protease activity were unable to enhance β cell proliferation in vitro. This observation suggests that SerpinB1 neutralizes a protease that would otherwise interfere with proliferation. In fact, the small-molecule inhibitors of elastases, GW311616A and sivelestat, directly enhanced proliferation of mouse and human insulin-producing cells. The parallel findings for GW311616A, sivelestat, and SerpinB1 make elastases strong candidates. While SerpinB1 action could be explained by its ability to modulate phosphorylation of key molecules (e.g., MAPK3, GSK3β/α, and PKA) of the insulin/IGF-1 growth/survival pathways, it is unclear how SerpinB1

precisely regulates these pathways. One possibility is that these pathways are activated through SerpinB1-mediated protease inhibition, particularly inhibition of elastase molecules known to be expressed in pancreatic β cells (Kutlu et al., 2009). This idea is consistent with previous reports suggesting the role for neutrophil elastase in modulating proteins in the insulin/IGF-1 signaling pathway (Bristow et al., 2008; Houghton et al., 2010; Talukdar et al., 2012). Elucidation of interactions with other proteases such as proteinase-3 and cathepsin G in the β cell and its potential role in regulating insulin sensitivity will further assist in deciphering the signaling pathways activated by SerpinB1. Alternative possibilities that require further investigation include interactions with protease-activated receptors (PARs), which are expressed in islets (J.S., A.E.O., and R.N.K., unpublished data).

Using zebrafish, we determined that serpinB1's ability to potentiate β cell proliferation is conserved from fish to mammals. Moreover, in zebrafish we showed that serpinB1 can potentiate β cell proliferation in vivo analogous to the in vivo effects we observed in mouse and human islets. By ablating the β cells in zebrafish, we also observed that serpinB1 can stimulate β cell regeneration and warrants studies to examine its role during β cell development.

In sum, the identification of SerpinB1 as a conserved endogenous secretory protein that promotes proliferation of β cells across species constitutes an important step to achieve regeneration of functional β cells. While it is likely that additional factors will be identified, the next challenge will be to explore whether one or a combination of these factors can safely, specifically, and reversibly enhance human β cell mass with the long-term goal of restoring normoglycemia in patients with diabetes.

EXPERIMENTAL PROCEDURES

Animals

All mice studied were 6- to 8-week-old males on the C57BL/6 background, except where indicated otherwise. Mice were housed in pathogen-free facilities and maintained in the Animal Care Facilities at Joslin Diabetes Center, Boston, MA; Foster Biomedical Research Laboratory, Brandeis University, Waltham, MA; or Boston Children's Hospital. Studies conducted and protocols used were approved by the Institutional Animal Care and Use Committees of the Joslin Diabetes Center and/or Brandeis University and/or Boston Children's Hospital and were in accordance with National Institute of Health guidelines. See the Supplemental Experimental Procedures for details of the animal genotypes. For short-term studies, 16-week-old serpinB1KO and age-matched wild-type male mice were challenged with HFD (Research Diet, catalog# D12492) for 10 weeks. For long-term studies, 8-week-old serpinB1KO and age-matched wild-type male mice were fed with low-fat diet (Research Diet, catalog# D12450J) or HFD (Research Diet, catalog# D12492) for 30 weeks.

LECM and HCM Preparation

The preparation of liver explant-conditioned media (LECM) and hepatocyte-conditioned media (HCM) have been described previously (El Ouaamari et al., 2013). See Supplemental Experimental Procedures for additional information.

LC-MS/MS-Based Proteomics

Proteomic analyses were performed as previously described (Zhou et al., 2010). See Supplemental Experimental Procedures for additional information.

Mouse Islet Studies

Islets were isolated from 6- to 8-week-old male C57BL/6 mice using intraductal collagenase technique (El Ouaamari et al., 2013). Islets were hand-picked and cultured overnight in RPMI 1640 media containing 7 mM glucose and 10% fetal bovine serum (FBS) and penicillin/streptomycin (1% v/v). After 3 hr starvation in RPMI 1640 media containing 3 mM glucose and 0.1% BSA, islets were stimulated as indicated (with recombinant protein or small molecules) for 48 hr and then embedded in agarose and paraffin, sectioned, and used for immunostaining studies as described below and in El Ouaamari et al. (2013).

Human Islet Studies

Human islets were obtained from the Integrated Islet Distribution Program. All studies and protocols used were approved by the Joslin Diabetes Center's Committee on Human Studies (CHS#5-05). Upon receipt, islets were cultured overnight in Miami Media #1A (Cellgro). The islets were then starved in Final Wash/Culture Media (Cellgro) for 3 hr before being stimulated with Miami Media #1A supplemented with sivelestat or GW311616A. 24 hr later, islets were embedded in agarose and used for immunostaining studies (described below).

Immunostaining Studies

Pancreases and in vitro stimulated islets were analyzed by immunostaining using anti-Ki67 (BD), anti-phospho-histone H3 (pHH3) (Millipore), anti-BrdU (Dako), anti-insulin (Abcam), or anti-glucagon (Sigma-Aldrich) antibodies. Quantification of replicating β and α cells and calculation of β cell mass were performed as described previously (El Ouaamari et al., 2013).

Phosphoproteomics Analysis

Phosphoproteomics analyses were performed as described in the Supplemental Experimental Procedures. To validate the phosphoproteomics findings, frozen SerpinB1-treated and ovalbumin-treated islets were lysed in RIPA buffer (150 mM NaCl, 10 mM Tris [pH 7.2], 1% Triton X-100, 1% deoxycholate, 5 mM EDTA) containing 200 μM orthovanadate, protease, and phosphatase inhibitors (Sigma-Aldrich) (Liew et al., 2014) and subjected to western blot analyses. pMAPK3, total MAPK3, and total GSK3 antibodies are from Cell Signaling. pPRKAR2B and total PRKAR2B are from Santa Cruz. pGSK3 antibody is from Millipore.

RT-PCR

Total RNA was extracted and reverse transcribed, and qPCR was performed as outlined in the Supplemental Experimental Procedures.

Statistical Analysis

All data are presented as mean ± SEM. Data were analyzed using unpaired, two-tailed Student's t test, ANOVA, or multivariate analyses as appropriate, and a p value < 0.05 was considered statistically significant.

ACCESSION NUMBERS

The accession number for the mass spectrometry phosphoproteomics dataset reported in this paper is ProteomeXchange: PXD003182.

SUPPLEMENTAL INFORMATION

Supplemental Information includes Supplemental Experimental Procedures, five figures, and three tables and can be found with this article online at http://dx.doi.org/10.1016/j.cmet.2015.12.001.

AUTHOR CONTRIBUTIONS

A.E.O. and R.N.K. conceived of the idea, designed experiments, analyzed the data, and wrote/edited the manuscript. Individual experimental contributions are as follows: E.R.-O. and W.-J.Q. contributed equally to design of experiments, providing reagents, and writing/editing the manuscript; J.-Y.Z., M.A.G., R.D.S., and W.-J.Q. were responsible for proteomics and phosphoproteomics experiments; E.D. contributed to islet isolation and transplantation studies; N.G., J.H., J.B., J.S., D.F.D.J., S.K., S.B., G.Q., and C.W.L. provided technical assistance; H.-D.B. conducted serpinB1 secretion studies in keratinocytes; R.M. assisted with mouse experiments; L.H., J.G., and Y.G. conducted mouse experiments and ELISA and biochemical assays; A.B.G. provided

human samples and contributed to analysis of human ELISA assays; A.D. and P.J. provided data on the serpinB1 variant; C.K. and O.A. conducted zebrafish studies. All authors read and approved the manuscript.

ACKNOWLEDGMENTS

We thank C. Ronald Kahn, MD for sharing the LIRKO mouse model, Ping Li, MD for assistance with statistical analyses, Dr. Lauge Schäffer (Novo Nordisk) for providing the S961 compound, Drs. Wei-Min Chen and Michele Sale (University of Virginia) for useful discussions, and Sandra Roger for technical assistance. This work was supported by NIH RO1 DK67536 and RO1 DK103215 (to R.N.K.); RO1 DK55523 (to A.D. and R.N.K.); NIH RO1 HL066548, R21 AI103407, and an RRRC award from Boston Children's Hospital (to E.R.O); R01 DK 074795 and P41 GM103493 (to R.D.S.); UC4 DK104167 (to W.-J.Q. and R.N.K.); Société Francophone du Diabète, Association Française des Diabétiques, American Diabetes Association, and JDRF (3-APF-2014-182-A-N) (to A.E.O.); a grant from the Juvenile Diabetes Research Foundation/Sanofi Aventis Strategic Alliance (17-2011-644) (R.N.K.), and P30 DK036836 (DRC). Zebrafish experiments were performed at the Karolinska Institute and supported by the Ragnar Söderbergs Foundation and the Swedish Research Council (O.A.). Proteomics and phosphoproteomics experiments were performed in the Environmental Molecular Sciences Laboratory, a national scientific user facility sponsored by Department of Energy and located at Pacific Northwest National Laboratory, which is operated by Battelle Memorial Institute for the DOE under Contract DE-AC05-76RL0 1830. A.E.O. and R.N.K. are listed as inventors on a patent that is based on these studies.

Received: April 14, 2015
Revised: October 20, 2015
Accepted: November 30, 2015
Published: December 14, 2015

REFERENCES

Amrein, P.C., and Stossel, T.P. (1980). Prevention of degradation of human polymorphonuclear leukocyte proteins by diisopropylfluorophosphate. Blood *56*, 442–447.

Andersson, O., Adams, B.A., Yoo, D., Ellis, G.C., Gut, P., Anderson, R.M., German, M.S., and Stainier, D.Y. (2012). Adenosine signaling promotes regeneration of pancreatic β cells in vivo. Cell Metab. *15*, 885–894.

Becker, C.E., Creagh, E.M., and O'Neill, L.A. (2009). Rab39a binds caspase-1 and is required for caspase-1-dependent interleukin-1beta secretion. J. Biol. Chem. *284*, 34531–34537.

Benarafa, C., and Remold-O'Donnell, E. (2005). The ovalbumin serpins revisited: perspective from the chicken genome of clade B serpin evolution in vertebrates. Proc. Natl. Acad. Sci. USA *102*, 11367–11372.

Bernal-Mizrachi, E., Kulkarni, R.N., Scott, D.K., Mauvais-Jarvis, F., Stewart, A.F., and Garcia-Ocaña, A. (2014). Human β-cell proliferation and intracellular signaling part 2: still driving in the dark without a road map. Diabetes *63*, 819–831.

Boitard, C. (2012). Pancreatic islet autoimmunity. Presse Med. *41* (12 P 2), e636–e650.

Bristow, C.L., Wolkowicz, R., Trucy, M., Franklin, A., Di Meo, F., Kozlowski, M.T., Winston, R., and Arnold, R.R. (2008). NF-kappaB signaling, elastase localization, and phagocytosis differ in HIV-1 permissive and nonpermissive U937 clones. J. Immunol. *180*, 492–499.

Butler, A.E., Janson, J., Bonner-Weir, S., Ritzel, R., Rizza, R.A., and Butler, P.C. (2003). Beta-cell deficit and increased beta-cell apoptosis in humans with type 2 diabetes. Diabetes *52*, 102–110.

Chakraborty, R., Bhatt, K.H., and Sodhi, A. (2013). Ultraviolet B induces high mobility group box 1 release from mouse peritoneal macrophages in vitro via caspase-1 mediated secretion pathway. Immunobiology *218*, 135–144.

Cooley, J., Mathieu, B., Remold-O'Donnell, E., and Mandle, R.J. (1998). Production of recombinant human monocyte/neutrophil elastase inhibitor (rM/NEI). Protein Expr. Purif. *14*, 38–44.

Cooley, J., Takayama, T.K., Shapiro, S.D., Schechter, N.M., and Remold-O'Donnell, E. (2001). The serpin MNEI inhibits elastase-like and chymotrypsin-like serine proteases through efficient reactions at two active sites. Biochemistry *40*, 15762–15770.

D'Amour, K.A., Bang, A.G., Eliazer, S., Kelly, O.G., Agulnick, A.D., Smart, N.G., Moorman, M.A., Kroon, E., Carpenter, M.K., and Baetge, E.E. (2006). Production of pancreatic hormone-expressing endocrine cells from human embryonic stem cells. Nat. Biotechnol. *24*, 1392–1401.

Dirice, E., Kahraman, S., Jiang, W., El Ouaamari, A., De Jesus, D.F., Teo, A.K., Hu, J., Kawamori, D., Gaglia, J.L., Mathis, D., and Kulkarni, R.N. (2014). Soluble factors secreted by T cells promote β-cell proliferation. Diabetes *63*, 188–202.

Dor, Y., Brown, J., Martinez, O.I., and Melton, D.A. (2004). Adult pancreatic beta-cells are formed by self-duplication rather than stem-cell differentiation. Nature *429*, 41–46.

El Ouaamari, A., Kawamori, D., Dirice, E., Liew, C.W., Shadrach, J.L., Hu, J., Katsuta, H., Hollister-Lock, J., Qian, W.J., Wagers, A.J., and Kulkarni, R.N. (2013). Liver-derived systemic factors drive β cell hyperplasia in insulin-resistant states. Cell Rep. *3*, 401–410.

Feldmeyer, L., Keller, M., Niklaus, G., Hohl, D., Werner, S., and Beer, H.D. (2007). The inflammasome mediates UVB-induced activation and secretion of interleukin-1beta by keratinocytes. Curr. Biol. *17*, 1140–1145.

Flier, S.N., Kulkarni, R.N., and Kahn, C.R. (2001). Proc Natl Acad Sci *98*, 7475–7480.

Gregg, B.E., Moore, P.C., Demozay, D., Hall, B.A., Li, M., Husain, A., Wright, A.J., Atkinson, M.A., and Rhodes, C.J. (2012). Formation of a human β-cell population within pancreatic islets is set early in life. J. Clin. Endocrinol. Metab. *97*, 3197–3206.

Greiner, D.L., Brehm, M.A., Hosur, V., Harlan, D.M., Powers, A.C., and Shultz, L.D. (2011). Humanized mice for the study of type 1 and type 2 diabetes. Ann. N Y Acad. Sci. *1245*, 55–58.

Härndahl, L., Jing, X.J., Ivarsson, R., Degerman, E., Ahrén, B., Manganiello, V.C., Renström, E., and Holst, L.S. (2002). Important role of phosphodiesterase 3B for the stimulatory action of cAMP on pancreatic beta-cell exocytosis and release of insulin. J. Biol. Chem. *277*, 37446–37455.

Hayes, H.L., Moss, L.G., Schisler, J.C., Haldeman, J.M., Zhang, Z., Rosenberg, P.B., Newgard, C.B., and Hohmeier, H.E. (2013). Pdx-1 activates islet α- and β-cell proliferation via a mechanism regulated by transient receptor potential cation channels 3 and 6 and extracellular signal-regulated kinases 1 and 2. Mol. Cell. Biol. *33*, 4017–4029.

Henquin, J.C., and Rahier, J. (2011). Pancreatic alpha cell mass in European subjects with type 2 diabetes. Diabetologia *54*, 1720–1725.

Houghton, A.M., Rzymkiewicz, D.M., Ji, H., Gregory, A.D., Egea, E.E., Metz, H.E., Stolz, D.B., Land, S.R., Marconcini, L.A., Kliment, C.R., et al. (2010). Neutrophil elastase-mediated degradation of IRS-1 accelerates lung tumor growth. Nat. Med. *16*, 219–223.

Hussain, M.A., Porras, D.L., Rowe, M.H., West, J.R., Song, W.J., Schreiber, W.E., and Wondisford, F.E. (2006). Increased pancreatic beta-cell proliferation mediated by CREB binding protein gene activation. Mol. Cell. Biol. *26*, 7747–7759.

Jhala, U.S., Canettieri, G., Screaton, R.A., Kulkarni, R.N., Krajewski, S., Reed, J., Walker, J., Lin, X., White, M., and Montminy, M. (2003). cAMP promotes pancreatic beta-cell survival via CREB-mediated induction of IRS2. Genes Dev. *17*, 1575–1580.

Jiao, Y., Le Lay, J., Yu, M., Naji, A., and Kaestner, K.H. (2014). Elevated mouse hepatic betatrophin expression does not increase human β-cell replication in the transplant setting. Diabetes *63*, 1283–1288.

Jung, Y., Miura, M., and Yuan, J. (1996). Suppression of interleukin-1 beta-converting enzyme-mediated cell death by insulin-like growth factor. J. Biol. Chem. *271*, 5112–5117.

Kassem, S.A., Ariel, I., Thornton, P.S., Scheimberg, I., and Glaser, B. (2000). Beta-cell proliferation and apoptosis in the developing normal human pancreas and in hyperinsulinism of infancy. Diabetes *49*, 1325–1333.

Kawabata, K., Suzuki, M., Sugitani, M., Imaki, K., Toda, M., and Miyamoto, T. (1991). ONO-5046, a novel inhibitor of human neutrophil elastase. Biochem. Biophys. Res. Commun. *177*, 814–820.

Keller, M., Rüegg, A., Werner, S., and Beer, H.D. (2008). Active caspase-1 is a regulator of unconventional protein secretion. Cell *132*, 818–831.

Kondegowda, N.G., Fenutria, R., Pollack, I.R., Orthofer, M., Garcia-Ocaña, A., Penninger, J.M., and Vasavada, R.C. (2015). Osteoprotegerin and Denosumab Stimulate Human Beta Cell Proliferation through Inhibition of the Receptor Activator of NF-κB Ligand Pathway. Cell Metab. *22*, 77–85.

Kroon, E., Martinson, L.A., Kadoya, K., Bang, A.G., Kelly, O.G., Eliazer, S., Young, H., Richardson, M., Smart, N.G., Cunningham, J., et al. (2008). Pancreatic endoderm derived from human embryonic stem cells generates glucose-responsive insulin-secreting cells in vivo. Nat. Biotechnol. *26*, 443–452.

Kubota, N., Terauchi, Y., Tobe, K., Yano, W., Suzuki, R., Ueki, K., Takamoto, I., Satoh, H., Maki, T., Kubota, T., et al. (2004). Insulin receptor substrate 2 plays a crucial role in beta cells and the hypothalamus. J. Clin. Invest. *114*, 917–927.

Kulkarni, R.N., Mizrachi, E.B., Ocana, A.G., and Stewart, A.F. (2012). Human β-cell proliferation and intracellular signaling: driving in the dark without a road map. Diabetes *61*, 2205–2213.

Kutlu, B., Burdick, D., Baxter, D., Rasschaert, J., Flamez, D., Eizirik, D.L., Welsh, N., Goodman, N., and Hood, L. (2009). Detailed transcriptome atlas of the pancreatic beta cell. BMC Med. Genomics *2*, 3.

Liew, C.W., Assmann, A., Templin, A.T., Raum, J.C., Lipson, K.L., Rajan, S., Qiang, G., Hu, J., Kawamori, D., Lindberg, I., et al. (2014). Insulin regulates carboxypeptidase E by modulating translation initiation scaffolding protein eIF4G1 in pancreatic β cells. Proc. Natl. Acad. Sci. USA *111*, E2319–E2328.

Liu, Y., Tanabe, K., Baronnier, D., Patel, S., Woodgett, J., Cras-Méneur, C., and Permutt, M.A. (2010). Conditional ablation of Gsk-3β in islet beta cells results in expanded mass and resistance to fat feeding-induced diabetes in mice. Diabetologia *53*, 2600–2610.

Lysy, P.A., Weir, G.C., and Bonner-Weir, S. (2013). Curr Dia Report *13*, 695–703.

Macdonald, S.J., Dowle, M.D., Harrison, L.A., Shah, P., Johnson, M.R., Inglis, G.G., Clarke, G.D., Smith, R.A., Humphreys, D., Molloy, C.R., et al. (2001). The discovery of a potent, intracellular, orally bioavailable, long duration inhibitor of human neutrophil elastase–GW311616A a development candidate. Bioorg. Med. Chem. Lett. *11*, 895–898.

Matsuda, M., and DeFronzo, R.A. (1999). Insulin sensitivity indices obtained from oral glucose tolerance testing: comparison with the euglycemic insulin clamp. Diabetes Care *22*, 1462–1470.

Mertins, P., Yang, F., Liu, T., Mani, D.R., Petyuk, V.A., Gillette, M.A., Clauser, K.R., Qiao, J.W., Gritsenko, M.A., Moore, R.J., et al. (2014). Ischemia in tumors induces early and sustained phosphorylation changes in stress kinase pathways but does not affect global protein levels. Mol. Cell. Proteomics *13*, 1690–1704.

Muoio, D.M., and Newgard, C.B. (2008). Mechanisms of disease:Molecular and metabolic mechanisms of insulin resistance and beta-cell failure in type 2 diabetes. Nat. Rev. Mol. Cell Biol. *9*, 193–205.

Nickel, W. (2010). Pathways of unconventional protein secretion. Curr. Opin. Biotechnol. *21*, 621–626.

Pagliuca, F.W., Millman, J.R., Gürtler, M., Segel, M., Van Dervort, A., Ryu, J.H., Peterson, Q.P., Greiner, D., and Melton, D.A. (2014). Generation of functional human pancreatic β cells in vitro. Cell *159*, 428–439.

Remold-O'Donnell, E. (1993). The ovalbumin family of serpin proteins. FEBS Lett. *315*, 105–108.

Rezania, A., Bruin, J.E., Arora, P., Rubin, A., Batushansky, I., Asadi, A., O'Dwyer, S., Quiskamp, N., Mojibian, M., Albrecht, T., et al. (2014). Reversal of diabetes with insulin-producing cells derived in vitro from human pluripotent stem cells. Nat. Biotechnol. *32*, 1121–1133.

Rieck, S., Zhang, J., Li, Z., Liu, C., Naji, A., Takane, K.K., Fiaschi-Taesch, N.M., Stewart, A.F., Kushner, J.A., and Kaestner, K.H. (2012). Overexpression of hepatocyte nuclear factor-4α initiates cell cycle entry, but is not sufficient to promote β-cell expansion in human islets. Mol. Endocrinol. *26*, 1590–1602.

Rutti, S., Sauter, N.S., Bouzakri, K., Prazak, R., Halban, P.A., and Donath, M.Y. (2012). In vitro proliferation of adult human beta-cells. PLoS ONE *7*, e35801.

Silverman, G.A., Bird, P.I., Carrell, R.W., Church, F.C., Coughlin, P.B., Gettins, P.G., Irving, J.A., Lomas, D.A., Luke, C.J., Moyer, R.W., et al. (2001). The serpins are an expanding superfamily of structurally similar but functionally diverse proteins. Evolution, mechanism of inhibition, novel functions, and a revised nomenclature. J. Biol. Chem. *276*, 33293–33296.

Stewart, A.F., Hussain, M.A., García-Ocaña, A., Vasavada, R.C., Bhushan, A., Bernal-Mizrachi, E., and Kulkarni, R.N. (2015). Human β-cell proliferation and intracellular signaling: part 3. Diabetes *64*, 1872–1885.

Talukdar, S., Oh, Y., Bandyopadhyay, G., Li, D., Xu, J., McNelis, J., Lu, M., Li, P., Yan, Q., Zhu, Y., et al. (2012). Neutrophils mediate insulin resistance in mice fed a high-fat diet through secreted elastase. Nat. Med. *18*, 1407–1412.

Walpita, D., Hasaka, T., Spoonamore, J., Vetere, A., Takane, K.K., Fomina-Yadlin, D., Fiaschi-Taesch, N., Shamji, A., Clemons, P.A., Stewart, A.F., et al. (2012). A human islet cell culture system for high-throughput screening. J. Biomol. Screen. *17*, 509–518.

Wang, P., Alvarez-Perez, J.C., Felsenfeld, D.P., Liu, H., Sivendran, S., Bender, A., Kumar, A., Sanchez, R., Scott, D.K., Garcia-Ocaña, A., and Stewart, A.F. (2015). A high-throughput chemical screen reveals that harmine-mediated inhibition of DYRK1A increases human pancreatic beta cell replication. Nat. Med. *21*, 383–388.

Withers, D.J., Gutierrez, J.S., Towery, H., Burks, D.J., Ren, J.M., Previs, S., Zhang, Y., Bernal, D., Pons, S., Shulman, G.I., et al. (1998). Disruption of IRS-2 causes type 2 diabetes in mice. Nature *391*, 900–904.

Yi, P., Park, J.S., and Melton, D.A. (2013). Betatrophin: a hormone that controls pancreatic β cell proliferation. Cell *153*, 747–758.

Zhou, J.Y., Schepmoes, A.A., Zhang, X., Moore, R.J., Monroe, M.E., Lee, J.H., Camp, D.G., Smith, R.D., and Qian, W.J. (2010). Improved LC-MS/MS spectral counting statistics by recovering low-scoring spectra matched to confidently identified peptide sequences. J. Proteome Res. *9*, 5698–5704.

Appendix A7

Publication

Shirakawa J*, **De Jesus DF***, and Kulkarni RN. Exploring inter-organ crosstalk to uncover mechanisms that regulate β-cell function and mass. Eur J Clin Nutr 7(7): 896- 903, 2017. (*co-first authors).

Contribution

I am co-first author in this review article.

European Journal of Clinical Nutrition (2017) **71**, 896–903

www.nature.com/ejcn

REVIEW

Exploring inter-organ crosstalk to uncover mechanisms that regulate β-cell function and mass

J Shirakawa[1,3], DF De Jesus[1,2,3] and RN Kulkarni[1]

Impaired β-cell function and insufficient β-cell mass compensation are twin pathogenic features that underlie type 2 diabetes (T2D). Current therapeutic strategies continue to evolve to improve treatment outcomes in different ethnic populations and include approaches to counter insulin resistance and improve β-cell function. Although the effects of insulin secretion on metabolic organs such as liver, skeletal muscle and adipose is directly relevant for improving glucose uptake and reduce hyperglycemia, the ability of pancreatic β-cells to crosstalk with multiple non-metabolic tissues is providing novel insights into potential opportunities for improving β-cell function and/or mass that could have beneficial effects in patients with diabetes. For example, the role of the gastrointestinal system in the regulation of β-cell biology is well recognized and has been exploited clinically to develop incretin-related antidiabetic agents. The microbiome and the immune system are emerging as important players in regulating β-cell function and mass. The rich innervation of islet cells indicates it is a prime organ for regulation by the nervous system. In this review, we discuss the potential implications of signals from these organ systems as well as those from bone, placenta, kidney, thyroid, endothelial cells, reproductive organs and adrenal and pituitary glands that can directly impact β-cell biology. An added layer of complexity is the limited data regarding the relative relevance of one or more of these systems in different ethnic populations. It is evident that better understanding of this paradigm would provide clues to enhance β-cell function and/or mass *in vivo* in the long-term goal of treating or curing patients with diabetes.

European Journal of Clinical Nutrition (2017) **71,** 896–903; doi:10.1038/ejcn.2017.13; published online 15 March 2017

INTRODUCTION

The prevalence of type 2 diabetes (T2D) is rapidly accelerating in Asian countries and the large numbers are especially noticeable given the large population density in these countries.[1] The increased incidence is the result of an aging society, compounded by lifestyle changes and epigenetic modifications, especially in developing Asian countries. Furthermore, studies suggest that the susceptibility to develop T2D is genetically higher in Asian populations when compared to populations of European origin.[2] Notably, genetic variants associated with T2D from genome-wide association studies are related to reduced pancreatic β-cell function, rather than peripheral insulin resistance.[3] 'Diabetes' is manifest when β-cells are unable to compensate for increasing insulin demand to maintain normoglycemia by enhancing their proliferation, mass and/or function. Most autopsy studies have revealed a positive correlation between β-cell mass and body-mass index in European, North American and Asian populations.[4–6] Since Asian subjects generally show a lower body-mass index than Caucasians, β-cell mass is expected to be smaller in Asians. However, it is becoming evident that curiously Asians easily develop insulin resistance and diabetes without morbid obesity.[3] Thus, therapeutic strategies that protect and enhance 'functional β-cell mass' are essential to promote appropriate glycemic control and to potentially cure diabetes in Asian populations.

Considerable effort has been invested to progress our understanding of the complex intracellular signaling mechanisms and pathways that regulate human β-cell function and mass including those that modulate insulin secretion, islet cell replication, apoptosis, dedifferentiation, autophagy, and endoplasmic reticulum (ER) and oxidative stress. It is also evident that metabolites (for example, glucose and free fatty acids) and hormones (for example, glucagon-like peptide-1 (GLP-1) and glucose-dependent insulinotropic polypeptide (GIP)) continue to be important regulators of human islet function.[7–9] However, recent studies have been steadily accumulating evidence to point to the concept of *in vivo* regulation of islet cell function and mass secondary to organ crosstalk. This relatively new area has become a focus to explore novel targets to influence regeneration of 'functional β-cells'. This review focuses on the different metabolic tissues that can crosstalk with β-cells to impact whole-body glucose homeostasis.

MATERIALS AND METHODS

Search strategy and article selection

A systematic literature search was performed using the PubMed database. The search terms used were 'pancreatic beta cells' AND ('crosstalk' OR 'inter-organ' OR 'communication'). Studies were restricted to those in the English language published between

[1]Islet Cell and Regenerative Biology, Joslin Diabetes Center, Department of Medicine, Brigham and Women's Hospital, Harvard Stem Cell Institute, Harvard Medical School, Boston, MA, USA and [2]Graduate Program in Areas of Basic and Applied Biology (GABBA), Abel Salazar Biomedical Sciences Institute, University of Porto, Porto, Portugal. Correspondence: Professor RN Kulkarni, Islet Cell and Regenerative Biology, Joslin Diabetes Center, Department of Medicine, Brigham and Women's Hospital, Harvard Stem Cell Institute, Harvard Medical School, One Joslin Place, Boston, MA 02215, USA.
E-mail: rohit.kulkarni@joslin.harvard.edu
[3]These two authors contributed equally to this work.
Received 19 January 2017; accepted 24 January 2017; published online 15 March 2017

January 2000 and 31 December 2016. In all, 441 articles were found in those search terms. First the journal name, the title and then the abstract of each listed article was examined and only those with the significant impact on this area of research were retained. We selected 11 distinct publications that represent a significant advance in the understanding of the regulation of β-cell inter-organ crosstalk. Furthermore, reference lists of reviews, original papers and our personal knowledge were reviewed, and an additional 16 publications were selected.

CROSSTALK BETWEEN β-CELLS AND METABOLIC TISSUES

Liver

The existence of circulating β-cell growth factors was hypothesized more than a decade ago, when Flier *et al.* demonstrated an increase in β-cell mass in response to insulin resistance independent of glucose or obesity.[10] The liver is an ideal candidate for crosstalk with islet β-cells for several reasons. First, the liver and the islets have a common embryonic origin and teleologically it is conceivable that alterations in one or the other organ would elicit signals to restore homeostasis. Second, multiple metabolites and hormones regulate complex transcriptional networks that modulate hepatic glucose metabolism that can impact whole-body metabolism; and finally, being a major organ of energy storage and in glucose and lipid metabolism the liver is directly involved in development of insulin resistance and T2D.[11]

Thus it is not surprising that several reports point to the liver as a source of factors that can directly impact the islets and contribute to organismal metabolism. For example, hepatic growth factor (HGF), which is produced in the liver is known to be involved in the regeneration capabilities in different tissues[12] and acts via the c-Met receptor, expressed on β-cells. Conditional ablation of *c-Met* is not detrimental in normal conditions but is crucial for adaptatin of β-cell mass in response to multiple low doses of streptozotocin[12] and partial prancreatectomy.[13]

El Ouaamari and colleagues used parabiosis and transplantation experiments to specifically demonstrate the existence of hepatocyte-derived factors that drive mouse and human β-cell proliferation.[14] The leukocyte-neutrophil elastase inhibitor (SerpinB1) was identified as a hepatocyte-derived secretory protease inhibitor protein that regulates mouse, zebrafish and human β-cell proliferation.[15] In a proof of concept, the authors shown that Silvestat—a small-molecule compound that acts like SperbinB1-inhibiting elastase activity, was able to increase β-cell proliferation in *in vitro* cultured islets and *in vivo* transplanted islets.[15,16] The conserved and defined activity of SerpinB1 among different species argues for potential as a therapeutic to promote β-cell regeneration in diabetes states.

The KISS-1 metastasis-supressor gene (*KISS-1*) known as kisspeptin was first discovered to be enriched in non-metastatic melanoma cells and found to have metastatic-suppressive properties.[17] It is widely expressed in different tissues, particularly in placenta and in the central nervous system.[17] Kisspeptin is involved in several phases of puberty and reproduction. Estradiol and testosterone regulate *Kiss1* gene expression while kisspeptin stimulates the release of gonadotropin releasing-hormone.[17] The role of kisspeptin in glucose homeostasis is new and of great interest. Kisspeptin is augmented in livers and sera of patients with T2D and in rodent models of obesity and diabetes.[18] Glucagon acts on the liver by stimulating the cAMP-PKA-CREAB signaling pathway and increasing the hepatic production of kisspeptin.[18] Nutritional and genetic models of insulin resistance-lacking *Kiss1* gene present augmented glucose-stimulated insulin secretion (GSIS) and improved glucose tolerance,[18] and provide insights on the role of Kisspeptin on glucagon regulation of insulin secretion.

Insulin-like growth factor binding proteins (IGFBPs) play a central role in insulin signaling and are expressed in a widespread variety of tissues, including the liver. Low concentrations of circulating IGFBP1 are associated with T2D and increasing its levels in mice has positive effects on insulin sensitivity.[19] Hepatic *IGFBP1* expression is positively regulated by fibroblast growth factor 21 (*FGF21*) and causes bone loss by acting on integrin β1 receptors on osteoclasts.[20] Interestingly, IGFBP1 was shown to promote β-cell regeneration by inducing α-to-β-cell transdifferentiation in zebrafish, mouse and human islets.[21] *In vitro* treatment of mouse and human islets with recombinant IGFBP1 increased the number of cells co-expressing insulin and glucagon.[21]

Liver has a central role in regulating metabolism and is constituted by a complex and vast proteome. Further work is necessary to identify additional novel hepatocyte-derived signaling peptides that regulate β-cell function and/or mass.

Adipose tissue

Although adipose tissue was considered as a mere energy reservoir for several decades, it has emerged as an active endocrine organ that integrates multiple systemic signals and secretes various adipokines.[22] Adiponectin is one of the major secreted adipokines that is important for the overall regulation of lipid homeostasis and metabolic flexibility. While, adiponectin seems to be dispensable in normal physiological conditions, recent work revealed its importance in β-cell regeneration.[23,24] Adiponectin promotes β-cell proliferation in response to experimental β-cell ablation[23] and improves islet lipid metabolism to enhance β-cell regeneration.[24]

Leptin is a hormone produced by adipocytes in proportion to the total fat mass and acts on multiple circuits, namely on central nervous system controlling food-intake and energy expenditure. Mice and humans lacking leptin exhibit hyperphagia and consequently obesity and T2D.[25] Leptin acts on β-cells and inhibits insulin secretion[26] in a K^+_{ATP}-dependent manner.[27] The effects of leptin on β-cells may be indirect and further studies are needed to elucidate the mechanisms of its action.[22]

Adipsin was among the adipokines identified early and observed to be reduced in obesity and diabetes.[28] Mice genetically manipulated to lack adipsin, present decreased insulin secretion and glucose intolerance.[29] Adipsin generates the C3a peptide, which acts on islets by increasing ATP and Ca^{2+} levels boosting insulin secretion.[29] Finally, recent work has shown that brown adipose tissue, which is rich in mitochondria and regulates thermogenesis by expressing high amounts of uncoupling protein-1, also secretes factors able to influence overall glucose and lipid metabolism. Some examples include FGF21, bone morphogenetic protein, interleukin (IL)-6 and vascular endothelial growth factor (VEGF; reviewed in Wang *et al.*[30]). Further work is warranted to examine whether the brown adipose tissue secretome can directly impact β-cell biology.

Skeletal and cardiac muscle

Physical activity reduces the risk of a myriad of health disorders ranging from cancer to obesity. The concept of skeletal muscle as an active signaling organ with the capacity to modulate the function of other organs has gained relevance with the development of high throughput methodologies.[31] IL-6 is one of the well characterized myokines[22] and acts on α-cells to induce the production of GLP-1 through increased expression of proglugacon and prohormone convertase 1/3.[32] Consequently, exercise increases the expression of IL-6 in skeletal muscle which crosstalks to β-cells via GLP-1 and potentiating GSIS.[32]

Exosome-mediated crosstalk is an attractive cell-to-cell communication system and microRNAs are being recognized as key regulators of β-cell function (reviewed in Guay and Regazzi[33]). Recently, Jalabert *et al.* isolated skeletal muscle-derived exosomes from mice fed chow or a palmitate-enriched diet for 16 weeks and

analyzed if pancreas could take up exosome cargoes.[34] The authors showed that pancreas could not only take up these muscle-derived exosome but also that these cargoes affected MIN6B1 and isolated islet cell proliferation.[34] miR-16 was identified as one of the principal mediators of this effects and MIN6B1 cells transfected with miR-16 exhibited decreased *Ptch1* gene expression—a gene involved in proliferation.[34] It would be of great interest to validate these findings in human islets.

While peripheral tissues such as adipose, may increase the risk of myocardial infarction as a consequence of obesity and an altered adipokinome,[35] the role of heart itself as a metabolic modulator has been neglected until recently.[35] Ischemic stress can lead to infiltration and inflammation of the myocardium, affecting a myriad of different inflammatory cytokines, known as cardiokines.[35] Most of the known cardiokines act in a paracrine manner and modulate cardiac metabolism, response to stress, and angiogenesis. The discovery and understanding of new human myokines constitute an interesting and active area of research that can lead to the identification of novel therapeutical targets including effects on β-cell function and/or mass.[36]

THE β-CELL AND INTRA-ISLET ENDOTHELIAL CELL INTERACTION

Pancreas is constituted by an endocrine component that secrete hormones directly into the bloodstream, and an exocrine component that secretes enzymes through a duct network into the gastrointestinal tract, likely favored by evolution to improve homeostatic responses via endocrine and paracrine communication.[37] Although the total islet mass represents between 1 and 2% of the total pancreatic mass, islets receive a significant part of the pancreatic blood flow.[38] Indeed, islets are intensely vascularized and endothelial cells play a role in β-cell glucose sensing and insulin secretion.[38] VEGF-A is a major modulator of islet vascularization. Islets secrete large amounts of VEGF-A that acts on endothelial cells to stimulate cell migration and proliferation.[38] Mice genetically modified to have reduced levels of β-cell VEGF-A present normal β-cell mass but decreased GSIS.[39] It is also notable that endothelial cells secrete multiple factors that regulate β-cell function and survival (reviewed in Peiris *et al*.[38]). Among them, thrombospondin-1 (*TSP-1*) regulates β-cell function partially via transforming growth factor-1 (*TGF-β1*) signaling.[40] Recently, *TSP-1* was reported to induce a protective antioxidant response against palmitate in β-cells via the PERK-NRF2 pathway.[41] Other factors secreted by endothelial cells include endothelin-1 and hepatic growth factor acting on β-cells to stimulate insulin secretion and proliferation respectively.[38] In T2D, endothelial cells are exposed to diverse stress factors that induce inflammatory responses which ultimately leads to fibrosis, destruction of islet microvasculature and consequent β-cell dysfunction. Thus, islet microvasculature is important for maintenance of islet function and alterations in islet blood supply appear to be related to the development of T2D.

GASTROINTESTINAL SYSTEM-MEDIATED REGULATION OF β-CELLS

Incretins and decretins

The term incretin was coined from observations in which oral administration of glucose leads to a greater amount of secreted insulin in comparison to an intravenous administration of glucose.[42] GLP-1 and GIP are among the most famous incretins.[22] GIP and GLP-1 are released from intestinal K and L cells, respectively, in response to glucose and lipids and improve GSIS.[42] GLP-1 stimulates insulin secretion in response to glucose and also acts on α-cells through glucagon like peptide 1 receptor (GLP-1R) to inhibit glucagon secretion.[22,42] Interestingly, ablation of GLP-1R in β-cells does not disrupt GLP-1 effects on insulin secretion, suggesting that GLP-1 acts on β-cells through a neuronal mechanism.[22,43] Variants in the GIP receptor gene locus have been associated with higher susceptibility for T2D[42] but its mechanism of action in β-cells are complex.[22] Transgenic mice lacking glucose-dependent insulinotropic polypeptide receptor selectively on β-cells present with decreased GSIS in response to meals but preserve their insulin sensitivity.[44] Nonetheless, β-cells lacking glucose-dependent insulinotropic polypeptide receptor are more susceptible to apoptosis and exhibit lower expression of T-cell specific transcription factor-1 (from Tcf7 gene).[44] Tcf7 has been relatively recently reported to be decreased in diabetic rodent islets and in T2D islets and suggested to be important for the anti-apoptotic effects of GIP.[44] Although incretins stimulate insulin secretion in response to nutrients, decretins act by inhibiting insulin secretion in fasting conditions. Using the same conceptual experiment for incretins, decretins were discovered by their inability to reduce insulin secretion after an intravenous injection of glucose in the fasting state.[22] Neuromedin U, ghrelin and galanin are among the most studied decretins secreted by the gastrointestinal tract. The mechanism by which they reduce β-cell GSIS is largely unknown and this topic has been reviewed recently.[22]

Microbiome

The human gut is colonized by thousands of different anaerobic bacterial genomes that play an important physiological role in modulating digestion and playing a role in the synthesis of vitamins and other metabolites[45] (reviewed in Baothman *et al*.[45]). Alterations in the gut microbiota are known to be associated with obesity, T2D and other diseases. Transfer of microbiota from lean humans to individuals with metabolic syndrome improves insulin sensitivity after only 6 weeks.[46] Short-chain fatty acids are produced in the distal gut by bacterial fermentation of different substrates that escape digestion in the upper part of the gastrointerstinal tract and is considered to be an important mediator of the microbiome effects on metabolism.[47] Receptors for short-chain fatty acids are widely expressed and include two G-protein coupled proteins: free fatty acid receptor 2 (also known as GPR43) and FFAR3 (also known as GPR41).[47] β-cells express free fatty acid receptor 2 and mice genetically lacking free fatty acid receptor 2 present glucose intolerance, impaired insulin secretion and decreased β-cell mass when challenged with a high-fat diet.[48] Indeed, *in vitro* treatment of mouse and human islets with a free fatty acid receptor 2 agonist potentiates insulin secretion[48] constituting a promising therapeutic intervention strategy.

NEURAL CONTROL OF β-CELLS

It is well established that the brain regulates global metabolic and energy homeostasis by integrating multiple signals, such as hormones and nutrients from different metabolic organs and exerts a continuous and coordinated control of most metabolic organs. The β-cell is one of the major targets of neurons. Indeed, β-cells are highly innervated by sympathetic and parasympathetic neurons, and expresses multiple neurotransmitters and neuropeptide receptors.[49] Parasympathetic nerve activation provokes increased GSIS and β-cell proliferation probably through muscarinic acethylcholine receptor-3 (m3AChR).[50,51] In mice, genetic ablation of sympathetic innervation by tyrosine hydroxylase promoter-driven cre-induced TrkA receptor conditional knockout or pharmacological ablation by administration with the neurotoxin 6-hydroxydopamine has been reported to result in disorganized islet architecture, impaired insulin secretion and glucose intolerance during development.[52] Intriguingly, leptin negatively regulates parasympathetic innervation of pancreatic islets and causes impaired glucose tolerance.[53] Interestingly, the

innervation patterns of human islets and mouse islets are different.[54] Mouse islets being densely innervated with parasympathetic neurons in the core, and with sympathetic neuron in the periphery, compared to the exocrine tissues. In contrast, human islets show minimal penetration by parasympathetic neurons while sympathetic nerves mainly project to blood vessels within islets.[54] Instead, human α-cells release acetylcholine and provide cholinergic input on surrounding β-cells in human islets.[55] Thus, neural regulation of β-cell function and mass likely differ between mouse and man.

An interesting observation links the brain and the liver in the inter-organ regulation of β-cell function and mass. Imai *et al.* injected the liver with an adenovirus that expresses constitutively active MEK-1 in mice[56] and observed that the animals exhibited enhanced GSIS and β-cell proliferation. Furthermore, ablation of efferent vagal signals by pancreatic vagotomy, the selective blockade of afferent splanchnic nerve with capsaicin, or bilateral mid brain transection markedly blunted the effects of ERK on β-cell function and proliferation.[56] These results suggest that the nerve-mediated liver–brain–pancreas axis is an attractive pathway to replenish functional β-cell in addition to hepatic humoral factors such as SerpinB1. However, the precise mechanism by which hepatic ERK activation affects neural control of β-cells warrants selective activation of liver-mediated afferent splanchnic nerve.

Brain is a physiological sensor for glucose particularly in response to hypoglycemia. The neuronal counter-regulatory response to hypoglycemia suppresses insulin release and induces glucagon and catecholamine release to restore normoglycemia. In mouse β-cells, glucose uptake and sensing are mediated by glucose transporter 2 (Glut2), the major glucose transporter, and glucokinase, a low affinity hexokinase, whereas human β-cells predominantly express GLUT1 rather than GLUT2.[57] The β-cell glucokinase is a rate-limiting enzyme in the induction of glycolysis, glucose oxidation, ATP production, calcium influx and GSIS through ATP-gated potassium (K_{ATP}) channel. The brain also expresses Glut2, glucokinase and K_{ATP} channel, and those three molecules in the brain play crucial roles in the regulation of glucagon secretion in response to glucose.[58–61] Tarussio *et al.* generated neuron-specific Glut2 knockout (NG2KO)[62] and demonstrated they exhibit glucose intolerance due to impaired insulin secretion in response to aging and high-fat diet-induced obesity. β-cell mass and proliferation were also reduced in NG2KO mice in the postnatal period.[62] Thus, in mice glut2-mediated glucose sensing in neurons regulates β-cell function and mass mainly through modulating parasympathetic activity.

Acetylcholine is a major neurotransmitter for the parasympathetic action on β-cells. Interestingly, Rodriguez-Diaz *et al.* demonstrated that pancreatic α-cells secrete acetylcholine in response to kinate stimulation or a decline in ambient glucose, and have a cholinergic effect on neighboring β-cells in human islets.[55] These studies indicate that paracrine signals from islet endocrine cells contribute to neuroendocrine regulation of β-cells. In addition to autonomic nerves, islets reportedly receive sensory innervation[63] and functional modulation of β-cells by neuropeptides such as encephalin, neuropeptide Y, cholecystokinin, substance P or PACAP have also been reported. Further investigation of neuron/neurotransmitter-mediated regulation of β-cells would contribute to a better understanding of how one could potentially replenish β-cells through activation of proteins in the central nervous system.

CROSSTALK BETWEEN β-CELLS AND OTHER TISSUES

In addition to the aforementioned tissues, the β-cell has been reported to interact with multiple other tissues including the bone, placenta, reproductive glands, kidney, the immune system, thyroid, endothelial cells, adrenal and pituitary glands. We will discuss recent research only on some of these tissues due to space limitations.

Bone

Bone, now recognized as an endocrine tissue, is known to secrete humoral factors that are involved in systemic metabolism. Lee *et al.* generated a mouse with a osteoblast-specific knockout of a receptor-like protein phosphatase,[64] and observed that the animals showed an increase in β-cell proliferation and insulin secretion.[64] Osteocalcin is an osteoblast-specific secreting protein and osteocalcin knockout mice exhibit a reduction in β-cell proliferation and insulin secretion.[64] Osteocalcin haploinsufficiency reversed both metabolic and β-cell phenotypes of osteoblast-specific knockout of a receptor-like protein phosphatase knockout mice.[64] They also showed that the receptor-like protein phosphatase regulates osteocalcin activity by modulating γ-carboxylation.[64] A recent study revealed that effects of osteocalcin on β-cells is mediated by Gprc6a, an osteocalcin receptor.[65] These studies have positioned osteoblast-derived osteocalcin as a prominent regulator of β-cell function and mass. Conversely, β-cell-derived insulin stimulates osteocalcin production through insulin receptor mediated suppression of Twist2, a Runx2 inhibitor, in osteoblasts.[66] Osteoblast-specific insulin receptor knockout mice showed low circulating osteocalcin levels and decreased β-cell mass and function.[66,67] Interestingly, this osteocalcin activity is also regulated by sympathetic nerves and is modulated by adipose tissue-derived leptin.[68] Since leptin and sympathetic nerves directly regulate β-cell function,[49,69] this interplay between the adipocyte, brain, sympathetic nerve, osteoblast and β-cells represents a complex inter-organ network in the regulation of whole-body homeostasis.

Pregnancy and sex hormones

In rodents, an increase in β-cell mass during pregnancy occurs primarily as a result of enhanced cell replication. Since the prolactin receptor is required for β-cell adaptation during pregnancy, prolactin secreted from the pituitary and placental lactogen have been reported to contribute to the expansion of β-cell mass during pregnancy.[70] Prolactin and lactogen mediate their actions on β-cell proliferation through hepatic growth factor, menin, serotonin and/or osteoprotegerin pathways.[71–75] However, the factors that promote β-cell adaptation that potentially occurs during pregnancy in humans are still unclear and is a timely area for additional studies. Women after menopause are more susceptible to diabetes compared to men and postmenopausal diabetes has been associated with β-cell dysfunction in addition to insulin resistance.[76] Hormone replacement therapy in postmenopausal women improves glycemic control.[77] Meanwhile, men with testosterone deficiency exhibit impaired insulin secretion and T2D. These observations indicate significant effects of reproductive hormones in the maintenance of β-cell function. The receptors for estrogen, ERα, ERβ and G-protein coupled ER, are all expressed on β-cells and contribute to β-cell function and mass. ERα contributes to reduction in apoptosis, allevaites ER stress, and decrease in fatty acid synthesis, and enhances proliferation and survival in β-cells.[78,79] ERα is required for the generation of Neurogenin-3-mediated β-cell regeneration during development and pregnancy, and following partial duct ligation.[80] ERβ and G-protein coupled ER play roles in GSIS and β-cell proliferation.[79,81] An involvement of estrogen in prevention of T1D by modulating iNKT cell function has also been reported.[82] The activation of androgen receptors in β-cell potentiates glucose-stimulated insulin secretion in co-operation with GLP-1 receptor activation and altering cAMP levels.[83] Progesterone reportedly facilitates insulin secretion and β-cell proliferation; however, progesterone receptor knockout mice also show enhanced β-cell proliferation.[84,85] These examples of communication between

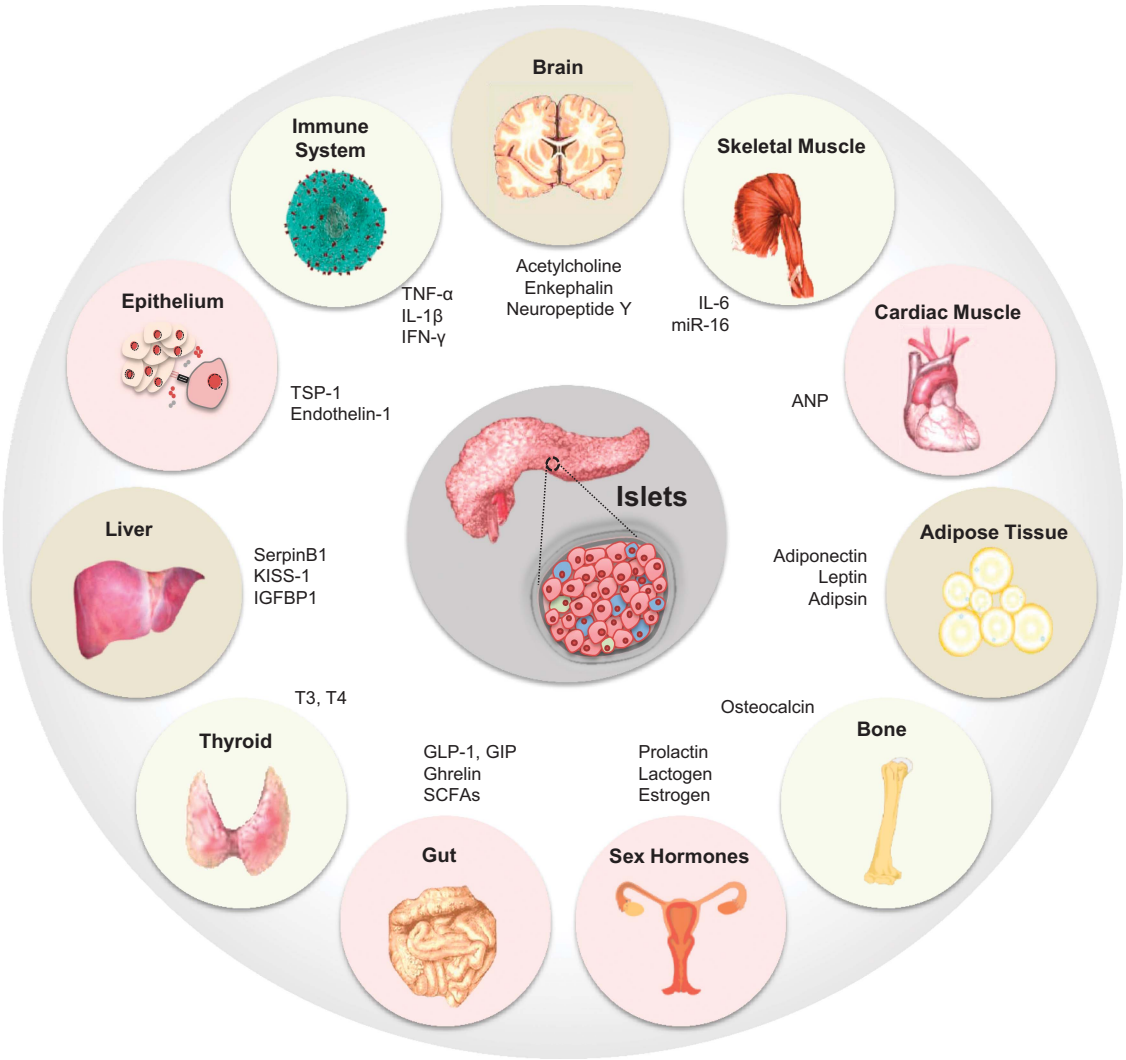

Figure 1. Inter-organ crosstalk impacting β-cell function and/or mass. The figure represents different factors that are secreted by diverse metabolic organs and tissues with the potential to regulate glucose-stimulated insulin secretion and β-cell proliferation. Each of the pathways denoted are discussed briefly in the text. ANP, atrial natriuretic peptide; IGFBP1, insulin-like growth factor-binding protein 1 IFN-γ, interferon γ; miR-16, microRNA 16; SCF, short-chain fatty acids; SerpinB1, leukocyte elastase inhibitor; T3, triiodothyronine; T4, thyroxine; TNF-α, tumor necrosis factor α.

β-cells and reproductive organs indicate the potential for gender-specific approaches for replenishment of functional β-cell mass and is discussed in a recent review.[81]

Thyroid

Hyperthyroidism due to Graves' Disease, or due other causes of thyrotoxicosis, is known to cause hyperinsulinemia associated with various metabolic changes. Thyroid hormone has been linked to altered GSIS in people with prediabetes, suggesting that thyroid hormones are involved in the regulation of insulin secretion from β-cells.[86] Aguayo-Mazzucato *et al.* demonstrated that β-cells express thyroid hormone receptors and that thyroid hormone enhances β-cell maturation by enhancing expression of MAFA.[87] Recently, Bruin *et al.* investigated the impact of thyroid dysregulation on the development of encapsulated human embryonic stem cell-derived progenitor cells in mice.[88] Hypothyroidism showed a negative effect on human embryonic stem cell-derived β-cell development and induced higher numbers of human embryonic stem cell-derived glucagon-positive α- and ghrelin-positive ε-cells.[88] Thus, thyroid hormone contributes to the maintenance of β cell function as well as the differentiation and maturation steps during development of β cells.

Immune system

The innate immune system and inflammatory pathways have been recognized to play important roles during the onset and development of T2D. Chronic inflammation has been observed in adipose tissue, liver, vascular endothelial cells, circulating leukocytes as well as in pancreatic islets in obese and/or diabetic subjects. Islet inflammation has been suggested to be a factor in the decline of β-cell mass in both T1D and T2D.[89] Currently, islet macrophages are recognized as important and emerging regulators of islet inflammation, and saturated fatty acid and TLR4/Myd88 signaling are considered to be involved in crosstalk between macrophages and islets in the development of β-cell dysfunction.[90] Increased islet macrophages in human T2D have been reported in pathological studies[91] and accumulating evidence suggests that islet-infiltrated macrophages exhibit a wide range of functional heterogeneity in the interaction with β-cells in terms of cytokine expression. In addition to β-cell failure or death, islet macrophages reportedly contribute to β-cell

differentiation, regeneration and proliferation.[92] For example, Brissova *et al.* showed that inducible vascular endothelial growth factor-A (VEGF-A) expression in β-cells led to islet endothelial cell expansion, β-cell loss and bone marrow-derived macrophage recruitment into the injured islets.[93] Interestingly, the macrophage infiltration was essential for the β-cell proliferation after this VEGF-A-induced β-cell loss.[93] Thus, crosstalk between β-cells and macrophages is complex and contribute to different roles in the patho-physiology underlying β-cell dysfunction in diabetes. Further studies are necessary to clarify the origin and subtypes of macrophages in pathological and physiological situations to define whether islet macrophages can serve as appropriate targets for diabetes therapy.

It is well-known that adaptive immune system components including cytotoxic, helper, and regulatory T-cells, B-cells, and dendritic cells play roles in autoimmunity leading to β-cell destruction in T1D. However, cytokines or chemokines released from $CD4^+$ and $CD8^+$ T cells have also been shown to enhance β-cell proliferation in mouse islets.[94] Furthermore, stimulation with a combination of TNF-a, IL-1b and IFN-g led to an induction of Neurogenin-3 expression in pancreatic ductal cells to promote differentiation to endocrine cells in NOD mice.[95] These observations point to inflammatory cells as potential therapeutic targets for the prevention of β-cell failure as well as for expanding β-cell mass. Butcher *et al.* investigated immune cells within human islets from non-diabetes or T2D donors.[96] The islets from T2D donors showed increased infiltration of $CD45^+$ leukocytes and an elevated ratio of B cells in those leukocytes, suggesting an involvement of adaptive immune response in T2D.[96] Jaeckle Santos *et al.* demonstrated that intrauterine growth restriction causes T2D in rat by inducing inflammation by recruitment of T-helper 2 (Th) lymphocytes and macrophages in fetal islets.[97] Neutralizing Th2 response with IL-4 antibody during the neonatal period restored inflammation and β-cell function in intrauterine growth restricted rats. The adaptive Th2 response might be involved in epigenetic control of β-cell function in T2D. Thus, both innate and adaptive immune systems closely interact with β-cells in both T1D and T2D. The unifying models that account for mechanistic integration of the innate and adaptive immune responses in β-cells in T1D and T2D would greatly benefit in dissecting their respective pathogenesis.

DISCUSSION

In this review, we highlight crosstalk between β-cells and multiple tissues (Figure 1). An issue that requires urgent attention in this field of research relates to the significance of inter-organ communication in regulating human β-cells *in vivo*. This is especially significant given that human β-cells exhibit features that are distinct from rodents in regard to structure, function and gene expression.[98,99] Furthermore, an understanding of the crosstalk between β-cells and other tissues in the context of altered glycemia and overt diabetes is particularly necessary as β-cells are exposed to variable 'diabetes niches' such as hyperglycemia (glucotoxicity), hyperlipidemia (lipotoxicity), inflammatory cytokines and other factors for prolonged periods in patients susceptible to diabetes or the metabolic syndrome. Each of these conditions potentially trigger epigenetic changes in islet cells and other organs[75] and warrant investigations focused on examining the impact of epigenetics in the context of inter-organ crosstalk. A related topic that is not fully explored is the ability of antidiabetic drugs or factors that can differentially influence organ-crosstalk and treatment outcomes in diverse ethnic backgrounds. Investigations in these and associated areas over the next several years are likely to provide therapeutic opportunities that can be targeted to improve glycemia and/or prevent the onset of diabetes in susceptible populations.

CONFLICT OF INTEREST

The authors declare no conflict of interest.

ACKNOWLEDGEMENTS

This review was supported by R01 DK67536 and R01 DK103215 (to RNK). JS is supported by a Post-doctoral Fellowship for Research Abroad, the Japan Society for the Promotion of Science (JSPS) and the Uehara Memorial Foundation.

REFERENCES

1 Nanditha A, Ma RC, Ramachandran A, Snehalatha C, Chan JC, Chia KS *et al.* Diabetes in Asia and the Pacific: implications for the Global Epidemic. *Diabetes Care* 2016; **39**: 472–485.
2 Chan JC, Malik V, Jia W, Kadowaki T, Yajnik CS, Yoon KH *et al.* Diabetes in Asia: epidemiology, risk factors, and pathophysiology. *JAMA* 2009; **301**: 2129–2140.
3 Ramachandran A, Ma RC, Snehalatha C. Diabetes in Asia. *Lancet* 2010; **375**: 408–418.
4 Saisho Y, Butler AE, Manesso E, Elashoff D, Rizza RA, Butler PC. Beta-cell mass and turnover in humans: effects of obesity and aging. *Diabetes Care* 2013; **36**: 111–117.
5 Yoon KH, Ko SH, Cho JH, Lee JM, Ahn YB, Song KH *et al.* Selective beta-cell loss and alpha-cell expansion in patients with type 2 diabetes mellitus in Korea. *J Clin Endocrinol Metab* 2003; **88**: 2300–2308.
6 Rahier J, Guiot Y, Goebbels RM, Sempoux C, Henquin JC. Pancreatic beta-cell mass in European subjects with type 2 diabetes. *Diabetes Obes Metab* 2008; **10**: 32–42.
7 Kulkarni RN, Mizrachi EB, Ocana AG, Stewart AF. Human beta-cell proliferation and intracellular signaling: driving in the dark without a road map. *Diabetes* 2012; **61**: 2205–2213.
8 Bernal-Mizrachi E, Kulkarni RN, Scott DK, Mauvais-Jarvis F, Stewart AF, Garcia-Ocana A. Human beta-cell proliferation and intracellular signaling part 2: still driving in the dark without a road map. *Diabetes* 2014; **63**: 819–831.
9 Stewart AF, Hussain MA, Garcia-Ocana A, Vasavada RC, Bhushan A, Bernal-Mizrachi E *et al.* Human beta-cell proliferation and intracellular signaling: part 3. *Diabetes* 2015; **64**: 1872–1885.
10 Flier SN, Kulkarni RN, Kahn CR. Evidence for a circulating islet cell growth factor in insulin-resistant states. *Proc Natl Acad Sci USA* 2001; **98**: 7475–7480.
11 Tilg H, Moschen AR, Roden M. NAFLD and diabetes mellitus. *Nat Rev Gastroenterol Hepatol* 2016; **14**: 32–42.
12 Mellado-Gil J, Rosa TC, Demirci C, Gonzalez-Pertusa JA, Velazquez-Garcia S, Ernst S *et al.* Disruption of hepatocyte growth factor/c-Met signaling enhances pancreatic β-cell death and accelerates the onset of diabetes. *Diabetes* 2011; **60**: 525–536.
13 Alvarez-Perez JC, Ernst S, Demirci C, Casinelli GP, Mellado-Gil JMD, Rausell-Palamos F *et al.* Hepatocyte growth factor/c-Met signaling is required for β-cell regeneration. *Diabetes* 2014; **63**: 216–223.
14 El Ouaamari A, Kawamori D, Dirice E, Liew Chong W, Shadrach Jennifer L, Hu J *et al.* Liver-derived systemic factors drive beta cell hyperplasia in insulin-resistant states. *Cell Rep* 2013; **3**: 401–410.
15 El Ouaamari A, Dirice E, Gedeon N, Hu J, Zhou J-Y, Shirakawa J *et al.* SerpinB1 promotes pancreatic beta cell proliferation. *Cell Metab* 2016; **23**: 194–205.
16 Shirakawa J, Kulkarni RN. Novel factors modulating human beta-cell proliferation. *Diabetes Obes Metab* 2016; **18**: 71–77.
17 Hussain MA, Song W-J, Wolfe A. There is kisspeptin—and then there is kisspeptin. *Trends Endocrinol Metab* 2015; **26**: 564–572.
18 Song W-J, Mondal P, Wolfe A, Alonso Laura C, Stamateris R, Ong Benny WT *et al.* Glucagon regulates hepatic kisspeptin to impair insulin secretion. *Cell Metab* 2014; **19**: 667–681.
19 Rajwani A, Ezzat V, Smith J, Yuldasheva NY, Duncan ER, Gage M *et al.* Increasing circulating IGFBP1 levels improves insulin sensitivity, promotes nitric oxide production, lowers blood pressure, and protects against atherosclerosis. *Diabetes* 2012; **61**: 915–924.
20 Wang X, Wei W, Krzeszinski Jing Y, Wang Y, Wan Y. A liver-bone endocrine relay by IGFBP1 promotes osteoclastogenesis and mediates FGF21-induced bone resorption. *Cell Metab* 2015; **22**: 811–824.
21 Lu J, Liu K-C, Schulz N, Karampelias C, Charbord J, Hilding A *et al.* IGFBP1 increases β-cell regeneration by promoting α- to β-cell transdifferentiation. *EMBO J* 2016; **35**: 2026–2044.
22 Hussain MA, Akalestou E, Song W-j. Inter-organ communication and regulation of beta cell function. *Diabetologia* 2016; **59**: 659–667.
23 Ye R, Holland WL, Gordillo R, Wang M, Wang QA, Shao M *et al.* Adiponectin is essential for lipid homeostasis and survival under insulin deficiency and promotes β-cell regeneration. *eLife* 2014; **3**: e03851.

24 Ye R, Wang M, Wang QA, Scherer PE. Adiponectin-mediated antilipotoxic effects in regenerating pancreatic islets. *Endocrinology* 2015; **156**: 2019–2028.
25 Amitani M, Asakawa A, Amitani H, Inui A. The role of leptin in the control of insulin-glucose axis. *Front Neurosci* 2013; **7**: 51.
26 Kulkarni RN, Wang ZL, Wang RM, Hurley JD, Smith DM, Ghatei MA *et al.* Leptin rapidly suppresses insulin release from insulinoma cells, rat and human islets and, in vivo, in mice. *J Clin Invest* 1997; **100**: 2729–2736.
27 Chen P-C, Kryukova YN, Shyng S-L. Leptin regulates KATP channel trafficking in pancreatic β-cells by a signaling mechanism involving amp-activated protein kinase (AMPK) and cAMP-dependent protein kinase (PKA). *J Biol Chem* 2013; **288**: 34098–34109.
28 Polyzos SA, Kountouras J, Mantzoros CS. Adipokines in nonalcoholic fatty liver disease. *Metabolism* 2016; **65**: 1062–1079.
29 Lo James C, Ljubicic S, Leibiger B, Kern M, Leibiger Ingo B, Moede T *et al.* Adipsin is an adipokine that improves β cell function in diabetes. *Cell* 2014; **158**: 41–53.
30 Wang G-X, Zhao X-Y, Lin JD. The brown fat secretome: metabolic functions beyond thermogenesis. *Trends Endocrinol Metab* 2015; **26**: 231–237.
31 Whitham M, Febbraio MA. The ever-expanding myokinome: discovery challenges and therapeutic implications. *Nat Rev Drug Discov* 2016; **15**: 719–729.
32 Ellingsgaard H, Hauselmann I, Schuler B, Habib AM, Baggio LL, Meier DT *et al.* Interleukin-6 enhances insulin secretion by increasing glucagon-like peptide-1 secretion from L cells and alpha cells. *Nat Med* 2011; **17**: 1481–1489.
33 Guay C, Regazzi R. New emerging tasks for microRNAs in the control of β-cell activities. *Biochim Biophys Acta* 2016; **1861**: 2121–2129.
34 Jalabert A, Vial G, Guay C, Wiklander OPB, Nordin JZ, Aswad H *et al.* Exosome-like vesicles released from lipid-induced insulin-resistant muscles modulate gene expression and proliferation of beta recipient cells in mice. *Diabetologia* 2016; **59**: 1049–1058.
35 Jahng JWS, Song E, Sweeney G. Crosstalk between the heart and peripheral organs in heart failure. *Exp Mol Med* 2016; **48**: e217.
36 Baskin Kedryn K, Winders Benjamin R, Olson Eric N. Muscle as a 'mediator' of systemic metabolism. *Cell Metab* 2015; **21**: 237–248.
37 Hayden MR, Patel K, Habibi J, Gupta D, Tekwani SS, Whaley-Connell A *et al.* Attenuation of endocrine-exocrine pancreatic communication in type 2 diabetes: pancreatic extracellular matrix ultrastructural abnormalities. *J Cardiometab Syndr* 2008; **3**: 234–243.
38 Peiris H, Bonder CS, Coates PTH, Keating DJ, Jessup CF. The β-cell/EC axis: how do islet cells talk to each other? *Diabetes* 2014; **63**: 3–11.
39 Brissova M, Shostak A, Shiota M, Wiebe PO, Poffenberger G, Kantz J *et al.* Pancreatic islet production of vascular endothelial growth factor-a is essential for islet vascularization, revascularization, and function. *Diabetes* 2006; **55**: 2974–2985.
40 Olerud J, Mokhtari D, Johansson M, Christoffersson G, Lawler J, Welsh N *et al.* Thrombospondin-1: an islet endothelial cell signal of importance for β-cell function. *Diabetes* 2011; **60**: 1946–1954.
41 Cunha DA, Cito M, Carlsson P-O, Vanderwinden J-M, Molkentin JD, Bugliani M *et al.* Thrombospondin 1 protects pancreatic [beta]-cells from lipotoxicity via the PERK-NRF2 pathway. *Cell Death Differ* 2016; **23**: 1995–2006.
42 Kulkarni RN. GIP: no longer the neglected incretin twin? *Sci Transl Med* 2010; **2**: 49ps7.
43 Smith Eric P, An Z, Wagner C, Lewis Alfor G, Cohen Eric B, Li B *et al.* The role of β cell glucagon-like peptide-1 signaling in glucose regulation and response to diabetes drugs. *Cell Metab* 2014; **19**: 1050–1057.
44 Campbell JE, Ussher JR, Mulvihill EE, Kolic J, Baggio LL, Cao X *et al.* TCF1 links GIPR signaling to the control of beta cell function and survival. *Nat Med* 2016; **22**: 84–90.
45 Baothman OA, Zamzami MA, Taher I, Abubaker J, Abu-Farha M. The role of Gut Microbiota in the development of obesity and Diabetes. *Lipids Health Dis* 2016; **15**: 108.
46 Vrieze A, Van Nood E, Holleman F, Salojärvi J, Kootte RS, Bartelsman JFWM *et al.* Transfer of intestinal microbiota from lean donors increases insulin sensitivity in individuals with metabolic syndrome. *Gastroenterology* 2012; **143**: 913–6.e7.
47 Puddu A, Sanguineti R, Montecucco F, Viviani GL. Evidence for the gut microbiota short-chain fatty acids as key pathophysiological molecules improving diabetes. *Mediators Inflamm* 2014; **2014**: 9.
48 McNelis JC, Lee YS, Mayoral R, van der Kant R, Johnson AM, Wollam J *et al.* GPR43 potentiates beta-cell function in obesity. *Diabetes* 2015; **64**: 3203–3217.
49 Thorens B. Neural regulation of pancreatic islet cell mass and function. *Diabetes Obes Metab* 2014; **16**: 87–95.
50 Lausier J, Diaz WC, Roskens V, LaRock K, Herzer K, Fong CG *et al.* Vagal control of pancreatic β-cell proliferation. *Am J Physiol Endocrinol Metab* 2010; **299**: E786–E793.
51 Gautam D, Han SJ, Duttaroy A, Mears D, Hamdan FF, Li JH *et al.* Role of the M3 muscarinic acetylcholine receptor in beta-cell function and glucose homeostasis. *Diabetes Obes Metab* 2007; **9**: 158–169.
52 Borden P, Houtz J, Leach SD, Kuruvilla R. Sympathetic innervation during development is necessary for pancreatic islet architecture and functional maturation. *Cell Rep* 2013; **4**: 287–301.
53 Croizier S, Prevot V, Bouret SG. Leptin controls parasympathetic wiring of the pancreas during embryonic life. *Cell Rep* 2016; **15**: 36–44.
54 Rodriguez-Diaz R, Abdulreda MH, Formoso AL, Gans I, Ricordi C, Berggren PO *et al.* Innervation patterns of autonomic axons in the human endocrine pancreas. *Cell Metab* 2011; **14**: 45–54.
55 Rodriguez-Diaz R, Dando R, Jacques-Silva MC, Fachado A, Molina J, Abdulreda MH *et al.* Alpha cells secrete acetylcholine as a non-neuronal paracrine signal priming beta cell function in humans. *Nat Med* 2011; **17**: 888–892.
56 Imai J, Katagiri H, Yamada T, Ishigaki Y, Suzuki T, Kudo H *et al.* Regulation of pancreatic beta cell mass by neuronal signals from the liver. *Science* 2008; **322**: 1250–1254.
57 De Vos A, Heimberg H, Quartier E, Huypens P, Bouwens L, Pipeleers D *et al.* Human and rat beta cells differ in glucose transporter but not in glucokinase gene expression. *J Clin Invest* 1995; **96**: 2489–2495.
58 McCrimmon RJ, Evans ML, Fan X, McNay EC, Chan O, Ding Y *et al.* Activation of ATP-sensitive K+ channels in the ventromedial hypothalamus amplifies counter-regulatory hormone responses to hypoglycemia in normal and recurrently hypoglycemic rats. *Diabetes* 2005; **54**: 3169–3174.
59 Thorens B, Guillam MT, Beermann F, Burcelin R, Jaquet M. Transgenic reexpression of GLUT1 or GLUT2 in pancreatic beta cells rescues GLUT2-null mice from early death and restores normal glucose-stimulated insulin secretion. *J Biol Chem* 2000; **275**: 23751–23758.
60 Marty N, Dallaporta M, Foretz M, Emery M, Tarussio D, Bady I *et al.* Regulation of glucagon secretion by glucose transporter type 2 (glut2) and astrocyte-dependent glucose sensors. *J Clin Invest* 2005; **115**: 3545–3553.
61 Ogunnowo-Bada EO, Heeley N, Brochard L, Evans ML. Brain glucose sensing, glucokinase and neural control of metabolism and islet function. *Diabetes Obes Metab* 2014; **16**(Suppl 1): 26–32.
62 Tarussio D, Metref S, Seyer P, Mounien L, Vallois D, Magnan C *et al.* Nervous glucose sensing regulates postnatal beta cell proliferation and glucose homeostasis. *J Clin Invest* 2014; **124**: 413–424.
63 Razavi R, Chan Y, Afifiyan FN, Liu XJ, Wan X, Yantha J *et al.* TRPV1+ sensory neurons control beta cell stress and islet inflammation in autoimmune diabetes. *Cell* 2006; **127**: 1123–1135.
64 JUN regulation of energy metabolism by the skeleton. *Cell* 2007; **130**: 456–469.
65 Wei J, Hanna T, Suda N, Karsenty G, Ducy P. Osteocalcin promotes beta-cell proliferation during development and adulthood through Gprc6a. *Diabetes* 2014; **63**: 1021–1031.
66 Fulzele K, Riddle RC, DiGirolamo DJ, Cao X, Wan C, Chen D *et al.* Insulin receptor signaling in osteoblasts regulates postnatal bone acquisition and body composition. *Cell* 2010; **142**: 309–319.
67 Wei J, Ferron M, Clarke CJ, Hannun YA, Jiang H, Blaner WS *et al.* Bone-specific insulin resistance disrupts whole-body glucose homeostasis via decreased osteocalcin activation. *J Clin Invest* 2014; **124**: 1–13.
68 Hinoi E, Gao N, Jung DY, Yadav V, Yoshizawa T, Myers MG Jr. *et al.* The sympathetic tone mediates leptin's inhibition of insulin secretion by modulating osteocalcin bioactivity. *J Cell Biol* 2008; **183**: 1235–1242.
69 Morioka T, Asilmaz E, Hu J, Dishinger JF, Kurpad AJ, Elias CF *et al.* Disruption of leptin receptor expression in the pancreas directly affects beta cell growth and function in mice. *J Clin Invest* 2007; **117**: 2860–2868.
70 Huang C, Snider F, Cross JC. Prolactin receptor is required for normal glucose homeostasis and modulation of beta-cell mass during pregnancy. *Endocrinology* 2009; **150**: 1618–1626.
71 Karnik SK, Chen H, McLean GW, Heit JJ, Gu X, Zhang AY *et al.* Menin controls growth of pancreatic beta-cells in pregnant mice and promotes gestational diabetes mellitus. *Science* 2007; **318**: 806–809.
72 Kim H, Toyofuku Y, Lynn FC, Chak E, Uchida T, Mizukami H *et al.* Serotonin regulates pancreatic beta cell mass during pregnancy. *Nat Med* 2010; **16**: 804–808.
73 Demirci C, Ernst S, Alvarez-Perez JC, Rosa T, Valle S, Shridhar V *et al.* Loss of HGF/c-Met signaling in pancreatic beta-cells leads to incomplete maternal beta-cell adaptation and gestational diabetes mellitus. *Diabetes* 2012; **61**: 1143–1152.
74 Kondegowda NG, Fenutria R, Pollack IR, Orthofer M, Garcia-Ocana A, Penninger JM *et al.* Osteoprotegerin and denosumab stimulate human beta cell proliferation through inhibition of the receptor activator of NF-kappaB ligand pathway. *Cell Metab* 2015; **22**: 77–85.
75 De Jesus DF, Kulkarni RN. Epigenetic modifiers of islet function and mass. *Trends Endocrinol Metab* 2014; **25**: 628–636.
76 Ahren B. Beta- and alpha-cell dysfunction in subjects developing impaired glucose tolerance: outcome of a 12-year prospective study in postmenopausal Caucasian women. *Diabetes* 2009; **58**: 726–731.

77 Ferrara A, Karter AJ, Ackerson LM, Liu JY, Selby JV. Hormone replacement therapy is associated with better glycemic control in women with type 2 diabetes: The Northern California Kaiser Permanente Diabetes Registry. *Diabetes Care* 2001; **24**: 1144–1150.
78 Tiano JP, Delghingaro-Augusto V, Le May C, Liu S, Kaw MK, Khuder SS *et al.* Estrogen receptor activation reduces lipid synthesis in pancreatic islets and prevents beta cell failure in rodent models of type 2 diabetes. *J Clin Invest* 2011; **121**: 3331–3342.
79 Tiano JP, Mauvais-Jarvis F. Importance of oestrogen receptors to preserve functional beta-cell mass in diabetes. *Nat Rev Endocrinol* 2012; **8**: 342–351.
80 Yuchi Y, Cai Y, Legein B, De Groef S, Leuckx G, Coppens V *et al.* Estrogen receptor alpha regulates beta-cell formation during pancreas development and following injury. *Diabetes* 2015; **64**: 3218–3228.
81 Mauvais-Jarvis F. Role of sex steroids in beta cell function, growth, and survival. *Trends Endocrinol Metab* 2016; **27**: 844–855.
82 Gourdy P, Bourgeois EA, Levescot A, Pham L, Riant E, Ahui ML *et al.* Estrogen therapy delays autoimmune diabetes and promotes the protective efficiency of natural killer T-cell activation in female nonobese diabetic mice. *Endocrinology* 2016; **157**: 258–267.
83 Navarro G, Xu W, Jacobson DA, Wicksteed B, Allard C, Zhang G *et al.* Extranuclear actions of the androgen receptor enhance glucose-stimulated insulin secretion in the male. *Cell Metab* 2016; **23**: 837–851.
84 Costrini NV, Kalkhoff RK. Relative effects of pregnancy, estradiol, and progesterone on plasma insulin and pancreatic islet insulin secretion. *J Clin Invest* 1971; **50**: 992–999.
85 Picard F, Wanatabe M, Schoonjans K, Lydon J, O'Malley BW, Auwerx J. Progesterone receptor knockout mice have an improved glucose homeostasis secondary to beta -cell proliferation. *Proc Natl Acad Sci USA* 2002; **99**: 15644–15648.
86 Oda T, Taneichi H, Takahashi K, Togashi H, Hangai M, Nakagawa R *et al.* Positive association of free triiodothyronine with pancreatic beta-cell function in people with prediabetes. *Diabet Med* 2015; **32**: 213–219.
87 Aguayo-Mazzucato C, Zavacki AM, Marinelarena A, Hollister-Lock J, El Khattabi I, Marsili A *et al.* Thyroid hormone promotes postnatal rat pancreatic beta-cell development and glucose-responsive insulin secretion through MAFA. *Diabetes* 2013; **62**: 1569–1580.
88 Bruin JE, Saber N, O'Dwyer S, Fox JK, Mojibian M, Arora P *et al.* Hypothyroidism impairs human stem cell-derived pancreatic progenitor cell maturation in mice. *Diabetes* 2016; **65**: 1297–1309.
89 Donath MY, Halban PA. Decreased beta-cell mass in diabetes: significance, mechanisms and therapeutic implications. *Diabetologia* 2004; **47**: 581–589.
90 Eguchi K, Manabe I, Oishi-Tanaka Y, Ohsugi M, Kono N, Ogata F *et al.* Saturated fatty acid and TLR signaling link beta cell dysfunction and islet inflammation. *Cell Metab* 2012; **15**: 518–533.
91 Ehses JA, Perren A, Eppler E, Ribaux P, Pospisilik JA, Maor-Cahn R *et al.* Increased number of islet-associated macrophages in type 2 diabetes. *Diabetes* 2007; **56**: 2356–2370.
92 Morris DL. Minireview: emerging concepts in islet macrophage biology in type 2 diabetes. *Mol Endocrinol* 2015; **29**: 946–962.
93 Brissova M, Aamodt K, Brahmachary P, Prasad N, Hong JY, Dai C *et al.* Islet microenvironment, modulated by vascular endothelial growth factor-A signaling, promotes beta cell regeneration. *Cell Metab* 2014; **19**: 498–511.
94 Dirice E, Kahraman S, Jiang W, El Ouaamari A, De Jesus DF, Teo AK *et al.* Soluble factors secreted by T cells promote beta-cell proliferation. *Diabetes* 2014; **63**: 188–202.
95 Valdez IA, Dirice E, Gupta MK, Shirakawa J, Teo AK, Kulkarni RN. Proinflammatory cytokines induce endocrine differentiation in pancreatic ductal cells via STAT3-dependent NGN3 activation. *Cell Rep* 2016; **15**: 460–470.
96 Butcher MJ, Hallinger D, Garcia E, Machida Y, Chakrabarti S, Nadler J *et al.* Association of proinflammatory cytokines and islet resident leucocytes with islet dysfunction in type 2 diabetes. *Diabetologia* 2014; **57**: 491–501.
97 Jaeckle Santos LJ, Li C, Doulias PT, Ischiropoulos H, Worthen GS, Simmons RA. Neutralizing Th2 inflammation in neonatal islets prevents beta-cell failure in adult IUGR rats. *Diabetes* 2014; **63**: 1672–1684.
98 Cabrera O, Berman DM, Kenyon NS, Ricordi C, Berggren PO, Caicedo A. The unique cytoarchitecture of human pancreatic islets has implications for islet cell function. *Proc Natl Acad Sci USA* 2006; **103**: 2334–2339.
99 Fiaschi-Taesch NM, Kleinberger JW, Salim FG, Troxell R, Wills R, Tanwir M *et al.* Human pancreatic beta-cell G1/S molecule cell cycle atlas. *Diabetes* 2013; **62**: 2450–2459.